

**STUDY OF STATIC STABILITY AND VIBRATIONS OF CIRCULAR
AND ANNULAR PLATES ON GENERALIZED ELASTIC MEDIUM**

LOKAVARAPU BHASKARA RAO



**Thesis Submitted To Osmania University
For The Award of Degree of**

Doctor of Philosophy

IN MECHANICAL ENGINEERING

2008

**STUDY OF STATIC STABILITY AND VIBRATIONS OF CIRCULAR
AND ANNULAR PLATES ON GENERALIZED ELASTIC MEDIUM**

LOKAVARAPU BHASKARA RAO



**Thesis Submitted To Osmania University
For The Award of Degree of
Doctor of Philosophy**

IN MECHANICAL ENGINEERING

2008

DEDICATED TO
MY BELOVED FATHER
LATE L. S. PATRUDU [BABULU]

DEPARTMENT OF MECHANICAL ENGINEERING
UNIVERSITY COLLEGE OF ENGINEERING
(AUTONOMOUS)
OSMANIA UNIVERSITY
HYDERABAD, INDIA



CERTIFICATE

This is to certify that the Thesis or Dissertation entitled “**STUDY OF STATIC STABILITY AND VIBRATIONS OF CIRCULAR AND ANNULAR PLATES ON GENERALIZED ELASTIC MEDIUM**” submitted to Osmania University, Hyderabad by **LOKAVARAPU BHASKARA RAO** for the award of the degree of Doctor of Philosophy in Mechanical Engineering is a record of bonafide research work carried out by him. The contents of this thesis have not been submitted to any other University/Institution for the award of any degree.

HEAD

Prof. V. Nageswara Rao,
Department of Mechanical Engineering,
University College of Engineering,
Osmania University, Hyderabad, India.

INTERNAL GUIDE,
Dr. G. Rama Murty,
Department of Mechanical Engineering,
M. J. College of Engineering & Technology,
Hyderabad, India.

EXTERNAL GUIDE,
Dr. C. Kameswara Rao,
Client Manager (Mechanical),
SciTech Patent Services (P) Ltd,
Hyderabad, India.

DECLARATION

This is to certify that the thesis entitled “**STUDY OF STATIC STABILITY AND VIBRATIONS OF CIRCULAR AND ANNULAR PLATES ON GENERALIZED**

ELASTIC MEDIUM” does not constitute any part of another thesis / dissertation / monograph submitted to this or any other University / Institution.

LOKAVARAPU BHASKARA RAO

Associate Professor,
Department of Mechanical Engineering,
DRK College of Science & Technology,
Bowrampet (V), Via Air Force Academy,
Hyderabad, India.

ACKNOWLEDGEMENTS

I would like to express my sincere appreciation and gratitude to my supervisor Dr. C. Kameswara Rao, Client Manager (Mechanical), SciTech Patent (Pvt) Ltd, Hyderabad for suggesting the problem. His invaluable knowledge and support were indispensable for this work. I am grateful for his help, cooperation, constant encouragement, thoughtfulness, supervision and advice often beyond the scope of my thesis work. Working under his able guidance for the Ph.D. degree was not only a mere academic pursuit but also a thorough education for me. He has been that of a friend, philosopher and guide.

I thank Dr. G. Ramamurty, Professor, M. J. College of Engineering & Technology, Hyderabad for all his suggestions and guidance in the for working for the thesis

Finally, I would like to express my deep gratitude and sincere appreciation to my family. This work would not have come to an end without their patience, sacrifice and insistence that I acquire a higher research degree. I am also deeply indebted to my wife and daughter for their patience and support. I am forever grateful to my family, friends for their love, kindness and belief in me.

ABSTRACT

The present study is to theoretically investigate the effect of elastically restrained edges on buckling and transverse vibrations of circular and annular plates resting on elastic foundation and also to investigate the effect of internal elastic/rigid ring type support on buckling. The general equations of motions are derived for each of the cases studied in the thesis and exact expressions for buckling and natural frequencies are derived. This method is also utilized in analyzing the stability criterion of circular and annular plates under the presence of elastic foundation and internal elastic/rigid ring support. The previous works contributed by many researchers had restricted themselves to study of circular and annular plates with classical boundary conditions and obtained buckling load and frequency parameters. It is also observed that no provision has been made to include the effect of generalized elastic edge conditions, while determining the buckling load and frequency parameters and also to determine mode switching as well.

The influence of the rotational, translational elastic restraint parameters (R_{11}, R_{22}, T_{11} & T_{22}), elastic foundation parameters (ξ) and internal elastic/rigid ring type support are studied in details in this thesis both for circular and annular plates. It is seen that the effect of these parameters on buckling loads and natural frequencies is quite significant. The results obtained thereon by solving the exact closed form stability and frequency equations are then confirmed numerically by comparing with earlier results. Numerical results are obtained for various combinations of parameters and are plotted stating the influence of variation of rotational stiffness parameter R_{11} , translational stiffness parameter T_{11} , elastic ring support stiffness parameter T_{22} , and elastic foundation stiffness parameters ξ , on buckling load and frequency parameters of both circular and annular plates. From the various case studies carried out important conclusions are drawn and suggestions are made for future work that can be taken up in this area of research.

LIST OF FIGURES

Figure	Description	Page
1.1	Winkler Model	9
2.1	Laterally loaded Rectangular Plate	15
2.2	External and Internal Forces on the element of the middle surface.	16
2.3	Stresses on a Plate element	20
2.4	Section before and after Deflection	21
2.5	Angular Distortion	21
2.6a	Relationship between Cartesian and Polar Coordinates.	26
2.6b	Plate element.	26
2.7a	Various boundary conditions Fixed Edge	32
2.7b	Various boundary conditions Free Edge	32
2.7c	Various boundary conditions Simple Support	32
2.7d	Various boundary conditions Elastic Support	32
2.7e	Various boundary conditions Elastic Restraint	32
2.7f	Various boundary conditions Elastic Support and Restraint	33
2.8	Applied in-plane Forces and Moments in a Plate Element	37

2.9	Transformation Between Rectangular and Polar Coordinate Systems	39
2.10	Moments and Shear Forces on an Element of a Circular Plate	40
3.1	Buckling of a Circular Plate with an Elastically Restrained edge against Rotation and Translation and Resting on Elastic Foundation	51
3.2	Buckling Load Parameter k , versus foundation Stiffness Parameter ξ , for Rotational and Translational Parameters of $R_{11} = T_{11} = 1$	70
3.3	Buckling Load Parameter k , versus foundation Stiffness Parameter ξ , for Rotational and Translational Parameters of $R_{11} = T_{11} = 10$	71
3.4	Buckling Load Parameter k , versus foundation Stiffness Parameter ξ , for Rotational and Translational Parameters of $R_{11} = T_{11} = 100$	72
3.5	Buckling Load Parameter k , versus foundation Stiffness Parameter ξ , for Clamped boundary condition	73
4.1	Buckling of a Circular Plate with an Internal <i>Elastic Ring</i> Support and Elastically Restrained Edge against Rotation and Translation	75
4.2	Buckling of a Circular Plate with an Internal <i>Elastic Ring</i> Support and Restrained Edge against Rotation	86
4.3	Buckling of a Circular Plate with an Internal <i>Elastic Ring</i> Support and Restrained Guided Edge against Translation	87
4.4	Buckling of a Circular Plate with an Internal <i>Elastic Ring</i> Support and Restrained Edge against Translation	89
4.5	Buckling of a Circular Plate with an Internal <i>Elastic Ring</i> Support and Guided Edge	89
4.6	Buckling of a Circular Plate with an Internal <i>Elastic Ring</i> Support and Simply Supported Edge	90
4.7	Buckling of a Circular Plate with an Internal <i>Elastic Ring</i> Support and Clamped Edge	90
4.8	Buckling of a Circular Plate with an Internal <i>Elastic Ring</i> Support and Free Edge	91
4.9	Buckling of a Circular Plate with an Internal Ring Support and Elastically Restrained Edge against Rotation and Translation	92
4.10	Buckling of a Circular plate with an <i>Internal ring</i> Support and Restrained Guided Edge against Translation	95
4.11	Buckling of a Circular plate with an <i>Internal ring</i> Support and Restrained Edge against Translation	95

4.12	Buckling of a Circular plate with an <i>Internal ring</i> Support and Guided Edge	97
4.13	Buckling of a Circular plate with an <i>Internal ring</i> Support and Simply Supported Edge	97
4.14	Buckling of a Circular plate with an <i>Internal ring</i> Support and Clamped Edge	98
4.15	Buckling Load Parameter k , versus Internal <i>Elastic Ring</i> Support Radius b , for various values of R_{11} & $T_{11} = T_{22} = 1000$	105
4.16	Buckling Load Parameter k , versus Internal <i>Elastic Ring</i> Support Radius b , for various values of T_{22} & $R_{11} = T_{11} = 1000$	106
4.17	Buckling Load Parameter k , versus Internal <i>Elastic Ring</i> Support Radius b , for various values of T_{11} & $R_{11} = T_{22} = 1000$	106
4.18	Buckling Load Parameter k , versus Internal <i>Elastic Ring</i> Support Radius b , for various values of R_{11}, T_{11} & T_{22}	107
4.19	Buckling Load Parameter k , versus Internal Elastic Ring Support Radius b , for various values of $R_{11} = 0.5$ & $T_{22} = 100000$	110
4.20	Buckling Load Parameter k , versus Internal Elastic Ring Support Radius b , for various values of $R_{11} = 10$ & $T_{22} = 100000$	110
4.21	Buckling Load Parameter k , versus Internal Elastic Ring Support Radius b , for various values of $R_{11} = 100$ & $T_{22} = 100000$	111
4.22	Buckling Load Parameter k , versus Internal Elastic Ring Support Radius b , for various values of $R_{11} = \infty$ & $T_{22} = 100000$	111
4.23	Buckling Load Parameter k , versus Internal Elastic Ring Support Radius b , for various values of $T_{22} = 1000$ & $R_{11} = 1000$	113
4.24	Buckling Load Parameter k , versus Internal Elastic Ring Support Radius b , for various values of $T_{22} = 100000$ & $R_{11} = 1000$	114
4.25	Buckling Load Parameter k , versus Internal Elastic Ring Support Radius b , for various values of $T_{22} = \infty$ & $R_{11} = 1000$	114
4.26	Buckling Load Parameter k , versus Internal Elastic Ring Support Radius b , for various values of $T_{11} = T_{22} = 1000$	117
4.27	Buckling Load Parameter k , versus Internal Elastic Ring Support	117

	Radius b , for various values of $T_{11} = \infty$ & $T_{22} = 1000$	
4.28	Buckling Load Parameter k , versus Internal Elastic Ring Support Radius b , for various values of $T_{11} = T_{22} = 1000$	120
4.29	Buckling Load Parameter k , versus Internal Elastic Ring Support Radius b , for various values of $T_{11} = 1000$ & $T_{22} = \infty$	120
4.30	Buckling Load Parameter k , versus Internal Elastic Ring Support Radius b , for various values of $T_{22} (=100)$ when $T_{11} = 10000$	123
4.31	Buckling Load Parameter k , versus Internal Elastic Ring Support Radius b , for various values of $T_{22} (=10^{16})$ when $T_{11} = 10000$	124
4.32	Buckling Load Parameter k , versus Internal Elastic Ring Support Radius b , for Translational Spring Stiffness Parameter of an internal Elastic Ring, $T_{22}=100$	127
4.33	Percentage of Increase in Buckling Load Parameter k , versus Internal Elastic Ring Support Radius b , for Translational Spring Stiffness Parameter of an Internal Elastic Ring, $T_{22}=100$	127
4.34	Buckling Load Parameter k , versus Internal Elastic Ring Support Radius b , for Translational Spring Stiffness Parameter of an internal Elastic Ring, $T_{22} = 10^{16}$	128
4.35	Percentage of Increase in Buckling Load Parameter k , versus Internal Elastic Ring Support Radius b , for Translational Spring Stiffness Parameter of an Internal Elastic Ring, $T_{22} = 10^{16}$	128
4.36	Buckling Load Parameter k , versus Internal Elastic Ring Support Parameter b , for Translational Spring Stiffness Parameter of an internal Elastic Ring, $T_{22}=100$	131
4.37	Percentage of Increase in Buckling Load Parameter k , versus Internal Elastic Ring Support Parameter b , for Translational Spring Stiffness Parameter of an Internal Elastic Ring, $T_{22}=100$	132
4.38	Buckling Load Parameter k , versus Internal Elastic Ring Support Parameter b , for Translational Spring Stiffness Parameter of an Internal Elastic Ring, $T_{22} = 10^{16}$	132
4.39	Percentage of Increase in Buckling Load Parameter k , versus Internal Elastic Ring Support Parameter b , for Translational Spring Stiffness Parameter of an Internal Elastic Ring, $T_{22} = 10^{16}$	133
4.40	Buckling Load Parameter k , versus <i>Internal ring</i> Support Radius b , for $R_{11} = 0.3$ & $T_{11} = 100$	135

4.41	Buckling Load Parameter k , versus <i>Internal ring</i> Support Radius b , for $R_{11} = 0.5$ & $T_{11} = 1000$	135
4.42	Buckling Load Parameter k , versus <i>Internal ring</i> Support Radius b , for $R_{11} = 50$ & $T_{11} = 1000$	136
4.43	Buckling Load Parameter k , versus <i>Internal ring</i> Support Radius b , for $R_{11} = T_{11} = \infty$	136
4.44	Buckling Load Parameter, k versus <i>Internal ring</i> Support Radius, b for $T_{11} = 1000$	142
4.45	Buckling Load Parameter, k versus <i>Internal ring</i> Support Radius, b for $T_{11} = 100000$	142
4.46	Buckling Load Parameter, k versus <i>Internal ring</i> Support Radius, b for $T_{11} = \infty$	143
4.47	Buckling Load Parameter, k versus Poisson's Ratio, ν , for $T_{11} = 1000$ and internal <i>ring</i> support radius parameter, b	143
4.48	Buckling Load Parameter k , versus <i>Internal ring</i> Support Radius b , for $T_{11} = 10$	146
4.49	Buckling Load Parameter k , versus <i>Internal ring</i> Support Radius b , for $T_{11} = \infty$	146
4.50	Buckling Load Parameter k , versus <i>Internal ring</i> Support Radius b , for Simply Supported Plate	149
4.51	Buckling Load Parameter k , versus <i>Internal ring</i> Support Radius b , for Clamped Plate	150
5.1	Buckling of an Annular Plate with Elastically Restrained Edges against Rotation and Translation	152
5.2	Buckling Load Parameter k , versus Internal Radius Parameter b , for $R_{11} = 0.001$ and $R_{22} = T_{11} = T_{22} = 10$ ($n = 0$ for <i>axisymmetric</i> mode and $n = 1$ for <i>asymmetric</i> mode).	171
5.3	Buckling Load Parameter k , versus Internal Radius Parameter b , for $R_{11} = 0.5$ and $R_{22} = T_{11} = T_{22} = 10$ ($n = 0$ for <i>axisymmetric</i> mode and $n = 1$ for <i>asymmetric</i> mode).	172
5.4	Buckling Load Parameter k , versus Internal Radius Parameter b , for $R_{11} = 10$ and $R_{22} = T_{11} = T_{22} = 10$ ($n = 0$ for <i>axisymmetric</i> mode and $n = 1$ for <i>asymmetric</i> mode).	172

5.5	Buckling Load Parameter k , versus Internal Radius Parameter b , for $R_{11} = 100$ and $R_{22} = T_{11} = T_{22} = 10$ ($n = 0$ for <i>axisymmetric</i> mode and $n = 1$ for <i>asymmetric</i> mode).	173
5.6	Buckling Load Parameter k , versus Internal Radius Parameter b , for $R_{11} = \infty$ and $R_{22} = T_{11} = T_{22} = 10$ ($n = 0$ for <i>axisymmetric</i> mode and $n = 1$ for <i>asymmetric</i> mode).	173
5.7	Buckling Load Parameter k , versus Internal Radius Parameter b , for $R_{22} = 5$ and $R_{11} = T_{11} = T_{22} = 10$ ($n = 0$ for <i>axisymmetric</i> mode and $n = 1$ for <i>asymmetric</i> mode).	175
5.8	Buckling Load Parameter k , versus Internal Radius Parameter b , for $R_{22} = 10$ and $R_{11} = T_{11} = T_{22} = 10$ ($n = 0$ for <i>axisymmetric</i> mode and $n = 1$ for <i>asymmetric</i> mode).	175
5.9	Buckling Load Parameter k , versus Internal Radius Parameter b , for $R_{22} = 100$ and $R_{11} = T_{11} = T_{22} = 10$ ($n = 0$ for <i>axisymmetric</i> mode and $n = 1$ for <i>asymmetric</i> mode).	176
5.10	Buckling Load Parameter k , versus Internal Radius Parameter b , for $R_{22} = \infty$ and $R_{11} = T_{11} = T_{22} = 10$ ($n = 0$ for <i>axisymmetric</i> mode and $n = 1$ for <i>asymmetric</i> mode).	176
5.11	Buckling Load Parameter k , versus Internal Radius Parameter b , for $T_{11} = 5$ and $R_{11} = R_{22} = T_{22} = 10$ ($n = 0$ for <i>axisymmetric</i> mode and $n = 1$ for <i>asymmetric</i> mode).	178
5.12	Buckling Load Parameter k , versus Internal Radius Parameter b , for $T_{11} = 10$ and $R_{11} = R_{22} = T_{22} = 10$ ($n = 0$ for <i>axisymmetric</i> mode and $n = 1$ for <i>asymmetric</i> mode).	179
5.13	Buckling Load Parameter k , versus Internal Radius Parameter b , for $T_{11} = 100$ and $R_{11} = R_{22} = T_{22} = 10$ ($n = 0$ for <i>axisymmetric</i> mode and $n = 1$ for <i>asymmetric</i> mode).	179
5.14	Buckling Load Parameter k , versus Internal Radius Parameter b , for $T_{11} = \infty$ and $R_{11} = R_{22} = T_{22} = 10$ ($n = 0$ for <i>axisymmetric</i> mode and $n = 1$ for <i>asymmetric</i> mode).	180
5.15	Buckling Load Parameter k , versus Internal Radius Parameter b , for $R_{11} = 0.2$ ($n = 0$ for <i>axisymmetric</i> mode and $n = 1$ for <i>asymmetric</i> mode).	183
5.16	Buckling Load Parameter k , versus Internal Radius Parameter b , for $R_{11} = 5$ ($n = 0$ for <i>axisymmetric</i> mode and $n = 1$ for	183

	<i>asymmetric mode</i>).	
5.17	Buckling Load Parameter k , versus Internal Radius Parameter b , for $R_{11} = 100$ ($n=0$ for <i>axisymmetric mode</i> and $n=1$ for <i>asymmetric mode</i>).	184
5.18	Buckling Load Parameter k , versus Internal Radius Parameter b , for $R_{11} = 10^{16}$ ($n=0$ for <i>axisymmetric mode</i> and $n=1$ for <i>asymmetric mode</i>).	184
5.19	Buckling Load Parameter k , versus Internal Radius Parameter b , for $R_{11} = 0.2$ & $\nu = 0$ ($n=0$ for <i>axisymmetric mode</i> and $n=1$ for <i>asymmetric mode</i>).	187
5.20	Buckling Load Parameter k , versus Internal Radius Parameter b , for $R_{11} = 0.2$ & $\nu = 0.1$ ($n=0$ for <i>axisymmetric mode</i> and $n=1$ for <i>asymmetric mode</i>).	188
5.21	Buckling Load Parameter k , versus Internal Radius Parameter b , for $R_{11} = 0.2$ & $\nu = 0.2$ ($n=0$ for <i>axisymmetric mode</i> and $n=1$ for <i>asymmetric mode</i>).	188
5.22	Buckling Load Parameter k , versus Internal Radius Parameter b , for $R_{11} = 0.2$ & $\nu = 0.3$ ($n=0$ for <i>axisymmetric mode</i> and $n=1$ for <i>asymmetric mode</i>).	189
5.23	Buckling Load Parameter k , versus Internal Radius Parameter b , for $R_{11} = 0.2$ & $\nu = 0.4$ ($n=0$ for <i>axisymmetric mode</i> and $n=1$ for <i>asymmetric mode</i>).	189
5.24	Buckling Load Parameter k , versus Internal Radius Parameter b , for <i>axisymmetric mode</i> ($n=0$) and <i>asymmetric mode</i> ($n=1$) when $R_{11} = 0.2$ & $\nu = 0.5$.	190
5.25	Critical Buckling Load Parameter, k versus Poisson Ratio, ν for <i>axisymmetric mode</i> ($n=0$) and <i>asymmetric mode</i> ($n=1$)	190
6.1	A thin circular plate with rotational K_{R1} and translational K_{T1} elastic edge constraints and supporting on full elastic foundation.	193
6.2	A thin circular plate with translational K_{T1} elastic edge constraints and supported on full elastic foundation	198
6.3	A thin circular plate with rotational K_R elastic edge constraints and supported on full elastic foundation	199

6.4	A thin circular plate with guided edge and supported on full elastic foundation	200
6.5	Effect of Rotational stiffness ratio, R_{11} on eigenvalues, λ_{mn}	204
6.5a(i)-(iv)	Mode shape parameters C_{mn} , for different Rotational constraint for $T_{11}=100$; $\xi=100$ & $\nu=0.33$	207
6.5b(i)-(iv)	Normalization constants A_{mn} , for different Rotational constraint for $T_{11}=100$; $\xi=100$ & $\nu=0.33$	210
6.6	Effect of Translational constraint, T_{11} on eigenvalues, λ_{mn}	212
6.6a(i)-(iv)	Mode shape parameters C_{mn} , for different Translational constraint for $R_{11}=100$; $\xi=100$ & $\nu=0.33$	214
6.6b(i)-(iv)	Normalization constant A_{mn} , for different Translational constraint for $R_{11}=100$; $\xi=100$ & $\nu=0.33$	217
6.7	Effect of Foundation constraint, ξ on eigenvalues, λ_{mn}	218
6.8	Effect of Foundation constraint, ξ on eigenvalues, λ_{mn}	219
6.8a(i)-(iv)	Mode shape parameters C_{mn} , for different foundation stiffness for $R_{11}=10$; $T_{11}=1000$ & $\nu=0.33$	222
6.8b(i)-(iv)	Normalization constant A_{mn} , for different foundation stiffness for $R_{11}=10$; $T_{11}=1000$ & $\nu=0.33$	224
6.9	Effect of Poisson ratio on Eigenvalues	225
6.10	Effect of translational constraint, T_{11} on eigenvalues, λ_{mn}	227
6.11	A simply supported thin circular plate resting on full elastic foundation	227
6.12	Effect of Foundation constraint, ξ on eigenvalues, λ_{mn}	229
6.13	Effect of translational, T_{11} and foundation, ξ constraints on eigenvalues, λ_{mn}	230
6.14	Effect of Poisson ratio, ν on eigenvalues, λ_{mn}	231
6.15	Effect of Rotational constraint, T_{11} on eigenvalues, λ_{mn}	233

6.16	A clamped thin circular plate resting on full elastic foundation	233
6.17	Effect of Foundation constraint, ξ on eigenvalues, λ_{mn}	235
6.18	Effect of Rotational, R and foundation, ξ constraints on eigenvalues, λ_{mn}	236
6.19	Effect of Poisson ratio, ν on eigenvalues, λ_{mn}	237
6.20	Effect of Foundation constraint, ξ on eigenvalues, λ_{mn}	239
6.21	Effect of Poisson ratio, ν on eigenvalues, λ_{mn}	240
7.1	Annular Plate with Rotational and Translational Constraints at inner and outer Edge and Resting on Elastic Foundation	242
7.2	Annular plate with Translational Constraints at inner Edge and Rotational and Translational constraints at outer edge and Resting on Elastic Foundation	260
7.3	Annular plate with Rotational Constraint and simply supported at inner edge and Rotational and Translational Constraints at outer Edge and Resting on Elastic Foundation	262
7.4	Effect of Non-Dimensional Rotational Spring Stiffness R_{11} , on Frequency Parameter for $T_{11} = R_{22} = T_{22} = 100$ & $\xi = 10$	265
7.5	Effect of Non-Dimensional Translational Spring Stiffness Parameter T_{11} , on Frequency Parameter for $R_{11} = R_{22} = T_{22} = 100$ & $\xi = 10$	266
7.6	Effect of Non-Dimensional Foundation Stiffness ξ , on Frequency Parameter for $R_{11} = T_{11} = R_{22} = T_{22} = 100$	268
7.7	Effect of Non-Dimensional Rotational R_{11} , Translational T_{11} , and Foundation ξ , Stiffness Parameters on Frequency Parameter for $R_{22} = T_{22} = 100$	269
7.8	Effect of Non-Dimensional Rotational Stiffness R_{11} , Translational Stiffness T_{11} , and Foundation Stiffness ξ , Parameters on Frequency Parameter for $R_{22} = T_{22} = 100$	270
7.9	Effect of Non-Dimensional Rotational Spring Stiffness R_{22} , on Frequency Parameter for $R_{11} = T_{11} = T_{22} = 100$ & $\xi = 10$	272

7.10	Effect of Non-Dimensional Translational Spring Stiffness Parameter T_{22} , on Natural Frequency for $R_{11} = R_{22} = T_{11} = 100$ & $\xi = 10$	273

LIST OF TABLES

Table	Description	Page
-------	-------------	------

2.1	Mathematical expressions for various boundary conditions	35
3.1	Buckling (for axisymmetric and asymmetric modes) Load Parameters for various Rotational, Translational and Foundation Parameters (R_{11}, T_{11} & ξ) and $\nu=0.33$	70
3.2	Comparison of Mode Switches with Wang [13] Clamped boundary and Poisson's ratio = 0.3.	73
4.1	Buckling (for axisymmetric and asymmetric modes) Load Parameters for different values of Rotational Stiffness Parameters, R_{11} and constant Translational Stiffness Parameter, T_{11} and Translational Stiffness Parameter of Internal <i>Elastic Ring</i> , T_{22} ($T_{11} = T_{22} = 1000$) when $\nu = 0.3$	100
4.2	Optimal Locations of an Internal <i>Elastic Ring</i> Support b_{opt} , the Corresponding Buckling Load Parameter k_{opt} and the Percentage Increase in Buckling Load Parameter	101
4.3	Buckling (for axisymmetric and asymmetric modes) Load Parameters for different values of Translational Stiffness Parameter of Internal <i>Elastic Ring</i> , T_{22} and Constant Rotational Stiffness Parameters, $R_{11} = 100$ & Translational Stiffness Parameter, $T_{11} = 1000$ when $\nu = 0.3$	102
4.4	Optimal Locations of an Internal <i>Elastic Ring</i> Support b_{opt} , the Corresponding Buckling Load Parameter and Percentage Increase in Buckling Parameter	102
4.5	Buckling (for axisymmetric and asymmetric modes) Load Parameters for different values of Translational Stiffness Parameter, T_{11} and Constant Rotational Stiffness Parameters, $R_{11} = 1000$ & T_{11} Translational Stiffness Parameter of Internal T_{11} <i>Elastic Ring</i> , $T_{22} = 1000$, when $\nu = 0.3$	103
4.6	Optimal Locations of an Internal <i>Elastic Ring</i> Support b_{opt} , the Corresponding Buckling Load Parameter and Percentage Increase in Buckling Load Parameter	103
4.7	Buckling (for axisymmetric and asymmetric modes) Load Parameters for different values of Rotational Stiffness Parameters, R_{11} , Translational Stiffness Parameter, T_{11} and Translational Stiffness Parameter of Internal <i>Elastic Ring</i> , T_{22} , when $\nu = 0.3$	104

4.8	Optimal Locations of an Internal <i>Elastic Ring</i> Support b_{opt} , the Corresponding Buckling Load Parameter k_{opt} and Percentage Increase in Buckling Load Parameter	105
4.9	Comparison of Buckling Load Parameter k , with Wang et al. [68] for various Rotational Stiffness Parameters R_{11} and Poisson's ratio = 0.3	107
4.10	Buckling (for axisymmetric and asymmetric modes) Load Parameters for different values of Rotational Stiffness Parameters, R_{11} and constant Translational Stiffness Parameter of Internal <i>Elastic Ring</i> , $T_{22} = 10000$, when $\nu = 0.3$	109
4.11	Optimal location of an internal elastic ring support b_{opt} , the corresponding buckling load parameter k_{opt} and Percentage Increase in Buckling Load Parameter	109
4.12	Buckling (for axisymmetric and asymmetric modes) Load Parameters for different values of Translational Stiffness Parameter of Internal <i>Elastic Ring</i> , T_{22} and Constant Rotational Stiffness Parameters, $R_{11} = 1000$, when $\nu = 0.3$	113
4.13	Optimal locations of an internal elastic ring support b_{opt} , the corresponding buckling load parameter k_{opt} and Percentage Increase in Buckling Load Parameter	115
4.14	Buckling (for axisymmetric and asymmetric modes) Load Parameters for different values of Translational Stiffness Parameters, T_{11} when $T_{22} = 1000$ and $\nu = 0.3$	116
4.15	Buckling (for axisymmetric and asymmetric modes) Load Parameters for different values of Translational Stiffness Parameters of Elastic Ring support, T_{22} when $T_{11} = 1000$ and $\nu = 0.3$	118
4.16	Optimal location of an internal elastic ring support b_{opt} , the corresponding buckling load parameter k_{opt} and Percentage Increase in Buckling Load Parameter	121
4.17	Optimal locations of an internal elastic ring support b_{opt} , the corresponding buckling load parameter k_{opt} and Percentage increase in Buckling Load Parameter	121
4.18	Buckling (for axisymmetric and asymmetric modes) Load Parameters for different values of Translational Stiffness of Elastic Ring parameter, T_{22} when $T_{11} = 10000$ and $\nu = 0.3$	123

4.19	Buckling (for axisymmetric and asymmetric modes) Load Parameters for different values of Translational Spring Stiffness Parameter of an Internal Elastic Ring, T_{22} when $\nu = 0.3$	126
4.20	Buckling (for axisymmetric and asymmetric modes) Load Parameters for different values of Translational Stiffness Parameter of Internal Elastic Ring, T_{22} when $\nu = 0.3$	131
4.21	Buckling (for axisymmetric and asymmetric modes) Load Parameters for different values of Rotational, R_{11} and Translational Stiffness, T_{11} Parameters when $\nu = 0.3$	134
4.22	The cross over radius of the ring support for various values of Rotational, R_{11} and Translational Stiffness, T_{11} Parameters when $\nu = 0.3$	134
4.23	Optimum location of the ring support, the corresponding buckling Load parameters and Percentage Increase in Buckling Load Parameters	137
4.24	Comparison of Buckling Load Parameter k , with Laura et al. [2] and Wang et al. [69] for Rotational stiffness Parameter $R_{11} = 0$ & $\nu = 0.3$	138
4.25	Comparison of Buckling Load Parameter k , with Laura et al. [2] for Rotational stiffness Parameter $R_{11} = \infty$ & $\nu = 0.3$	138
4.26	Comparison of Buckling Load Parameter k , with Wang et al. [69] for Rotational stiffness Parameter $R_{11} = 10^5$ & $\nu = 0.3$	138
4.27	Comparison of Buckling Load Parameter k , with Wang et al. [67] and Wang et al [69] for Clamped Edge for Rotational stiffness Parameter $R_{11} = 10^5$ & $\nu = 0.3$	139
4.28	Comparison of Buckling Load Parameter k , with Wang et al. [67] and Wang et al [69] for Simply Supported Edge for Rotational Stiffness Parameter $R_{11} = 0$ & $\nu = 0.3$	139
4.29	Optimum location of the ring support and the corresponding Buckling load parameters	139
4.30	Buckling (for axisymmetric and asymmetric modes) Load Parameters for different values of Translational Stiffness, T_{11} Parameters when $\nu = 0.3$	144
4.31	Optimum location of the ring support, the corresponding buckling Load parameters and Percentage of Increase in Buckling Load Parameters	144

4.32	Buckling (for axisymmetric and asymmetric modes) Load Parameters for different values of Translational Stiffness, T_{11} Parameters when $\nu = 0.3$	145
4.33	Optimum location of the ring support, the corresponding buckling load parameters, cross - over radius (switching of mode) and percentage increase in buckling load	146
4.34	Buckling (for axisymmetric and asymmetric modes) Load Parameters for Simply Supported Plate, when $\nu = 0.3$	148
4.35	Buckling (for axisymmetric and asymmetric modes) Load Parameters for Clamped Plate, when $\nu = 0.3$	149
5.1	Buckling ($n=0$ for <i>axisymmetric</i> mode and $n=1$ for <i>asymmetric</i> mode) Load Parameters for different values of Rotational Spring Stiffness Parameter, R_{11} when $R_{22} = T_{11} = T_{22} = 10$ & $\nu = 0.3$	171
5.2	Buckling ($n=0$ for <i>axisymmetric</i> mode and $n=1$ for <i>asymmetric</i> mode) Load Parameters for different values of Rotational Stiffness Parameter, R_{22} when $R_{11} = T_{11} = T_{22} = 10$ & $\nu = 0.3$	174
5.3	Buckling ($n=0$ for <i>axisymmetric</i> mode and $n=1$ for <i>asymmetric</i> mode) Load Parameters for different values of Rotational Stiffness Parameter, T_{11} when $R_{11} = R_{22} = T_{22} = 10$ & $\nu = 0.3$	178
5.4	Buckling Load Parameter, k ($n=0$ for <i>axisymmetric</i> mode and $n=1$ for <i>asymmetric</i> mode) for Various Values of Rotational Restraint, R_{11} and Poisson's ratio, ν is 0.3.	181
5.5	Critical Buckling Load Parameters ($n=0$ for <i>axisymmetric</i> mode and $n=1$ for <i>asymmetric</i> mode), k for Various Values of Poisson's Ratio and Rotational Restraint, $R_{11} = 0.2$	186
5.6	Critical Buckling Load Parameter (<i>axisymmetric</i> mode), k for Various Values of Poisson's Ratio and Rotational Restraint, $R_{11} = 0.2$	186
5.7	Critical Buckling Load Parameter (<i>asymmetric</i> mode), k for Various Values of Poisson's Ratio and Rotational Restraint, $R_{11} = 0.2$	187
5.8	Cross Over Radius (Switching of mode) Parameter, b_{co} for Various Values of Poisson's Ratio and Rotational Restraint, $R_{11} = 0.2$	187

5.9	Comparison of Critical Buckling Load Parameter k , with Yamaki [14] for an Annular Plate with both Edges Simply Supported and Poisson's ratio = 0.3.	191
5.10	Comparison of Critical Buckling Load Parameter k , with Yamaki [14] for an Annular Plate with Outer Edge Clamped and Inner Edge Simply Supported and Poisson's ratio = 0.3.	191
6.1	Frequency for the mode 00 and Poisson ratio 0.3	203
6.2	Eigenvalues for different Rotational constraint for $T_{11}=100$; $\xi=100$ & $\nu=0.33$	203
6.2a	Mode shape parameters C_{mn} , for different Rotational constraint for $T_{11}=100$; $\xi=100$ &	204
6.2b	Normalization Constants A_{mn} , for different Rotational constraint for $T_{11}=100$; $\xi=100$ & $\nu=0.33$	207
6.3	Eigenvalues for different Translational constraint for $R_{11}=100$; $\xi=100$ & $\nu=0.33$	211
6.3a	Mode shape parameters C_{mn} , for different Translational constraint for $R_{11}=100$; $\xi=100$ & $\nu=0.33$	212
6.3b	Normalization constant A_{mn} , for different Translational constraint for $R_{11}=100$; $\xi=100$ & $\nu=0.33$	215
6.4	Eigenvalues for different foundation stiffness for $R_{11}=10$; $T_{11}=1000$ & $\nu=0.33$	218
6.5	Eigenvalues for different foundation stiffness for $R_{11}=100$; $T_{11}=100$ & $\nu=0.33$	219
6.5a	Mode shape parameters C_{mn} , for different foundation stiffness for $R_{11}=10$; $T_{11}=1000$ & $\nu=0.33$	220
6.5b	Normalization constant A_{mn} , for different foundation stiffness for $R_{11}=10$; $T_{11}=1000$ & $\nu=0.33$	222
6.6	Eigenvalues for different set of Poisson ratio, R_{11} , T_{11} & ξ	225
6.7	Eigenvalues for different Translational stiffness ratio for $\xi=100$ & $\nu=0.33$	226
6.8	Eigenvalues for different Foundation stiffness ratio for $T_{11}=100$ &	228

	$\nu=0.33$	
6.9	Eigenvalues for different Translational and Foundation stiffness ratios for $\nu=0.33$	230
6.10	Eigenvalues for different Poisson ratios	231
6.10a	Eigenvalues for different Rotational stiffness ratio for $\xi=100$ & $\nu=0.33$	232
6.11	Eigenvalues for different Foundation stiffness ratio for $R_{11}=100$ & $\nu=0.33$	234
6.12	Eigenvalues for different Rotational and Foundation stiffness ratios for $\nu=0.33$	236
6.13	Eigenvalues for different Poisson ratios	237
6.14	Eigenvalues for different Foundation stiffness ratio for $\nu=0.33$	238
6.15	Eigenvalues for different Poisson ratios	239
7.1	Frequency Parameter For Different Rotational Stiffness Parameters R_{11} , when $T_{11} = R_{22} = T_{22} = 100$ & $\xi = 10$ & $\nu = 0.3$	265
7.2	Comparison of Frequency Parameter for $R_{11} = 20, T_{11} = R_{22} = T_{22} = 100$ & $\xi = 0$	265
7.3	Frequency for Different Translational stiffness Parameter T_{11} , when $R_{11} = R_{22} = T_{22} = 100$ & $\xi = 10$ & $\nu = 0.3$	266
7.4	Frequency for Different Foundation Stiffness Parameters ξ , when $T_{11} = R_{11} = R_{22} = T_{22} = 100$ & $\nu = 0.3$	267
7.5	Frequency for Different Rotational R_{11} , Translational T_{11} , and Foundation ξ , Stiffness Parameters when $R_{22} = T_{22} = 100$ & $\nu = 0.3$	269
7.6	Frequency For Different Rotational Stiffness Parameters R_{22} , when $R_{11} = T_{11} = T_{22} = 100$, $\xi = 10$ & $\nu = 0.3$	272
7.7	Frequency for Different Translational Stiffness Parameters T_{22} when $R_{11} = R_{22} = T_{11} = 100$ & $\xi = 10$ & $\nu = 0.3$	273
7.8	Comparison of Frequency Parameters when Both the Boundaries of the Plate are Rigidly Clamped	274
7.9	Comparison of Frequency Parameters when both the Inner	274

	Boundary of the Plate is Simply Supported and Outer Boundary of the Plate is Rigidly Clamped	
7.10	Comparison of Frequency Parameters when Outer Boundary is Clamped and Inner Boundary is Free	275
7.11	Comparison of Frequency Parameters when Both Edges are Free	275

LIST OF SYMBOLS

R	Radius of a plate
h	Thickness of a plate
a	Radius of a plate
b	Non-dimensional radius of ring support/elastic ring support/inner radius of Annular Plate
ρ	Density of a plate material
E	Modulus of elasticity of the plate/ Young's modulus of a material
ν	Poisson's ratio
D	Flexural rigidity of a plate material
r, θ	Polar co-ordinates

$w(r, \theta)$	Transverse deflection of the plate
w	Transverse deflection of the plate
n	Number of nodal diameters
\tilde{w}	Normalized transverse deflection of the plate
T	Tensile Force
∇^2	Laplace operator
P_z	External Load
m_{xy}	Torsional Moments in xy Plane
m_{yz}	Torsional Moments in yz Plane
τ_{xy}	In-Plane Shear Stress in xy Plane
τ_{yx}	In-Plane Shear Stress in yz Plane
ε_x	Strain due to normal stress in the X direction
ε_y	Strain due to normal stress in the Y direction
χ	Warping of the Plate
q_x	Transverse shear force in the X - direction
q_y	Transverse shear force in the Y - direction
$\sigma_{xz}, \sigma_{yz}, \sigma_{zz}$	Transverse stresses*
$\gamma_{xz}, \gamma_{yz}, \gamma_{zz}$	Transverse strains
N_{xx}, N_{yy}, N_{xy}	Applied in-plane compressive and shear forces
$N_{rr}, N_{\theta\theta}, N_{r\theta}$	In-plane compressive forces
\bar{m}	Represents the mass of the plate per unit area.
ω	Natural circular frequency of the plate
K_{R1}	Torsional spring constant per unit length located along external edge of the plate or Rotational Spring Stiffness at Outer Edge

K_{R2}	Torsional spring constant per unit length located along internal edge of the Plate
K_{T1}	Linear spring constant per unit length located along external edge of the Plate or Translational Spring Stiffness at Outer Edge
K_{T2}	Linear spring constant per unit length located along internal edge of the Plate / Translational Spring Stiffness of Internal <i>elastic ring</i>
R_{11}	Non-Dimensional rotational flexibility parameter at outer edge of the plate
R_{22}	Non-Dimensional rotational flexibility parameter at inner edge of the plate
T_{11}	Non-Dimensional translational flexibility parameter at outer edge of the Plate
T_{22}	Non-Dimensional translational flexibility parameter at inner edge of the Plate / Non-dimensional translational Flexibility parameter of internal <i>elastic ring</i>
N	Uniform In-Plane compressive load per unit length at the edge of the plate
N_1	In-plane compressive load per unit length along external edge
N_2	In-plane compressive load per unit length along internal edge
k	Non-Dimensional buckling load parameter at the edge of the plate
k_1	Non-Dimensional buckling load parameter at external edge
k_2	Non-Dimensional buckling load parameter at internal edge
K_w	Modulus of sub grade reaction or Deflection modulus of the foundation or Winkler Parameter or Winkler Foundation Stiffness Constant
ξ	Non-Dimensional modulus of Winkler foundation /Non-Dimensional Foundation Stiffness Parameter
\bar{k}_1	Non-Dimensional frequency parameter without foundation
\bar{k}_2	Non-Dimensional frequency parameter due to modulus of sub grade reaction or Winkler Foundation
λ_1	Eigenvalue without foundation

λ_2	Eigenvalue with Winkler foundation
a	Radius of the Plate
A	Normalization Constant
C	Mod Shape Parameter
ω	Angular frequency

LIST OF PAPERS CONTRIBUTED ON THIS RESEARCH WORK

1. **Bhaskara Rao. L & Kameswara Rao. C.** “Vibrations Of Elastically Restrained Circular Plates On Winkler Foundation”, Paper communicated to International Journal of Thin Walled Structures, Elsevier Applied Sciences Publishers, Great Britain.
2. **Bhaskara Rao. L & Kameswara Rao. C.** “Buckling Of Circular Plates with an Elastically Restrained Edges and an Internal Elastic Ring Support”, Paper communicated to International Journal of Thin Walled Structures, Elsevier Applied Sciences Publishers, Great Britain.
3. **Bhaskara Rao. L & Kameswara Rao. C.** “Vibrations of Circular Plates With an Internal Ring Support and Flexible Edge Conditions”, Proceedings of International Conference on Advances in Machine Design and Industry Automation (ICAMDIA-2007), 10-12 Jan 2007, pp. 182-186, College of Engineering, Pune, India.
4. **Bhaskara Rao. L & Kameswara Rao. C.** “Frequency Analysis of Annular Plate With Internal and External Elastically Restrained Edge”, Proceedings of International Conference on Advances in Machine Design and Industry Automation (ICAMDIA-2007), 10-12 Jan 2007, pp. 171-175, College of Engineering, Pune, India.
5. **Bhaskara Rao. L & Kameswara Rao. C.** “Natural Frequency of Circular Plate Elastically Restrained Against Rotation and Resting on Winkler Foundation”, Proceedings of Eight International Conference on Vibration Problems (ICOVP-2007), 31 Jan-3 Feb 2007, Bengal Engineering & Science University, Howrah, India.
6. **Bhaskara Rao. L & Kameswara Rao. C.** “Vibrations Of Elastically Restrained Circular Plates Against Rotation and Supported by Partial Foundation”, Proceedings of Eight International Conference on Vibration Problems (ICOVP-2007), 31 Jan-3 Feb 2007, Bengal Engineering & Science University, Howrah, India.

7. **Bhaskara Rao. L & Kameswara Rao. C.** “Vibrations of Elastically Restrained Annular Plates on Elastic Foundation”, Fifteenth International Conference On Nuclear Engineering (ICONE15), ASME Paper ICONE15-10744, April 22-26, 2007, Japan.
8. **Bhaskara Rao. L & Kameswara Rao. C.** “Buckling Of Circular Plates with an Internal Ring Support and Elastically Restrained Edge Against Rotation and Translation”, Fifteenth International Conference On Nuclear Engineering (ICONE15), ASME Paper ICONE15-10864, April 22-26, 2007, Japan.
9. **Bhaskara Rao. L & Kameswara Rao. C.** “Vibrations Of Elastically Restrained Circular Plates on Winkler-Pasternak Foundation”, Fifteenth International Conference On Nuclear Engineering (ICONE15), ASME Paper ICONE15-10340, April 22-26, 2007, Japan.
10. **Bhaskara Rao. L & Kameswara Rao. C.** “Buckling of Annular Plate With an Elastically Restrained Outer Edge Against Rotation And Simply Supported”, International Conference On Computer Aided Engineering 2007 (CAE 2007), December 13 -15, 2007, IIT Chennai, India.
11. **Bhaskara Rao. L & Kameswara Rao. C.** “Buckling Of Circular Plates with an Internal Elastic Ring Support and Elastically Restrained Guided Edge Against Translation”, International Conference On Vibration Engineering and Technology Of Machinery (VETOMAC-IV), December 17-19, 2007, pp. 393-400, Osmania University, Hyderabad, India.
12. **Bhaskara Rao. L & Kameswara Rao. C.** “Vibrations Of Circular Plates on Elastic Foundation With an Internal Elastic Ring Support and Restrained Edge Against Rotation”, International Conference On Vibration Engineering and Technology Of Machinery (VETOMAC-IV), December 17-19, 2007, pp. 381-392, Osmania University, Hyderabad, India.
13. **Bhaskara Rao. L & Kameswara Rao. C.** “Frequency Analysis of Circular Plates With an Internal Elastic Ring Support and Flexible Edge”, 16th International Conference on Nuclear Engineering (ICONE16), ASME Paper ICONE16-48520, May 11-15, 2008, Orlando, Florida, USA.
14. **Bhaskara Rao. L & Kameswara Rao. C.** “Buckling of Annular Plates with an Elastically Restrained Guided Edge Against Trnaslation”, 16th International Conference on Nuclear Engineering (ICONE16), ASME Paper ICONE16-48427, May 11-15, 2008, Orlando, Florida, USA.

TABLE OF CONTENTS

PRELIMINARIES	PAGE NO
CERTIFICATE	
DECLARATION	
ACKNOWLEDGEMENTS	
ABSTRACT	
TABLE OF CONTENTS	
LIST OF FIGURES	
LIST OF TABLES	
LIST OF SYMBOLS	
LIST OF PAPERS CONTRIBUTED	
CHAPTER 1	1
1.0 INTRODUCTION	1
1.1 Introduction to Buckling	1
1.1.1 Review of the Literature	2
1.2 Introduction to Vibration	3
1.2.1 Review of the Literature	4
1.3 Introduction to Elastic Foundation	6
1.3.1 Review Of The Literature	7
1.4 Objects and Scope of the Study	10
1.5 Summary of the Study	11
CHAPTER 2	13
2.0 DERIVATION OF EQUATION OF MOTION OF PLATES IN CARTESIAN COORDINATE SYSTEM	
2.1 Assumptions	13
2.2 Coordinate System and Sign Convention	15
2.3 Equilibrium of Plate Element	17

2.4	Relation Between Stress, Strain and Displacements	19
2.5	Internal Forces Expressed in Terms of w	23
2.6	Equation of Motion for Circular Plates	25
2.7	Bending Theory and Boundary Conditions	31
2.7.1	Geometrical Boundary Conditions	33
2.7.2	Statistical Boundary Conditions (Free Edges)	33
2.7.3	Mixed Boundary Conditions	34
2.7.4	Elastic Support and Restraint	34
2.8	Differential Equation in Static Equilibrium	35
2.8.1	Governing Equations in Rectangular Coordinates	36
2.8.2	Governing Equations in Polar Coordinates	38
2.9	Differential Equation of Lateral Motion	43
2.9.1	Free Flexural Vibration of Circular Plates	45
2.10	Study of Possible Methods of Solution	45
2.10.1	Solution of the Homogeneous Equation	47
2.10.2	Particular Solution of the Homogeneous Equation	47
CHAPTER 3		49
3.0	BUCKLING OF CIRCULAR PLATES WITH ELASTICALLY RESTRAINED EDGES AND RESTING ON ELASTIC FOUNDATION	
3.1	Theoretical Background	49
3.2	Problem Definition	50
3.3	Mathematical Formulation	51
3.4	Solution	69
3.5	Results and Discussions	69
CHAPTER 4		74
4.0	BUCKLING OF CIRCULAR PLATES WITH ELASTICALLY RESTRAINED EDGES AND RESTING ON INTERNAL ELASTIC RING SUPPORT	
4.1	Background	74
4.2	Problem Definition	75
4.3	Analytical Formulation of the Problem	76
4.4	Solution	98
4.5	Results and Discussions	98

CHAPTER 5	151
5.0 BUCKLING OF ANNULAR PLATES WITH ELASTICALLY RESTRAINED EXTERNAL AND INTERNAL EDGES	
5.1 History	151
5.2 Definition of the Problem	151
5.3 Mathematical Formulation of the System	152
5.4 Solution	169
5.5 Results and Discussions	169
CHAPTER 6	192
6.0 VIBRATIONS OF ELASTICALLY RESTRIANED CIRCULAR PLATES ON WINKLER FOUNDATION	
6.1 Definition of the Problem	191
6.2 Derivation of Frequency of Transverse Vibration of Elastically Rrestrained circular Plates	193
6.3 Solution	201
6.4 Results	202
CHAPTER 7	241
7.0 FREQUENCY ANALYSIS OF ANNULAR PLATES WITH ELASTICALLY RESTRAINED INNER AND OUTER EDGES AND RESTING ON ELASTIC FOUNDATION	
7.1 Theoretical Background	241
7.2 Problem Definition	241
7.3 Derivation of Frequency Equation of Transverse Vibrations of Elastically Restrained Edges	242
7.4 Solution	263
7.5 Results	263
CHAPTER 8	276
8.0 CONCLUSIONS	

8.1	Conclusions	276
8.2	Future Scope of Studies	277
REFERENCES		279

CHAPTER 1

INTRODUCTION

1.1 Introduction to Buckling

Thin plate elements used in naval and aeronautical structures are often subjected to normal and shearing forces acting in the plane of the plate. If these in-plane forces are sufficiently small, the equilibrium is stable and the resulting deformations are characterized by the absence of lateral displacements ($w = 0, u \neq 0, v \neq 0$). As the magnitude of these in-plane forces increases, at certain load intensity, a marked change in the character of the deformation pattern takes place. That is, simultaneously with the in-plane deformations, lateral displacements are introduced. In this condition, the originally stable equilibrium becomes unstable and the plate is said to have buckled. The load producing this condition is called the critical load. The importance of the critical load is the initiation of a deflection pattern, which, if the load is further increased, rapidly leads to very large lateral deflections and eventually to complete failure of the plate. This is a dangerous condition, which must be avoided.

Design of structures is often based on strength and stiffness considerations. The buckling load governs the design before the strength criterion does. Therefore, buckling is an important consideration in structural design, particularly when the structure is slender and light weight. Linear elastic bifurcation buckling of structural members is the most elementary form of buckling, and its study is an essential step towards understanding the buckling behavior of complex structures, including structures incorporating elastic behavior, initial imperfections, residual stresses, etc. The load at which linear elastic buckling occurs is important, because it provides the basis for commonly used buckling formulas used in design codes.

Buckling also known as structural instability may be classified into two categories, i.e., bifurcation buckling and limit load buckling. In bifurcation buckling, the deflection under compressive load changes from one direction to a different direction (e.g. from axial shorting

to lateral deflection). The load at which the bifurcation occurs is the load-deflection space is called the critical buckling load or simply critical load. In limit load buckling, the structure attains a maximum load without any previous bifurcation, i.e., with only a single mode of deflection. The smallest buckling load is termed the critical buckling load.

1.1.1 Review of the Literature

The buckling of plates is an important topic in structural engineering and several authors have studied it in the past (Brush and Almoth [1]). Laura et al. [2] investigated the elastic buckling problem of circular plates with an additional concentric ring support at the interior, which modeled the plate using the classical thin plate theory. In recent steady, Wang and Wang [3] showed that when the ring support has a small radius, the buckling mode takes the asymmetric form instead. In practice, the edge is neither fully clamped nor simply supported and hence usually a rotational elastically restrained boundary condition is applied for analysis by Reismann [4], Kerr [5] and Thevendran and Wang [6]. Several authors (see, e.g., Yu [7], Galletly [8], Kline [9] and Wolkowisky [10]) studied the buckling of circular plates on elastic foundation. However, these studies considered only axisymmetric buckling, which may not lead to the correct buckling load. Elishakoff and Tang [11] studied the buckling of a circular plate on Winkler foundation by using the Rayleigh's method. Wang et al. [12] presented relationships between the buckling loads determined using classical Kirchhoff plate theory and shear deformable plate theories on Pasternak foundation. The relationships of Kirchhoff, Mindlin and Reddy polygonal plates on a Pasternak foundation obtained are found to be exact simply supported boundary conditions under an isotropic in-plane load. The relationships are also applicable for Winkler foundation as this foundation model is a special case of the Pasternak foundation. Wang [13] studied the buckling of a circular plate on elastic foundation by including the non-axisymmetric modes also. Yamaki [14] solved the elastic buckling problem of thin annular plates under uniform compression.

He presented the stability criteria for twelve combinations of standard boundary conditions for the inner and outer edges of the annular plate.

1.2 Introduction to Vibration

Continuous circular plates have received considerable attention due to their numerous applications. They are widely used as structural elements in many aerospace, marine, mechanical and structural engineering applications. When subjected to the dynamic load, structures incorporating circular plates often exhibit several vibration modes, which may be associated with this structural element. As a result, vibrations of continuous uniform circular plates have been extensively studied for several decades showing that straightforward and relatively simple analytical solutions exist for many complex problems. Although the circular symmetry of the problem allows for its significant simplification, additional difficulties often arise due to uncertainty of boundary conditions. This uncertainty occurs because, in many practical applications, the edge of the plate is not necessarily classical such as free, clamped or simply supported. When the plate's boundary conditions depart from classical cases, elastic translational and rotational constraints should be considered. Perforated plates constitute important components in structural, aerospace and mechanical engineering. Submarines, disc brakes, micro pumps and nuclear reactors are but a few examples. The knowledge of natural frequencies of components is of great interest in the study of responses of structures to various excitations. Among perforated plates, annular plates have a particular importance, due to their axial symmetry.

1.2.1 Review of the Literature

The free vibrations of circular plates have been of practical and academic interest for at least two centuries, Chlandni [15] and Poisson [16]. A thorough summary of the previously published literature through the year 1965 by Leissa [17] revealed that a reasonable number

of numerical results had been obtained for the two cases when the plate boundary is either clamped or free, but that a few results were available for the simply supported boundary. Leissa [18] revealed one significant publication on the simply supported case. A contributory study by Pardoen [19], wherein 12 frequencies previously given by Leissa [17] for a Poisson's ratio of 0.3 were compared against results obtained from a finite element method.

One of the earliest formulations of elastic edge was presented by Leissa [17], who formulated a frequency parameter for four vibration modes of a simply supported circular plate with varying rotational stiffness parameters. Further extension of the work by Leissa et al. [20] included numerical results obtained using the Fourier solution and the Ritz method. Avalos et al. [21] and [22] studied vibrations of stepped circular plates elastically restrained against both translational and rotational. Authors presented an approximate solution in terms of polynomial coordinate function and tabulated results for a number of vibration modes. Tabulations provided by these authors are perhaps the most comprehensive reference available on the subject. It should be noted, however, that only four values of translational and rotational stiffness parameters were considered (two of which are 0 & ∞) and a very limited number of vibration modes were presented. It is worth noting that circular plates are widely used in modeling various fluid-structure interaction problems previously with assumptions of the classical boundary conditions (for example free plate) by Amabili et al. [23], recently expanded by Rdzanek, who included effects of rotational and translational edge stiffness parameters in the analytical formulations for the radiated sound power. Kang and Kim [24] studied the modal properties of the elastically restrained beams and plates.

Circular plates mounted on several intermediate ring supports are commonly observed in structures such as boilers, ships and pressure vessels. Kunukkasseril and Swamidas [25] are probably the first to consider elastic ring supports. They formulated the equations in

general, but presented only the case of a circular plate with a free edge. As in Bodine [26] who studied rigid supports, a change of the fundamental mode from symmetric to asymmetric was noted in certain cases where the radius of the support is small. Later authors Singh and Mirza [27], Azimi [28], Ding [29] and Chou et al [30] tend to study only the symmetric modes. Azimi [28] reported a broader range of results for both edge and interior supports, but rotational constraints were not included in the study. Wang [31] studied the effect of internal elastic translational support and also observed that the switching between axisymmetric and asymmetric vibration modes.

The literature shows that although vibration of elastically restrained circular plates is of a considerable interest, availability of tabulated data is scarce. In particular, previous studies considered circular plates with both translational and rotational constraints were restricted to a few low frequency vibration modes. For these modes, the frequency parameter was calculated using only several translational and rotational stiffness parameters in a $0 - \infty$ range (4 in Avalos [21 & 22]) and 2 in Rdzanek et al. [32]). Thus, it is very difficult to use these results in establishing potential data trends. In contrast to studies on the free edge plates by Amabili [23] and Itao and Crandall [33], no data are available for a mode shape parameter and on the effect of the Poisson's ratio. Southwell [34] derived equations for an annular plate clamped around the inner boundary and free at the outside edge. Some numerical investigations have been made with notable work in this direction accomplished by Hort and Koenig [35] and Narayana Raju [36]. There are also in the literature some interesting numerical investigations, such as the one by Vogel and Skinner [37], who studied nine combinations of boundary conditions; they considered simply supported, clamped and free edges at the inner and outer boundaries. Data and also references have also given in Leissa [17].

1.3 Introduction to Elastic Foundation

Treatment of soil and structure as a whole is a major concern of many engineering applications. Foundations very often represent a complex medium. It is often difficult to find suitable analytical models for foundation problems. An acceptable analysis must include the behavior of foundation properly. By using certain assumptions there exist some simplified models to represent the behavior of foundations. One of the most elementary models is based on the assumption that foundation behaves elastically. This implies not only that the foundation elements return to their original position after removing loads, but it is also accepted that their resistance is proportional to the deformation they experience. This assumption can be acceptable if displacement and pressure underneath foundation are small and approximately linearly related to each other. For “generalized” foundations the model assumes that at the point of contact between plate and foundation there is not only pressure but also distributed moments caused by the interactions between linear springs.

1.3.1 Review of the Literature

Plates on elastic foundations have received a considerable attention due to their wide applications, ranging from more conventional civil engineering and mechanical engineering to aerospace engineering. Since the interaction between structural foundations and supporting soil has a great importance in many engineering applications, a considerable amount of research has been conducted on plates on elastic foundations. Good amount of research has been conducted to deal with bending, buckling and vibration problems of plates on elastic foundation. The main aim of most of these is to solve some real engineering problems such as structural foundation analysis of buildings, pavements of highways, water tanks, airport runways, buried pipe lines, structural elements resting on foundations, such as building footings, base of machines and heavy duty machines [45, 46]. Because the intent of this subsection is to give a synoptic overview of research accomplishments to date, it is necessarily brief.

Many studies have been done to find a convenient representation of physical behavior of a real structural component supported on a foundation. The usual approach in formulating problems of beams, plates and shells continuously supported by elastic media is based on the inclusion of the foundation reaction in the corresponding differential equation of the beam, plate or shell.

In order to include behavior of foundation properly into the mathematically simple representation, it is necessary to make some assumptions. The most common soil model used in practical applications is Winkler model (one parameter model) proposed by Winkler [38]. One of the most useful simplified models known as the Winkler model assumes that the foundation behaves elastically, and that the vertical displacement and pressure underneath it are linearly related to each other. That is, it is assumed that the supporting medium is isotropic, homogeneous and linearly elastic, provided that the displacements are “small”. This simplest simulation of an elastic foundation is considered to provide vertical displacement by a composition of closely spaced independent vertical linearly elastic springs. The physical representation of this mechanical model is shown in Fig.1.1. Thus the relation between the pressure and deflection of the foundation can be expressed as follows

$$p(x, y) = k_w w(x, y) \quad (1.1)$$

Where

$p(x, y)$ Distributed reaction from the foundation due to applied load at point x, y

k_w Winkler parameter

$w(x, y)$ Vertical deflection at point x, y

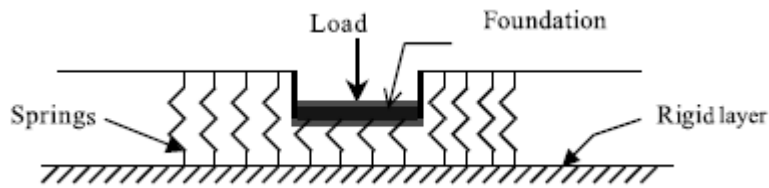


Fig. 1.1 Winkler Model

A number of studies by Hetenyi [39], Popov [40], Baker [41], Vesic [42], Kramrisch and Rogers [43] and Brown et al [44], in the area of soil – structure interaction have been conducted on the basis of Winkler hypothesis because of its simplicity.

Although the circular symmetry of the problem allows for its significant simplification, many difficulties very often arise due to complexity and uncertainty of boundary conditions. This uncertainty could be due to practical engineering applications where the edge of the plate does not fall into the classical boundary conditions. It is accepted fact that the condition on a periphery often tends to be part way between the classical boundary conditions (free, clamped and simply supported) and may correspond more closely to some form of elastic restraints, i.e., rotational and translational restraints [47, 48 & 49].

The solutions of the plate problems with classical methods that provide mathematically exact solutions are available for a limited number of cases. The vibration of a plate supported laterally by an elastic foundation was discussed by Leissa [50]. Leissa deduced that the effect of a full (Winkler) foundation merely increases the square of the natural frequency of the plate by a constant. The same conclusion was conjectured by Salari et al. [51]. The vibration of plate supported by a partial elastic foundation was considered by Laura et al. [52], in which case a simple frequency relation no longer holds. Celep [53] studied the contact region of circular plates resting on unilateral Winkler foundation and subjected to arbitrary loads by using the minimization of total potential energy. Zheng and Zhou [54] studied the large

deflection of a circular plate resting on Winkler foundation and subjected to a concentrated load at the center by means of a step-by-step iterative technique. Ghosh [55] studied the free and forced vibration of circular plates on Winkler foundation by an exact analytical method.

1.4 Objects and Scope of the Study

The scope of the present work is to theoretically investigate the effect of elastically restrained edges on buckling and transverse vibrations of circular plates resting on elastic foundation and also to investigate the effect of internal ring and elastic ring support on buckling mode.

The general method followed in deriving exact frequency equations in the present work is based on “separation of variables” approach in order to find the transverse natural frequencies of circular plates. This method is also well adopted in analyzing the stability criterion of circular plates i.e., to determine the buckling load parameters.

The previous works contributed by many researchers as mentioned in the previous section show that they had paid more attention to study the effect of classical boundary conditions and obtained frequency parameters. It is also observed that no provision has been made to include the effect of elastic edge i.e., rotational and translational stiffness parameters, while determining the frequency parameters and also to determine the buckling load parameters, mode switching as well.

The influence of the rotational and translational elastic restraint parameters $(R_{11}, R_{22}, T_{11} \text{ \& } T_{22})$, elastic foundation parameters (ξ) is studied. It is seen that the effect of these parameters on natural frequencies is quite significant. The results obtained thereon by solving the closed form frequency equations and stability criteria are then confirmed numerically by comparing with earlier results.

All the results are thereon plotted for variation of rotational stiffness parameter R_{11} , translational stiffness parameter T_{11} , elastic ring support parameter T_{22} and elastic foundation stiffness parameters (ξ) versus frequency parameter. Similarly, the results are thereon plotted for variation of rotational stiffness parameter R_{11} , translational stiffness parameter T_{11} , elastic ring support parameter T_{22} and elastic foundation stiffness parameters (ξ) versus buckling load parameter. At various stages of this thesis the results obtained in the chapters have been reported in references [.]

1.5 Summary of the Study

There are eight chapters in the thesis. Chapter 1 covers an overview and scope of the work of the thesis and presents extensive literature search on the subject.

In Chapter 2 the differential equation of plates in Cartesian coordinate system as well as in polar coordinate system are formulated. A review of various boundary conditions is presented. A review on solution methods is also presented.

In Chapter 3 the problem of buckling of circular plates with an elastically restrained edges and resting on elastic foundation is studied. The influence of rotational spring stiffness parameter, translational spring stiffness parameter and foundation stiffness parameter are portrayed graphically.

In Chapter 4 the problem of buckling of circular plates with an elastically restrained edges and resting on internal elastic ring support is studied. The influence of elastic edge constraints on buckling mode is studied. Also the influence of elastic ring restraint on mode switching is studied.

In Chapter 5 the problem of buckling of annular plates with an elastically restrained external and internal edges is studied. The influence of elastic edge constraints at inner and outer edge on buckling mode is studied.

Chapter 6 contains the solution of vibration problem of circular plates with elastically restrained edges and resting on elastic foundation. The results are compared with the well known analytical and the other numerical solutions.

Chapter 7 contains the solution of vibration problem of annular plates resting on elastic foundation. The results are compared with that of earlier published results.

Chapter 8 presents the conclusions and the suggestions for further studies.

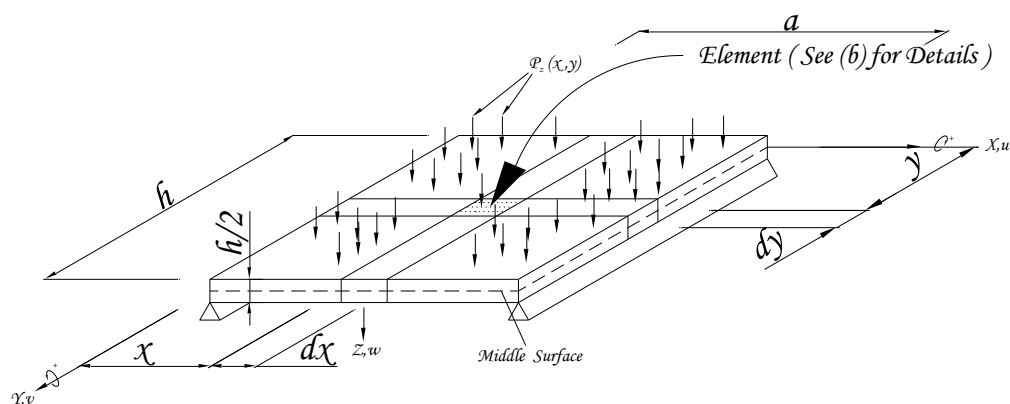
CHAPTER 2

DERIVATION OF EQUATION OF MOTION OF PLATES IN CARTESIAN COORDINATE SYSTEM

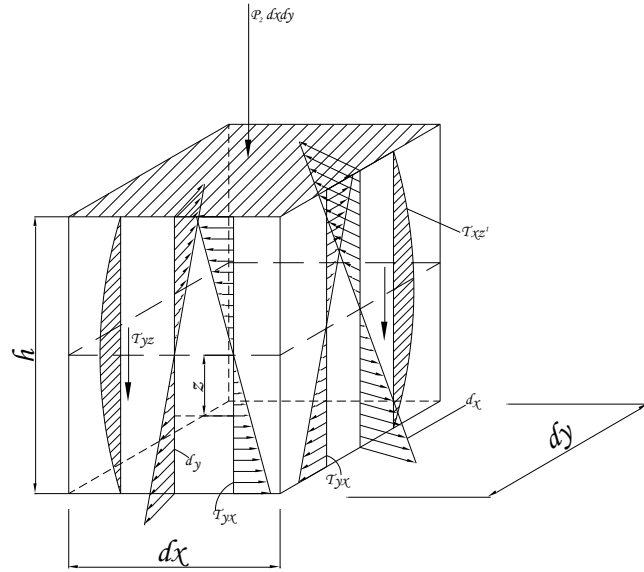
2.1 Assumptions

The shape of a plate is adequately defined by describing the geometry of its middle surface, which is a surface that bisects the plate thickness h at each point as shown in Fig. 2.1. The small deflection plate theory generally attributed to Kirchhoff [58] and Love [59] is based on the following assumptions.

- (i) The material of the plate is homogeneous, isotropic and elastic.
- (ii) The deflection of the midplane is small compared with the thickness of the plate.
- (iii) The plate is initially flat.
- (iv) The thickness of the plate is small compared to its other dimensions. The smallest lateral dimension of the plate is at least ten times larger than its thickness.
- (v) There is no deformation in the middle plane of the plate.
- (vi) The midplane remains unstrained subsequent to bending.
- (vii) The slopes of the deflected middle surface are small and the square of the slope is negligible in comparison to unity.
- (viii) The deflection of the plate is produced by displacement of points of the middle surface normal to its initial plane.
- (ix) The deformations are such that straight lines, initially normal to the middle surface, remain straight lines and normal to the middle surface (deformations due to transverse shear being neglected).
- (x) The stresses normal to the middle surface are of a negligible order of magnitude in comparison with the other stress components.



(a) Laterally Loaded Rectangular Plate



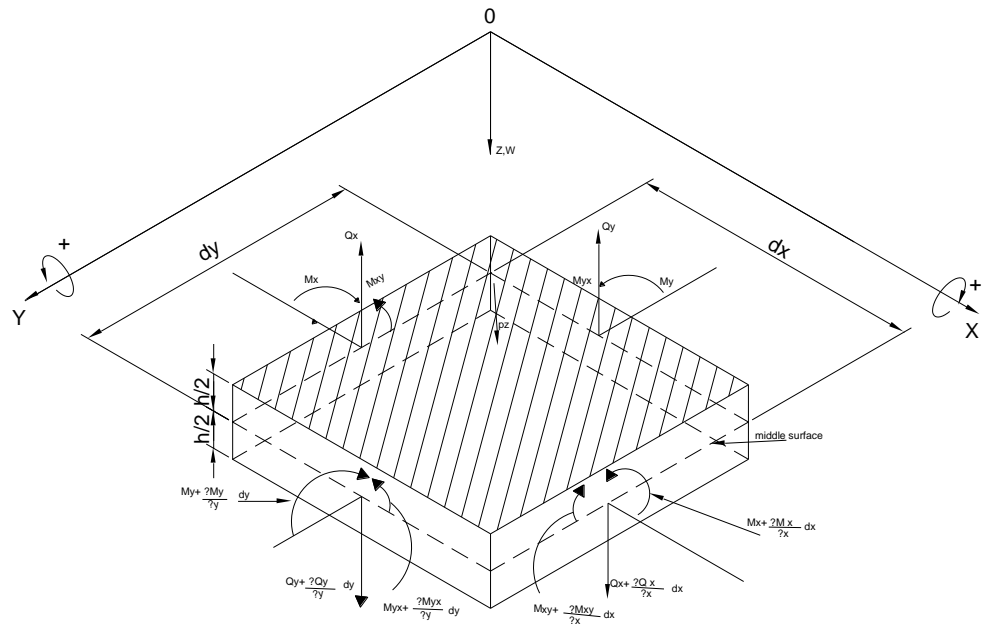
(b) Stress Components on a Plate Element

Fig. 2.1 Laterally Loaded Rectangular Plates

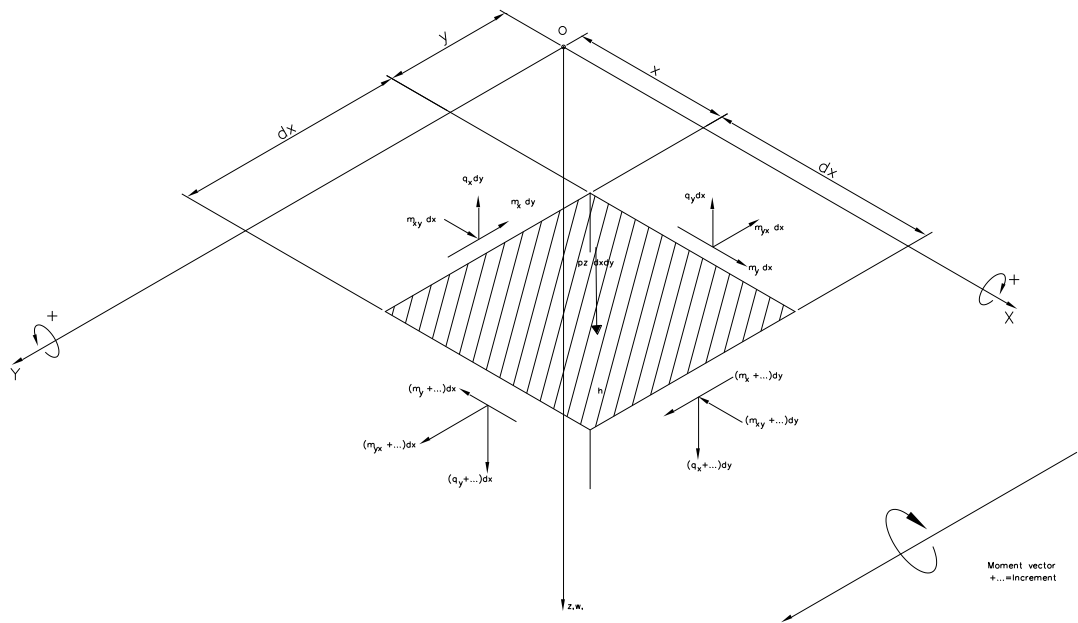
2.2 Coordinate System and Sign Convention

Small and large-scale tests have proved the validity of the assumptions given in section 2.1. For rectangular plates, the use of Cartesian coordinate system is the most convenient as shown in Fig. 2.1. The external and internal forces and deflection components u, v and w are considered positive when they point toward the positive direction of the coordinate axes X, Y and Z . In general engineering practice, positive moments produce tension in the fibers at the bottom part of the structure. The sign convention is maintained for the plates.

Considering an elemental parallelepiped cut out of the plate, as shown in Fig. 2.2, we assign positive internal forces and moments to the near faces. To satisfy the equilibrium of the element, negative internal forces and moments must act on its far sides. The first subscript of the internal forces indicates the direction of the surface-normal pertinent to the section on which the force or the moment acts.



(a) Detailed Illustration



(b) Schematic Illustration

Fig. 2.2 External and Internal Forces On The Element Of The Middle Surface.

2.3 Equilibrium of Plate Element

Assuming that the plate is subjected to lateral forces only, from the six fundamental equilibrium equations, the following three can be used.

$$\sum M_x = 0, \quad \sum M_y = 0, \quad \text{and} \quad \sum P_z = 0 \quad (2.1)$$

The behavior of the plate is in many respects analogous to that of a two-dimensional grid work of beams. Thus the external load P_z is carried by Q_x and Q_y transverse shear forces and by M_x and M_y as shown in Fig. 2.2a. In the theory of plates it is customary to deal with internal forces and moments per unit length of the middle surface as shown in Fig. 2.2b. To distinguish these internal forces from the above mentioned resultants, the notations $q_x, q_y, m_x, m_y, m_{xy}$ and m_{yx} are introduced. The procedure involved in setting up the differential equation of equilibrium is as follows.

1. Select a convenient coordinate system and draw a sketch of a plate element as shown in Fig. 2.2.
2. Show all external and internal forces acting on the element.
3. Assign positive internal forces with increments to the near sides.
4. Assign negative internal forces to the far sides.
5. Express the increments by a truncated Taylor's series in the form

$$q_x + dq_x = q_x + \frac{\partial q_x}{\partial x} dx, \quad m_y + dm_y = m_y + \frac{\partial m_y}{\partial y} dy \text{ etc.} \quad (2.2)$$

6. Express the equilibrium of the internal and external forces acting on the element.

Consider the sum of moments of all forces acting along the Y axis is zero as shown in Fig. 2.2b.

$$\left(m_x + \frac{\partial m_x}{\partial x} dx \right) dy - m_x dy + \left(m_{yx} + \frac{\partial m_{yx}}{\partial y} dy \right) dx - m_{yx} dx - \left(q_x + \frac{\partial q_x}{\partial x} dx \right) dy \frac{dx}{2} - q_x dy \frac{dx}{2} = 0 \quad (2.3)$$

After simplification, we neglect the term containing $\frac{1}{2} \left(\frac{\partial q_x}{\partial x} \right) (dx)^2 dy$, since it is a small quantity of higher order. Thus equation (2.3) becomes

$$\frac{\partial m_x}{\partial x} dx dy + \frac{\partial m_{yx}}{\partial y} dy dx - q_x dx dy = 0 \quad (2.4)$$

Divide the equation (2.4) by $dx dy$, yields the following

$$\frac{\partial m_x}{\partial x} + \frac{\partial m_{yx}}{\partial y} = q_x \quad (2.5)$$

In a similar manner the sum of the moments along the X axis gives the following equilibrium equation

$$\frac{\partial m_y}{\partial y} dx dy + \frac{\partial m_{xy}}{\partial x} dy dx - q_y dx dy = 0 \quad (2.6)$$

Divide the equation (2.6) by $dx dy$, yields the following

$$\frac{\partial m_y}{\partial y} + \frac{\partial m_{xy}}{\partial x} = q_y \quad (2.7)$$

Similarly, the sum of the moments along the Z axis gives the following equilibrium equation.

$$\frac{\partial q_x}{\partial x} dx dy + \frac{\partial q_y}{\partial y} dy dx + P_z dx dy = 0 \quad (2.8)$$

Divide the equation (2.8) by $dx dy$ yields the following

$$\frac{\partial q_x}{\partial x} + \frac{\partial q_y}{\partial y} = -P_z \quad (2.9)$$

Substituting equations (2.5), (2.7) into equation (2.9) and also observe that $m_{xy} = m_{yx}$, we obtain the following equation.

$$\frac{\partial^2 m_x}{\partial x^2} + 2 \frac{\partial^2 m_{xy}}{\partial x \partial y} + \frac{\partial^2 m_y}{\partial y^2} = -P_z(x, y) \quad (2.10)$$

It is clear from the equation (2.10) that the bending moment and twisting moments depend on the strains and the strains are the functions of the displacement components (u, v, w) .

2.4 Relation Between Stress, Strain and Displacements

The assumption that the material is elastic permits the use of the two-dimensional Hook's law. The following equations are relates stress and strain in a plate element.

$$\sigma_x = E\varepsilon_x + \nu\sigma_y \quad (2.11)$$

$$\sigma_y = E\varepsilon_y + \nu\sigma_x \quad (2.12)$$

Substitute equation (2.12) into equation. (2.11) gives the following

$$\sigma_x = \frac{E}{1-\nu^2}(\varepsilon_x + \nu\varepsilon_y) \quad (2.13)$$

Similarly substituting equation (2.11) into equation (2.12) gives the following

$$\sigma_y = \frac{E}{1-\nu^2}(\varepsilon_y + \nu\varepsilon_x) \quad (2.14)$$

The torsional moments m_{xy} and m_{yx} produce in plane shear stresses τ_{xy} and τ_{yx} as shown in Fig. 2.3, which are again related to the shear strain γ by the pertinent Hookean relationship given by the following

$$\tau_{xy} = G\gamma_{xy} = \frac{E}{2(1+\nu)}\gamma_{xy} = \tau_{yx} \quad (2.15)$$

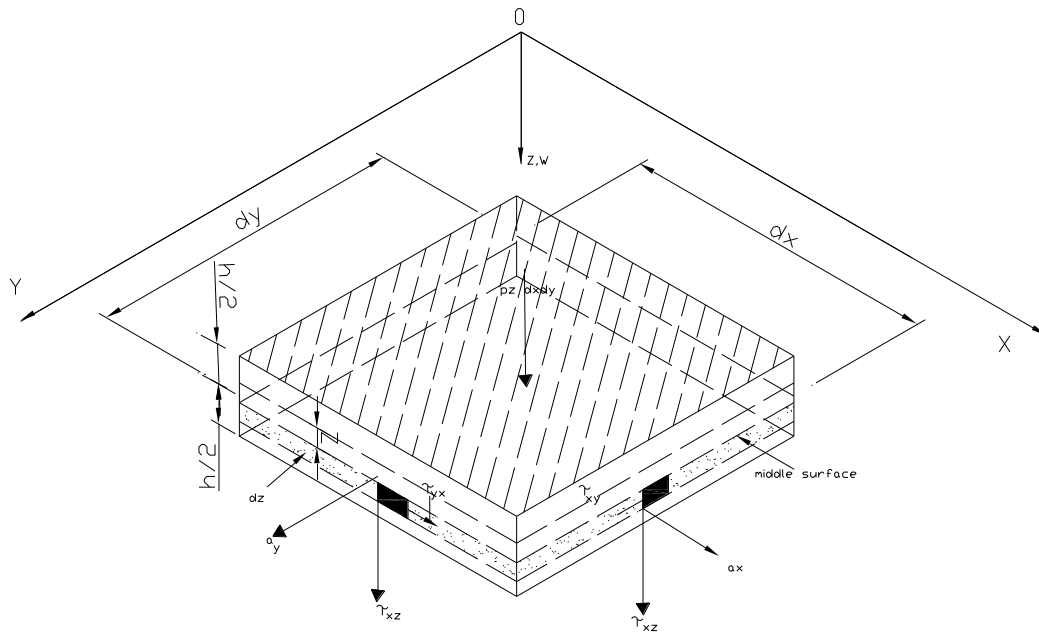


Fig. 2.3 Stresses On a Plate Element

Next, we consider the geometry of the deflected plate to express the strains in terms of the displacement coefficients. Taking a section at a constant y , as shown in Fig. 2.4, we compare the section before and after deflection. Using assumptions 6 and 8, we express the angle of rotation of lines I - I and II - II by

$$\vartheta = -\frac{\partial w}{\partial x} \text{ and } \vartheta + \dots = \vartheta + \frac{\partial \vartheta}{\partial x} dx \quad (2.16)$$

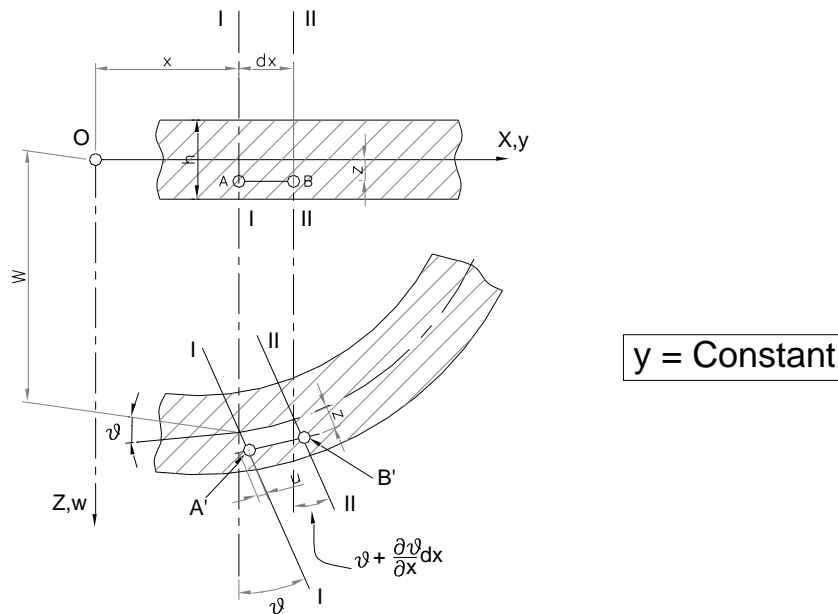


Fig. 2.4 Section Before and After Deflection

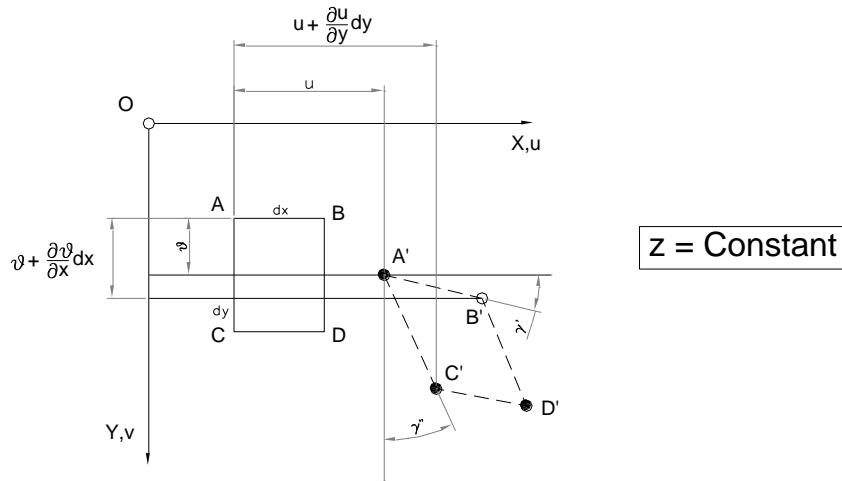


Fig. 2.5 Angular Distortion

respectively. After the deformation the length \overline{AB} of a fiber, located at z distance from the middle surface, becomes $\overline{A'B'}$ as shown in Fig. 2.4. Using the deflection of strain given by the equation $\varepsilon_x = \frac{\Delta dx}{dx}$, can be write this as

$$\varepsilon_x = \frac{\Delta dx}{dx} = \frac{\overline{A'B'} - \overline{AB}}{\overline{AB}} = \frac{\left[dx + z \frac{\partial g}{\partial x} dx \right] - dx}{dx} = z \frac{\partial g}{\partial x} \quad (2.17)$$

Substituting the first of the equation (2.16) into equation (2.17) gives the following

$$\varepsilon_x = -z \frac{\partial^2 w}{\partial x^2} \quad (2.18)$$

Similarly the strain ε_y , due to normal stresses in the Y direction yields the following

$$\varepsilon_y = -z \frac{\partial^2 w}{\partial y^2} \quad (2.19)$$

Angular distortion $\gamma_{xy} = \gamma' + \gamma''$ by comparing $ABCD$ rectangular parallelogram as shown in Fig. 2.5, located at a constant distance z from the middle surface, by its deformed shape

$A'B'C'D'$ on the deflected plate surface. From the two small triangles in Fig. 2.5 and from the

$$\text{following equation } \gamma_{xy} = \gamma' + \gamma'' = \frac{\partial v}{\partial x} + \frac{\partial u}{\partial y} = \gamma_{yx} \quad (2.20)$$

$$\text{And it is evident that } \gamma' = \frac{\partial v}{\partial x} \text{ and } \gamma'' = \frac{\partial u}{\partial y} \quad (2.21)$$

But from the Fig. 2.4

$$u = z\theta = -z \frac{\partial w}{\partial x} \quad (2.22)$$

$$\text{Similarly } v = z\theta = -z \frac{\partial w}{\partial y} \quad (2.23)$$

From equations (2.20), (2.21), (2.22) and (2.23) gives the following

$$\gamma_{xy} = \gamma' + \gamma'' = -2z \frac{\partial^2 w}{\partial x \partial y} \quad (2.24)$$

The curvature changes of the deflected middle surface are defined by

$$\kappa_x = -\frac{\partial^2 w}{\partial x^2}, \kappa_y = -\frac{\partial^2 w}{\partial y^2}, \text{ and } \chi = -\frac{\partial^2 w}{\partial x \partial y} \quad (2.25)$$

Where χ represent the warping of the plate.

2.5 Internal Forces Expressed in Terms of w

The stress components σ_x and σ_y as shown in Fig. 2.3, produce bending moments in the plate element in a manner similar to that the elementary beam theory. Thus, by integration of the normal stress components, the bending moments, acting on the plate element, are obtained

$$m_x = \int_{-(h/2)}^{+(h/2)} \sigma_x z dz \text{ and } m_y = \int_{-(h/2)}^{+(h/2)} \sigma_y z dz \quad (2.26)$$

Similarly, the twisting moments produced by the shear stresses $\tau = \tau_{xy} = \tau_{yx}$ can be determined from the following equations

$$m_{xy} = \int_{-(h/2)}^{+(h/2)} \tau_{xy} z dz \text{ and } m_x = \int_{-(h/2)}^{+(h/2)} \tau_{xy} z dz \quad (2.27)$$

but $\tau_{xy} = \tau_{yx} = \tau$ and therefore $m_{xy} = m_{yx}$

Substituting equations (2.18) and (2.19) into equations (2.13) and (2.14), yields the following expressions.

$$\sigma_x = -\frac{Ez}{1-\nu^2} \left(\frac{\partial^2 w}{\partial x^2} + \nu \frac{\partial^2 w}{\partial y^2} \right) \quad (2.28)$$

$$\sigma_y = -\frac{Ez}{1-\nu^2} \left(\frac{\partial^2 w}{\partial y^2} + \nu \frac{\partial^2 w}{\partial x^2} \right) \quad (2.29)$$

The above equations are expressed in terms of the lateral deflection w . Substitute the above Eqs. (2.28) and (2.29) in Eqs. (2.26). Then integration of Eqs. (2.26), gives the following expressions.

$$m_x = -\frac{Eh^3}{12(1-\nu^2)} \left(\frac{\partial^2 w}{\partial x^2} + \nu \frac{\partial^2 w}{\partial y^2} \right) = -D \left(\frac{\partial^2 w}{\partial x^2} + \nu \frac{\partial^2 w}{\partial y^2} \right) = D(\kappa_x + \nu \kappa_y) \quad (2.30)$$

$$m_y = -\frac{Eh^3}{12(1-\nu^2)} \left(\frac{\partial^2 w}{\partial y^2} + \nu \frac{\partial^2 w}{\partial x^2} \right) = -D \left(\frac{\partial^2 w}{\partial y^2} + \nu \frac{\partial^2 w}{\partial x^2} \right) = D(\kappa_y + \nu \kappa_x) \quad (2.31)$$

Where $D = \frac{Eh^3}{12(1-\nu^2)}$, represents the bending or flexural rigidity of the plate.

Substituting equations (2.24) into equation (2.15) yields the following expressions.

$$\tau_{xy} = -2Gz \frac{\partial^2 w}{\partial x \partial y} = \tau_{yx} = \tau \quad (2.32)$$

Substituting equations (2.32) into equation (2.27) yields the following

$$m_{xy} = m_{yx} = \int_{-(h/2)}^{+(h/2)} \tau z dz = -2G \int_{-(h/2)}^{+(h/2)} \frac{\partial^2 w}{\partial x \partial y} z^2 dz = -(1-\nu)D \frac{\partial^2 w}{\partial x \partial y} = D(1-\nu)\chi \quad (2.33)$$

Substituting equations (2.30), (2.31) and (2.33) into equation (2.10) yields the governing differential equation of the plate subjected to lateral loads.

$$\frac{\partial^4 w}{\partial x^4} + 2\frac{\partial^4 w}{\partial x^2 \partial y^2} - \frac{\partial^4 w}{\partial y^4} = \frac{p_z(x, y)}{D} \quad (2.34)$$

Using the two-dimensional Laplacian operator $\nabla^2 = \frac{\partial^2}{\partial x^2} + \frac{\partial^2}{\partial y^2}$, equation (2.34) can be written as follows

$$D\nabla^2 \nabla^2 w = p_z \quad (2.35)$$

This equation is a fourth-order, nonhomogeneous, partial differential equation of the elliptic type with constant coefficients, often called a nonhomogeneous biharmonic equation. The equation (1.34) is a linear since the derivatives of w do not have exponents of higher than one.

The transverse shear forces in terms of the lateral deflections. Substituting equations (2.30), (2.31) and (2.33) into equations (2.5) and (2.7) gives the following equations

$$q_x = \frac{\partial m_x}{\partial x} + \frac{\partial m_{yx}}{\partial y} = -D \frac{\partial}{\partial x} \left(\frac{\partial^2 w}{\partial x^2} + \frac{\partial^2 w}{\partial y^2} \right) = -D \frac{\partial}{\partial x} \nabla^2 w \quad (2.36)$$

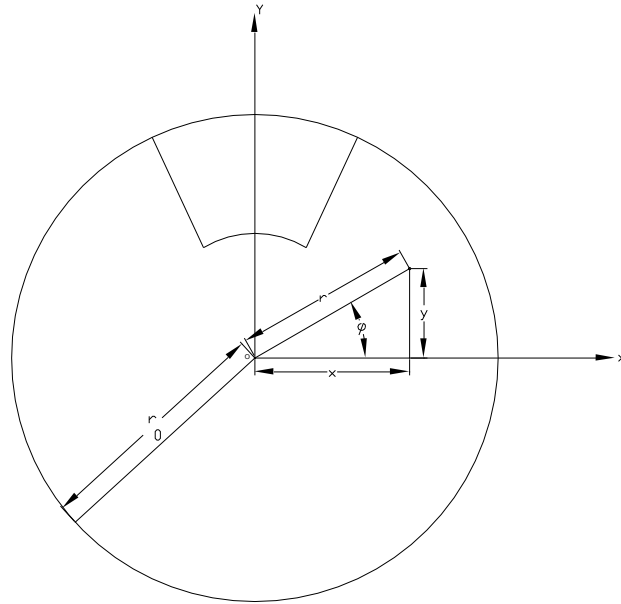
$$q_y = \frac{\partial m_y}{\partial y} + \frac{\partial m_{xy}}{\partial x} = -D \frac{\partial}{\partial y} \left(\frac{\partial^2 w}{\partial x^2} + \frac{\partial^2 w}{\partial y^2} \right) = -D \frac{\partial}{\partial y} \nabla^2 w \quad (2.37)$$

The plate problem is considered solved if a suitable expression for the deflected plate surface $w(x, y)$ is found which simultaneously satisfies the differential equation of equilibrium (equation 2.34) and the boundary conditions. Consequently, it can be stated that the solution of plate problems is a specific case of a boundary value problem of mathematical physics.

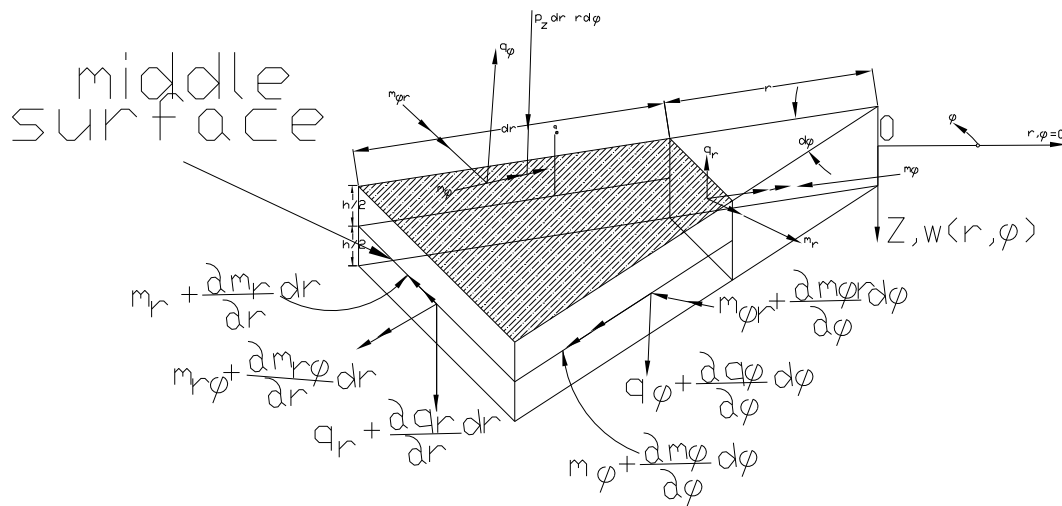
2.6 Equation of Motion for Circular Plates

For circular plates, the use of polar coordinates system is most convenient. When circular plates are analyzed, it is convenient to express the governing differential equation 2.34 in a polar coordinate system as shown in Fig. 2.6a. This can be readily accomplished by

a coordinate transformation. An alternative approach based on the equilibrium condition of an infinitesimally small plate element as shown in Fig. 2.6b, is analogous to the derivation given in [derivation for Cartesian coordinate system].



(a) Relationship Between Cartesian and Polar Coordinates.



(b) Plate Element.

Fig. 2.6 Circular Plate

If the coordinate transformation technique is used, the following geometrical relationships between the Cartesian and polar coordinates are applicable as shown in Fig.2.6a.

$$(x, y) \rightarrow (r, \theta) \quad (2.38)$$

$$x = r \cos \theta, y = r \sin \theta \quad (2.39)$$

$$r^2 = x^2 + y^2, \tan \theta = \frac{y}{x} \Rightarrow \theta = \tan^{-1}\left(\frac{y}{x}\right) \quad (2.40)$$

Since x is a function of r and θ , the derivative of $w(r, \theta)$ with respect to x can be transformed into derivatives with respect to r and θ .

$$\frac{\partial w}{\partial x} = \frac{\partial w}{\partial r} \frac{\partial r}{\partial x} + \frac{\partial w}{\partial \theta} \frac{\partial \theta}{\partial x} \quad (2.41)$$

Differentiate the equation $r^2 = x^2 + y^2$, with respect to x , we obtain the following

$$2x = 2r \frac{\partial r}{\partial x} \Rightarrow \frac{\partial r}{\partial x} = \frac{x}{r} = \frac{r \cos \theta}{r} = \cos \theta \quad (2.42)$$

Similarly differentiate equation $\theta = \tan^{-1}\left(\frac{y}{x}\right)$, with respect to x , we obtain the following

$$\frac{\partial \theta}{\partial x} = \frac{1}{1 + (y/x)^2} \left(\frac{-y}{x^2} \right) = \frac{-y}{x^2 + y^2} = \frac{-r \sin \theta}{r^2} = \frac{-\sin \theta}{r} \quad (2.43)$$

From Equation (2.41)

$$\frac{\partial w}{\partial x} = \cos \theta \frac{\partial w}{\partial r} - \frac{\sin \theta}{r} \frac{\partial w}{\partial \theta} \quad (2.44)$$

$$\frac{\partial^2 w}{\partial x^2} = \frac{\partial}{\partial x} \left(\frac{\partial w}{\partial x} \right) = \frac{\partial}{\partial r} \left[\cos \theta \frac{\partial w}{\partial r} - \frac{\sin \theta}{r} \frac{\partial w}{\partial \theta} \right] \frac{\partial r}{\partial x} + \frac{\partial}{\partial \theta} \left[\cos \theta \frac{\partial w}{\partial r} - \frac{\sin \theta}{r} \frac{\partial w}{\partial \theta} \right] \frac{\partial \theta}{\partial x} \quad (2.45)$$

$$\begin{aligned}
& \left[\cos \theta \frac{\partial^2 w}{\partial r^2} + \frac{\partial w}{\partial r} \frac{\partial}{\partial r} \cos \theta - \frac{\sin \theta}{r} \frac{\partial^2 w}{\partial r \partial \theta} - \frac{\partial w}{\partial \theta} \frac{\partial}{\partial r} \frac{\sin \theta}{r} \right] \cos \theta + \\
& = \left[\cos \theta \frac{\partial^2 w}{\partial \theta \partial r} + \frac{\partial w}{\partial r} \frac{\partial}{\partial \theta} \cos \theta - \frac{\sin \theta}{r} \frac{\partial^2 w}{\partial \theta^2} - \frac{\partial w}{\partial \theta} \frac{\partial}{\partial \theta} \frac{\sin \theta}{r} \right] \cdot -\frac{\sin \theta}{r}
\end{aligned} \tag{2.46}$$

$$\left[\cos^2 \theta \frac{\partial^2 w}{\partial r^2} - \frac{\sin \theta \cos \theta}{r} \frac{\partial^2 w}{\partial r \partial \theta} + \frac{\partial w}{\partial \theta} \frac{\sin \theta \cos \theta}{r^2} - \frac{\sin \theta \cos \theta}{r} \frac{\partial^2 w}{\partial r \partial \theta} + \frac{\partial w}{\partial r} \frac{\sin^2 \theta}{r} + \frac{\sin^2 \theta}{r^2} \frac{\partial^2 w}{\partial \theta^2} + \frac{\partial w}{\partial \theta} \frac{\sin \theta \cos \theta}{r^2} \right]$$

=

$$\left[\cos^2 \theta \frac{\partial^2 w}{\partial r^2} - \frac{2 \sin \theta \cos \theta}{r} \frac{\partial^2 w}{\partial r \partial \theta} + \frac{\partial w}{\partial \theta} \frac{2 \sin \theta \cos \theta}{r^2} + \frac{\partial w}{\partial r} \frac{\sin^2 \theta}{r} + \frac{\sin^2 \theta}{r^2} \frac{\partial^2 w}{\partial \theta^2} \right]$$

$$\frac{\partial^2 w}{\partial x^2} = \left[\cos^2 \theta \frac{\partial^2 w}{\partial r^2} + \frac{\sin^2 \theta}{r^2} \frac{\partial^2 w}{\partial \theta^2} + \frac{\sin^2 \theta}{r} \frac{\partial w}{\partial r} - \frac{\sin 2\theta}{r} \frac{\partial^2 w}{\partial r \partial \theta} + \frac{\sin 2\theta}{r^2} \frac{\partial w}{\partial \theta} \right] \tag{2.47}$$

Similarly y is a function of r and θ , the derivative of $w(r, \theta)$ with respect to y can be transformed into derivatives with respect to r and θ .

$$\frac{\partial w}{\partial y} = \frac{\partial w}{\partial r} \frac{\partial r}{\partial y} + \frac{\partial w}{\partial \theta} \frac{\partial \theta}{\partial y} \tag{2.48}$$

Differentiate the equation $r^2 = x^2 + y^2$, with respect to y , we obtain the following

$$2y = 2r \frac{\partial r}{\partial y} \Rightarrow \frac{\partial r}{\partial y} = \frac{y}{r} = \frac{r \sin \theta}{r} = \sin \theta \tag{2.49}$$

Similarly differentiate equation $\theta = \tan^{-1}\left(\frac{y}{x}\right)$, with respect to y , we obtain the following

$$\frac{\partial \theta}{\partial y} = \frac{1}{1 + (y/x)^2} \left(\frac{1}{x} \right) = \frac{x}{x^2 + y^2} = \frac{r \cos \theta}{r^2} = \frac{\cos \theta}{r} \tag{2.50}$$

From Equation (2.48)

$$\frac{\partial w}{\partial y} = \sin \theta \frac{\partial w}{\partial r} + \frac{\cos \theta}{r} \frac{\partial w}{\partial \theta} \tag{2.51}$$

$$\frac{\partial^2 w}{\partial y^2} = \frac{\partial}{\partial y} \left(\frac{\partial w}{\partial y} \right) = \frac{\partial}{\partial r} \left[\sin \theta \frac{\partial w}{\partial r} + \frac{\cos \theta}{r} \frac{\partial w}{\partial \theta} \right] \frac{\partial r}{\partial y} + \frac{\partial}{\partial \theta} \left[\sin \theta \frac{\partial w}{\partial r} + \frac{\cos \theta}{r} \frac{\partial w}{\partial \theta} \right] \frac{\partial \theta}{\partial y} \tag{2.52}$$

$$\begin{aligned}
&= \left[\sin \theta \frac{\partial^2 w}{\partial r^2} + \frac{\partial w}{\partial r} \frac{\partial}{\partial r} \sin \theta + \frac{\cos \theta}{r} \frac{\partial^2 w}{\partial r \partial \theta} + \frac{\partial w}{\partial \theta} \frac{\partial}{\partial r} \frac{\cos \theta}{r} \right] \sin \theta + \\
&\quad \left[\sin \theta \frac{\partial^2 w}{\partial \theta \partial r} + \frac{\partial w}{\partial r} \frac{\partial}{\partial \theta} \sin \theta + \frac{\cos \theta}{r} \frac{\partial^2 w}{\partial \theta^2} + \frac{\partial w}{\partial \theta} \frac{\partial}{\partial \theta} \frac{\cos \theta}{r} \right] \frac{\cos \theta}{r} \quad (2.53) = \\
&\quad \left[\sin^2 \theta \frac{\partial^2 w}{\partial r^2} + \frac{\sin \theta \cos \theta}{r} \frac{\partial^2 w}{\partial r \partial \theta} - \frac{\partial w}{\partial \theta} \frac{\sin \theta \cos \theta}{r^2} + \frac{\sin \theta \cos \theta}{r} \frac{\partial^2 w}{\partial r \partial \theta} + \frac{\partial w}{\partial r} \frac{\cos^2 \theta}{r} + \frac{\cos^2 \theta}{r^2} \frac{\partial^2 w}{\partial \theta^2} - \frac{\partial w}{\partial \theta} \frac{\sin \theta \cos \theta}{r^2} \right] \\
&= \left[\sin^2 \theta \frac{\partial^2 w}{\partial r^2} + \frac{2 \sin \theta \cos \theta}{r} \frac{\partial^2 w}{\partial r \partial \theta} - \frac{2 \sin \theta \cos \theta}{r^2} \frac{\partial w}{\partial \theta} + \frac{\cos^2 \theta}{r} \frac{\partial w}{\partial r} + \frac{\cos^2 \theta}{r^2} \frac{\partial^2 w}{\partial \theta^2} \right] \\
&\quad \frac{\partial^2 w}{\partial y^2} = \left[\sin^2 \theta \frac{\partial^2 w}{\partial r^2} + \frac{\cos^2 \theta}{r^2} \frac{\partial^2 w}{\partial \theta^2} + \frac{\cos^2 \theta}{r} \frac{\partial w}{\partial r} + \frac{\sin 2\theta}{r} \frac{\partial^2 w}{\partial r \partial \theta} - \frac{\sin 2\theta}{r^2} \frac{\partial w}{\partial \theta} \right] \quad (2.54)
\end{aligned}$$

From equations (2.41) and (2.48) yields the following

$$\begin{aligned}
\frac{\partial^2 w}{\partial x \partial y} &= \frac{\partial}{\partial x} \left(\frac{\partial w}{\partial y} \right) = \frac{\partial}{\partial x} \left[\sin \theta \frac{\partial w}{\partial r} + \frac{\cos \theta}{r} \frac{\partial w}{\partial \theta} \right] \\
&= \frac{\partial}{\partial r} \left[\sin \theta \frac{\partial w}{\partial r} + \frac{\cos \theta}{r} \frac{\partial w}{\partial \theta} \right] \frac{\partial r}{\partial x} + \frac{\partial}{\partial \theta} \left[\sin \theta \frac{\partial w}{\partial r} + \frac{\cos \theta}{r} \frac{\partial w}{\partial \theta} \right] \frac{\partial \theta}{\partial x} \\
&= \left[\sin \theta \frac{\partial^2 w}{\partial r^2} + \frac{\partial w}{\partial r} \frac{\partial}{\partial r} \sin \theta + \frac{\cos \theta}{r} \frac{\partial^2 w}{\partial r \partial \theta} + \frac{\partial w}{\partial \theta} \frac{\partial}{\partial r} \frac{\cos \theta}{r} \right] \cos \theta + \\
&\quad \left[\sin \theta \frac{\partial^2 w}{\partial r \partial \theta} + \frac{\partial w}{\partial r} \frac{\partial}{\partial \theta} \sin \theta + \frac{\cos \theta}{r} \frac{\partial^2 w}{\partial \theta^2} + \frac{\partial w}{\partial \theta} \frac{\partial}{\partial \theta} \frac{\cos \theta}{r} \right] \frac{-\sin \theta}{r} \\
&= \left[\sin \theta \cos \theta \frac{\partial^2 w}{\partial r^2} + \frac{\cos^2 \theta}{r} \frac{\partial^2 w}{\partial r \partial \theta} - \frac{\cos^2 \theta}{r^2} \frac{\partial w}{\partial \theta} - \frac{\sin^2 \theta}{r} \frac{\partial^2 w}{\partial r \partial \theta} - \frac{\sin \theta \cos \theta}{r} \frac{\partial w}{\partial r} - \frac{\sin \theta \cos \theta}{r^2} \frac{\partial^2 w}{\partial \theta^2} + \frac{\sin^2 \theta}{r^2} \frac{\partial w}{\partial r} \right] \\
&= \left[\frac{\sin 2\theta}{2} \frac{\partial^2 w}{\partial r^2} - \frac{\sin 2\theta}{2r^2} \frac{\partial^2 w}{\partial \theta^2} + \frac{\cos 2\theta}{r} \frac{\partial^2 w}{\partial r \partial \theta} - \frac{\cos 2\theta}{r^2} \frac{\partial w}{\partial \theta} - \frac{\sin 2\theta}{2r} \frac{\partial w}{\partial r} \right] \\
&\quad \frac{\partial^2 w}{\partial x \partial y} = \left[\frac{\sin 2\theta}{2} \frac{\partial^2 w}{\partial r^2} - \frac{\sin 2\theta}{2r^2} \frac{\partial^2 w}{\partial \theta^2} + \frac{\cos 2\theta}{r} \frac{\partial^2 w}{\partial r \partial \theta} - \frac{\cos 2\theta}{r^2} \frac{\partial w}{\partial \theta} - \frac{\sin 2\theta}{2r} \frac{\partial w}{\partial r} \right] \quad (2.55)
\end{aligned}$$

Therefore the Laplace operator $\nabla^2 = \frac{\partial^2}{\partial x^2} + \frac{\partial^2}{\partial y^2}$, in terms of polar coordinates, becomes

$$\begin{aligned}
\nabla^2 &= \left[\cos^2 \theta \frac{\partial^2 w}{\partial r^2} + \frac{\sin^2 \theta}{r^2} \frac{\partial^2 w}{\partial \theta^2} + \frac{\sin^2 \theta}{r} \frac{\partial w}{\partial r} - \frac{\sin 2\theta}{r} \frac{\partial^2 w}{\partial r \partial \theta} + \frac{\sin 2\theta}{r^2} \frac{\partial w}{\partial \theta} \right] + \\
&\left[\sin^2 \theta \frac{\partial^2 w}{\partial r^2} + \frac{\cos^2 \theta}{r^2} \frac{\partial^2 w}{\partial \theta^2} + \frac{\cos^2 \theta}{r} \frac{\partial w}{\partial r} + \frac{\sin 2\theta}{r} \frac{\partial^2 w}{\partial r \partial \theta} - \frac{\sin 2\theta}{r^2} \frac{\partial w}{\partial \theta} \right] \\
&= \left[\frac{\partial^2 w}{\partial r^2} + \frac{1}{r^2} \frac{\partial^2 w}{\partial \theta^2} + \frac{1}{r} \frac{\partial w}{\partial r} \right] \\
\nabla_r^2 &= \left[\frac{\partial^2 w}{\partial r^2} + \frac{1}{r^2} \frac{\partial^2 w}{\partial \theta^2} + \frac{1}{r} \frac{\partial w}{\partial r} \right] \tag{2.56}
\end{aligned}$$

When the Laplacian operator ∇^2 is replaced by ∇_r^2 in the equation $D\nabla^2\nabla^2 w = P_z$, the plate equation in Polar coordinates is obtained as

$$\nabla_r^2 \nabla_r^2 w = \frac{P_z(r, \theta)}{D} \tag{2.57}$$

The expressions for internal moments and shear forces, derived earlier can be also transformed into Polar coordinates,

$$M_r = -D \left[\frac{\partial^2 w}{\partial r^2} + \nu \left(\frac{1}{r^2} \frac{\partial^2 w}{\partial \theta^2} + \frac{1}{r} \frac{\partial w}{\partial r} \right) \right] \tag{2.58}$$

$$M_\theta = -D \left[\frac{1}{r} \frac{\partial w}{\partial r} + \frac{1}{r^2} \frac{\partial^2 w}{\partial \theta^2} + \nu \frac{\partial^2 w}{\partial r^2} \right] \tag{2.59}$$

$$M_{r\theta} = M_{\theta r} = -(1-\nu)D \frac{\partial}{\partial r} \left(\frac{1}{r} \frac{\partial w}{\partial \theta} \right) = -(1-\nu) \left[\frac{1}{r} \frac{\partial^2 w}{\partial r \partial \theta} - \frac{1}{r^2} \frac{\partial w}{\partial \theta} \right] \tag{2.60}$$

$$Q_r = -D \frac{\partial}{\partial r} \nabla_r^2 w \tag{2.61}$$

$$Q_\theta = -D \frac{1}{r} \frac{\partial}{\partial \theta} \nabla_r^2 w \tag{2.62}$$

Similarly, transformations of equations of the shearing force at the edge of the plate into polar coordinates gives the lateral edge forces.

$$V_r = Q_r + \frac{1}{r} \frac{\partial M_{r\theta}}{\partial \theta} \tag{2.63}$$

$$V_\theta = Q_\theta + \frac{1}{r} \frac{\partial M_\theta}{\partial r} \quad (2.64)$$

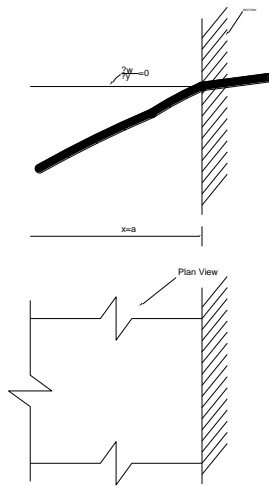
These equations for an edge with outward normal in the r or θ direction become

$$V_r = -D \left[\frac{\partial}{\partial r} \nabla_r^2 w + \frac{1-\nu}{r} \frac{\partial}{\partial \theta} \left(\frac{1}{r} \frac{\partial^2 w}{\partial r \partial \theta} - \frac{1}{r^2} \frac{\partial w}{\partial \theta} \right) \right] \quad (2.65)$$

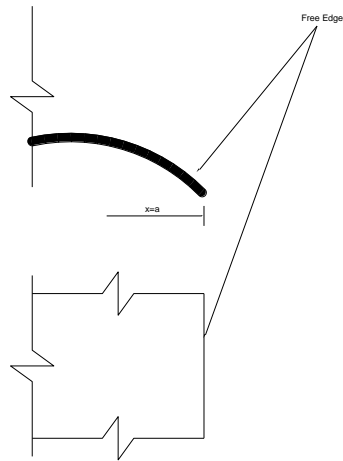
$$V_\theta = -D \left[\frac{1}{r} \frac{\partial}{\partial \theta} \nabla_r^2 w + 1-\nu \frac{\partial}{\partial r} \left(\frac{1}{r} \frac{\partial^2 w}{\partial r \partial \theta} - \frac{1}{r^2} \frac{\partial w}{\partial \theta} \right) \right] \quad (2.66)$$

2.7 Bending Theory and Boundary Conditions

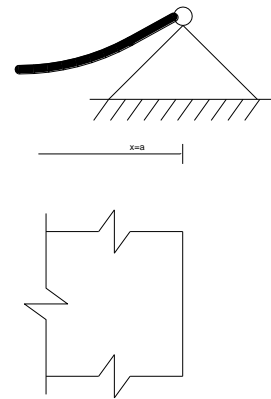
An exact solution of the governing plate equation (Eq. 2.34) must simultaneously satisfy the differential equation and the boundary conditions of any given problem. Since Eq. (2.34) is a fourth-order differential equation, two boundary conditions, either for the displacements or for the internal forces, are required at each boundary condition. In the bending theory of plates, three internal force components are to be considered, and are represented by bending moment, torsional moment and transverse shear. Similarly, the displacement components to be used in formulating the boundary conditions are lateral deflections and slope. Boundary conditions of the plates in bending can be generally classified as one of the following.



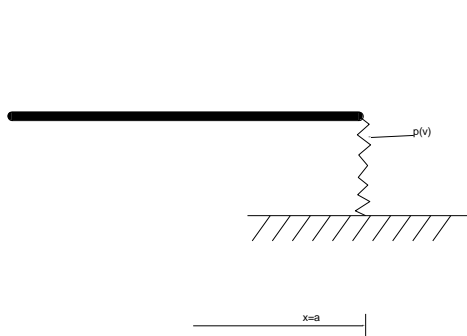
2.7(a) Fixed Edge



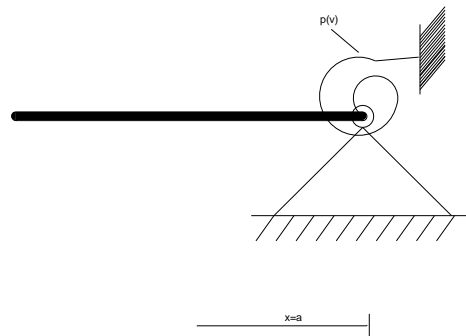
2.7(b) Free Edge



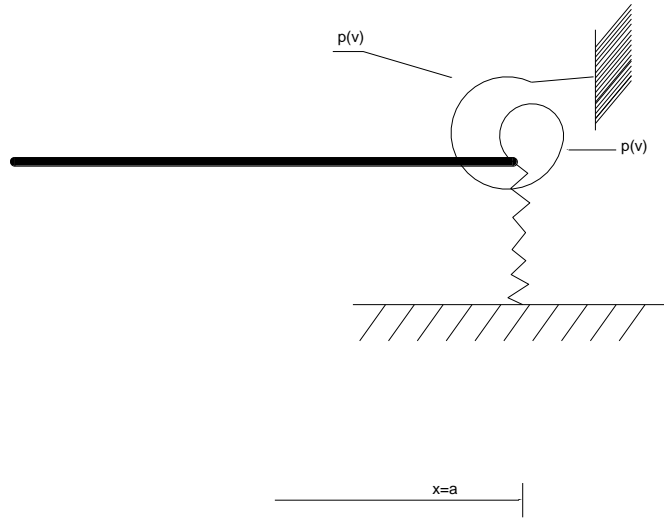
2.7(c) Simply Support



2.7(d) Elastic Support



2.7(e) Elastic Restraint



2.7(f) Elastic Support and Restraint

Fig. 2.7 Various Boundary Conditions

2.7.1 Geometrical Boundary Conditions

Certain geometrical conditions provided by the magnitude of displacements (rotation and translation) can be used to formulate the boundary conditions in mathematical form. At fixed edges as shown in Fig. 2.7a, for instance, the deflection and the slope of the deflected plate surface are zero. Thus we can write

$$(w)_x = 0, \left(\frac{\partial w}{\partial x} \right)_x = 0 \quad (x = 0 \text{ or } x = a) \quad (2.67)$$

$$\text{and } (w)_y = 0, \left(\frac{\partial w}{\partial y} \right)_y = 0 \quad (y = 0 \text{ or } y = a) \quad (2.68)$$

2.7.2 Statistical Boundary Conditions (Free Edges)

For statistical boundary conditions the edge forces provide the required mathematical expressions. At an unloaded free edge as shown in Fig 2.7b, for instance, it is seen that the edge moment and the transverse shear force (v) are zero and given by

$$(m_x)_x = (v_x)_x = 0 \quad x = 0, a \quad (2.69)$$

$$\text{or } (m_x)_x = (v_x)_x = 0 \quad y = 0, a \quad (2.70)$$

2.7.3 Mixed Boundary Conditions

A simply supported edge as shown in Fig. 2.7c, represents mixed boundary conditions. Since the deflection and the bending moment along the boundary is zero, formulation of this type of boundary condition involves statements concerning displacements and forces. Thus

$$(w)_x = 0, (m_x)_x = \left(\frac{\partial^2 w}{\partial x^2} + \nu \frac{\partial^2 w}{\partial y^2} \right) = 0 \quad (2.71)$$

$$\text{and } (w)_x = 0, (m_y)_y = \left(\frac{\partial^2 w}{\partial y^2} + \nu \frac{\partial^2 w}{\partial x^2} \right) = 0 \quad (2.72)$$

2.7.4 Elastic Support and Restraint

A special case of the mixed boundary condition occurs when the plate is resting on yielding support as shown in Fig. 2.7d, such as provided by an edge beam without torsional rigidity. Assuming that the support is elastic and that its translational stiffness or spring constant is K_T and the torsional rigidity is K_R . The boundary with torsional rigidity is shown in Fig. 2.7e. If the edge beam has torsional rigidity K_R , it also provides partial restraint (fixity) as shown in Fig. 2.7f. The geometrical boundary conditions of elastic support and restraint along the edges at $x = 0$ and $x = a$ are

$$(w)_{x=0,a} = \pm \frac{D}{K_T} \left[\frac{\partial^3 w}{\partial x^3} + (2 - \nu) \frac{\partial^3 w}{\partial x \partial y^2} \right]_{x=0,a} \quad (2.73)$$

$$\left(\frac{\partial w}{\partial x} \right)_{x=0,a} = \pm \frac{D}{K_R} \left[\frac{\partial^2 w}{\partial x^2} + \nu \frac{\partial^2 w}{\partial y^2} \right]_{x=0,a} \quad (2.74)$$

The analytical formulations of the various boundary conditions are listed in Table. 2.1

Table. 2.1 Mathematical expressions for various boundary conditions

S.No	Type Of Support	Mathematical Expression
------	-----------------	-------------------------

1	Simple Support	$(w)_{x=a} = 0, (m_x)_{x=a} = \left(\frac{\partial^2 w}{\partial x^2} + \nu \frac{\partial^2 w}{\partial y^2} \right)_{x=a} = 0$
2	Fixed Edge	$(w)_{x=a} = 0, \left(\frac{\partial w}{\partial x} \right)_{x=a} = 0$
3	Free Edge	$(m_x)_{x=a} = \left(\frac{\partial^2 w}{\partial x^2} + \nu \frac{\partial^2 w}{\partial y^2} \right)_{x=a} = 0$ $(v)_{x=a} = \left[\frac{\partial^3 w}{\partial x^3} + (2 - \nu) \frac{\partial^3 w}{\partial x \partial y^2} \right]_{x=a} = 0$
4	Partially Fixed Edge	$(w)_{x=a} = 0$ $\left(\frac{\partial w}{\partial x} \right)_{x=a} = \frac{D}{K_R} \left[\frac{\partial^2 w}{\partial x^2} + \nu \frac{\partial^2 w}{\partial y^2} \right]_{x=a}$
5	Elastic Support	$(m_x)_{x=a} = \left(\frac{\partial^2 w}{\partial x^2} + \nu \frac{\partial^2 w}{\partial y^2} \right)_{x=a} = 0$ $(w)_{x=a} = \frac{D}{K_T} \left[\frac{\partial^3 w}{\partial x^3} + (2 - \nu) \frac{\partial^3 w}{\partial x \partial y^2} \right]_{x=a}$
6	Elastic Support and Restraint	$(w)_{x=a} = \frac{D}{K_T} \left[\frac{\partial^3 w}{\partial x^3} + (2 - \nu) \frac{\partial^3 w}{\partial x \partial y^2} \right]_{x=a}$ $\left(\frac{\partial w}{\partial x} \right)_{x=a} = \frac{D}{K_R} \left[\frac{\partial^2 w}{\partial x^2} + \nu \frac{\partial^2 w}{\partial y^2} \right]_{x=a}$

2.8 Differential Equation in Static Equilibrium

Classical buckling problems of plates can be formulated using the following methods.

- (i) The differential equation of static equilibrium
- (ii) Various energy methods
- (iii) Dynamic approaches

2.8.1 Governing Equations in Rectangular Coordinates

Consider the classical thin plate theory, which is based on the Kirchhoff hypothesis

1. Straight lines perpendicular to the mid-surface (i.e., transverse normals) before deformation remain straight after deformation.
2. The transverse normals do not experience elongation (i.e., they are inextensible).
3. The transverse normals rotate such that they remain perpendicular to the mid-surface after deformation.

The consequence of the Kirchhoff hypothesis is that the transverse strains ($\gamma_{xz}, \gamma_{yz}, \gamma_{zz}$) are zero, and consequently, the transverse stresses ($\sigma_{xz}, \sigma_{yz}, \sigma_{zz}$) do not enter the theory. The equation governing buckling of plates under in-plane compressive and shear forces is

$$\frac{\partial^2 M_{xx}}{\partial x^2} + 2 \frac{\partial^2 M_{xy}}{\partial x \partial y} + \frac{\partial^2 M_{yy}}{\partial y^2} = \frac{\partial}{\partial x} \left(N_{xx} \frac{\partial w}{\partial x} + N_{xy} \frac{\partial w}{\partial y} \right) + \frac{\partial}{\partial y} \left(N_{xy} \frac{\partial w}{\partial x} + N_{yy} \frac{\partial w}{\partial y} \right) \quad (2.75)$$

Where (M_{xx}, M_{yy}) are the bending moments per unit length, M_{xy} is the twisting moment per unit length and (N_{xx}, N_{yy}, N_{xy}) are the applied in-plane compressive and shear forces measured per unit length as shown in Fig. 2.8.

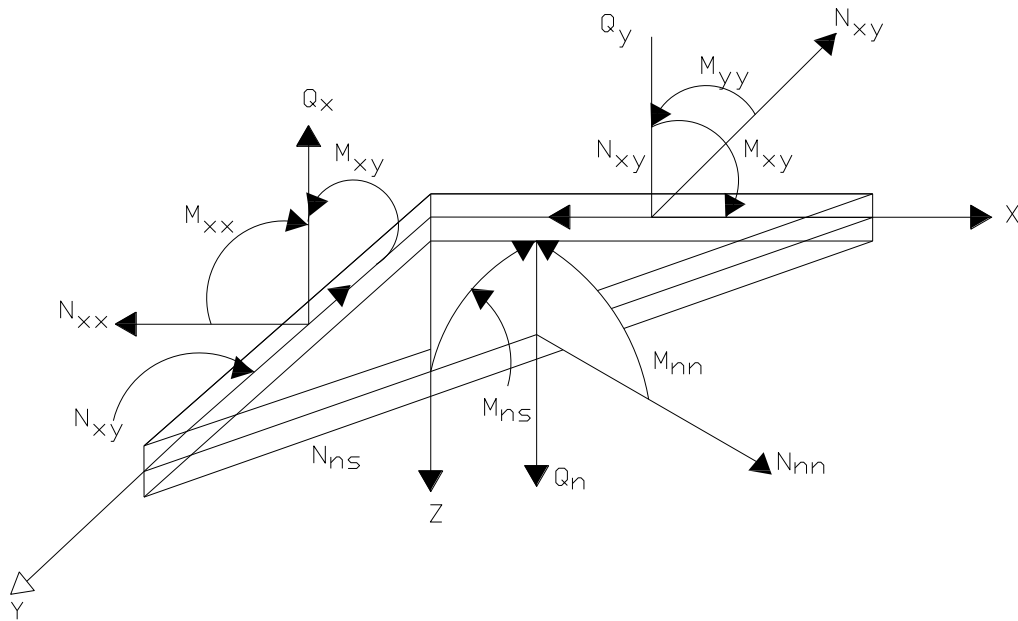


Fig.2.8 Applied in-plane Forces and Moments in a plane element

Eq. (2.75) must be solved in conjunction with boundary conditions that may be classified as essential and natural

Essential: $w, \frac{\partial w}{\partial n}$ Natural: V_n, M_{nn}

Where

$$V_n = Q_n + \frac{\partial M_{ns}}{\partial s} - \left(N_{xx} \frac{\partial w}{\partial x} + N_{xy} \frac{\partial w}{\partial y} \right) n_x - \left(N_{xy} \frac{\partial w}{\partial x} + N_{yy} \frac{\partial w}{\partial y} \right) n_y \quad (2.76)$$

$$Q_n = (M_{xx,x} + M_{xy,y}) n_x + (M_{yy,y} + M_{xy,x}) n_y \quad (2.77)$$

$$M_{nn} = n_x^2 M_{nn} + n_y^2 M_{yy} + 2n_x n_y M_{xy} \quad (2.78)$$

$$M_{ns} = (M_{yy} - M_{xx}) n_x n_y + (n_x^2 - n_y^2) M_{xy} \quad (2.79)$$

and (n_x, n_y) are the direction cosines of the unit outward normal vector \hat{n} that is oriented at an angle θ from the positive x -axis, hence, its direction cosines are, $n_x = \cos \theta$ and $n_y = \sin \theta$.

Thus, at every boundary point one must know one element in each of the two pairs; (w, V_n) and $(\partial w / \partial n, M_{nn})$.

For an orthographic material with principal materials axes (x_1, x_2, x_3) coinciding with the plate coordinates (x, y, z) , the bending moments are related to the deflection $w(x, y)$ as follows.

$$\begin{Bmatrix} M_{xx} \\ M_{yy} \\ M_{xy} \end{Bmatrix} = - \begin{bmatrix} D_{11} & D_{12} & 0 \\ D_{12} & D_{22} & 0 \\ 0 & 0 & D_{66} \end{bmatrix} \begin{Bmatrix} \frac{\partial^2 w}{\partial x^2} \\ \frac{\partial^2 w}{\partial y^2} \\ 2 \frac{\partial^2 w}{\partial x \partial y} \end{Bmatrix} \quad (2.80)$$

$$D_{11} = \frac{E_1 h^3}{12(1 - \nu_{12}\nu_{21})}, D_{12} = \nu_{21}D_{11}, D_{22} = \frac{E_2}{E_1}D_{11}, D_{66} = \frac{G_{12}h^3}{12} \quad (2.81)$$

The equation of equilibrium (Eq. 2.75) can be expressed in terms of displacement (w) by substituting for the moments from Eq. (2.80). For homogeneous plates (i.e., for plates with constant D_s), the equation of equilibrium takes the form

$$D_{11} \frac{\partial^4 w}{\partial x^4} + 2(D_{12} + 2D_{66}) \frac{\partial^4 w}{\partial x^2 \partial y^2} + D_{22} \frac{\partial^4 w}{\partial y^4} + \frac{\partial}{\partial x} \left(N_{xx} \frac{\partial w}{\partial x} + N_{xy} \frac{\partial w}{\partial y} \right) + \frac{\partial}{\partial y} \left(N_{xy} \frac{\partial w}{\partial x} + N_{yy} \frac{\partial w}{\partial y} \right) = 0 \quad (2.82)$$

2.8.2 Governing Equations in Polar Coordinates

The equations governing circular plates may be obtained using the transformation relations ($x = r \cos \theta$, $y = r \sin \theta$) between the polar coordinates (r, θ) and the rectangular coordinates (x, y) as shown in Fig. 2.9.

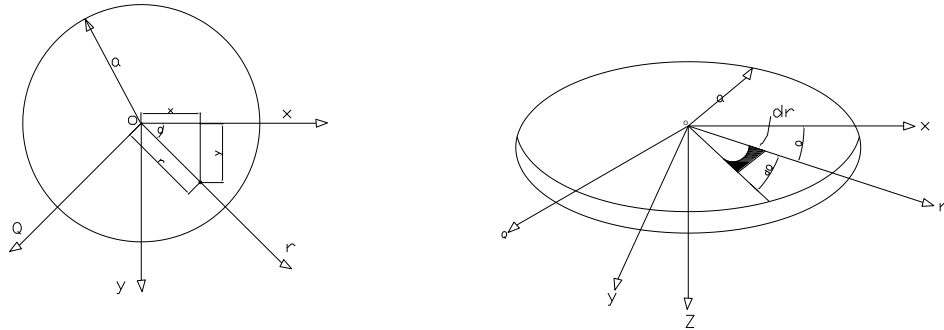


Fig.

2.9 Transformation Between Rectangular and Polar Coordinate Systems

With the help of these transformations we can express the equation of equilibrium (Eq. 2.75) governing the buckling of a circular plate as

$$\frac{1}{r} \left[\frac{\partial}{\partial r} (r Q_r) + \frac{\partial Q_\theta}{\partial \theta} - \frac{\partial}{\partial r} \left(r N_{rr} \frac{\partial w}{\partial r} \right) - \frac{1}{r} \frac{\partial}{\partial \theta} \left(N_{\theta\theta} \frac{\partial w}{\partial \theta} \right) \right] = 0 \quad (2.83)$$

Where (Q_r, Q_θ) are the scalar forces, $(M_r, M_\theta, M_{r\theta})$ are the bending moments, and

$(N_{rr}, N_{\theta\theta}, N_{r\theta})$ are the inplane compressive forces as shown in Fig. 2.9.

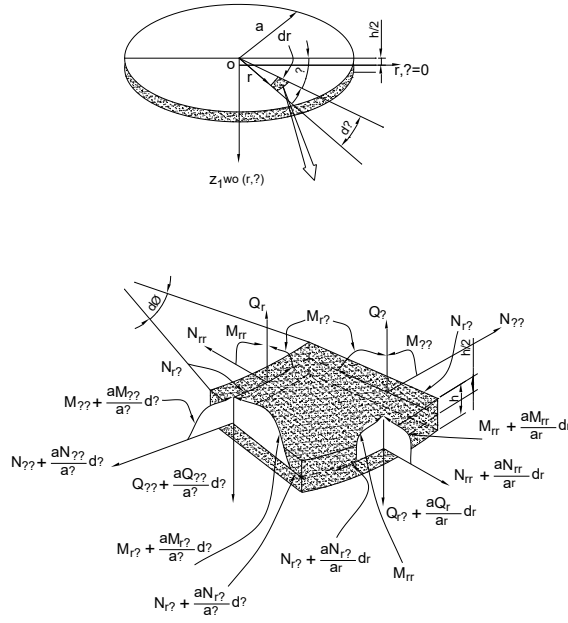


Fig. 2.10. Moments and Shear Forces on an Element of a Circular Plate

$$Q_r = \frac{1}{r} \left[\frac{\partial}{\partial r} (r M_{r\theta}) + \frac{\partial M_{\theta\theta}}{\partial \theta} - M_{\theta\theta} \right] \quad (2.84)$$

$$Q_\theta = \frac{1}{r} \left[\frac{\partial}{\partial r} (r M_{r\theta}) + \frac{\partial M_{\theta\theta}}{\partial \theta} + M_{r\theta} \right] \quad (2.85)$$

$$M_{rr} = -D \left[\frac{\partial^2 w}{\partial r^2} + \nu \left(\frac{1}{r^2} \frac{\partial^2 w}{\partial \theta^2} + \frac{1}{r} \frac{\partial w}{\partial r} \right) \right] \quad (2.86)$$

$$M_{\theta\theta} = -D \left[\frac{1}{r} \frac{\partial w}{\partial r} + \frac{1}{r^2} \frac{\partial^2 w}{\partial \theta^2} + \nu \frac{\partial^2 w}{\partial r^2} \right] \quad (2.87)$$

$$M_{r\theta} = M_{\theta r} = -(1-\nu)D \frac{\partial}{\partial r} \left(\frac{1}{r} \frac{\partial w}{\partial \theta} \right) = -(1-\nu) \left[\frac{1}{r} \frac{\partial^2 w}{\partial r \partial \theta} - \frac{1}{r^2} \frac{\partial w}{\partial \theta} \right] \quad (2.88)$$

Similarly, transformations of equations of the shearing force at the edge of the plate into

Polar coordinates gives the lateral edge forces.

$$V_r = Q_r + \frac{1}{r} \frac{\partial M_{r\theta}}{\partial \theta} - N_{rr} \frac{\partial w}{\partial r} - \frac{1}{r} N_{r\theta} \frac{\partial w}{\partial \theta} \quad (2.89)$$

$$V_\theta = Q_\theta + \frac{1}{r} \frac{\partial M_{\theta r}}{\partial r} - \frac{1}{r} N_{\theta\theta} \frac{\partial w}{\partial \theta} - N_{r\theta} \frac{\partial w}{\partial r} \quad (2.90)$$

The moments are related to the deflection w , by the following

$$M_{rr} = - \left[D_{11} \frac{\partial^2 w}{\partial r^2} + D_{12} \left(\frac{1}{r^2} \frac{\partial^2 w}{\partial \theta^2} + \frac{1}{r} \frac{\partial w}{\partial r} \right) \right] \quad (2.91)$$

$$M_{\theta\theta} = - \left[D_{22} \left(\frac{1}{r} \frac{\partial w}{\partial r} + \frac{1}{r^2} \frac{\partial^2 w}{\partial \theta^2} \right) + D_{12} \frac{\partial^2 w}{\partial r^2} \right] \quad (2.92)$$

$$M_{r\theta} = M_{\theta r} = -2D_{66} \left[\frac{1}{r} \frac{\partial^2 w}{\partial r \partial \theta} - \frac{1}{r^2} \frac{\partial w}{\partial \theta} \right] \quad (2.93)$$

For isotropic plates, set $D_{11} = D_{22} = D$, $D_{12} = \nu D$ and $2D_{66} = (1-\nu)D$ and the bending moment-deflection relationships (Eqs. (2.91)-(2.93) reduce to the following

$$M_{rr} = -D \left[\frac{\partial^2 w}{\partial r^2} + \nu \left(\frac{1}{r^2} \frac{\partial^2 w}{\partial \theta^2} + \frac{1}{r} \frac{\partial w}{\partial r} \right) \right] \quad (2.94)$$

$$M_{\theta\theta} = -D \left[\frac{1}{r} \frac{\partial w}{\partial r} + \frac{1}{r^2} \frac{\partial^2 w}{\partial \theta^2} + \nu \frac{\partial^2 w}{\partial r^2} \right] \quad (2.95)$$

$$M_{r\theta} = M_{\theta r} = -(1-\nu)D \frac{\partial}{\partial r} \left(\frac{1}{r} \frac{\partial w}{\partial \theta} \right) = -(1-\nu) \left[\frac{1}{r} \frac{\partial^2 w}{\partial r \partial \theta} - \frac{1}{r^2} \frac{\partial w}{\partial \theta} \right] \quad (2.96)$$

Equation of equilibrium (Eq.2.75) for an isotropic plate can be written in terms of the displacement with the aid of Eqs. (2.94), (2.95) and (2.96) as

$$D \left[\frac{1}{r} \frac{\partial}{\partial r} \left(r \frac{\partial}{\partial r} \right) + \frac{1}{r^2} \frac{\partial^2}{\partial \theta^2} \right] \left[\frac{1}{r} \frac{\partial}{\partial r} \left(r \frac{\partial w}{\partial r} \right) + \frac{1}{r^2} \frac{\partial^2 w}{\partial \theta^2} \right] = -\frac{1}{r} \frac{\partial}{\partial r} \left(r N_{rr} \frac{\partial w}{\partial r} \right) - \frac{1}{r^2} \frac{\partial}{\partial \theta} \left(N_{\theta\theta} \frac{\partial w}{\partial \theta} \right) \quad (2.97)$$

Using the Laplace operator $\nabla^2 = \left[\frac{\partial^2 w}{\partial r^2} + \frac{1}{r^2} \frac{\partial^2 w}{\partial \theta^2} + \frac{1}{r} \frac{\partial w}{\partial r} \right]$ (2.98)

Equation (2.97) can be written as

$$D \nabla^2 \nabla^2 w + \frac{1}{r} \frac{\partial}{\partial r} \left(r N_{rr} \frac{\partial w}{\partial r} \right) + \frac{1}{r^2} \frac{\partial}{\partial \theta} \left(N_{\theta\theta} \frac{\partial w}{\partial \theta} \right) = 0 \quad (2.99)$$

For axisymmetric buckling of circular plates, all variables are independent of the angular coordinate θ , and they are only functions of the radial coordinate r . Hence, in specializing the governing equations to the axisymmetric case, we omit terms involving differentiation with respect to θ . The moment-deflection relationships for the axisymmetric case are

$$M_{rr} = - \left[D_{11} \frac{d^2 w}{dr^2} + D_{12} \frac{1}{r} \frac{dw}{dr} \right] \quad (2.100)$$

$$M_{\theta\theta} = - \left[D_{22} \frac{1}{r} \frac{dw}{dr} + D_{12} \frac{d^2 w}{dr^2} \right] \quad (2.101)$$

$$Q_r = -D_{11} \frac{1}{r} \frac{d}{dr} \left(r \frac{d^2 w}{dr^2} \right) + D_{22} \frac{1}{r^2} \frac{dw}{dr} \quad (2.102)$$

Therefore, the equation of equilibrium for the axisymmetric case can be deduced from equation (2.75) as

$$- \frac{1}{r} \frac{d}{dr} (r Q_r) + \frac{1}{r} \frac{d}{dr} \left(r N_{rr} \frac{dw}{dr} \right) = 0 \quad (2.103)$$

From equations (2.102) for $r Q_r$ in equation (2.103) yields

$$D_{11} \frac{1}{r} \frac{d}{dr} \left\{ r \frac{d}{dr} \left[\frac{1}{r} \frac{d}{dr} \left(r \frac{dw}{dr} \right) \right] \right\} + \left(\frac{D_{11} - D_{22}}{D_{11}} \right) \frac{1}{r} \frac{dw}{dr} + \frac{1}{r} \frac{d}{dr} \left(r N_{rr} \frac{dw}{dr} \right) = 0 \quad (2.104)$$

For isotropic plates set $D_{11} = D_{22} = D$,

Equations (2.100), (2.101) and (2.102) can be written as

$$M_{rr} = -D \left[\frac{d^2 w}{dr^2} + \nu \left(\frac{1}{r} \frac{dw}{dr} \right) \right] \quad (2.105)$$

$$M_{\theta\theta} = -D \left[\frac{1}{r} \frac{dw}{dr} + \nu \frac{d^2 w}{dr^2} \right] \quad (2.106)$$

$$Q_r = -D \frac{d}{dr} \left[\frac{1}{r} \frac{d}{dr} \left(r \frac{dw}{dr} \right) \right] \quad (2.107)$$

and the equilibrium equation (2.104) simplifies to

$$\frac{D}{r} \frac{d}{dr} \left\{ r \frac{d}{dr} \left[\frac{1}{r} \frac{d}{dr} \left(r \frac{dw}{dr} \right) \right] \right\} + \frac{1}{r} \frac{d}{dr} \left(r N_{rr} \frac{dw}{dr} \right) = 0 \quad (2.108)$$

2.9 Differential Equation of Lateral Motion

Since lateral vibration is of interest, we can reduce the number of degrees of freedom by neglecting the effects of rotational inertia; hence the inertia forces along with the lateral translation of the plate is considered. Damping effects are caused either by internal friction of the surrounding media. Although structural damping is theoretically present in all plate vibrations, it has little or no effect on the natural frequencies and steady-state amplitudes; therefore, it is ignored in the initial treatment of the problem.

The governing differential equations of motion are written by considering two approaches. We may either apply D'Alembert's dynamic equilibrium principle or use a work formulation based on the conservation of energy. The present study deals with the dynamic equilibrium of a plate element for writing the governing differential equation of motions, since it is simple. The inertia force, associated with the lateral translation of a plate element as shown in Fig. 2.2, can be expressed by

$$p_z = -\bar{m} \frac{\partial^2 w}{\partial t^2} = -\bar{m} \ddot{w} \quad (2.109)$$

Where \bar{m} represents the mass of the plate per unit area.

In the dynamic analysis of plates, the lateral loads, and therefore the resulting deflections, are time-dependent. A convenient way for expressing such time dependency is by means of the Fourier series, as follows

$$p_z(x, y, t) = p_z(x, y)(\theta_t) = p_z(x, y) \sum_n P_n \sin p_n t \quad (2.110)$$

The differential equation of static equilibrium (Eq. 2.34) is extended by adding the inertia force, the differential equation of forced, undamped motion of plates is obtained

$$D\nabla^2\nabla^2 w(x, y, t) = p_z(x, y, t) - \bar{m} \frac{\partial^2 w(x, y, t)}{\partial t^2} \quad (2.111)$$

Where x and y are Cartesian coordinates in the plane of the middle surface. For the case of a freely vibrating plate, the external force, p_z , is zero, and the differential equation of the undamped motion becomes

$$D\nabla^2\nabla^2 w + \bar{m} \frac{\partial^2 w}{\partial t^2} = 0 \quad (2.112)$$

Assuming harmonic vibration, we may write

$$w(x, y, t) = W(x, y) \sin \omega t \quad (2.113)$$

Where $W(x, y)$ is the shape function describing the modes of the vibration and ω is the natural circular frequency of the plate. Substituting equation (2.113) into equation (2.112) gives

$$D\nabla^2\nabla^2 w(x, y) - \frac{\bar{m} \omega^2}{D} W(x, y) = 0 \quad (2.114)$$

Similarly, the extension of the governing plate equation, expressed in polar coordinates (Eq. 2.57), yields

$$D\nabla_r^2\nabla_r^2 w(r, \theta, t) = p_z(r, \theta, t) - \bar{m} \frac{\partial^2 w(r, \theta, t)}{\partial t^2} \quad (2.115)$$

From which the differential equation of free undamped vibration is

$$D\nabla_r^2\nabla_r^2 w(r, \theta, t) + \bar{m} \frac{\partial^2 w(r, \theta, t)}{\partial t^2} = 0 \quad (2.116)$$

If the plate is subjected to simultaneous, static, in-plane loadings, the differential equation of lateral motion becomes

$$D\nabla^2\nabla^2 w(x, y, t) = p_z(x, y, t) + n_x \frac{\partial^2 w}{\partial x^2} + n_y \frac{\partial^2 w}{\partial y^2} + 2n_{xy} \frac{\partial^2 w}{\partial x \partial y} - \bar{m} \frac{\partial^2 w(x, y, t)}{\partial t^2} \quad (2.117)$$

$$D\nabla^2\nabla^2 w + \frac{1}{r} \frac{\partial}{\partial r} \left(r N_{rr} \frac{\partial w}{\partial r} \right) + \frac{1}{r^2} \frac{\partial}{\partial \theta} \left(N_{\theta\theta} \frac{\partial w}{\partial \theta} \right) = 0 \quad (2.118)$$

2.9.1 Free Flexural Vibration of Circular Plates

The governing differential equation of the undamped, free vibration of circular plates is (Eq. 2.116). The solution to this differential equation is assumed in the form

$$w(r, \theta, t) = R(r) \cdot \Theta(\theta) \cdot \theta(t) = R(r) \cdot \Theta(\theta) \cdot \sin \omega t \quad (2.119)$$

Where $\Theta(\theta)$ can be represented by $\cos m\theta$, for instance, here m denotes the number of nodal diameters. Functions $R(r)$ must satisfy the governing differential equation (Eq. 2.116) and the boundary conditions. In the case of the lowest mode, the shape function is symmetric. Modified or hyperbolic Bessel functions can also be used to obtain higher modes and pertinent frequencies. The nodal lines for plates are either concentric circles or diameters.

2.10 Study of Possible Methods of Solution

Mathematically, the differential equation of plates (Eq. 2.34) is classified as linear partial differential equation of the fourth order having constant coefficients as expressed in equations (2.120) and (2.121). Its homogeneous form

$$\nabla^2\nabla^2 w = 0 \quad (2.120)$$

Is called the biharmonic equation.

In general, there are four types of mathematically “exact” solutions available for plate problems. They are as follows

1. Closed form solution

2. Solution of the biharmonic equation upon which a particular solution of the governing equation of plate (Eq. 2.34) is superimposed.
3. Double trigonometric series solution.
4. Single series solution.

The rigorous solution of Eq. (2.34) must satisfy the boundary conditions characterizing each problem and the governing differential equation of the plate. Consequently, the rigorous solution of plate problems is essentially a boundary value problem of mathematical physics. Since the fulfillment of the boundary conditions usually presents considerable mathematical difficulties, in general, rigorous solution of plate problems is rare. In the few cases, which lend themselves to exact analysis, the linearity of Eq. (2.34) can be used to permit the linear combination of solutions in form of superposition. Thus the most general form the rigorous solution of the governing differential equation can be expressed as

$$x(x, y) = w_H(x, y) + w_P(x, y) \quad (2.121)$$

Where w_H represents the solution of the homogeneous equation (2.120), and w_P is a particular solution of the nonhomogeneous differential equation of the plate (Eq. 2.34). There are a few cases, however, when the solution can be obtained directly, without employing the above mentioned superposition principle. Certain boundary conditions permit the use of special solutions, such as Navier solution.

2.10.1 Solution of the Homogeneous Equation

The physical interpretations of the solution of the biharmonic equation (2.120) are to obtain the deflection of the plate $w_H(x, y)$ when only edge forces are acting. Consequently, the solution of the homogeneous equation fulfills the prescribed boundary conditions and maintains the equilibrium with the external boundary forces. The fundamental difficulty of the rigorous solution is the proper choice of functions $w_H(x, y)$ for a given problem. The

biharmonic equation (1.120) permits the use of the solutions of the Laplace equation

$\nabla^2 w = 0$, which are

$$x, xy, \cos \alpha x, \cosh \alpha x, x^2 - y^2, x^3 - 3xy^2 \quad (2.122)$$

Where α represents an arbitrary constant. Worch [60] gives an extensive listing of functions that can be used for solution of the biharmonic equation.

A special method for finding solutions of the biharmonic equation is based on separation of variables.

2.10.2 Particular Solution of the Homogeneous Equation

Although the solution w_H of the biharmonic equation effectively describes the equilibrium conditions of the plate subjected to edge forces, the expression of the deflection $w(x, y)$ is not complete without considering the equilibrium of the lateral forces p_z . For this purpose, a particular solution w_p of the nonhomogeneous differential equation (2.34) must be determined. The particular solution shall satisfy the differential equation of the plate (2.34), but satisfying the boundary conditions is not mandatory.

CHAPTER 3

BUCKLING OF CIRCULAR PLATES WITH ELASTICALLY RESTRAINED EDGES AND RESTING ON ELASTIC FOUNDATION

3.1 Theoretical Background

Based on the Kirchhoff's theory, many authors have studied the elastic buckling of thin circular plates, but the pioneering work was done by Bryan [61]. Extensive studies on the subject cover various aspects like different materials of construction under various boundary

and loading conditions. The prediction of buckling of structural members restrained laterally is important in the design of engineering components when they are supported on elastic foundation. Holanda [62] studied the influence of elastic foundation on the stability. The buckling of beams on an elastic foundation has also been well studied by Hetenyi [39]. It was found that for stiffer foundations, the buckling load corresponds to a mode with increased number of nodes. Various researchers studied the buckling behavior of plates considering unilateral contact constraints. Seide [63] studied an infinitely long simply supported plate and found that a rigid lateral constraint may increase the critical load by as much as 33% relative to an unconstrained plate. Analytical solution for the buckling loads for a rectangular plate is possible if two opposite sides are simply supported (Warren [64]), otherwise numerical solutions are necessary (Raju et al. [65]). Yu [7], Gallety [8], Kline et al. [9], Wolkowisky [10] studied the buckling of circular plates. Although the circular symmetry of the problem allows for its significant simplification, many difficulties arise due to complexity and uncertainty of boundary conditions. This uncertainty could be due to practical engineering applications where the edge of the plate does not fall into the classical boundary conditions. It is an accepted fact that the condition on a periphery often tends to be between the classical boundary conditions (free, clamped and simply supported) and correspond more closely to some form of elastic restraints, i.e., rotational and translational restraints (Wang et al [3], Kim et al [66], Yamaki [14]). In a recent study, Wang [13] found buckling load not only by the axisymmetric modes considered by earlier authors, but also by the asymmetric modes as well.

The present work is carried out to compute buckling loads of circular plates with elastically restrained edges against rotation and translation and resting on elastic foundation and by including the asymmetric modes, thus determining the buckling loads more exactly.

3.2 Problem Definition

Consider a thin circular plate of radius, R , uniform thickness, h , Young's modulus E , and Poisson's ratio, ν and subjected to a uniform in-plane load, N along its boundary, as shown in Fig.3.1. This circular plate is assumed to be made of linearly elastic, homogeneous and isotropic material and the effects of shear deformation and rotary inertia are neglected. The edge of the circular plate is elastically restrained against rotation and translation and supported by an elastic foundation, as shown in Fig. 3.1. The problem at hand is to determine the elastic critical buckling load of a circular plate with an elastically restrained edges and supported on elastic foundation.

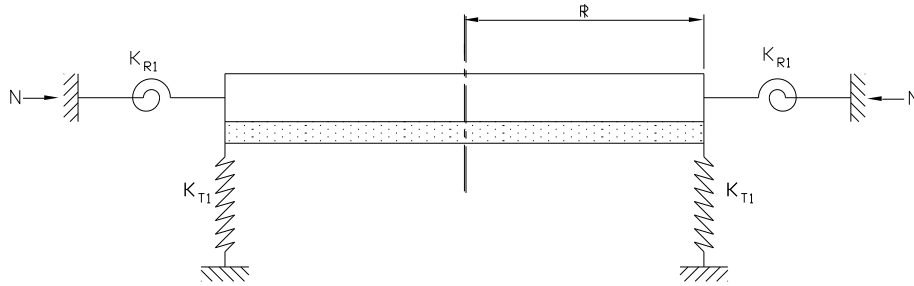


Fig.

3.1 Buckling of a Circular plate with an Elastically Restrained edge against Rotation and Translation and Resting on Elastic Foundation.

3.3 Mathematical Formulation

The plate is elastically restrained against rotation and translation at the edge of radius R and supported on an elastic foundation as shown in Fig.3.1. According to Yu [7], the fourth order differential equation proposed by the Classical Plate Theory (Kirchhof's theory), for a plate resting on elastic foundation is given by the following

$$D\nabla^4 w + N\nabla^2 w + K_w w = 0 \quad (3.1)$$

Where w is the lateral displacement, N is the uniform compressive load at the edge of the plate, D is the flexural rigidity, and K_w is the Modulus of sub grade reaction or Deflection modulus of the foundation. Here, all lengths are normalized by R , and then Eq. (3.1) can be written as

$$\nabla^4 \bar{w} + k^2 \nabla^2 \bar{w} + \xi^4 \bar{w} = 0 \quad (3.2)$$

$$\nabla^2 (\nabla^2 + k^2) \bar{w} + \xi^4 \bar{w} = 0 \quad (3.3)$$

Where, $k^2 = NR^2 / D$ is a non-dimensional buckling load parameter and $\xi^4 = K_w R^4 / D$ is a non-dimensional foundation stiffness parameter, $\nabla^2 = \frac{\partial^2}{\partial \bar{r}^2} + \frac{1}{\bar{r}} \frac{\partial}{\partial \bar{r}} + \frac{1}{\bar{r}^2} \frac{\partial^2}{\partial \theta^2}$ is the Laplacian parameter in the polar coordinates r and θ , \bar{r} is the radial distance normalized by R , and $\bar{w} = w / R$, is normalized transverse displacement of the plate. Suppose there are n nodal diameters. In polar coordinates (r, θ) set

$$\bar{w}(\bar{r}, \theta) = \bar{u}(\bar{r}) \cos(n\theta) \quad (3.4)$$

Where, n is the number of nodal diameters, the general solution which is bounded at the origin is as follows. Let J_n be the Bessel function of order n . The general solution to the Eq. (3.3) is more complicated. Therefore, the following three cases are considered.

Case (i) If $k > \sqrt{2}\xi$, the solution to equation (3.3) is given by

$$u(\bar{r}) = AJ_n(\alpha \bar{r}) + BJ_n(\beta \bar{r}) \quad (3.5)$$

Substituting equation (3.5) into equation (3.4) yields the following

$$\bar{w}(\bar{r}, \theta) = (AJ_n(\alpha \bar{r}) + BJ_n(\beta \bar{r})) \cos(n\theta) \quad (3.6)$$

$$\text{Where } \alpha = \left(\frac{k^2 + \sqrt{k^4 - 4\xi^4}}{2} \right)^{1/2}, \beta = \left(\frac{k^2 - \sqrt{k^4 - 4\xi^4}}{2} \right)^{1/2} \quad (3.7)$$

Case (ii) If $k = \sqrt{2}\xi$, the solution to equation (3.3) is given by

$$u(\bar{r}) = AJ_n(\xi \bar{r}) + B\bar{r}J_{n+1}(\xi \bar{r}) \quad (3.8)$$

Substituting equation (3.8) into equation (3.4) yields the following

$$\bar{w}(\bar{r}, \theta) = (AJ_n(\xi\bar{r}) + B\bar{r}J_{n+1}(\xi\bar{r}))\cos(n\theta) \quad (3.9)$$

Case (iii) If $k < \sqrt{2}\xi$, the solution to equation (3.3) is given by

$$u(\bar{r}) = A \operatorname{Re}[J_n(i\delta\bar{r})] + B \operatorname{Im}[J_n(i\delta\bar{r})] \quad (3.10)$$

Substituting equation (3.10) into equation (3.4) yields the following

$$\bar{w}(\bar{r}, \theta) = (A \operatorname{Re}[J_n(i\delta\bar{r})] + B \operatorname{Im}[J_n(i\delta\bar{r})])\cos(n\theta) \quad (3.11)$$

$$\text{Where } i = \sqrt{-1} \text{ and } \delta = \left(\frac{-k^2 + \sqrt{4\xi^4 - k^4}i}{2} \right)^{1/2} \quad (3.12)$$

The boundary conditions at the edge of the circular plate in terms of rotational stiffness (K_{R1})

and translational stiffness (K_{T1}) is given by the following expressions

$$M_r(\bar{r}, \theta) = K_{R1} \frac{\partial \bar{w}(\bar{r}, \theta)}{\partial \bar{r}} \quad (3.13)$$

$$V_r(\bar{r}, \theta) = -K_{T1} \bar{w}(\bar{r}, \theta) \quad (3.14)$$

Where the bending moment and the Kelvin-Kirchhoff shearing forces are defined as follows

$$M_r(\bar{r}, \theta) = -\frac{D}{R^3} \left[\frac{\partial^2 \bar{w}(\bar{r}, \theta)}{\partial \bar{r}^2} + \nu \left(\frac{1}{\bar{r}} \frac{\partial \bar{w}(\bar{r}, \theta)}{\partial \bar{r}} + \frac{1}{\bar{r}^2} \frac{\partial^2 \bar{w}(\bar{r}, \theta)}{\partial \theta^2} \right) \right] \quad (3.15)$$

$$V_r(\bar{r}, \theta) = -\frac{D}{R^3} \left[\frac{\partial}{\partial \bar{r}} \nabla^2 \bar{w}(\bar{r}, \theta) + (1-\nu) \frac{1}{\bar{r}} \frac{\partial}{\partial \theta} \left(\frac{1}{\bar{r}} \frac{\partial^2 \bar{w}(\bar{r}, \theta)}{\partial \bar{r} \partial \theta} - \frac{1}{\bar{r}^2} \frac{\partial \bar{w}(\bar{r}, \theta)}{\partial \theta} \right) \right] \quad (3.16)$$

From Eqs. (3.13) and (3.15) yields the following

$$\left[\frac{\partial^2 \bar{w}(\bar{r}, \theta)}{\partial \bar{r}^2} + \nu \left(\frac{1}{\bar{r}} \frac{\partial \bar{w}(\bar{r}, \theta)}{\partial \bar{r}} + \frac{1}{\bar{r}^2} \frac{\partial^2 \bar{w}(\bar{r}, \theta)}{\partial \theta^2} \right) \right] = -\frac{K_{R1} R^2}{D} \frac{\partial \bar{w}(\bar{r}, \theta)}{\partial \bar{r}} \quad (3.17)$$

$$\left[\frac{\partial^2 \bar{w}(\bar{r}, \theta)}{\partial \bar{r}^2} + \nu \left(\frac{1}{\bar{r}} \frac{\partial \bar{w}(\bar{r}, \theta)}{\partial \bar{r}} + \frac{1}{\bar{r}^2} \frac{\partial^2 \bar{w}(\bar{r}, \theta)}{\partial \theta^2} \right) \right] = -R_{11} \frac{\partial \bar{w}(\bar{r}, \theta)}{\partial \bar{r}} \quad (3.18)$$

From Eqs. (3.14) and (3.16) yields the following

$$\left[\frac{\partial}{\partial \bar{r}} \nabla^2 \bar{w}(\bar{r}, \theta) + (1-\nu) \frac{1}{\bar{r}} \frac{\partial}{\partial \theta} \left(\frac{1}{\bar{r}} \frac{\partial^2 \bar{w}(\bar{r}, \theta)}{\partial \bar{r} \partial \theta} - \frac{1}{\bar{r}^2} \frac{\partial \bar{w}(\bar{r}, \theta)}{\partial \theta} \right) \right] = \frac{K_{T1} R^3}{D} \bar{w}(\bar{r}, \theta) \quad (3.19)$$

$$\left[\frac{\partial}{\partial \bar{r}} \nabla^2 \bar{w}(\bar{r}, \theta) + (1-\nu) \frac{1}{\bar{r}} \frac{\partial}{\partial \theta} \left(\frac{1}{\bar{r}} \frac{\partial^2 \bar{w}(\bar{r}, \theta)}{\partial \bar{r} \partial \theta} - \frac{1}{\bar{r}^2} \frac{\partial \bar{w}(\bar{r}, \theta)}{\partial \theta} \right) \right] = T_{11} \bar{w}(\bar{r}, \theta) \quad (3.20)$$

Where $R_{11} = \frac{K_{R1} R^2}{D}$ and $T_{11} = \frac{K_{T1} R^3}{D}$

Case (i) If $k > \sqrt{2}\xi$

Boundary conditions when the outer edges are elastically restrained against rotation.

From equations (3.6) and (3.18) yields the following

$$\frac{\partial \bar{w}(\bar{r}, \theta)}{\partial \bar{r}} = \left\{ \frac{\alpha}{2} [J_{n-1}(\alpha \bar{r}) - J_{n+1}(\alpha \bar{r})]A + \frac{\beta}{2} [J_{n-1}(\beta \bar{r}) - J_{n+1}(\beta \bar{r})]B \right\} \cos(n\theta) \quad (3.21)$$

$$\frac{\partial \bar{w}(\bar{r}, \theta)}{\partial \bar{r}} \bigg|_{\bar{r}=1} = \left\{ \frac{\alpha}{2} [J_{n-1}(\alpha) - J_{n+1}(\alpha)]A + \frac{\beta}{2} [J_{n-1}(\beta) - J_{n+1}(\beta)]B \right\} \cos(n\theta) \quad (3.22)$$

$$\frac{\partial \bar{w}(\bar{r}, \theta)}{\partial \bar{r}} = \left\{ \frac{\alpha}{2} [P_{77}]A + \frac{\beta}{2} [P_{77}']B \right\} \cos(n\theta) \quad (3.23)$$

Where $\mathbb{B}^{\mathbb{J}} = \gamma^{\mathbb{J}-1}(\alpha) - \gamma^{\mathbb{J}+1}(\alpha)$; $P_{77}' = J_{n-1}(\beta) - J_{n+1}(\beta)$

$$\frac{\partial^2 \bar{w}(\bar{r}, \theta)}{\partial \bar{r}^2} = \left\{ \frac{\alpha^2}{4} [(J_{n-2}(\alpha \bar{r}) - J_n(\alpha \bar{r})) - (J_n(\alpha \bar{r}) - J_{n+2}(\alpha \bar{r}))]A + \frac{\beta^2}{4} [(J_{n-2}(\beta \bar{r}) - J_n(\beta \bar{r})) - (J_n(\beta \bar{r}) - J_{n+2}(\beta \bar{r}))]B \right\} \cos(n\theta) \quad (3.24)$$

$$\frac{\partial^2 \bar{w}(\bar{r}, \theta)}{\partial \bar{r}^2} = \left\{ \frac{\alpha^2}{4} [J_{n-2}(\alpha \bar{r}) + J_{n+2}(\alpha \bar{r}) - 2J_n(\alpha \bar{r})]A + \frac{\beta^2}{4} [(J_{n-2}(\beta \bar{r}) + J_{n+2}(\beta \bar{r}) - 2J_n(\beta \bar{r}))]B \right\} \cos(n\theta) \quad (3.25)$$

$$\frac{\partial^2 \bar{w}(\bar{r}, \theta)}{\partial \bar{r}^2} \bigg|_{\bar{r}=1} = \left\{ \frac{\alpha^2}{4} [J_{n-2}(\alpha) + J_{n+2}(\alpha) - 2J_n(\alpha)]A + \frac{\beta^2}{4} [(J_{n-2}(\beta) + J_{n+2}(\beta) - 2J_n(\beta))]B \right\} \cos(n\theta) \quad (3.26)$$

$$\frac{\partial^2 \bar{w}(\bar{r}, \theta)}{\partial \bar{r}^2} \bigg|_{\bar{r}=1} = \left\{ \frac{\alpha^2}{4} [P_{88} - 2J_n(\alpha)]A + \frac{\beta^2}{4} [P_{88}' - 2J_n(\beta)]B \right\} \cos(n\theta) \quad (3.27)$$

Where $P_{88} = J_{n-2}(\alpha) + J_{n+2}(\alpha)$; $P_{88}' = (J_{n-2}(\beta) + J_{n+2}(\beta))$

$$\begin{aligned}
\frac{1}{\bar{r}} \frac{\partial \bar{w}(\bar{r}, \theta)}{\partial \bar{r}} &= \frac{1}{\bar{r}} \left\{ \frac{\alpha}{2} [J_{n-1}(\alpha \bar{r}) - J_{n+1}(\alpha \bar{r})] A + \frac{\beta}{2} [J_{n-1}(\beta \bar{r}) - J_{n+1}(\beta \bar{r})] B \right\} \cos(n\theta) \\
\frac{1}{\bar{r}} \frac{\partial \bar{w}(\bar{r}, \theta)}{\partial \bar{r}} \bigg|_{\bar{r}=1} &= \frac{1}{1} \left\{ \frac{\alpha}{2} [J_{n-1}(\alpha) - J_{n+1}(\alpha)] A + \frac{\beta}{2} [J_{n-1}(\beta) - J_{n+1}(\beta)] B \right\} \cos(n\theta) \\
&= \left\{ \frac{\alpha}{2} [P_{77}] A + \frac{\beta}{2} [P_{77}'] B \right\} \cos(n\theta)
\end{aligned} \tag{3.28}$$

$$\frac{\partial \bar{w}(\bar{r}, \theta)}{\partial \theta} = -n [AJ_n(\alpha \bar{r}) + BJ_n(\beta \bar{r})] \sin(n\theta) \tag{3.29}$$

$$\frac{\partial^2 \bar{w}(\bar{r}, \theta)}{\partial \theta^2} = -n^2 [AJ_n(\alpha \bar{r}) + BJ_n(\beta \bar{r})] \cos(n\theta) \tag{3.30}$$

$$\frac{1}{\bar{r}^2} \frac{\partial^2 \bar{w}(\bar{r}, \theta)}{\partial \theta^2} = -\frac{n^2}{\bar{r}^2} [AJ_n(\alpha \bar{r}) + BJ_n(\beta \bar{r})] \cos(n\theta) \tag{3.31}$$

$$\begin{aligned}
\frac{1}{\bar{r}^2} \frac{\partial^2 \bar{w}(\bar{r}, \theta)}{\partial \theta^2} \bigg|_{\bar{r}=1} &= -\frac{n^2}{1^2} [AJ_n(\alpha) + BJ_n(\beta)] \cos(n\theta) \\
&= n^2 [AJ_n(\alpha) + BJ_n(\beta)] \cos(n\theta)
\end{aligned} \tag{3.32}$$

Substituting equations (3.23), (3.27), (3.28) and (3.32) into equation (3.18) gives the following

$$\begin{aligned}
&\left[\frac{\alpha^2}{4} P_{88} + \frac{\alpha}{2} (\nu + R_{11}) P_{77} - \left(\frac{\alpha^2}{2} + m^2 \right) J_n(\alpha) \right] A + \\
&\left[\frac{\beta^2}{4} P_{88}' + \frac{\beta}{2} (\nu + R_{11}) P_{77}' - \left(\frac{\beta^2}{2} + m^2 \right) J_n(\beta) \right] B = 0
\end{aligned} \tag{3.33}$$

where $P_{77} = J_{n-1}(\alpha) - J_{n+1}(\alpha)$; $P_{77}' = J_{n-1}(\beta) - J_{n+1}(\beta)$; $P_{88} = J_{n-2}(\alpha) + J_{n+2}(\alpha)$; $P_{88}' = J_{n-2}(\beta) + J_{n+2}(\beta)$

Boundary conditions when the outer edges are elastically restrained against translation.

From equations (3.6) and (3.20) yields the following

$$\frac{\partial}{\partial \bar{r}} \nabla^2 \bar{w}(\bar{r}, \theta) = \frac{\partial}{\partial \bar{r}} \left[\frac{\partial^2 \bar{w}(\bar{r}, \theta)}{\partial \bar{r}^2} + \frac{1}{\bar{r}^2} \frac{\partial^2 \bar{w}(\bar{r}, \theta)}{\partial \theta^2} + \frac{1}{\bar{r}} \frac{\partial \bar{w}(\bar{r}, \theta)}{\partial \bar{r}} \right] \tag{3.34}$$

$$\frac{\partial}{\partial \bar{r}} \left[\frac{\partial^2 \bar{w}(\bar{r}, \theta)}{\partial \bar{r}^2} \right] = \frac{\partial}{\partial \bar{r}} \left\{ \frac{\alpha^2}{4} [J_{n-2}(\alpha \bar{r}) + J_{n+2}(\alpha \bar{r}) - 2J_n(\alpha \bar{r})] A + \frac{\beta^2}{4} [(J_{n-2}(\beta \bar{r}) + J_{n+2}(\beta \bar{r}) - 2J_n(\beta \bar{r})) B] \right\} \cos(n\theta)$$

$$\begin{aligned}
&= \left\{ \frac{\alpha^3}{8} [(J_{n-3}(\alpha\bar{r}) - J_{n-1}(\alpha\bar{r})) + (J_{n+1}(\alpha\bar{r}) - J_{n+3}(\alpha\bar{r})) - 2(J_{n-1}(\alpha\bar{r}) - J_{n+1}(\alpha\bar{r}))]A + \right. \\
&\quad \left. \frac{\beta^3}{8} [(J_{n-3}(\beta\bar{r}) - J_{n-1}(\beta\bar{r})) + (J_{n+1}(\beta\bar{r}) - J_{n+3}(\beta\bar{r})) - 2(J_{n-1}(\beta\bar{r}) - J_{n+1}(\beta\bar{r}))]B \right\} \cos(n\theta) \\
&= \left\{ \frac{\alpha^3}{8} [(J_{n-3}(\alpha\bar{r}) - J_{n+3}(\alpha\bar{r})) - 3(J_{n-1}(\alpha\bar{r}) - J_{n+1}(\alpha\bar{r}))]A + \right. \\
&\quad \left. \frac{\beta^3}{8} [(J_{n-3}(\beta\bar{r}) - J_{n+3}(\beta\bar{r})) - 3(J_{n-1}(\beta\bar{r}) - J_{n+1}(\beta\bar{r}))]B \right\} \cos(n\theta) \tag{3.35}
\end{aligned}$$

$$\frac{\partial}{\partial \bar{r}} \left[\frac{\partial^2 w(\bar{r}, \theta)}{\partial \bar{r}^2} \right]_{\bar{r}=1} = \left\{ \frac{\alpha^3}{8} [(J_{n-3}(\alpha) - J_{n+3}(\alpha)) - 3(J_{n-1}(\alpha) - J_{n+1}(\alpha))]A + \right. \tag{3.36}$$

$$\left. \frac{\beta^3}{8} [(J_{n-3}(\beta) - J_{n+3}(\beta)) - 3(J_{n-1}(\beta) - J_{n+1}(\beta))]B \right\} \cos(n\theta)
= \left\{ \frac{\alpha^3}{8} [P_{99} - 3P_{77}]A + \frac{\beta^3}{8} [P_{99}' - 3P_{77}']B \right\} \cos(n\theta) \tag{3.37}$$

Where $P_{99} = (J_{n-3}(\alpha) - J_{n+3}(\alpha))$; $P_{77} = (J_{n-1}(\alpha) - J_{n+1}(\alpha))$

$$P_{99}' = (J_{n-3}(\beta) - J_{n+3}(\beta)); P_{77}' = (J_{n-1}(\beta) - J_{n+1}(\beta))$$

$$\frac{\partial}{\partial \bar{r}} \left[\frac{1}{\bar{r}^2} \frac{\partial^2 w(\bar{r}, \theta)}{\partial \theta^2} \right] = \frac{1}{\bar{r}^2} \frac{\partial}{\partial \bar{r}} \left[\frac{\partial^2 w(\bar{r}, \theta)}{\partial \theta^2} \right] - \frac{2}{\bar{r}^3} \frac{\partial^2 w(\bar{r}, \theta)}{\partial \theta^2} \tag{3.38}$$

$$\begin{aligned}
&= \frac{1}{\bar{r}^2} \left\{ -n^2 \left\{ \frac{\alpha}{2} [J_{n-1}(\alpha\bar{r}) - J_{n+1}(\alpha\bar{r})]A + \frac{\beta}{2} [J_{n-1}(\beta\bar{r}) - J_{n+1}(\beta\bar{r})]B \right\} \cos(n\theta) \right\} - \\
&\quad \frac{2}{\bar{r}^3} \left\{ -n^2 [AJ_n(\alpha\bar{r}) + BJ_n(\beta\bar{r})] \cos(n\theta) \right\}
\end{aligned}$$

$$\begin{aligned}
\frac{\partial}{\partial \bar{r}} \left[\frac{1}{\bar{r}^2} \frac{\partial^2 w(\bar{r}, \theta)}{\partial \theta^2} \right]_{\bar{r}=1} &= \frac{1}{1^2} \left\{ -n^2 \left\{ \frac{\alpha}{2} [J_{n-1}(\alpha) - J_{n+1}(\alpha)]A + \frac{\beta}{2} [J_{n-1}(\beta) - J_{n+1}(\beta)]B \right\} \cos(n\theta) \right\} - \\
&\quad \frac{2}{1^3} \left\{ -n^2 [AJ_n(\alpha) + BJ_n(\beta)] \cos(n\theta) \right\} \\
&= -n^2 \left\{ \frac{\alpha}{2} [P_{77}]A + \frac{\beta}{2} [P_{77}']B \right\} \cos(n\theta) + 2n^2 \{J_n(\alpha)A + J_n(\beta)B\} \cos(n\theta) \tag{3.39}
\end{aligned}$$

$$\frac{\partial}{\partial \bar{r}} \left[\frac{1}{\bar{r}} \frac{\partial w(\bar{r}, \theta)}{\partial \bar{r}} \right] = \frac{1}{\bar{r}} \frac{\partial}{\partial \bar{r}} \left[\frac{\partial w(\bar{r}, \theta)}{\partial \bar{r}} \right] + \frac{\partial w(\bar{r}, \theta)}{\partial \bar{r}} \frac{\partial}{\partial \bar{r}} \left[\frac{1}{\bar{r}} \right] = \frac{1}{\bar{r}} \frac{\partial^2 w(\bar{r}, \theta)}{\partial \bar{r}^2} - \frac{1}{\bar{r}^2} \frac{\partial w(\bar{r}, \theta)}{\partial \bar{r}} \tag{3.40}$$

$$\begin{aligned}
&= \frac{1}{\bar{r}} \left\{ \frac{\alpha^2}{4} [J_{n-2}(\alpha\bar{r}) + J_{n+2}(\alpha\bar{r}) - 2J_n(\alpha\bar{r})]A + \frac{\beta^2}{4} [(J_{n-2}(\beta\bar{r}) + J_{n+2}(\beta\bar{r}) - 2J_n(\beta\bar{r}))]B \right\} \cos(n\theta) \\
&\quad - \frac{1}{\bar{r}^2} \left\{ \frac{\alpha}{2} [J_{n-1}(\alpha\bar{r}) - J_{n+1}(\alpha\bar{r})]A + \frac{\beta}{2} [J_{n-1}(\beta\bar{r}) - J_{n+1}(\beta\bar{r})]B \right\} \cos(n\theta)
\end{aligned}$$

$$\begin{aligned}
& \frac{\partial}{\partial \bar{r}} \left[\frac{1}{\bar{r}} \frac{\partial w(\bar{r}, \theta)}{\partial \bar{r}} \right]_{\bar{r}=1} = \\
& = \frac{1}{1} \left\{ \frac{\alpha^2}{4} [J_{n-2}(\alpha) + J_{n+2}(\alpha) - 2J_n(\alpha)]A + \frac{\beta^2}{4} [(J_{n-2}(\beta) + J_{n+2}(\beta) - 2J_n(\beta))]B \right\} \cos(n\theta) \\
& - \frac{1}{1^2} \left\{ \frac{\alpha}{2} [J_{n-1}(\alpha) - J_{n+1}(\alpha)]A + \frac{\beta}{2} [J_{n-1}(\beta) - J_{n+1}(\beta)]B \right\} \cos(n\theta) \\
& = \left\{ \frac{\alpha^2}{4} [P_{88} - 2J_n(\alpha)]A + \frac{\beta^2}{4} [P_{88}' - 2J_n(\beta)]B \right\} \cos(n\theta) - \left\{ \frac{\alpha}{2} [P_{77}]A + \frac{\beta}{2} [P_{77}']B \right\} \cos(n\theta) \quad (3.41)
\end{aligned}$$

$$\begin{aligned}
& \left[\frac{\partial^2 w(\bar{r}, \theta)}{\partial \bar{r} \partial \theta} \right] = \frac{\partial}{\partial \bar{r}} \left[\frac{\partial w(\bar{r}, \theta)}{\partial \theta} \right] = \frac{\partial}{\partial \bar{r}} \{ -n[AJ_n(\alpha \bar{r}) + BJ_n(\beta \bar{r})] \sin(n\theta) \} \\
& = -n \left\{ \frac{\alpha}{2} [J_{n-1}(\alpha \bar{r}) - J_{n+1}(\alpha \bar{r})]A + \frac{\beta}{2} [J_{n-1}(\beta \bar{r}) - J_{n+1}(\beta \bar{r})]B \right\} \sin(n\theta) \quad (3.42)
\end{aligned}$$

$$\frac{1}{\bar{r}^2} \frac{\partial w(\bar{r}, \theta)}{\partial \theta} = \frac{-n}{\bar{r}^2} [AJ_n(\alpha \bar{r}) + BJ_n(\beta \bar{r})] \sin(n\theta) \quad (3.43)$$

$$\begin{aligned}
& \frac{\partial}{\partial \theta} \left[\frac{1}{\bar{r}} \frac{\partial^2 w(\bar{r}, \theta)}{\partial \bar{r} \partial \theta} - \frac{1}{\bar{r}^2} \frac{\partial w(\bar{r}, \theta)}{\partial \theta} \right] \\
& = -\frac{n^2}{\bar{r}} \left\{ \frac{\alpha}{2} [J_{n-1}(\alpha \bar{r}) - J_{n+1}(\alpha \bar{r})]A + \frac{\beta}{2} [J_{n-1}(\beta \bar{r}) - J_{n+1}(\beta \bar{r})]B \right\} \cos(n\theta) + \\
& \frac{n^2}{\bar{r}^2} [AJ_n(\alpha \bar{r}) + BJ_n(\beta \bar{r})] \cos(n\theta)
\end{aligned}$$

The above equation can be written as

$$\begin{aligned}
& (1-\nu) \frac{1}{\bar{r}} \frac{\partial}{\partial \theta} \left[\frac{1}{\bar{r}} \frac{\partial^2 w(\bar{r}, \theta)}{\partial \bar{r} \partial \theta} - \frac{1}{\bar{r}^2} \frac{\partial w(\bar{r}, \theta)}{\partial \theta} \right]_{\bar{r}=1} \\
& = (1-\nu) \frac{1}{1} \left\{ -\frac{n^2}{1} \left\{ \frac{\alpha}{2} [J_{n-1}(\alpha) - J_{n+1}(\alpha)]A + \frac{\beta}{2} [J_{n-1}(\beta) - J_{n+1}(\beta)]B \right\} \cos(n\theta) + \right. \\
& \left. \frac{n^2}{1^2} [AJ_n(\alpha) + BJ_n(\beta)] \cos(n\theta) \right\} \\
& = (1-\nu) \left\{ -n^2 \left[\frac{\alpha}{2} P_{77}A + \frac{\beta}{2} P_{77}'B \right] \cos(n\theta) + n^2 [AJ_n(\alpha) + BJ_n(\beta)] \cos(n\theta) \right\} \quad (3.44)
\end{aligned}$$

Substituting equations (3.37), (3.39), (3.41) and (3.44) into equation (3.20) gives the following

$$\begin{aligned} & \left[\frac{\alpha^3}{8} (P_{99} - 3P_{77}) + \frac{\alpha^2}{4} P_{88} + \frac{\alpha}{2} (n^2(\nu - 2) - 1)P_{77} + \left(n^2(3 - \nu) - \frac{\alpha^2}{2} - T_{11} \right) J_n(\alpha) \right] A + \\ & \left[\frac{\beta^3}{8} (P'_{99} - 3P'_{77}) + \frac{\beta^2}{4} P'_{88} + \frac{\beta}{2} (n^2(\nu - 2) - 1)P'_{77} + \left(n^2(3 - \nu) - \frac{\beta^2}{2} - T_{11} \right) J_n(\beta) \right] B = 0 \end{aligned} \quad (3.45)$$

Where

$$\begin{aligned} P_{77} &= J_{n-1}(\alpha) - J_{n+1}(\alpha); P'_{77} = J_{n-1}(\beta) - J_{n+1}(\beta); P_{88} = J_{n-2}(\alpha) + J_{n+2}(\alpha); \\ P'_{88} &= J_{n-2}(\beta) + J_{n+2}(\beta); P_{99} = J_{n-3}(\alpha) - J_{n+3}(\alpha); P'_{99} = J_{n-3}(\beta) - J_{n+3}(\beta); \end{aligned}$$

Case (ii) If $k = \sqrt{2}\xi$

Boundary conditions when the outer edges are elastically restrained against rotation

From equations (3.9) and (3.18) yields the following expressions

$$\bar{w}(\bar{r}, \theta)_{\bar{r}=1} = (AJ_n(\xi) + BJ_{n+1}(\xi))\cos(n\theta) \quad (3.46)$$

$$\begin{aligned} \frac{\partial w(\bar{r}, \theta)}{\partial \bar{r}} = & \left\{ \frac{\xi}{2} (J_{n-1}(\xi\bar{r}) - J_{n+1}(\xi\bar{r}))A + J_{n+1}(\xi\bar{r})B + \bar{r} \frac{\xi}{2} (J_n(\xi\bar{r}) - J_{n+2}(\xi\bar{r}))B \right\} \cos(n\theta) \end{aligned} \quad (3.47)$$

$$\frac{\partial w(\bar{r}, \theta)}{\partial \bar{r}}_{\bar{r}=1} = \left\{ \frac{\xi}{2} (J_{n-1}(\xi) - J_{n+1}(\xi))A + J_{n+1}(\xi)B + \frac{\xi}{2} (J_n(\xi) - J_{n+2}(\xi))B \right\} \cos(n\theta) \quad (3.48)$$

$$\frac{\partial w(\bar{r}, \theta)}{\partial \bar{r}}_{\bar{r}=1} = \left\{ \frac{\xi}{2} P_{12}A + (J_{n+1}(\xi) + \frac{\xi}{2} P_{12}')B \right\} \cos(n\theta) \quad (3.49)$$

Where $P_{12} = (J_{n-1}(\xi) - J_{n+1}(\xi)); P_{12}' = (J_n(\xi) - J_{n+2}(\xi))$

$$\begin{aligned} \frac{\partial^2 w(\bar{r}, \theta)}{\partial \bar{r}^2} = & \left\{ \frac{\xi^2}{4} [(J_{n-2}(\xi\bar{r}) - J_n(\xi\bar{r})) - (J_n(\xi\bar{r}) - J_{n+2}(\xi\bar{r}))]A + \frac{\xi}{2} (J_n(\xi\bar{r}) - J_{n+2}(\xi\bar{r}))B \right. \\ & \left. + \frac{\xi}{2} (J_n(\xi\bar{r}) - J_{n+2}(\xi\bar{r}))B + \bar{r} \frac{\xi^2}{4} [(J_{n-1}(\xi\bar{r}) - J_{n+1}(\xi\bar{r})) - (J_{n+1}(\xi\bar{r}) - J_{n+3}(\xi\bar{r}))]B \right\} \cos(n\theta) \\ \frac{\partial^2 w(\bar{r}, \theta)}{\partial \bar{r}^2} = & \left\{ \frac{\xi^2}{4} [(J_{n-2}(\xi\bar{r}) + J_{n+2}(\xi\bar{r}) - 2J_n(\xi\bar{r}))]A + \xi (J_n(\xi\bar{r}) - J_{n+2}(\xi\bar{r}))B \right. \\ & \left. + \bar{r} \frac{\xi^2}{4} [(J_{n-1}(\xi\bar{r}) - J_{n+1}(\xi\bar{r})) - (J_{n+1}(\xi\bar{r}) - J_{n+3}(\xi\bar{r}))]B \right\} \cos(n\theta) \end{aligned} \quad (3.50)$$

$$\frac{\partial^2 w(\bar{r}, \theta)}{\partial \bar{r}^2}_{\bar{r}=1} = \left\{ \frac{\xi^2}{4} [(J_{n-2}(\xi) + J_{n+2}(\xi) - 2J_n(\xi))]A + \xi (J_n(\xi) - J_{n+2}(\xi))B \right. \\ \left. + \frac{\xi^2}{4} [(J_{n-1}(\xi) - J_{n+1}(\xi)) - (J_{n+1}(\xi) - J_{n+3}(\xi))]B \right\} \cos(n\theta)$$

$$\begin{aligned}\frac{\partial^2 w(\bar{r}, \theta)}{\partial \bar{r}^2} \bigg|_{\bar{r}=1} &= \left\{ \frac{\xi^2}{4} [P_{13} - 2J_n(\xi)]A + \xi P_{12}' B + \frac{\xi^2}{4} [P_{12} - P_{14}]B \right\} \cos(n\theta) \\ \frac{\partial^2 w(\bar{r}, \theta)}{\partial \bar{r}^2} \bigg|_{\bar{r}=1} &= \left\{ \frac{\xi^2}{4} [P_{13} - 2J_n(\xi)]A + \left[\xi P_{12}' + \frac{\xi^2}{4} [P_{12} - P_{14}] \right] B \right\} \cos(n\theta)\end{aligned}\quad (3.51)$$

Where $P_{13} = J_{n-2}(\xi) + J_{n+2}(\xi)$; $P_{14} = J_{n+1}(\xi) - J_{n+3}(\xi)$

$$\begin{aligned}\frac{1}{\bar{r}} \frac{\partial w(\bar{r}, \theta)}{\partial \bar{r}} \bigg|_{\bar{r}=1} &= \frac{1}{\bar{r}} \left\{ \frac{\xi}{2} (J_{n-1}(\xi\bar{r}) - J_{n+1}(\xi\bar{r}))A + J_{n+1}(\xi\bar{r})B + \bar{r} \frac{\xi}{2} (J_n(\xi\bar{r}) - J_{n+2}(\xi\bar{r}))B \right\} \cos(n\theta) \\ \frac{1}{\bar{r}} \frac{\partial w(\bar{r}, \theta)}{\partial \bar{r}} \bigg|_{\bar{r}=1} &= \frac{1}{\bar{r}} \left\{ \frac{\xi}{2} (J_{n-1}(\xi) - J_{n+1}(\xi))A + J_{n+1}(\xi)B + \frac{\xi}{2} (J_n(\xi) - J_{n+2}(\xi))B \right\} \cos(n\theta) \\ \frac{1}{\bar{r}} \frac{\partial w(\bar{r}, \theta)}{\partial \bar{r}} \bigg|_{\bar{r}=1} &= \left\{ \frac{\xi}{2} P_{12}A + J_{n+1}(\xi)B + \frac{\xi}{2} P_{12}' B \right\} \cos(n\theta) \\ \frac{1}{\bar{r}} \frac{\partial w(\bar{r}, \theta)}{\partial \bar{r}} \bigg|_{\bar{r}=1} &= \left\{ \frac{\xi}{2} P_{12}A + \left[J_{n+1}(\xi) + \frac{\xi}{2} P_{12}' \right] B \right\} \cos(n\theta)\end{aligned}\quad (3.52)$$

$$\begin{aligned}\frac{1}{\bar{r}^2} \frac{\partial^2 w(\bar{r}, \theta)}{\partial \theta^2} &= \frac{1}{\bar{r}^2} \frac{\partial}{\partial \theta} \left\{ -n[J_n(\xi\bar{r})A + \bar{r}J_{n+1}(\xi\bar{r})B] \sin(n\theta) \right\} \\ &= -\frac{n^2}{\bar{r}^2} [J_n(\xi\bar{r})A + \bar{r}J_{n+1}(\xi\bar{r})B] \cos(n\theta) \\ \frac{1}{\bar{r}^2} \frac{\partial^2 w(\bar{r}, \theta)}{\partial \theta^2} \bigg|_{\bar{r}=1} &= -\frac{n^2}{1^2} [J_n(\xi)A + J_{n+1}(\xi)B] \cos(n\theta) = -n^2 [J_n(\xi)A + J_{n+1}(\xi)B] \cos(n\theta)\end{aligned}\quad (3.53)$$

Substituting equations (3.49), (3.51), (3.52), (3.53) into equation (3.18) gives the following

$$\begin{aligned}\left[\frac{\xi^2}{4} P_{13} + \frac{\xi}{2} (\nu + R_{11})P_{12} - \left(\frac{\xi^2}{2} + \nu n^2 \right) J_n(\xi) \right] A_1 + \\ \left[\frac{\xi^2}{4} (P_{12} - P_{14}) + \frac{\xi}{2} (\nu + R_{11} + 2)P_{12}' + (\nu(1 - n^2) + R_{11})J_{n+1}(\xi) \right] B = 0\end{aligned}\quad (3.54)$$

Boundary conditions when the outer edges are elastically restrained against translation

From equations (3.9) and (3.20) yields the following expressions

$$\frac{\partial}{\partial \bar{r}} \nabla^2 \bar{w}(\bar{r}, \theta) = \frac{\partial}{\partial \bar{r}} \left[\frac{\partial^2 w(\bar{r}, \theta)}{\partial \bar{r}^2} + \frac{1}{\bar{r}^2} \frac{\partial^2 w(\bar{r}, \theta)}{\partial \theta^2} + \frac{1}{\bar{r}} \frac{\partial w(\bar{r}, \theta)}{\partial \bar{r}} \right] \quad (3.55)$$

$$\frac{\partial}{\partial \bar{r}} \left[\frac{\partial^2 w(\bar{r}, \theta)}{\partial \bar{r}^2} \right] = \frac{\partial}{\partial \bar{r}} \left\{ \begin{aligned} & \frac{\xi^2}{4} [(J_{n-2}(\xi\bar{r}) + J_{n+2}(\xi\bar{r}) - 2J_n(\xi\bar{r}))A + \xi(J_n(\xi\bar{r}) - J_{n+2}(\xi\bar{r}))B] \\ & + \bar{r} \frac{\xi^2}{4} [(J_{n-1}(\xi\bar{r}) - J_{n+1}(\xi\bar{r})) - (J_{n+1}(\xi\bar{r}) - J_{n+3}(\xi\bar{r}))B] \end{aligned} \right\} \cos(n\theta) \quad (3.56)$$

$$= \left\{ \begin{aligned} & \frac{\xi^3}{8} [(J_{n-3}(\xi\bar{r}) - J_{n-1}(\xi\bar{r})) + (J_{n+1}(\xi\bar{r}) - J_{n+3}(\xi\bar{r})) - 2(J_{n-1}(\xi\bar{r}) - J_{n+1}(\xi\bar{r}))]A + \\ & \frac{\xi^2}{2} [(J_{n-1}(\xi\bar{r}) - J_{n+1}(\xi\bar{r})) - (J_{n+1}(\xi\bar{r}) - J_{n+3}(\xi\bar{r}))]B + \\ & \frac{\xi^2}{4} [(J_{n-1}(\xi\bar{r}) - J_{n+1}(\xi\bar{r})) + (J_{n+3}(\xi\bar{r}) - J_{n+1}(\xi\bar{r}))]B + \\ & + \bar{r} \frac{\xi^3}{8} [(J_{n-2}(\xi\bar{r}) - J_n(\xi\bar{r})) - (J_n(\xi\bar{r}) - J_{n+2}(\xi\bar{r})) + (J_{n+2}(\xi\bar{r}) - J_{n+4}(\xi\bar{r})) - \\ & (J_n(\xi\bar{r}) - J_{n+2}(\xi\bar{r}))]B \end{aligned} \right\} \cos(n\theta) \quad (3.57)$$

$$\begin{aligned} \frac{\partial}{\partial \bar{r}} \left[\frac{\partial^2 w(\bar{r}, \theta)}{\partial \bar{r}^2} \right]_{\bar{r}=1} &= \left\{ \begin{aligned} & \frac{\xi^3}{8} [(J_{n-3}(\xi) - J_{n-1}(\xi)) + (J_{n+1}(\xi) - J_{n+3}(\xi)) - 2(J_{n-1}(\xi) - J_{n+1}(\xi))]A + \\ & \frac{\xi^2}{2} [(J_{n-1}(\xi) - J_{n+1}(\xi)) - (J_{n+1}(\xi) - J_{n+3}(\xi))]B + \\ & \frac{\xi^2}{4} [(J_{n-1}(\xi) - J_{n+1}(\xi)) + (J_{n+3}(\xi) - J_{n+1}(\xi))]B + \\ & + \frac{\xi^3}{8} [(J_{n-2}(\xi) - J_n(\xi)) - (J_n(\xi) - J_{n+2}(\xi)) + (J_{n+2}(\xi) - J_{n+4}(\xi)) - \\ & (J_n(\xi) - J_{n+2}(\xi))]B \end{aligned} \right\} \cos(n\theta) \\ &= \left\{ \begin{aligned} & \frac{\xi^3}{8} [(J_{n-3}(\xi) - J_{n+3}(\xi)) - (J_{n-1}(\xi) - J_{n+1}(\xi)) - 2(J_{n-1}(\xi) - J_{n+1}(\xi))]A + \\ & \frac{\xi^2}{2} [(J_{n-1}(\xi) - J_{n+1}(\xi)) - (J_{n+1}(\xi) - J_{n+3}(\xi))]B + \\ & \frac{\xi^2}{4} [(J_{n-1}(\xi) - J_{n+1}(\xi)) - (J_{n+1}(\xi) - J_{n+3}(\xi))]B + \\ & + \frac{\xi^3}{8} [(J_{n-2}(\xi) - J_{n+4}(\xi)) - 3(J_n(\xi) - J_{n+2}(\xi))]B \end{aligned} \right\} \cos(n\theta) \end{aligned} \quad (3.58)$$

$$\frac{\partial}{\partial \bar{r}} \left[\frac{\partial^2 w(\bar{r}, \theta)}{\partial \bar{r}^2} \right]_{\bar{r}=1} = \left\{ \begin{aligned} & \frac{\xi^3}{8} [P_{15} - P_{12} - 2P_{12}]A + \frac{\xi^2}{2} [P_{12} - P_{14}]B + \\ & \frac{\xi^2}{4} [P_{12} - P_{14}]B + \frac{\xi^3}{8} [P_{16} - 3P_{12}]B \end{aligned} \right\} \cos(n\theta) \quad (3.59)$$

Where $P_{14} = J_{n-1}(\xi) - J_{n+1}(\xi)$; $P_{15} = J_{n-3}(\xi) - J_{n+3}(\xi)$; $P_{16} = J_{n-2}(\xi) - J_{n+4}(\xi)$

$$\frac{\partial}{\partial \bar{r}} \left[\frac{\partial^2 w(\bar{r}, \theta)}{\partial \bar{r}^2} \right]_{\bar{r}=1} = \left\{ \begin{aligned} & \frac{\xi^3}{8} [P_{15} - 3P_{12}]A + \frac{\xi^3}{8} [P_{16} - 3P_{12}]B + \\ & \frac{\xi^2}{4} [P_{12} - P_{14}]B + \frac{\xi^2}{2} [P_{12} - P_{14}]B \end{aligned} \right\} \cos(n\theta) \quad (3.60)$$

$$\frac{\partial}{\partial \bar{r}} \left[\frac{1}{\bar{r}^2} \frac{\partial^2 w(\bar{r}, \theta)}{\partial \theta^2} \right] = \frac{1}{\bar{r}^2} \frac{\partial}{\partial \bar{r}} \left[\frac{\partial^2 w(\bar{r}, \theta)}{\partial \theta^2} \right] - \frac{2}{\bar{r}^3} \frac{\partial^2 w(\bar{r}, \theta)}{\partial \theta^2} \quad (3.61)$$

$$= \frac{1}{\bar{r}^2} \left\{ -n^2 \left\{ \frac{\xi}{2} (J_{n-1}(\xi\bar{r}) - J_{n+1}(\xi\bar{r}))A + J_{n+1}(\xi\bar{r})B + \bar{r} \frac{\xi}{2} (J_n(\xi\bar{r}) - J_{n+2}(\xi\bar{r}))B \right\} \cos(n\theta) \right\} -$$

$$\frac{2}{\bar{r}^3} \left\{ -n^2 [AJ_n(\xi\bar{r}) + B\bar{r}J_{n+1}(\xi\bar{r})] \cos(n\theta) \right\}$$

$$\frac{\partial}{\partial \bar{r}} \left[\frac{1}{\bar{r}^2} \frac{\partial^2 w(\bar{r}, \theta)}{\partial \theta^2} \right]_{\bar{r}=1} =$$

$$= \frac{1}{1^2} \left\{ -n^2 \left\{ \frac{\xi}{2} (J_{n-1}(\xi) - J_{n+1}(\xi))A + J_{n+1}(\xi)B + \frac{\xi}{2} (J_n(\xi) - J_{n+2}(\xi))B \right\} \cos(n\theta) \right\} -$$

$$\frac{2}{1^3} \left\{ -n^2 [AJ_n(\xi) + BJ_{n+1}(\xi)] \cos(n\theta) \right\}$$

$$= \left\{ -n^2 \left\{ \frac{\xi}{2} P_{12}A + J_{n+1}(\xi)B + \frac{\xi}{2} P_{12}B \right\} \cos(n\theta) \right\} + 2n^2 [AJ_n(\xi) + BJ_{n+1}(\xi)] \cos(n\theta) \quad (3.62)$$

$$\frac{\partial}{\partial \bar{r}} \left[\frac{1}{\bar{r}} \frac{\partial w(\bar{r}, \theta)}{\partial \bar{r}} \right] = \frac{1}{\bar{r}} \frac{\partial}{\partial \bar{r}} \left[\frac{\partial w(\bar{r}, \theta)}{\partial \bar{r}} \right] + \frac{\partial w(\bar{r}, \theta)}{\partial \bar{r}} \frac{\partial}{\partial \bar{r}} \left[\frac{1}{\bar{r}} \right] = \frac{1}{\bar{r}} \frac{\partial^2 w(\bar{r}, \theta)}{\partial \bar{r}^2} - \frac{1}{\bar{r}^2} \frac{\partial w(\bar{r}, \theta)}{\partial \bar{r}} \quad (3.63)$$

$$= \frac{1}{\bar{r}} \left\{ \begin{aligned} & \frac{\xi^2}{4} [(J_{n-2}(\xi\bar{r}) + J_{n+2}(\xi\bar{r}) - 2J_n(\xi\bar{r}))A + \xi(J_n(\xi\bar{r}) - J_{n+2}(\xi\bar{r}))B] \\ & + \bar{r} \frac{\xi^2}{4} [(J_{n-1}(\xi\bar{r}) - J_{n+1}(\xi\bar{r})) - (J_{n+1}(\xi\bar{r}) - J_{n+3}(\xi\bar{r}))]B \end{aligned} \right\} \cos(n\theta) -$$

$$\frac{1}{\bar{r}^2} \left\{ \frac{\xi}{2} (J_{n-1}(\xi\bar{r}) - J_{n+1}(\xi\bar{r}))A + J_{n+1}(\xi\bar{r})B + \bar{r} \frac{\xi}{2} (J_n(\xi\bar{r}) - J_{n+2}(\xi\bar{r}))B \right\} \cos(n\theta)$$

$$\frac{\partial}{\partial \bar{r}} \left[\frac{1}{\bar{r}} \frac{\partial w(\bar{r}, \theta)}{\partial \bar{r}} \right]_{\bar{r}=1} =$$

$$\begin{aligned}
&= \frac{1}{1} \left\{ \frac{\xi^2}{4} [(J_{n-2}(\xi) + J_{n+2}(\xi) - 2J_n(\xi))]A + \xi(J_n(\xi) - J_{n+2}(\xi))B \right. \\
&\quad \left. + \frac{\xi^2}{4} [(J_{n-1}(\xi) - J_{n+1}(\xi)) - (J_{n+1}(\xi) - J_{n+3}(\xi))]B \right\} \cos(n\theta) - \\
&\quad \frac{1}{1^2} \left\{ \frac{\xi}{2} (J_{n-1}(\xi) - J_{n+1}(\xi))A + J_{n+1}(\xi)B + \frac{\xi}{2} (J_n(\xi) - J_{n+2}(\xi))B \right\} \cos(n\theta) \\
&= \left\{ \frac{\xi^2}{4} [P_{13} - 2J_n(\xi)]A + \xi P_{12}^1 B + \frac{\xi^2}{4} [P_{12} - P_{14}]B \right\} \cos(n\theta) - \\
&\quad \left\{ \frac{\xi}{2} P_{12} A + (J_{n+1}(\xi) + \frac{\xi}{2} P_{12}^1)B \right\} \cos(n\theta) \\
&= \left\{ -\frac{\xi}{2} P_{12} A - J_{n+1}(\xi)B - \frac{\xi}{2} P_{12}^1 B + \frac{\xi^2}{4} [P_{13} - 2J_n(\xi)]A + \xi P_{12}^1 B + \frac{\xi^2}{4} [P_{12} - P_{14}]B \right\} \cos(n\theta)
\end{aligned} \tag{3.64}$$

$$\left[\frac{\partial^2 w(\bar{r}, \theta)}{\partial \bar{r} \partial \theta} \right] = \frac{\partial}{\partial \bar{r}} \left[\frac{\partial w(\bar{r}, \theta)}{\partial \theta} \right] = \frac{\partial}{\partial \bar{r}} \{ -n[AJ_n(\xi\bar{r}) + B\bar{r}J_{n+1}(\xi\bar{r})] \sin(n\theta) \} \tag{3.65}$$

$$= -n \left\{ \frac{\xi}{2} (J_{n-1}(\xi\bar{r}) - J_{n+1}(\xi\bar{r}))A + J_{n+1}(\xi\bar{r})B + \bar{r} \frac{\xi}{2} (J_n(\xi\bar{r}) - J_{n+2}(\xi\bar{r}))B \right\} \sin(n\theta) \tag{3.66}$$

$$\frac{1}{\bar{r}^2} \frac{\partial w(\bar{r}, \theta)}{\partial \theta} = \frac{-n}{\bar{r}^2} [AJ_n(\alpha\bar{r}) + BJ_n(\beta\bar{r})] \sin(n\theta) \tag{3.67}$$

From equations (3.66) and (3.67) yields the following

$$\begin{aligned}
&\frac{\partial}{\partial \theta} \left[\frac{1}{\bar{r}} \frac{\partial^2 w(\bar{r}, \theta)}{\partial \bar{r} \partial \theta} - \frac{1}{\bar{r}^2} \frac{\partial w(\bar{r}, \theta)}{\partial \theta} \right] \\
&= -\frac{n^2}{\bar{r}} \left\{ \frac{\xi}{2} (J_{n-1}(\xi\bar{r}) - J_{n+1}(\xi\bar{r}))A + J_{n+1}(\xi\bar{r})B + \bar{r} \frac{\xi}{2} (J_n(\xi\bar{r}) - J_{n+2}(\xi\bar{r}))B \right\} \cos(n\theta) + \\
&\quad \frac{n^2}{\bar{r}^2} [AJ_n(\xi\bar{r}) + B\bar{r}J_{n+1}(\xi\bar{r})] \cos(n\theta)
\end{aligned}$$

The above equation can be written as

$$\begin{aligned}
&(1-\nu) \frac{1}{\bar{r}} \frac{\partial}{\partial \theta} \left[\frac{1}{\bar{r}} \frac{\partial^2 w(\bar{r}, \theta)}{\partial \bar{r} \partial \theta} - \frac{1}{\bar{r}^2} \frac{\partial w(\bar{r}, \theta)}{\partial \theta} \right]_{\bar{r}=1} \\
&= (1-\nu) \frac{1}{1} \left\{ -\frac{n^2}{1} \left\{ \frac{\xi}{2} (J_{n-1}(\xi) - J_{n+1}(\xi))A + J_{n+1}(\xi)B + \frac{\xi}{2} (J_n(\xi) - J_{n+2}(\xi))B \right\} \cos(n\theta) + \right. \\
&\quad \left. \frac{n^2}{1^2} [AJ_n(\xi) + BJ_{n+1}(\xi)] \cos(n\theta) \right\} \\
&= (1-\nu) \left\{ -n^2 \left\{ \frac{\xi}{2} P_{12} A + J_{n+1}(\xi)B + \frac{\xi}{2} P_{12}^1 B \right\} \cos(n\theta) + n^2 [AJ_n(\xi) + BJ_{n+1}(\xi)] \cos(n\theta) \right\} \tag{3.68}
\end{aligned}$$

Substituting equations (3.46), (3.60), (3.62), (3.64) and (3.68) into equation (3.20) gives the following

$$\begin{aligned} & \left[\frac{\xi^3}{8} (P_{15} - 3P_{12}) + \frac{\xi^2}{4} P_{13} + \frac{\xi}{2} (n^2(\nu - 2) - 1)P_{12} + \left(n^2(3 - \nu) - \frac{\xi^2}{2} - T_{11} \right) J_n(\xi) \right] A + \\ & \left[\frac{\xi^3}{8} (P_{16} - 3P'_{12}) + \xi^2 (P_{12} - P_{14}) + \frac{\xi}{2} (n^2(\nu - 2) + 1)P'_{12} + (n^2 - 1 - T_{11}) J_{n+1}(\xi) \right] B = 0 \end{aligned} \quad (3.69)$$

where

$$\begin{aligned} P_{12} &= J_{n-1}(\xi) - J_{n+1}(\xi); P'_{12} = J_n(\xi) - J_{n+1}(\xi); P_{13} = J_{n-2}(\xi) + J_{n+2}(\xi); \\ P_{14} &= J_{n+2}(\xi) - J_{n+3}(\xi); P_{15} = J_{n-3}(\xi) - J_{n+3}(\xi); P_{16} = J_{n-2}(\xi) - J_{n+4}(\xi); \end{aligned}$$

Case (iii) If $k < \sqrt{2}\xi$

Boundary conditions when the outer edges are elastically restrained against rotation

From equations (3.11) and (3.18) yields the following expressions

$$\bar{w}(\bar{r}, \theta)_{\bar{r}=1} = (A \operatorname{Re}[J_n(i\delta)] + B \operatorname{Im}[J_n(i\delta)]) \cos(n\theta) \quad (3.70)$$

$$\frac{\partial w(\bar{r}, \theta)}{\partial \bar{r}} = \left\{ \operatorname{Re} \left[(J_{n-1}(i\delta\bar{r}) - J_{n+1}(i\delta\bar{r})) \frac{i\delta}{2} \right] A + \operatorname{Im} \left[(J_{n-1}(i\delta\bar{r}) - J_{n+1}(i\delta\bar{r})) \frac{i\delta}{2} \right] B \right\} \cos(n\theta) \quad (3.71)$$

$$\frac{\partial w(\bar{r}, \theta)}{\partial \bar{r}}_{\bar{r}=1} = \left\{ \operatorname{Re} \left[(J_{n-1}(i\delta) - J_{n+1}(i\delta)) \frac{i\delta}{2} \right] A + \operatorname{Im} \left[(J_{n-1}(i\delta) - J_{n+1}(i\delta)) \frac{i\delta}{2} \right] B \right\} \cos(n\theta) \quad (3.72)$$

$$\frac{\partial w(\bar{r}, \theta)}{\partial \bar{r}}_{\bar{r}=1} = \left\{ \operatorname{Re} \left[(P_{21}) \frac{i\delta}{2} \right] A + \operatorname{Im} \left[(P_{21}) \frac{i\delta}{2} \right] B \right\} \cos(n\theta) \quad (3.73)$$

Where $P_{21} = J_{n-1}(i\delta) - J_{n+1}(i\delta)$;

$$\frac{\partial^2 w(\bar{r}, \theta)}{\partial \bar{r}^2} = \left\{ \begin{aligned} & \operatorname{Re} \left[(J_{n-2}(i\delta\bar{r}) + J_{n+2}(i\delta\bar{r}) - 2J_n(i\delta\bar{r})) \frac{i^2\delta^2}{4} \right] A + \\ & \operatorname{Im} \left[(J_{n-2}(i\delta\bar{r}) + J_{n+2}(i\delta\bar{r}) - 2J_n(i\delta\bar{r})) \frac{i^2\delta^2}{4} \right] B \end{aligned} \right\} \cos(n\theta) \quad (3.74)$$

$$\frac{\partial^2 w(\bar{r}, \theta)}{\partial \bar{r}^2} \bigg|_{\bar{r}=1} = \left\{ \begin{aligned} &\text{Re} \left[(J_{n-2}(i\delta) + J_{n+2}(i\delta) - 2J_n(i\delta)) \frac{i^2 \delta^2}{4} \right] A + \\ &\text{Im} \left[(J_{n-2}(i\delta) + J_{n+2}(i\delta) - 2J_n(i\delta)) \frac{i^2 \delta^2}{4} \right] B \end{aligned} \right\} \cos(n\theta) \quad (3.75)$$

$$\frac{\partial^2 w(\bar{r}, \theta)}{\partial \bar{r}^2} \bigg|_{\bar{r}=1} = \left\{ \text{Re} \left[(P_{31} - 2J_n(i\delta)) \frac{i^2 \delta^2}{4} \right] A + \text{Im} \left[(P_{31} - 2J_n(i\delta)) \frac{i^2 \delta^2}{4} \right] B \right\} \cos(n\theta) \quad (3.76)$$

$$P_{31} = J_{n-2}(i\delta) + J_{n+2}(i\delta);$$

$$\begin{aligned} \frac{1}{\bar{r}} \frac{\partial w(\bar{r}, \theta)}{\partial \bar{r}} &= \frac{1}{\bar{r}} \left\{ \text{Re} \left[(J_{n-1}(i\delta\bar{r}) - J_{n+1}(i\delta\bar{r})) \frac{i\delta}{2} \right] A + \text{Im} \left[(J_{n-1}(i\delta\bar{r}) - J_{n+1}(i\delta\bar{r})) \frac{i\delta}{2} \right] B \right\} \cos(n\theta) \\ \frac{1}{\bar{r}} \frac{\partial w(\bar{r}, \theta)}{\partial \bar{r}} \bigg|_{\bar{r}=1} &= \frac{1}{1} \left\{ \text{Re} \left[(J_{n-1}(i\delta) - J_{n+1}(i\delta)) \frac{i\delta}{2} \right] A + \text{Im} \left[(J_{n-1}(i\delta) - J_{n+1}(i\delta)) \frac{i\delta}{2} \right] B \right\} \cos(n\theta) \\ \frac{1}{\bar{r}} \frac{\partial w(\bar{r}, \theta)}{\partial \bar{r}} \bigg|_{\bar{r}=1} &= \left\{ \text{Re} \left[(P_{21}) \frac{i\delta}{2} \right] A + \text{Im} \left[(P_{21}) \frac{i\delta}{2} \right] B \right\} \cos(n\theta) \end{aligned} \quad (3.77)$$

$$\begin{aligned} \frac{1}{\bar{r}^2} \frac{\partial^2 w(\bar{r}, \theta)}{\partial \theta^2} &= \frac{1}{\bar{r}^2} \frac{\partial}{\partial \theta} \{ -n(A \text{Re}[J_n(i\delta\bar{r})] + B \text{Im}[J_n(i\delta\bar{r})]) \sin(n\theta) \} \\ &= -\frac{n^2}{\bar{r}^2} (A \text{Re}[J_n(i\delta\bar{r})] + B \text{Im}[J_n(i\delta\bar{r})]) \cos(n\theta) \end{aligned}$$

$$\begin{aligned} \frac{1}{\bar{r}^2} \frac{\partial^2 w(\bar{r}, \theta)}{\partial \theta^2} \bigg|_{\bar{r}=1} &= -\frac{n^2}{1^2} (A \text{Re}[J_n(i\delta)] + B \text{Im}[J_n(i\delta)]) \cos(n\theta) \\ &= -n^2 (A \text{Re}[J_n(i\delta)] + B \text{Im}[J_n(i\delta)]) \cos(n\theta) \end{aligned} \quad (3.78)$$

Substituting equations (3.76), (3.77) and (3.78) into equation (3.18) gives the following

$$\begin{aligned} &\left[\text{Re} \left[(P_{31}) \frac{i^2 \delta^2}{4} \right] + (\nu + R_{11}) \text{Re} \left[(P_{21}) \frac{i\delta}{2} \right] + \left(\frac{\delta^2}{2} - \nu n^2 \right) \text{Re}[J_n(i\delta)] \right] A_1 + \\ &\left[\text{Im} \left[(P_{31}) \frac{i^2 \delta^2}{4} \right] + (\nu + R_{11}) \text{Im} \left[(P_{21}) \frac{i\delta}{2} \right] + \left(\frac{\delta^2}{2} - \nu n^2 \right) \text{Im}[J_n(i\delta)] \right] B = 0 \end{aligned} \quad (3.79)$$

Boundary conditions when the outer edges are elastically restrained against translation.

From equations (3.11) and (3.20) yields the following

$$\frac{\partial}{\partial \bar{r}} \nabla^2 \bar{w}(\bar{r}, \theta) = \frac{\partial}{\partial \bar{r}} \left[\frac{\partial^2 w(\bar{r}, \theta)}{\partial \bar{r}^2} + \frac{1}{\bar{r}^2} \frac{\partial^2 w(\bar{r}, \theta)}{\partial \theta^2} + \frac{1}{\bar{r}} \frac{\partial w(\bar{r}, \theta)}{\partial \bar{r}} \right] \quad (3.80)$$

$$\frac{\partial}{\partial \bar{r}} \left[\frac{\partial^2 w(\bar{r}, \theta)}{\partial \bar{r}^2} \right] = \frac{\partial}{\partial \bar{r}} \left\{ \begin{aligned} &\text{Re} \left[\left(J_{n-2}(i\delta\bar{r}) + J_{n+2}(i\delta\bar{r}) - 2J_n(i\delta\bar{r}) \right) \frac{i^2 \delta^2}{4} \right] A + \\ &\text{Im} \left[\left(J_{n-2}(i\delta\bar{r}) + J_{n+2}(i\delta\bar{r}) - 2J_n(i\delta\bar{r}) \right) \frac{i^2 \delta^2}{4} \right] B \end{aligned} \right\} \cos(n\theta) \quad (3.81)$$

$$= \left\{ \begin{aligned} &\text{Re} \left[\left((J_{n-3}(i\delta\bar{r}) - J_{n+3}(i\delta\bar{r})) - 3(J_{n-1}(i\delta\bar{r}) - J_{n+1}(i\delta\bar{r})) \right) \frac{i^3 \delta^3}{8} \right] A + \\ &\text{Im} \left[\left((J_{n-3}(i\delta\bar{r}) - J_{n+3}(i\delta\bar{r})) - 3(J_{n-1}(i\delta\bar{r}) - J_{n+1}(i\delta\bar{r})) \right) \frac{i^3 \delta^3}{8} \right] B \end{aligned} \right\} \cos(n\theta) \quad (3.82)$$

$$\begin{aligned} \frac{\partial}{\partial \bar{r}} \left[\frac{\partial^2 w(\bar{r}, \theta)}{\partial \bar{r}^2} \right]_{\bar{r}=1} &= \\ \left\{ \begin{aligned} &\text{Re} \left[\left((J_{n-3}(i\delta) - J_{n+3}(i\delta)) - 3(J_{n-1}(i\delta) - J_{n+1}(i\delta)) \right) \frac{i^3 \delta^3}{8} \right] A + \\ &\text{Im} \left[\left((J_{n-3}(i\delta) - J_{n+3}(i\delta)) - 3(J_{n-1}(i\delta) - J_{n+1}(i\delta)) \right) \frac{i^3 \delta^3}{8} \right] B \end{aligned} \right\} \cos(n\theta) \end{aligned}$$

$$\frac{\partial}{\partial \bar{r}} \left[\frac{\partial^2 w(\bar{r}, \theta)}{\partial \bar{r}^2} \right]_{\bar{r}=1} = \left\{ \text{Re} \left[(P_{41} - 3P_{21}) \frac{i^3 \delta^3}{8} \right] A + \text{Im} \left[(P_{41} - 3P_{21}) \frac{i^3 \delta^3}{8} \right] B \right\} \cos(n\theta) \quad (3.83)$$

where $P_{41} = J_{n-3}(i\delta) - J_{n+3}(i\delta)$;

$$\frac{\partial}{\partial \bar{r}} \left[\frac{1}{\bar{r}^2} \frac{\partial^2 w(\bar{r}, \theta)}{\partial \theta^2} \right] = \frac{1}{\bar{r}^2} \frac{\partial}{\partial \bar{r}} \left[\frac{\partial^2 w(\bar{r}, \theta)}{\partial \theta^2} \right] - \frac{2}{\bar{r}^3} \frac{\partial^2 w(\bar{r}, \theta)}{\partial \theta^2} \quad (3.84)$$

$$\begin{aligned} &= \frac{1}{\bar{r}^2} \frac{\partial}{\partial \bar{r}} \left\{ -n^2 \{ A \text{Re}[J_n(i\delta\bar{r})] + B \text{Im}[J_n(i\delta\bar{r})] \} \cos(n\theta) \right\} - \\ &\frac{2}{\bar{r}^3} \left\{ -n^2 \{ A \text{Re}[J_n(i\delta\bar{r})] + B \text{Im}[J_n(i\delta\bar{r})] \} \cos(n\theta) \right\} \\ &= \frac{-n^2}{\bar{r}^2} \left\{ \text{Re} \left[(J_{n-1}(i\delta\bar{r}) - J_{n+1}(i\delta\bar{r})) \frac{i\delta}{2} \right] A + \text{Im} \left[(J_{n-1}(i\delta\bar{r}) - J_{n+1}(i\delta\bar{r})) \frac{i\delta}{2} \right] B \right\} \cos(n\theta) - \\ &\frac{2}{\bar{r}^3} \left\{ -n^2 \{ A \text{Re}[J_n(i\delta\bar{r})] + B \text{Im}[J_n(i\delta\bar{r})] \} \cos(n\theta) \right\} \end{aligned}$$

$$\begin{aligned}
& \frac{\partial}{\partial \bar{r}} \left[\frac{1}{\bar{r}^2} \frac{\partial^2 w(\bar{r}, \theta)}{\partial \theta^2} \right]_{\bar{r}=1} = \\
& \frac{-n^2}{1^2} \left\{ \operatorname{Re} \left[(J_{n-1}(i\delta) - J_{n+1}(i\delta)) \frac{i\delta}{2} \right] A + \operatorname{Im} \left[(J_{n-1}(i\delta) - J_{n+1}(i\delta)) \frac{i\delta}{2} \right] B \right\} \cos(n\theta) - \\
& \frac{2}{1^3} \left\{ -n^2 \{ A \operatorname{Re}[J_n(i\delta)] + B \operatorname{Im}[J_n(i\delta)] \} \cos(n\theta) \right\} \\
& = \frac{-n^2}{1^2} \left\{ \operatorname{Re} \left[(J_{n-1}(i\delta) - J_{n+1}(i\delta)) \frac{i\delta}{2} \right] A + \operatorname{Im} \left[(J_{n-1}(i\delta) - J_{n+1}(i\delta)) \frac{i\delta}{2} \right] B \right\} \cos(n\theta) - \\
& \frac{2}{1^3} \left\{ -n^2 \{ A \operatorname{Re}[J_n(i\delta)] + B \operatorname{Im}[J_n(i\delta)] \} \cos(n\theta) \right\} \\
& = -n^2 \left\{ \operatorname{Re} \left[(J_{n-1}(i\delta) - J_{n+1}(i\delta)) \frac{i\delta}{2} \right] A + \operatorname{Im} \left[(J_{n-1}(i\delta) - J_{n+1}(i\delta)) \frac{i\delta}{2} \right] B \right\} \cos(n\theta) - \\
& 2 \left\{ -n^2 \{ A \operatorname{Re}[J_n(i\delta)] + B \operatorname{Im}[J_n(i\delta)] \} \cos(n\theta) \right\} \\
& = -n^2 \left\{ \operatorname{Re} \left[(J_{n-1}(i\delta) - J_{n+1}(i\delta)) \frac{i\delta}{2} \right] A + \operatorname{Im} \left[(J_{n-1}(i\delta) - J_{n+1}(i\delta)) \frac{i\delta}{2} \right] B \right\} \cos(n\theta) + \\
& 2n^2 \{ A \operatorname{Re}[J_n(i\delta)] + B \operatorname{Im}[J_n(i\delta)] \} \cos(n\theta) \\
& = -n^2 \left\{ \operatorname{Re} \left[(P_{21}) \frac{i\delta}{2} \right] A + \operatorname{Im} \left[(P_{21}) \frac{i\delta}{2} \right] B \right\} \cos(n\theta) + 2n^2 \{ A \operatorname{Re}[J_n(i\delta)] + B \operatorname{Im}[J_n(i\delta)] \} \cos(n\theta)
\end{aligned} \tag{3.85}$$

$$\begin{aligned}
& \frac{\partial}{\partial \bar{r}} \left[\frac{1}{\bar{r}} \frac{\partial w(\bar{r}, \theta)}{\partial \bar{r}} \right] = \frac{1}{\bar{r}} \frac{\partial}{\partial \bar{r}} \left[\frac{\partial w(\bar{r}, \theta)}{\partial \bar{r}} \right] + \frac{\partial w(\bar{r}, \theta)}{\partial \bar{r}} \frac{\partial}{\partial \bar{r}} \left[\frac{1}{\bar{r}} \right] = \frac{1}{\bar{r}} \frac{\partial^2 w(\bar{r}, \theta)}{\partial \bar{r}^2} - \frac{1}{\bar{r}^2} \frac{\partial w(\bar{r}, \theta)}{\partial \bar{r}} \\
& = \frac{1}{\bar{r}} \left\{ \operatorname{Re} \left[(J_{n-2}(i\delta\bar{r}) + J_{n+2}(i\delta\bar{r}) - 2J_n(i\delta\bar{r})) \frac{i^2 \delta^2}{4} \right] A + \right. \\
& \left. \operatorname{Im} \left[(J_{n-2}(i\delta\bar{r}) + J_{n+2}(i\delta\bar{r}) - 2J_n(i\delta\bar{r})) \frac{i^2 \delta^2}{4} \right] B \right\} \cos(n\theta) - \\
& \frac{1}{\bar{r}^2} \left\{ \operatorname{Re} \left[(J_{n-1}(i\delta\bar{r}) - J_{n+1}(i\delta\bar{r})) \frac{i\delta}{2} \right] A + \operatorname{Im} \left[(J_{n-1}(i\delta\bar{r}) - J_{n+1}(i\delta\bar{r})) \frac{i\delta}{2} \right] B \right\} \cos(n\theta) \\
& \frac{\partial}{\partial \bar{r}} \left[\frac{1}{\bar{r}} \frac{\partial w(\bar{r}, \theta)}{\partial \bar{r}} \right]_{\bar{r}=1} =
\end{aligned} \tag{3.86}$$

$$\begin{aligned}
&= \frac{1}{1} \left\{ \text{Re} \left[\left(J_{n-2}(i\delta) + J_{n+2}(i\delta) - 2J_n(i\delta) \right) \frac{i^2 \delta^2}{4} \right] A + \text{Im} \left[\left(J_{n-2}(i\delta) + J_{n+2}(i\delta) - 2J_n(i\delta) \right) \frac{i^2 \delta^2}{4} \right] B \right\} \cos(n\theta) - \\
&\frac{1}{1^2} \left\{ \text{Re} \left[\left(J_{n-1}(i\delta) - J_{n+1}(i\delta) \right) \frac{i\delta}{2} \right] A + \text{Im} \left[\left(J_{n-1}(i\delta) - J_{n+1}(i\delta) \right) \frac{i\delta}{2} \right] B \right\} \cos(n\theta) \\
&= \left\{ \text{Re} \left[\left(P_{31} - 2J_n(i\delta) \right) \frac{i^2 \delta^2}{4} \right] A + \text{Im} \left[\left(P_{31} - 2J_n(i\delta) \right) \frac{i^2 \delta^2}{4} \right] B \right\} \cos(n\theta) - \\
&\left\{ \text{Re} \left[\left(P_{21} \right) \frac{i\delta}{2} \right] A + \text{Im} \left[\left(P_{21} \right) \frac{i\delta}{2} \right] B \right\} \cos(n\theta)
\end{aligned} \tag{3.87}$$

$$\left[\frac{\partial^2 w(\bar{r}, \theta)}{\partial \bar{r} \partial \theta} \right] = \frac{\partial}{\partial \bar{r}} \left[\frac{\partial w(\bar{r}, \theta)}{\partial \theta} \right] = \frac{\partial}{\partial \bar{r}} \left\{ -n(A \text{Re}[J_n(i\delta\bar{r})] + B \text{Im}[J_n(i\delta\bar{r})]) \sin(n\theta) \right\} \tag{3.88}$$

$$= -n \left\{ \text{Re} \left[\left(J_{n-1}(i\delta\bar{r}) - J_{n+1}(i\delta\bar{r}) \right) \frac{i\delta}{2} \right] A + \text{Im} \left[\left(J_{n-1}(i\delta\bar{r}) - J_{n+1}(i\delta\bar{r}) \right) \frac{i\delta}{2} \right] B \right\} \sin(n\theta) \tag{3.89}$$

$$\frac{1}{\bar{r}^2} \frac{\partial w(\bar{r}, \theta)}{\partial \theta} = \frac{-n}{\bar{r}^2} (A \text{Re}[J_n(i\delta\bar{r})] + B \text{Im}[J_n(i\delta\bar{r})]) \sin(n\theta) \tag{3.90}$$

From equations (3.89) and (3.90) yields the following

$$\begin{aligned}
&\frac{\partial}{\partial \theta} \left[\frac{1}{\bar{r}} \frac{\partial^2 w(\bar{r}, \theta)}{\partial \bar{r} \partial \theta} - \frac{1}{\bar{r}^2} \frac{\partial w(\bar{r}, \theta)}{\partial \theta} \right] \\
&= -\frac{n^2}{\bar{r}} \left\{ \text{Re} \left[\left(J_{n-1}(i\delta\bar{r}) - J_{n+1}(i\delta\bar{r}) \right) \frac{i\delta}{2} \right] A + \text{Im} \left[\left(J_{n-1}(i\delta\bar{r}) - J_{n+1}(i\delta\bar{r}) \right) \frac{i\delta}{2} \right] B \right\} \cos(n\theta) + \\
&\frac{n^2}{\bar{r}^2} (A \text{Re}[J_n(i\delta\bar{r})] + B \text{Im}[J_n(i\delta\bar{r})]) \cos(n\theta)
\end{aligned} \tag{3.91}$$

Equation (3.91) can be written as

$$\begin{aligned}
&(1-\nu) \frac{1}{\bar{r}} \frac{\partial}{\partial \theta} \left[\frac{1}{\bar{r}} \frac{\partial^2 w(\bar{r}, \theta)}{\partial \bar{r} \partial \theta} - \frac{1}{\bar{r}^2} \frac{\partial w(\bar{r}, \theta)}{\partial \theta} \right]_{\bar{r}=1} \\
&= (1-\nu) \frac{1}{1} \left\{ -\frac{n^2}{1} \left\{ \text{Re} \left[\left(J_{n-1}(i\delta) - J_{n+1}(i\delta) \right) \frac{i\delta}{2} \right] A + \text{Im} \left[\left(J_{n-1}(i\delta) - J_{n+1}(i\delta) \right) \frac{i\delta}{2} \right] B \right\} \cos(n\theta) + \right. \\
&\left. \frac{n^2}{1^2} (A \text{Re}[J_n(i\delta)] + B \text{Im}[J_n(i\delta)]) \cos(n\theta) \right\} \\
&= (1-\nu) \left\{ -n^2 \left\{ \text{Re} \left[\left(P_{12} \right) \frac{i\delta}{2} \right] A + \text{Im} \left[\left(P_{12} \right) \frac{i\delta}{2} \right] B \right\} \cos(n\theta) + \right. \\
&\left. n^2 (A \text{Re}[J_n(i\delta)] + B \text{Im}[J_n(i\delta)]) \cos(n\theta) \right\}
\end{aligned} \tag{3.92}$$

Substituting equations (3.70), (3.83), (3.85), (3.87) and (3.92) into equation (3.20) gives the following

$$\begin{aligned} & \left[\operatorname{Re} \left[(P_{41}) \frac{i^3 \delta^3}{8} \right] + \operatorname{Re} \left[(P_{31}) \frac{i^2 \delta^2}{4} \right] + \frac{i\delta}{2} \left(\frac{3\delta^2}{4} + n^2(\nu-2) - 1 \right) \operatorname{Re}[P_{21}] + \left(\frac{\delta^2}{2} + n^2(3-\nu) - T_{11} \right) \operatorname{Re}[J_n(i\delta)] \right] A + \\ & \left[\operatorname{Im} \left[(P_{41}) \frac{i^3 \delta^3}{8} \right] + \operatorname{Im} \left[(P_{31}) \frac{i^2 \delta^2}{4} \right] + \frac{i\delta}{2} \left(\frac{3\delta^2}{4} + n^2(\nu-2) - 1 \right) \operatorname{Im}[P_{21}] + \left(\frac{\delta^2}{2} + n^2(3-\nu) - T_{11} \right) \operatorname{Im}[J_n(i\delta)] \right] B = 0 \end{aligned} \quad (3.93)$$

The above equations listed in above three cases are used for axisymmetric buckling ($n = 0$) and for asymmetric buckling ($n \neq 0$), A & B are constants, and $J_n(.)$ are the Bessel functions of the first kind of order n .

3.4 Solution

For the given values of n, ν, R_{11}, T_{11} & ξ the above set of equations, gives an exact characteristic equation for non-trivial solutions of the coefficients A & B . For non-trivial solution, the determinant of $[A]_{2 \times 2}$ must vanish. The value of k is calculated from the characteristic equation by a simple root search method. Using Mathematica, computer software with symbolic capabilities, the problem is solved.

3.5 Results and Discussions

The buckling loads are calculated for various rotational spring stiffness parameter, translational spring stiffness parameter and foundation stiffness parameters of an elastic foundation. Poisson's ratio used in these calculations is 0.3.

Buckling load parameters for axisymmetric and asymmetric modes and for various rotational, translational and foundation parameters are presented in Table. 3.2. Fig. 3.2 shows the variations of buckling load parameter k , with respect to the foundation parameter, ξ for various values of rotational and translational spring stiffness parameters, i.e., $R_{11} = T_{11} = 1$. It is observed from the Fig. 3.2 the curve is composed of two segments. This is due to the

switching of buckling modes. Fig. 3.2 shows buckling load parameter, k , rises monotonically with the foundation stiffness parameter, ξ . It is observed that the symmetric (*i.e.*, $n = 0$) solution weaves with the asymmetric solution (*i.e.*, $n = 1$). When foundation stiffness is zero, the plate buckles axisymmetrically with $k = 2.52051$. When ξ increased beyond 4.67891 ($k = 7.35415$), the asymmetric mode $n = 1$ gives the correct lower buckling load. This persists until $\xi = 5.17926$ ($k = 8.022311$) where the $n = 0$ mode again determines the lower buckling load. The next three switches are at $\xi = 10.05204$ ($k = 14.5642$), $\xi = 15.2891$ ($k = 22.4873$) and $\xi = 18.5192$ ($k = 26.962$).

Table 3.1 Buckling (for axisymmetric and asymmetric modes) Load Parameters for various Rotational, Translational and Foundation Parameters (R_{11}, T_{11} & ξ) and $\nu = 0.33$

ξ	$R_{11} = T_{11} = 1$		$R_{11} = T_{11} = 10$		$R_{11} = T_{11} = 100$	
	$n = 0$	$n = 1$	$n = 0$	$n = 1$	$n = 0$	$n = 1$
0	2.52051	2.74951	3.48887	2.74951	3.79365	2.74951
2.5	4.38057	5.10167	4.23479	4.65156	4.39922	5.27624
5	7.78999	7.6852	7.73659	7.34844	7.75413	7.39619
7.5	11.1116	12.4921	10.9502	12.3471	11.6795	10.8835
10	14.4752	14.4927	15.3885	15.1862	15.333	14.4861
12.5	18.8247	17.9778	17.9051	18.5461	18.5706	18.2913
15	22.1629	22.0849	22.0444	22.0627	21.4294	21.9807
17.5	24.9567	25.5571	24.9517	25.5522	26.4594	25.5071
20	29.8829	29.007	29.8341	28.9668	28.8349	28.4275

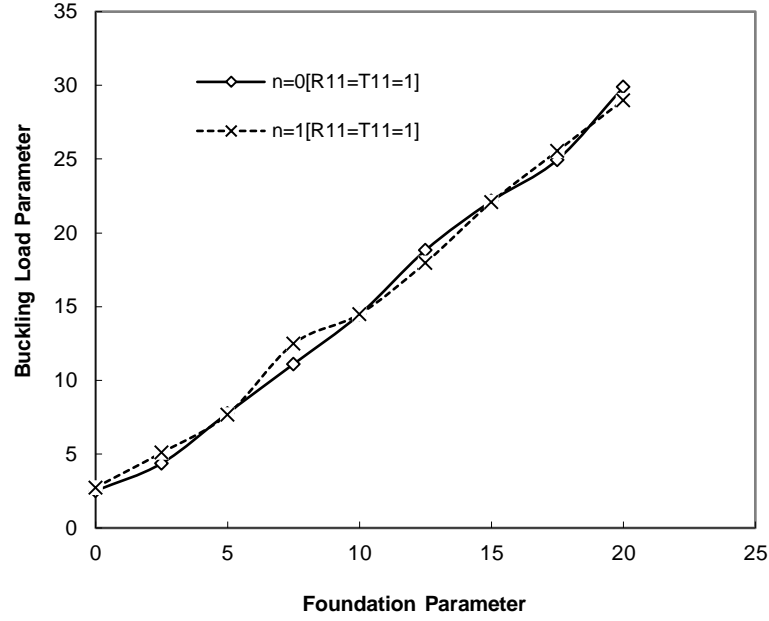


Fig. 3.2 Buckling Load Parameter k , versus foundation Stiffness Parameter ξ , for Rotational and Translational Parameters of $R_{11} = T_{11} = 1$

Fig. 3.3 shows buckling load parameter, k , increases monotonically with the foundation stiffness parameter, ξ . It is observed that the asymmetric (*i.e.*, $n = 1$) solution weaves with the symmetric solution (*i.e.*, $n = 0$). When foundation stiffness is zero, the plate buckles asymmetrically with $k = 2.74951$. When ξ increased beyond 1.60085 ($k = 3.9656$), the symmetric mode $n = 0$ gives the correct lower buckling load. This persists until $\xi = 3.7944$ ($k = 6.05096$) where the $n = 1$ mode again determines the lower buckling load. The next four switches are at $\xi = 5.5486$ ($k = 8.4391$), $\xi = 9.6868$ ($k = 14.8302$), $\xi = 10.596$ ($k = 15.9952$) and $\xi = 18.5240$ ($k = 26.9427$).

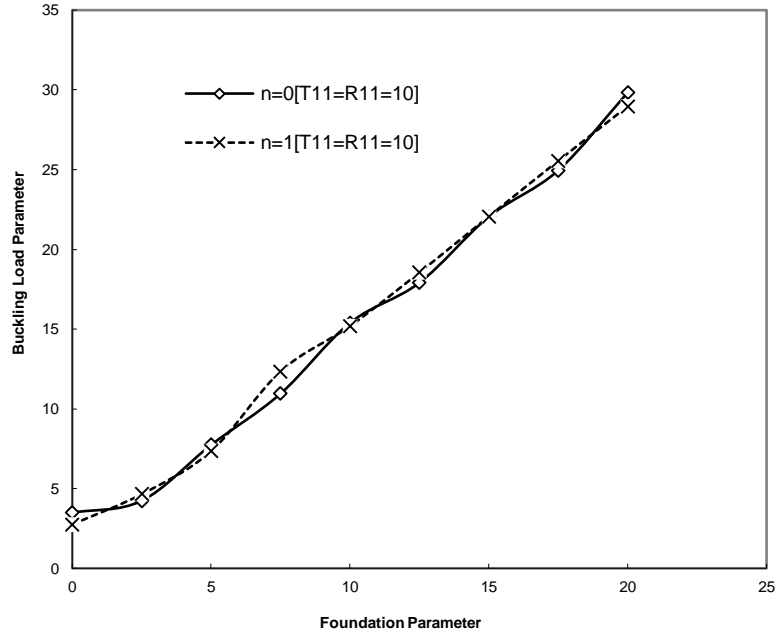


Fig. 3.3 Buckling Load Parameter k , versus foundation Stiffness Parameter ξ , for Rotational and Translational Parameters of $R_{11} = T_{11} = 10$

Fig. 3.4 shows buckling load parameter, k , increases with the foundation stiffness parameter, ξ . It is observed that the asymmetric (*i.e.*, $n = 1$) solution weaves with the symmetric solution (*i.e.*, $n = 0$). When foundation stiffness is zero, the plate buckles asymmetrically with $k = 2.74951$. When ξ increased beyond 1.35405 ($k = 4.118$), the symmetric mode $n = 0$ gives the correct lower buckling load. When ξ increases beyond 4.27350 the $n = 1$ mode again gives the lower buckling load. The next two switches are at $\xi = 13.3435$ ($k = 19.5308$) and $\xi = 15.9176$ ($k = 23.2749$).

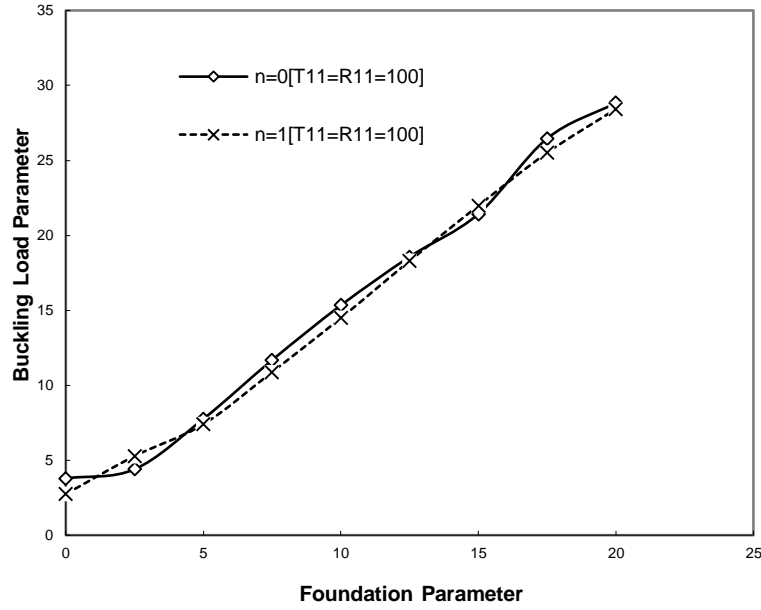


Fig. 3.4 Buckling Load Parameter k , versus foundation Stiffness Parameter ξ , for Rotational and Translational Parameters of $R_{11} = T_{11} = 100$

The results of this kind were scarce in the literature. However, the results are compared with the clamped boundary condition as shown in Fig. 3.5. Table 3.2 shows the comparison of mode switches against those obtained by Wang [11]. Kline and Hancock [9] obtained only the symmetric $n = 0$ curve, thus overestimated the lower buckling load where the asymmetric $n = 1$ mode gives the correct buckling load. The buckling load of a circular plate with elastically restrained edges and resting on elastic foundation is now correctly estimated. This data would be useful in the basic design of embedded circular plates. Also, in this work the characteristic equations are exact, and the solutions can be found to any accuracy and can be used to check numerical or approximate results.

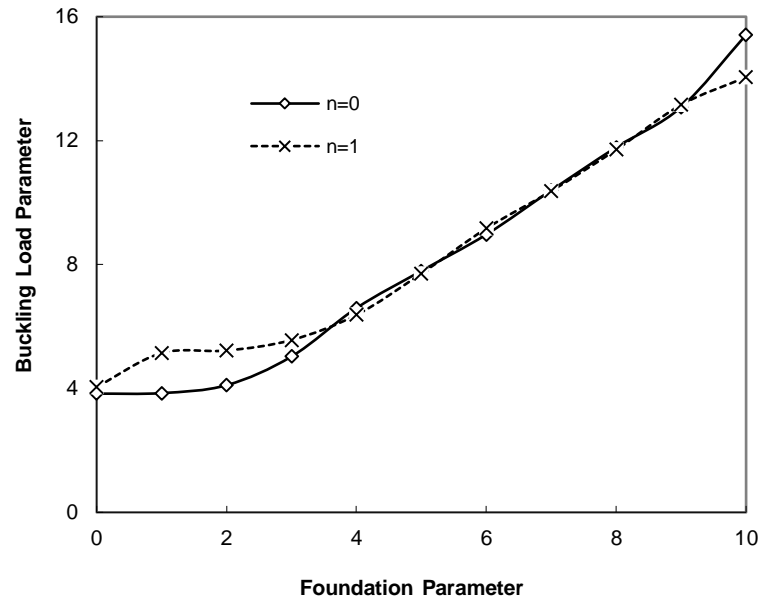


Fig. 3.5 Buckling Load Parameter k , versus foundation Stiffness Parameter ξ , for Clamped boundary condition

Table 3.2 Comparison of Mode Switches with Wang [13] Clamped boundary and Poisson's ratio = 0.3.

	$n = 0$		$n = 1$		$n = 0$		$n = 1$		$n = 0$		$n = 1$	
	ξ	k	ξ	k	ξ	k	ξ	k	ξ	k	ξ	k
Wang [13]	0	3.8317	3.644	6.022	5.185	7.994	6.912	10.265	8.446	12.355	9.059	13.213
Thesis	0	3.8317	3.644	6.022	5.185	7.994	6.912	10.265	8.446	12.355	9.059	13.213

CHAPTER 4

BUCKLING OF CIRCULAR PLATES WITH ELASTICALLY RESTRAINED EDGES AND RESTING ON INTERNAL ELASTIC RING SUPPORT

4.1 Background

In particular, the circular plates with an internal *elastic ring* supports find applications in aeronautical (instrument mounting bases for space vehicles), rocket launching pads, aircrafts and naval vessels (instrument mounting bases). Based on the Kirchhoff's theory, the elastic buckling of thin circular plates has been extensively studied by many authors. However, the previous works considered only the axisymmetric cases, which may not lead to the exact buckling load. Introducing an internal *elastic ring* supports may increase the elastic buckling capacity of in-plane loaded circular plates significantly. Some difficulties were arisen due to complexity and uncertainty of boundary conditions. This uncertainty could be due to the nature of real life applications where the edge of the plate does not fall into the classical boundary conditions. It is an accepted fact that the condition on a periphery often tends to be in between the classical boundary conditions (free, clamped and simply supported) and corresponds more closely to some form of elastic restraints, i.e., rotational and translational restraints (Wang and Wang [3]), Kim and Dickinson [66] and Yamaki [14]). In a recent study, Wang and Wang [67] showed that when the ring support has a small radius, the buckling mode takes the asymmetric form. But they have studied only the circular plate with elastically restrained edge against rotation.

4.2 Problem Definition

Consider a thin circular plate of radius R , uniform thickness h , Young's modulus E , and Poisson's ratio ν and subjected to a uniform in-plane load, N along its boundary, as shown in Fig. 4.1. This circular plate is assumed to be made of linearly elastic, homogeneous and isotropic material and the effects of shear deformation and rotary inertia are neglected. The edge of the circular plate is elastically restrained against rotation, translation and

supported by an internal *elastic ring* support, as shown in Fig. 4.1. The purpose of the present work is to complete the results of the buckling of circular plates with an internal *elastic ring* support and elastically restrained edge against rotation and translation by including the asymmetric modes, thus correctly determining the buckling loads.

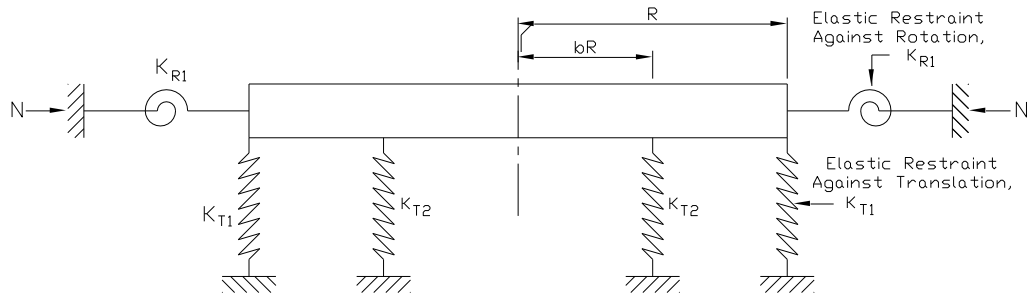


Fig. 4.1. Buckling of a Circular Plate with an Internal *Elastic Ring* Support and Elastically Restrained Edge Against Rotation and Translation

4.3 Analytical Formulation of the Problem

The plate is elastically restrained against rotation and translation at the edge of radius, R and supported on an internal *elastic ring* of smaller radius bR as shown in Fig. 4.1. Let subscript I denote the inner region $0 \leq \bar{r} \leq b$ and the subscript II denote the outer region $b \leq \bar{r} \leq 1$. Here, all lengths are normalized by R . Using classical (Kirchhoff's) plate theory, the following fourth order differential equation for buckling in polar coordinates (r, θ) .

$$D\nabla^4 w + N\nabla^2 w = 0 \quad (4.1)$$

where w is the lateral displacement, N is the uniform compressive load at the edge. After normalizing the lengths by the radius of the plate R , equation (4.1) can be written as

$$D\nabla^4 \bar{w} + k^2 \nabla^2 \bar{w} = 0 \quad (4.2)$$

Where $\nabla^2 = \frac{\partial^2}{\partial \bar{r}^2} + \frac{1}{\bar{r}} \frac{\partial}{\partial \bar{r}} + \frac{1}{\bar{r}^2} \frac{\partial^2}{\partial \theta^2}$ is the Laplace operator in the polar coordinates r and θ .

where \bar{r} is the radial distance normalized by R . After normalization, the inner and outer radius parameters are b and 1 respectively. $\bar{D} = Eh^3/12(1-\nu^2)$ is the flexural rigidity, $\bar{w} = w/R$, is normalized transverse displacement of the plate. $k^2 = R^2 N / \bar{D}$ is non-dimensional load parameter. Suppose there are n nodal diameters. In polar coordinates (r, θ) set

$$\bar{w}(\bar{r}, \theta) = \bar{u}(\bar{r}) \cos(n\theta) \quad (4.3)$$

Considering the boundness at the origin, the general solution (Yamaki [14]) for the two regions is

$$\bar{u}_I(r) = C_1 J_n(k\bar{r}) + C_2 Y_n(k\bar{r}) + C_3 \bar{r}^n + C_4 \begin{Bmatrix} \log \bar{r} \\ \bar{r}^{-n} \end{Bmatrix} \quad (4.4)$$

$$\bar{u}_{II}(r) = C_5 J_n(k\bar{r}) + C_6 \bar{r}^n \quad (4.5)$$

Where top form of the equation (4.4) is used for $n=0$ (Axisymmetric) and the bottom form is used for $n \neq 0$ (Asymmetric), C_1, C_2, C_3, C_4, C_5 & C_6 are constants, $J_n(.)$ & $Y_n(.)$ are the Bessel functions of the first and second kinds of order n , respectively. Substituting equation (4.4) into equation (4.3), gives the following

$$\bar{w}_I(\bar{r}, \theta) = \left[C_1 J_n(k\bar{r}) + C_2 Y_n(k\bar{r}) + C_3 \bar{r}^n + C_4 \begin{Bmatrix} \log \bar{r} \\ \bar{r}^{-n} \end{Bmatrix} \right] \cos(n\theta) \quad (5.6)$$

The boundary conditions at outer region of the circular plate in terms of rotational stiffness (K_{R1}) and translational stiffness (K_{T1}) is given by the following expressions

$$M_r(\bar{r}, \theta) = K_{R1} \frac{\partial \bar{w}_I(\bar{r}, \theta)}{\partial \bar{r}} \quad (4.7)$$

$$V_r(\bar{r}, \theta) = -K_{T1} \bar{w}_I(\bar{r}, \theta) \quad (4.8)$$

The radial moment and the radial Kirchhoff shear at outer edge are defined as follows

$$M_r(\bar{r}, \theta) = -\frac{D}{R^3} \left[\frac{\partial^2 \bar{w}_I(\bar{r}, \theta)}{\partial \bar{r}^2} + \nu \left(\frac{1}{\bar{r}} \frac{\partial \bar{w}_I(\bar{r}, \theta)}{\partial \bar{r}} + \frac{1}{\bar{r}^2} \frac{\partial^2 \bar{w}_I(\bar{r}, \theta)}{\partial \theta^2} \right) \right] \quad (4.9)$$

$$V_r(\bar{r}, \theta) = -\frac{D}{R^3} \left[\frac{\partial}{\partial \bar{r}} \nabla^2 \bar{w}_I(\bar{r}, \theta) + (1-\nu) \frac{1}{\bar{r}} \frac{\partial}{\partial \theta} \left(\frac{1}{\bar{r}} \frac{\partial^2 \bar{w}_I(\bar{r}, \theta)}{\partial \bar{r} \partial \theta} - \frac{1}{\bar{r}^2} \frac{\partial \bar{w}_I(\bar{r}, \theta)}{\partial \theta} \right) \right] \quad (4.10)$$

Equations (4.7) and (4.9) yield the following

$$\left[\frac{\partial^2 \bar{w}_I(\bar{r}, \theta)}{\partial \bar{r}^2} + \nu \left(\frac{1}{\bar{r}} \frac{\partial \bar{w}_I(\bar{r}, \theta)}{\partial \bar{r}} + \frac{1}{\bar{r}^2} \frac{\partial^2 \bar{w}_I(\bar{r}, \theta)}{\partial \theta^2} \right) \right] = -\frac{K_{R1} R^2}{D} \frac{\partial^2 \bar{w}_I(\bar{r}, \theta)}{\partial \bar{r}^2} \quad (4.11)$$

$$\left[\frac{\partial^2 \bar{w}_I(\bar{r}, \theta)}{\partial \bar{r}^2} + \nu \left(\frac{1}{\bar{r}} \frac{\partial \bar{w}_I(\bar{r}, \theta)}{\partial \bar{r}} + \frac{1}{\bar{r}^2} \frac{\partial^2 \bar{w}_I(\bar{r}, \theta)}{\partial \theta^2} \right) \right] = -R_{11} \frac{\partial \bar{w}_I(\bar{r}, \theta)}{\partial \bar{r}} \quad (4.12)$$

From equations (4.8) and (4.10), we get the following

$$\left[\frac{\partial}{\partial \bar{r}} \nabla^2 \bar{w}_I(\bar{r}, \theta) + (1-\nu) \frac{1}{\bar{r}} \frac{\partial}{\partial \theta} \left(\frac{1}{\bar{r}} \frac{\partial^2 \bar{w}_I(\bar{r}, \theta)}{\partial \bar{r} \partial \theta} - \frac{1}{\bar{r}^2} \frac{\partial \bar{w}_I(\bar{r}, \theta)}{\partial \theta} \right) \right] = \frac{K_{T1} R^3}{D} \bar{w}_I(\bar{r}, \theta) \quad (4.13)$$

$$\left[\frac{\partial}{\partial \bar{r}} \nabla^2 \bar{w}_I(\bar{r}, \theta) + (1-\nu) \frac{1}{\bar{r}} \frac{\partial}{\partial \theta} \left(\frac{1}{\bar{r}} \frac{\partial^2 \bar{w}_I(\bar{r}, \theta)}{\partial \bar{r} \partial \theta} - \frac{1}{\bar{r}^2} \frac{\partial \bar{w}_I(\bar{r}, \theta)}{\partial \theta} \right) \right] = T_{11} \bar{w}_I(\bar{r}, \theta) \quad (4.14)$$

$$\text{where } R_{11} = \frac{K_{R1} R^2}{D} \text{ and } T_{11} = \frac{K_{T1} R^3}{D}$$

Apart from the elastically restrained edge against rotation and translation, there is an internal *elastic ring* support constraint and the continuity requirements of slope and curvature at the support, i.e. $\bar{r} = b$

$$\bar{w}_I(b, \theta) = \bar{w}_{II}(b, \theta) \quad (4.15)$$

$$\bar{w}_I'(b, \theta) = \bar{w}_{II}'(b, \theta) \quad (4.16)$$

$$\bar{w}_I''(b, \theta) = \bar{w}_{II}''(b, \theta) \quad (4.17)$$

$$\bar{w}_I'''(b, \theta) = \bar{w}_{II}'''(b, \theta) - T_{22} \bar{w}_{II}(b, \theta) \quad (4.18)$$

where $T_{22} = \frac{K_{T2} R^3}{D}$ is the normalized spring constant, K_{T2} of the translational spring.

Non-trivial solutions to equations (4.12), (4.14), (4.15) - (4.18) are sought. The lowest value of k is the square root of the normalized buckling load.

For **region I**, Plate edges are elastically restrained against rotation and translation

Boundary conditions when the edges are elastically restrained against rotation.

From equations (4.6) and (4.12) we get the following

$$\frac{\partial \bar{w}(\bar{r}, \theta)}{\partial \bar{r}} = \left[\frac{k}{2} [J_{n-1}(k\bar{r}) - J_{n+1}(k\bar{r})] C_1 + \frac{k}{2} [Y_{n-1}(k\bar{r}) - Y_{n+1}(k\bar{r})] C_2 + n\bar{r}^{n-1} C_3 + \left\{ \frac{1}{\bar{r}} \right. \right. \\ \left. \left. - n\bar{r}^{-n-1} \right\} C_4 \right] \cos(n\theta) \quad (4.19)$$

$$\frac{\partial \bar{w}(\bar{r}, \theta)}{\partial \bar{r}} \Big|_{\bar{r}=1} = \left[\frac{k}{2} [J_{n-1}(k) - J_{n+1}(k)] C_1 + \frac{k}{2} [Y_{n-1}(k) - Y_{n+1}(k)] C_2 + n C_3 + \left\{ \frac{1}{-n} \right\} C_4 \right] \cos(n\theta) \quad (4.20)$$

$$\frac{\partial \bar{w}(\bar{r}, \theta)}{\partial \bar{r}} \Big|_{\bar{r}=1} = \left[\frac{k}{2} [P_1] C_1 + \frac{k}{2} [Q_1] C_2 + n C_3 + \left\{ \frac{1}{-n} \right\} C_4 \right] \cos(n\theta) \quad (4.21)$$

where $P_1 = J_{n-1}(k) - J_{n+1}(k)$; $Q_1 = Y_{n-1}(k) - Y_{n+1}(k)$

$$\frac{\partial^2 \bar{w}(\bar{r}, \theta)}{\partial \bar{r}^2} = \left[\frac{k^2}{4} [(J_{n-2}(k\bar{r}) - J_n(k\bar{r})) - (J_n(k\bar{r}) - J_{n+2}(k\bar{r}))] C_1 + \right. \\ \left. \frac{k^2}{4} [(Y_{n-2}(k\bar{r}) - Y_n(k\bar{r})) - (Y_n(k\bar{r}) - Y_{n+2}(k\bar{r}))] C_2 + n(n-1)\bar{r}^{n-2} C_3 + \left\{ -\frac{1}{\bar{r}^2} \right. \right. \\ \left. \left. - \frac{n(n+1)}{\bar{r}^{n-2}} \right\} C_4 \right] \cos(n\theta) \quad (4.22)$$

$$\frac{\partial^2 \bar{w}(\bar{r}, \theta)}{\partial \bar{r}^2} = \left[\frac{k^2}{4} [(J_{n-2}(k\bar{r}) + J_{n+2}(k\bar{r}) - 2J_n(k\bar{r}))] C_1 + \right. \\ \left. \frac{k^2}{4} [(Y_{n-2}(k\bar{r}) + Y_{n+2}(k\bar{r}) - 2Y_n(k\bar{r}))] C_2 + n(n-1)\bar{r}^{n-2} C_3 + \left\{ -\frac{1}{\bar{r}^2} \right. \right. \\ \left. \left. - \frac{n(n+1)}{\bar{r}^{n-2}} \right\} C_4 \right] \cos(n\theta) \quad (4.23)$$

$$\frac{\partial^2 \bar{w}(\bar{r}, \theta)}{\partial \bar{r}^2} \Big|_{\bar{r}=1} = \left[\frac{k^2}{4} [(J_{n-2}(k) + J_{n+2}(k) - 2J_n(k))] C_1 + \right. \\ \left. \frac{k^2}{4} [(Y_{n-2}(k) + Y_{n+2}(k) - 2Y_n(k))] C_2 + n(n-1) C_3 + \left\{ -\frac{1}{n(n+1)} \right\} C_4 \right] \cos(n\theta) \quad (4.24)$$

$$\frac{\partial^2 \bar{w}(\bar{r}, \theta)}{\partial \bar{r}^2} \Big|_{\bar{r}=1} = \left[\frac{k^2}{4} [(P_2 - 2J_n(k))] C_1 + \right. \\ \left. \frac{k^2}{4} [(Q_2 - 2Y_n(k))] C_2 + n(n-1) C_3 + \left\{ -\frac{1}{n(n+1)} \right\} C_4 \right] \cos(n\theta) \quad (4.25)$$

where $P_2 = J_{n-2}(k) + J_{n+2}(k)$; $Q_2 = Y_{n-2}(k) + Y_{n+2}(k)$

$$\frac{1}{\bar{r}} \frac{\partial \bar{w}(\bar{r}, \theta)}{\partial \bar{r}} = \frac{1}{\bar{r}} \left[\frac{k}{2} [J_{n-1}(k\bar{r}) - J_{n+1}(k\bar{r})] C_1 + \frac{k}{2} [Y_{n-1}(k\bar{r}) - Y_{n+1}(k\bar{r})] C_2 + n\bar{r}^{n-1} C_3 \right. \\ \left. + \left\{ \frac{1}{\bar{r}} \right. \right. \\ \left. \left. - n\bar{r}^{-n-1} \right\} C_4 \right] \cos(n\theta) \quad (4.26)$$

$$\frac{1}{\bar{r}} \frac{\partial \bar{w}(\bar{r}, \theta)}{\partial \bar{r}} \bigg|_{\bar{r}=1} = \left[\frac{k}{2} [J_{n-1}(k) - J_{n+1}(k)] C_1 + \frac{k}{2} [Y_{n-1}(k) - Y_{n+1}(k)] C_2 + nC_3 + \left\{ \frac{1}{-n} \right\} C_4 \right] \cos(n\theta) \quad (4.27)$$

$$\frac{1}{\bar{r}} \frac{\partial \bar{w}(\bar{r}, \theta)}{\partial \bar{r}} \bigg|_{\bar{r}=1} = \left[\frac{k}{2} [P_1] C_1 + \frac{k}{2} [Q_1] C_2 + nC_3 + \left\{ \frac{1}{-n} \right\} C_4 \right] \cos(n\theta) \quad (4.28)$$

$$\frac{\partial \bar{w}(\bar{r}, \theta)}{\partial \theta} = -n \left[C_1 J_n(k\bar{r}) + C_2 Y_n(k\bar{r}) + C_3 \bar{r}^n + C_4 \left\{ \frac{\log \bar{r}}{\bar{r}^{-n}} \right\} \right] \sin(n\theta) \quad (4.29)$$

$$\frac{\partial^2 \bar{w}(\bar{r}, \theta)}{\partial \theta^2} = -n^2 \left[C_1 J_n(k\bar{r}) + C_2 Y_n(k\bar{r}) + C_3 \bar{r}^n + C_4 \left\{ \frac{\log \bar{r}}{\bar{r}^{-n}} \right\} \right] \cos(n\theta) \quad (4.30)$$

$$\frac{1}{\bar{r}^2} \frac{\partial^2 \bar{w}(\bar{r}, \theta)}{\partial \theta^2} = -\frac{n^2}{\bar{r}^2} \left[C_1 J_n(k\bar{r}) + C_2 Y_n(k\bar{r}) + C_3 \bar{r}^n + C_4 \left\{ \frac{\log \bar{r}}{\bar{r}^{-n}} \right\} \right] \cos(n\theta) \quad (4.31)$$

$$\frac{1}{\bar{r}^2} \frac{\partial^2 \bar{w}(\bar{r}, \theta)}{\partial \theta^2} \bigg|_{\bar{r}=1} = -n^2 \left[C_1 J_n(k) + C_2 Y_n(k) + C_3 \cdot 1 + C_4 \left\{ \frac{0}{1} \right\} \right] \cos(n\theta) \quad (4.32)$$

Substituting equations (4.21), (4.25), (4.28), (4.32) into equation (4.12) gives the following

$$\left[\frac{k^2}{4} P_2 + \frac{k}{2} (\nu + R_{11}) P_1 - \left(\frac{k^2}{2} + \nu n^2 \right) J_n(k) \right] C_1 + \\ \left[\frac{k^2}{4} Q_2 + \frac{k}{2} (\nu + R_{11}) Q_1 - \left(\frac{k^2}{2} + \nu n^2 \right) Y_n(k) \right] C_2 + \\ [n((n-1)(1-\nu) + R_{11})] C_3 + \left\{ \frac{(\nu + R_{11}) - 1}{n((n+1)(1-\nu) - R_{11})} \right\} C_4 = 0 \quad (4.33)$$

Boundary conditions when the edges are elastically restrained against translation.

Equations (4.6) and (4.14) yield the following

$$\frac{\partial}{\partial \bar{r}} \nabla^2 \bar{w}(\bar{r}, \theta) = \frac{\partial}{\partial \bar{r}} \left[\frac{\partial^2 \bar{w}(\bar{r}, \theta)}{\partial \bar{r}^2} + \frac{1}{\bar{r}^2} \frac{\partial^2 \bar{w}(\bar{r}, \theta)}{\partial \theta^2} + \frac{1}{\bar{r}} \frac{\partial \bar{w}(\bar{r}, \theta)}{\partial \bar{r}} \right] \quad (4.34)$$

$$\frac{\partial}{\partial \bar{r}} \left[\frac{\partial^2 w(\bar{r}, \theta)}{\partial \bar{r}^2} \right] = \frac{\partial}{\partial \bar{r}} \left[\frac{k^2}{4} [(J_{n-2}(\bar{k}\bar{r}) + J_{n+2}(\bar{k}\bar{r}) - 2J_n(\bar{k}\bar{r}))]C_1 + \right. \\ \left. \frac{k^2}{4} [(Y_{n-2}(\bar{k}\bar{r}) + Y_{n+2}(\bar{k}\bar{r}) - 2Y_n(\bar{k}\bar{r}))]C_2 + n(n-1)\bar{r}^{n-2}C_3 + \left\{ -\frac{1}{\bar{r}^2} \right\} C_4 \right] \cos(n\theta) \quad (4.35)$$

$$= \left\{ \begin{aligned} & \frac{k^3}{8} [(J_{n-3}(\bar{k}\bar{r}) - J_{n-1}(\bar{k}\bar{r})) + (J_{n+1}(\bar{k}\bar{r}) - J_{n+3}(\bar{k}\bar{r})) - 2(J_{n-1}(\bar{k}\bar{r}) - J_{n+1}(\bar{k}\bar{r}))]C_1 + \\ & \frac{k^3}{8} [(Y_{n-3}(\bar{k}\bar{r}) - Y_{n-1}(\bar{k}\bar{r})) + (Y_{n+1}(\bar{k}\bar{r}) - Y_{n+3}(\bar{k}\bar{r})) - 2(Y_{n-1}(\bar{k}\bar{r}) - Y_{n+1}(\bar{k}\bar{r}))]C_2 + \\ & n(n-1)(n-2)\bar{r}^{n-3}C_3 + \left\{ \frac{2}{\bar{r}^3} \right\} C_4 \\ & - n(n+1)(n+2)\bar{r}^{-n-3} \end{aligned} \right\} \cos(n\theta) \quad (4.36)$$

$$= \left\{ \begin{aligned} & \frac{k^3}{8} [(J_{n-3}(\bar{k}\bar{r}) - J_{n+3}(\bar{k}\bar{r})) - 3(J_{n-1}(\bar{k}\bar{r}) - J_{n+1}(\bar{k}\bar{r}))]C_1 + \\ & \frac{k^3}{8} [(Y_{n-3}(\bar{k}\bar{r}) - Y_{n+3}(\bar{k}\bar{r})) - 3(Y_{n-1}(\bar{k}\bar{r}) - Y_{n+1}(\bar{k}\bar{r}))]C_2 + \\ & n(n-1)(n-2)\bar{r}^{n-3}C_3 + \left\{ \frac{2}{\bar{r}^3} \right\} C_4 \\ & - n(n+1)(n+2)\bar{r}^{-n-3} \end{aligned} \right\} \cos(n\theta) \quad (4.37)$$

$$\frac{\partial}{\partial \bar{r}} \left[\frac{\partial^2 w(\bar{r}, \theta)}{\partial \bar{r}^2} \right]_{\bar{r}=1} = \left\{ \begin{aligned} & \frac{k^3}{8} [(J_{n-3}(k) - J_{n+3}(k)) - 3(J_{n-1}(k) - J_{n+1}(k))]C_1 + \\ & \frac{k^3}{8} [(Y_{n-3}(k) - Y_{n+3}(k)) - 3(Y_{n-1}(k) - Y_{n+1}(k))]C_2 + \\ & n(n-1)(n-2)C_3 + \left\{ 2 \right\} C_4 \\ & - n(n+1)(n+2) \end{aligned} \right\} \cos(n\theta) \quad (4.38)$$

$$= \left\{ \frac{k^3}{8} [P_3 - 3P_1]C_1 + \frac{k^3}{8} [Q_3 - 3Q_1]C_2 + n(n-1)(n-2)C_3 + \left\{ 2 \right\} C_4 - n(n+1)(n+2) \right\} \cos(n\theta) \quad (4.39)$$

where $P_3 = J_{n-3}(k) - J_{n+3}(k)$; $Q_3 = Y_{n-3}(k) - Y_{n+3}(k)$

$$\frac{\partial}{\partial \bar{r}} \left[\frac{1}{\bar{r}^2} \frac{\partial^2 w(\bar{r}, \theta)}{\partial \theta^2} \right] = \frac{1}{\bar{r}^2} \frac{\partial}{\partial \bar{r}} \left[\frac{\partial^2 w(\bar{r}, \theta)}{\partial \theta^2} \right] - \frac{2}{\bar{r}^3} \frac{\partial^2 w(\bar{r}, \theta)}{\partial \theta^2} \quad (4.40)$$

$$\begin{aligned}
&= \frac{1}{\bar{r}^2} \left\{ -n^2 \left[\frac{k}{2} [J_{n-1}(k\bar{r}) - J_{n+1}(k\bar{r})] C_1 + \frac{k}{2} [Y_{n-1}(k\bar{r}) - Y_{n+1}(k\bar{r})] C_2 + n\bar{r}^{n-1} C_3 + \left\{ \frac{1}{\bar{r}} \right. \right. \right. \\
&\quad \left. \left. \left. - n\bar{r}^{-n-1} \right\} C_4 \right] \cos(n\theta) \right\} - \\
&\frac{2}{\bar{r}^3} \left\{ -n^2 \left[C_1 J_n(k\bar{r}) + C_2 Y_n(k\bar{r}) + C_3 \bar{r}^n + C_4 \left\{ \frac{\log \bar{r}}{\bar{r}^{-n}} \right\} \right] \cos(n\theta) \right\}
\end{aligned}
\tag{4.41}$$

$$\begin{aligned}
\frac{\partial}{\partial \bar{r}} \left[\frac{1}{\bar{r}^2} \frac{\partial^2 w(\bar{r}, \theta)}{\partial \theta^2} \right]_{\bar{r}=1} &= \left\{ -n^2 \left[\frac{k}{2} [J_{n-1}(k) - J_{n+1}(k)] C_1 + \frac{k}{2} [Y_{n-1}(k) - Y_{n+1}(k)] C_2 + n C_3 \right. \right. \\
&\quad \left. \left. + \left\{ \begin{matrix} 1 \\ -n \end{matrix} \right\} C_4 \right] \cos(n\theta) \right\} - \\
2 \left\{ -n^2 \left[C_1 J_n(k) + C_2 Y_n(k) + C_3 + C_4 \left\{ \begin{matrix} 0 \\ 1 \end{matrix} \right\} \right] \cos(n\theta) \right\}
\end{aligned}
\tag{4.42}$$

$$\begin{aligned}
\frac{\partial}{\partial \bar{r}} \left[\frac{1}{\bar{r}^2} \frac{\partial^2 w(\bar{r}, \theta)}{\partial \theta^2} \right]_{\bar{r}=1} &= -n^2 \left[\frac{k}{2} [P_1] C_1 + \frac{k}{2} [Q_1] C_2 + n C_3 + \left\{ \begin{matrix} 1 \\ -n \end{matrix} \right\} C_4 \right] \cos(n\theta) + \\
2n^2 \left[C_1 J_n(k) + C_2 Y_n(k) + C_3 + C_4 \left\{ \begin{matrix} 0 \\ 1 \end{matrix} \right\} \right] \cos(n\theta)
\end{aligned}
\tag{4.43}$$

$$\frac{\partial}{\partial \bar{r}} \left[\frac{1}{\bar{r}} \frac{\partial w(\bar{r}, \theta)}{\partial \bar{r}} \right] = \frac{1}{\bar{r}} \frac{\partial}{\partial \bar{r}} \left[\frac{\partial w(\bar{r}, \theta)}{\partial \bar{r}} \right] + \frac{\partial w(\bar{r}, \theta)}{\partial \bar{r}} \frac{\partial}{\partial \bar{r}} \left[\frac{1}{\bar{r}} \right] = \frac{1}{\bar{r}} \frac{\partial^2 w(\bar{r}, \theta)}{\partial \bar{r}^2} - \frac{1}{\bar{r}^2} \frac{\partial w(\bar{r}, \theta)}{\partial \bar{r}}
\tag{4.44}$$

$$\begin{aligned}
&= \frac{1}{\bar{r}} \left[\frac{k^2}{4} [(J_{n-2}(k\bar{r}) + J_{n+2}(k\bar{r}) - 2J_n(k\bar{r}))] C_1 + \right. \\
&\quad \left. \frac{k^2}{4} [(Y_{n-2}(k\bar{r}) + Y_{n+2}(k\bar{r}) - 2Y_n(k\bar{r}))] C_2 + n(n-1)\bar{r}^{n-2} C_3 + \left\{ \begin{matrix} -\frac{1}{\bar{r}^2} \\ n(n+1)\bar{r}^{-n-2} \end{matrix} \right\} C_4 \right] \cos(n\theta) \\
&- \frac{1}{\bar{r}^2} \left[\frac{k}{2} [J_{n-1}(k\bar{r}) - J_{n+1}(k\bar{r})] C_1 + \frac{k}{2} [Y_{n-1}(k\bar{r}) - Y_{n+1}(k\bar{r})] C_2 + n\bar{r}^{n-1} C_3 + \left\{ \begin{matrix} \frac{1}{\bar{r}} \\ -n\bar{r}^{-n-1} \end{matrix} \right\} C_4 \right] \cos(n\theta)
\end{aligned}
\tag{4.45}$$

$$\frac{\partial}{\partial \bar{r}} \left[\frac{1}{\bar{r}} \frac{\partial w(\bar{r}, \theta)}{\partial \bar{r}} \right]_{\bar{r}=1} =$$

$$\begin{aligned}
&= \left[\frac{k^2}{4} [J_{n-2}(k) + J_{n+2}(k) - 2J_n(k)] C_1 + \right. \\
&\quad \left. \frac{k^2}{4} [Y_{n-2}(k) + Y_{n+2}(k) - 2Y_n(k)] C_2 + n(n-1)C_3 + \left\{ \frac{-1}{n(n+1)} \right\} C_4 \right] \cos(n\theta) \\
&- \left[\frac{k}{2} [J_{n-1}(k) - J_{n+1}(k)] C_1 + \frac{k}{2} [Y_{n-1}(k) - Y_{n+1}(k)] C_2 + nC_3 + \left\{ \frac{1}{-n} \right\} C_4 \right] \cos(n\theta)
\end{aligned} \tag{4.46}$$

$$\begin{aligned}
&= \left[\frac{k^2}{4} [P_2 - 2J_n(k)] C_1 + \frac{k^2}{4} [Q_2 - 2Y_n(k)] C_2 + n(n-1)C_3 + \left\{ \frac{-1}{n(n+1)} \right\} C_4 \right] \cos(n\theta) \\
&- \left[\frac{k}{2} [P_1] C_1 + \frac{k}{2} [Q_1] C_2 + nC_3 + \left\{ \frac{1}{-n} \right\} C_4 \right] \cos(n\theta)
\end{aligned} \tag{4.47}$$

$$\left[\frac{\partial^2 w(\bar{r}, \theta)}{\partial \bar{r} \partial \theta} \right] = \frac{\partial}{\partial \bar{r}} \left[\frac{\partial w(\bar{r}, \theta)}{\partial \theta} \right] = \frac{\partial}{\partial \bar{r}} \left\{ -n \left[C_1 J_n(k\bar{r}) + C_2 Y_n(k\bar{r}) + C_3 \bar{r}^n + C_4 \left\{ \frac{\log \bar{r}}{\bar{r}^{-n}} \right\} \right] \sin(n\theta) \right\} \tag{4.48}$$

$$= -n \left[\frac{k}{2} [J_{n-1}(k\bar{r}) - J_{n+1}(k\bar{r})] C_1 + \frac{k}{2} [Y_{n-1}(k\bar{r}) - Y_{n+1}(k\bar{r})] C_2 + n\bar{r}^{n-1} C_3 + \left\{ \frac{1}{\bar{r}} \right\} C_4 \right] \sin(n\theta) \tag{4.49}$$

$$\frac{1}{\bar{r}^2} \frac{\partial w(\bar{r}, \theta)}{\partial \theta} = \frac{-n}{\bar{r}^2} \left[C_1 J_n(k\bar{r}) + C_2 Y_n(k\bar{r}) + C_3 \bar{r}^n + C_4 \left\{ \frac{\log \bar{r}}{\bar{r}^{-n}} \right\} \right] \sin(n\theta) \tag{4.50}$$

Equations (4.49) and (4.50) yield the following

$$\begin{aligned}
&\frac{\partial}{\partial \theta} \left[\frac{1}{\bar{r}} \frac{\partial^2 w(\bar{r}, \theta)}{\partial \bar{r} \partial \theta} - \frac{1}{\bar{r}^2} \frac{\partial w(\bar{r}, \theta)}{\partial \theta} \right] \\
&= -\frac{n^2}{\bar{r}} \left[\frac{k}{2} [J_{n-1}(k\bar{r}) - J_{n+1}(k\bar{r})] C_1 + \frac{k}{2} [Y_{n-1}(k\bar{r}) - Y_{n+1}(k\bar{r})] C_2 + n\bar{r}^{n-1} C_3 + \left\{ \frac{1}{\bar{r}} \right\} C_4 \right] \cos(n\theta) + \\
&\frac{n^2}{\bar{r}^2} \left[C_1 J_n(k\bar{r}) + C_2 Y_n(k\bar{r}) + C_3 \bar{r}^n + C_4 \left\{ \frac{\log \bar{r}}{\bar{r}^{-n}} \right\} \right] \cos(n\theta)
\end{aligned} \tag{4.51}$$

Equation (4.51) can be written as

$$\begin{aligned}
&(1-\nu) \frac{1}{\bar{r}} \frac{\partial}{\partial \theta} \left[\frac{1}{\bar{r}} \frac{\partial^2 w(\bar{r}, \theta)}{\partial \bar{r} \partial \theta} - \frac{1}{\bar{r}^2} \frac{\partial w(\bar{r}, \theta)}{\partial \theta} \right]_{\bar{r}=1} \\
&= (1-\nu) \left\{ -n^2 \left[\frac{k}{2} [J_{n-1}(k) - J_{n+1}(k)] C_1 + \frac{k}{2} [Y_{n-1}(k) - Y_{n+1}(k)] C_2 + nC_3 + \left\{ \frac{1}{-n} \right\} C_4 \right] \cos(n\theta) + \right. \\
&\quad \left. n^2 \left[C_1 J_n(k) + C_2 Y_n(k) + C_3 + C_4 \left\{ \frac{0}{1} \right\} \right] \cos(n\theta) \right\}
\end{aligned}$$

(4.52)

$$= (1-\nu) \left\{ \begin{aligned} & -n^2 \left[\frac{k}{2} [P_1] C_1 + \frac{k}{2} [Q_1] C_2 + n C_3 + \left\{ \begin{matrix} 1 \\ -n \end{matrix} \right\} C_4 \right] \cos(n\theta) + \\ & n^2 \left[C_1 J_n(k) + C_2 Y_n(k) + C_3 + C_4 \left\{ \begin{matrix} 0 \\ 1 \end{matrix} \right\} \right] \cos(n\theta) \end{aligned} \right\} \quad (4.53)$$

Equation (5.6) gives the following at $\bar{r} = 1$

$$\bar{w}(\bar{r}, \theta)_{\bar{r}=1} = \left[C_1 J_n(k) + C_2 Y_n(k) + C_3 + C_4 \left\{ \begin{matrix} 0 \\ 1 \end{matrix} \right\} \right] \cos(n\theta) \quad (4.54)$$

Substituting equations (4.39), (4.43), (4.47), (4.53), (4.54) into equation (4.14) gives the following

$$\begin{aligned} & \left[\frac{k^3}{8} P_3 + \frac{k^2}{4} P_2 - \frac{k}{2} \left(\frac{3}{4} k^2 + n^2 (2-\nu) + 1 \right) P_1 + \left(n^2 (3-\nu) - \frac{k^2}{2} - T_{11} \right) J_n(k) \right] C_1 + \\ & \left[\frac{k^3}{8} Q_3 + \frac{k^2}{4} Q_2 - \frac{k}{2} \left(\frac{3}{4} k^2 + n^2 (2-\nu) + 1 \right) Q_1 + \left(n^2 (3-\nu) - \frac{k^2}{2} - T_{11} \right) Y_n(k) \right] C_2 + \\ & \left[n^2 (n-1) \nu - n^3 - T_{11} \right] C_3 - \left\{ \begin{matrix} n^2 (2-\nu) \\ -n^2 (n+1) \nu + n^3 - T_{11} \end{matrix} \right\} C_4 = 0 \end{aligned} \quad (4.55)$$

where $P_1 = J_{n-1}(k) - J_{n+1}(k); P_2 = J_{n-2}(k) + J_{n+2}(k); P_3 = J_{n-3}(k) - J_{n+3}(k);$
 $Q_1 = Y_{n-1}(k) - Y_{n+1}(k); Q_2 = Y_{n-2}(k) + Y_{n+2}(k); Q_3 = Y_{n-3}(k) - Y_{n+3}(k);$

For **region II**, we delete the singular terms

$$\bar{u}_{II}(r) = C_5 J_n(k\bar{r}) + C_6 \bar{r}^n \quad (4.56)$$

Substituting equation (4.56) into equation (4.3) yields the following

$$\bar{w}_{II}(\bar{r}, \theta) = [C_5 J_n(k\bar{r}) + C_6 \bar{r}^n] \cos(n\theta) \quad (4.57)$$

Consider the boundary condition (equation (4.15)) at $\bar{r} = b$, i.e., $\bar{w}_I(b, \theta) = \bar{w}_{II}(b, \theta)$

$$J_n(kb)C_1 + Y_n(kb)C_2 + b^n C_3 + \left\{ \begin{matrix} \log b \\ b^{-n} \end{matrix} \right\} C_4 - J_n(kb)C_5 - b^n C_6 = 0 \quad (4.58)$$

Consider the boundary condition (equation (4.16)) at $\bar{r} = b$, i.e., $\bar{w}_I(b, \theta) = \bar{w}_{II}(b, \theta)$

$$\frac{k}{2} P_1' C_1 + \frac{k}{2} Q_1' C_2 + n b^{n-1} C_3 + \left\{ \begin{matrix} \frac{1}{b} \\ -n b^{-n-1} \end{matrix} \right\} C_4 - \frac{k}{2} P_1' C_5 - n b^{n-1} C_6 = 0 \quad (4.59)$$

Consider the boundary condition (equation (4.17)) at $\bar{r} = b$, i.e., $\bar{w}_I''(b, \theta) = \bar{w}_{II}''(b, \theta)$

$$\begin{aligned} & \frac{k^2}{4} (P_2' - 2J_n(kb))C_1 + \frac{k^2}{4} (Q_2' - 2Y_n(kb))C_2 + n(n-1)b^{n-2}C_3 - \left\{ \frac{1}{b^2} \right. \\ & \left. - \frac{1}{n(n+1)b^{n-2}} \right\} C_4 \\ & - \frac{k^2}{4} (P_2' - 2J_n(kb))C_5 - n(n-1)b^{n-2}C_6 = 0 \end{aligned} \quad (4.60)$$

Consider the boundary condition (equation (4.18)) at $\bar{r} = b$, i.e.,

$$\begin{aligned} & \bar{w}_I'''(b, \theta) = \bar{w}_{II}'''(b, \theta) - T_{22}\bar{w}_{II}(b, \theta) \\ & \frac{k^2}{8} (P_3' - 3P_1')C_1 + \frac{k^2}{8} (Q_3' - Q_1')C_2 + n(n-1)(n-2)b^{n-3}C_3 + \left\{ \frac{2}{b^3} \right. \\ & \left. - \frac{1}{n(n+1)(n+2)b^{n-3}} \right\} C_4 \\ & - \left[\frac{k^2}{8} (P_3' - 3P_1') - T_{22}J_n(kb) \right] C_5 - \left[n(n-1)(n-2)b^{n-3} - T_{22}b^n \right] C_6 = 0 \end{aligned} \quad (4.61)$$

where $P_1' = J_{n-1}(kb) - J_{n+1}(kb); P_2' = J_{n-2}(kb) + J_{n+2}(kb); P_3' = J_{n-3}(kb) - J_{n+3}(kb);$
 $Q_1' = Y_{n-1}(kb) - Y_{n+1}(kb); Q_2' = Y_{n-2}(kb) + Y_{n+2}(kb); Q_3' = Y_{n-3}(kb) - Y_{n+3}(kb);$

The top form of equations (4.33), (4.55) and (4.58)-(4.61) are used for $n = 0$ (axisymmetric buckling) and the bottom form is used for $n \neq 0$ (asymmetric buckling).

The foregoing general closed-form solution includes the following subset problems.

(i) Buckling of circular plates with internal *elastic ring* support and restrained edge against rotation as shown in Fig. 5.2. Set $T_{11} \rightarrow \infty$ and Eq. (4.55) yields the following.

$$[J_n(k)]C_1 + [Y_n(k)]C_2 + [1]C_3 + \left\{ \begin{matrix} 0 \\ -1 \end{matrix} \right\} C_4 = 0 \quad (4.62)$$

Therefore, the set of equations for this case are (4.33), (4.62) and (4.58) – (4.61).

(ii) Buckling of circular plates with internal *elastic ring* support and restrained guided edge against translation as shown in Fig. 4.3. Set $R_{11} \rightarrow \infty$ and Eq. (4.33) yields the following.

$$\left[\frac{k}{2} P_1 \right] C_1 + \left[\frac{k}{2} Q_1 \right] C_2 + [1]C_3 + \left\{ \begin{matrix} 1 \\ -n \end{matrix} \right\} C_4 = 0 \quad (4.63)$$

Therefore, the set of equations for this case are (4.63), (4.55) and (4.58) – (4.61)

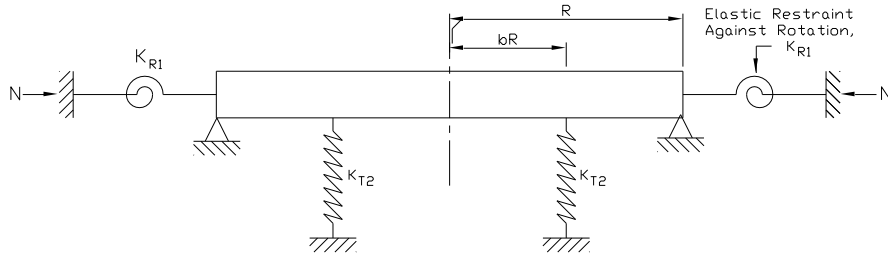


Fig. 4.2. Buckling of a Circular Plate with an Internal *Elastic Ring* Support and Restrained Edge Against Rotation

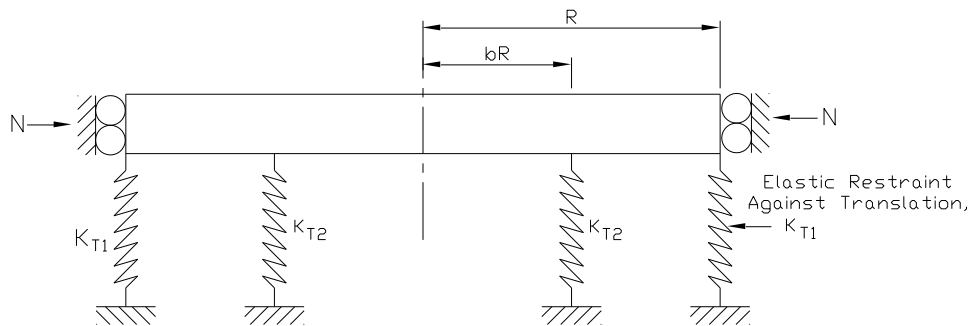


Fig. 4.3. Buckling of a Circular Plate with an Internal *Elastic Ring* Support and Restrained Guided Edge Against Translation

(iii) Buckling of circular plates with internal *elastic ring* support and restrained edge against translation as shown in Fig. 4.4. **Set** $R_{11} \rightarrow 0$ and from Eq. (4.33) yields the following

$$\begin{aligned} & \left[\frac{k^2}{4} P_2 + \frac{k}{2} (\nu) P_1 - \left(\frac{k^2}{2} + \nu n^2 \right) J_n(k) \right] C_1 + \left[\frac{k^2}{4} Q_2 + \frac{k}{2} (\nu) Q_1 - \left(\frac{k^2}{2} + \nu n^2 \right) Y_n(k) \right] C_2 + \\ & [n((n-1)(1-\nu))] C_3 + \left\{ \frac{(\nu)-1}{n((n+1)(1-\nu))} \right\} C_4 = 0 \end{aligned} \quad (4.64)$$

Therefore, the set of equations for this case are (4.64), (4.55) and (4.58) – (4.61).

(iv) Buckling of circular plates with internal *elastic ring* support and guided edge, as shown in Fig. 4.5. **Set** $R_{11} \rightarrow \infty$ & $T_{11} \rightarrow 0$ and **from Eq. (4.33) and (4.55)** yields the following

$$\left[\frac{k}{2} P_1 \right] C_1 + \left[\frac{k}{2} Q_1 \right] C_2 + [1] C_3 + \left\{ \frac{1}{-n} \right\} C_4 = 0 \quad (4.65)$$

$$\begin{aligned} & \left[\frac{k^3}{8} P_3 + \frac{k^2}{4} P_2 - \frac{k}{2} \left(\frac{3}{4} k^2 + n^2(2-\nu) + 1 \right) P_1 + \left(n^2(3-\nu) - \frac{k^2}{2} \right) J_n(k) \right] C_1 + \\ & \left[\frac{k^3}{8} Q_3 + \frac{k^2}{4} Q_2 - \frac{k}{2} \left(\frac{3}{4} k^2 + n^2(2-\nu) + 1 \right) Q_1 + \left(n^2(3-\nu) - \frac{k^2}{2} \right) Y_n(k) \right] C_2 + \\ & [n^2(n-1)\nu - n^3] C_3 - \left\{ \frac{n^2(2-\nu)}{-n^2(n+1)\nu + n^3} \right\} C_4 = 0 \end{aligned} \quad (4.66)$$

Therefore, the set of equations for this case are (4.65), (4.66) and (4.58) – (4.61).

(v) Buckling of circular plates with internal *elastic ring* support and simply supported edge, as shown in Fig. 4.6. **Set** $R_{11} \rightarrow 0$ & $T_{11} \rightarrow \infty$ and **from Eq. (4.33) and (4.55)** yields the following

$$\begin{aligned} & \left[\frac{k^2}{4} P_2 + \frac{k}{2} (\nu) P_1 - \left(\frac{k^2}{2} + \nu n^2 \right) J_n(k) \right] C_1 + \left[\frac{k^2}{4} Q_2 + \frac{k}{2} (\nu) Q_1 - \left(\frac{k^2}{2} + \nu n^2 \right) Y_n(k) \right] C_2 + \\ & [n((n-1)(1-\nu))] C_3 + \left\{ \frac{(\nu)-1}{n((n+1)(1-\nu))} \right\} C_4 = 0 \end{aligned} \quad (4.67)$$

$$[J_n(k)] C_1 + [Y_n(k)] C_2 + [1] C_3 + \left\{ \frac{0}{-1} \right\} C_4 = 0 \quad (4.68)$$

Therefore, the set of equations for this case are (4.67), (4.68) and (4.58) – (4.61).

(vi) Buckling of circular plates with internal *elastic ring* support and clamped edge, as shown in Fig. 4.7. **Large** R_{11} & T_{11} (**i.e.**, $R_{11} \rightarrow \infty$ & $T_{11} \rightarrow \infty$) **in the Fig. 4.1** exemplify the

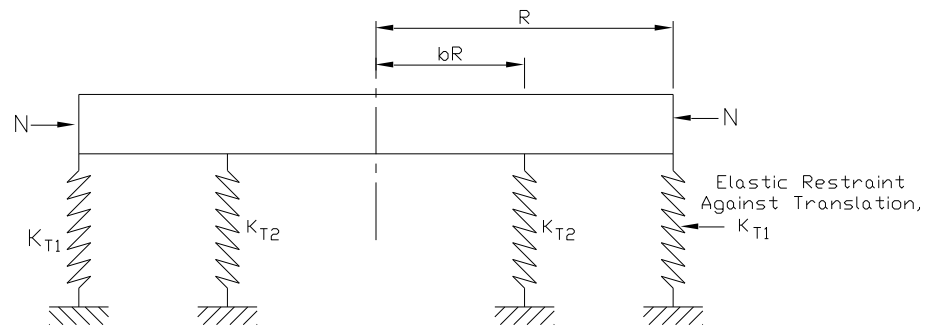


Fig. 4.4. Buckling of a Circular Plate with an Internal *Elastic Ring* Support and Restrained Edge Against Translation

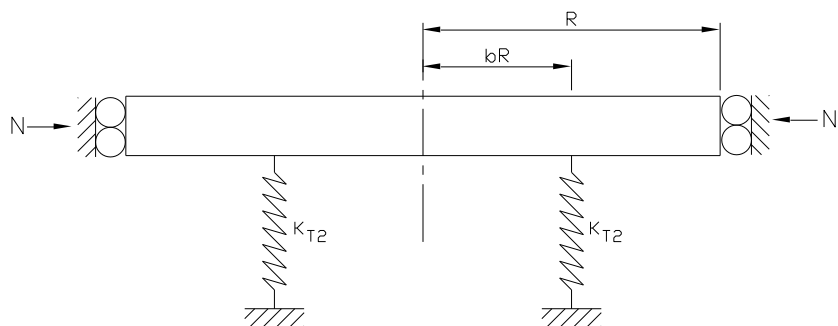


Fig. 4.5. Buckling of a Circular Plate with an Internal *Elastic Ring* Support and Guided Edge

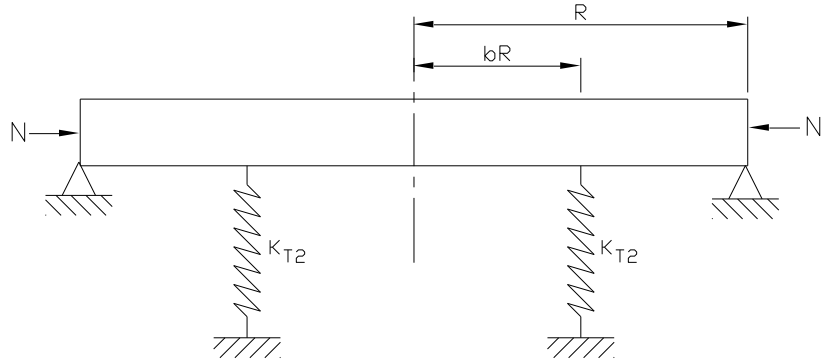


Fig. 4.6. Buckling of a Circular Plate with an Internal *Elastic Ring* Support and Simply Supported Edge

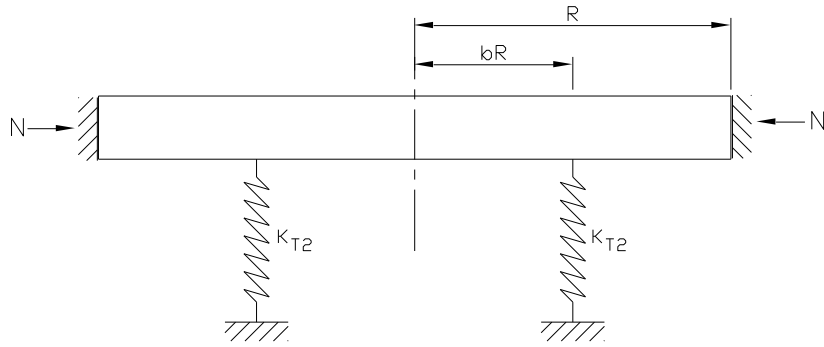


Fig. 4.7. Buckling of a Circular Plate with an Internal *Elastic Ring* Support and Clamped Edge

Clamped boundary condition. Set $R_{11} \rightarrow \infty$ & $T_{11} \rightarrow \infty$ and from Eqs. (4.33) and (4.55) yields the following

$$\left[\frac{k}{2}P_1\right]C_1 + \left[\frac{k}{2}Q_1\right]C_2 + [1]C_3 + \left\{\begin{matrix} 1 \\ -n \end{matrix}\right\}C_4 = 0 \quad (4.69)$$

$$[J_n(k)]C_1 + [Y_n(k)]C_2 + [1]C_3 + \left\{\begin{matrix} 0 \\ -1 \end{matrix}\right\}C_4 = 0 \quad (4.70)$$

Therefore, the set of equations for this case are (4.69), (4.70) and (4.58) to (4.61).

(vii) Buckling of circular plates with internal *elastic ring* support and free edge, as shown in

Fig. 4.8. **Small** R_{11} & T_{11} (**i.e.**, $R_{11} \rightarrow 0$ & $T_{11} \rightarrow 0$) **in the Fig. 4.1** exemplify the free boundary condition. Set $R_{11} \rightarrow 0$ & $T_{11} \rightarrow 0$ and from Eqs. (4.33) and (4.55) yields the following

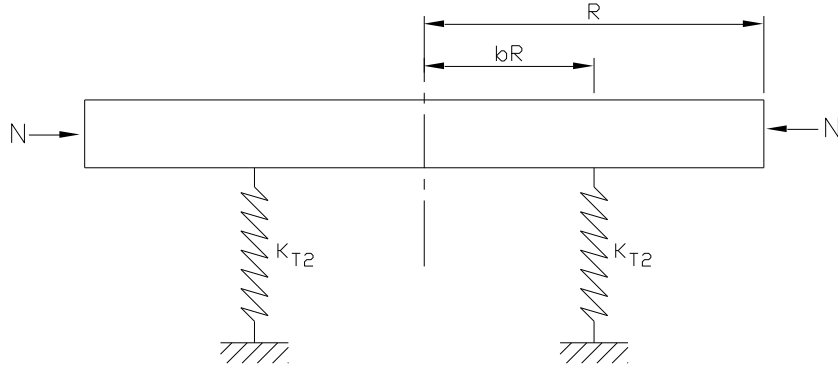


Fig. 4.8 Buckling of a Circular Plate with an Internal *Elastic Ring* Support and Free Edge

$$\left[\frac{k^2}{4}P_2 + \frac{k}{2}(\nu)P_1 - \left(\frac{k^2}{2} + \nu n^2\right)J_n(k)\right]C_1 + \left[\frac{k^2}{4}Q_2 + \frac{k}{2}(\nu)Q_1 - \left(\frac{k^2}{2} + \nu n^2\right)Y_n(k)\right]C_2 + [n((n-1)(1-\nu))]C_3 + \left\{\begin{matrix} (\nu)-1 \\ n((n+1)(1-\nu)) \end{matrix}\right\}C_4 = 0 \quad (4.71)$$

$$\begin{aligned}
& \left[\frac{k^3}{8} P_3 + \frac{k^2}{4} P_2 - \frac{k}{2} \left(\frac{3}{4} k^2 + n^2(2-\nu) + 1 \right) P_1 + \left(n^2(3-\nu) - \frac{k^2}{2} \right) J_n(k) \right] C_1 + \\
& \left[\frac{k^3}{8} Q_3 + \frac{k^2}{4} Q_2 - \frac{k}{2} \left(\frac{3}{4} k^2 + n^2(2-\nu) + 1 \right) Q_1 + \left(n^2(3-\nu) - \frac{k^2}{2} \right) Y_n(k) \right] C_2 + \\
& \left[n^2(n-1)\nu - n^3 \right] C_3 - \left\{ \begin{matrix} n^2(2-\nu) \\ -n^2(n+1)\nu + n^3 \end{matrix} \right\} C_4 = 0
\end{aligned} \tag{4.72}$$

Therefore, the set of equations for this case are (4.71), (4.72) and (4.58) to (4.61).

SPECIAL CASE: When $K_{T2} \rightarrow \infty$ in Fig. 4.1, the above problem becomes buckling of circular plates with internal *rigid ring* support and elastically restrained edge against rotation and translation as shown in Fig. 4.9.

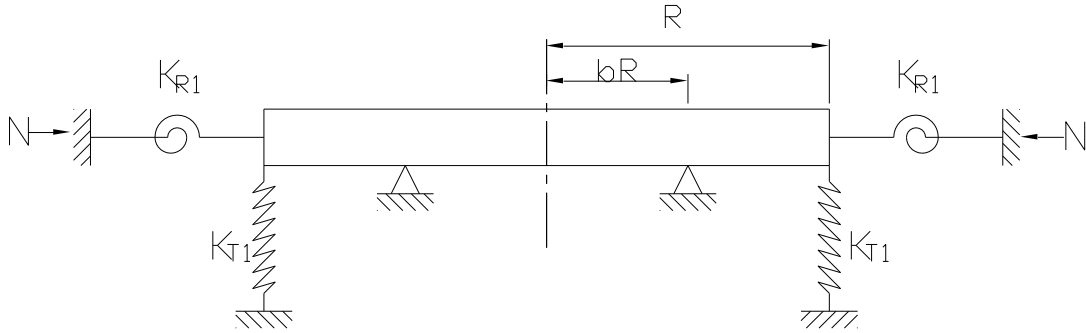


Fig. 4.9 Buckling of a Circular Plate with an *Internal Ring* Support and Elastically Restrained Edge against Rotation and Translation

The boundary conditions at outer edge of the plate are

$$\left[\frac{\partial^2 \bar{w}_I(\bar{r}, \theta)}{\partial \bar{r}^2} + \nu \left(\frac{1}{\bar{r}} \frac{\partial \bar{w}_I(\bar{r}, \theta)}{\partial \bar{r}} + \frac{1}{\bar{r}^2} \frac{\partial^2 \bar{w}_I(\bar{r}, \theta)}{\partial \theta^2} \right) \right] = -R_{11} \frac{\partial \bar{w}_I(\bar{r}, \theta)}{\partial \bar{r}} \tag{4.73}$$

$$\left[\frac{\partial}{\partial \bar{r}} \nabla^2 \bar{w}_I(\bar{r}, \theta) + (1-\nu) \frac{1}{\bar{r}} \frac{\partial}{\partial \theta} \left(\frac{1}{\bar{r}} \frac{\partial^2 \bar{w}_I(\bar{r}, \theta)}{\partial \bar{r} \partial \theta} - \frac{1}{\bar{r}^2} \frac{\partial \bar{w}_I(\bar{r}, \theta)}{\partial \theta} \right) \right] = T_{11} \bar{w}_I(\bar{r}, \theta) \tag{4.74}$$

Apart from the elastically restrained edge against rotation and translation, there is an *internal ring* support constraint and the continuity requirements of slope and curvature at the support, i.e. $\bar{r} = b$

$$\bar{w}_I(b, \theta) = 0 \quad (4.75)$$

$$\bar{w}_{II}(b, \theta) = 0 \quad (4.76)$$

$$\bar{w}'_I(b, \theta) = \bar{w}'_{II}(b, \theta) \quad (4.77)$$

$$\bar{w}''_I(b, \theta) = \bar{w}''_{II}(b, \theta) \quad (4.78)$$

The non-trivial solutions to equations (4.73), (4.74), (4.75) to (4.78) are sought. The lowest value of k is the square root of the normalized buckling load.

The set of equations for this case are

$$\begin{aligned} & \left[\frac{k^2}{4} P_2 + \frac{k}{2} (\nu + R_{11}) P_1 - \left(\frac{k^2}{2} + m^2 \right) J_n(k) \right] C_1 + \\ & \left[\frac{k^2}{4} Q_2 + \frac{k}{2} (\nu + R_{11}) Q_1 - \left(\frac{k^2}{2} + m^2 \right) Y_n(k) \right] C_2 + \\ & [n((n-1)(1-\nu) + R_{11})] C_3 + \left\{ \frac{(\nu + R_{11}) - 1}{n((n+1)(1-\nu) - R_{11})} \right\} C_4 = 0 \end{aligned} \quad (4.79)$$

$$\begin{aligned} & \left[\frac{k^3}{8} P_3 + \frac{k^2}{4} P_2 - \frac{k}{2} \left(\frac{3}{4} k^2 + n^2(2-\nu) + 1 \right) P_1 + \left(n^2(3-\nu) - \frac{k^2}{2} - T_{11} \right) J_n(k) \right] C_1 + \\ & \left[\frac{k^3}{8} Q_3 + \frac{k^2}{4} Q_2 - \frac{k}{2} \left(\frac{3}{4} k^2 + n^2(2-\nu) + 1 \right) Q_1 + \left(n^2(3-\nu) - \frac{k^2}{2} - T_{11} \right) Y_n(k) \right] C_2 + \\ & [n^2(n-1)\nu - n^3 - T_{11}] C_3 - \left\{ \frac{n^2(2-\nu)}{-n^2(n+1)\nu + n^3 - T_{11}} \right\} C_4 = 0 \end{aligned} \quad (4.80)$$

where $P_1 = J_{n-1}(k) - J_{n+1}(k); P_2 = J_{n-2}(k) + J_{n+2}(k); P_3 = J_{n-3}(k) - J_{n+3}(k);$
 $Q_1 = Y_{n-1}(k) - Y_{n+1}(k); Q_2 = Y_{n-2}(k) + Y_{n+2}(k); Q_3 = Y_{n-3}(k) - Y_{n+3}(k);$

$$J_n(kb)C_1 + Y_n(kb)C_2 + b^n C_3 + \left\{ \frac{\log b}{b^{-n}} \right\} C_4 = 0 \quad (4.81)$$

$$J_n(kb)C_5 + b^n C_6 \quad (4.82)$$

$$\frac{k}{2}P_1' C_1 + \frac{k}{2}Q_1' C_2 + nb^{n-1}C_3 + \left\{ \frac{1}{b} \right. \\ \left. - nb^{-n-1} \right\} C_4 - \frac{k}{2}P_1' C_5 - nb^{n-1}C_6 = 0 \quad (4.83)$$

$$\frac{k^2}{4}(P_2' - 2J_n(kb))C_1 + \frac{k^2}{4}(Q_2' - 2Y_n(kb))C_2 + n(n-1)b^{n-2}C_3 - \left\{ \frac{1}{b^2} \right. \\ \left. - \frac{1}{n(n+1)b^{-n-2}} \right\} C_4 \\ - \frac{k^2}{4}(P_2' - 2J_n(kb))C_5 - n(n-1)b^{n-2}C_6 = 0 \quad (4.84)$$

where $P_1' = J_{n-1}(kb) - J_{n+1}(kb); P_2' = J_{n-2}(kb) + J_{n+2}(kb);$
 $Q_1' = Y_{n-1}(kb) - Y_{n+1}(kb); Q_2' = Y_{n-2}(kb) + Y_{n+2}(kb);$

The top form of equations (4.79), (4.80) and (4.81) to (4.84) is used for $n = 0$ (axisymmetric buckling) and the bottom form is used for $n \neq 0$ (asymmetric buckling).

The foregoing general closed-form solution includes the following subset problems in this case.

(i) Buckling of circular plates with internal ring support and restrained guided edge against translation as shown in Fig. 4.10. **Set $R_{11} \rightarrow \infty$ and Eq. (4.79)** yields the following.

$$\left[\frac{k}{2}P_1 \right] C_1 + \left[\frac{k}{2}Q_1 \right] C_2 + [1]C_3 + \left\{ \frac{1}{-n} \right\} C_4 = 0 \quad (4.85)$$

Therefore, the set of equations for this case are (4.85), (4.80) and (4.81) – (4.84).

(ii) Buckling of circular plates with internal ring support and restrained edge against translation as shown in Fig. 4.11. **Set $R_{11} \rightarrow 0$ and from Eq. (4.79)** yields the following

$$\left[\frac{k^2}{4}P_2 + \frac{k}{2}(\nu)P_1 - \left(\frac{k^2}{2} + \nu n^2 \right) J_n(k) \right] C_1 + \left[\frac{k^2}{4}Q_2 + \frac{k}{2}(\nu)Q_1 - \left(\frac{k^2}{2} + \nu n^2 \right) Y_n(k) \right] C_2 + \\ [n((n-1)(1-\nu))]C_3 + \left\{ \frac{(\nu)-1}{n((n+1)(1-\nu))} \right\} C_4 = 0 \quad (4.86)$$

Therefore, the set of equations for this case are (4.86), (4.80) and (4.81) to (4.84).

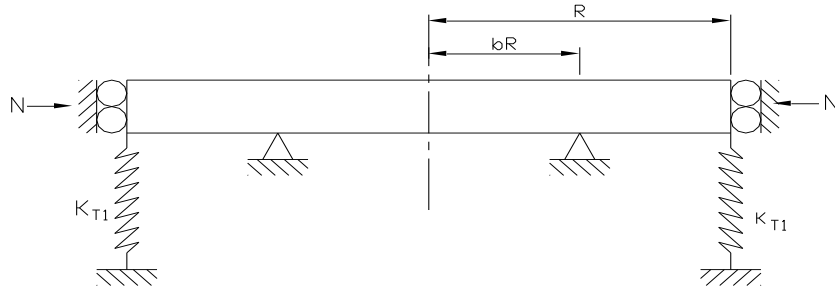


Fig. 4.10 Buckling of a Circular Plate with an *Internal Ring* Support and Restrained Guided Edge Against Translation

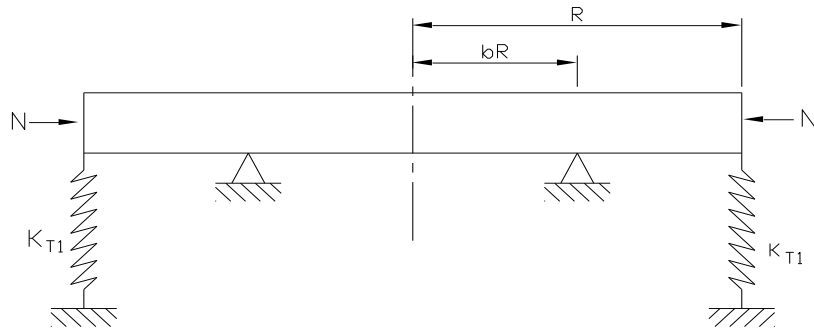


Fig. 4.11 Buckling of a Circular Plate with an *Internal Ring* Support and Restrained Edge Against Translation
(iii) Buckling of circular plates with internal ring support and guided edge, as shown in Fig.

4.12. **Set** $R_{11} \rightarrow \infty$ & $T_{11} \rightarrow 0$ **and from Eq. (4.79) and (4.80), we get the following**

$$\left[\frac{k}{2} P_1 \right] C_1 + \left[\frac{k}{2} Q_1 \right] C_2 + [1] C_3 + \left\{ \begin{matrix} 1 \\ -n \end{matrix} \right\} C_4 = 0 \quad (4.87)$$

$$\begin{aligned}
& \left[\frac{k^3}{8} P_3 + \frac{k^2}{4} P_2 - \frac{k}{2} \left(\frac{3}{4} k^2 + n^2(2-\nu) + 1 \right) P_1 + \left(n^2(3-\nu) - \frac{k^2}{2} \right) J_n(k) \right] C_1 + \\
& \left[\frac{k^3}{8} Q_3 + \frac{k^2}{4} Q_2 - \frac{k}{2} \left(\frac{3}{4} k^2 + n^2(2-\nu) + 1 \right) Q_1 + \left(n^2(3-\nu) - \frac{k^2}{2} \right) Y_n(k) \right] C_2 + \\
& \left[n^2(n-1)\nu - n^3 \right] C_3 - \left\{ \begin{matrix} n^2(2-\nu) \\ -n^2(n+1)\nu + n^3 \end{matrix} \right\} C_4 = 0
\end{aligned} \tag{4.88}$$

Therefore, the set of equations for this case are (4.87), (4.88) and (4.81) to (4.84).

(iv) Buckling of circular plates with internal ring support and simply supported edge, as shown in Fig. 4.13. Set $R_{11} \rightarrow 0$ & $T_{11} \rightarrow \infty$ and from Eq. (4.79) and (4.80), we get the following

$$\begin{aligned}
& \left[\frac{k^2}{4} P_2 + \frac{k}{2}(\nu) P_1 - \left(\frac{k^2}{2} + m^2 \right) J_n(k) \right] C_1 + \left[\frac{k^2}{4} Q_2 + \frac{k}{2}(\nu) Q_1 - \left(\frac{k^2}{2} + m^2 \right) Y_n(k) \right] C_2 + \\
& [n((n-1)(1-\nu))] C_3 + \left\{ \begin{matrix} (\nu) - 1 \\ n((n+1)(1-\nu)) \end{matrix} \right\} C_4 = 0
\end{aligned} \tag{4.89}$$

$$[J_n(k)] C_1 + [Y_n(k)] C_2 + [1] C_3 + \left\{ \begin{matrix} 0 \\ -1 \end{matrix} \right\} C_4 = 0 \tag{4.90}$$

Therefore, the set of equations for this case are (4.89), (4.89) and (4.81) – (4.84).

(v) Buckling of circular plates with internal ring support and clamped edge, as shown in Fig. 4.14. Large R_{11} & T_{11} (i.e., $R_{11} \rightarrow \infty$ & $T_{11} \rightarrow \infty$) in the Fig. 4.9 exemplify the clamped boundary

condition. Set $R_{11} \rightarrow \infty$ & $T_{11} \rightarrow \infty$ and from Eqs. (4.79) and (4.80) yields the following

$$\left[\frac{k}{2} P_1 \right] C_1 + \left[\frac{k}{2} Q_1 \right] C_2 + [1] C_3 + \left\{ \begin{matrix} 1 \\ -n \end{matrix} \right\} C_4 = 0 \tag{4.91}$$

$$[J_n(k)] C_1 + [Y_n(k)] C_2 + [1] C_3 + \left\{ \begin{matrix} 0 \\ -1 \end{matrix} \right\} C_4 = 0 \tag{4.92}$$

Therefore, the set of equations for this case are (4.91), (4.92) and (4.81) – (4.84).

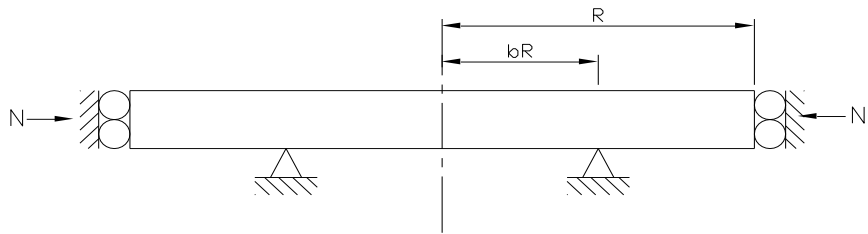


Fig. 4.12 Buckling of a Circular Plate with an *Internal Ring* Support and Guided Edge

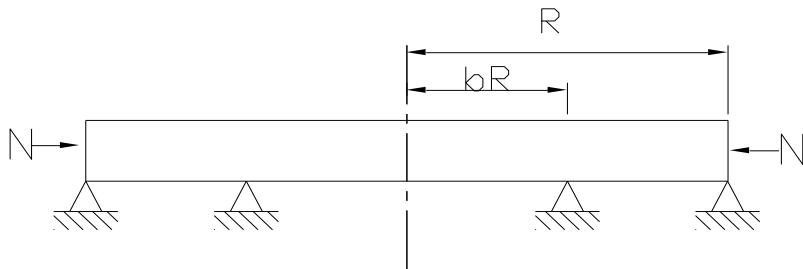


Fig. 4.13 Buckling of a Circular Plate with an *Internal Ring* Support and Simply Supported Edge

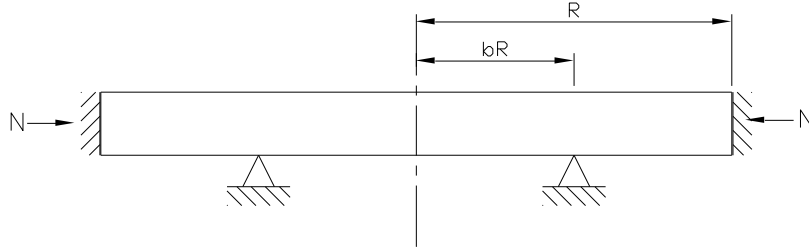


Fig. 4.14 Buckling of a Circular Plate with an *Internal Ring* Support and Clamped Edge

4.4 Solution

For the given values of $n, \nu, R_{11}, T_{11}, T_{22}$ & b the above set of equations, gives an exact characteristic equation for non-trivial solutions of the coefficients C_1, C_2, C_3, C_4, C_5 & C_6 . For non-trivial solution, the determinant of $[C]_{6 \times 6}$ vanish. The value of k , calculated from the characteristic equation by a simple root search method. Using Mathematica, computer software with symbolic capabilities, solves this problem.

4.5 Results and Discussions

There is a lot of flexibility of the code developed in Mathematica. It is used to determine the buckling load parameter for any range of rotational and translational constraints and also various translational spring stiffness constraints of an internal *elastic ring* support. The findings are presented in both tabular and graphical form. Buckling loads are calculated for various internal *elastic ring* support radii b , rotational spring stiffness parameter R_{11} , translational spring stiffness parameter T_{11} , and translational spring stiffness

parameters of an internal *elastic ring* support T_{22} . Poisson's ratio used in the calculations is 0.3.

The buckling load parameters for axisymmetric and asymmetric modes and for various values of rotational spring stiffness parameters, R_{11} and keeping translational spring stiffness parameter, T_{11} and translational spring stiffness parameter, T_{22} constant, are presented in Table 4.1. It is observed from the Figs. 4.15 to 18, for a given value of R_{11}, T_{11} & T_{22} , the curve is composed of two segments. This is due to the switching of buckling modes. For a smaller internal *elastic ring* support radius b , the plate buckles in an asymmetric mode (*i.e.*, $n = 1$). In this segment (as shown by dotted lines in Figs. 4.15 to 5.18) the buckling load decreases as b decreases in value. For larger internal *elastic ring* support radius b , the plate buckles in an axisymmetric mode (*i.e.*, $n = 0$). In this segment (as shown by continuous lines in Figs. 4.15 to 4.18) the buckling load increases as b decreases up to a peak point corresponds to maximum buckling load and thereafter decrease as b decreases in value as shown in Figs. 4.15 to 4.18. Fig. 4.15, shows the variation of buckling load parameter k , with respect to the internal *elastic ring* support radius b , for various values of rotational spring stiffness parameters ($R_{11} = 0.5, 10 \text{ \& } \infty$) and keeping translational spring stiffness parameter and translational spring stiffness parameter of an internal *elastic ring* support are constant ($T_{11} = T_{22} = 1000$). The cross over radius varies from $b = 0.233$ for $R_{11} = 0.5 \text{ \& } T_{11} = T_{22} = 1000$ to $b = 0.234$ for $R_{11} = \infty \text{ \& } T_{11} = T_{22} = 1000$ as shown in Fig. 4.15. It is observed from the Fig. 5.15 that the buckling is governed by the asymmetric mode $n = 1$, when $b \leq 0.233$ for $R_{11} = 0.5 \text{ \& } T_{11} = T_{22} = 1000$. When b is increased beyond 0.233, the $n = 0$ axisymmetric mode gives the correct lower buckling load. Similarly, the buckling is governed by the asymmetric mode $n = 1$, when $b \leq 0.234$ for $R_{11} = \infty \text{ \& } T_{11} = T_{22} = 1000$. When b is increased beyond 0.234, the $n = 0$ axisymmetric mode gives the correct lower buckling load. Optimal location of

internal elastic ring support for maximum buckling load is of interest in the design of supported circular plates. The optimal solutions (optimal location of internal elastic ring support and corresponding buckling load) for this case are presented in Table 4.2. It is observed that the optimum-buckling load parameter increases with increase in rotational spring stiffness parameter, R_{11} . Introducing internal elastic ring support, when placed at an optimal position increases the elastic buckling capacity significantly, and the percentage of increase in buckling loads is presented in Table 4.2. It is observed that the percentage increase in buckling load parameter decreases with increase in R_{11} . This is due to the amount of increase in buckling load without elastic ring support with R_{11} is more than that of increase in buckling load with elastic ring support with R_{11} .

Table 4.1 Buckling (for axisymmetric and asymmetric modes) Load Parameters for different values of Rotational Stiffness Parameters, R_{11} and Constant Translational Stiffness Parameter, T_{11} and Translational Stiffness Parameter of Internal Elastic Ring, T_{22} ($T_{11} = T_{22} = 1000$) when $\nu = 0.3$

b	$R_{11} = 0.5, T_{11} = T_{22} = 1000[n = 0]$	$R_{11} = 0.5, T_{11} = T_{22} = 1000[n = 1]$	$R_{11} = 10, T_{11} = T_{22} = 1000[n = 0]$	$R_{11} = 10, T_{11} = T_{22} = 1000[n = 1]$	$R_{11} = \infty, T_{11} = T_{22} = 1000[n = 0]$	$R_{11} = \infty, T_{11} = T_{22} = 1000[n = 1]$
0	2.34422	3.77555	3.51188	4.70945	3.8531	5.13048
0.1	4.67684	4.0601	6.1039	5.06033	6.69782	5.52023
0.2	4.96006	4.81372	6.32317	6.00965	6.94504	6.61564
0.3	5.25523	5.55305	6.43411	6.88999	6.99121	7.66182
0.4	5.4671	6.29013	6.24905	7.59267	6.60737	8.37771
0.5	5.40957	6.90851	5.7695	7.67119	5.95379	3.12889
0.6	5.0828	6.8419	5.2116	7.03001	5.29611	3.86641
0.7	4.65656	6.27244	4.68264	6.29575	4.70433	4.64511
0.8	4.18204	5.60991	4.18626	5.61847	4.19007	5.09741
0.9	3.46153	4.75036	3.71744	5.01776	3.87304	5.15389
1	2.31723	3.77684	3.4889	4.71475	3.83163	5.13591

Table 4.2 Optimal Locations of an Internal Elastic Ring Support b_{opt} ; the Corresponding Buckling Load Parameter k_{opt} and the Percentage Increase in Buckling Load Parameter

$T_{11} = T_{22} = 1000$			
R_{11}	0.5	10	∞
b_{opt}	0.4050	0.3003	0.2340
k_{opt}	5.464	6.434	6.971
%	135.82	84.41	81.93

The buckling load parameters for axisymmetric and asymmetric modes and for various values of translational spring stiffness parameters of an internal *elastic ring* support ($T_{22} = 1000 \& \infty$) and keeping rotational spring stiffness parameters, R_{11} and translational spring stiffness parameter, T_{11} constant, are presented in Table 4.3. Fig. 4.16 shows the variations of buckling load parameter k , with respect to the internal *elastic ring* support radius b , for various values of translational spring stiffness parameters of an internal *elastic ring* support ($T_{22} = 1000 \& \infty$) and keeping rotational spring stiffness parameters R_{11} and translational spring stiffness parameters T_{11} are constant ($R_{11} = 100 \& T_{11} = 1000$). The cross over radius (switching of buckling mode) varies from $b = 0.1537$ to 0.2341 as shown in Fig. 4.16.

It is observed from the Fig. 4.16 that the buckling is governed by the asymmetric mode $n = 1$, when $b \leq 0.1537$ for $T_{22} = 1000 \& R_{11} = 100, T_{11} = 1000$. When b is increased beyond 0.1537 , the $n = 0$ axisymmetric mode gives the correct lower buckling load. Similarly, the buckling is governed by the asymmetric mode $n = 1$, when $b \leq 0.2341$ for $T_{22} = 10^{16} \& R_{11} = 100, T_{11} = 1000$. When b is increased beyond 0.2341 , the $n = 0$ axisymmetric mode gives the correct lower buckling load. Of interest in the design of supported circular plates is the optimal location of the internal *elastic ring* support for maximum buckling load. The optimal solutions for this case are presented in Table 5.4. Introducing internal elastic ring support, when placed at an optimal position increases the elastic buckling capacity significantly, and the percentage of increase in buckling loads is presented in Table 4.4. It is found that the percentage increase in buckling load is negligible due to the fact that there is less influence of T_{22} on buckling load parameter.

Table 4.3 Buckling (for axisymmetric and asymmetric modes) Load Parameters for different values of Translational Stiffness Parameter of Internal *Elastic Ring*, T_{22} and Constant Rotational Stiffness Parameters, $R_{11} = 100$ & Translational Stiffness Parameter, $T_{11} = 1000$ when $\nu = 0.3$

b	$T_{22} = 1000, R_{11} = 100 \& T_{11} = 1000 [n = 0]$	$T_{22} = 1000, R_{11} = 100 \& T_{11} = 1000 [n = 1]$	$T_{22} = \infty, R_{11} = 100 \& T_{11} = 1000 [n = 0]$	$T_{22} = \infty, R_{11} = 100 \& T_{11} = 1000 [n = 1]$
0	3.81535	5.07899	6.57733	5.34015

0.1	6.6333	5.46437	6.69453	6.42772
0.2	6.87437	6.54262	6.88357	7.12049
0.3	6.92542	7.56651	6.92777	7.80417
0.4	6.56336	8.2795	6.60053	8.29339
0.5	5.92915	7.97692	6.00578	8.0656
0.6	5.28363	7.12069	5.38818	7.31334
0.7	4.70083	6.3111	4.82919	6.53979
0.8	4.18947	5.62491	4.32015	5.83674
0.9	3.85064	5.17693	3.89536	5.25568
1	3.79368	5.08212	3.79368	5.08516

Table 4.4 Optimal Locations of an Internal *Elastic Ring* Support b_{opt} , the Corresponding Buckling Load Parameter and Percentage Increase in Buckling Parameter

k_{opt}	$R_{11} = 100 \text{ \& } T_{11} = 1000$	
T_{22}	1000	∞
b_{opt}	0.2905	0.2824
k_{opt}	6.921	6.928
%	82.43	82.62

The buckling load parameters for axisymmetric and asymmetric modes and for various values of translational spring stiffness parameters ($T_{11} = 1000 \text{ \& } \infty$) and keeping rotational spring stiffness parameter, R_{11} and translational spring stiffness parameter of the internal *elastic ring* support T_{22} constant are presented in Table 4.5. Fig. 4.17 show the variations of buckling load parameter k , with respect to the internal *elastic ring* support radius b , for various values of translational spring stiffness parameters ($T_{11} = 1000 \text{ \& } \infty$) and keeping rotational spring stiffness parameters R_{11} and translational spring stiffness parameters of the internal *elastic ring* support T_{22} are constant ($R_{11} = 100 \text{ \& } T_{22} = 1000$). The optimal solutions for this case are presented in Table 4.6. Introducing internal elastic ring support, when placed at an optimal position increases the elastic buckling capacity significantly, and the percentage of increase in buckling loads is presented in Table 4.6. It is observed that the percentage increase in buckling load is negligible this is due to the minute influence of T_{22} on buckling load parameter.

Table 4.5 Buckling (for axisymmetric and asymmetric modes) Load Parameters for different values of Translational Stiffness Parameter, T_{11} and Constant Rotational Stiffness Parameters, $R_{11} = 1000$ & Translational Stiffness Parameter of Internal *Elastic Ring*, $T_{22} = 1000$, when $\nu = 0.3$

b	$T_{11} = 1000, R_{11} = T_{22} = 1000[n = 0]$	$T_{11} = 1000, R_{11} = T_{22} = 1000[n = 1]$	$T_{11} = \infty, R_{11} = T_{22} = 1000[n = 0]$	$T_{11} = \infty, R_{11} = T_{22} = 1000[n = 1]$
0	3.84932	5.12531	3.84932	5.13048
0.1	6.69136	5.51456	6.69848	5.51788
0.2	6.93798	6.60828	6.93984	6.60877
0.3	6.98455	7.65218	6.98562	7.65225
0.4	6.60289	8.3678	6.6202	8.37255
0.5	5.9513	8.01422	5.99288	8.05125
0.6	5.29481	7.13382	5.36053	7.20067
0.7	4.70393	6.31373	4.7949	6.40582
0.8	4.19007	5.62602	4.28826	5.718
0.9	3.87065	5.20212	3.90033	5.22168
1	3.82784	5.12785	3.82784	5.13048

Table 4.6 Optimal Locations of an Internal *Elastic Ring* Support b_{opt} , the Corresponding Buckling Load Parameter and Percentage Increase in Buckling Load Parameter

k_{opt}	$R_{11} = 100 \& T_{22} = 1000$	
T_{11}	1000	∞
b_{opt}	0.3011	0.2893
k_{opt}	6.98	6.984
%	82.35	82.45

The buckling load parameters for axisymmetric and asymmetric modes and for various values of three spring stiffness parameters R_{11} , T_{11} & T_{22} are presented in Table 4.7. Fig. 4.18 shows the variations of buckling load parameter k , with respect to the internal *elastic ring* support radius b , for various values of translational spring stiffness parameters ($T_{11} = 1000 \& \infty$) and keeping rotational spring stiffness parameters ($R_{11} = 10 \& \infty$), translational spring stiffness parameters of the internal ring elastic support ($T_{22} = 1000 \& \infty$). The cross over radius (switching of mode) varies from $b = 0.1514$ to 0.2414 as shown in Fig. 4.18. The optimal solutions for this case are presented in Table 4.8. Introducing internal elastic ring support, when placed at an optimal position increases the elastic buckling capacity significantly, and the percentage of increase in buckling loads is presented in Table 4.8. The results of this kind were scarce in the literature. However, the results are compared with the

following cases. Table 4.9, presents the buckling load parameters k , for a circular plate with simply supported edge and rotational restraint, against those obtained by Wang et. al. [68].

Table 4.7 Buckling (for axisymmetric and asymmetric modes) Load Parameters for different values of Rotational Stiffness Parameters, R_{11} , Translational Stiffness Parameter, T_{11} and Translational Stiffness Parameter of Internal Elastic Ring, T_{22} , when $\nu = 0.3$

b	$R_{11} = 10, T_{11} = T_{22} = 1000[n = 0]$	$R_{11} = 10, T_{11} = T_{22} = 1000[n = 1]$	$R_{11} = T_{11} = T_{22} = \infty[n = 0]$	$R_{11} = T_{11} = T_{22} = \infty[n = 1]$
0	3.51188	4.70945	6.64780	5.39854
0.1	6.1039	5.06033	6.76632	6.50105
0.2	6.32317	6.00965	6.95592	7.20716
0.3	6.43411	6.88999	6.99485	7.90409
0.4	6.24905	7.59267	6.66257	8.39426
0.5	5.76950	7.67119	6.07454	8.15012
0.6	5.21160	7.03001	5.47550	7.40994
0.7	4.68264	6.29575	4.95263	6.68062
0.8	4.18626	5.61847	4.51266	6.06546
0.9	3.71744	5.01776	4.14357	5.55732
1	3.48890	4.71475	3.83194	5.13594

Table 4.8 Optimal Locations of an Internal Elastic Ring Support b_{opt} , the Corresponding Buckling Load Parameter k_{opt} and Percentage Increase in Buckling Load Parameter

T_{22}	$R_{11} = 10, T_{11} = 1000 = T_{22} = 1000$	$R_{11} = T_{11} = T_{22} = \infty$
b_{opt}	0.3003	0.2801
k_{opt}	6.434	6.987
%	84.41	82.35

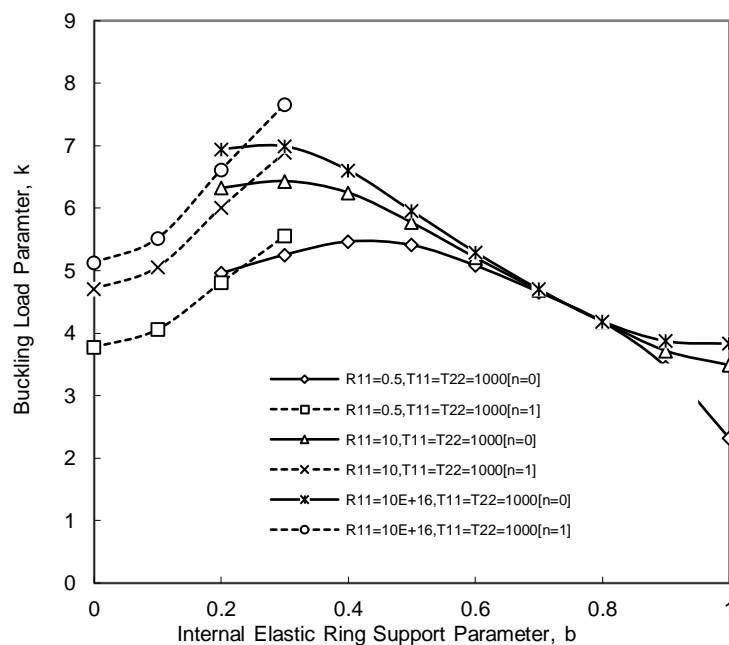


Fig. 4.15 Buckling Load Parameter k , versus Internal Elastic Ring Support Radius b , for various values of R_{11} & $T_{11} = T_{22} = 1000$

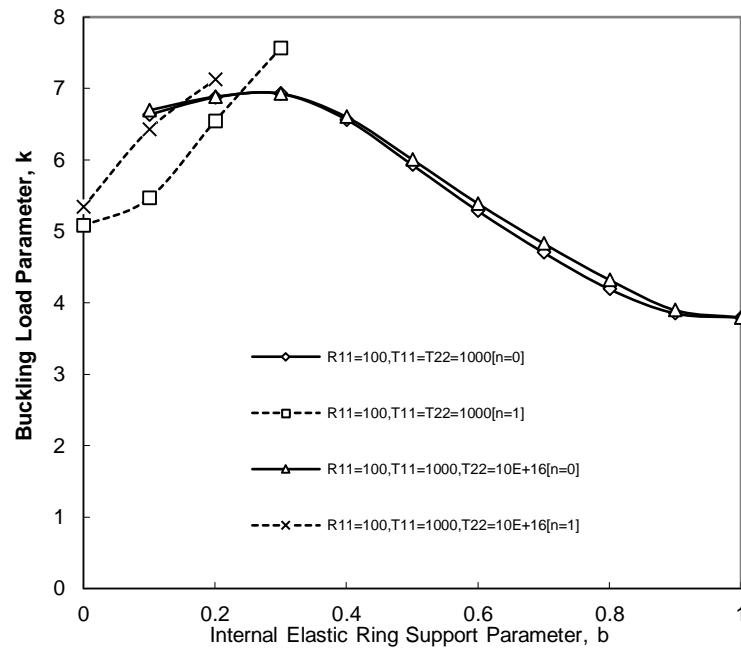


Fig. 4.16 Buckling Load Parameter k , versus Internal Elastic Ring Support Radius b , for various values of T_{22} & $R_{11} = T_{11} = 1000$

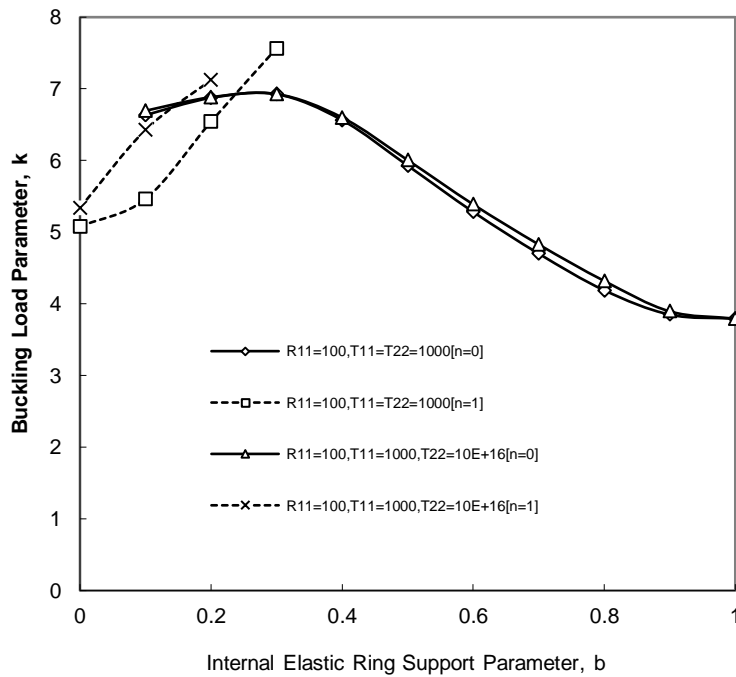


Fig. 4.17 Buckling Load Parameter k , versus Internal Elastic Ring Support Radius b , for Various Values of T_{11} & $R_{11} = T_{22} = 1000$

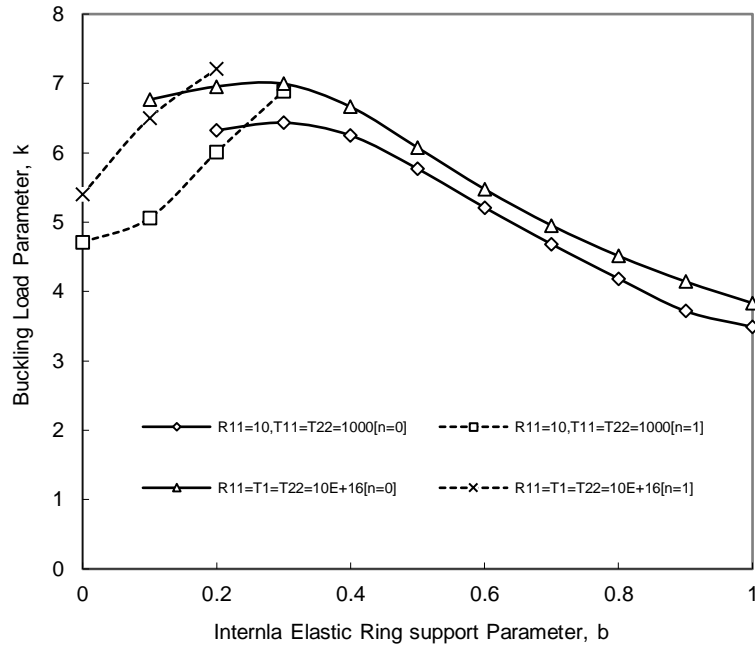


Fig. 4.18 Buckling Load Parameter k , versus Internal Elastic Ring Support Radius b , for various values of R_{11} , T_{11} & T_{22}

Table 4.9 Comparison of Buckling Load Parameter k , with Wang et al. [68] for various Rotational Stiffness Parameters R_{11} and Poisson's ratio = 0.3

R_{11}	0	0.1	5	10	100	∞
Wang et al.	4.198	4.449	10.462	12.173	14.392	14.682
Present	4.19766	4.44864	10.46134	12.17242	14.392	14.6813

Subset problems:

(i) Buckling of circular plates with internal elastic ring support and restrained edge against rotation

The buckling load parameters for axisymmetric and asymmetric modes and for various values of rotational spring stiffness parameters, R_{11} and keeping translational spring stiffness parameter, T_{22} constant, are presented in Table 4.10. Figs. 4.19 – 4.22, show the variations of buckling load parameter k , with respect to the internal elastic ring support radius b , for various values of rotational spring stiffness parameters ($R_{11} = 0, 0.5, 10, 100 & \infty$) and keeping translational spring stiffness parameter of an internal elastic ring support is constant ($T_{22} = 100000$). It is observed from Figs. 4.19 - 4.22, for a given value of R_{11} and by keeping T_{22} constant, the curve is composed of two segments. This is due to the switching of buckling

modes. For a smaller internal elastic ring support radius b , the plate buckles in an asymmetric mode (*i.e.*, $n = 1$). In this segment (as shown by dotted lines in Figs. 4.19 - 4.22) the buckling load decreases as b decreases in value. For larger internal elastic ring support radius b , the plate buckles in an axisymmetric mode (*i.e.*, $n = 0$). In this segment (as shown by continuous lines in Figs. 4.19 - 4.22) the buckling load increases as b decreases up to a peak point corresponds to maximum buckling load and thereafter decrease as b decreases in value as shown in Figs. 4.19 to 4.22.

The cross over radius (switching of mode) varies from $b = 0.09891$ for $R_{11} = 0$ & $T_{22} = 100000$ to $b = 0.1545$ for $R_{11} = \infty$ & $T_{22} = 100000$ as shown in Figs. 4.19 and 4.22 respectively. Of interest in the design of supported circular plates is the optimal location of the internal elastic ring support for maximum buckling load. The optimal solutions for this case are presented in Table 4.11. It is observed that the optimal ring support radius parameter decrease with increase in rotational spring stiffness parameter and also the optimal buckling load capacity increases with rotational spring stiffness parameter. Introducing internal elastic ring support, when placed at an optimal position increases the elastic buckling capacity significantly, and the percentage of increase in buckling loads is presented in Table 4.11. It is observed that the percentage increase in buckling load parameter decreases with increase in R_{11} . This is due to the amount of increase in buckling load without elastic ring support with R_{11} is more than that of increase in buckling load with elastic ring support with R_{11} .

Table 4.10 Buckling (for axisymmetric and asymmetric modes) Load Parameters for Different Values of Rotational Stiffness Parameters, R_{11} and Constant Translational Stiffness Parameter of Internal Elastic Ring, $T_{22} = 10000$, when $\nu = 0.3$

b	$R_{11} = 0.5,$ $T_{22} = 100000$ [$n = 0$]	$R_{11} = 0.5,$ $T_{22} = 100000$ [$n = 1$]	$R_{11} = 10,$ $T_{22} = 100000$ [$n = 0$]	$R_{11} = 10,$ $T_{22} = 100000$ [$n = 1$]	$R_{11} = 100,$ $T_{22} = 100000$ [$n = 0$]	$R_{11} = 100,$ $T_{22} = 100000$ [$n = 1$]	$R_{11} = 10^{16},$ $T_{22} = 100000$ [$n = 0$]	$R_{11} = 10^{16},$ $T_{22} = 100000$ [$n = 1$]
0	3.7306	3.77764	4.9839	4.71989	5.2932	5.08516	5.32691	5.13556
0.1	4.73024	4.70314	6.14335	5.88716	6.69638	6.40305	6.76581	6.47374
0.2	4.96415	5.21695	6.32316	6.50479	6.8834	7.11616	6.95581	7.20116
0.3	5.24126	5.76937	6.43334	7.11478	6.92927	7.80481	6.99483	7.90226

0.4	5.45584	6.37614	6.2853	7.64903	6.61681	8.30315	6.66217	8.39422
0.5	5.43249	6.89771	5.85628	7.73551	6.04508	8.09967	6.07384	8.1494
0.6	5.15166	6.90439	5.34264	7.21865	5.45473	7.3816	5.47431	7.40794
0.7	4.78153	6.45711	4.8667	6.57103	4.93636	6.65972	4.95093	6.67763
0.8	4.4232	5.95313	4.4571	5.99556	4.49839	6.04669	4.50947	6.06037
0.9	4.1023	5.50365	4.10998	5.51323	4.12642	5.53378	4.1334	5.54256
1	2.31704	3.77794	3.4889	4.71995	3.79368	5.08516	3.83163	5.13557

Table 4.11 Optimal Location of an Internal Elastic Ring Support b_{opt} , the Corresponding Buckling Load Parameter k_{opt} and Percentage Increase in Buckling Load Parameter

$T_{22} = 100000$					
R_{11}	0	0.5	10	100	∞
b_{opt}	0.4998	0.4010	0.3001	0.2982	0.2966
k_{opt}	5.3669	5.4571	6.4333	6.9313	6.9989
%	161.95	135.52	84.39	82.71	82.66

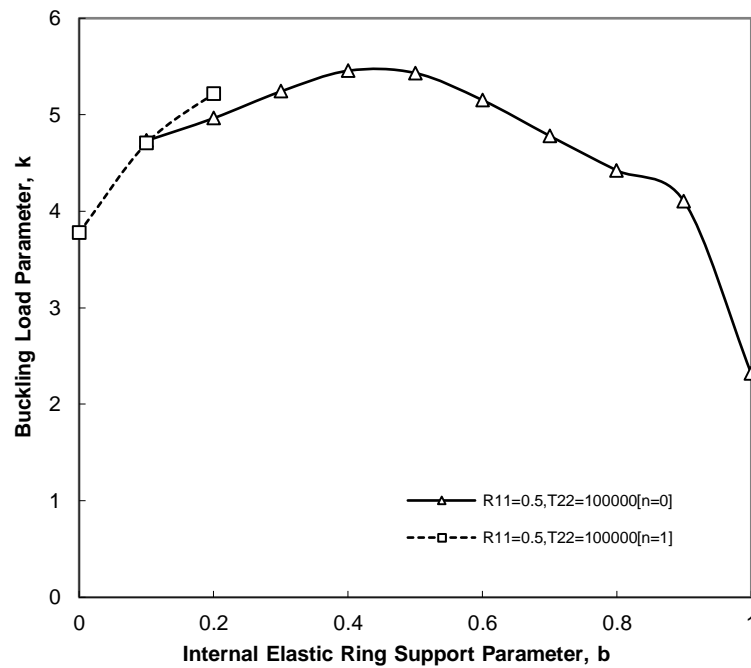


Fig. 4.19 Buckling Load Parameter k , versus Internal Elastic Ring Support Radius b , for various values of $R_{11} = 0.5$ & $T_{22} = 100000$

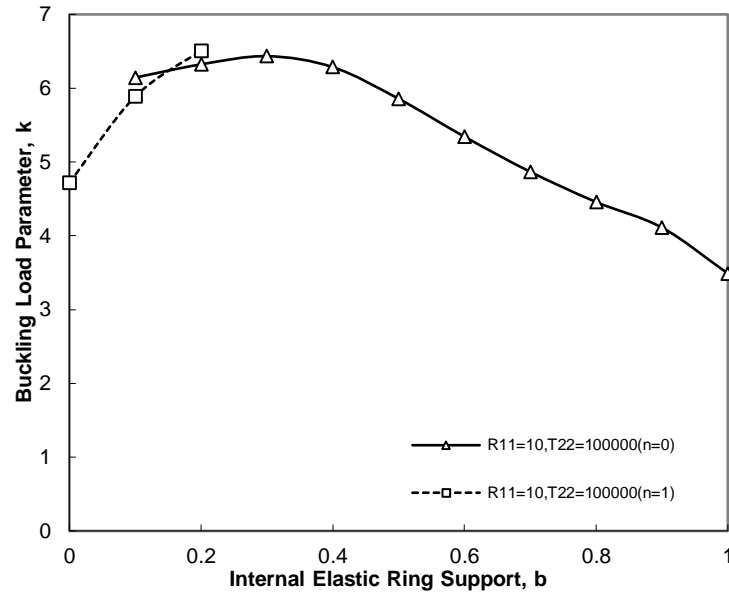


Fig. 4.20 Buckling Load Parameter k , versus Internal Elastic Ring Support Radius b , for various values of $R_{11} = 10$ & $T_{22} = 100000$

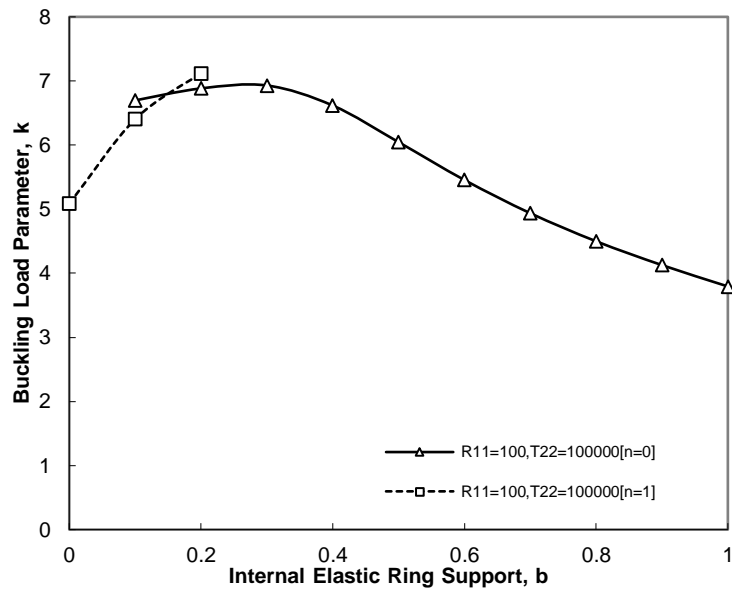


Fig. 4.21 Buckling Load Parameter k , versus Internal Elastic Ring Support Radius b , for various values of $R_{11} = 100$ & $T_{22} = 100000$

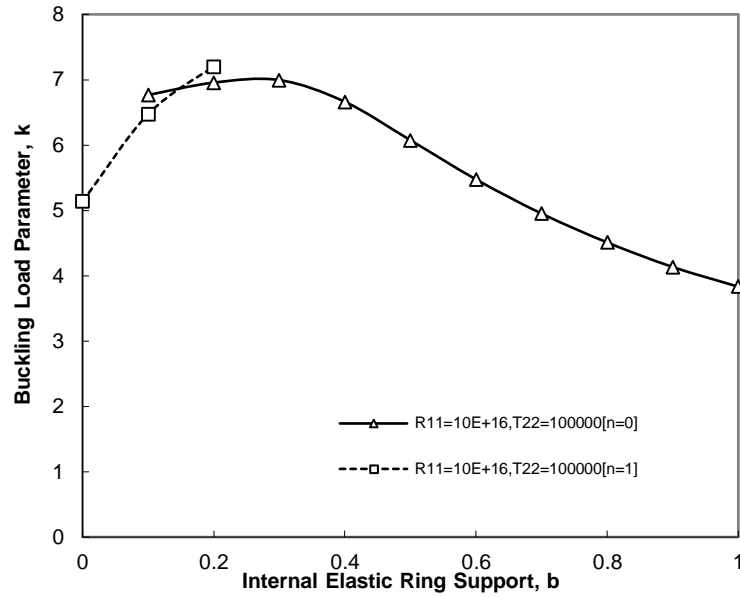


Fig. 4.22 Buckling Load Parameter k , versus Internal Elastic Ring Support Radius b , for various values of $R_{11} = \infty$ & $T_{22} = 100000$

The buckling load parameters for axisymmetric and asymmetric modes and for various values of translational spring stiffness parameter, T_{22} , and keeping rotational spring stiffness parameters, R_{11} constant, are presented in Table 4.12. The influence of translational spring stiffness parameter of an elastic ring support on buckling load for a given rotational spring stiffness parameter is shown in Figs. 4.23 – 4.25. Figs. 4.23 – 4.25 show the variations of buckling load parameter k , with respect to the internal elastic ring support radius b , for various values of translational spring stiffness parameters of an elastic ring support ($T_{22} = 1000, 100000$ & ∞) and for a given value of rotational spring stiffness parameters ($R_{11} = 1000$). It is observed from the Fig. 4.23 – 4.25, for a given value of T_{22} and by keeping R_{11} constant, the curve is composed of two segments. This is due to the switching of buckling modes. For a smaller internal elastic ring support radius b , the plate buckles in an asymmetric mode (*i.e.*, $n = 1$). In this segment (as shown by dotted lines in Fig. 4.23 – 4.25) the buckling load decreases as b decreases in value. For larger internal elastic ring support radius b , the plate buckles in an axisymmetric mode (*i.e.*, $n = 0$). In this segment (as shown

by continuous lines in Figs. 4.23 – 4.25) the buckling load increases as b decreases up to a peak point corresponds to maximum buckling load and thereafter decrease as b decreases in value as shown in Fig. 4.23 – 4.25. The cross over radius varies from $b=0.2333$ to $b=0.1518$ as shown in Figs. 4.23 and 4.25 respectively. The optimal solutions for this case are presented in Table 4.13. Introducing internal elastic ring support, when placed at an optimal position increases the elastic buckling capacity significantly, and the percentage of increase in buckling loads is presented in Table 4.13.

Table 4.12 Buckling (for axisymmetric and asymmetric modes) Load Parameters for different values of Translational Stiffness Parameter of Internal *Elastic Ring*, T_{22} and Constant Rotational Stiffness Parameters, $R_{11} = 1000$, when $\nu = 0.3$

b	$T_{22} = 1000, R_{11} = 1000$		$T_{22} = 100000, R_{11} = 1000$		$T_{22} = 10^{16}, R_{11} = 1000$	
	$[n = 0]$	$[n = 1]$	$[n = 0]$	$[n = 1]$	$[n = 0]$	$[n = 1]$
0	3.84932	5.13049	5.32351	5.13049	6.64114	5.39316
0.1	6.69848	5.51788	6.75885	6.46667	6.75936	6.49378
0.2	6.93984	6.60877	6.94855	7.1925	6.94866	7.19859
0.3	6.98562	7.65225	6.98817	7.89242	6.98818	7.89424
0.4	6.6202	8.37255	6.65758	8.38497	6.65789	8.38511
0.5	5.99288	8.05125	6.07084	8.1443	6.07154	8.14503
0.6	5.36053	7.20067	5.47231	7.40523	5.47341	7.40714
0.7	4.7949	6.40582	4.94933	6.67573	4.95103	6.67872
0.8	4.28826	5.718	4.50827	6.05878	4.51146	6.06386
0.9	3.90033	5.22168	4.13251	5.54146	4.14257	5.55602
1	3.82784	5.13048	3.82784	5.13048	3.83165	5.13595

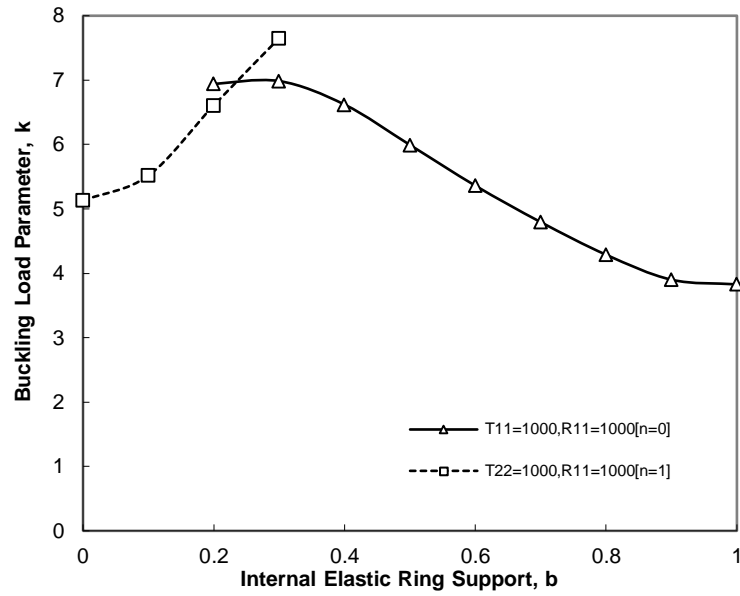


Fig. 4.23 Buckling Load Parameter k , versus Internal Elastic Ring Support Radius b , for various values of $T_{22} = 1000$ & $R_{11} = 1000$

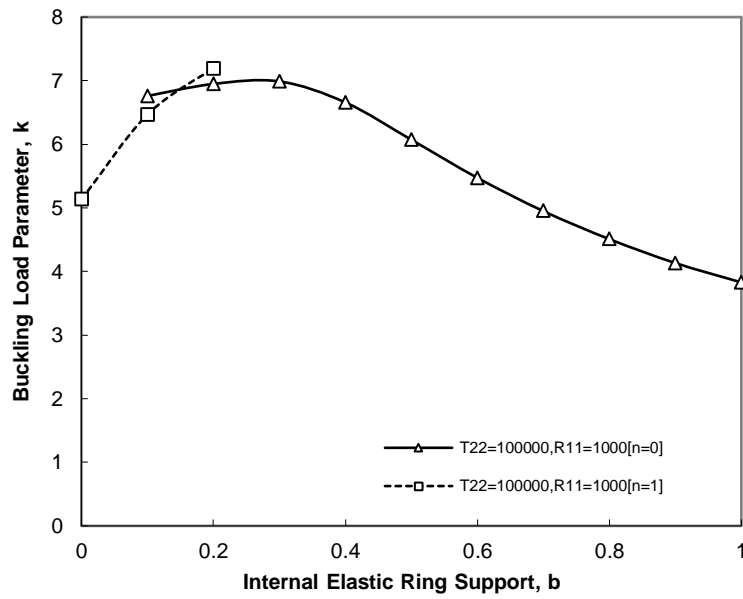


Fig. 4.24 Buckling Load Parameter k , versus Internal Elastic Ring Support Radius b , for Various Values of $T_{22} = 100000$ & $R_{11} = 1000$

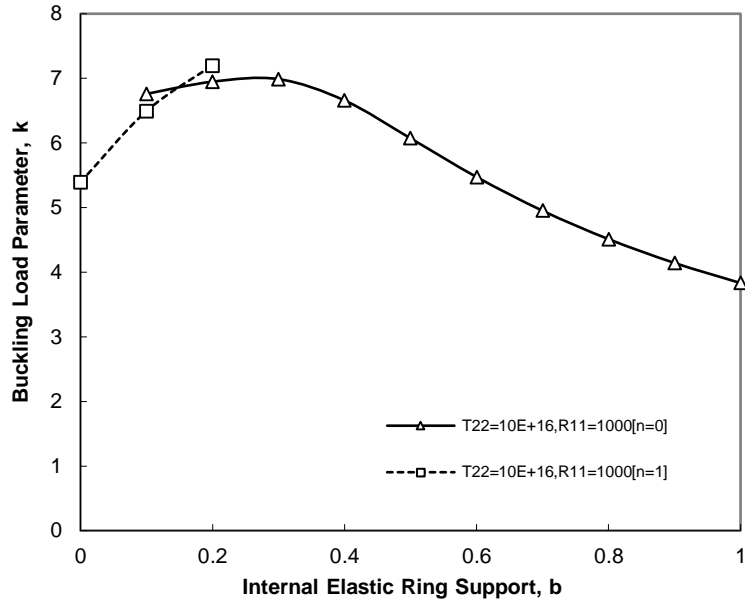


Fig. 4.25 Buckling Load Parameter k , versus Internal Elastic Ring Support Radius b , for Various Values of $T_{22} = \infty$ & $R_{11} = 1000$

Table 4.13 Optimal Locations of an Internal Elastic Ring Support b_{opt} , the Corresponding Buckling Load Parameter k_{opt} and Percentage Increase in Buckling Load Parameter

$R_{11} = 1000$			
T_{22}	1000	100000	∞
b_{opt}	0.2999	0.2987	0.2984
k_{opt}	6.9857	6.9898	6.9901
%	82.49	82.60	82.61

(ii) Buckling of circular plates with internal elastic ring support and restrained guided edge against translation

The buckling load parameters for axisymmetric and asymmetric modes and for various values of translational spring stiffness parameter, T_{11} and keeping translational spring stiffness parameter of elastic ring, T_{22} constant, is presented in Table 4.14. Figs. 4.26 and 4.27 show the variations of buckling load parameter k , with respect to the internal elastic ring support radius b , for various values of translational spring stiffness parameters ($T_{11} = 1000$ & ∞) and for a given translational spring stiffness parameters of an elastic ring support ($T_{22} = 1000$). It is

observed from Figs. 4.26 and 4.27, for a given value of T_{11} & T_{22} , the curve is composed of two segments. This is due to the switching of buckling modes. For a smaller internal elastic ring support radius b , the plate buckles in an asymmetric mode (*i.e.*, $n = 1$). In this segment (as shown by dotted lines in Figs. 4.26 and 4.27) the buckling load decreases as b decreases in value. For larger internal elastic ring support radius b , the plate buckles in an axisymmetric mode (*i.e.*, $n = 0$). In this segment (as shown by continuous lines in Figs. 4.26 and 4.27) the buckling load increases as b decreases up to a peak point corresponds to maximum buckling load and thereafter decrease as b decreases in value as shown in Figs. 4.26 and 4.27.

The cross over radius (switching of mode) varies from $b=0.2333$ for $T_{11}=1000$ & $T_{22}=1000$ to $b=0.2341$ for $T_{11}=\infty$ & $T_{22}=1000$ as shown in Figs. 4.26 and 4.27. Note that when $b \rightarrow 1$, all curves (as shown in Figs. 4.26 and 4.27) converge to $k = 3.83163$ which is the first root of $J_1(k) = 0$ of the clamped plate *i.e.*, the buckling solution approaches that of a clamped plate without any internal ring support (*i.e.*, $k = 3.83163$). This is in well agreement with those of Wang et al. [69]. The optimal solutions for this case are presented in Table 4.16. Introducing internal elastic ring support, when placed at an optimal position increases the elastic buckling capacity significantly, and the percentage of increase in buckling loads is presented in Table 4.16. It is observed that percentage increase in buckling load parameter is negligible with increase in T_{11} and this is due to the influence of T_{11} on buckling load is marginal.

Table 4.14 Buckling (for axisymmetric and asymmetric modes) Load Parameters for different values of Translational Stiffness Parameters, T_{11} when $T_{22} = 1000$ and $\nu = 0.3$

b	$T_{11} = 1000,$ $T_{22} = 1000[n = 0]$	$T_{11} = 1000,$ $T_{22} = 1000[n = 1]$	$T_{11} = 10^{16},$ $T_{22} = 1000[n = 0]$	$T_{11} = 10^{16},$ $T_{22} = 1000[n = 1]$
-----	--	--	---	---

0	3.8531	5.13048	3.8531	5.13557
0.1	6.69782	5.52023	6.70524	5.52346
0.2	6.94504	6.61564	6.9471	6.61603
0.3	6.99121	7.66182	6.99209	7.66179
0.4	6.60737	8.37771	6.62449	8.38207
0.5	5.95379	8.01841	5.99538	8.05506
0.6	5.29611	7.13542	5.36193	7.20208
0.7	4.70433	6.31403	4.7955	6.40633
0.8	4.19007	5.62621	4.28826	5.718
0.9	3.87304	5.20511	3.90202	5.22407
1	3.83163	5.13303	3.83163	5.13557

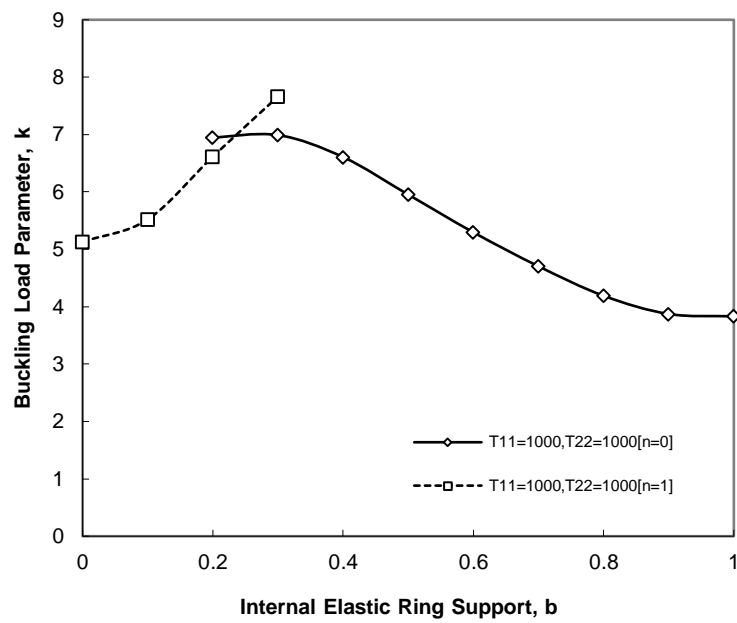


Fig. 4.26 Buckling Load Parameter k , versus Internal Elastic Ring Support Radius b , for various values of $T_{11} = T_{22} = 1000$

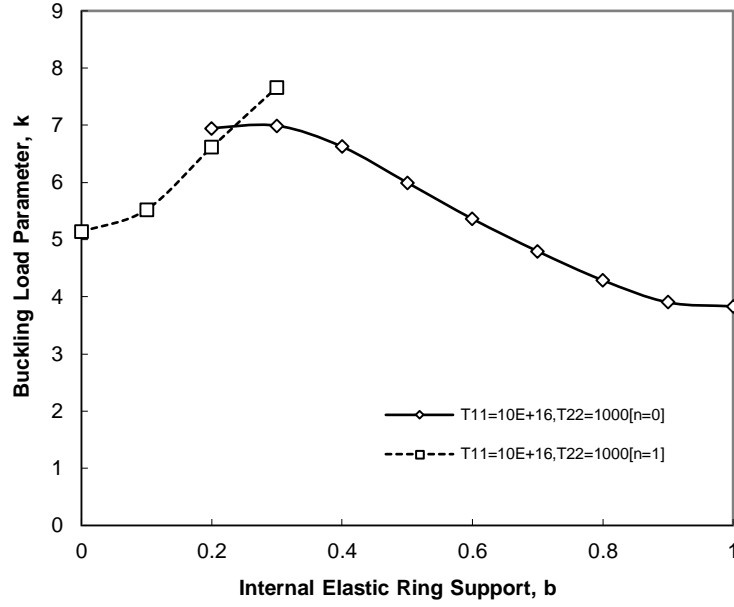


Fig. 4.27 Buckling Load Parameter k , versus Internal Elastic Ring Support Radius b , for various values of $T_{11} = \infty$ & $T_{22} = 1000$

The buckling load parameters for axisymmetric and asymmetric modes and for various values of Translational Stiffness Parameters of Elastic Ring support, T_{22} and keeping translational spring stiffness parameter, T_{11} constant, is presented in Table 4.15. Figs. 4.28 and 4.29 show the variations of buckling load parameter k , with respect to the internal elastic ring support radius b , for various values of translational spring stiffness parameters of an elastic ring support ($T_{22} = 1000$ & ∞) and for a given value of translational spring stiffness parameters ($T_{11} = 1000$). It is observed from the Figs. 4.28 and 4.29, for a given value of T_{11} & T_{22} , the curve is composed of two segments. This is due to the switching of buckling modes. For a smaller internal elastic ring support radius b , the plate buckles in an asymmetric mode (*i.e.*, $n = 1$). In this segment (as shown by dotted lines in Figs. 4.28 and 4.29) the buckling load decreases as b decreases in value. For larger internal elastic ring support radius b , the plate buckles in an axisymmetric mode (*i.e.*, $n = 0$). In this segment (as shown by continuous lines in Figs. 4.28 and 4.29) the buckling load increases as b decreases

up to a peak point corresponds to maximum buckling load and thereafter decrease as b decreases in value as shown in Figs.4.28 and 4.29.

Table 4.15 Buckling (for axisymmetric and asymmetric modes) Load Parameters for Different Values of Translational Stiffness Parameters of Elastic Ring Support, T_{22} when $T_{11} = 1000$ and $\nu = 0.3$

b	$T_{22} = 1000, T_{11} = 1000$		$T_{22} = 10^{16}, T_{11} = 1000$	
	$[n = 0]$	$[n = 1]$	$[n = 0]$	$[n = 1]$
0	3.8531	5.13048	6.64071	5.39473
0.1	6.69782	5.52023	6.76119	6.49999
0.2	6.94504	6.61564	6.95429	7.20665
0.3	6.99121	7.66182	6.99411	7.90328
0.4	6.60737	2.51093	6.64804	8.38855
0.5	5.95379	3.12889	6.0357	8.1203
0.6	5.29611	3.86641	5.40693	7.34148
0.7	4.70433	4.64511	4.83916	6.55393
0.8	4.19007	5.09741	4.32123	5.8383
0.9	3.87304	5.15389	3.9079	5.26939
1	3.83163	5.13591	3.83163	5.13557

The cross over radius (switching of mode) varies from $b=0.2333$ for $T_{22}=1000 \& T_{11}=1000$ to $b=0.1514$ for $T_{22}=\infty \& T_{11}=1000$ as shown in Figs. 4.28 and 4.29. Note that when $b \rightarrow 1$, all curves (as shown in Figs. 4.28 and 4.29) converge to $k = 3.83163$ which is the first root of $J_1(k) = 0$ of the clamped plate i.e., the buckling solution approaches that of a clamped plate without any internal ring support (i.e., $k = 3.83163$). This is in well agreement with those of Wang et al. [69]. The optimal solutions for this case are presented in Table 4.17. Introducing internal elastic ring support, when placed at an optimal position increases the elastic buckling capacity significantly, and the percentage of increase in buckling loads is presented in Table 4.17. It is observed that percentage increase in buckling load parameter is negligible with increase in T_{22} and this is due to the influence of T_{22} on buckling load is marginal.

The results of this kind were scarce in the literature. However, the results are compared with the following case i.e., the buckling load parameters k , for a circular plate with clamped

edge, against those obtained by Wang et. al. [69]. For $K_{T1} \rightarrow 0$, this case becomes the sliding edge with an internal elastic ring support and the buckling load for this case is $k = 3.83163$.

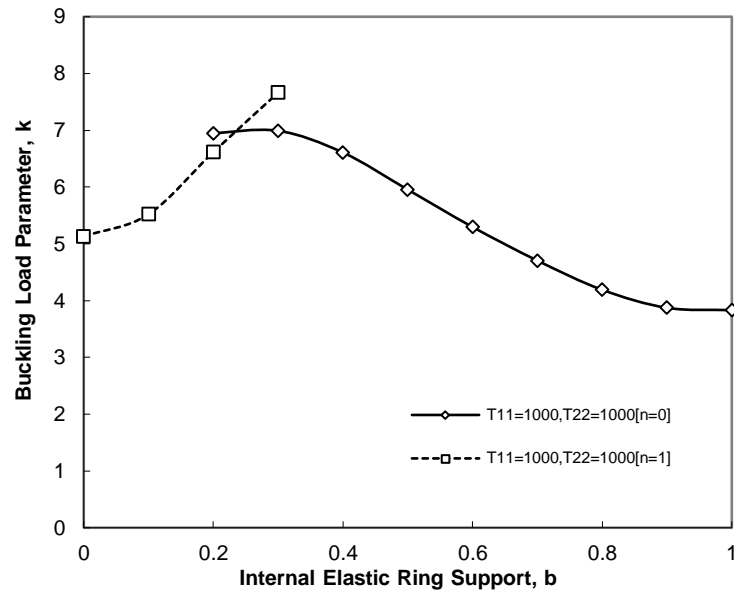


Fig. 4.28 Buckling Load Parameter k , versus Internal Elastic Ring Support Radius b , for various values of $T_{11} = T_{22} = 1000$

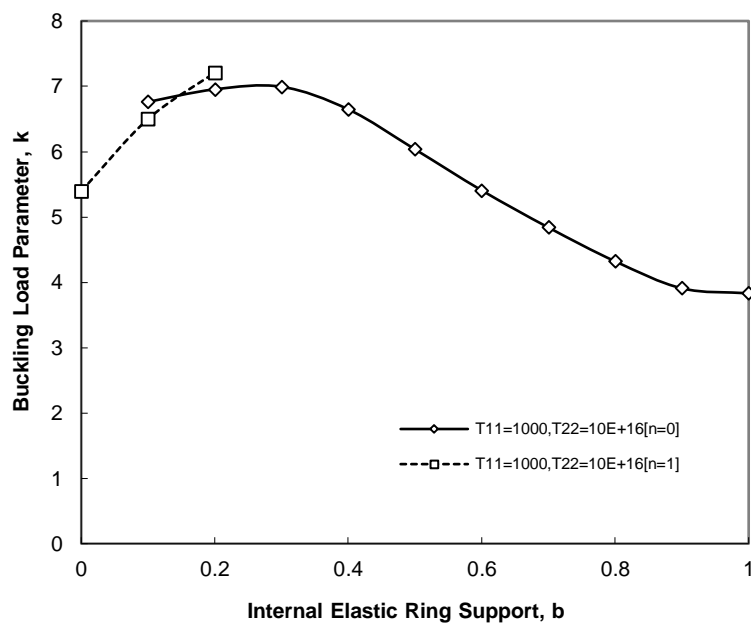


Fig. 4.29 Buckling Load Parameter k , versus Internal Elastic Ring Support Radius b , for Various Values of $T_{11} = 1000$ & $T_{22} = \infty$

Table 4.16 Optimal Location of an Internal Elastic Ring Support b_{opt} , the Corresponding Buckling Load Parameter k_{opt} and Percentage Increase in Buckling Load Parameter

$T_{22} = 1000$		
T_{11}	1000	∞
b_{opt}	0.300	0.2993
k_{opt}	6.991	6.99308
%	82.45	82.51

Table 4.17 Optimal Locations of an Internal Elastic Ring Support b_{opt} , the Corresponding Buckling Load Parameter k_{opt} and Percentage Increase in Buckling Load Parameter

$T_{11} = 1000$		
T_{22}	1000	∞
b_{opt}	0.3	0.2993
k_{opt}	6.991	6.995
%	82.45	82.56

(iii) Buckling of circular plates with internal *elastic ring* support and *restrained edge against translation*

The buckling load parameters for *axisymmetric* and *asymmetric* modes and for various values of Translational Stiffness Parameters of Elastic Ring support, T_{22} and keeping translational spring stiffness parameter, T_{11} constant, is presented in Table 4.18. Fig. 4.30 shows the variation of buckling load parameter, k versus elastic ring support parameter, b for translational spring stiffness parameter of an elastic ring support ($T_{22} = 100$) and translational spring stiffness parameter ($T_{11} = 10000$). It is observed that the $n = 0$ symmetric solution weaves with $n = 1$ asymmetric solution. When $\nu = 0$, the untethered plate buckles axisymmetrically with $k = 2.05171$. When b increased beyond 0.125 ($k = 3.71692$), the $n = 1$ asymmetric mode gives the correct lower buckling load. This persists until $b = 0.5161$ ($k = 5.13575$) where the $n = 0$ mode again determines the buckling load. It is observed from

the Fig. 4.24 that the buckling is governed by the *axisymmetric* mode $n = 0$, when $b \leq 0.125$ and $b \geq 0.5161$. The optimal location of an internal elastic ring support (b_{opt}) is 0.5161 and the corresponding buckling load parameter (k_{opt}) is 5.13575. For this case, an internal elastic ring support, when placed at an optimal position, can increase the buckling load capacity by 34%.

Fig. 4.31 shows the variation of buckling load parameter k , with respect to the internal elastic ring support radius b , for translational spring stiffness parameter of an elastic ring support ($T_{22} = 10^{16}$) and translational spring stiffness parameter ($T_{11} = 10000$). It is observed from the Fig. 4.31, for a given value of T_{11} & T_{22} , the curve is composed of two segments. This is due to the switching of buckling modes. For a smaller internal elastic ring support radius b , the plate buckles in an asymmetric mode (*i.e.*, $n = 1$). In this segment (as shown by dotted lines in Fig. 4.31) the buckling load decreases as b decreases in value. For larger internal elastic ring support radius b , the plate buckles in an axisymmetric mode (*i.e.*, $n = 0$). In this segment (as shown by continuous lines in Fig. 4.31) the buckling load increases as b decreases up to a peak point corresponds to maximum buckling load and thereafter decrease as b decreases in value as shown in Fig. 4.31. The cross over radius is 0.09371 ($k = 4.508325$). It is observed from the Fig. 4.31 that the *asymmetric* buckling mode dominates small elastic ring support radius parameter b , situation *i.e.*, $b \leq 0.09371$. The optimal location of an internal elastic ring support (b_{opt}) is 0.48980 and the corresponding buckling load parameter (k_{opt}) is 5.363089. Similarly for this case, an internal elastic ring support, when placed at an optimal position, can increase the buckling load capacity by 40%.

Table 4.18 Buckling (for axisymmetric and asymmetric modes) Load Parameters for Different Values of Translational Stiffness of Elastic Ring Parameter, T_{22} when $T_{11} = 10000$ and $\nu = 0.3$

b	$T_{22} = 100, T_{11} = 10000$		$T_{22} = 10^{16}, T_{11} = 10000$	
	$[n = 0]$	$[n = 1]$	$[n = 0]$	$[n = 1]$

0	2.05171	3.62463	4.40403	3.81036
0.1	3.54546	3.66107	4.52668	4.55422
0.2	4.17149	3.86098	4.77366	5.05184
0.3	4.66723	4.22897	5.07429	5.60533
0.4	5.16055	4.68984	5.33153	6.22488
0.5	5.23921	5.11781	5.36541	6.7861
0.6	4.5961	5.22724	5.1224	6.85729
0.7	3.94715	4.90345	4.7666	6.43801
0.8	3.25764	4.40407	4.40967	5.93723
0.9	2.50951	3.89459	4.06498	5.45838
1	2.04882	3.62463	2.04912	3.62512

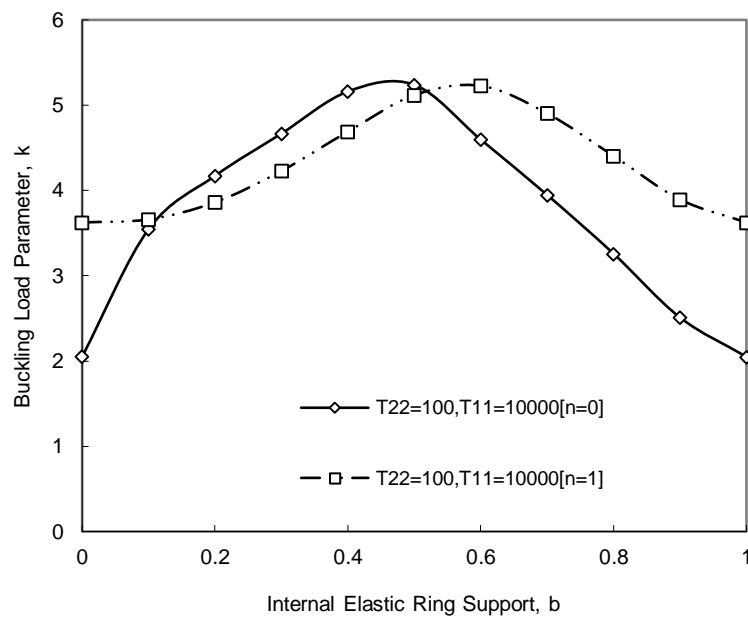


Fig. 4.30 Buckling Load Parameter k , versus Internal Elastic Ring Support Radius b , for various values of T_{22} ($=100$) when $T_{11} = 10000$

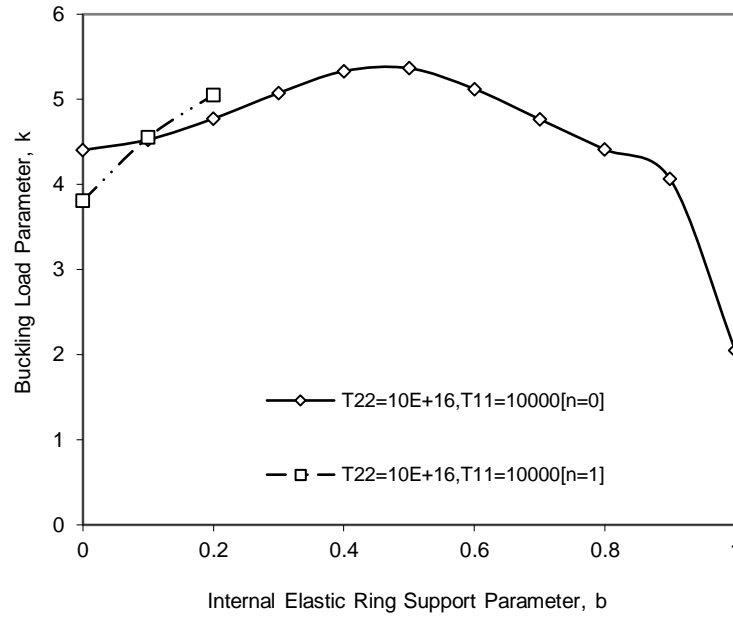


Fig. 4.31 Buckling Load Parameter k , versus Internal Elastic Ring Support Radius b , for various values of $T_{22} (= 10^{16})$ when $T_{11} = 10000$

(iv) Buckling of circular plates with internal *elastic ring* support and *guided edge*

It is observed that the buckling is independent of the internal elastic ring support if the buckling mode is axisymmetric. It gives a constant buckling load parameter and the buckling load is $k = 3.83163$. And it is also observed that the *asymmetric* buckling mode dominates small values of elastic ring support parameter, b and stiffness parameter of elastic ring support, T_{22} situations.

(v) Buckling of circular plates with internal *elastic ring* support and *simply supported edge*

The buckling load parameters for axisymmetric and asymmetric modes and for various values of translational stiffness parameters of elastic ring support T_{22} are presented in Table 4.19. Fig. 4.32 shows the variation of buckling load parameter, k versus elastic ring support parameter, b for a given translational spring stiffness parameter of an elastic ring support ($T_{22} = 100$). It is observed that the $n = 0$ *axisymmetric* solution weaves with $n = 1$ *asymmetric*

solution. When $\nu=0$, the untethered plate buckles axisymmetrically with $k=2.04882$. When b increased beyond 0.12611 ($k=3.71692$), the $n=1$ asymmetric mode gives the correct lower buckling load. This persists until $b=0.5179$ ($k=5.13137$) where the $n=0$ mode again determines the buckling load. When $b=1$, the buckling load is $k=2.04882$, which is the first root of the following equation,

$$kJ_0(k) - (1-\nu)J_1(k) = 0$$

(4.93)

And it is corresponding to the axisymmetric mode as shown in Fig. 4.32. It is observed from the Fig. 4.32 that the buckling is governed by the *axisymmetric* mode $n=0$, when $b \leq 0.12611$ and $b \geq 0.5179$. The optimal location of an internal elastic ring support (b_{opt}) is 0.5179 and the corresponding buckling load parameter (k_{opt}) is 5.13137. For this case, an internal elastic ring support, when placed at an optimal position, can increase the buckling load capacity by 150%. Percentage of increase in buckling loads k , for a given translational spring stiffness parameter of an internal elastic ring ($T_{22}=100$) by providing internal elastic ring support is shown in Fig. 4.33.

Fig. 4.34 shows the variation of buckling load parameter k , with respect to the internal elastic ring support radius b , for translational spring stiffness parameter of an elastic ring support ($T_{22}=10^{16}$). It is observed from the Fig. 4.34, for a given value of T_{22} , the curve is composed of two segments. This is due to the switching of buckling modes. For a smaller internal elastic ring support radius b , the plate buckles in an *asymmetric* mode (*i.e.*, $n=1$). In this segment (as shown by dotted lines in Fig. 4.34) the buckling load decreases as b decreases in value. For larger internal elastic ring support radius b , the plate buckles in an *axisymmetric* mode (*i.e.*, $n=0$). In this segment (as shown by continuous lines in Fig. 4.34) the buckling load increases as b decreases up to a peak point corresponds to maximum

buckling load and thereafter decrease as b decreases in value as shown in Fig. 4.34. The cross over radius is 0.09508 ($k = 4.5375$). It is noticed that the *asymmetric* buckling mode dominates small elastic ring support radius parameter b , situation i.e., $b \leq 0.09508$. The optimal location of an internal elastic ring support (b_{opt}) is 0.50 and the corresponding buckling load parameter (k_{opt}) is 5.36659. Similarly for this case, an internal elastic ring support, when placed at an optimal position, can increase the buckling load capacity by 162%. Percentage of increase in buckling loads k , for a given translational spring stiffness parameter of an internal elastic ring ($T_{22} = 100$) by providing internal elastic ring support is shown in Fig. 4.35. The influence of stiffness parameter of elastic ring support is not very much on buckling load at lower values of T_{22} . And also it is observed that the influence of stiffness parameter of elastic ring support is more on buckling load at higher values of T_{22} . The buckling loads increases with increase in value of T_{22} .

Table 4.19 Buckling (for axisymmetric and asymmetric modes) Load Parameters for Different Values of Translational Spring Stiffness Parameter of an Internal Elastic Ring, T_{22} when $\nu = 0.3$

b	$T_{22} = 0.5$		$T_{22} = 100$		$T_{22} = 10^{16}$	
	$[n = 0]$	$[n = 1]$	$[n = 0]$	$[n = 1]$	$[n = 0]$	$[n = 1]$
0	2.04882	3.62463	2.05171	3.62463	4.40095	3.81016
0.1	2.06297	3.62482	3.54368	3.66107	4.52341	4.55263
0.2	2.07492	3.62592	4.16821	3.86059	4.77018	5.04915
0.3	2.08289	3.62841	4.66238	4.22788	5.07091	5.60095
0.4	2.08588	3.63159	5.15444	4.68745	5.32964	6.21912
0.5	2.08378	3.63408	5.2427	5.11365	5.36659	6.78183
0.6	2.07731	3.63478	4.59865	5.22337	5.12606	6.85994
0.7	2.06835	3.63299	3.94953	4.90126	4.77266	6.44514
0.8	2.05898	3.6295	3.25983	4.40258	4.42141	5.95154
0.9	2.05161	3.62612	2.51061	3.8931	4.10629	5.50984
1	2.04882	3.62463	2.04882	3.62463	3.83192	5.13596

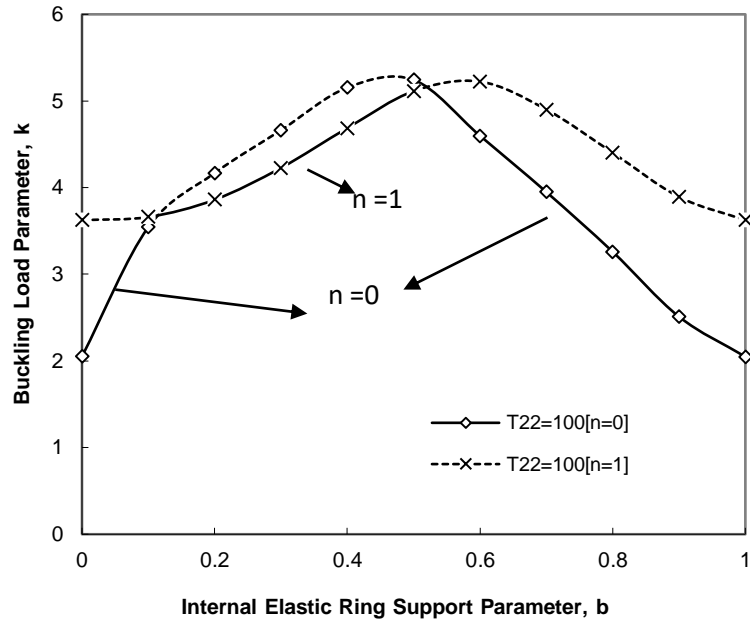


Fig. 4.32 Buckling Load Parameter k , versus Internal Elastic Ring Support Radius b , for Translational Spring Stiffness Parameter of an internal Elastic Ring, $T_{22}=100$

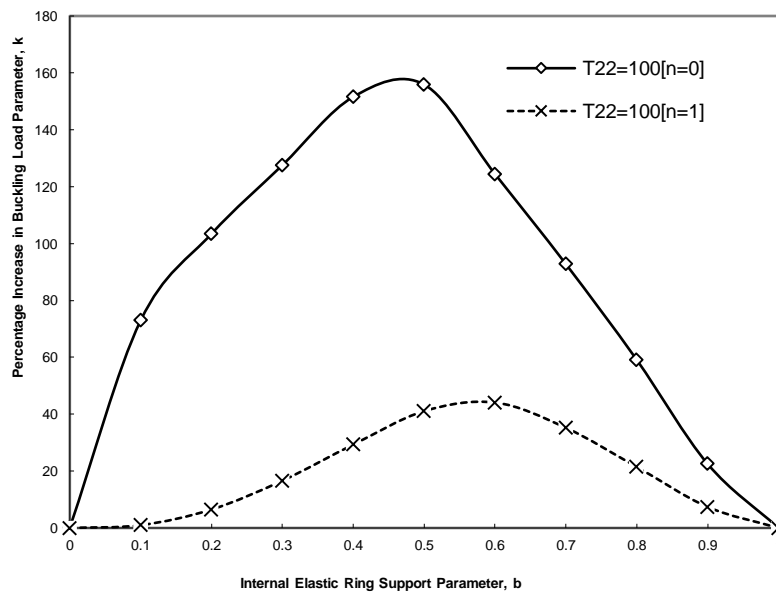


Fig. 4.33 Percentage of Increase in Buckling Load Parameter k , versus Internal Elastic Ring Support Radius b , for Translational Spring Stiffness Parameter of an internal Elastic Ring, $T_{22}=100$

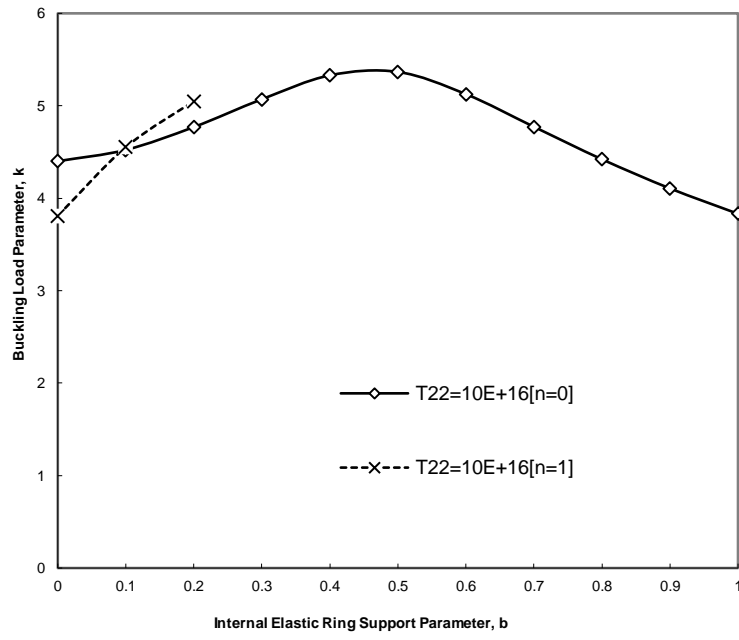


Fig. 4.34 Buckling Load Parameter k , versus Internal Elastic Ring Support Radius b , for Translational Spring Stiffness Parameter of an internal Elastic Ring, $T_{22} = 10^{16}$

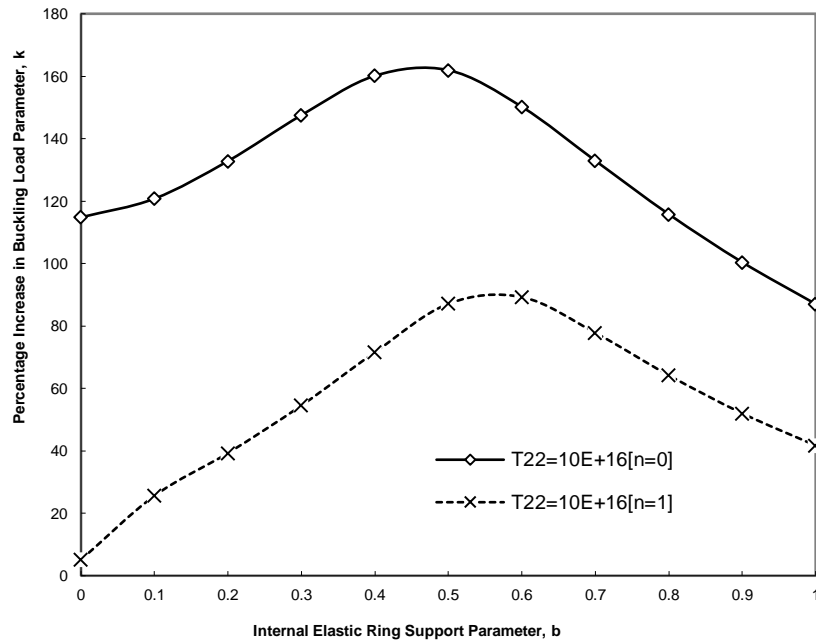


Fig. 4.35 Percentage of Increase in Buckling Load Parameter k , versus Internal Elastic Ring Support Radius b , for Translational Spring Stiffness Parameter of an internal Elastic Ring, $T_{22} = 10^{16}$

(vi) Buckling of circular plates with internal *elastic ring* support and *clamped edge*

The buckling load parameters for axisymmetric and asymmetric modes and for various values of Translational Stiffness Parameter of Elastic Ring support T_{22} are presented in Table 4.20. Fig. 4.36 shows the variation of buckling load parameter, k versus elastic ring support parameter, b for translational spring stiffness parameter of an elastic ring support ($T_{22} = 100$). It is observed that the $n = 0$ axisymmetric solution weaves with $n = 1$ asymmetric solution. When $\nu = 0$, the untethered plate buckles axisymmetrically with $k = 3.83381$. When b increased beyond 0.087562 ($k = 5.16957$), the $n = 1$ asymmetric mode gives the correct lower buckling load. This persists until $b = 0.3666$ ($k = 6.15977$) where the $n = 0$ mode again determines the buckling load. When $b = 1$, the buckling load is $k = 3.83163$, which is the first root of the following equation,

$$J_1(k) = 0 \quad (4.94)$$

And it is corresponding to the axisymmetric mode as shown in Fig. 4.36. It is observed from the Fig. 4.36 that the buckling is governed by the *axisymmetric* mode $n = 0$, when $b \leq 0.087562$ and $b \geq 0.3666$. The optimal location of an internal elastic ring support (b_{opt}) is 0.3666 and the corresponding buckling load parameter (k_{opt}) is 6.15977. For this case, an internal elastic ring support, when placed at an optimal position, can increase the buckling load capacity by 61%. Percentage of increase in buckling load versus internal elastic ring support parameter, for a given $T_{22} = 100$, by providing internal elastic ring support is shown in Fig. 4.37.

Fig. 4.38 shows the variation of buckling load parameter k , with respect to the internal elastic ring support parameter b , for a given translational spring stiffness parameter of an elastic ring support ($T_{22} = 10^{16}$). It is observed from the Fig. 4.38, for a given value of T_{22} , the curve is composed of two segments. This is due to the switching of buckling modes. For a smaller internal elastic ring support radius b , the plate buckles in an asymmetric mode

(i.e., $n = 1$). In this segment (as shown by dotted lines in Fig. 4.38) the buckling load decreases as b decreases in value. For larger internal elastic ring support radius b , the plate buckles in an axisymmetric mode (i.e., $n = 0$). In this segment (as shown by continuous lines in Fig. 4.38) the buckling load increases as b decreases up to a peak point corresponds to maximum buckling load and thereafter decrease as b decreases in value as shown in Fig. 4.38. The cross over radius is 0.1532 ($k = 6.87049$). It is noticed from the Fig. 5.38 that the *asymmetric* buckling mode dominates small elastic ring support radius parameter b , situation i.e., $b \leq 0.1532$. The optimal location of an internal elastic ring support (b_{opt}) is 0.2968 and the corresponding buckling load parameter (k_{opt}) is 6.9987. For this case, an internal elastic ring support, when placed at an optimal position, can increase the buckling load capacity by 83%. Percentage of increase in buckling load versus internal elastic ring support parameter, for a given $T_{22} = 10^{16}$, by providing internal elastic ring support is shown in Fig. 4.39.

It is observed that the effect of the supporting elastic ring is absent if the ring radius b is one, because at $b = 1$ the outer fixed edge dominates. Similarly the effect of the internal elastic ring support is negligible for $b = 0$. The influence of stiffness parameter of elastic ring support is not very much on buckling load at lower values of T_{22} . And also it is observed that the influence of stiffness parameter of elastic ring support is more on buckling load at higher values of T_{22} . The buckling loads increases with increase in value of T_{22} . When $T_{22} \rightarrow \infty$, i.e., when the support is rigid, the buckling is governed by the asymmetric mode $n = 1$ when $b \leq 0.152$ and this is in well agreement with the results of Wang and Wang [3]. When $T_{22} \rightarrow \infty$, i.e., rigid ring support, the optimum location is at a radius of $b = 0.2663$, with a buckling load of $k = 7.0156$ that is in well agreement with the results of Wang and Wang [3].

Table 4.20 Buckling (for axisymmetric and asymmetric modes) Load Parameters for Different Values of Translational Stiffness Parameter of Internal Elastic Ring, T_{22} when $\nu = 0.3$

b	$T_{22} = 0.5$		$T_{22} = 100$		$T_{22} = 10^{16}$	
	$[n = 0]$	$[n = 1]$	$[n = 0]$	$[n = 1]$	$[n = 0]$	$[n = 1]$

0	3.83163	5.13556	3.83381	5.13556	6.6478	5.39854
0.1	3.84187	5.13586	5.35271	5.18509	6.76632	6.50105
0.2	3.84903	5.13726	6.25771	5.4449	6.95592	7.20716
0.3	3.85141	5.13984	6.57573	5.88086	6.99485	7.90409
0.4	3.84923	5.14203	5.92394	6.27428	6.66257	8.39426
0.5	3.84416	5.14232	5.24445	6.28338	6.07454	8.15012
0.6	3.83859	5.14064	4.66576	5.93642	5.4755	7.40994
0.7	3.83441	5.13805	4.22013	5.54137	4.95263	6.68062
0.8	3.83232	5.13626	3.9416	5.25944	4.51266	6.06546
0.9	3.83173	5.13566	3.84049	5.14642	4.14357	5.55732
1	3.83163	5.13557	3.83163	5.13557	3.83193	5.13594

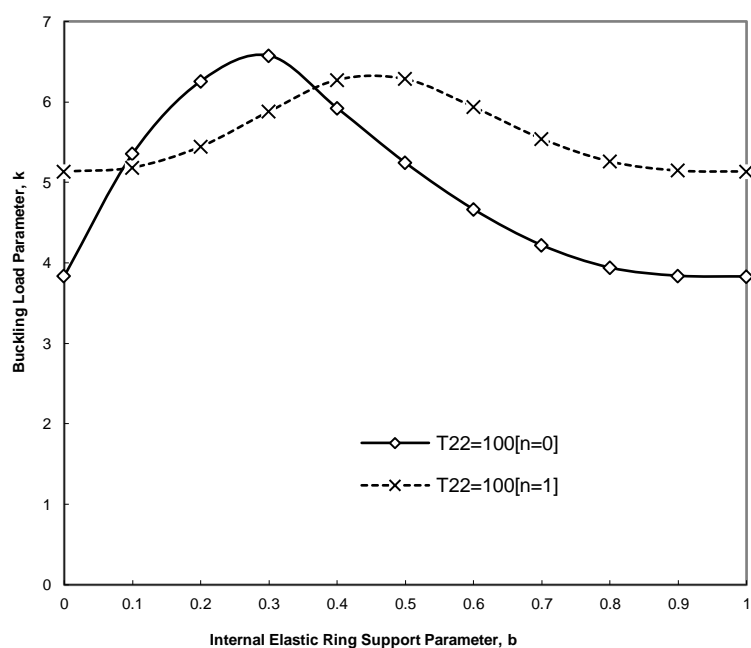


Fig. 4.36 Buckling Load Parameter k , versus Internal Elastic Ring Support Parameter b , for Translational Spring Stiffness Parameter of an Internal Elastic Ring, $T_{22}=100$

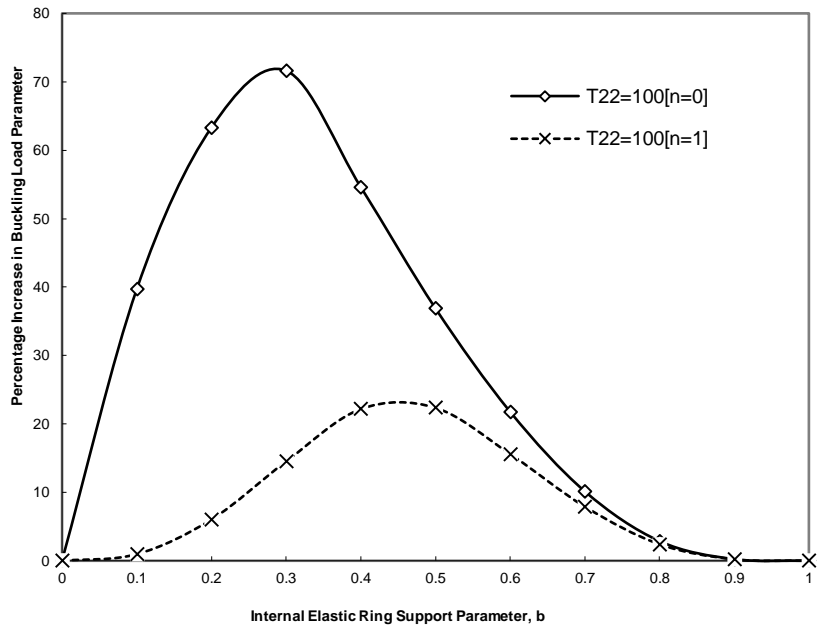


Fig. 4.37 Percentage of Increase in Buckling Load Parameter k , versus Internal Elastic Ring Support Parameter b , for Translational Spring Stiffness Parameter of an Internal Elastic Ring, $T_{22}=100$

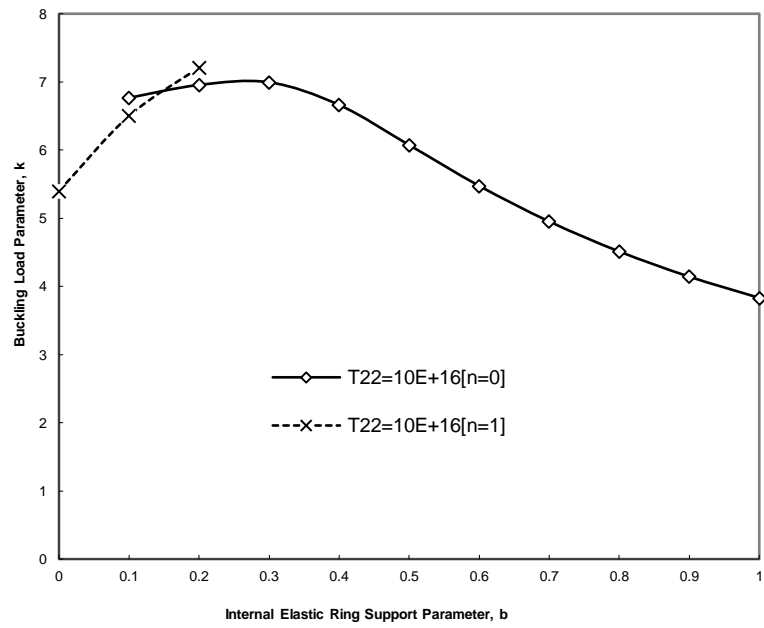


Fig. 4.38 Buckling Load Parameter k , versus Internal Elastic Ring Support Parameter b , for Translational Spring Stiffness Parameter of an Internal Elastic Ring, $T_{22} = 10^{16}$

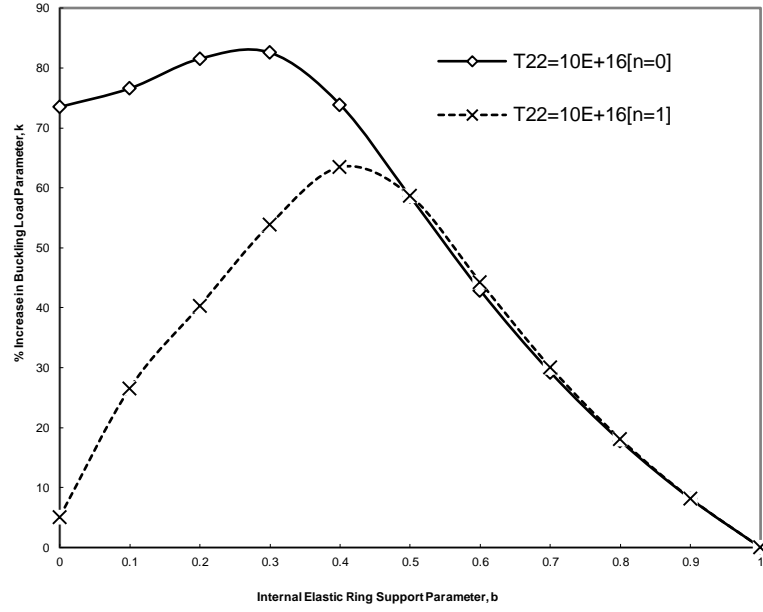


Fig. 4.39 Percentage of Increase in Buckling Load Parameter k , versus Internal Elastic Ring Support Parameter b , for Translational Spring Stiffness Parameter of an Internal Elastic Ring, $T_{22} = 10^{16}$

SPECIAL CASE: When $K_{T2} \rightarrow \infty$ in Fig. 4.1, the above problem becomes buckling of circular plates with internal **rigid ring** support and elastically restrained edge against rotation and translation as shown in Fig. 4.9.

Buckling load parameters for axisymmetric and asymmetric modes and for various values of rotational and translational spring stiffness parameters are presented in Table 4.21. Figs. 4.40 – 4.43 show the variations of buckling load parameter k , with respect to the *internal ring* support radius b , for various values of rotational and translational spring stiffness parameters. It is observed from Figs. 4.40-4.43, that for a given value of rotational and translational spring stiffness parameters, the curve is composed of two segments. This is due to the switching of buckling modes. For a smaller *internal ring* support radius b , the plate buckles in an asymmetric mode (i.e. $n \neq 0$). In this segment (as shown by dotted lines in Figs. 4.40-4.43) the buckling load decreases as b decreases in value. For a larger *internal ring* support radius b , the plate buckles in an axisymmetric mode (i.e. $n = 0$). In this segment (as

shown by continuous lines in Figs. 4.40-4.43) the buckling load increases as b decreases up to a peak point corresponds to maximum buckling load and thereafter decreases as b decreases in value as shown in Figs. 4.40-4.43. The cross over radius i.e., mode switching for various values of rotational and translational spring stiffness parameters are presented in Table 4.22. As $R_{11} \& T_{11} \rightarrow \infty$, the edge of the plate becomes clamped and as $b \rightarrow 1$, the buckling solution for this case is 3.83163. This is in good agreement with that of Wang and Wang [3].

Table 4.21 Buckling (for axisymmetric and asymmetric modes) Load Parameters for Different Values of Rotational, R_{11} and Translational Stiffness, T_{11} Parameters when $\nu = 0.3$

b	$R_{11} = 0.3, T_{11} = 100$		$R_{11} = 0.5, T_{11} = 1000$		$R_{11} = T_{11} = \infty$	
	$n = 0$	$n = 1$	$n = 0$	$n = 1$	$n = 0$	$n = 1$
0	4.89743	3.91863	4.64572	3.96743	6.6478	5.39854
0.1	5.02685	4.80513	4.763	4.73549	6.76632	6.50105
0.2	5.27558	5.43758	4.9979	5.24637	6.95592	7.20716
0.3	5.50412	6.16939	5.27144	5.81058	6.99485	7.90409
0.4	5.53837	6.89897	5.46841	6.42815	6.66257	8.39426
0.5	5.29439	7.11677	5.41565	6.9268	6.07454	8.15012
0.6	4.86967	6.70441	5.11353	6.87217	5.4755	7.40994
0.7	4.35806	6.05246	4.72154	6.38876	4.95263	6.68062
0.8	3.73599	5.30321	4.3109	5.82344	4.51266	6.06546
0.9	2.90043	4.43422	3.75851	5.11814	4.14357	5.55732
1.0	2.21924	3.7201	2.31704	3.77804	3.83163	5.13594

Table 4.22 The Cross Over Radius (switching of. buckling mode) of the Ring Support for Various Values of Rotational, R_{11} and Translational Stiffness, T_{11} Parameters when $\nu = 0.3$

	$R_{11} = 0.3, T_{11} = 100$	$R_{11} = 0.5, T_{11} = 1000$	$R_{11} = 50, T_{11} = 1000$	$R_{11} = T_{11} = \infty$
b	0.1589	0.1102	0.1557	0.1523

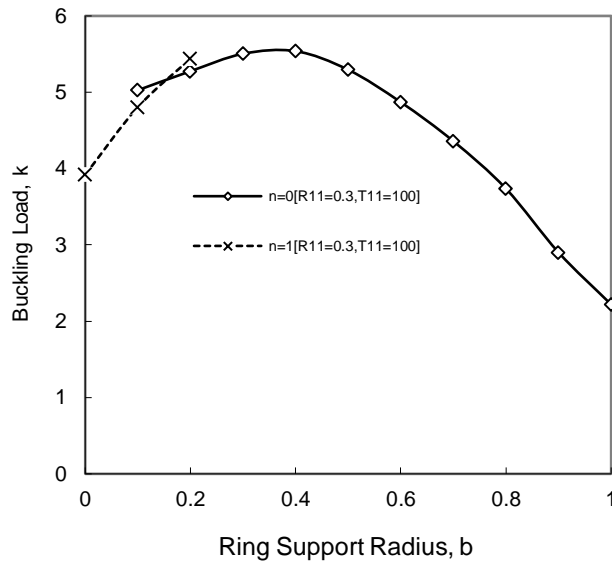


Fig 4.40 Buckling Load Parameter k , versus *Internal Ring Support Radius* b , for $R_{11} = 0.3$ & $T_{11} = 100$

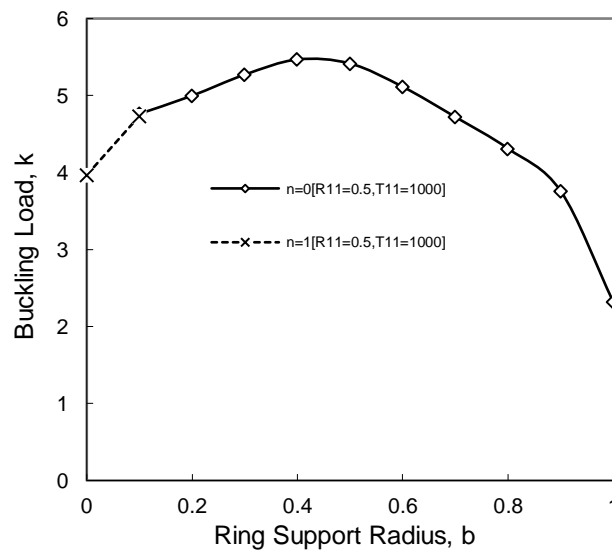


Fig 4.41 Buckling Load Parameter k , versus *Internal Ring Support Radius* b , for $R_{11} = 0.5$ & $T_{11} = 1000$

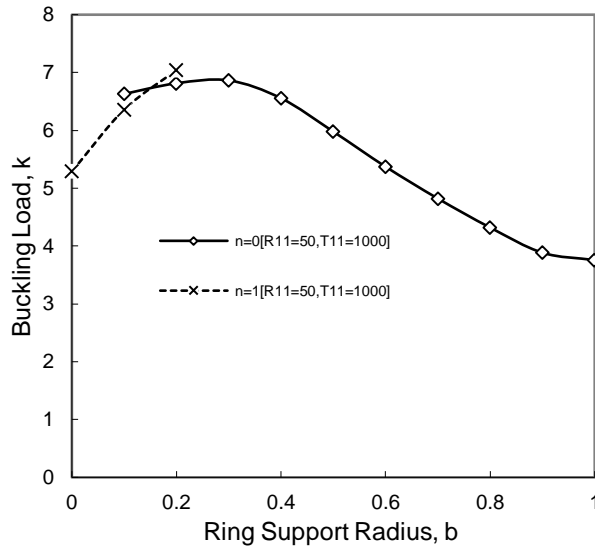


Fig 4.42 Buckling Load Parameter k , versus Internal Ring Support Radius b , for $R_{11} = 50$ & $T_{11} = 1000$

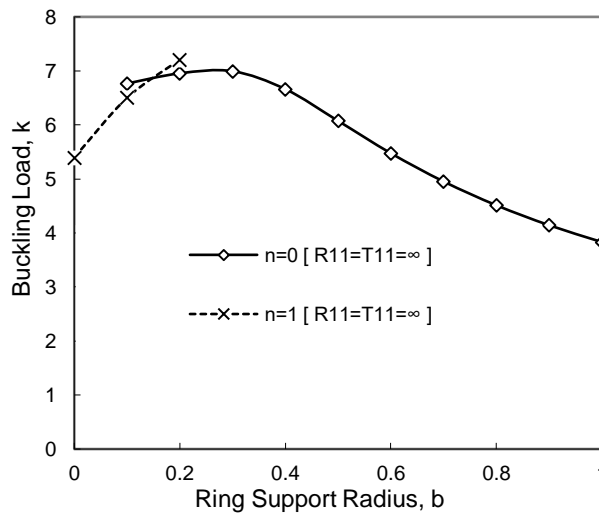


Fig 4.43 Buckling Load Parameter k , versus Internal Ring Support Radius b , for $R_{11} = T_{11} = \infty$

The optimum location of the ring support and the corresponding buckling load parameters for various rotational spring stiffness parameters ($R_{11} = 0.3, 50$ & ∞) and translational spring stiffness parameters ($T_{11} = 100, 1000$ & ∞) are presented in the Table 4.33. It is observed that the optimal ring support radius parameter decrease with increase in rotational spring stiffness parameter and also the optimal buckling load capacity increases with rotational spring stiffness parameter. Introducing internal ring support, when placed at an optimal position increases the elastic buckling capacity significantly, and the percentage of increase in buckling loads is presented in Table 4.23. It is observed that the percentage

increase in buckling load parameter decreases with increase in R_{11} . This is due to the amount of increase in buckling load without ring support with R_{11} is more than that of increase in buckling load with ring support with R_{11} .

The results of this kind were scarce in the literature. However, the results are compared with the following cases. Tables 4.24, 4.25 and 4.26, presents the buckling load parameters k , for a circular plate with an *internal ring* support and elastically restrained edge against rotation, against those obtained by Wang et al, [67], Laura et al. [2] and Wang et al. [69]. Reference [67] is considered because the plate can be considered as thin for $\tau = h/R = 0.001$. It shows that the present results are in good agreement. The buckling load parameters k , for clamped and simply supported edges are compared with those obtained by Wang et al. [67] and Wang et al. [69] as shown in Tables 4.27 and 4.28 respectively. Also the optimum location of the ring support and the corresponding buckling load parameters for rotational spring stiffness parameter 0.3, 50 and ∞ are calculated by substituting $T_{11} = 0$ and it is in good agreement with earlier results obtained by Wang et al [3] as shown in Table 4.29.

Table 4.23 Optimum Location of the Ring Support; the Corresponding Buckling Load Parameters and Percentage Increase in Buckling Load Parameters

R_{11}	0.3	50	∞
T_{11}	100	1000	∞
b_{opt}	0.3211	0.27022	0.2600
k_{opt}	5.53449	6.87832	7.01485
% age increase in Buckling Load	149.39	83.11	83.07

Table 4.24 Comparison of Buckling Load Parameter k , with Laura et al. [2] and Wang et al. [69] for Rotational Stiffness Parameter $R_{11} = 0$ & $\nu = 0.3$

Ring support radius, b	Laura et al [2]	Wang et al. [69]	Present
0.1	4.5244	4.5235	4.52341
0.2	4.7718	4.7702	4.77018
0.3	5.0725	5.071	5.07091
0.4	5.3301	5.3296	5.32964
0.5	5.3666	5.3666	5.36659

0.6	5.1284	5.1261	5.12606
0.7	4.7789	4.7727	4.77266
0.8	4.4249	4.4215	4.42141
0.9	4.1122	4.1063	4.10629

Table 4.25 Comparison of Buckling Load Parameter k , with Laura et al. [2] for Rotational Stiffness Parameter $R_{11} = \infty$ & $\nu = 0.3$

Ring support radius, b	Laura et al [2]	Present
0.1	6.772	6.50105
0.2	6.9649	6.95592
0.3	6.9964	6.99485
0.4	6.6693	6.66257
0.5	6.0852	6.07454
0.6	5.4845	5.4755
0.7	4.9588	4.95263
0.8	4.5277	4.51266
0.9	4.1509	4.14357

Table 4.26 Comparison of Buckling Load Parameter k , with Wang et al. [69] for Rotational stiffness Parameter $R_{11} = 10^5$ & $\nu = 0.3$

Ring support radius, b	Wang et al [69]	Present
0.1	6.5009*	6.50095*
0.2	6.9558	6.95582
0.3	6.9947	6.99475
0.4	6.6625	6.66248
0.5	6.0745	6.07454
0.6	5.4755	5.4755
0.7	4.9526	4.95263
0.8	4.5127	4.51266
0.9	4.1436	4.14357

* Asymmetric buckling load parameters

Table 4.27 Comparison of Buckling Load Parameter k , with Wang et al. [67] and Wang et al [69] for Clamped Edge for Rotational stiffness Parameter $R_{11} = 10^5$ & $\nu = 0.3$

Ring support radius, b	Wang et al [67]	Wang et al [69]	Present
0.1	----	6.5009*	6.50095*
0.2	6.9559	6.9558	6.95582
0.3	6.9948	6.9947	6.99475
0.4	6.6627	6.6625	6.66248
0.5	6.0749	6.0745	6.07454
0.6	5.476	5.4755	5.4755
0.7	4.9532	4.9526	4.95263
0.8	4.5134	4.5127	4.51266

0.9	4.1448	4.1436	4.14357
0.99	3.8667	3.8604	3.86061

* Asymmetric buckling load parameters

Table 4.28 Comparison of Buckling Load Parameter k , with Wang et al. [67] and Wang et al [69] for Simply Supported Edge for Rotational stiffness Parameter $R_{11} = 0$ & $\nu = 0.3$

Ring support radius, b	Wang et al [67]	Wang et al [69]	Present
0.1	---	4.5235	4.52341
0.2	4.7703	4.7702	4.77018
0.3	5.0711	5.071	5.07091
0.4	5.3297	5.3296	5.32964
0.5	5.3667	5.3666	5.36659
0.6	5.1264	5.1261	5.12606
0.7	4.773	4.7727	4.77266
0.8	4.4219	4.4215	4.42141
0.9	4.1069	4.1063	4.10629
0.99	3.8603	3.8573	3.85742

Table 4.29 Optimum Locations of The Ring Support and The Corresponding Buckling Load Parameters

R_{11}	0.3		50		∞	
b_{opt}	Wang [3]	Present	Wang [3]	Present	Wang [3]	Present
	0.463	0.463	0.271	0.271	0.265	0.265
k_{opt}	5.38929	5.38929	6.87741	6.87741	7.01554	7.01554

Subset problems:

(i) Buckling of circular plates with internal ring support and restrained guided edge against translation

The buckling load parameters for axisymmetric and asymmetric modes and for various values of translational spring stiffness parameters are presented in Table 4.30. Figs. 4.44-4.46 show the variations of buckling load parameter, k with respect to the internal *ring* support radius, b for various values of translational spring stiffness parameters. It is observed from Figs. 4.44-4.46 that for a given value of translational spring stiffness parameters, the curve in each case is composed of two segments. This is due to the switching of buckling modes. For a smaller internal *ring* support radius b , the plate buckles in an asymmetric mode (i.e. $n \neq 0$). In this segment (as shown by dotted lines in Figs. 4.44-4.46) the buckling load decreases as b decreases in value. For a larger internal *ring* support radius b , the plate buckles in an

axisymmetric mode (i.e. $n=0$). In this segment (as shown by continuous lines in Figs. 4.44-4.46) the buckling load increases as b decreases up to a peak point corresponds to maximum buckling load and thereafter decreases as b decreases in value as shown in Figs. 4.44-4.46. As $T_{11} \rightarrow \infty$, the edge of the plate becomes clamped and as $b \rightarrow 1$, the buckling solution for this case is 3.83163. This is in good agreement with that of Wang et al [69]. It is also observed from Figs. 4.44-4.46 that all curves converge to $k = 3.83163$ as $b \rightarrow 1$.

Fig. 4.44, shows the variations of buckling load parameter k , with respect to the internal *ring* support radius b , for translational spring stiffness parameter $T_{11}=1000$. The cross over radius (switching of. buckling mode) in this case is $b=0.1514$. It is noticed from the Fig. 5.44 that the buckling is governed by the asymmetric mode $n=1$, when $b \leq 0.1514$ for $T_{11}=10000$. When b is increased beyond 0.1514, the $n=0$ axisymmetric mode gives the correct lower buckling load. Fig. 4.45, shows the variations of buckling load parameter k , with respect to the internal *ring* support radius b , for translational spring stiffness parameter $T_{11}=100000$. The cross over radius (switching of. buckling mode) in this case is $b=0.15226$. It is observed from the Fig. 4.45 that the buckling is governed by the asymmetric mode $n=1$, when $b \leq 0.15226$ for $T_{11}=1000000$. When b is increased beyond 0.15226, the $n=0$ axisymmetric mode gives the correct lower buckling load. Fig. 4.46 shows the variations of buckling load parameter k , with respect to the internal *ring* support radius b , for translational spring stiffness parameter $T_{11} = \infty$. The cross over radius (switching of. buckling mode) in this case is $b=0.1532$. Similarly, it is observed from the Fig. 4.46 that the buckling is governed by the asymmetric mode $n=1$, when $b \leq 0.1532$ for $T_{11} = \infty$. When b is increased beyond 0.1532, the $n=0$ axisymmetric mode gives the correct lower buckling load. The optimal solutions for this case are presented in Table 4.31, for various translational spring stiffness parameters ($T_{11}=1000, 100000 \& \infty$). It is observed that the optimal ring support

radius parameter slightly decrease with increase in translational spring stiffness parameter and also the optimal buckling load capacity slightly increases with translational spring stiffness parameter. Introducing internal ring support, when placed at an optimal position increases the elastic buckling capacity significantly, and the percentage of increase in buckling loads is presented in Table 4.31. It is observed that percentage increase in buckling load parameter is negligible with increase in T_{11} and this is due to the influence of T_{11} on buckling load is marginal.

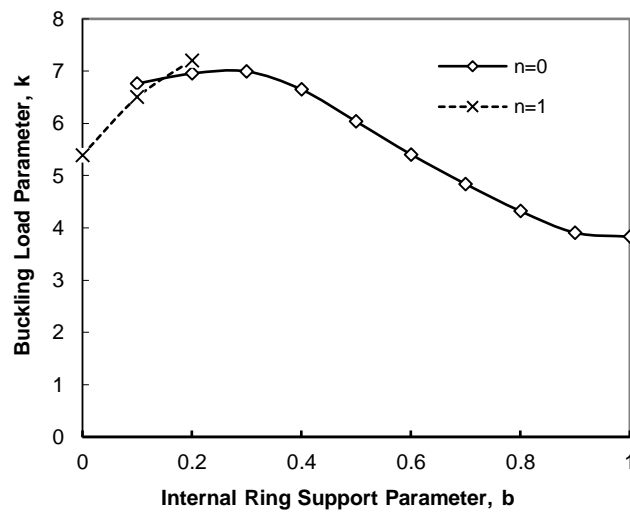


Fig. 4.44 Buckling Load Parameter, k versus Internal *Ring* Support Radius, b for $T_{11} = 1000$

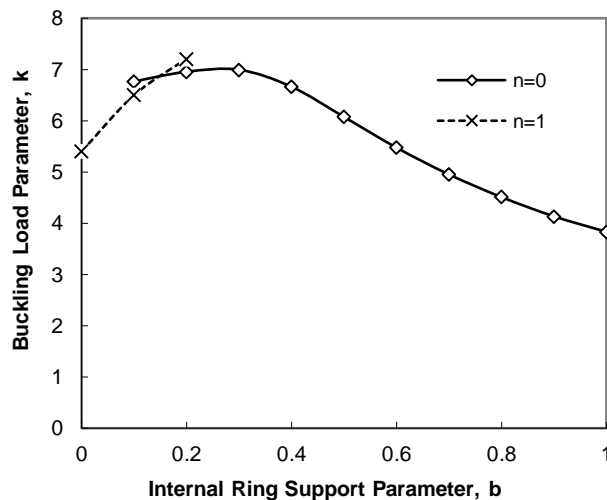


Fig. 4.45 Buckling Load Parameter, k versus Internal *Ring* Support Radius, b for $T_{11} = 100000$

The optimal internal *ring* support radius is found to be independent of the Poisson's ratio and it is affected by the translational spring stiffness parameter. There is no influence of Poisson's ratio on buckling load parameters, for a given values of translational spring stiffness parameters and internal *ring* support radius parameter, as shown in Fig. 4.47.

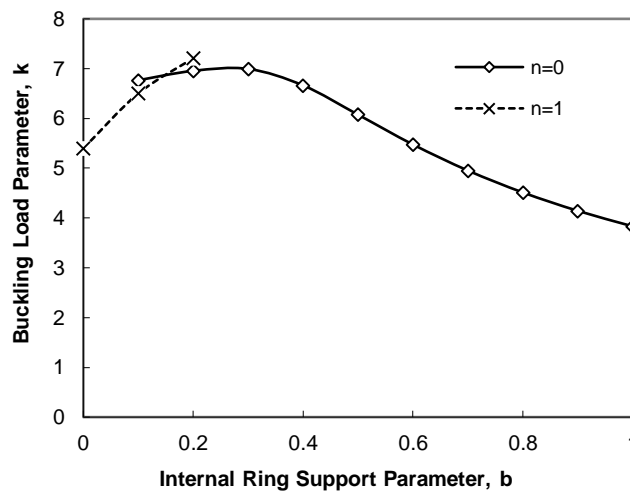


Fig. 4.46 Buckling Load Parameter, k versus Internal *Ring* Support Radius, b for $T_{11} = \infty$

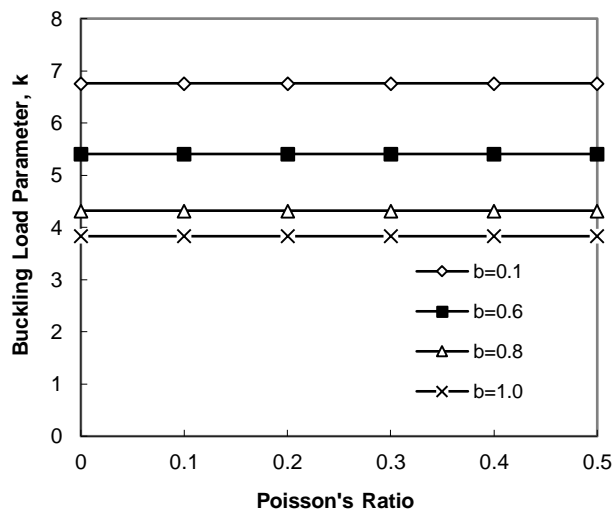


Fig. 4.47 Buckling Load Parameter, k versus Poisson's Ratio, ν , for $T_{11} = 1000$ and internal *Ring* Support Radius Parameter, b

However, it is observed from Figs. 4.44-4.46, that the affect of translational spring stiffness parameters, on buckling load parameter is less as compared to rotational spring stiffness parameter [70].

Table 4.30 Buckling (for axisymmetric and asymmetric modes) Load Parameters for different values of Translational Stiffness, T_{11} Parameters when $\nu = 0.3$

b	$T_{11} = 100000$		$T_{11} = \infty$	
	$n = 0$	$n = 1$	$n = 0$	$n = 1$
0	6.6477	5.39853	6.6478	5.39854
0.1	6.76622	6.50104	6.76632	6.50105
0.2	6.95582	7.20715	6.95592	7.20716
0.3	6.99484	7.90408	6.99485	7.90409
0.4	6.66237	8.39425	6.66257	8.39426
0.5	6.07414	8.14981	6.07454	8.15012
0.6	5.4748	7.40924	5.4755	7.40994
0.7	4.95143	6.67932	4.95263	6.68062
0.8	4.51016	6.06237	4.51266	6.06546
0.9	4.1344	5.54575	4.14357	5.55732
1.0	3.83163	5.13557	3.83192	5.13594

Table 4.31 Optimum Location of The Ring Support, The Corresponding Buckling Load Parameters and Percentage of Increase in Buckling Load Parameters

T_{11}	1000	100000	∞
b_{opt}	0.3001	0.2995	0.2994
k_{opt}	6.994	6.995	6.996
% age increase in buckling load	82.53	82.56	82.59

(ii) Buckling of circular plates with internal ring support and restrained edge against translation.

The buckling load parameters for axisymmetric and asymmetric modes and for various values of translational spring stiffness parameters are presented in Table 4.32. Figs. 4.48 and 4.49 show the variations of buckling load parameter, k with respect to the internal *ring* support radius, b for various values of translational spring stiffness parameters (i.e., $T_{11} = 100000$ and $T_{11} = \infty$). It is observed from Figs. 4.48 and 4.49 that for a given value of translational spring stiffness parameters, the curve in each case is composed of two segments.

This is due to the switching of buckling modes. For a smaller internal *ring* support radius b , the plate buckles in an asymmetric mode (i.e. $n \neq 0$). In this segment (as shown by dotted lines in Figs. 4.48 and 4.49 the buckling load decreases as b decreases in value. For a larger internal *ring* support radius b , the plate buckles in an axisymmetric mode (i.e. $n = 0$). In this segment (as shown by continuous lines in Figs. 4.48 and 4.49) the buckling load increases as b decreases up to a peak point corresponds to maximum buckling load and thereafter decreases as b decreases in value as shown in Figs. 4.48 and 4.49. As $T_{11} \rightarrow \infty$, the edge of the plate becomes clamped and as $b \rightarrow 1$, the buckling solution for this case is 3.83163. This is in good agreement with that of Wang and Wang [3]. Of interest in the design of supported circular plates is the optimal location of the internal *ring* support for maximum buckling load. The optimal solutions for this case are presented in Table 4.33, for various translational spring stiffness parameters ($T_{11} = 100000 \& \infty$). The cross over radius (b_{co}) i.e., mode switching for various values of translational spring stiffness parameters are presented in Table 4.33. Introducing internal ring support, when placed at an optimal position increases the elastic buckling capacity significantly, and the percentage of increase in buckling loads is presented in Table 4.33. It is found that the maximum percentage increase in buckling load parameter due to ring support is 193.14%.

Table 4.32 Buckling (for axisymmetric and asymmetric modes) Load Parameters for Different Values of Translational Stiffness, T_{11} Parameters when $\nu = 0.3$

b	$T_{11} = 100000$		$T_{11} = \infty$	
	$n = 0$ [Axisymmetric]	$n = 1$ [Asymmetric]	$n = 0$ [Axisymmetric]	$n = 1$ [Asymmetric]
0	4.7656	3.83453	4.40095	3.81016
0.1	4.90217	4.71841	4.52341	4.55263
0.2	5.1673	5.35521	4.77018	5.04915
0.3	5.42375	6.09953	5.07091	5.60095
0.4	5.49383	6.85631	5.32964	6.21912
0.5	5.27835	7.10461	5.36659	6.78183
0.6	4.86833	6.70653	5.12606	6.85994
0.7	4.3598	6.05772	4.77266	6.44514
0.8	3.72178	5.29709	4.42141	5.95154
0.9	2.81381	4.38238	4.10629	5.50984
1	2.04902	3.62502	3.83192	5.13596

Table 4.33 Optimum Location of The Ring Support, The Corresponding Buckling Load Parameters, cross - over Radius (switching of mode) and Percentage Increase in Buckling Load

T_{11}	10	∞
b_{opt}	0.39552	0.49179
k_{opt}	6.00598	5.37541
%	193.14	162.366
b_{co}	0.14850	0.09253

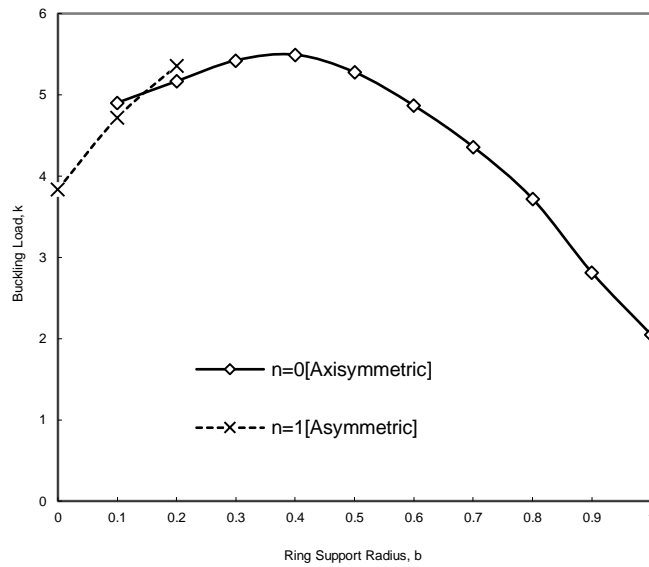


Fig 4.48 Buckling Load Parameter k , versus *Internal Ring* Support Radius b , for $T_{11} = 10$

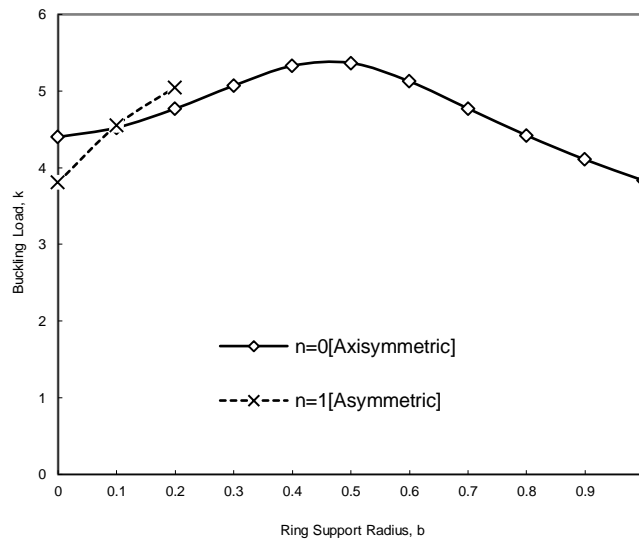


Fig 4.49 Buckling Load Parameter k , versus *Internal Ring* Support Radius b , for $T_{11} = \infty$

(iii) Buckling of circular plates with internal ring support and guided edge.

The buckling load parameter is 3.83163 and it is observed that the buckling load capacity is independent on ring support radius parameter.

(iv) Buckling of circular plates with internal ring support and *simply supported edge*.

The buckling load parameters for axisymmetric and asymmetric modes are presented in Table 4.34. Fig. 4.50 shows the variations of buckling load parameter, k with respect to the internal *ring* support radius, b . It is observed from Fig. 4.50 that the curve is composed of two segments. This is due to the switching of buckling modes. For a smaller internal *ring* support radius b , the plate buckles in an asymmetric mode (i.e. $n \neq 0$). In this segment (as shown by dotted lines in Fig. 4.50) the buckling load decreases as b decreases in value. For a larger internal *ring* support radius b , the plate buckles in an axisymmetric mode (i.e. $n = 0$). In this segment (as shown by continuous lines the Fig. 4.50) the buckling load increases as b decreases up to a peak point corresponds to maximum buckling load and thereafter decreases as b decreases in value as shown in Fig. 4.50. The cross-over radius (switching of buckling mode) is 0.094776. It is observed from the Fig. 5.50 that the buckling is governed by the asymmetric mode $n = 1$, when $b \leq 0.094776$. When b is increased beyond 0.094776, the $n = 0$ axisymmetric mode gives the correct lower buckling load. The optimal ring support b_{opt} is 0.49776 and the corresponding buckling load parameter, k_{opt} is 5.36926. An internal ring support, when placed at an optimal position, can increase the elastic buckling load capacity by 162.065%.

(v) Buckling of circular plates with internal ring support and *clamped edge*.

The buckling load parameters for axisymmetric and asymmetric modes are presented in Table 4.35. Fig. 4.51 shows the variations of buckling load parameter, k with respect to the internal *ring* support radius, b . It is observed from Figs. 4.51 that the curve is composed of two segments. This is due to the switching of buckling modes. For a smaller internal *ring* support radius b , the plate buckles in an asymmetric mode (i.e. $n \neq 0$). In this segment (as

shown by dotted lines in Fig. 4.51) the buckling load decreases as b decreases in value. For a larger internal *ring* support radius b , the plate buckles in an axisymmetric mode (i.e. $n=0$). In this segment (as shown by continuous lines the Fig. 4.51) the buckling load increases as b decreases up to a peak point corresponds to maximum buckling load and thereafter decreases as b decreases in value as shown in Fig. 4.51. The cross-over radius (switching of. buckling mode) is 0.15522.

It is observed from the Figure 4.51 that the buckling is governed by the asymmetric mode $n=1$, when $b \leq 0.15522$. When b is increased beyond 0.15522, the $n=0$ axisymmetric mode gives the correct lower buckling load. The optimal ring support b_{opt} is 0.28507 and the corresponding buckling load parameter, k_{opt} is 7.00931. An internal ring support, when placed at an optimal position, can increase the elastic buckling load capacity by 82.93%.

Table 4.34 Buckling (for axisymmetric and asymmetric modes) Load Parameters for Simply Supported Plate, When $\nu = 0.3$

b	$n = 0$ [Axisymmetric]	$n = 1$ [Asymmetric]
0	4.40095	3.81016
0.1	4.52341	4.55263
0.2	4.77018	5.04915
0.3	5.07091	5.60095
0.4	5.32964	6.21912
0.5	5.36659	6.78183
0.6	5.12606	6.85994
0.7	4.77266	6.44514
0.8	4.42141	5.95154
0.9	4.10629	5.50984
1	3.83192	5.13596

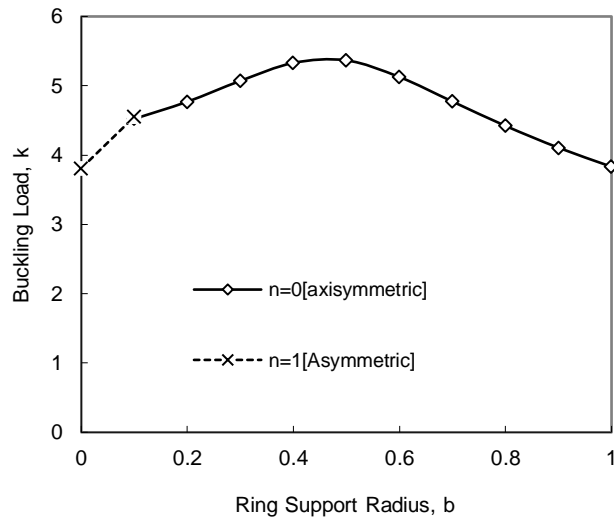


Fig 4.50 Buckling Load Parameter k , versus *Internal Ring Support Radius* b , for Simply Supported Plate

Table 4.35 Buckling (for axisymmetric and asymmetric modes) Load Parameters for Clamped Plate, when $\nu = 0.3$

b	$n = 0$ [Axisymmetric]	$n = 1$ [Asymmetric]
0	6.6478	5.39854
0.1	6.76632	6.50105
0.2	6.95592	7.20716
0.3	6.99485	7.90409
0.4	6.66257	8.39426
0.5	6.07454	8.15012
0.6	5.4755	7.40994
0.7	4.95263	6.68062
0.8	4.51266	6.06546
0.9	4.14357	5.55732
1	3.83193	5.13594

The optimal ring support is affected by the rotational stiffness parameters, translational stiffness parameters and translational spring stiffness parameters of an internal *elastic ring* support. However, it is observed that the influence of rotational spring stiffness parameters on buckling load is more predominant than that of translational spring stiffness parameters and elastic ring support constraints.

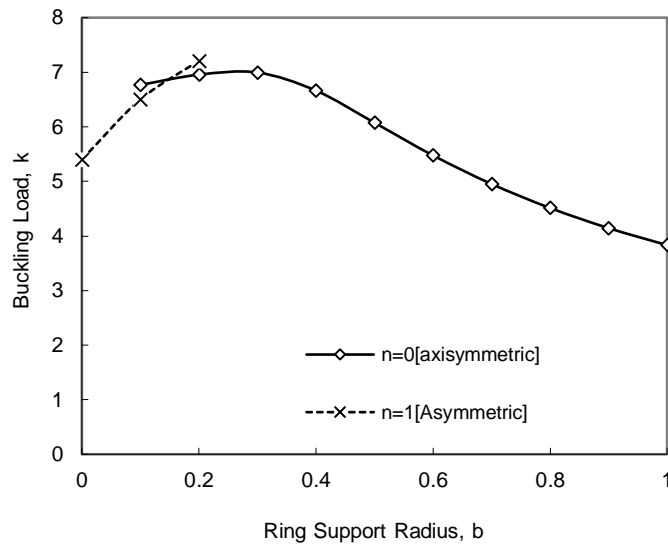


Fig 4.51 Buckling Load Parameter k , versus *Internal Ring* Support Radius b , for Clamped Plate

CHAPTER 5

BUCKLING OF ANNULAR PLATES WITH AN ELASTICALLY RESTRAINED EXTERNAL AND INTERNAL EDGES

5.1 History

Buckling of annular plates is an important in applications, like, in naval structures, aerospace, nuclear reactors, mechanical structures, civil structures etc. The earlier works based on the classical thin plate theory done by Yamaki [14], Mansfield [71] and Laura et al [2]. Laura et al. [2] investigated the elastic buckling problem of the aforesaid type of annular plates and has modeled the plate using the Classical Thin Plate theory, where axisymmetric modes were considered. It is an accepted fact that the condition on a periphery often tends to be in between the classical boundary conditions (free, clamped and simply supported) and may correspond more closely to some form of elastic restraints, i.e., rotational and translational restraints (Timoshenko and Gere [72] and Pflunger [73]). The purpose of the present work is to complete the results of the buckling of annular plates with outer and inner edges are elastically restrained against rotation and translation by including the asymmetric modes, thus correctly determining the buckling loads.

5.2 Definition of the Problem

Consider a thin circular annular plate of outer radius R , and inner radius bR , uniform thickness h , Young's modulus E , and Poisson's ratio ν . It is subjected to a uniform in-plane load, N along its boundary i.e., along the inner edge at $r = b$, and along the outer edge at $r = 1$, as shown in Fig. 5.1. This circular annular plate is assumed to be

made of linearly elastic, homogeneous and isotropic material and the effects of shear deformation and rotary inertia are neglected. The outer and inner edges of the annular plate are elastically restrained against rotation and translation as shown in Fig. 5.1. The problem at hand is to determine the elastic critical buckling loads of an annular plate with outer and inner edges are elastically restrained against rotation and translation.

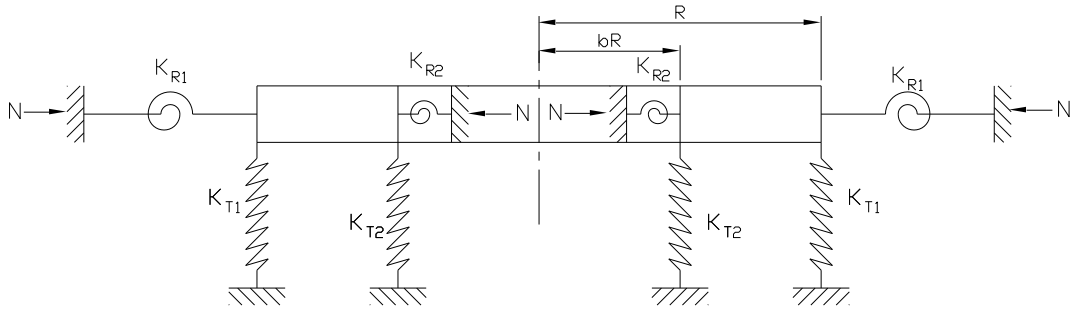


Fig. 5.1. Buckling of an Annular Plate with Elastically Restrained Edges against Rotation and Translation

5.3 Mathematical Formulation of the System

The annular plate is elastically restrained edge against rotation and translation at outer edge of radius R and at inner edge of radius bR . The annular plate under consideration is subjected to a uniformly distributed in-plane load N , along the inner edge $r = b$ and along the outer edge $r = 1$, as shown in Fig. 5.1. Let subscript I denote the inner region $0 \leq \bar{r} \leq b$ and the subscript II denote the outer region $b \leq \bar{r} \leq 1$. Here, all lengths are normalized by R . Based on the Classical Thin Plate theory (Kirchhoff

theory), the governing fourth order differential equation for elastic buckling of an annular plate may be expressed in polar coordinates (r, θ) as

$$D\nabla^4 w + N\nabla^2 w = 0 \quad (5.1)$$

Where w is the lateral displacement, D is the flexural rigidity, N is the uniform compressive load at inner and outer edge. After normalize lengths by the radius of the plate R , equation (6.1) can be written as

$$D\nabla^4 \bar{w} + k^2 \nabla^2 \bar{w} = 0 \quad (5.2)$$

$$\nabla^2 (\nabla^2 + k^2) \bar{w} = 0 \quad (5.3)$$

$$\text{Where the Laplacian operator, } \nabla^2 = \frac{\partial^2}{\partial \bar{r}^2} + \frac{1}{\bar{r}} \frac{\partial}{\partial \bar{r}} + \frac{1}{\bar{r}^2} \frac{\partial^2}{\partial \theta^2} \quad (5.4)$$

Where \bar{r} is the radial distance normalized by R . $\bar{D} = Eh^3/12(1-\nu^2)$ is the flexural rigidity, $\bar{w} = w/R$, is normalized transverse displacement of the plate. $\mathfrak{K}_5 = \mathfrak{B}_5 \mathfrak{A} \setminus \underline{\mathfrak{D}}$ is non-dimensional load parameter. Suppose there are n nodal diameters. In polar coordinates (r, θ) set

$$\bar{w}(\bar{r}, \theta) = \bar{u}(\bar{r}) \cos(n\theta) \quad (5.5)$$

Where n is the number of nodal diameters. The general solution for the governing buckling equation may be expressed as

$$\bar{u}_I(r) = C_1 J_n(k\bar{r}) + C_2 Y_n(k\bar{r}) + C_3 \bar{r}^n + C_4 \left\{ \frac{\log \bar{r}}{\bar{r}^{-n}} \right\} \quad (5.6)$$

Substituting equation (5.6) into equation (5.5) gives the following

$$\bar{w}_I(\bar{r}, \theta) = \left[C_1 J_n(k\bar{r}) + C_2 Y_n(k\bar{r}) + C_3 \bar{r}^n + C_4 \left\{ \frac{\log \bar{r}}{\bar{r}^{-n}} \right\} \right] \cos(n\theta) \quad (5.7)$$

Where top form of the equation (5.7) is used for $n=0$ (symmetric) and the bottom form is used for $n \neq 0$ (asymmetric), C_1, C_2, C_3 & C_4 are constants, $J_n(.)$ & $Y_n(.)$ are the Bessel

functions of the first and second kinds of order n , respectively. Let the subscript I denote outer domain $b \leq \bar{r} \leq 1$ and the subscript II denote the inner domain $0 \leq \bar{r} \leq b$.

CASE (i): Outer Edge of an Annular Plate Elastically Restrained Against Rotation and Translation

The boundary conditions at outer region of the annular plate in terms of rotational stiffness (K_{R1}) and translational stiffness (K_{T1}) is given by the following expressions

$$M_r(\bar{r}, \theta) = K_{R1} \frac{\partial \bar{w}_I(\bar{r}, \theta)}{\partial \bar{r}} \quad (5.8)$$

$$V_r(\bar{r}, \theta) = -K_{T1} \bar{w}_I(\bar{r}, \theta) \quad (5.9)$$

The radial moment and the radial Kirchhoff shear at outer edge are defined as follows

$$M_r(\bar{r}, \theta) = -\frac{D}{R^3} \left[\frac{\partial^2 \bar{w}_I(\bar{r}, \theta)}{\partial \bar{r}^2} + \nu \left(\frac{1}{\bar{r}} \frac{\partial \bar{w}_I(\bar{r}, \theta)}{\partial \bar{r}} + \frac{1}{\bar{r}^2} \frac{\partial^2 \bar{w}_I(\bar{r}, \theta)}{\partial \theta^2} \right) \right] \quad (5.10)$$

$$V_r(\bar{r}, \theta) = -\frac{D}{R^3} \left[\frac{\partial}{\partial \bar{r}} \nabla^2 \bar{w}_I(\bar{r}, \theta) + (1-\nu) \frac{1}{\bar{r}} \frac{\partial}{\partial \theta} \left(\frac{1}{\bar{r}} \frac{\partial^2 \bar{w}_I(\bar{r}, \theta)}{\partial \bar{r} \partial \theta} - \frac{1}{\bar{r}^2} \frac{\partial \bar{w}_I(\bar{r}, \theta)}{\partial \theta} \right) \right] \quad (5.11)$$

From equations (5.8) and (5.10) yields the following

$$\left[\frac{\partial^2 \bar{w}_I(\bar{r}, \theta)}{\partial \bar{r}^2} + \nu \left(\frac{1}{\bar{r}} \frac{\partial \bar{w}_I(\bar{r}, \theta)}{\partial \bar{r}} + \frac{1}{\bar{r}^2} \frac{\partial^2 \bar{w}_I(\bar{r}, \theta)}{\partial \theta^2} \right) \right] = -\frac{K_{R1} R^2}{D} \frac{\partial \bar{w}_I(\bar{r}, \theta)}{\partial \bar{r}} \quad (5.12)$$

$$\left[\frac{\partial^2 \bar{w}_I(\bar{r}, \theta)}{\partial \bar{r}^2} + \nu \left(\frac{1}{\bar{r}} \frac{\partial \bar{w}_I(\bar{r}, \theta)}{\partial \bar{r}} + \frac{1}{\bar{r}^2} \frac{\partial^2 \bar{w}_I(\bar{r}, \theta)}{\partial \theta^2} \right) \right] = -R_{11} \frac{\partial \bar{w}_I(\bar{r}, \theta)}{\partial \bar{r}} \quad (5.13)$$

Where $R_{11} = \frac{K_{R1} R^2}{D}$

From equations (5.9) and (5.11) yields the following

$$\left[\frac{\partial}{\partial \bar{r}} \nabla^2 \bar{w}_I(\bar{r}, \theta) + (1-\nu) \frac{1}{\bar{r}} \frac{\partial}{\partial \theta} \left(\frac{1}{\bar{r}} \frac{\partial^2 \bar{w}_I(\bar{r}, \theta)}{\partial \bar{r} \partial \theta} - \frac{1}{\bar{r}^2} \frac{\partial \bar{w}_I(\bar{r}, \theta)}{\partial \theta} \right) \right] = \frac{K_{T1} R^3}{D} \bar{w}_I(\bar{r}, \theta) \quad (5.14)$$

$$\left[\frac{\partial}{\partial \bar{r}} \nabla^2 \bar{w}_I(\bar{r}, \theta) + (1-\nu) \frac{1}{\bar{r}} \frac{\partial}{\partial \theta} \left(\frac{1}{\bar{r}} \frac{\partial^2 \bar{w}_I(\bar{r}, \theta)}{\partial \bar{r} \partial \theta} - \frac{1}{\bar{r}^2} \frac{\partial \bar{w}_I(\bar{r}, \theta)}{\partial \theta} \right) \right] = T_{11} \bar{w}_I(\bar{r}, \theta) \quad (5.15)$$

Where $T_{11} = \frac{K_{T1} R^3}{D}$

Boundary conditions when the edges are elastically restrained against rotation.

From equations (5.7) and (5.13) yield the following

$$\frac{\partial \bar{w}(\bar{r}, \theta)}{\partial \bar{r}} = \left[\frac{k}{2} [J_{n-1}(k\bar{r}) - J_{n+1}(k\bar{r})] C_1 + \frac{k}{2} [Y_{n-1}(k\bar{r}) - Y_{n+1}(k\bar{r})] C_2 + n\bar{r}^{n-1} C_3 + \left\{ \frac{1}{\bar{r}} \right. \right. \\ \left. \left. - n\bar{r}^{-n-1} \right\} C_4 \right] \cos(n\theta) \quad (5.16)$$

$$\frac{\partial \bar{w}(\bar{r}, \theta)}{\partial \bar{r}} \Big|_{\bar{r}=1} = \left[\frac{k}{2} [J_{n-1}(k) - J_{n+1}(k)] C_1 + \frac{k}{2} [Y_{n-1}(k) - Y_{n+1}(k)] C_2 + n C_3 + \left\{ \frac{1}{-n} \right\} C_4 \right] \cos(n\theta) \quad (5.17)$$

$$\frac{\partial \bar{w}(\bar{r}, \theta)}{\partial \bar{r}} \Big|_{\bar{r}=1} = \left[\frac{k}{2} [P_1] C_1 + \frac{k}{2} [Q_1] C_2 + n C_3 + \left\{ \frac{1}{-n} \right\} C_4 \right] \cos(n\theta) \quad (5.18)$$

where $P_1 = J_{n-1}(k) - J_{n+1}(k)$; $Q_1 = Y_{n-1}(k) - Y_{n+1}(k)$

$$\frac{\partial^2 \bar{w}(\bar{r}, \theta)}{\partial \bar{r}^2} = \left[\frac{k^2}{4} [(J_{n-2}(k\bar{r}) - J_n(k\bar{r})) - (J_n(k\bar{r}) - J_{n+2}(k\bar{r}))] C_1 + \right. \\ \left. \frac{k^2}{4} [(Y_{n-2}(k\bar{r}) - Y_n(k\bar{r})) - (Y_n(k\bar{r}) - Y_{n+2}(k\bar{r}))] C_2 + n(n-1)\bar{r}^{n-2} C_3 + \left\{ -\frac{1}{\bar{r}^2} \right. \right. \\ \left. \left. - \frac{1}{n(n+1)\bar{r}^{-n-2}} \right\} C_4 \right] \cos(n\theta) \quad (5.19)$$

$$\frac{\partial^2 \bar{w}(\bar{r}, \theta)}{\partial \bar{r}^2} = \left[\frac{k^2}{4} [(J_{n-2}(k\bar{r}) + J_{n+2}(k\bar{r}) - 2J_n(k\bar{r}))] C_1 + \right. \\ \left. \frac{k^2}{4} [(Y_{n-2}(k\bar{r}) + Y_{n+2}(k\bar{r}) - 2Y_n(k\bar{r}))] C_2 + n(n-1)\bar{r}^{n-2} C_3 + \left\{ -\frac{1}{\bar{r}^2} \right. \right. \\ \left. \left. - \frac{1}{n(n+1)\bar{r}^{-n-2}} \right\} C_4 \right] \cos(n\theta) \quad (5.20)$$

$$\frac{\partial^2 \bar{w}(\bar{r}, \theta)}{\partial \bar{r}^2} \Big|_{\bar{r}=1} = \left[\frac{k^2}{4} [(J_{n-2}(k) + J_{n+2}(k) - 2J_n(k))] C_1 + \right. \\ \left. \frac{k^2}{4} [(Y_{n-2}(k) + Y_{n+2}(k) - 2Y_n(k))] C_2 + n(n-1) C_3 + \left\{ \frac{-1}{n(n+1)} \right\} C_4 \right] \cos(n\theta) \quad (5.21)$$

$$\frac{\partial^2 \bar{w}(\bar{r}, \theta)}{\partial \bar{r}^2} \bigg|_{\bar{r}=1} = \left[\frac{k^2}{4} [(P_2 - 2J_n(k))] C_1 + \frac{k^2}{4} [(Q_2 - 2Y_n(k))] C_2 + n(n-1) C_3 + \left\{ \frac{-1}{n(n+1)} \right\} C_4 \right] \cos(n\theta) \quad (5.22)$$

where $P_2 = J_{n-2}(k) + J_{n+2}(k)$; $Q_2 = Y_{n-2}(k) + Y_{n+2}(k)$

$$\frac{1}{\bar{r}} \frac{\partial \bar{w}(\bar{r}, \theta)}{\partial \bar{r}} \bigg|_{\bar{r}=1} = \frac{1}{\bar{r}} \left[\frac{k}{2} [J_{n-1}(k\bar{r}) - J_{n+1}(k\bar{r})] C_1 + \frac{k}{2} [Y_{n-1}(k\bar{r}) - Y_{n+1}(k\bar{r})] C_2 + n\bar{r}^{n-1} C_3 + \left\{ \frac{1}{-n\bar{r}^{-n-1}} \right\} C_4 \right] \cos(n\theta) \quad (5.23)$$

$$\frac{1}{\bar{r}} \frac{\partial \bar{w}(\bar{r}, \theta)}{\partial \bar{r}} \bigg|_{\bar{r}=1} = \left[\frac{k}{2} [J_{n-1}(k) - J_{n+1}(k)] C_1 + \frac{k}{2} [Y_{n-1}(k) - Y_{n+1}(k)] C_2 + n C_3 + \left\{ \frac{1}{-n} \right\} C_4 \right] \cos(n\theta) \quad (5.24)$$

$$\frac{1}{\bar{r}} \frac{\partial \bar{w}(\bar{r}, \theta)}{\partial \bar{r}} \bigg|_{\bar{r}=1} = \left[\frac{k}{2} [P_1] C_1 + \frac{k}{2} [Q_1] C_2 + n C_3 + \left\{ \frac{1}{-n} \right\} C_4 \right] \cos(n\theta) \quad (5.25)$$

$$\frac{\partial \bar{w}(\bar{r}, \theta)}{\partial \theta} = -n \left[C_1 J_n(k\bar{r}) + C_2 Y_n(k\bar{r}) + C_3 \bar{r}^n + C_4 \left\{ \frac{\log \bar{r}}{\bar{r}^{-n}} \right\} \right] \sin(n\theta) \quad (5.26)$$

$$\frac{\partial^2 \bar{w}(\bar{r}, \theta)}{\partial \theta^2} = -n^2 \left[C_1 J_n(k\bar{r}) + C_2 Y_n(k\bar{r}) + C_3 \bar{r}^n + C_4 \left\{ \frac{\log \bar{r}}{\bar{r}^{-n}} \right\} \right] \cos(n\theta) \quad (5.27)$$

$$\frac{1}{\bar{r}^2} \frac{\partial^2 \bar{w}(\bar{r}, \theta)}{\partial \theta^2} = -\frac{n^2}{\bar{r}^2} \left[C_1 J_n(k\bar{r}) + C_2 Y_n(k\bar{r}) + C_3 \bar{r}^n + C_4 \left\{ \frac{\log \bar{r}}{\bar{r}^{-n}} \right\} \right] \cos(n\theta) \quad (5.28)$$

$$\frac{1}{\bar{r}^2} \frac{\partial^2 \bar{w}(\bar{r}, \theta)}{\partial \theta^2} \bigg|_{\bar{r}=1} = -n^2 \left[C_1 J_n(k) + C_2 Y_n(k) + C_3 \cdot 1 + C_4 \left\{ \frac{0}{1} \right\} \right] \cos(n\theta) \quad (5.29)$$

Substituting equations (5.18), (5.22), (5.25), (5.29) into equation (5.13) gives the following

$$\begin{aligned} & \left[\frac{k^2}{4} P_2 + \frac{k}{2} (\nu + R_{11}) P_1 - \left(\frac{k^2}{2} + m^2 \right) J_n(k) \right] C_1 + \\ & \left[\frac{k^2}{4} Q_2 + \frac{k}{2} (\nu + R_{11}) Q_1 - \left(\frac{k^2}{2} + m^2 \right) Y_n(k) \right] C_2 + \\ & [n((n-1)(1-\nu) + R_{11})] C_3 + \left\{ \frac{(\nu + R_{11}) - 1}{n((n+1)(1-\nu) - R_{11})} \right\} C_4 = 0 \end{aligned} \quad (5.30)$$

Boundary conditions when the edges are elastically restrained against translation.

From equations (5.7) and (5.15) yields the following

$$\frac{\partial}{\partial \bar{r}} \nabla^2 \bar{w}(\bar{r}, \theta) = \frac{\partial}{\partial \bar{r}} \left[\frac{\partial^2 w(\bar{r}, \theta)}{\partial \bar{r}^2} + \frac{1}{\bar{r}^2} \frac{\partial^2 w(\bar{r}, \theta)}{\partial \theta^2} + \frac{1}{\bar{r}} \frac{\partial w(\bar{r}, \theta)}{\partial \bar{r}} \right] \quad (5.31)$$

$$\frac{\partial}{\partial \bar{r}} \left[\frac{\partial^2 w(\bar{r}, \theta)}{\partial \bar{r}^2} \right] = \frac{\partial}{\partial \bar{r}} \left[\frac{k^2}{4} [(J_{n-2}(k\bar{r}) + J_{n+2}(k\bar{r}) - 2J_n(k\bar{r}))]C_1 + \right. \\ \left. \frac{k^2}{4} [(Y_{n-2}(k\bar{r}) + Y_{n+2}(k\bar{r}) - 2Y_n(k\bar{r}))]C_2 + n(n-1)\bar{r}^{n-2}C_3 + \left\{ -\frac{1}{\bar{r}^2} \right\} C_4 \right] \cos(n\theta) \quad (5.32)$$

$$= \left\{ \begin{aligned} & \frac{k^3}{8} [(J_{n-3}(k\bar{r}) - J_{n-1}(k\bar{r})) + (J_{n+1}(k\bar{r}) - J_{n+3}(k\bar{r})) - 2(J_{n-1}(k\bar{r}) - J_{n+1}(k\bar{r}))]C_1 + \\ & \frac{k^3}{8} [(Y_{n-3}(k\bar{r}) - Y_{n-1}(k\bar{r})) + (Y_{n+1}(k\bar{r}) - Y_{n+3}(k\bar{r})) - 2(Y_{n-1}(k\bar{r}) - Y_{n+1}(k\bar{r}))]C_2 + \\ & n(n-1)(n-2)\bar{r}^{n-3}C_3 + \left\{ \frac{2}{\bar{r}^3} \right\} C_4 \\ & - n(n+1)(n+2)\bar{r}^{-n-3} \end{aligned} \right\} \cos(n\theta) \quad (5.33)$$

$$= \left\{ \begin{aligned} & \frac{k^3}{8} [(J_{n-3}(k\bar{r}) - J_{n+3}(k\bar{r})) - 3(J_{n-1}(k\bar{r}) - J_{n+1}(k\bar{r}))]C_1 + \\ & \frac{k^3}{8} [(Y_{n-3}(k\bar{r}) - Y_{n+3}(k\bar{r})) - 3(Y_{n-1}(k\bar{r}) - Y_{n+1}(k\bar{r}))]C_2 + \\ & n(n-1)(n-2)\bar{r}^{n-3}C_3 + \left\{ \frac{2}{\bar{r}^3} \right\} C_4 \\ & - n(n+1)(n+2)\bar{r}^{-n-3} \end{aligned} \right\} \cos(n\theta) \quad (5.34)$$

$$\frac{\partial}{\partial \bar{r}} \left[\frac{\partial^2 w(\bar{r}, \theta)}{\partial \bar{r}^2} \right]_{\bar{r}=1} = \left\{ \begin{aligned} & \frac{k^3}{8} [(J_{n-3}(k) - J_{n+3}(k)) - 3(J_{n-1}(k) - J_{n+1}(k))]C_1 + \\ & \frac{k^3}{8} [(Y_{n-3}(k) - Y_{n+3}(k)) - 3(Y_{n-1}(k) - Y_{n+1}(k))]C_2 + \\ & n(n-1)(n-2)C_3 + \left\{ 2 \right\} C_4 \\ & - n(n+1)(n+2) \end{aligned} \right\} \cos(n\theta) \quad (5.35)$$

$$= \left\{ \frac{k^3}{8} [P_3 - 3P_1] C_1 + \frac{k^3}{8} [Q_3 - 3Q_1] C_2 + n(n-1)(n-2) C_3 + \left\{ \begin{matrix} 2 \\ -n(n+1)(n+2) \end{matrix} \right\} C_4 \right\} \cos(n\theta) \quad (5.36)$$

where $P_3 = J_{n-3}(k) - J_{n+3}(k)$; $Q_3 = Y_{n-3}(k) - Y_{n+3}(k)$

$$\frac{\partial}{\partial \bar{r}} \left[\frac{1}{\bar{r}^2} \frac{\partial^2 w(\bar{r}, \theta)}{\partial \theta^2} \right] = \frac{1}{\bar{r}^2} \frac{\partial}{\partial \bar{r}} \left[\frac{\partial^2 w(\bar{r}, \theta)}{\partial \theta^2} \right] - \frac{2}{\bar{r}^3} \frac{\partial^2 w(\bar{r}, \theta)}{\partial \theta^2} \quad (5.37)$$

$$= \frac{1}{\bar{r}^2} \left\{ -n^2 \left[\frac{k}{2} [J_{n-1}(k\bar{r}) - J_{n+1}(k\bar{r})] C_1 + \frac{k}{2} [Y_{n-1}(k\bar{r}) - Y_{n+1}(k\bar{r})] C_2 + n\bar{r}^{n-1} C_3 + \left\{ \begin{matrix} 1 \\ -n\bar{r}^{-n-1} \end{matrix} \right\} C_4 \right] \cos(n\theta) \right\} -$$

$$\frac{2}{\bar{r}^3} \left\{ -n^2 \left[C_1 J_n(k\bar{r}) + C_2 Y_n(k\bar{r}) + C_3 \bar{r}^n + C_4 \left\{ \begin{matrix} \log \bar{r} \\ \bar{r}^{-n} \end{matrix} \right\} \right] \cos(n\theta) \right\} \quad (5.38)$$

$$\frac{\partial}{\partial \bar{r}} \left[\frac{1}{\bar{r}^2} \frac{\partial^2 w(\bar{r}, \theta)}{\partial \theta^2} \right]_{\bar{r}=1} = \left\{ -n^2 \left[\frac{k}{2} [J_{n-1}(k) - J_{n+1}(k)] C_1 + \frac{k}{2} [Y_{n-1}(k) - Y_{n+1}(k)] C_2 + n C_3 \right] \cos(n\theta) \right\} -$$

$$+ \left\{ \begin{matrix} 1 \\ -n \end{matrix} \right\} C_4 \cos(n\theta) \quad (5.39)$$

$$2 \left\{ -n^2 \left[C_1 J_n(k) + C_2 Y_n(k) + C_3 + C_4 \left\{ \begin{matrix} 0 \\ 1 \end{matrix} \right\} \right] \cos(n\theta) \right\}$$

$$\frac{\partial}{\partial \bar{r}} \left[\frac{1}{\bar{r}^2} \frac{\partial^2 w(\bar{r}, \theta)}{\partial \theta^2} \right]_{\bar{r}=1} = -n^2 \left[\frac{k}{2} [P_1] C_1 + \frac{k}{2} [Q_1] C_2 + n C_3 + \left\{ \begin{matrix} 1 \\ -n \end{matrix} \right\} C_4 \right] \cos(n\theta) +$$

$$2n^2 \left[C_1 J_n(k) + C_2 Y_n(k) + C_3 + C_4 \left\{ \begin{matrix} 0 \\ 1 \end{matrix} \right\} \right] \cos(n\theta) \quad (5.40)$$

$$\frac{\partial}{\partial \bar{r}} \left[\frac{1}{\bar{r}} \frac{\partial w(\bar{r}, \theta)}{\partial \bar{r}} \right] = \frac{1}{\bar{r}} \frac{\partial}{\partial \bar{r}} \left[\frac{\partial w(\bar{r}, \theta)}{\partial \bar{r}} \right] + \frac{\partial w(\bar{r}, \theta)}{\partial \bar{r}} \frac{\partial}{\partial \bar{r}} \left[\frac{1}{\bar{r}} \right] = \frac{1}{\bar{r}} \frac{\partial^2 w(\bar{r}, \theta)}{\partial \bar{r}^2} - \frac{1}{\bar{r}^2} \frac{\partial w(\bar{r}, \theta)}{\partial \bar{r}} \quad (5.41)$$

$$\begin{aligned}
&= \frac{1}{\bar{r}} \left[\frac{k^2}{4} [(J_{n-2}(\bar{k}\bar{r}) + J_{n+2}(\bar{k}\bar{r}) - 2J_n(\bar{k}\bar{r}))]C_1 + \right. \\
&\quad \left. \frac{k^2}{4} [(Y_{n-2}(\bar{k}\bar{r}) + Y_{n+2}(\bar{k}\bar{r}) - 2Y_n(\bar{k}\bar{r}))]C_2 + n(n-1)\bar{r}^{n-2}C_3 + \left\{ -\frac{1}{\bar{r}^2} \right\} C_4 \right] \cos(n\theta) \quad (5.42) \\
&- \frac{1}{\bar{r}^2} \left[\frac{k}{2} [J_{n-1}(\bar{k}\bar{r}) - J_{n+1}(\bar{k}\bar{r})]C_1 + \frac{k}{2} [Y_{n-1}(\bar{k}\bar{r}) - Y_{n+1}(\bar{k}\bar{r})]C_2 + n\bar{r}^{n-1}C_3 + \left\{ \frac{1}{\bar{r}} \right\} C_4 \right] \cos(n\theta)
\end{aligned}$$

$$\frac{\partial}{\partial \bar{r}} \left[\frac{1}{\bar{r}} \frac{\partial w(\bar{r}, \theta)}{\partial \bar{r}} \right]_{\bar{r}=1} =$$

$$\begin{aligned}
&= \left[\frac{k^2}{4} [(J_{n-2}(k) + J_{n+2}(k) - 2J_n(k))]C_1 + \right. \\
&\quad \left. \frac{k^2}{4} [(Y_{n-2}(k) + Y_{n+2}(k) - 2Y_n(k))]C_2 + n(n-1)C_3 + \left\{ -\frac{1}{n(n+1)} \right\} C_4 \right] \cos(n\theta) \quad (5.43) \\
&- \left[\frac{k}{2} [J_{n-1}(k) - J_{n+1}(k)]C_1 + \frac{k}{2} [Y_{n-1}(k) - Y_{n+1}(k)]C_2 + nC_3 + \left\{ \frac{1}{-n} \right\} C_4 \right] \cos(n\theta)
\end{aligned}$$

$$\begin{aligned}
&= \left[\frac{k^2}{4} [P_2 - 2J_n(k)]C_1 + \frac{k^2}{4} [Q_2 - 2Y_n(k)]C_2 + n(n-1)C_3 + \left\{ -\frac{1}{n(n+1)} \right\} C_4 \right] \cos(n\theta) \quad (5.44) \\
&- \left[\frac{k}{2} [P_1]C_1 + \frac{k}{2} [Q_1]C_2 + nC_3 + \left\{ \frac{1}{-n} \right\} C_4 \right] \cos(n\theta)
\end{aligned}$$

$$\left[\frac{\partial^2 w(\bar{r}, \theta)}{\partial \bar{r} \partial \theta} \right] = \frac{\partial}{\partial \bar{r}} \left[\frac{\partial w(\bar{r}, \theta)}{\partial \theta} \right] = \frac{\partial}{\partial \bar{r}} \left\{ -n \left[C_1 J_n(\bar{k}\bar{r}) + C_2 Y_n(\bar{k}\bar{r}) + C_3 \bar{r}^n + C_4 \left\{ \frac{\log \bar{r}}{\bar{r}^{-n}} \right\} \right] \sin(n\theta) \right\} \quad (5.45)$$

$$= -n \left[\frac{k}{2} [J_{n-1}(\bar{k}\bar{r}) - J_{n+1}(\bar{k}\bar{r})]C_1 + \frac{k}{2} [Y_{n-1}(\bar{k}\bar{r}) - Y_{n+1}(\bar{k}\bar{r})]C_2 + n\bar{r}^{n-1}C_3 + \left\{ \frac{1}{\bar{r}} \right\} C_4 \right] \sin(n\theta) \quad (5.46)$$

$$\frac{1}{\bar{r}^2} \frac{\partial w(\bar{r}, \theta)}{\partial \theta} = \frac{-n}{\bar{r}^2} \left[C_1 J_n(\bar{k}\bar{r}) + C_2 Y_n(\bar{k}\bar{r}) + C_3 \bar{r}^n + C_4 \left\{ \frac{\log \bar{r}}{\bar{r}^{-n}} \right\} \right] \sin(n\theta) \quad (5.47)$$

From equations (5.46) and (5.47) yields the following

$$\begin{aligned}
& \frac{\partial}{\partial \theta} \left[\frac{1}{\bar{r}} \frac{\partial^2 w(\bar{r}, \theta)}{\partial \bar{r} \partial \theta} - \frac{1}{\bar{r}^2} \frac{\partial w(\bar{r}, \theta)}{\partial \theta} \right] \\
&= -\frac{n^2}{\bar{r}} \left[\frac{k}{2} [J_{n-1}(k\bar{r}) - J_{n+1}(k\bar{r})] C_1 + \frac{k}{2} [Y_{n-1}(k\bar{r}) - Y_{n+1}(k\bar{r})] C_2 + n\bar{r}^{n-1} C_3 + \left\{ \frac{1}{\bar{r}} \right. \right. \\
&\quad \left. \left. - n\bar{r}^{-n-1} \right\} C_4 \right] \cos(n\theta) + \\
&\frac{n^2}{\bar{r}^2} \left[C_1 J_n(k\bar{r}) + C_2 Y_n(k\bar{r}) + C_3 \bar{r}^n + C_4 \left\{ \frac{\log \bar{r}}{\bar{r}^{-n}} \right\} \right] \cos(n\theta)
\end{aligned} \tag{5.48}$$

Equation (5.48) can be written as

$$\begin{aligned}
& (1-\nu) \frac{1}{\bar{r}} \frac{\partial}{\partial \theta} \left[\frac{1}{\bar{r}} \frac{\partial^2 w(\bar{r}, \theta)}{\partial \bar{r} \partial \theta} - \frac{1}{\bar{r}^2} \frac{\partial w(\bar{r}, \theta)}{\partial \theta} \right]_{\bar{r}=1} \\
&= (1-\nu) \left\{ \begin{aligned} & -n^2 \left[\frac{k}{2} [J_{n-1}(k) - J_{n+1}(k)] C_1 + \frac{k}{2} [Y_{n-1}(k) - Y_{n+1}(k)] C_2 + n C_3 + \left\{ \frac{1}{-n} \right\} C_4 \right] \cos(n\theta) + \\ & n^2 \left[C_1 J_n(k) + C_2 Y_n(k) + C_3 + C_4 \left\{ \frac{0}{1} \right\} \right] \cos(n\theta) \end{aligned} \right\} \tag{5.49}
\end{aligned}$$

$$\begin{aligned}
&= (1-\nu) \left\{ \begin{aligned} & -n^2 \left[\frac{k}{2} [P_1] C_1 + \frac{k}{2} [Q_1] C_2 + n C_3 + \left\{ \frac{1}{-n} \right\} C_4 \right] \cos(n\theta) + \\ & n^2 \left[C_1 J_n(k) + C_2 Y_n(k) + C_3 + C_4 \left\{ \frac{0}{1} \right\} \right] \cos(n\theta) \end{aligned} \right\} \tag{5.50}
\end{aligned}$$

Equation (5.7) gives the following at $\bar{r} = 1$

$$\bar{w}(\bar{r}, \theta)_{\bar{r}=1} = \left[C_1 J_n(k) + C_2 Y_n(k) + C_3 + C_4 \left\{ \frac{0}{1} \right\} \right] \cos(n\theta) \tag{5.51}$$

Substituting equations (5.36), (5.40), (5.44), (5.50), (5.51) into equation (5.15) gives the following

$$\begin{aligned}
& \left[\frac{k^3}{8} P_3 + \frac{k^2}{4} P_2 - \frac{k}{2} \left(\frac{3}{4} k^2 + n^2(2-\nu) + 1 \right) P_1 + \left(n^2(3-\nu) - \frac{k^2}{2} - T_{11} \right) J_n(k) \right] C_1 + \\
& \left[\frac{k^3}{8} Q_3 + \frac{k^2}{4} Q_2 - \frac{k}{2} \left(\frac{3}{4} k^2 + n^2(2-\nu) + 1 \right) Q_1 + \left(n^2(3-\nu) - \frac{k^2}{2} - T_{11} \right) Y_n(k) \right] C_2 + \\
& \left[n^2(n-1)\nu - n^3 - T_{11} \right] C_3 - \left\{ \frac{n^2(2-\nu)}{-n^2(n+1)\nu + n^3 - T_{11}} \right\} C_4 = 0
\end{aligned} \tag{5.52}$$

where , $P_1 = J_{n-1}(k) - J_{n+1}(k); P_2 = J_{n-2}(k) + J_{n+2}(k); P_3 = J_{n-3}(k) - J_{n+3}(k);$
 $Q_1 = Y_{n-1}(k) - Y_{n+1}(k); Q_2 = Y_{n-2}(k) + Y_{n+2}(k); Q_3 = Y_{n-3}(k) - Y_{n+3}(k);$

CASE (ii): Inner Edge of an Annular Plate Elastically Restrained Against Rotation and Translation

The boundary conditions at inner region of the annular plate in terms of rotational stiffness (K_{R2}) and translational stiffness (K_{T2}) is given by the following expressions

$$M_r(\bar{r}, \theta) = -K_{R2} \frac{\partial \bar{w}_I(\bar{r}, \theta)}{\partial \bar{r}} \quad (5.53)$$

$$V_r(\bar{r}, \theta) = K_{T2} \bar{w}_I(\bar{r}, \theta) \quad (5.54)$$

The radial moment and the radial Kirchhoff shear at outer edge are defined as follows

$$M_r(\bar{r}, \theta) = -\frac{D}{R^3} \left[\frac{\partial^2 \bar{w}_I(\bar{r}, \theta)}{\partial \bar{r}^2} + \nu \left(\frac{1}{\bar{r}} \frac{\partial \bar{w}_I(\bar{r}, \theta)}{\partial \bar{r}} + \frac{1}{\bar{r}^2} \frac{\partial^2 \bar{w}_I(\bar{r}, \theta)}{\partial \theta^2} \right) \right] \quad (5.55)$$

$$V_r(\bar{r}, \theta) = -\frac{D}{R^3} \left[\frac{\partial}{\partial \bar{r}} \nabla^2 \bar{w}_I(\bar{r}, \theta) + (1-\nu) \frac{1}{\bar{r}} \frac{\partial}{\partial \theta} \left(\frac{1}{\bar{r}} \frac{\partial^2 \bar{w}_I(\bar{r}, \theta)}{\partial \bar{r} \partial \theta} - \frac{1}{\bar{r}^2} \frac{\partial \bar{w}_I(\bar{r}, \theta)}{\partial \theta} \right) \right] \quad (5.56)$$

From equations (5.53) and (5.55) yields the following

$$\left[\frac{\partial^2 \bar{w}_I(\bar{r}, \theta)}{\partial \bar{r}^2} + \nu \left(\frac{1}{\bar{r}} \frac{\partial \bar{w}_I(\bar{r}, \theta)}{\partial \bar{r}} + \frac{1}{\bar{r}^2} \frac{\partial^2 \bar{w}_I(\bar{r}, \theta)}{\partial \theta^2} \right) \right] = \frac{K_{R2} R^2}{D} \frac{\partial^2 \bar{w}_I(\bar{r}, \theta)}{\partial \bar{r}^2} \quad (5.57)$$

$$\left[\frac{\partial^2 \bar{w}_I(\bar{r}, \theta)}{\partial \bar{r}^2} + \nu \left(\frac{1}{\bar{r}} \frac{\partial \bar{w}_I(\bar{r}, \theta)}{\partial \bar{r}} + \frac{1}{\bar{r}^2} \frac{\partial^2 \bar{w}_I(\bar{r}, \theta)}{\partial \theta^2} \right) \right] = R_{22} \frac{\partial \bar{w}_I(\bar{r}, \theta)}{\partial \bar{r}} \quad (5.58)$$

$$\text{where } R_{22} = \frac{K_{R2} R^2}{D}$$

From equations (5.54) and (5.56) yields the following

$$\left[\frac{\partial}{\partial \bar{r}} \nabla^2 \bar{w}_I(\bar{r}, \theta) + (1-\nu) \frac{1}{\bar{r}} \frac{\partial}{\partial \theta} \left(\frac{1}{\bar{r}} \frac{\partial^2 \bar{w}_I(\bar{r}, \theta)}{\partial \bar{r} \partial \theta} - \frac{1}{\bar{r}^2} \frac{\partial \bar{w}_I(\bar{r}, \theta)}{\partial \theta} \right) \right] = -\frac{K_{T2} R^3}{D} \bar{w}_I(\bar{r}, \theta) \quad (5.59)$$

$$\left[\frac{\partial}{\partial \bar{r}} \nabla^2 \bar{w}_I(\bar{r}, \theta) + (1-\nu) \frac{1}{\bar{r}} \frac{\partial}{\partial \theta} \left(\frac{1}{\bar{r}} \frac{\partial^2 \bar{w}_I(\bar{r}, \theta)}{\partial \bar{r} \partial \theta} - \frac{1}{\bar{r}^2} \frac{\partial \bar{w}_I(\bar{r}, \theta)}{\partial \theta} \right) \right] = -T_{22} \bar{w}_I(\bar{r}, \theta) \quad (5.60)$$

where $T_{22} = \frac{K_{r2} R^3}{D}$

Boundary conditions when the edges are elastically restrained against rotation.

From equations (5.7) and (5.58) yields the following

$$\frac{\partial \bar{w}(\bar{r}, \theta)}{\partial \bar{r}} = \left[\frac{k}{2} [J_{n-1}(k\bar{r}) - J_{n+1}(k\bar{r})] C_1 + \frac{k}{2} [Y_{n-1}(k\bar{r}) - Y_{n+1}(k\bar{r})] C_2 + n\bar{r}^{n-1} C_3 + \left\{ \frac{1}{\bar{r}} \right. \right. \\ \left. \left. - n\bar{r}^{-n-1} \right\} C_4 \right] \cos(n\theta) \quad (5.61)$$

$$\frac{\partial \bar{w}(\bar{r}, \theta)}{\partial \bar{r}} \Big|_{b=1} = \left[\frac{k}{2} [J_{n-1}(kb) - J_{n+1}(kb)] C_1 + \frac{k}{2} [Y_{n-1}(kb) - Y_{n+1}(kb)] C_2 + nC_3 b^{n-1} + \left\{ \frac{1}{b} \right. \right. \\ \left. \left. - nb^{-n-1} \right\} C_4 \right] \cos(n\theta) \quad (5.62)$$

$$\frac{\partial \bar{w}(\bar{r}, \theta)}{\partial \bar{r}} \Big|_{b=1} = \left[\frac{k}{2} [P'_1] C_1 + \frac{k}{2} [Q'_1] C_2 + nC_3 b^{n-1} + \left\{ \frac{1}{b} \right. \right. \\ \left. \left. - nb^{-n-1} \right\} C_4 \right] \cos(n\theta) \quad (5.63)$$

where $P'_1 = J_{n-1}(kb) - J_{n+1}(kb)$; $Q'_1 = Y_{n-1}(kb) - Y_{n+1}(kb)$

$$\frac{\partial^2 \bar{w}(\bar{r}, \theta)}{\partial \bar{r}^2} = \left[\frac{k^2}{4} [(J_{n-2}(k\bar{r}) - J_n(k\bar{r})) - (J_n(k\bar{r}) - J_{n+2}(k\bar{r}))] C_1 + \right. \\ \left. \frac{k^2}{4} [(Y_{n-2}(k\bar{r}) - Y_n(k\bar{r})) - (Y_n(k\bar{r}) - Y_{n+2}(k\bar{r}))] C_2 + n(n-1)\bar{r}^{n-2} C_3 + \left\{ -\frac{1}{\bar{r}^2} \right. \right. \\ \left. \left. + \frac{n(n+1)}{\bar{r}^{n-2}} \right\} C_4 \right] \cos(n\theta) \quad (5.64)$$

$$\frac{\partial^2 \bar{w}(\bar{r}, \theta)}{\partial \bar{r}^2} = \left[\frac{k^2}{4} [(J_{n-2}(k\bar{r}) + J_{n+2}(k\bar{r}) - 2J_n(k\bar{r}))] C_1 + \right. \\ \left. \frac{k^2}{4} [(Y_{n-2}(k\bar{r}) + Y_{n+2}(k\bar{r}) - 2Y_n(k\bar{r}))] C_2 + n(n-1)\bar{r}^{n-2} C_3 + \left\{ -\frac{1}{\bar{r}^2} \right. \right. \\ \left. \left. + \frac{n(n+1)}{\bar{r}^{n-2}} \right\} C_4 \right] \cos(n\theta) \quad (5.65)$$

$$\frac{\partial^2 \bar{w}(\bar{r}, \theta)}{\partial \bar{r}^2} \Big|_{b=1} = \left[\begin{aligned} & \frac{k^2}{4} [(J_{n-2}(kb) + J_{n+2}(kb) - 2J_n(kb))] C_1 + \\ & \frac{k^2}{4} [(Y_{n-2}(kb) + Y_{n+2}(kb) - 2Y_n(kb))] C_2 + n(n-1)b^{n-2} C_3 + \left\{ -\frac{1}{b^2} \right\} C_4 \end{aligned} \right] \cos(n\theta) \quad (5.66)$$

$$\frac{\partial^2 \bar{w}(\bar{r}, \theta)}{\partial \bar{r}^2} \Big|_{\bar{r}=1} = \left[\begin{aligned} & \frac{k^2}{4} [(P'_2 - 2J_n(kb))] C_1 + \\ & \frac{k^2}{4} [(Q'_2 - 2Y_n(kb))] C_2 + n(n-1)b^{n-2} C_3 + \left\{ -\frac{1}{b^2} \right\} C_4 \end{aligned} \right] \cos(n\theta) \quad (5.67)$$

where $P'_2 = J_{n-2}(kb) + J_{n+2}(kb)$; $Q'_2 = Y_{n-2}(kb) + Y_{n+2}(kb)$

$$\frac{1}{\bar{r}} \frac{\partial \bar{w}(\bar{r}, \theta)}{\partial \bar{r}} = \frac{1}{\bar{r}} \left[\begin{aligned} & \frac{k}{2} [J_{n-1}(k\bar{r}) - J_{n+1}(k\bar{r})] C_1 + \frac{k}{2} [Y_{n-1}(k\bar{r}) - Y_{n+1}(k\bar{r})] C_2 + n\bar{r}^{n-1} C_3 \\ & + \left\{ \frac{1}{\bar{r}} \right\} C_4 \\ & - n\bar{r}^{-n-1} \end{aligned} \right] \cos(n\theta) \quad (5.68)$$

$$\frac{1}{\bar{r}} \frac{\partial \bar{w}(\bar{r}, \theta)}{\partial \bar{r}} \Big|_{b=1} = \frac{1}{b} \left[\begin{aligned} & \frac{k}{2} [J_{n-1}(kb) - J_{n+1}(kb)] C_1 + \frac{k}{2} [Y_{n-1}(kb) - Y_{n+1}(kb)] C_2 + nb^{n-1} C_3 + \left\{ \frac{1}{b} \right\} C_4 \\ & - nb^{-n-1} \end{aligned} \right] \cos(n\theta) \quad (5.69)$$

$$\frac{1}{\bar{r}} \frac{\partial \bar{w}(\bar{r}, \theta)}{\partial \bar{r}} \Big|_{b=1} = \frac{1}{b} \left[\begin{aligned} & \frac{k}{2} [P'_1] C_1 + \frac{k}{2} [Q'_1] C_2 + nb^{n-1} C_3 + \left\{ \frac{1}{b} \right\} C_4 \\ & - nb^{-n-1} \end{aligned} \right] \cos(n\theta) \quad (5.70)$$

$$\frac{\partial \bar{w}(\bar{r}, \theta)}{\partial \theta} = -n \left[C_1 J_n(k\bar{r}) + C_2 Y_n(k\bar{r}) + C_3 \bar{r}^n + C_4 \left\{ \frac{\log \bar{r}}{\bar{r}^{-n}} \right\} \right] \sin(n\theta) \quad (5.71)$$

$$\frac{\partial^2 \bar{w}(\bar{r}, \theta)}{\partial \theta^2} = -n^2 \left[C_1 J_n(k\bar{r}) + C_2 Y_n(k\bar{r}) + C_3 \bar{r}^n + C_4 \left\{ \frac{\log \bar{r}}{\bar{r}^{-n}} \right\} \right] \cos(n\theta) \quad (5.72)$$

$$\frac{1}{\bar{r}^2} \frac{\partial^2 \bar{w}(\bar{r}, \theta)}{\partial \theta^2} = -\frac{n^2}{\bar{r}^2} \left[C_1 J_n(k\bar{r}) + C_2 Y_n(k\bar{r}) + C_3 \bar{r}^n + C_4 \left\{ \frac{\log \bar{r}}{\bar{r}^{-n}} \right\} \right] \cos(n\theta) \quad (5.73)$$

$$\frac{1}{\bar{r}^2} \frac{\partial^2 \bar{w}(\bar{r}, \theta)}{\partial \theta^2} \Big|_{b=1} = -\frac{n^2}{b^2} \left[C_1 J_n(kb) + C_2 Y_n(kb) + C_3 b^n + C_4 \left\{ \frac{\log b}{b^{-n}} \right\} \right] \cos(n\theta) \quad (5.74)$$

Substituting equations (5.63), (5.67), (5.70), (5.74) into equation (5.58) gives the following

$$\begin{aligned}
& \left[\frac{k^2}{4} P_2' + \frac{k}{2} \left(\frac{\nu}{b} - R_{22} \right) P_1' - \left(\frac{k^2}{2} + \frac{\nu n^2}{b^2} \right) J_n(kb) \right] C_1 + \\
& \left[\frac{k^2}{4} Q_2' + \frac{k}{2} \left(\frac{\nu}{b} - R_{22} \right) Q_1' - \left(\frac{k^2}{2} + \frac{\nu n^2}{b^2} \right) Y_n(kb) \right] C_2 + \\
& \left[n((n-1)(1-\nu) - bR_{22}) b^{n-2} \right] C_3 + \left\{ \frac{1}{b^2} [\nu(1-n^2 \log b) - 1 - bR_{22}] \right. \\
& \left. n[(n+1)(1-\nu) + R_{22} b^{-2n-3}] b^{-n-2} \right\} C_4 = 0
\end{aligned} \tag{5.75}$$

Boundary conditions when the edges are elastically restrained against translation.

From equations (5.7) and (5.15) yields the following

$$\frac{\partial}{\partial \bar{r}} \nabla^2 \bar{w}(\bar{r}, \theta) = \frac{\partial}{\partial \bar{r}} \left[\frac{\partial^2 \bar{w}(\bar{r}, \theta)}{\partial \bar{r}^2} + \frac{1}{\bar{r}^2} \frac{\partial^2 \bar{w}(\bar{r}, \theta)}{\partial \theta^2} + \frac{1}{\bar{r}} \frac{\partial \bar{w}(\bar{r}, \theta)}{\partial \bar{r}} \right] \tag{5.76}$$

$$\begin{aligned}
\frac{\partial}{\partial \bar{r}} \left[\frac{\partial^2 \bar{w}(\bar{r}, \theta)}{\partial \bar{r}^2} \right] &= \frac{\partial}{\partial \bar{r}} \left[\frac{k^2}{4} [(J_{n-2}(k\bar{r}) + J_{n+2}(k\bar{r}) - 2J_n(k\bar{r}))] C_1 + \right. \\
& \left. \frac{k^2}{4} [(Y_{n-2}(k\bar{r}) + Y_{n+2}(k\bar{r}) - 2Y_n(k\bar{r}))] C_2 + n(n-1)\bar{r}^{n-2} C_3 + \left\{ -\frac{1}{\bar{r}^2} \right. \right. \\
& \left. \left. n(n+1)\bar{r}^{-n-2} \right\} C_4 \right] \cos(n\theta)
\end{aligned} \tag{5.77}$$

$$= \left\{ \begin{aligned} & \frac{k^3}{8} [(J_{n-3}(k\bar{r}) - J_{n-1}(k\bar{r})) + (J_{n+1}(k\bar{r}) - J_{n+3}(k\bar{r})) - 2(J_{n-1}(k\bar{r}) - J_{n+1}(k\bar{r}))] C_1 + \\ & \frac{k^3}{8} [(Y_{n-3}(k\bar{r}) - Y_{n-1}(k\bar{r})) + (Y_{n+1}(k\bar{r}) - Y_{n+3}(k\bar{r})) - 2(Y_{n-1}(k\bar{r}) - Y_{n+1}(k\bar{r}))] C_2 + \\ & n(n-1)(n-2)\bar{r}^{n-3} C_3 + \left\{ \frac{2}{\bar{r}^3} \right. \\ & \left. - n(n+1)(n+2)\bar{r}^{-n-3} \right\} C_4 \end{aligned} \right\} \cos(n\theta) \tag{5.78}$$

$$= \left\{ \begin{aligned} & \frac{k^3}{8} [(J_{n-3}(k\bar{r}) - J_{n+3}(k\bar{r})) - 3(J_{n-1}(k\bar{r}) - J_{n+1}(k\bar{r}))] C_1 + \\ & \frac{k^3}{8} [(Y_{n-3}(k\bar{r}) - Y_{n+3}(k\bar{r})) - 3(Y_{n-1}(k\bar{r}) - Y_{n+1}(k\bar{r}))] C_2 + \\ & n(n-1)(n-2)\bar{r}^{n-3} C_3 + \left\{ \frac{2}{\bar{r}^3} \right. \\ & \left. - n(n+1)(n+2)\bar{r}^{-n-3} \right\} C_4 \end{aligned} \right\} \cos(n\theta) \quad (5.79)$$

$$\frac{\partial}{\partial \bar{r}} \left[\frac{\partial^2 w(\bar{r}, \theta)}{\partial \bar{r}^2} \right]_{b=1} = \left\{ \begin{aligned} & \frac{k^3}{8} [(J_{n-3}(kb) - J_{n+3}(kb)) - 3(J_{n-1}(kb) - J_{n+1}(kb))] C_1 + \\ & \frac{k^3}{8} [(Y_{n-3}(kb) - Y_{n+3}(kb)) - 3(Y_{n-1}(kb) - Y_{n+1}(kb))] C_2 + \\ & n(n-1)(n-2)b^{n-2} C_3 + \left\{ \frac{2}{b^3} \right. \\ & \left. - n(n+1)(n+2)b^{-n-3} \right\} C_4 \end{aligned} \right\} \cos(n\theta) \quad (5.80)$$

$$= \left\{ \frac{k^3}{8} [P'_3 - 3P'_1] C_1 + \frac{k^3}{8} [Q'_3 - 3Q'_1] C_2 + n(n-1)(n-2)b^{n-2} C_3 + \left\{ \frac{2}{b^3} \right. \right. \\ \left. \left. - n(n+1)(n+2)b^{-n-3} \right\} C_4 \right\} \cos(n\theta) \quad (5.81)$$

where $P'_3 = J_{n-3}(kb) - J_{n+3}(kb)$; $Q'_3 = Y_{n-3}(kb) - Y_{n+3}(kb)$

$$\frac{\partial}{\partial \bar{r}} \left[\frac{1}{\bar{r}^2} \frac{\partial^2 w(\bar{r}, \theta)}{\partial \theta^2} \right] = \frac{1}{\bar{r}^2} \frac{\partial}{\partial \bar{r}} \left[\frac{\partial^2 w(\bar{r}, \theta)}{\partial \theta^2} \right] - \frac{2}{\bar{r}^3} \frac{\partial^2 w(\bar{r}, \theta)}{\partial \theta^2} \quad (5.82)$$

$$= \frac{1}{\bar{r}^2} \left\{ -n^2 \left[\frac{k}{2} [J_{n-1}(k\bar{r}) - J_{n+1}(k\bar{r})] C_1 + \frac{k}{2} [Y_{n-1}(k\bar{r}) - Y_{n+1}(k\bar{r})] C_2 + n\bar{r}^{n-1} C_3 + \left\{ \frac{1}{\bar{r}} \right. \right. \right. \\ \left. \left. \left. - n\bar{r}^{-n-1} \right\} C_4 \right] \cos(n\theta) \right\} - \\ \frac{2}{\bar{r}^3} \left\{ -n^2 \left[C_1 J_n(k\bar{r}) + C_2 Y_n(k\bar{r}) + C_3 \bar{r}^n + C_4 \left\{ \frac{\log \bar{r}}{\bar{r}^{-n}} \right\} \right] \cos(n\theta) \right\} \quad (5.83)$$

$$\begin{aligned}
\frac{\partial}{\partial \bar{r}} \left[\frac{1}{\bar{r}^2} \frac{\partial^2 w(\bar{r}, \theta)}{\partial \theta^2} \right]_{b=1} &= \left\{ -n^2 \left[\begin{aligned} &\frac{k}{2} [J_{n-1}(kb) - J_{n+1}(kb)] C_1 + \frac{k}{2} [Y_{n-1}(kb) - Y_{n+1}(kb)] C_2 + \\ &nb^{n-1} C_3 + \left\{ \frac{1}{b} \right\} C_4 \\ &- nb^{-n-1} \end{aligned} \right] \cos(n\theta) \right\} - \\
\frac{2}{b^3} &\left\{ -n^2 \left[C_1 J_n(kb) + C_2 Y_n(kb) + C_3 b^n + C_4 \left\{ \frac{\log b}{b^{-n}} \right\} \right] \cos(n\theta) \right\}
\end{aligned} \tag{5.84}$$

$$\begin{aligned}
\frac{\partial}{\partial \bar{r}} \left[\frac{1}{\bar{r}^2} \frac{\partial^2 w(\bar{r}, \theta)}{\partial \theta^2} \right]_{\bar{r}=1} &= -n^2 \left[\frac{k}{2} [P'_1] C_1 + \frac{k}{2} [Q'_1] C_2 + nb^{n-1} C_3 + \left\{ \frac{1}{b} \right\} C_4 \right] \cos(n\theta) + \\
\frac{2n^2}{b^3} &\left[C_1 J_n(kb) + C_2 Y_n(kb) + C_3 b^n + C_4 \left\{ \frac{\log b}{b^{-n}} \right\} \right] \cos(n\theta)
\end{aligned} \tag{5.85}$$

$$\frac{\partial}{\partial \bar{r}} \left[\frac{1}{\bar{r}} \frac{\partial w(\bar{r}, \theta)}{\partial \bar{r}} \right] = \frac{1}{\bar{r}} \frac{\partial}{\partial \bar{r}} \left[\frac{\partial w(\bar{r}, \theta)}{\partial \bar{r}} \right] + \frac{\partial w(\bar{r}, \theta)}{\partial \bar{r}} \frac{\partial}{\partial \bar{r}} \left[\frac{1}{\bar{r}} \right] = \frac{1}{\bar{r}} \frac{\partial^2 w(\bar{r}, \theta)}{\partial \bar{r}^2} - \frac{1}{\bar{r}^2} \frac{\partial w(\bar{r}, \theta)}{\partial \bar{r}} \tag{5.86}$$

$$\begin{aligned}
&= \frac{1}{\bar{r}} \left[\frac{k^2}{4} [(J_{n-2}(k\bar{r}) + J_{n+2}(k\bar{r}) - 2J_n(k\bar{r}))] C_1 + \right. \\
&\left. \frac{k^2}{4} [(Y_{n-2}(k\bar{r}) + Y_{n+2}(k\bar{r}) - 2Y_n(k\bar{r}))] C_2 + n(n-1)\bar{r}^{n-2} C_3 + \left\{ -\frac{1}{\bar{r}^2} \right\} C_4 \right] \cos(n\theta) \\
&- \frac{1}{\bar{r}^2} \left[\frac{k}{2} [J_{n-1}(k\bar{r}) - J_{n+1}(k\bar{r})] C_1 + \frac{k}{2} [Y_{n-1}(k\bar{r}) - Y_{n+1}(k\bar{r})] C_2 + n\bar{r}^{n-1} C_3 + \left\{ \frac{1}{\bar{r}} \right\} C_4 \right] \cos(n\theta)
\end{aligned} \tag{5.87}$$

$$\frac{\partial}{\partial \bar{r}} \left[\frac{1}{\bar{r}} \frac{\partial w(\bar{r}, \theta)}{\partial \bar{r}} \right]_{\bar{r}=1} =$$

$$= \frac{1}{b} \left[\frac{k^2}{4} [(J_{n-2}(kb) + J_{n+2}(kb) - 2J_n(kb))] C_1 + \frac{k^2}{4} [(Y_{n-2}(kb) + Y_{n+2}(kb) - 2Y_n(kb))] C_2 + n(n-1)b^{n-2}C_3 + \left\{ \frac{1}{b^2} \right\}_{n(n+1)b^{-n-2}} C_4 \right] \cos(n\theta) \quad (5.88)$$

$$- \frac{1}{b^2} \left[\frac{k}{2} [J_{n-1}(kb) - J_{n+1}(kb)] C_1 + \frac{k}{2} [Y_{n-1}(kb) - Y_{n+1}(kb)] C_2 + nb^{n-1}C_3 + \left\{ \frac{1}{b} \right\}_{-nb^{-n-1}} C_4 \right] \cos(n\theta)$$

$$= \frac{1}{b} \left[\frac{k^2}{4} [P'_2 - 2J_n(kb)] C_1 + \frac{k^2}{4} [Q'_2 - 2Y_n(kb)] C_2 + n(n-1)b^{n-2}C_3 + \left\{ \frac{1}{b^2} \right\}_{n(n+1)b^{-n-2}} C_4 \right] \cos(n\theta)$$

$$- \frac{1}{b^2} \left[\frac{k}{2} [P'_1] C_1 + \frac{k}{2} [Q'_1] C_2 + nb^{n-1}C_3 + \left\{ \frac{1}{b} \right\}_{-nb^{-n-1}} C_4 \right] \cos(n\theta)$$

$$(5.89)$$

$$\left[\frac{\partial^2 w(\bar{r}, \theta)}{\partial \bar{r} \partial \theta} \right] = \frac{\partial}{\partial \bar{r}} \left[\frac{\partial w(\bar{r}, \theta)}{\partial \theta} \right] = \frac{\partial}{\partial \bar{r}} \left\{ -n \left[C_1 J_n(k\bar{r}) + C_2 Y_n(k\bar{r}) + C_3 \bar{r}^n + C_4 \left\{ \frac{\log \bar{r}}{\bar{r}^{-n}} \right\} \right] \sin(n\theta) \right\} \quad (5.90)$$

$$= -n \left[\frac{k}{2} [J_{n-1}(k\bar{r}) - J_{n+1}(k\bar{r})] C_1 + \frac{k}{2} [Y_{n-1}(k\bar{r}) - Y_{n+1}(k\bar{r})] C_2 + n\bar{r}^{n-1}C_3 + \left\{ \frac{1}{\bar{r}} \right\}_{-n\bar{r}^{-n-1}} C_4 \right] \sin(n\theta) \quad (6.91)$$

$$\frac{1}{\bar{r}^2} \frac{\partial w(\bar{r}, \theta)}{\partial \theta} = \frac{-n}{\bar{r}^2} \left[C_1 J_n(k\bar{r}) + C_2 Y_n(k\bar{r}) + C_3 \bar{r}^n + C_4 \left\{ \frac{\log \bar{r}}{\bar{r}^{-n}} \right\} \right] \sin(n\theta) \quad (5.92)$$

From equations (5.91) and (5.92) yields the following

$$\begin{aligned} & \frac{\partial}{\partial \theta} \left[\frac{1}{\bar{r}} \frac{\partial^2 w(\bar{r}, \theta)}{\partial \bar{r} \partial \theta} - \frac{1}{\bar{r}^2} \frac{\partial w(\bar{r}, \theta)}{\partial \theta} \right] \\ &= -\frac{n^2}{\bar{r}} \left[\frac{k}{2} [J_{n-1}(k\bar{r}) - J_{n+1}(k\bar{r})] C_1 + \frac{k}{2} [Y_{n-1}(k\bar{r}) - Y_{n+1}(k\bar{r})] C_2 + n\bar{r}^{n-1}C_3 + \left\{ \frac{1}{\bar{r}} \right\}_{-n\bar{r}^{-n-1}} C_4 \right] \cos(n\theta) + \\ & \frac{n^2}{\bar{r}^2} \left[C_1 J_n(k\bar{r}) + C_2 Y_n(k\bar{r}) + C_3 \bar{r}^n + C_4 \left\{ \frac{\log \bar{r}}{\bar{r}^{-n}} \right\} \right] \cos(n\theta) \end{aligned}$$

$$(5.93)$$

Equation (5.93) can be written as

$$\begin{aligned}
 & (1-\nu) \frac{1}{\bar{r}} \frac{\partial}{\partial \theta} \left[\frac{1}{\bar{r}} \frac{\partial^2 w(\bar{r}, \theta)}{\partial \bar{r} \partial \theta} - \frac{1}{\bar{r}^2} \frac{\partial w(\bar{r}, \theta)}{\partial \theta} \right]_{b=1} \\
 &= (1-\nu) \frac{1}{b} \left\{ -\frac{n^2}{b} \left[\frac{k}{2} [J_{n-1}(kb) - J_{n+1}(kb)] C_1 + \frac{k}{2} [Y_{n-1}(kb) - Y_{n+1}(kb)] C_2 + nb^{n-1} C_3 + \left\{ \frac{1}{b} \right. \right. \right. \\
 & \quad \left. \left. \left. - nb^{-n-1} \right\} C_4 \right] \cos(n\theta) + \right. \\
 & \quad \left. \frac{n^2}{b^2} \left[C_1 J_n(kb) + C_2 Y_n(kb) + C_3 b^n + C_4 \left\{ \frac{\log b}{b^{-n}} \right\} \right] \cos(n\theta) \right\}
 \end{aligned} \tag{5.94}$$

$$\begin{aligned}
 &= (1-\nu) \frac{1}{b} \left\{ -\frac{n^2}{b} \left[\frac{k}{2} [P'_1] C_1 + \frac{k}{2} [Q'_1] C_2 + nb^{n-1} C_3 + \left\{ \frac{1}{b} \right. \right. \right. \\
 & \quad \left. \left. \left. - nb^{-n-1} \right\} C_4 \right] \cos(n\theta) + \right. \\
 & \quad \left. \frac{n^2}{b^2} \left[C_1 J_n(kb) + C_2 Y_n(kb) + C_3 b^n + C_4 \left\{ \frac{\log b}{b^{-n}} \right\} \right] \cos(n\theta) \right\}
 \end{aligned} \tag{5.95}$$

Equation (5.7) gives following at $\bar{r} = 1$

$$\bar{w}(\bar{r}, \theta)_{b=1} = \left[C_1 J_n(kb) + C_2 Y_n(kb) + C_3 b^n + C_4 \left\{ \frac{\log b}{b^{-n}} \right\} \right] \cos(n\theta) \tag{6.96}$$

Substituting equations (5.81), (5.85), (5.89), (5.95), (5.96) into equation (.15) gives the following

$$\begin{aligned}
 & \left[\frac{k^3}{8} P'_3 + \frac{k^2}{4b} P'_2 - \frac{k}{2} \left(\frac{3}{4} k^2 + \frac{n^2(2-\nu)+1}{b^2} \right) P'_1 + \left(\frac{n^2(3-\nu)}{b^3} - \frac{k^2}{2b} + T_{22} \right) J_n(kb) \right] C_1 + \\
 & \left[\frac{k^3}{8} Q'_3 + \frac{k^2}{4b} Q'_2 - \frac{k}{2} \left(\frac{3}{4} k^2 + \frac{n^2(2-\nu)+1}{b^2} \right) Q'_1 + \left(\frac{n^2(3-\nu)}{b^3} - \frac{k^2}{2b} + T_{22} \right) Y_n(kb) \right] C_2 + \\
 & b^{n-3} \left[n^2(n-1)(\nu-1) + T_{22} b^3 \right] C_3 + \left\{ \frac{n^2}{b^3} [(\nu-2) + (3-\nu) \log b] + T_{22} \log b \right\} C_4 = 0
 \end{aligned} \tag{5.97}$$

$$\text{where } R_{22} = \frac{K_{R2} R^2}{D}, \quad T_{22} = \frac{K_{T2} R^3}{D}$$

$$\begin{aligned}
 & P'_1 = J_{n-1}(kb) - J_{n+1}(kb); P'_2 = J_{n-2}(kb) + J_{n+2}(kb); P'_3 = J_{n-3}(kb) - J_{n+3}(kb); \\
 & Q'_1 = Y_{n-1}(kb) - Y_{n+1}(kb); Q'_2 = Y_{n-2}(kb) + Y_{n+2}(kb); Q'_3 = Y_{n-3}(kb) - Y_{n+3}(kb);
 \end{aligned}$$

Set $K_{T_1} \rightarrow \infty, K_{T_2} \rightarrow \infty$ & $K_{R_2} \rightarrow 0$ in Figure 5.1, then problem becomes annular plate with restrained edge against rotation at outer edge and simply supported at both edges. The set of equations in this case are by setting $T_{11} \rightarrow \infty, T_{22} \rightarrow \infty$ & $R_{22} \rightarrow 0$ into equations (5.52), (5.75) and (5.97).

5.4 Solution

For the given values of $n, \nu, R_{11}, T_{11}, R_{22}, T_{22}$ the above set of equations, gives an exact characteristic equation for non-trivial solutions of the coefficients C_1, C_2, C_3 & C_4 . For non-trivial solution, the determinant of $[C]_{4 \times 4}$ vanish. Using Mathematica, computer software with symbolic capabilities, solves this problem.

5.5 Results and discussions

Buckling load parameters are calculated for various internal radii parameter b , rotational spring stiffness parameters R_{11} & R_{22} , translational spring stiffness parameters T_{11} & T_{22} . For these calculations, we adopt Poisson's ratio $\nu = 0.3$.

The buckling load parameters for axisymmetric and asymmetric modes and for various rotational spring stiffness parameters at outer edge R_{11} , and keeping constant rotational spring stiffness parameter R_{22} , and translational spring stiffness parameters T_{11} & T_{22} , ($R_{22} = T_{11} = T_{22} = 10$), are presented in Table 5.1 and graphically in Figs 5.2 – 5.6. It is observed from the Fig. 5.2, for a given value of $R_{11} = 0.001$ and $R_{22} = T_{11} = T_{22} = 10$, the curve is composed of two segments. This is due to the switching of buckling modes. For a smaller internal radius b , the plate buckles in an axisymmetric mode (*i.e.*, $n = 0$).

In this segment (as shown by continuous lines in Fig. 5.2) the buckling load decreases as b decreases in value. For larger internal radius b , the plate buckles in an asymmetric mode (*i.e.*, $n = 1$). In this segment (as shown by dotted lines in Fig. 5.2) the buckling load increases as b increases in value as shown in Fig. 5.2. The cross over radius (switching of mode) is $b = 0.32891$ *i.e.*, the buckling is governed by the axisymmetric mode $n = 0$ when $b \leq 0.32891$. When b is increased beyond 0.32891, the $n = 1$ asymmetric mode gives the correct lower buckling load. Fig. 5.3, shows the variation of buckling load parameter k , with respect to the internal radius parameter b , for a given value of $R_{11} = 0.5$ and $R_{22} = T_{11} = T_{22} = 10$. It is observed from the Fig. 5.3, the curve is composed of two segments. This is due to the switching of buckling modes. The cross over radius (switching of mode) is $b = 0.2598$ and the corresponding buckling load is $k = 3.5777$. The buckling is governed by the axisymmetric mode $n = 0$ when $b \leq 0.2598$. When b is increased beyond 0.2598, the $n = 1$ asymmetric mode gives the correct lower buckling load. The cross-over radius parameter varies from 0.32891 to 0.2598 as R_{11} increased from 0.001 to 0.5.

Fig. 5.4, shows the variation of buckling load parameter k , with respect to the internal radius parameter b , for a given values of $R_{11} = 10$ and $R_{22} = T_{11} = T_{22} = 10$. It is noticed that the buckling is completely governed by asymmetric mode $n = 1$ (as shown by dotted lines in Fig. 5.4) and the buckling load increases as b increases in value as shown in Fig. 5.4. Fig. 5.5 shows the variation of buckling load parameter k , with respect to the internal radius parameter b , for a given values of $R_{11} = 100$ and $R_{22} = T_{11} = T_{22} = 10$. It is noticed that the buckling is completely governed by asymmetric mode $n = 1$ (as shown by dotted lines in Fig. 5.5) and the buckling load increases as b

increases in value as shown in Fig. 5.5. Fig. 5.6, shows the variation of buckling load parameter k , with respect to the internal radius parameter b , for a given values of $R_{11} = \infty$ and $R_{22} = T_{11} = T_{22} = 10$. It is noticed that the buckling is completely governed by asymmetric mode $n = 1$ (as shown by dotted lines in Fig. 5.6) and the buckling load increases as b increases in value as shown in Fig. 5.6.

Table 5.1 Buckling ($n = 0$ for axisymmetric mode and $n = 1$ for asymmetric mode) Load Parameters for different values of Rotational Spring Stiffness Parameter, R_{11} when $R_{22} = T_{11} = T_{22} = 10$ & $\nu = 0.3$

b	$R_{11} = 0.001$		$R_{11} = 0.5$		$R_{11} = 10$		$R_{11} = 100$		$R_{11} = 10^{16}$	
	$[n = 0]$	$[n = 1]$	$[n = 0]$	$[n = 1]$	$[n = 0]$	$[n = 1]$	$[n = 0]$	$[n = 1]$	$[n = 0]$	$[n = 1]$
0	2.04986	3.62455	2.31751	3.59525	3.48925	3.44977	3.79385	3.39892	3.83184	3.39151
0.1	2.51953	3.61866	2.78811	3.59001	3.8877	3.44753	4.12692	3.39763	4.1552	3.39031
0.2	2.99333	3.58958	3.27022	3.56392	4.34119	3.4357	4.54703	3.39022	4.57077	3.38357
0.3	3.51119	3.62308	3.80159	3.59318	4.87509	3.44719	5.06483	3.39696	5.08641	3.3897
0.4	4.13835	3.84455	4.44833	3.78725	5.56585	3.52598	5.75441	3.44494	5.77562	3.43351
0.5	4.98519	4.36757	5.3215	4.23568	6.53843	3.69098	6.74155	3.54591	6.76439	3.52633
0.6	6.26967	5.38856	6.63843	5.08783	8.02657	3.9823	8.26475	3.7346	8.29143	3.70257
0.7	8.49521	7.31271	8.90093	6.65936	10.5599	4.54645	10.866	4.13491	10.9003	4.08295
0.8	13.1593	10.9636	13.6063	9.61489	15.7092	5.85539	16.1575	5.14108	16.2076	5.04988
0.9	27.7673	17.7729	28.2712	15.8321	31.306	9.88109	32.1917	8.44441	32.2919	8.24751

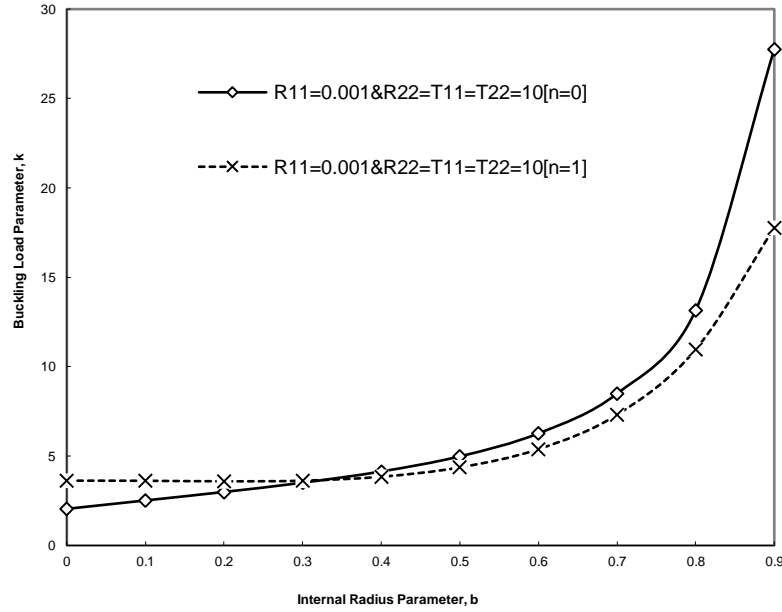


Fig. 5.2 Buckling Load Parameter k , versus Internal Radius Parameter b , for $R_{11} = 0.001$ and $R_{22} = T_{11} = T_{22} = 10$ ($n = 0$ for axisymmetric mode and $n = 1$ for asymmetric mode).

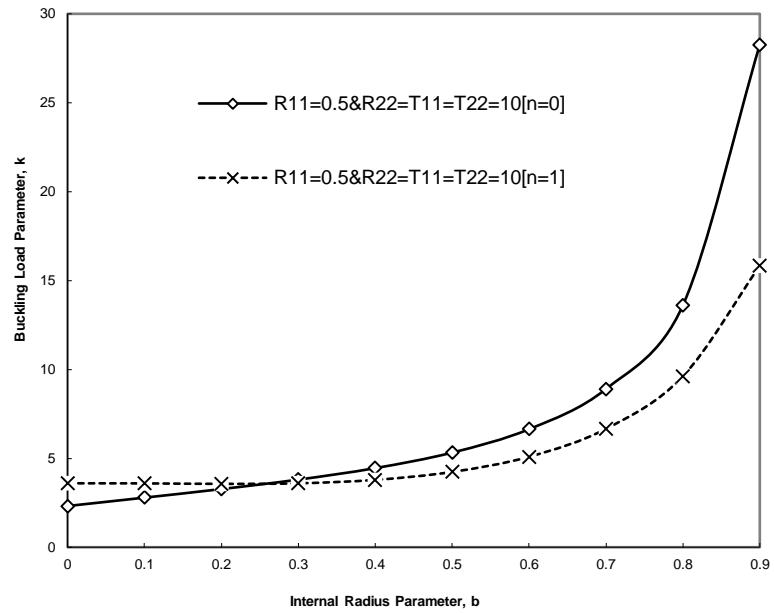


Fig. 5.3 Buckling Load Parameter k , versus Internal Radius Parameter b , for $R_{11} = 0.5$ and $R_{22} = T_{11} = T_{22} = 10$ ($n = 0$ for axisymmetric mode and $n = 1$ for asymmetric mode).

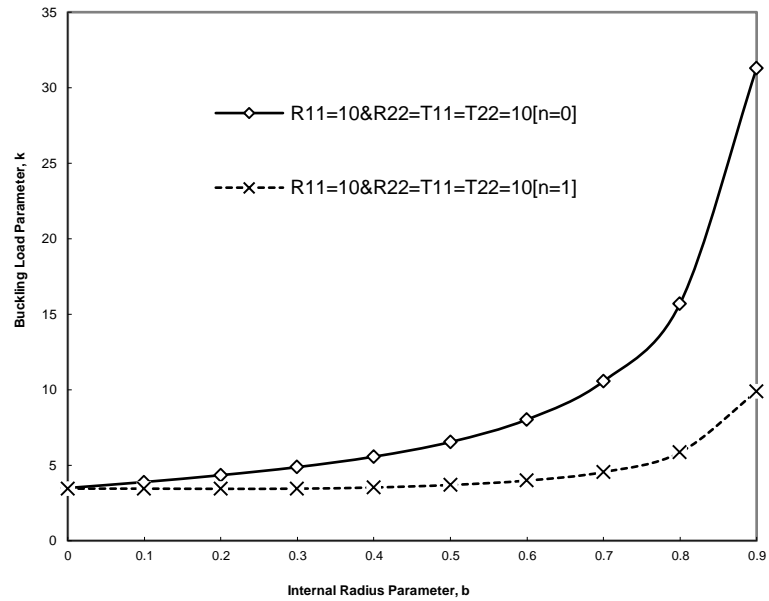


Fig. 5.4 Buckling Load Parameter k , versus Internal Radius Parameter b , for $R_{11} = 10$ and $R_{22} = T_{11} = T_{22} = 10$ ($n = 0$ for axisymmetric mode and $n = 1$ for asymmetric mode).

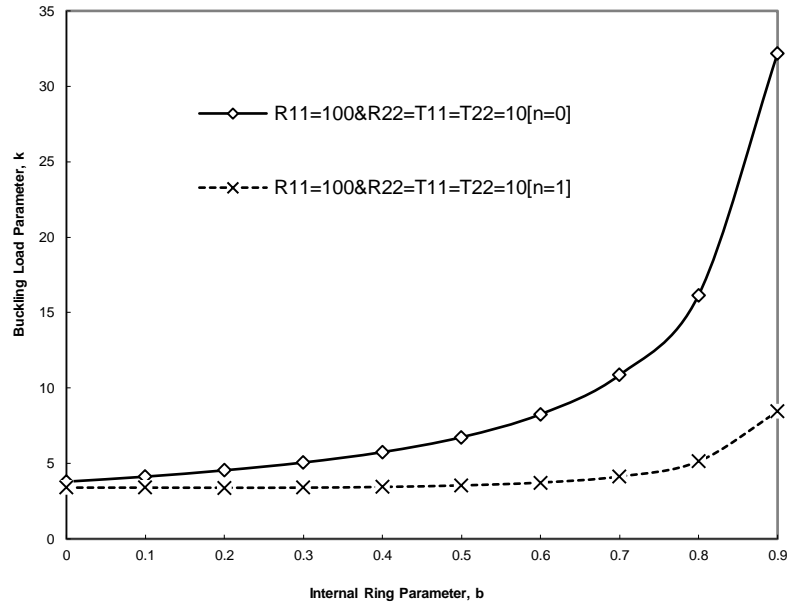


Fig. 5.5 Buckling Load Parameter k , versus Internal Radius Parameter b , for $R_{11} = 100$ and $R_{22} = T_{11} = T_{22} = 10$ ($n = 0$ for axisymmetric mode and $n = 1$ for asymmetric mode).

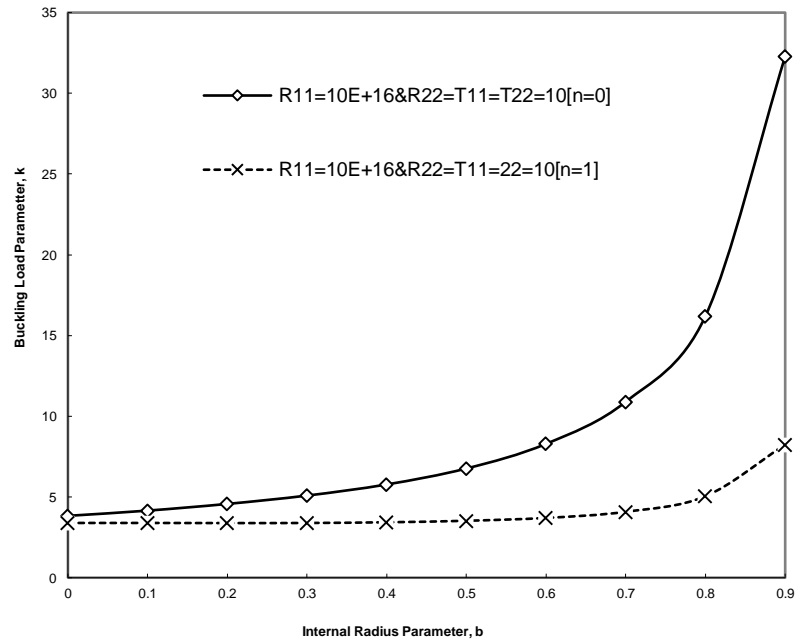


Fig. 5.6 Buckling Load Parameter k , versus Internal Radius Parameter b , for $R_{11} = \infty$ and $R_{22} = T_{11} = T_{22} = 10$ ($n = 0$ for axisymmetric mode and $n = 1$ for asymmetric mode).

The buckling load parameters for axisymmetric and asymmetric modes and for various rotational spring stiffness parameters at inner edge R_{22} , and keeping constant rotational spring stiffness parameter R_{11} , and translational spring stiffness parameters T_{11} & T_{22} , ($R_{11} = T_{11} = T_{22} = 10$), are presented in Table 5.2 and graphically in Fig. 5.7 – 5.10. Fig. 5.7 – 5.10 show the variation of buckling load parameter k , with respect to the internal radius parameter b , for various values of rotational spring stiffness parameters at inner edge ($R_{22} = 5, 10, 100$ & ∞) and $R_{11} = T_{11} = T_{22} = 10$. It is noticed from Fig. 5.6 – 5.10, the buckling is completely governed by asymmetric mode $n = 1$ (as shown by dotted lines in Fig. 5.7 – 5.10) irrespective of R_{22} . The buckling load increases as b increases in value as shown in Fig. 5.7 – 5.10.

Table 5.2 Buckling ($n = 0$ for axisymmetric mode and $n = 1$ for asymmetric mode) Load Parameters for different values of Rotational Stiffness Parameter, R_{22} when $R_{11} = T_{11} = T_{22} = 10$ & $\nu = 0.3$

b	$R_{22} = 5$		$R_{22} = 10$		$R_{22} = 100$		$R_{22} = 10^{16}$	
	$[n = 0]$	$[n = 1]$	$[n = 0]$	$[n = 1]$	$[n = 0]$	$[n = 1]$	$[n = 0]$	$[n = 1]$
0	3.49222	3.44977	3.49222	3.44977	3.49222	3.44977	3.49222	3.44977
0.1	3.90492	3.44753	3.8877	3.44753	3.85306	3.44753	3.84652	3.44753
0.2	4.39615	3.4357	4.34119	3.4357	4.26147	3.4357	4.2497	3.4357
0.3	4.96969	3.4472	4.87509	3.44719	4.75846	3.44709	4.74284	3.44709
0.4	5.69734	3.52668	5.56585	3.52598	5.41979	3.52538	5.40122	3.52538
0.5	6.7049	3.69497	6.53843	3.69098	6.3665	3.68738	6.34538	3.68698
0.6	8.23157	3.99995	8.02657	3.9823	7.82619	3.96595	7.80225	3.96415
0.7	10.8202	4.61191	10.5599	4.54645	10.3167	4.48418	10.2881	4.47711
0.8	16.0813	6.06545	15.7092	5.85539	15.379	5.63833	15.3406	5.61234
0.9	32.0635	10.4926	31.306	9.88109	30.7084	9.12756	30.6393	9.02702

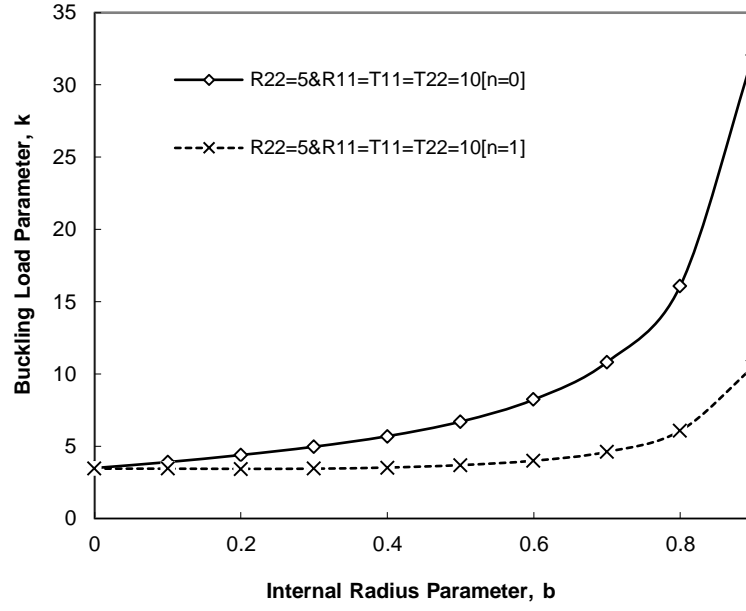


Fig. 5.7 Buckling Load Parameter k , versus Internal Radius Parameter b , for $R_{22} = 5$ and $R_{11} = T_{11} = T_{22} = 10$ ($n = 0$ for *axisymmetric* mode and $n = 1$ for *asymmetric* mode).

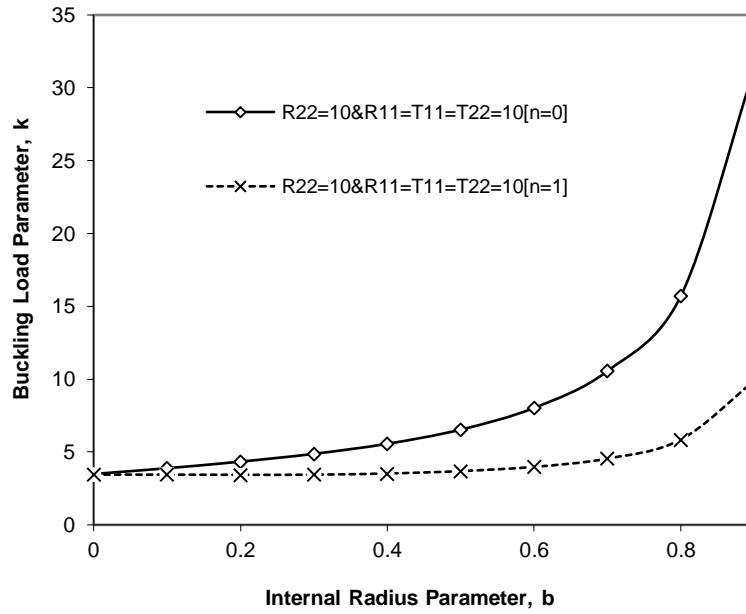


Fig. 5.8 Buckling Load Parameter k , versus Internal Radius Parameter b , for $R_{22} = 10$ and $R_{11} = T_{11} = T_{22} = 10$ ($n = 0$ for *axisymmetric* mode and $n = 1$ for *asymmetric* mode).

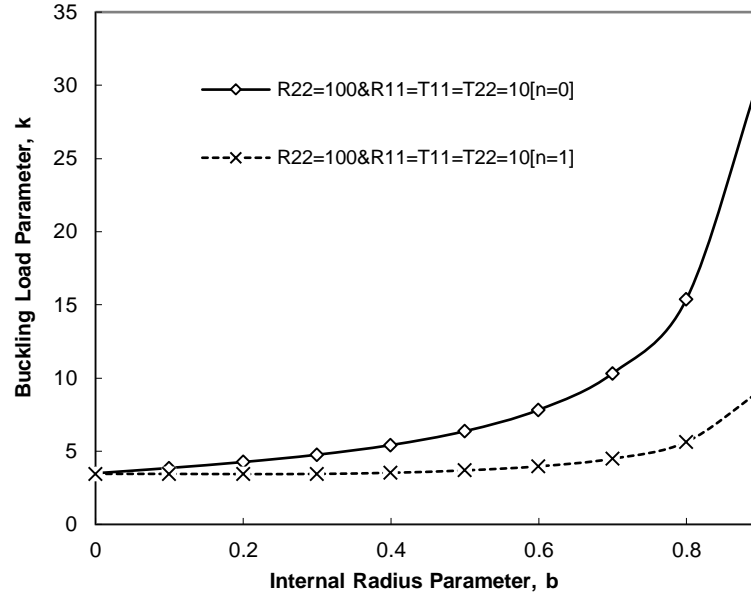


Fig. 5.9 Buckling Load Parameter k , versus Internal Radius Parameter b , for $R_{22} = 100$ and $R_{11} = T_{11} = T_{22} = 10$ ($n = 0$ for *axisymmetric* mode and $n = 1$ for *asymmetric* mode).

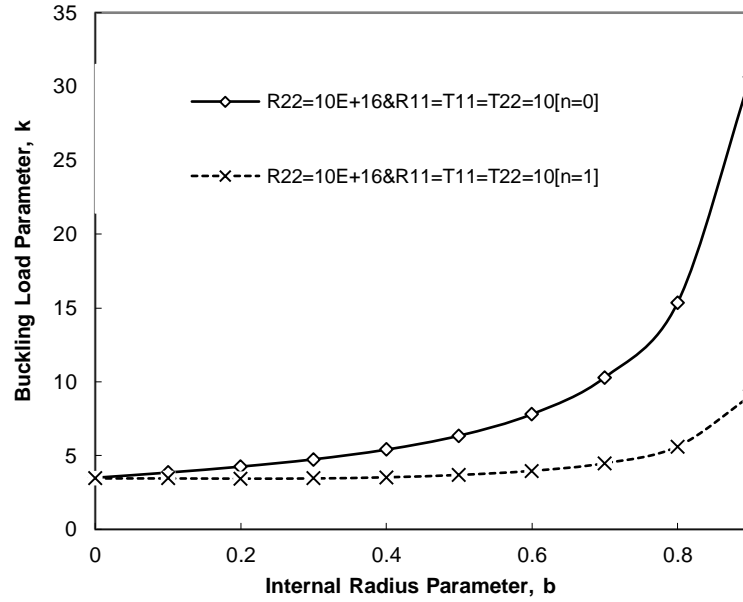


Fig. 5.10 Buckling Load Parameter k , versus Internal Radius Parameter b , for $R_{22} = \infty$ and $R_{11} = T_{11} = T_{22} = 10$ ($n = 0$ for *axisymmetric* mode and $n = 1$ for *asymmetric* mode).

The buckling load parameters for axisymmetric and asymmetric modes and for various translational spring stiffness parameters at outer edge T_{11} , and keeping constant rotational spring stiffness parameters R_{11} & R_{22} , and translational spring stiffness

parameter at inner edge T_{22} , ($R_{11} = R_{22} = T_{22} = 10$), are presented in Table 5.3 and graphically in Figs. 5.11 to 5.14. Figs. 5.11 to 5.12 show the variation of buckling load parameter k , with respect to the internal radius parameter b , for various values of translational spring stiffness parameters at outer edge ($T_{11} = 5 \& 10$) and $R_{11} = R_{22} = T_{22} = 10$. It is observed from Figs. 5.11 to 5.12, the buckling is completely governed by asymmetric mode $n = 1$ (as shown by dotted lines in Figs. 5.11 to 5.12) and the buckling load increases as the value of b increases and is shown in Figs. 5.11 to 5.12.

Fig. 5.13, shows the variation of buckling load parameter k , with respect to the internal radius b , for translational spring stiffness parameter of $T_{11} = 100$ and $R_{11} = R_{22} = T_{22} = 10$. It is observed from the Fig. 5.13, for a given value of $T_{11} = 100$ and $R_{11} = R_{22} = T_{22} = 10$, the curve is composed of two segments. This is due to the switching of buckling modes. For a smaller internal radius b , the plate buckles in an axisymmetric mode (*i.e.*, $n = 0$). In this segment (as shown by continuous lines in Fig. 5.13) the buckling load decreases as b decreases in value. For larger internal radius b , the plate buckles in an asymmetric mode (*i.e.*, $n = 1$). In this segment (as shown by dotted lines in Fig. 5.13) the buckling load increases as b increases in value as shown in Fig. 5.13. The cross over radius (switching of mode) is $b = 0.2598$. The buckling is governed by the axisymmetric mode $n = 0$ when $b \leq 0.2598$. When b is increased beyond 0.2598, the $n = 1$ asymmetric mode gives the correct lower buckling load. Fig. 5.14, shows the variation of buckling load parameter k , with respect to the internal radius parameter b , for a given value of $T_{11} = \infty$ and $R_{11} = R_{22} = T_{22} = 10$. It is observed from the Fig. 5.14, the curve is composed of two segments. This is due to the switching of buckling mode. The cross over radius (switching of mode) is $b = 0.28855$ and the corresponding buckling

load is $k = 4.6901$. The buckling is governed by the axisymmetric mode $n = 0$ when $b \leq 0.28855$. When b is increased beyond 0.28855, the $n = 1$ asymmetric mode gives the correct lower buckling load. The cross-over radius parameter varies from 0.2598 to 0.28855 as T_{11} increased from 100 to ∞ .

Table 5.3 Buckling ($n = 0$ for *axisymmetric* mode and $n = 1$ for *asymmetric* mode) Load Parameters for different values of Rotational Stiffness Parameter, T_{11} when $R_{11} = R_{22} = T_{22} = 10$ & $\nu = 0.3$

b	$T_{11} = 5$		$T_{11} = 10$		$T_{11} = 100$		$T_{11} = 10^{16}$	
	$[n = 0]$	$[n = 1]$	$[n = 0]$	$[n = 1]$	$[n = 0]$	$[n = 1]$	$[n = 0]$	$[n = 1]$
0	3.49321	2.87535	3.49222	3.44977	3.49133	4.60625	3.49123	4.71989
0.1	3.95424	2.87429	3.8877	3.44753	3.82302	4.59288	3.81549	4.70422
0.2	4.43535	2.86931	4.34119	3.4357	4.24301	4.53024	4.23112	4.63398
0.3	4.98857	2.88079	4.87509	3.44719	4.74727	4.56924	4.73103	4.68091
0.4	5.70569	2.94169	5.56585	3.52598	5.39511	4.82865	5.37225	4.97532
0.5	6.72291	3.07497	6.53843	3.69098	6.29576	5.34558	6.26151	5.57066
0.6	8.28941	3.32444	8.02657	3.9823	7.65985	6.20393	7.6055	6.59859
0.7	10.976	3.82623	10.5599	4.54645	9.96414	7.66448	9.87266	8.44754
0.8	16.5391	5.00498	15.7092	5.85539	14.6039	10.5826	14.433	12.3933
0.9	-	8.60323	31.306	9.88109	28.3987	18.9687	27.9788	24.9593

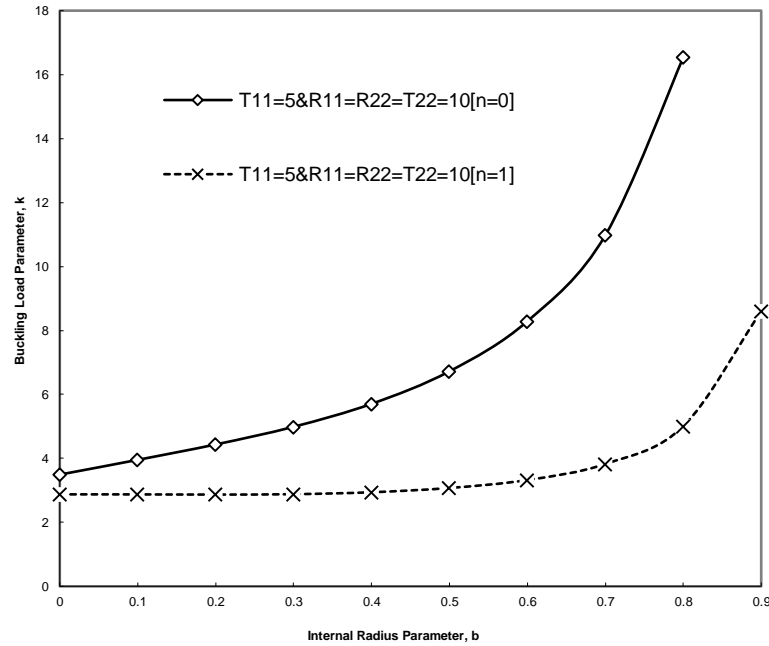


Fig. 5.11 Buckling Load Parameter k , versus Internal Radius Parameter b , for $T_{11} = 5$ and $R_{11} = R_{22} = T_{22} = 10$ ($n = 0$ for *axisymmetric* mode and $n = 1$ for *asymmetric* mode).

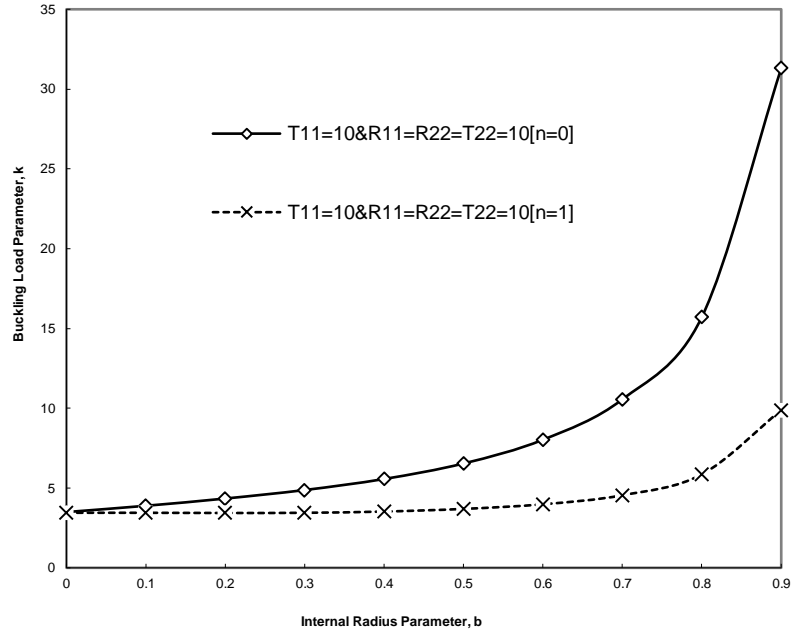


Fig. 5.12 Buckling Load Parameter k , versus Internal Radius Parameter b , for $T_{11}=10$ and $R_{11}=R_{22}=T_{22}=10$ ($n=0$ for axisymmetric mode and $n=1$ for asymmetric mode).

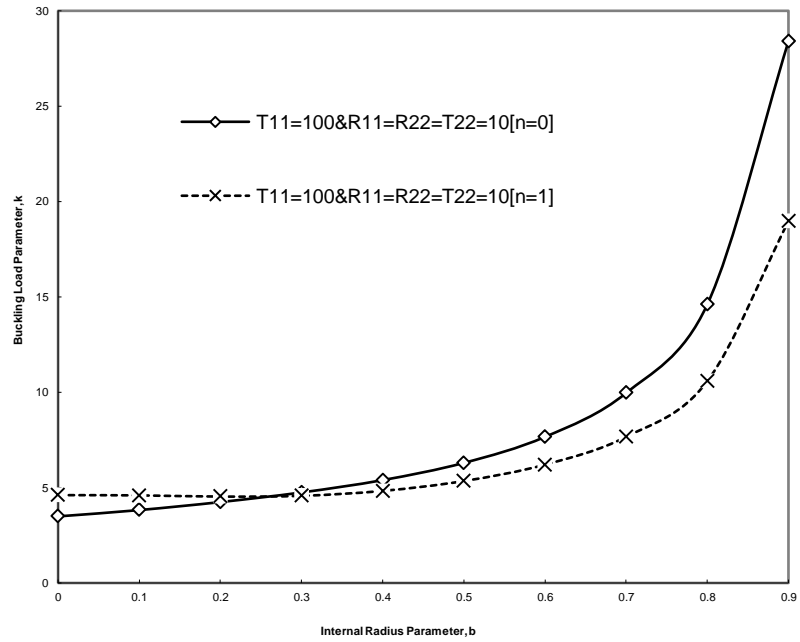


Fig. 5.13 Buckling Load Parameter k , versus Internal Radius Parameter b , for $T_{11}=100$ and $R_{11}=R_{22}=T_{22}=10$ ($n=0$ for axisymmetric mode and $n=1$ for asymmetric mode).

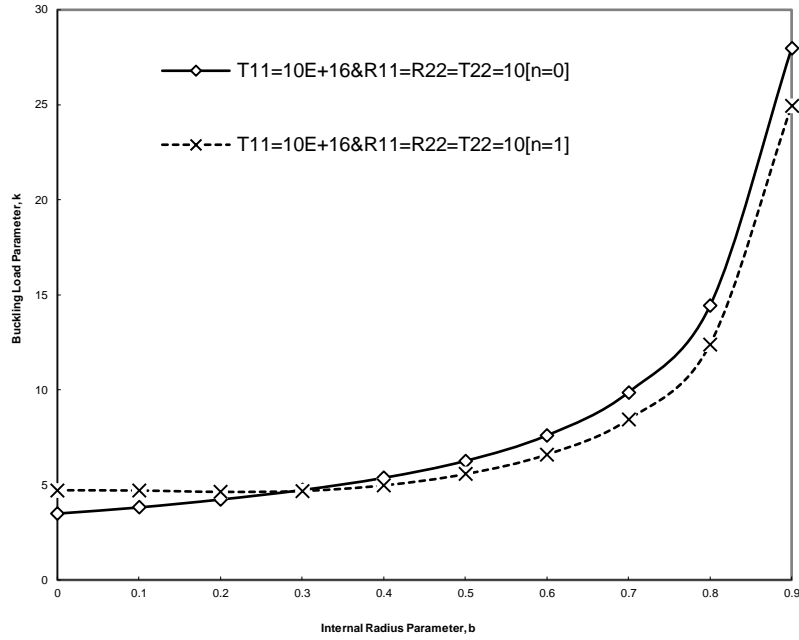


Figure 5.14 Buckling Load Parameter k , versus Internal Radius Parameter b , for $T_{11} = \infty$ and $R_{11} = R_{22} = T_{22} = 10$ ($n=0$ for axisymmetric mode and $n=1$ for asymmetric mode).

The subset problem is buckling of an annular plate with elastic outer edge against rotation and simply supported edge at both edges. The buckling load parameters for axisymmetric and asymmetric modes and for various rotational spring stiffness parameters at outer edge ($R_{11} = 0.2, 5, 100 \text{ \& } 10^{16}$), are presented in Table 5.4 and graphically in Figs. 5.15 – 5.18. It is observed from the Fig. 5.15, for a given value of $R_{11} = 0.2$, the curve is composed of two segments. This is due to the switching of buckling modes. For a smaller internal radius b , the plate buckles in an asymmetric mode (*i.e.*, $n=1$). In this segment (as shown by dotted lines in Fig. 5.15) the buckling load increases as b increases in value. For larger internal radius b , the plate buckles in an axisymmetric mode (*i.e.*, $n=0$). In this segment (as shown by continuous lines in Fig. 5.15) the buckling load increases as b increases in value as shown in Fig. 5.15. The cross over radius (switching of mode) is $b = 0.10625$ and the corresponding buckling load is

$k = 4.2872$. The buckling is governed by the asymmetric mode $n = 1$ when $b \leq 0.10625$. When b increased beyond 0.10625, the $n = 0$ axisymmetric mode gives the correct lower buckling load. Fig. 5.16 shows the variation of buckling load parameter k , with respect to the internal radius parameter b , for a given value of $R_{11} = 5$. It is observed from the Fig. 5.16, the curve is composed of two segments. This is due to the switching of buckling mode. The cross over radius (switching of mode) is $b = 0.19626$ and the corresponding buckling load is $k = 5.4708$. The buckling is governed by the asymmetric mode $n = 1$ when $b \leq 0.19626$. When b increased beyond 0.19626, the $n = 0$ axisymmetric mode $n = 0$ gives the correct lower buckling load.

Table 5.4 Buckling Load Parameter, k ($n = 0$ for *axisymmetric* mode and $n = 1$ for *asymmetric* mode) for Various Values of Rotational Restraint, R_{11} and Poisson's ratio, ν is 0.3.

b	$R_{11} = 0.2$		$R_{11} = 5$		$R_{11} = 100$		$R_{11} = \infty$	
	$n = 0$	$n = 1$	$n = 0$	$n = 1$	$n = 0$	$n = 1$	$n = 0$	$n = 1$
0.0	4.49052	3.82169	5.64025	4.61944	6.58125	5.26816	6.64775	5.32063
0.1	4.29207	4.28056	5.38283	5.15835	6.24522	5.92781	6.30692	5.99051
0.2	4.42233	4.57494	5.48141	5.49155	6.40391	6.36081	6.47597	6.43445
0.3	4.82781	5.00315	5.89575	5.96764	6.96671	6.99189	7.05846	7.08432
0.4	5.48534	5.64033	6.58153	6.66171	7.87805	7.91506	8.0012	8.03801
0.5	6.47496	6.59769	7.61143	7.68328	9.24087	9.27369	9.416	9.44842
0.6	8.00391	8.09587	9.19385	9.2524	11.3342	11.3592	11.604	11.6284
0.7	10.5919	10.6552	11.8455	11.8898	14.8345	14.8517	15.3047	15.321
0.8	15.8048	15.8433	17.1345	17.1644	21.7412	21.7519	22.7595	22.7691
0.9	31.4944	31.5119	32.9146	32.9299	41.5632	41.5689	45.199	45.2032

It is observed from the Fig. 5.17, for a given value of $R_{11} = 100$, the curve is composed of two segments. This is due to the switching of buckling modes. For a smaller internal radius b , the plate buckles in an asymmetric mode (*i.e.*, $n = 1$). In this segment (as shown by dotted lines in Fig. 5.17) the buckling load increases as b increases in value. For larger internal radius b , the plate buckles in an axisymmetric mode (*i.e.*, $n = 0$). In this segment (as shown by continuous lines in Fig. 5.17) the buckling load

increases as b increases in value as shown in Fig. 5.17. The cross over radius (switching of mode) is $b = 0.2633$ and the buckling load at cross over radius is $k = 6.7607$. The buckling is governed by the asymmetric mode $n = 1$ when $b \leq 0.2633$. When b increased beyond 0.2633, the $n = 0$ axisymmetric mode gives the correct lower buckling load. Fig. 5.18 shows the variation of buckling load parameter k , with respect to the internal radius parameter b , for a given value of $R_{11} = 10^{16}$. It is observed from the Fig. 5.18, the curve is composed of two segments. This is due to the switching of buckling mode. For a smaller internal radius b , the plate buckles in an asymmetric mode (*i.e.*, $n = 1$). In this segment (as shown by dotted lines in Fig. 5.18) the buckling load increases as b increases in value. For larger internal radius b , the plate buckles in an axisymmetric mode (*i.e.*, $n = 0$). In this segment (as shown by continuous lines in Fig. 5.18) the buckling load increases as b increases in value as shown in Fig. 5.18. The cross over radius (switching of mode) is $b = 0.26122$ and the buckling load at this cross over radius is $k = 6.8314$. The buckling is governed by the asymmetric mode $n = 1$ when $b \leq 0.26122$. When b increased beyond 0.26122, the $n = 0$ axisymmetric mode gives the correct lower buckling load. The cross-over radius parameter varies from 0.10625 to 0.2633 depending on the rotational stiffness of the elastic restraint at the edge.

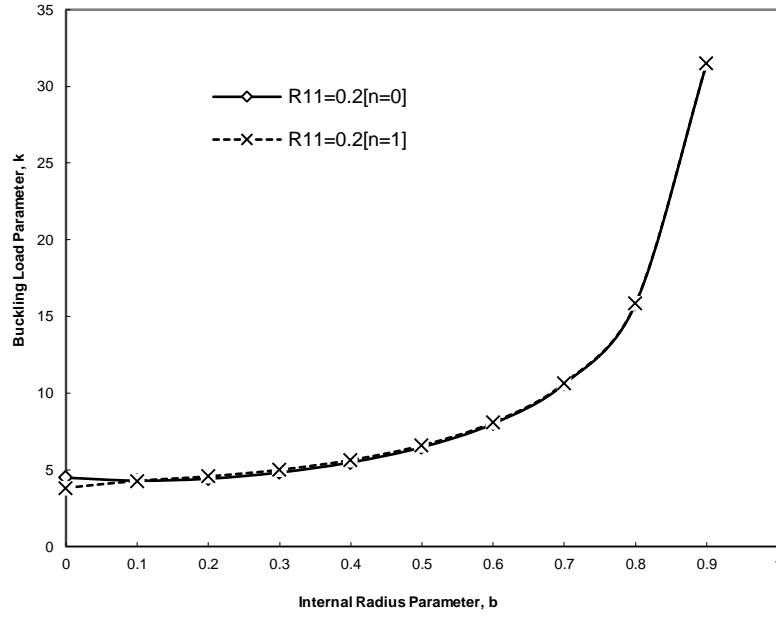


Fig. 5.15 Buckling Load Parameter k , versus Internal Radius Parameter b , for $R_{11} = 0.2$ ($n = 0$ for *axisymmetric* mode and $n = 1$ for *asymmetric* mode).

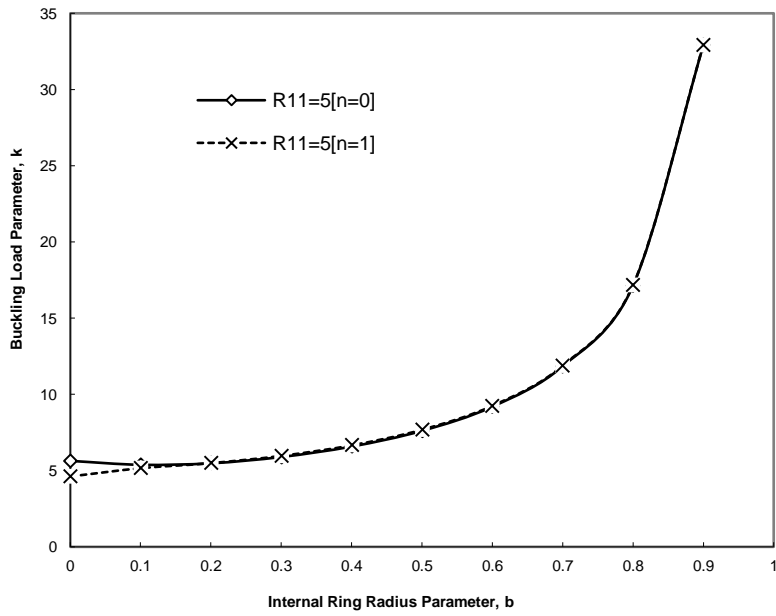


Fig. 5.16 Buckling Load Parameter k , versus Internal Radius Parameter b , for $R_{11} = 5$ ($n = 0$ for *axisymmetric* mode and $n = 1$ for *asymmetric* mode).

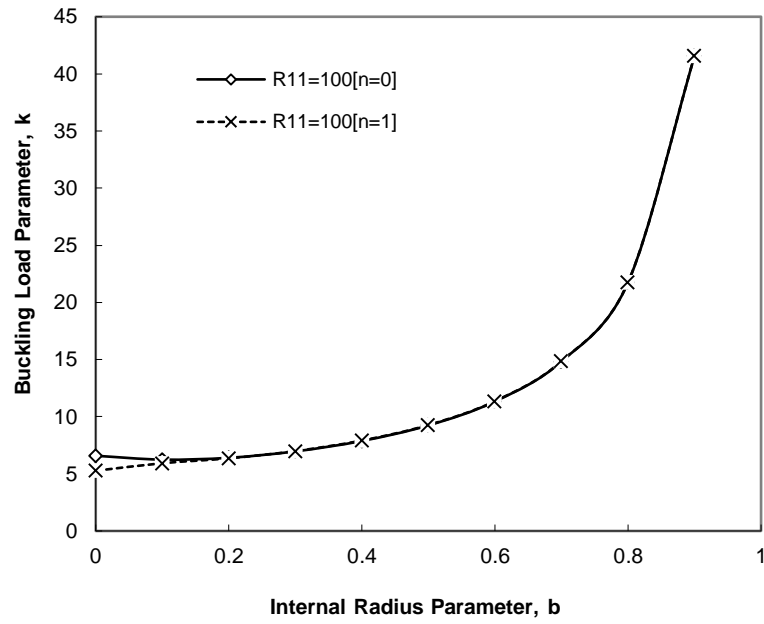


Fig. 5.17 Buckling Load Parameter k , versus Internal Radius Parameter b , for $R_{11} = 100$ ($n = 0$ for *axisymmetric* mode and $n = 1$ for *asymmetric* mode).

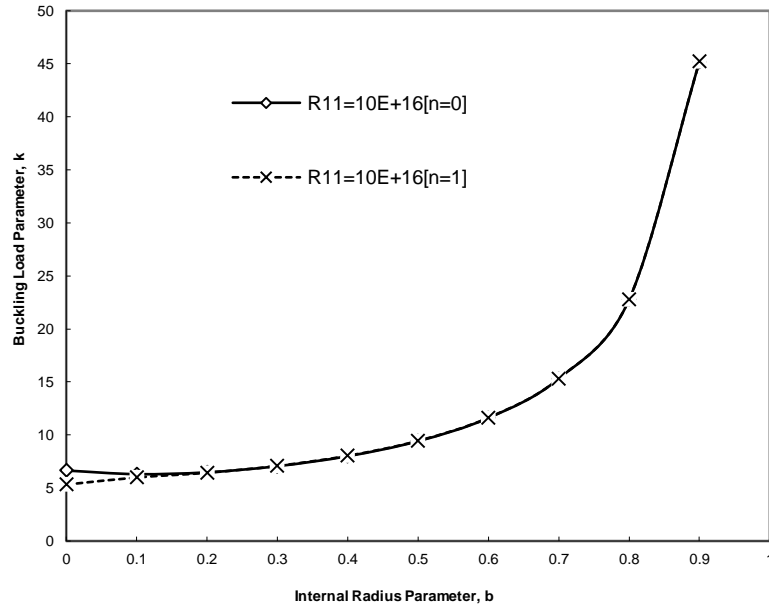


Fig. 5.18 Buckling Load Parameter k , versus Internal Radius Parameter b , for $R_{11} = 10^{16}$ ($n = 0$ for *axisymmetric* mode and $n = 1$ for *asymmetric* mode).

The critical buckling load parameters are calculated for various materials i.e., for different Poisson's ratios ν , by keeping rotational restraint constant ($R_{11} = 0.2$) and for

different inner radius parameter of an annular plate, b . The results (both axisymmetric and asymmetric modes) are presented in Table 5.5 and separately in Tables 5.6 and 5.7. Figs. 5.19 – 5.22, show the variation of buckling load parameter k , with respect to the internal radius b , for Poisson's ratios of $\nu = 0, 0.1, 0.2$ & 0.3 and $R_{II} = 0.2$. It is observed from Figs. 5.19 – 5.22, for a given value of Poisson ratio and R_{II} , the curve is composed of two segments. This is due to the switching of buckling modes. For a smaller internal radius b , the plate buckles in an asymmetric mode (*i.e.*, $n = 1$). In this segment (as shown by dotted lines in Figs. 5.19 – 5.22) the buckling load decreases as b decreases in value. For larger internal radius b , the plate buckles in an axisymmetric mode (*i.e.*, $n = 0$). In this segment (as shown by continuous lines as shown in Figs. 5.19 – 5.22) the buckling load increases as b increases in value as shown in Figs. 5.19 – 5.22. The cross over radius (switching of asymmetric mode to axisymmetric mode) for $\nu = 0, 0.1, 0.2$ & 0.3 and $R_{II} = 0.2$ is presented in Table 6.8. And also the buckling load parameter at this cross over radius is presented in Table 5.8. Figs. 5.23 – 5.24 show the variation of buckling load parameter k , with respect to the internal radius parameter b , for Poisson's ratios of $\nu = 0.4$ & 0.5 and $R_{II} = 0.2$. It is noticed from Figs. 5.23 and 5.24, the buckling is completely governed by axisymmetric mode $n = 0$ (as shown by continuous lines in Figs. 5.23 and 5.24) and the buckling load increases as b increases in value as shown in Figs. 5.23 and 5.24.

For a given inner radius parameter of the plate b , the critical buckling load parameter decreases slightly with increasing Poisson ratio, ν as shown in Fig. 5.25. The results of this kind were scarce in the literature. However, the results are compared

with the following cases. (i). Table 5.9, presents the comparison of critical buckling load parameters k , for the annular plate with both edges simply supported (by setting the rotational restraint with $R_{11} = 0$), against those obtained by Yamaki [14]. (ii). Table 5.10, presents the comparison of critical buckling load parameters k , for an annular plate with outer edge clamped and inner edge simply supported (by setting the rotational restraint with $R_{11} \rightarrow \infty$), against those obtained by Yamaki [14]. The optimal ring support is affected by the rotational stiffness parameters, translational stiffness parameters. However, it is observed that the influence of rotational spring stiffness parameters on buckling load is much more predominant than that of translational spring stiffness parameters

Table 5.5 Critical Buckling Load Parameters ($n = 0$ for *axisymmetric* mode and $n = 1$ for *asymmetric* mode), k for various values of Poisson's Ratio and Rotational Restraint, $R_{11} = 0.2$

	$\nu = 0$		$\nu = 0.1$		$\nu = 0.2$		$\nu = 0.3$		$\nu = 0.4$		$\nu = 0.5$	
b	$[n = 0]$	$[n = 1]$	$[n = 0]$	$[n = 1]$	$[n = 0]$	$[n = 1]$	$[n = 0]$	$[n = 1]$	$[n = 0]$	$[n = 1]$	$[n = 0]$	$[n = 1]$
0.1	4.29291	4.26249	4.3016	4.27348	4.30194	4.2798	4.29207	4.28056	4.26899	4.27487	4.22865	4.26145
0.2	4.46727	4.58841	4.46	4.58888	4.44528	4.58449	4.42233	4.57494	4.38995	4.55944	4.34645	4.53729
0.3	4.87422	5.02911	4.86408	5.02453	4.84877	5.01597	4.82781	5.00315	4.8009	4.98577	4.76733	4.96342
0.4	5.52399	5.66816	5.51474	5.66199	5.50192	5.65275	5.48534	5.64033	5.46478	5.62454	5.44015	5.60527
0.5	6.50377	6.62243	6.49631	6.61646	6.48638	6.60822	6.47396	6.59769	6.45896	6.58467	6.44118	6.56938
0.6	8.02567	8.11554	8.02011	8.11057	8.01285	8.10401	8.00391	8.09587	7.99329	8.08604	7.98087	8.07461
0.7	10.6067	10.6692	10.6028	10.6656	10.598	10.6609	10.5919	10.6552	10.5847	10.6483	10.5765	10.6404
0.8	15.8138	15.852	15.8114	15.8497	15.8084	15.8468	15.8048	15.8433	15.8006	15.839	15.7956	15.8342
0.9	31.4985	31.516	31.4974	31.5149	31.4961	31.5136	31.4944	31.5119	31.4925	31.51	31.4903	31.5078

Table 5.6 Critical Buckling Load Parameter (*axisymmetric* mode), k for Various Values of Poisson's Ratio and Rotational Restraint, $R_{11} = 0.2$

$R_{11} = 0.2 \& n = 0$						
b	$\nu = 0$	$\nu = 0.1$	$\nu = 0.2$	$\nu = 0.3$	$\nu = 0.4$	$\nu = 0.5$
0.2	4.46727	4.46	4.44528	4.42233	4.38995	4.34645
0.3	4.87422	4.86408	4.84877	4.82781	4.8009	4.76733
0.4	5.52399	5.51474	5.50192	5.48534	5.46478	5.44015
0.5	6.50377	6.49631	6.48638	6.47396	6.45896	6.44118
0.6	8.02567	8.02011	8.01285	8.00391	7.99329	7.98087
0.7	10.6067	10.6028	10.598	10.5919	10.5847	10.5765
0.8	15.8138	15.8114	15.8084	15.8048	15.8006	15.7956
0.9	31.4985	31.4974	31.4961	31.4944	31.4925	31.4903

Table 5.7 Critical Buckling Load Parameter (*asymmetric mode*), k for Various Values of Poisson's Ratio and Rotational Restraint, $R_{11} = 0.2$

$R_{11} = 0.2 \text{ \& } n = 1$						
b	$\nu = 0$	$\nu = 0.1$	$\nu = 0.2$	$\nu = 0.3$	$\nu = 0.4$	$\nu = 0.5$
0.2	4.58841	4.58888	4.58449	4.57494	4.55944	4.53729
0.3	5.02911	5.02453	5.01597	5.00315	4.98577	4.96342
0.4	5.66816	5.66199	5.65275	5.64033	5.62454	5.60527
0.5	6.62243	6.61646	6.60822	6.59769	6.58467	6.56938
0.6	8.11554	8.11057	8.10401	8.09587	8.08604	8.07461
0.7	10.6692	10.6656	10.6609	10.6552	10.6483	10.6404
0.8	15.852	15.8497	15.8468	15.8433	15.839	15.8342
0.9	31.516	31.5149	31.5136	31.5119	31.51	31.5078

Table 5.8 Cross Over Radius (Switching of mode) Parameter, b_{co} for Various Values of Poisson's Ratio and Rotational Restraint, $R_{11} = 0.2$

$R_{11} = 0.2$				
	$\nu = 0$	$\nu = 0.1$	$\nu = 0.2$	$\nu = 0.3$
Cross-Over Radius [b_{co}]	0.12605	0.12130	0.11388	0.10274
Buckling Load Parameter [k_{co}]	4.3279	4.3351	4.33824	4.3010

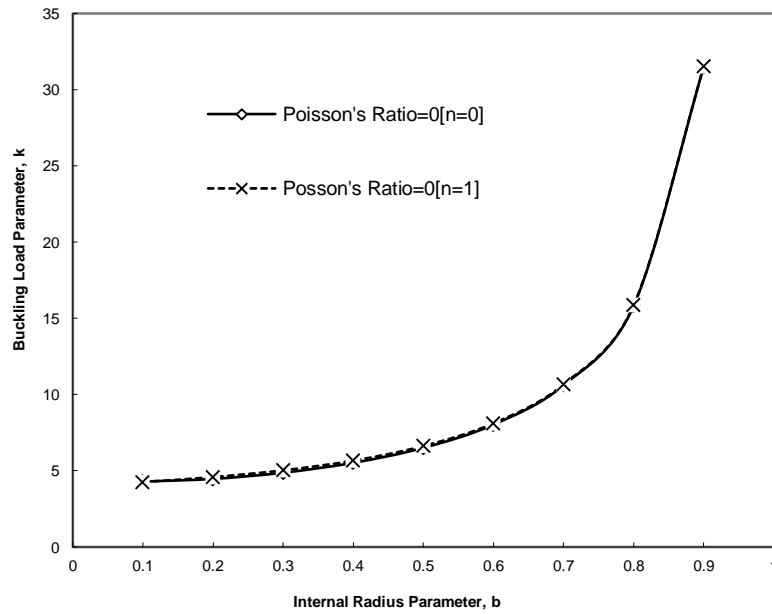


Fig. 5.19 Buckling Load Parameter k , versus Internal Radius Parameter b , for $R_{11} = 0.2$ & $\nu = 0$ ($n = 0$ for *axisymmetric mode* and $n = 1$ for *asymmetric mode*).

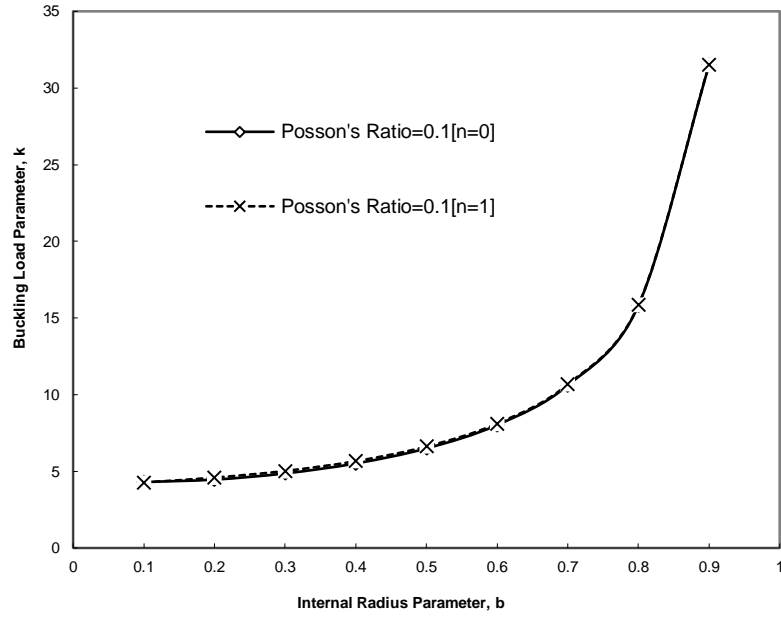


Fig. 5.20 Buckling Load Parameter k , versus Internal Radius Parameter b , for $R_{11} = 0.2$ & $\nu = 0.1$ ($n = 0$ for *axisymmetric* mode and $n = 1$ for *asymmetric* mode).

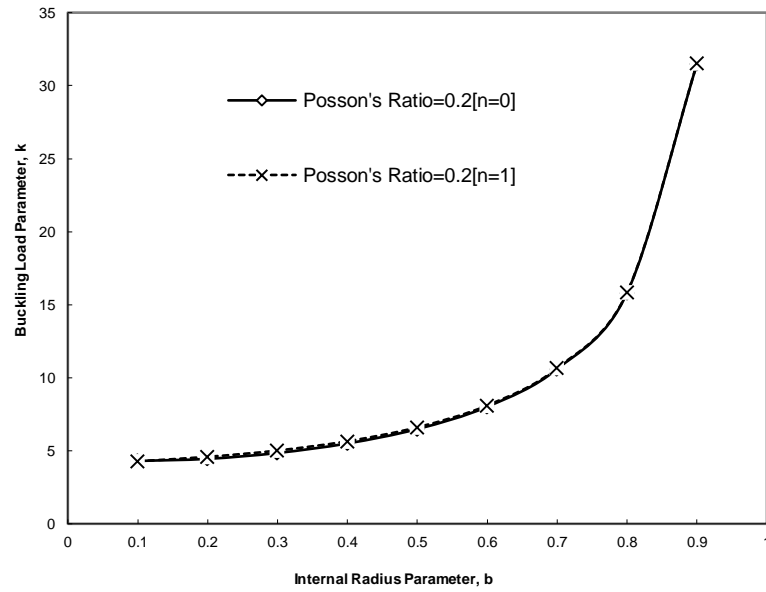


Fig. 5.21 Buckling Load Parameter k , versus Internal Radius Parameter b , for $R_{11} = 0.2$ & $\nu = 0.2$ ($n = 0$ for *axisymmetric* mode and $n = 1$ for *asymmetric* mode).

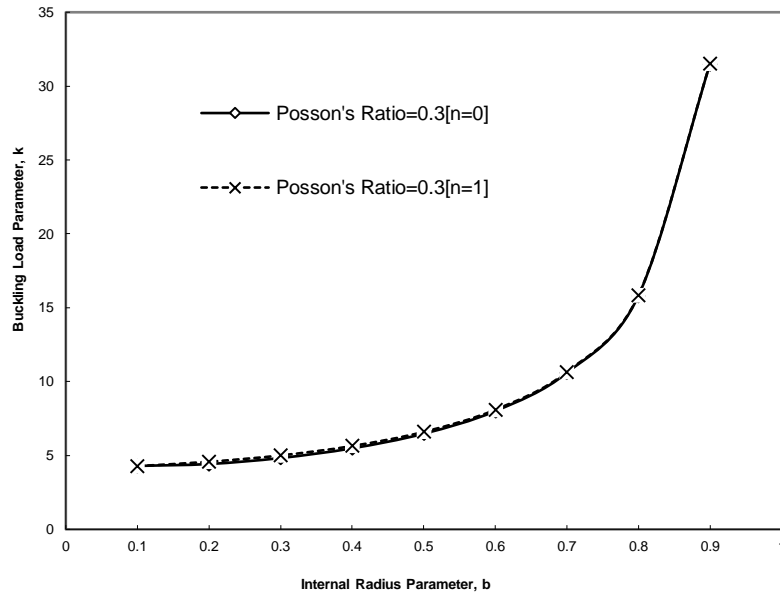


Fig. 5.22 Buckling Load Parameter k , versus Internal Radius Parameter b , for $R_{11} = 0.2$ & $\nu = 0.3$ ($n = 0$ for *axisymmetric* mode and $n = 1$ for *asymmetric* mode).

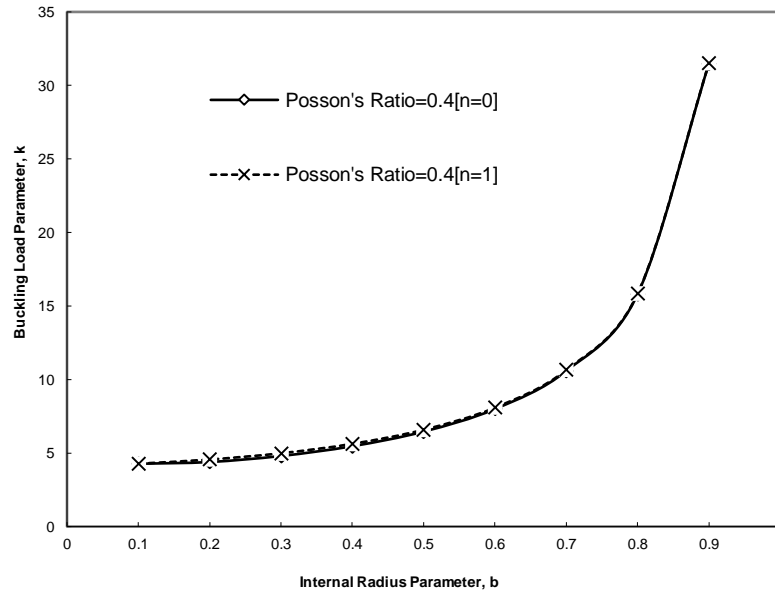


Fig. 5.23 Buckling Load Parameter k , versus Internal Radius Parameter b , for $R_{11} = 0.2$ & $\nu = 0.4$ ($n = 0$ for *axisymmetric* mode and $n = 1$ for *asymmetric* mode).

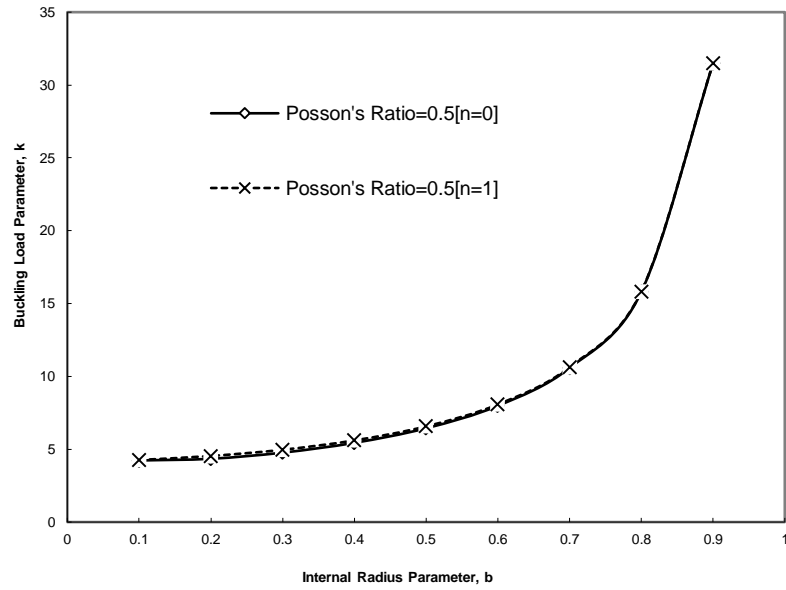


Fig. 5.24 Buckling Load Parameter k , versus Internal Radius Parameter b , for *axisymmetric* mode ($n = 0$) and *asymmetric* mode ($n = 1$) when $R_{11} = 0.2$ & $\nu = 0.5$.

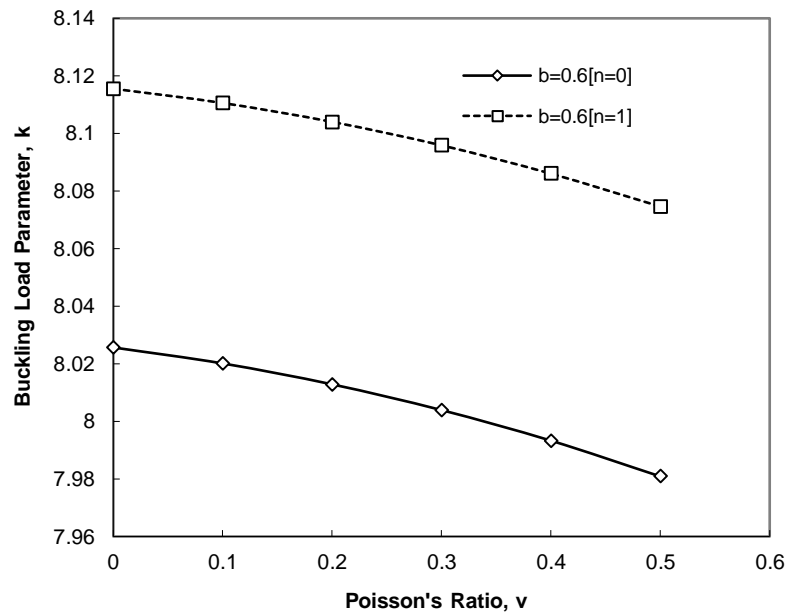


Fig. 5.25 Critical Buckling Load Parameter, k versus Poisson Ratio, ν for *axisymmetric* mode ($n = 0$) and *asymmetric* mode ($n = 1$)

Table 5.9 Comparison of Critical Buckling Load Parameter k , with Yamaki [14] for an Annular Plate with both Edges Simply Supported and Poisson's ratio = 0.3.

b	0	0.1	0.3	0.5	0.7	0.9
Yamaki - [14]	-	-	4.75	6.40	10.52	31.43
Present	4.40089	4.20507	4.74929	6.40088	10.5231	31.4292

Table 5.10 Comparison of Critical Buckling Load Parameter k , with Yamaki [14] for an Annular Plate with Outer Edge Clamped and Inner Edge Simply Supported and Poisson's ratio = 0.3.

b	0	0.1	0.3	0.5	0.7	0.9
Yamaki - [14]	-	-	7.06	9.42	15.31	45.20
Present	6.64775	6.30692	7.05846	9.416	15.3047	45.199

CHAPTER 6

VIBRATIONS OF ELASTICALLY RESTRIANED CIRCULAR PLATES ON WINKLER FOUNDATION

6.1. Definition of the Problem

The vibration characteristics of plates resting on an elastic medium are different from those of the plates supported only on the boundary. The most general soil model used in practical applications is the Winkler model [38] in which the soil layer is represented by unconnected closely spaced elastic springs. In general, papers dealing with vibrating plates, shells and beams are concerned with the determination of eigenvalues and mode shapes [81] [74, 75] solved by using Classical Plate theory with classical boundary conditions. The present work considers the problem of vibrations of circular plates elastically restrained against rotation and translation and resting on elastic foundation.

Consider a thin isotropic, circular plate of radius R , uniform thickness h , Young's modulus E , density ρ , flexural rigidity D and Poisson's ratio ν , as shown in Fig. 6.1. The plate edge is elastically restrained against rotation and translation and also resting on Winkler foundation. The present problem is to determine the eigenvalues of circular plate elastically restrained against rotation and translation and resting on elastic foundation i.e Winkler foundation.

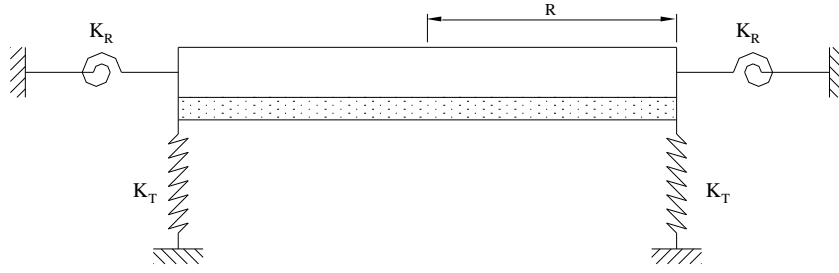


Fig. 6.1 A thin circular plate with rotational K_{R1} and translational K_{T1} elastic edge constraints and supporting on full elastic foundation.

6.2. Derivation of Frequency of Transverse Vibration of Elastically restrained circular Plates

The considered elastic thin circular plate supported on a Winkler foundation. The geometrical and loading configuration of the plate is axisymmetric and consequently, deflection shape of the plate will be axially symmetric as well. In the classical plate theory [17], the following fourth order differential equation describes free flexural vibrations of a thin circular uniform plate.

$$D.\nabla^4 w(r, \theta, t) + \rho h.\partial^2 w(r, \theta, t) / \partial t^2 = 0 \quad (6.1)$$

The homogeneous equation for Kirchoff plate on one parameter elastic foundation is given by the following equation

$$D.\nabla^4 w(r, \theta, t) + kw(r, \theta, t) + \rho h.\partial^2 w(r, \theta, t) / \partial t^2 = 0 \quad (6.2)$$

Displacement in equation (6.2) can be presented as a combination of spatial and time dependent components as follows;

$$\text{Let } w(r, \theta, t) = W(r, \theta)e^{i\omega t} \quad (6.3)$$

Now substitute the Eq. (6.3) in Eq. (6.2)

$$D.\nabla^4 \tilde{w} + (k - \rho h\omega^2).\tilde{w} = 0 \quad (6.4)$$

The solution of the equation takes the following form

$$W_{mn}(r, \theta) = A_{mn} \left[J_n \left(\frac{\lambda_{mn} r}{a} \right) + C_{mn} I_n \left(\frac{\lambda_{mn} r}{a} \right) \right] \cdot \cos n\theta, \quad \text{where } n > 0 \quad (6.5)$$

Where J_n Bessel is function of the first kind of first order and I_n is modified Bessel function of the first kind of first order.

Considering an elastically supported plate as shown in Fig. 6.1, boundary conditions can be formulated in terms of rotational stiffness (K_{R1}) and translational stiffness (K_{T1}) as follows

$$M_r(a, \theta) = K_{R1} \frac{\partial w(a, \theta)}{\partial r} \quad (6.6)$$

$$V_r(a, \theta) = -K_{T1} W(a, \theta) \quad (6.7)$$

Where the Kelvin-Kirchhoff and bending moment are defined as follows

$$M_r = -D \left[\frac{\partial^2 w}{\partial r^2} + \nu \left(\frac{1}{r} \frac{\partial w}{\partial r} + \frac{1}{r^2} \frac{\partial^2 w}{\partial \theta^2} \right) \right] \quad (6.8)$$

$$V_r = -D \left[\frac{\partial}{\partial r} \nabla^2 W + (1 - \nu) \cdot \frac{1}{r} \frac{\partial}{\partial \theta} \left(\frac{1}{r} \frac{\partial^2 W}{\partial r \partial \theta} - \frac{1}{r^2} \frac{\partial W}{\partial \theta} \right) \right] \quad (6.9)$$

From Eqs. (6.6) and (6.8), we get the following

$$-D \left[\frac{\partial^2 w}{\partial r^2} + \nu \left(\frac{1}{r} \frac{\partial w}{\partial r} + \frac{1}{r^2} \frac{\partial^2 w}{\partial \theta^2} \right) \right] = K_{R1} \cdot \frac{\partial w}{\partial r}(a, \theta) \quad (6.10)$$

From the Eq. (6.10), we derived the following equation

$$C_{mn} = \frac{-J_{P2} + \frac{2}{\lambda_{mn}} \left[\nu + \frac{aK_{R1}}{D} \right] J_{m1} + \left[2 + \frac{4\nu n^2}{\lambda_{mn}^2} \right] J_n(\lambda_{mn})}{I_{P2} + \frac{2}{\lambda_{mn}} \left[\nu + \frac{aK_{R1}}{D} \right] I_{P1} + \left[2 - \frac{4\nu n^2}{\lambda_{mn}^2} \right] I_n(\lambda_{mn})} \quad (6.11)$$

$$C_{mn} = \frac{-J_{P2} + \frac{2}{\lambda_{mn}} [\nu + R_{11}] J_{m1} + \left[2 + \frac{4\nu n^2}{\lambda_{mn}^2} \right] J_n(\lambda_{mn})}{I_{P2} + \frac{2}{\lambda_{mn}} [\nu + R_{11}] I_{P1} + \left[2 - \frac{4\nu n^2}{\lambda_{mn}^2} \right] I_n(\lambda_{mn})} \quad (6.11a)$$

where, $R_{11} = \frac{aK_{R1}}{D}$

$$J_{m1} = J_{n+1}(\lambda_{mn}) - J_{n-1}(\lambda_{mn}); J_{P2} = J_{n+2}(\lambda_{mn}) + J_{n-2}(\lambda_{mn});$$

$$I_{P1} = I_{n+1}(\lambda_{mn}) + I_{n-1}(\lambda_{mn}); I_{P2} = I_{n+2}(\lambda_{mn}) + I_{n-2}(\lambda_{mn});$$

From Eqs. (6.7) and (6.9), we get the following

$$-D \left[\frac{\partial}{\partial r} \nabla^2 W + (1-\nu) \cdot \frac{1}{r} \frac{\partial}{\partial \theta} \left(\frac{1}{r} \frac{\partial^2 W}{\partial r \partial \theta} - \frac{1}{r^2} \frac{\partial W}{\partial \theta} \right) \right] = -K_{T1} \cdot W(a, \theta) \quad (6.12)$$

From Eq. (6.12), we derived the following equation

$$C_{mn} = \frac{J_{m3} - \frac{2J_{P2}}{\lambda_{mn}} - \left[3 + \frac{4 + 4(2-\nu)n^2}{\lambda_{mn}^2} \right] \cdot J_{m1} - \left[\frac{8(3-\nu)n^2}{\lambda^3} - \frac{4}{\lambda_{mn}} - \frac{8a^3 K_T}{\lambda_{mn}^3 D} \right] \cdot J_n(\lambda_{mn})}{I_{P3} + \frac{2I_{P2}}{\lambda_{mn}} + \left[3 - \frac{4 - 4(2-\nu)n^2}{\lambda_{mn}^2} \right] \cdot I_{P1} + \left[\frac{8(3-\nu)n^2}{\lambda_{mn}^3} + \frac{4}{\lambda_{mn}} - \frac{8a^3 K_T}{\lambda_{mn}^3 D} \right] \cdot I_n(\lambda_{mn})} \quad (6.13)$$

$$C_{mn} = \frac{J_{m3} - \frac{2J_{P2}}{\lambda_{mn}} - \left[3 + \frac{4 + 4(2-\nu)n^2}{\lambda_{mn}^2} \right] \cdot J_{m1} - \left[\frac{8(3-\nu)n^2}{\lambda^3} - \frac{4}{\lambda_{mn}} - \frac{8T_{11}}{\lambda_{mn}^3} \right] \cdot J_n(\lambda_{mn})}{I_{P3} + \frac{2I_{P2}}{\lambda_{mn}} + \left[3 - \frac{4 - 4(2-\nu)n^2}{\lambda_{mn}^2} \right] \cdot I_{P1} + \left[\frac{8(3-\nu)n^2}{\lambda_{mn}^3} + \frac{4}{\lambda_{mn}} - \frac{8T_{11}}{\lambda_{mn}^3} \right] \cdot I_n(\lambda_{mn})} \quad (6.13a)$$

where, $T_{11} = \frac{a^3 K_{T1}}{D}$

$$J_{m1} = J_{n+1}(\lambda_{mn}) - J_{n-1}(\lambda_{mn}); J_{P2} = J_{n+2}(\lambda_{mn}) + J_{n-2}(\lambda_{mn}); J_{m3} = J_{n+3}(\lambda_{mn}) - J_{n-3}(\lambda_{mn});$$

$$I_{P1} = I_{n+1}(\lambda_{mn}) + I_{n-1}(\lambda_{mn}); I_{P2} = I_{n+2}(\lambda_{mn}) + I_{n-2}(\lambda_{mn}); I_{P3} = I_{n+3}(\lambda_{mn}) + I_{n-3}(\lambda_{mn});$$

The frequency equation can be calculated From Eqs. (6.11) And (6.13), which allows determining eigenvalues λ_{mn} . The mode shape parameters C_{mn} can be determined corresponding to these eigenvalues by using either Eq. (6.11) or Eq. (6.13). The amplitude of each vibration mode in Eq. (6.5) is set by the normalization constant A_{mn} determined from the following condition.

$$\int_0^{2\pi} \int_0^a W_{mn}(r, \theta) \cdot W_{pq}(r, \theta) r dr d\theta = M \delta_{mp} \delta_{nq} \quad (6.14)$$

Where, M is a mass of the plate, $\delta_{mp} = \delta_{nq} = 1$ if $m = p, n = q$ and $\delta_{mp} \delta_{nq} = 0$ if $m \neq p$ or $n \neq q$.

Dimensionless normalization constant A_{mn} from the Eq. (6.14) is given by following equation

$$A_{mn} = \left[\frac{1}{\pi a^2} \cdot \int_0^{2\pi} \int_0^a \left(J_n \left(\frac{\lambda_{mn} r}{a} \right) + C_{mn} \cdot I_n \left(\frac{\lambda_{mn} r}{a} \right) \right) \cdot \cos n\theta \right]^2 r dr d\theta \Bigg]^{-1} \quad (6.15)$$

$$\text{In Eq (6.4), } \omega_{mn} \text{ is the natural frequency of vibrations} = \left(\frac{\lambda_{mn}^2}{a^2} \right) \cdot \sqrt{\frac{D}{\rho h}} \quad (6.16)$$

It is clear from the Eq. (6.16) the natural frequency of vibrations is dependent on the plate radius and eigenvalues

$$\text{Equation (6.16) can be written as } \omega_{mn}^2 = \frac{\lambda_{mn}^4 \cdot D}{a^4 \rho h} \quad (6.17)$$

$$\text{From Eq. (6.17) } \lambda_{mn}^4 = \frac{\rho h \omega_{mn}^2}{D} \quad (6.18)$$

$$\lambda_{mn}^4 = \frac{\rho h \omega_{mn}^2}{D} - \frac{K a^4}{D} = \frac{\rho h \omega_{mn}^2}{D} - \xi^2 \quad (6.19)$$

$$\text{where } \xi^2 = \frac{K a^4}{D}$$

$$\lambda_{mn}^{*4} = \lambda_{mn}^4 + \xi^2 \quad (6.20)$$

$$\lambda_{mn}^* = \left[\lambda_{mn}^4 + \xi^2 \right]^{\frac{1}{4}} \quad (6.21)$$

where λ_{mn} is eigen value without foundation

λ_{mn}^* is eigen value with Winkler foundation

The following four cases are considered.

Case: 1 Plate with elastically restrained edge against rotation and translation and supporting on full foundation as shown in Fig.6.1. The boundary conditions used for this case are Eqs. (6.6) and (6.7). The set of equations for this case are Eqs. (6.10) and (6.12). From these equations we get the following equations

$$C_{mn} = \frac{-J_{P2} + \frac{2}{\lambda_{mn}} \left[\nu + \frac{aK_{R1}}{D} \right] J_{m1} + \left[2 + \frac{4\nu n^2}{\lambda_{mn}^2} \right] J_n(\lambda_{mn})}{I_{P2} + \frac{2}{\lambda_{mn}} \left[\nu + \frac{aK_{R1}}{D} \right] I_{P1} + \left[2 - \frac{4\nu n^2}{\lambda_{mn}^2} \right] I_n(\lambda_{mn})} \quad (6.22)$$

$$C_{mn} = \frac{-J_{P2} + \frac{2}{\lambda_{mn}} [\nu + R_{11}] J_{m1} + \left[2 + \frac{4\nu n^2}{\lambda_{mn}^2} \right] J_n(\lambda_{mn})}{I_{P2} + \frac{2}{\lambda_{mn}} [\nu + R_{11}] I_{P1} + \left[2 - \frac{4\nu n^2}{\lambda_{mn}^2} \right] I_n(\lambda_{mn})} \quad (6.22a)$$

$$C_{mn} = \frac{J_{m3} - \frac{2J_{P2}}{\lambda_{mn}} - \left[3 + \frac{4 + 4(2-\nu)n^2}{\lambda_{mn}^2} \right] J_{m1} - \left[\frac{8(3-\nu)n^2}{\lambda^3} - \frac{4}{\lambda_{mn}} - \frac{8a^3 K_{T1}}{\lambda_{mn}^3 D} \right] J_n(\lambda_{mn})}{I_{P3} + \frac{2I_{P2}}{\lambda_{mn}} + \left[3 - \frac{4 - 4(2-\nu)n^2}{\lambda_{mn}^2} \right] I_{P1} + \left[\frac{8(3-\nu)n^2}{\lambda_{mn}^3} + \frac{4}{\lambda_{mn}} - \frac{8a^3 K_{T1}}{\lambda_{mn}^3 D} \right] I_n(\lambda_{mn})} \quad (6.23)$$

$$C_{mn} = \frac{J_{m3} - \frac{2J_{P2}}{\lambda_{mn}} - \left[3 + \frac{4 + 4(2-\nu)n^2}{\lambda_{mn}^2} \right] J_{m1} - \left[\frac{8(3-\nu)n^2}{\lambda^3} - \frac{4}{\lambda_{mn}} - \frac{8T_{11}}{\lambda_{mn}^3} \right] J_n(\lambda_{mn})}{I_{P3} + \frac{2I_{P2}}{\lambda_{mn}} + \left[3 - \frac{4 - 4(2-\nu)n^2}{\lambda_{mn}^2} \right] I_{P1} + \left[\frac{8(3-\nu)n^2}{\lambda_{mn}^3} + \frac{4}{\lambda_{mn}} - \frac{8T_{11}}{\lambda_{mn}^3} \right] I_n(\lambda_{mn})} \quad (6.23a)$$

Case: 2 Plate with elastically restrained edge against translation and supporting on full Winkler foundation as shown in Fig.6.2. [$K_{R1} \rightarrow 0$ and K_{T1} vary]. Substituting $K_{R1} \rightarrow 0$ in Eqs. (6.6). Therefore, the boundary conditions from Eqs. (6.6) and (6.7) are

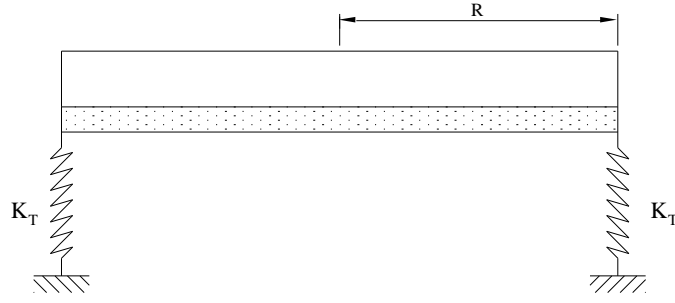


Fig. 6.2. A thin circular plate with translational K_{T1} elastic edge constraints and supported on full elastic foundation

$$M_r(a, \theta) = 0 \quad (6.24)$$

$$V_r(a, \theta) = -K_{T1}W(a, \theta) \quad (6.25)$$

From Eqs. (6.8), (6.9) and (6.24), (6.25), we get the following

$$-D \left[\frac{\partial^2 w}{\partial r^2} + \nu \left(\frac{1}{r} \frac{\partial w}{\partial r} + \frac{1}{r^2} \frac{\partial^2 w}{\partial \theta^2} \right) \right] = 0 \quad (6.26)$$

$$-D \left[\frac{\partial}{\partial r} \nabla^2 W + (1 - \nu) \cdot \frac{1}{r} \frac{\partial}{\partial \theta} \left(\frac{1}{r} \frac{\partial^2 W}{\partial r \partial \theta} - \frac{1}{r^2} \frac{\partial W}{\partial \theta} \right) \right] = -K_{T1} \cdot W(a, \theta) \quad (6.27)$$

From Eqs. (6.5), (6.26) and (6.27) we obtained the following

$$C_{mn} = \frac{-J_{P2} + \frac{2\nu}{\lambda_{mn}} \cdot J_{m1} + \left[2 + \frac{4\nu n^2}{\lambda_{mn}^2} \right] \cdot J_n(\lambda_{mn})}{I_{P2} + \frac{2\nu}{\lambda_{mn}} \cdot I_{P1} + \left[2 - \frac{4\nu n^2}{\lambda_{mn}^2} \right] \cdot I_n(\lambda_{mn})} \quad (6.28)$$

$$C_{mn} = \frac{J_{m3} - \frac{2J_{P2}}{\lambda_{mn}} - \left[3 + \frac{4 + 4(2 - \nu)n^2}{\lambda_{mn}^2} \right] \cdot J_{m1} - \left[\frac{8(3 - \nu)n^2}{\lambda^3} - \frac{4}{\lambda_{mn}} - \frac{8a^3 K_{T1}}{\lambda_{mn}^3 D} \right] \cdot J_n(\lambda_{mn})}{I_{P3} + \frac{2I_{P2}}{\lambda_{mn}} + \left[3 - \frac{4 - 4(2 - \nu)n^2}{\lambda_{mn}^2} \right] \cdot I_{P1} + \left[\frac{8(3 - \nu)n^2}{\lambda_{mn}^3} + \frac{4}{\lambda_{mn}} - \frac{8a^3 K_{T1}}{\lambda_{mn}^3 D} \right] \cdot I_n(\lambda_{mn})} \quad (6.29)$$

$$C_{mn} = \frac{J_{m3} - \frac{2J_{P2}}{\lambda_{mn}} - \left[3 + \frac{4 + 4(2-\nu)n^2}{\lambda_{mn}^2} \right] J_{m1} - \left[\frac{8(3-\nu)n^2}{\lambda^3} - \frac{4}{\lambda_{mn}} - \frac{8T_{11}}{\lambda_{mn}^3} \right] J_n(\lambda_{mn})}{I_{P3} + \frac{2I_{P2}}{\lambda_{mn}} + \left[3 - \frac{4 - 4(2-\nu)n^2}{\lambda_{mn}^2} \right] I_{P1} + \left[\frac{8(3-\nu)n^2}{\lambda_{mn}^3} + \frac{4}{\lambda_{mn}} - \frac{8T_{11}}{\lambda_{mn}^3} \right] I_n(\lambda_{mn})} \quad (6.29a)$$

If $K_{R1} \rightarrow 0$ and $K_{T1} \rightarrow \infty$, then this case becomes simply supported boundary condition.

Case: 3 Plate with elastically restrained edge against rotation and supported on full Winkler foundation as shown in Fig.6.3. [$K_{T1} \rightarrow \infty$ & K_{T1} Varies]. Substituting this condition in Eqs. (6.6) and (6.7) and we obtain the following.

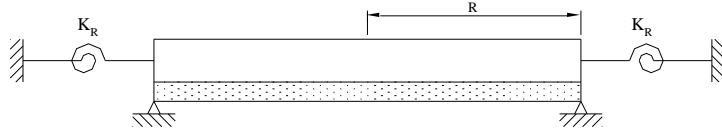


Fig. 6.3 A thin circular plate with rotational K_R elastic edge constraints and supported on full elastic foundation

$$M_r(a, \theta) = K_{R1} \frac{\partial w(a, \theta)}{\partial r} \quad (6.30)$$

$$W(a, \theta) = 0 \quad (6.31)$$

From Eqs. (6.8), (6.9) and (6.30), (6.31), we get the following

$$-D \left[\frac{\partial^2 w}{\partial r^2} + \nu \left(\frac{1}{r} \frac{\partial w}{\partial r} + \frac{1}{r^2} \frac{\partial^2 w}{\partial \theta^2} \right) \right] = K_{R1} \cdot \frac{\partial w}{\partial r}(a, \theta) \quad (6.32)$$

$$W(a, \theta) = 0 \quad (6.33)$$

From Eqs. (6.5), (6.32) and (6.33) we obtain the following expressions

$$C_{mn} = \frac{-J_{P2} + \frac{2}{\lambda_{mn}} \left[\nu + \frac{aK_{R1}}{D} \right] J_{m1} + \left[2 + \frac{4\nu n^2}{\lambda_{mn}^2} \right] J_n(\lambda_{mn})}{I_{P2} + \frac{2}{\lambda_{mn}} \left[\nu + \frac{aK_{R1}}{D} \right] I_{P1} + \left[2 - \frac{4\nu n^2}{\lambda_{mn}^2} \right] I_n(\lambda_{mn})} \quad (6.34)$$

$$C_{mn} = \frac{-J_{P2} + \frac{2}{\lambda_{mn}}[\nu + R_{11}]J_{m1} + \left[2 + \frac{4\nu n^2}{\lambda_{mn}^2}\right]J_n(\lambda_{mn})}{I_{P2} + \frac{2}{\lambda_{mn}}[\nu + R_{11}]I_{P1} + \left[2 - \frac{4\nu n^2}{\lambda_{mn}^2}\right]I_n(\lambda_{mn})} \quad (6.34a)$$

$$C_{mn} = -\frac{J_n(\lambda_{mn})}{I_n(\lambda_{mn})} \quad (6.35)$$

If $K_{R1} \rightarrow \infty$ & $K_{T1} \rightarrow \infty$, then this case becomes clamped edge boundary condition.

Case: 4 Plate with guided edge and supported fully on Winkler foundation as shown in Fig.

6.4. Substitute $K_{R1} \rightarrow \infty$ & $K_{T1} \rightarrow 0$ in Eqs. (6.6) and (6.7) we get the following equations.

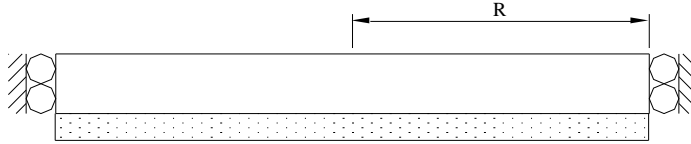


Fig. 6.4. A thin circular plate with guided edge and supported on full elastic foundation

$$\frac{\partial w}{\partial r}(a, \theta) = 0 \quad (6.36)$$

$$V_r(a, \theta) = 0 \quad (6.37)$$

From Eqs. (6.8), (6.9) and (6.36), (6.37), we get the following Equations

$$\frac{\partial w}{\partial r}(a, \theta) = 0 \quad (6.38)$$

$$-D \left[\frac{\partial}{\partial r} \nabla^2 W + (1 - \nu) \cdot \frac{1}{r} \frac{\partial}{\partial \theta} \left(\frac{1}{r} \frac{\partial^2 W}{\partial r \partial \theta} - \frac{1}{r^2} \frac{\partial W}{\partial \theta} \right) \right] = 0 \quad (6.39)$$

From Eqs. (6.5), (6.38) and (6.39) we obtain the following expressions.

$$C_{mn} = \frac{J_{m1}}{I_{P1}} \quad (6.40)$$

$$C_{mn} = \frac{J_{m3} - \frac{2J_{p2}}{\lambda_{mn}} - \left[3 + \frac{4 + 4(2-\nu)n^2}{\lambda_{mn}^2} \right] J_{m1} - \left[\frac{8(3-\nu)n^2}{\lambda_{mn}^3} - \frac{4}{\lambda_{mn}} \right] J_n(\lambda_{mn})}{I_{p3} + \frac{2I_{p2}}{\lambda_{mn}} + \left[3 - \frac{4 - 4(2-\nu)n^2}{\lambda_{mn}^2} \right] I_{p1} + \left[\frac{8(3-\nu)n^2}{\lambda_{mn}^3} + \frac{4}{\lambda_{mn}} \right] I_n(\lambda_{mn})} \quad (6.41)$$

6.3. Solution

The above each case is solved by using Matlab programming, computer software with symbolic capabilities. The program determines eigenvalues (λ_{mn}^*), for a given range of boundary conditions. The boundary conditions are defined as follows.

$$R_{11} = \frac{aK_{R1}}{D} \quad (6.22); \quad T_{11} = \frac{a^3 K_{T1}}{D} \quad (6.23) \quad \text{and} \quad \xi = \frac{K_w a^3}{D} \quad (6.24)$$

The following are the input parameters to the program;

(i) Rotational stiffness ratio (R_{11}) (ii) Translational stiffness ratio (T_{11}) (iii) Foundation ratio (ξ) (iv) Poisson ratio (ν) (v) Upper bound for eigenvalues (N) (vi) Suggested for eigenvalues (d) (vii) Number of mode shape parameters (n). The program finds eigenvalues λ_{mn}^* by using Matlab root finding function. The calculated eigenvalues are used for calculation of mode shape parameter C_{mn} and normalization constant A_{mn} . The program also allows for displaying the results in a desired format.

6.4. Results

Case: 1 Plates with edges elastically restrained against rotation and translation and resting on Winkler foundation

There is a lot of flexibility of the Matlab code developed. This is used to determine eigenvalues of any set or range of rotational, translational and foundation constraints. This code also implanted for various plate materials by adjusting Poisson ratio. The obtained results were compared with previously published data as shown in Table 6.1 depicting

eigenvalues, mode shape parameters and normalization constants for the first vibration mode. The results were not available for higher modes. For the squared eigenvalues (from Eq. $\Psi_{mn} = \lambda_{mn}^2$), the agreement with the previous results is 0.07% [55] and 0.14% [15]. The results obtained with the developed Matlab code are in very good agreement with these two references. For this case the set of Eqs, used are (6.22) and (6.23). The variation of eigenvalues with rotational stiffness ratio is presented in Table 6.2. As seen from the table 6.2, eigenvalues increases with rotational stiffness ratios. The effect of the rotational stiffness ratio is plotted in Fig. 6.5. As observed seen from Fig. 6.5, eigenvalues increases with an increment in the rotational stiffness. Twelve vibration modes presented in Fig. 6.5, position of the stepped region with respect to R_{11} changed very little and falls within 1-100 range and the plates become unstable in this region. The variation of mode shape parameters with rotational stiffness parameter is presented in Table 6.2a. Mode shape parameters are presented in Fig 6.5a (i) – (iv), for twelve vibration modes. The variation of normalization constants with rotational stiffness parameter is presented in Table 6.2b. Mode shape parameters are presented in Fig 6.5b (i) – (iv), for twelve vibration modes.

Table 6.1 Frequency for the mode 00 and Poisson ratio 0.3

$R_{11} \backslash T_{11}$	Thesis 1	Ref. [21,15] 1	Thesis 100	Ref. [21,15] 100
1	1.38820	1.387	-	-
0.01	1.3747	1.374	-	-
0	1.37446	1.373	4.76728	4.735

Table 6.2 Eigenvalues for different Rotational constraint for $T_{11}=100$; $\xi=100$ & $\nu=0.33$

Log R_{11}	λ_{00}	λ_{10}	λ_{20}	λ_{01}	λ_{11}	λ_{21}
-3	10.00568	10.1199	10.46889	10.2319	10.89099	12.52358
-2	10.00571	10.1199	10.46912	10.23194	10.89138	12.52413
-1	10.00597	10.11991	10.47132	10.23237	10.8952	12.52959
0	10.00816	10.11998	10.49012	10.23594	10.92848	12.57911
1	10.01515	10.12023	10.55811	10.24818	11.06059	12.81519
2	10.01882	10.12037	10.59848	10.25514	11.14761	13.01071
3	10.01934	10.12038	10.60451	10.25617	11.16109	13.04388
4	10.0194	10.12039	10.60514	10.25628	11.16252	13.04741
5	10.01941	10.12039	10.6052	10.25629	11.16266	13.04777
6	10.01941	10.12039	10.60521	10.25629	11.16266	13.0478

7	10.01941	10.12039	10.60521	10.25629	11.16267	13.04781
12	10.01941	10.12039	10.60521	10.25629	11.16267	13.04781

Continue...

λ_{02}	λ_{12}	λ_{22}	λ_{03}	λ_{13}	λ_{23}
10.42005	11.51596	13.57339	10.74588	12.31332	14.70778
10.42022	11.51644	13.57395	10.74617	12.31384	14.70832
10.42189	11.52117	13.57945	10.74904	12.31897	14.71364
10.43609	11.56327	13.62988	10.77389	12.3652	14.76286
10.48745	11.74611	13.8863	10.87126	12.58135	15.02657
10.51831	11.88102	14.12102	10.93587	12.78876	15.29071
10.52296	11.88102	14.12102	10.94601	12.78876	15.34008
10.52345	11.90524	14.16282	10.94709	12.79199	15.34542
10.52356	11.90547	14.16775	10.94719	12.79231	15.34595
10.5235	11.90547	14.16775	10.9472	12.79234	15.34601
10.5235	11.9055	14.1678	10.94721	12.79235	15.34601
10.5235	11.9055	14.1678	10.94721	12.79235	15.34601

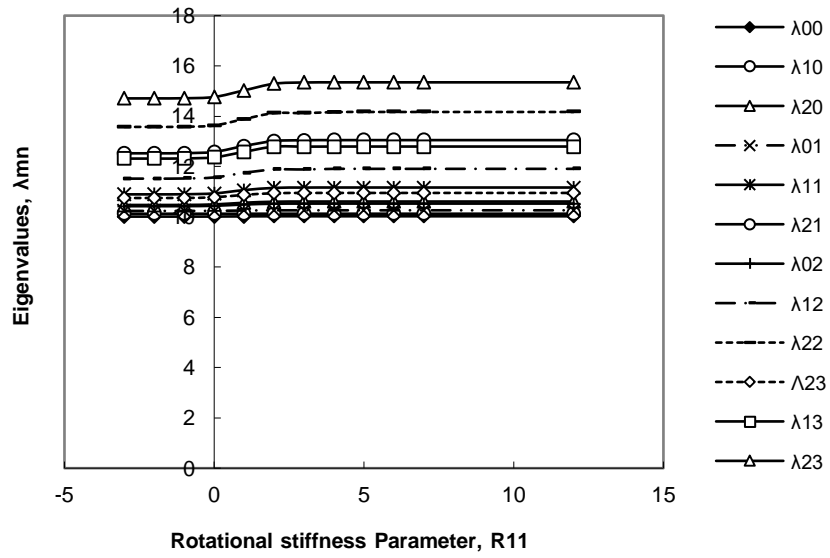


Fig. 6.5. Effect of Rotational stiffness ratio, R_{11} on eigenvalues, λ_{mn}

Table 6.2a Mode shape parameters C_{mn} , for different Rotational constraint for $T_{11}=100$; $\xi=100$ & $\nu=0.33$

$\text{Log } R_{11}$	C_{00}	C_{10}	C_{20}	C_{01}	C_{11}	C_{21}
-4	-2.77E-05	-1.39E-05	1.34E-05	-8.79E-05	-3.43E-05	5.73E-06
-3	-2.77E-05	-1.39E-05	1.34E-05	-8.79E-05	-3.43E-05	5.73E-06
-2	-2.77E-05	-1.39E-05	1.34E-05	-8.79E-05	-3.43E-05	5.73E-06
-1	-2.77E-05	-1.39E-05	1.35E-05	-8.78E-05	-3.41E-05	5.73E-06

0	-2.77E-05	-1.39E-05	1.34E-05	-8.79E-05	-3.43E-05	5.73E-06
1	-2.65E-05	-1.39E-05	1.74E-05	-8.64E-05	-2.44E-05	5.36E-06
2	-2.60E-05	-1.39E-05	1.90E-05	-8.57E-05	-1.99E-05	4.80E-06
3	-2.59E-05	-1.39E-05	1.92E-05	-8.56E-05	-1.93E-05	4.69E-06
4	-2.59E-05	-1.39E-05	1.92E-05	-8.56E-05	-1.92E-05	4.67E-06
5	-2.59E-05	-1.39E-05	1.92E-05	-8.56E-05	-1.92E-05	4.67E-06
6	-2.59E-05	-1.39E-05	1.92E-05	-8.56E-05	-1.92E-05	4.67E-06
7	-2.59E-05	-1.39E-05	1.92E-05	-8.56E-05	-1.92E-05	4.67E-06
12	-2.59E-05	-1.39E-05	1.92E-05	-8.56E-05	-1.92E-05	4.67E-06

continue

C_{02}	C_{12}	C_{22}	C_{03}	C_{13}	C_{23}
-2.95E-05	-2.68E-05	1.13E-06	4.75E-05	-1.14E-05	1.09E-07
-2.95E-05	-2.68E-05	1.13E-06	4.75E-05	-1.14E-05	1.09E-07
-2.95E-05	-2.67E-05	1.13E-06	4.74E-05	-1.14E-05	1.10E-07
-2.96E-05	-2.66E-05	1.14E-06	4.71E-05	-1.14E-05	1.16E-07
-2.95E-05	-2.68E-05	1.13E-06	4.75E-05	-1.14E-05	1.09E-07
-3.25E-05	-2.11E-05	1.45E-06	3.45E-05	-1.02E-05	3.44E-07
-3.36E-05	-1.79E-05	1.45E-06	2.86E-05	-8.96E-06	4.11E-07
-3.37E-05	-1.74E-05	1.43E-06	2.78E-05	-8.75E-06	4.14E-07
-3.37E-05	-1.73E-05	1.43E-06	2.77E-05	-8.72E-06	4.15E-07
-3.37E-05	-1.73E-05	1.43E-06	2.76E-05	-8.72E-06	4.15E-07
-3.37E-05	-1.73E-05	1.43E-06	2.76E-05	-8.72E-06	4.15E-07
-3.37E-05	-1.73E-05	1.43E-06	2.76E-05	-8.72E-06	4.15E-07
-3.37E-05	-1.73E-05	1.43E-06	2.76E-05	-8.72E-06	4.15E-07

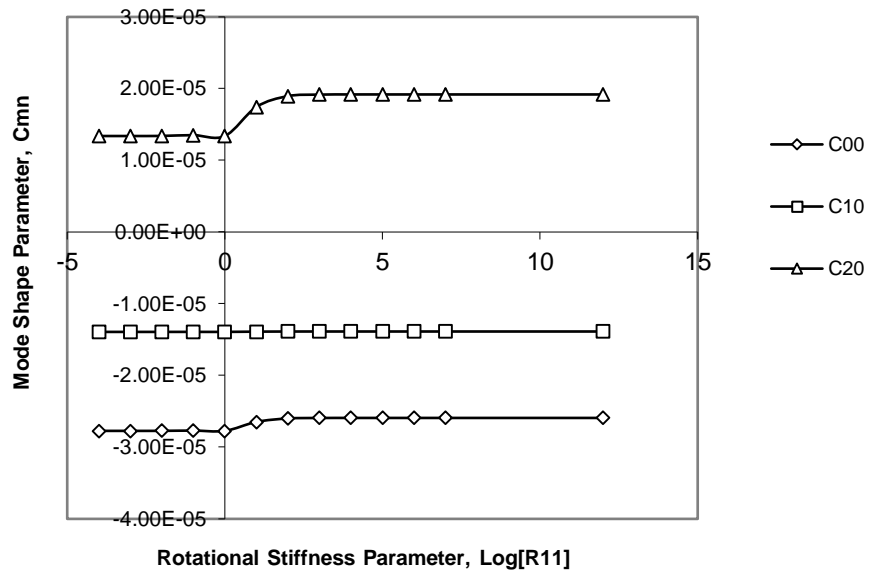


Fig. 6.5a (i)

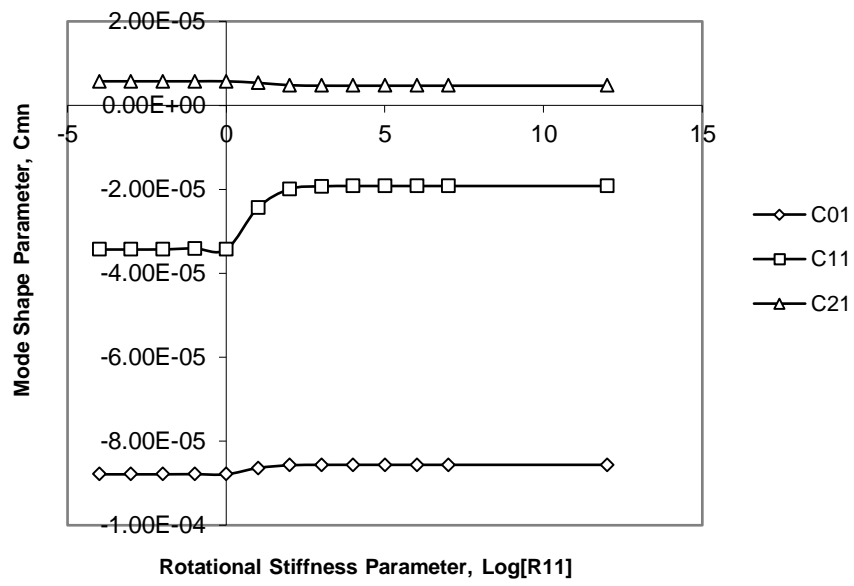


Fig. 6.5a (ii)

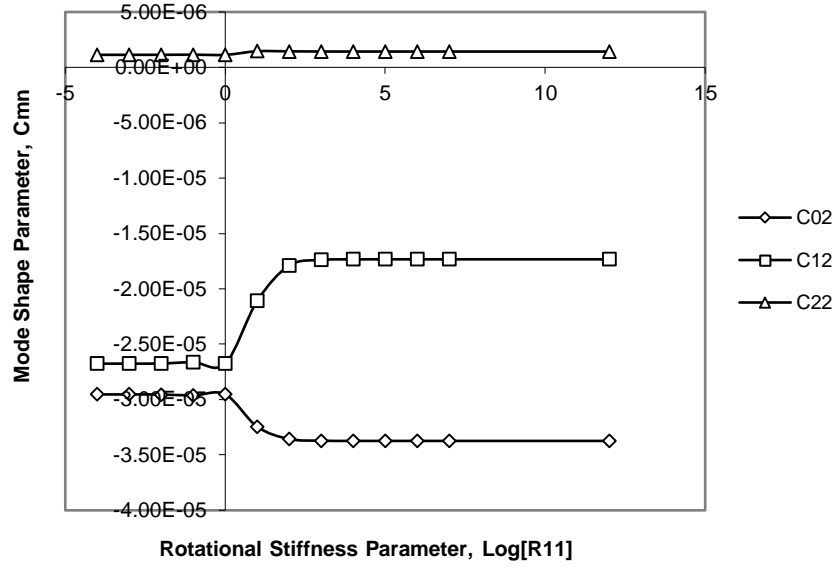


Fig. 6.5a (iii)

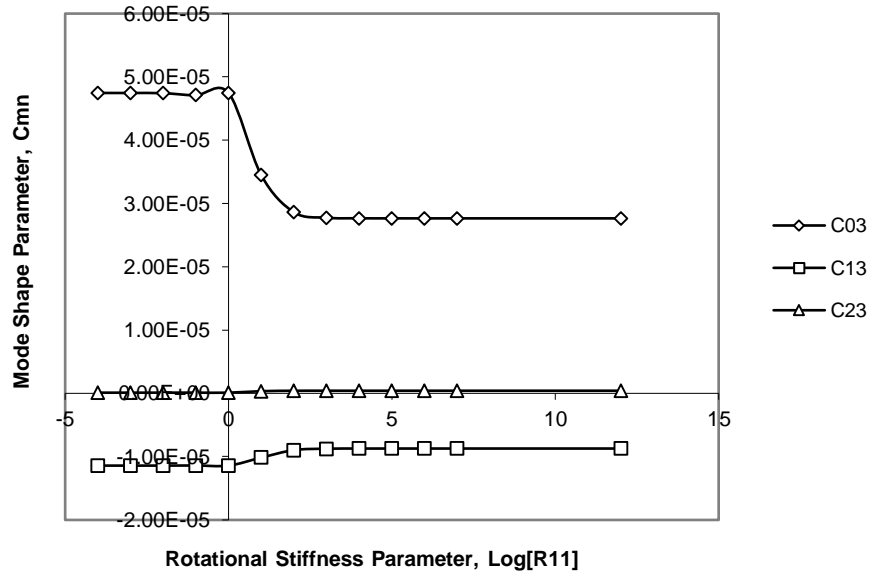


Fig. 6.5a (iv)

Fig. 6.5 a (i)-(iv) Mode shape parameters C_{mn} , for different Rotational constraint for $T_{11}=100$; $\xi=100$ & $\nu=0.33$

Table 6.2b Normalization Constants A_{mn} , for different Rotational constraint for $T_{11}=100$; $\xi=100$ & $\nu=0.33$

Log R_{11}	A_{00}	A_{10}	A_{20}	A_{01}	A_{11}	A_{21}
-4	3.89268	3.93802	4.10917	5.94463	5.82626	6.56489
-3	3.89269	3.93802	4.10918	5.94463	5.82626	6.56492

-2	3.8927	3.93802	4.1093	5.94462	5.82625	6.56636
-1	3.89279	3.93803	4.11048	5.94453	5.82611	6.57217
0	3.89268	3.93802	4.10916	5.94463	5.82626	6.56488
1	3.89618	3.93817	4.15727	5.94123	5.83015	6.69173
2	3.89755	3.93822	4.1791	5.93975	5.84068	6.73167
3	3.89775	3.93823	4.18236	5.93953	5.84285	6.73515
4	3.89777	3.93823	4.1827	5.93951	5.84309	6.73546
5	3.89777	3.93823	4.18273	5.93951	5.84311	6.73549
6	3.89777	3.93823	4.18273	5.93951	5.84311	6.7355
7	3.89777	3.93823	4.18273	5.93951	5.84311	6.7355
12	3.89777	3.93823	4.18273	5.93951	5.84311	6.7355

Continue

A_{02}	A_{12}	A_{22}	A_{03}	A_{13}	A_{23}
5.93716	6.37696	6.69458	5.81501	6.66791	6.89759
5.93717	6.37695	6.69461	5.81501	6.66793	6.89762
5.93731	6.37691	6.69496	5.81505	6.66815	6.89791
5.93862	6.37647	6.69844	5.81548	6.67033	6.90081
5.93716	6.37696	6.69458	5.81501	6.6679	6.89758
5.98975	6.34241	6.88394	5.84105	6.74916	7.08286
6.01336	6.31526	6.99721	5.85822	6.76679	7.23276
6.01691	6.30666	7.01263	5.86137	6.76724	7.258
6.01728	6.30963	7.01389	5.86171	6.76722	7.26065
6.01732	6.30959	7.01406	5.86175	6.76722	7.26092
6.01732	6.30958	7.01408	5.86175	6.76722	7.26095
6.01732	6.30958	7.01408	5.86175	6.76722	7.26095
6.01732	6.30958	7.01408	5.86175	6.76722	7.26095

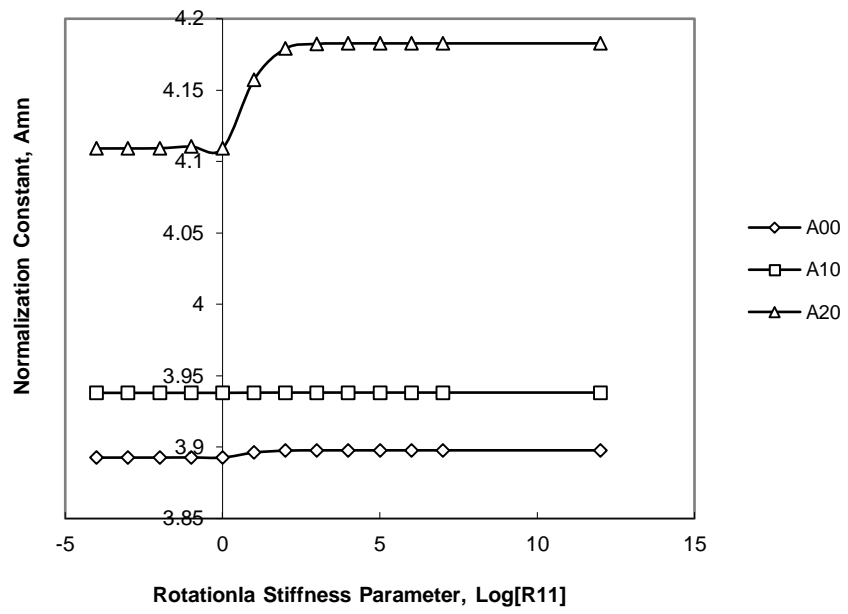


Fig. (i)

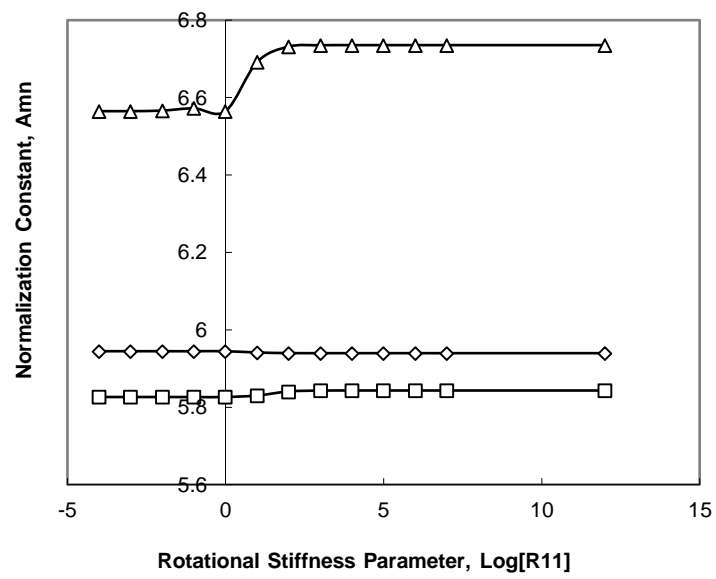


Fig. (ii)

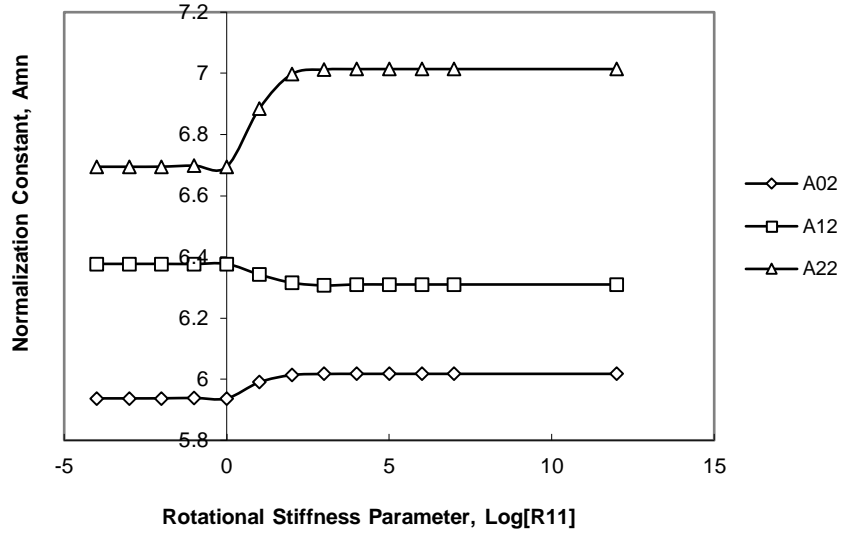


Fig. (iii)

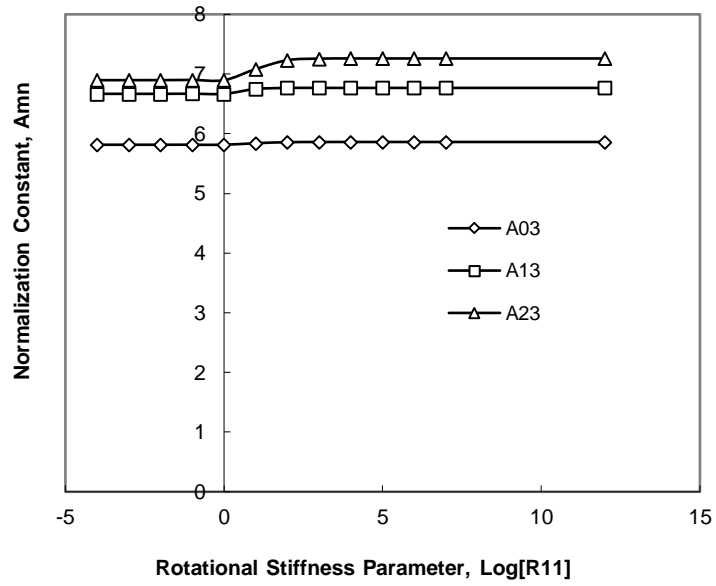


Fig. (iv)

Fig. 6.5 b(i)-(iv) Normalization constants A_{mn} , for different Rotational constraint for $T_{11}=100$; $\xi=100$ & $\nu=0.33$

The variation of eigenvalues with translational constraint is presented in Table 6.3. As seen from the table 6.2, eigenvalues increases with translational stiffness ratios. The effect of the

translational stiffness ratio is plotted in Fig. 6.6. As seen from Fig. 6.6, eigenvalues increases with an increment in the translational stiffness. Twelve vibration modes presented in Fig. 6.6, the position of the stepped region with respect to T_{11} moved steadily from $1-10^4$. Therefore, stepped variation of T_{11} is much more erudite than that of the R_{11} . The variation of mode shape parameters with rotational stiffness parameter is presented in Table 6.3a. Mode shape parameters are presented in Fig 6.6a (i) – (iv), for twelve vibration modes. The variation of normalization constants with rotational stiffness parameter is presented in Table 6.3b. Mode shape parameters are presented in Fig 6.6b (i) – (iv), for twelve vibration modes.

Table 6.3 Eigenvalues for different Translational constraint for $R_{11}=100$; $\xi=100$ & $\nu=0.33$

$\text{Log } T_{11}$	λ_{00}	λ_{10}	λ_{20}	λ_{01}	λ_{11}	λ_{21}
-3	10	10.05243	10.54743	10.19217	11.10502	12.98461
-2	10	10.05244	10.54743	10.19217	11.10502	12.98461
-1	10	10.05248	10.54747	10.19222	11.10505	12.98464
0	10.0005	10.05294	10.54788	10.19268	11.1054	12.98486
1	10.0045	10.05791	10.55201	10.19741	11.10902	12.98716
2	10.0189	10.12037	10.59848	10.25514	11.14761	13.01071
3	10.0243	10.31372	11.0944	10.62837	11.63183	13.30063
4	10.0249	10.3563	11.48645	10.77686	12.35162	14.5744
5	10.025	10.36037	11.52305	10.79064	12.42703	14.80018
6	10.025	10.36077	11.52656	10.7919	12.43407	14.81961
12	10.025	10.36081	11.52695	10.79214	12.43485	14.82173

Continue....

λ_{02}	λ_{12}	λ_{22}	λ_{03}	λ_{13}	λ_{23}
10.46173	11.84557	14.10027	10.88491	12.7292	15.27401
10.46174	11.84558	14.10028	10.88492	12.72928	15.27401
10.46178	11.84561	14.10029	10.88496	12.7293	15.27402
10.46223	11.84591	14.10048	10.88539	12.72956	15.27417
10.46682	11.84829	14.10231	10.8897	12.73213	15.27566
10.51831	11.88102	14.12102	10.93587	12.75857	15.29071
11.00942	12.28648	14.34046	11.45187	13.08037	15.46088
11.36392	13.31448	15.71133	12.08898	14.32869	16.83283
11.39769	13.44776	16.05237	12.15643	14.54171	17.31721
11.40095	13.45981	16.08062	12.16282	14.56035	17.3562
11.40131	13.46114	16.08368	12.16352	14.56239	17.36039

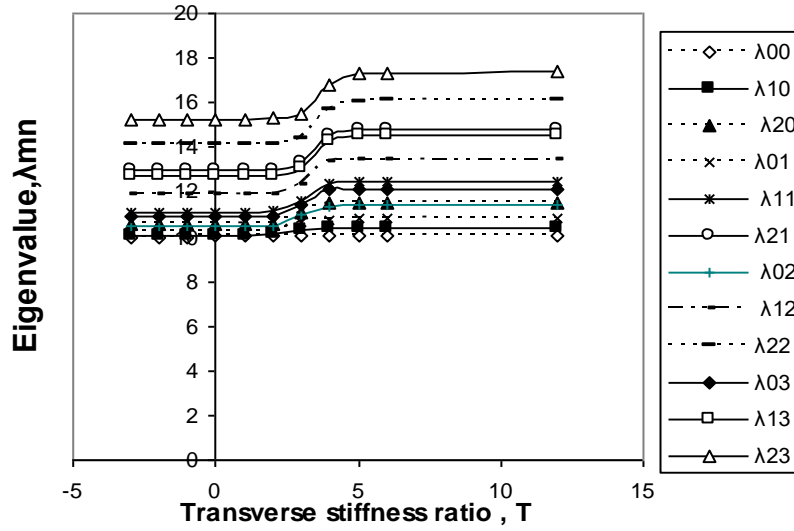


Fig. 6.6. Effect of Translational constraint, T_{11} on eigenvalues, λ_{mn}

Table 6.3a Mode shape parameters C_{mn} , for different Translational constraint for $R_{11}=100$; $\xi=100$ & $\nu=0.33$

$\text{Log } T_{11}$	C_{00}	C_{10}	C_{20}	C_{01}	C_{11}	C_{21}
-3	-1.63E-05	-1.08E-05	1.99E-05	-8.23E-05	-1.84E-05	4.72E-06
-2	-1.63E-05	-1.08E-05	1.99E-05	-8.23E-05	-1.84E-05	4.72E-06
-1	-1.63E-05	-1.08E-05	1.99E-05	-8.23E-05	-1.84E-05	4.72E-06
0	-1.63E-05	-1.08E-05	1.99E-05	-8.24E-05	-1.85E-05	4.72E-06
1	-1.69E-05	-1.12E-05	1.98E-05	-8.27E-05	-1.86E-05	4.73E-06
2	-2.60E-05	-1.39E-05	1.90E-05	-8.57E-05	-1.99E-05	4.80E-06
3	2.23E-03	-1.30E-03	4.41E-05	-5.29E-04	-4.05E-05	6.38E-06
4	9.61E-05	6.81E-05	3.65E-06	3.28E-05	7.76E-06	-1.42E-06
5	8.66E-05	6.24E-05	4.98E-06	2.54E-05	6.48E-06	-7.90E-07
6	8.57E-05	6.19E-05	5.09E-06	2.48E-05	6.38E-06	-7.53E-07
7	8.57E-05	6.19E-05	5.10E-06	2.47E-05	6.37E-06	-7.49E-07
12	8.56E-05	6.19E-05	5.10E-06	2.47E-05	6.37E-06	-7.49E-07

Continue

C_{02}	C_{12}	C_{22}	C_{03}	C_{13}	C_{23}
-3.44E-05	-1.73E-05	1.44E-06	2.63E-05	-8.82E-06	4.12E-07
-3.44E-05	-1.73E-05	1.44E-06	2.63E-05	-8.82E-06	4.12E-07
-3.44E-05	-1.73E-05	1.44E-06	2.63E-05	-8.82E-06	4.12E-07
-3.43E-05	-1.73E-05	1.44E-06	2.63E-05	-8.83E-06	4.12E-07
-3.42E-05	-1.74E-05	1.44E-06	2.65E-05	-8.84E-06	4.12E-07
-3.36E-05	-1.79E-05	1.45E-06	2.86E-05	-8.96E-06	4.11E-07
-8.53E-05	-2.86E-05	1.68E-06	6.30E-05	-1.21E-05	4.34E-07
-3.39E-06	4.77E-06	-5.55E-07	-1.33E-05	2.39E-06	-2.28E-07
-5.52E-06	3.32E-06	-2.42E-07	-1.15E-05	1.37E-06	-7.49E-08
-5.70E-06	3.22E-06	-2.26E-07	-1.14E-05	1.31E-06	-6.85E-08
-5.72E-06	3.21E-06	-2.24E-07	-1.13E-05	1.30E-06	-6.79E-08
-5.72E-06	3.21E-06	-2.24E-07	-1.13E-05	1.30E-06	-6.78E-08

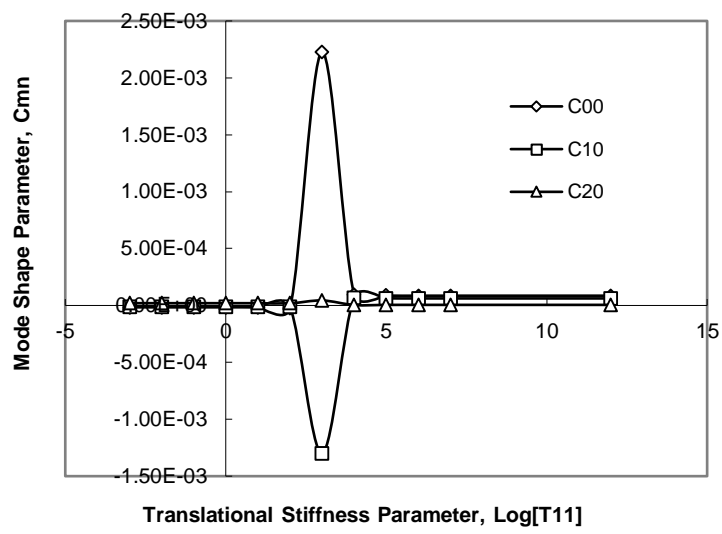


Fig. (i)

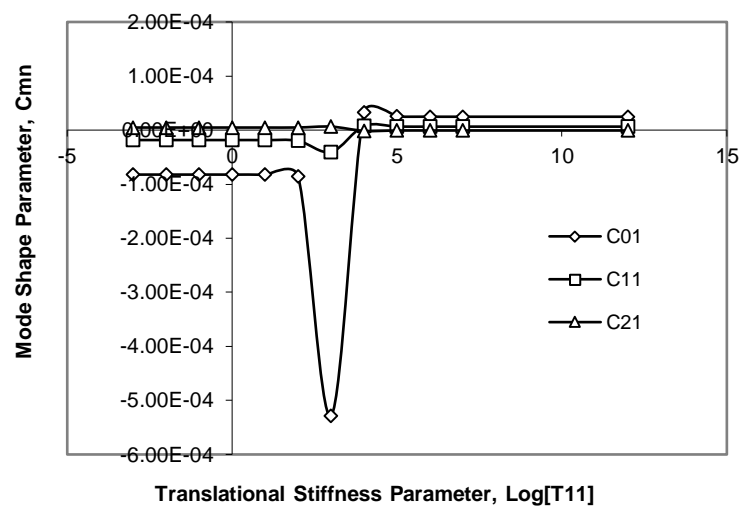


Fig. (ii)

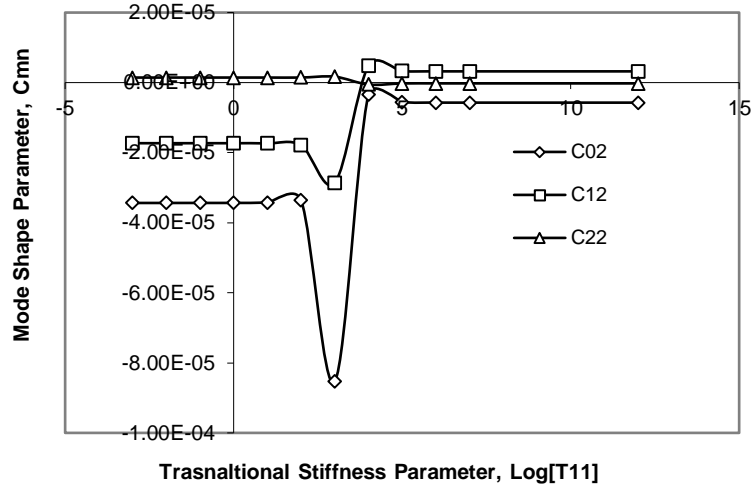


Fig. (iii)

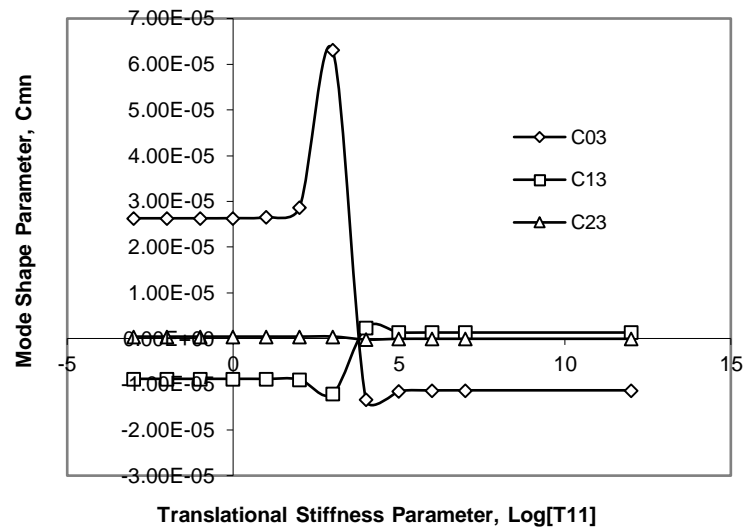


Fig. (iv)

Fig. 6.6a(i)-(iv) Mode shape parameters C_{mn} , for different Translational constraint for $R_{11}=100$; $\xi=100$ & $\nu=0.33$

Table 6.3b Normalization constant A_{mn} , for different Translational constraint for $R_{11}=100$; $\xi=100$ & $\nu=0.33$

$\text{Log } T_{11}$	A_{00}	A_{10}	A_{20}	A_{01}	A_{11}	A_{21}
-3	3.94286	3.96013	4.17229	5.96267	5.88606	6.72327

-2	3.94286	3.96013	4.17229	5.96267	5.88606	6.72327
-1	3.94283	3.96011	4.1723	5.96266	5.88602	6.72328
0	3.94257	3.95989	4.17233	5.96256	5.88566	6.72336
1	3.93978	3.95772	4.17265	5.96149	5.88201	6.72415
2	3.89755	3.93822	4.1791	5.93975	5.84068	6.73167
3	0.50459	0.6113	4.48291	1.79055	4.58722	6.55527
4	4.11188	4.26932	4.27047	5.69982	6.56477	6.77061
5	4.1247	4.26758	4.30984	5.78904	6.55418	7.04004
6	4.1256	4.26726	4.31332	5.79634	6.55386	7.05187
7	4.12569	4.26723	4.31366	5.79705	6.5538	7.05296
12	4.1257	4.26722	4.3137	5.79713	6.55379	7.05308

continue

A_{02}	A_{12}	A_{22}	A_{03}	A_{13}	A_{23}
5.99313	6.3372	6.98629	5.90799	6.76063	7.22578
5.99313	6.33719	6.9863	5.90798	6.76063	7.22578
5.99314	6.33718	6.98631	5.90794	6.76063	7.22579
5.99326	6.33702	6.9864	5.90754	6.7607	7.22585
5.99455	6.33542	6.98736	5.90338	6.76132	7.22645
6.01336	6.31526	6.99721	5.85822	6.76679	7.23276
6.21663	5.18006	7.10152	4.61377	6.43589	7.32741
6.02829	6.80304	6.72413	6.59869	6.85393	6.66128
6.09087	6.85591	7.26476	6.5868	7.08704	7.50833
6.09634	6.85779	7.28754	6.58626	7.09629	7.54289
6.09688	6.85796	7.28963	6.58621	7.09719	7.54603
6.09694	6.85798	7.28986	6.58621	7.09728	7.54637

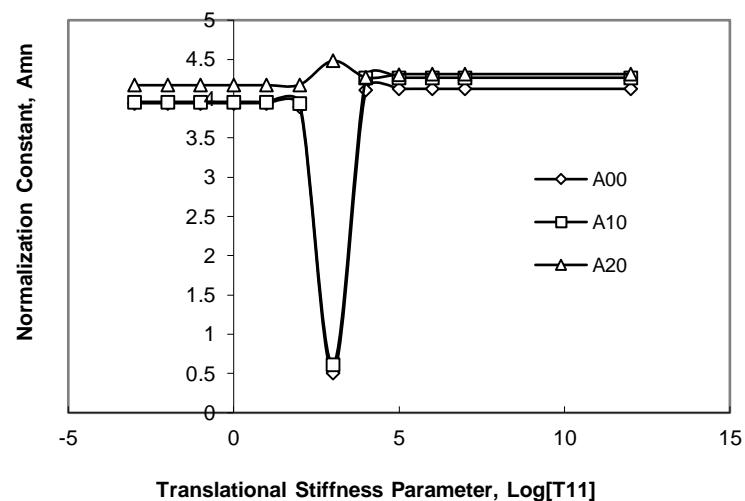


Fig. (i)

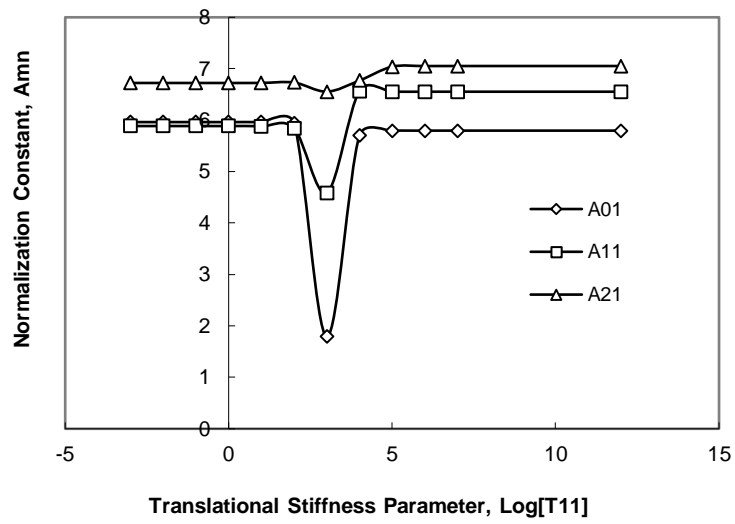


Fig. (ii)

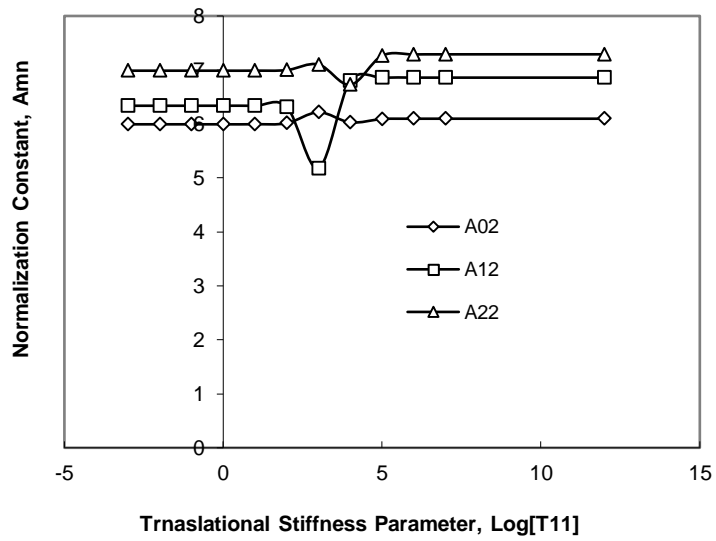


Fig. (iii)

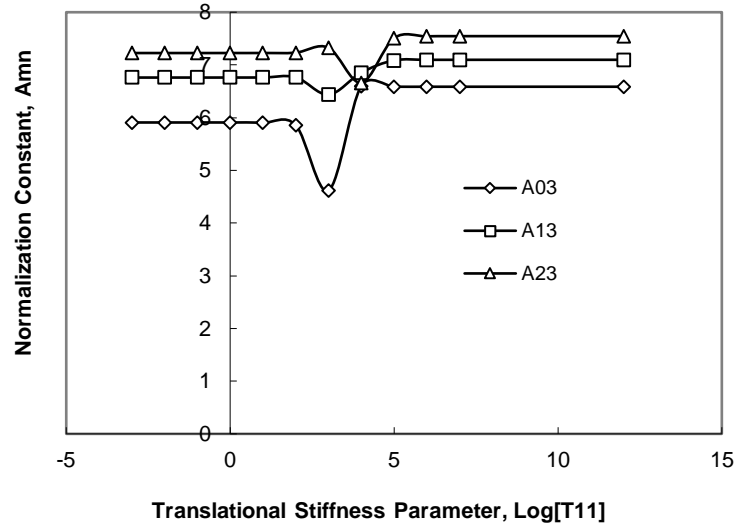


Fig. (iv)

Fig. 6.6 b(i)-(iv) Normalization constant A_{mn} , for different Translational constraint for $R_{11}=100$; $\xi=100$ & $\nu=0.33$

Similarly the variation of eigenvalues with foundation constraint is presented in Table 6.4 and 6.5. As seen from the table 6.4 and 6.5, eigenvalues increases with foundation stiffness. The effect of the foundation parameter is plotted in Fig. 6.7 and 6.8. As can be seen from Fig. 6.7 and 6.8, eigenvalues increases with an increment in the foundation stiffness. As observed from the Table 6.2, 6.3 and 6.4, 6.5, the influence of foundation parameter on eigenvalues is more predominant than that of transverse stiffness parameter or rotational stiffness parameter. As seen from Fig. 6.7 and 6.8, all the curves tend to converge as the value of foundation stiffness increases.

Table 6.4. Eigenvalues for different foundation stiffness for $R_{11}=10$; $T_{11}=1000$ & $\nu=0.33$

ξ	λ_{00}	λ_{01}	λ_{02}	λ_{10}	λ_{11}	λ_{12}	λ_{20}	λ_{21}	λ_{22}
0	2.94189	7.04771	8.1667	5.77006	9.53318	10.62846	8.37513	12.01027	13.26816
1	2.95166	7.04842	8.16716	5.77136	9.53347	10.62867	8.37555	12.01042	13.26887
5	3.16152	7.0655	8.17815	5.80232	9.54039	10.63366	8.38575	12.01388	13.27144
20	4.66822	7.31748	8.34441	6.23209	9.64656	10.71079	8.5404	12.06758	13.137
35	6.00451	7.79506	8.67875	6.95024	9.86854	10.87484	8.85382	12.18327	13.39796
50	7.12345	8.39511	9.12995	7.75051	10.18468	11.11463	9.28113	12.35583	13.52857
100	10.01867	10.56675	10.96361	10.01867	11.62444	12.2828	11.05204	13.24838	14.22946

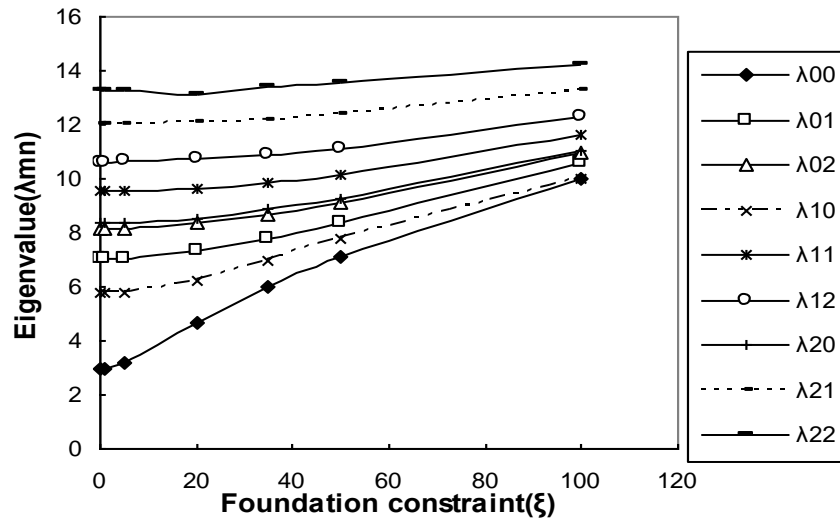


Fig. 6.7. Effect of Foundation constraint, ξ on eigenvalues, λ_{mn}

Table 6.5 Eigenvalues for different foundation stiffness for $R_{11}=100$; $T_{11}=100$ & $\nu=0.33$

Log ξ	λ_{00}	λ_{10}	λ_{20}	λ_{01}	λ_{11}	λ_{21}
-3	2.94751	4.70542	7.15274	5.70632	8.58927	11.68693
-2	2.94751	4.70542	7.15274	5.70632	8.58927	11.68693
-1	2.94761	4.70544	7.15274	5.70633	8.58927	11.68693
0	2.95723	4.70782	7.15342	5.70767	8.58966	11.68708
1	3.63962	4.92895	7.22009	5.83635	8.62845	11.70256
2	10.01882	10.12037	10.59848	10.25514	11.14761	13.01071
3	31.62337	31.62665	31.64345	31.63116	31.66572	31.76924
4	100	100.0001	100.0007	100.0003	100.0014	100.0047
5	316.2277	316.2277	316.2278	316.2277	316.2278	316.2279

Continue..

λ_{02}	λ_{12}	λ_{22}	λ_{03}	λ_{13}	λ_{23}
6.87962	9.98139	13.13452	8.09899	11.33328	14.53759
6.87962	9.98139	13.13452	8.09899	11.33328	14.53759
6.87963	9.9814	13.13452	8.099	11.33329	14.53759
6.88039	9.98164	13.13463	8.09946	11.33346	14.53767
6.95515	10.00644	13.14554	8.14565	11.35042	14.54572
10.51831	11.88102	14.12102	10.93507	12.75857	15.29071
31.64047	31.70096	31.85548	31.65674	31.7524	31.97012
100.0006	100.0025	100.0074	100.0011	100.0041	100.0112
316.2278	316.2278	316.228	316.2278	316.2279	316.2281

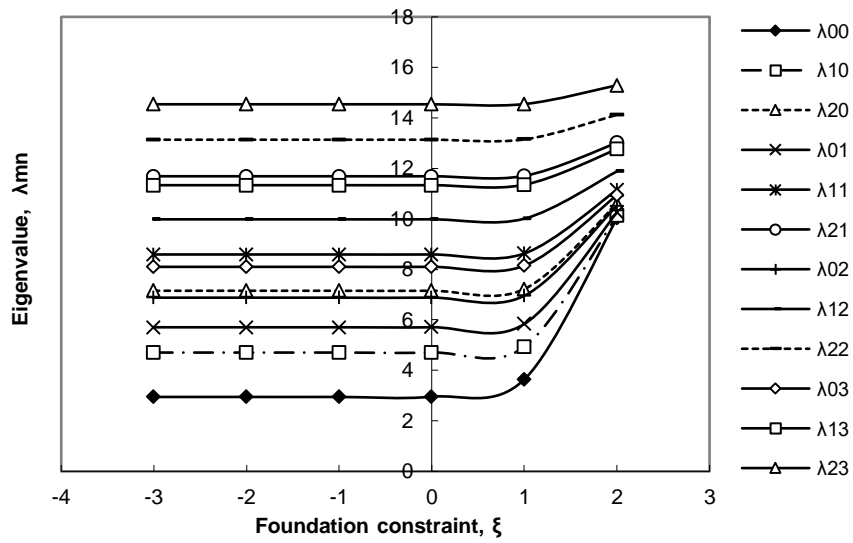


Fig. 6.8. Effect of Foundation constraint, ξ on eigenvalues, λ_{mn}

Table 6.5a. Mode shape parameters C_{mn} , for different foundation stiffness for $R_{11}=10$; $T_{11}=1000$ & $\nu=0.33$

Log ξ	C_{00}	C_{10}	C_{20}	C_{01}	C_{11}	C_{21}
-3	8.98E-02	-1.50E-02	3.20E-04	-2.97E-03	5.20E-05	-1.58E-06
-2	8.98E-02	-1.50E-02	3.20E-04	-2.97E-03	5.20E-05	-1.58E-06
-1	8.98E-02	-1.50E-02	3.20E-04	-2.97E-03	5.20E-05	-1.58E-06
0	9.03E-02	-1.63E-02	3.18E-04	-2.93E-03	5.18E-05	-1.58E-06
1	8.83E-02	1.05E-01	1.32E-04	2.62E-04	3.02E-05	-1.25E-06
2	-2.60E-05	-1.39E-05	1.90E-05	-8.57E-05	-1.99E-05	4.80E-06
3	2.02E-14	2.00E-14	1.92E-14	3.23E-14	3.19E-14	3.02E-14
4	7.22E-44	7.22E-44	7.22E-44	1.95E-44	1.96E-44	1.98E-44
5	-8.86E-138	-8.86E-138	-8.86E-138	2.60E-138	2.60E-138	2.60E-138

continue

C_{02}	C_{12}	C_{22}	C_{03}	C_{13}	C_{23}
-5.98E-04	1.16E-05	-3.94E-07	-1.48E-04	3.17E-06	-1.12E-07
-5.98E-04	1.16E-05	-3.94E-07	-1.48E-04	3.17E-06	-1.12E-07
-5.98E-04	1.16E-05	-3.94E-07	-1.48E-04	3.17E-06	-1.12E-07
-5.94E-04	1.15E-05	-3.94E-07	-1.47E-04	3.16E-06	-1.12E-07
-1.99E-04	7.95E-06	-3.35E-07	-7.32E-05	2.43E-06	-1.00E-07
-3.36E-05	-1.79E-05	1.45E-06	2.86E-05	-8.96E-06	4.11E-07
-1.85E-14	-1.54E-14	-8.60E-15	-3.89E-14	-3.65E-14	-3.06E-14
-7.32E-44	-7.31E-44	-7.26E-44	-2.34E-44	-2.35E-44	-2.39E-44
8.93E-138	8.93E-138	8.93E-138	-2.52E-138	-2.52E-138	-2.52E-138

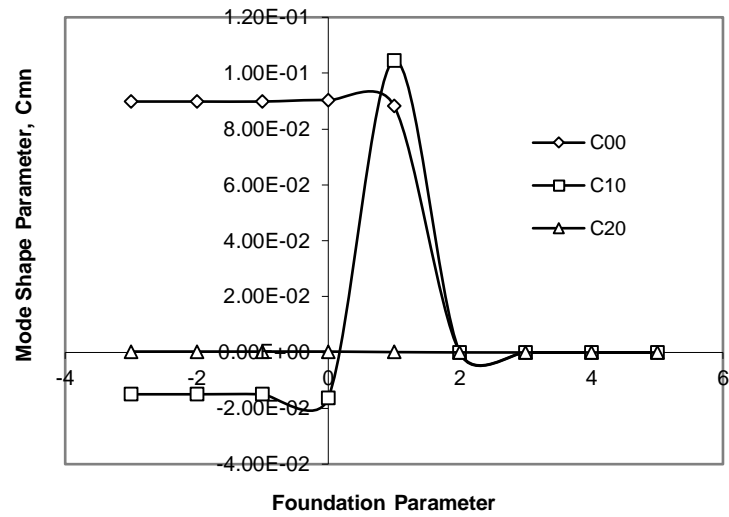


Fig. (i)

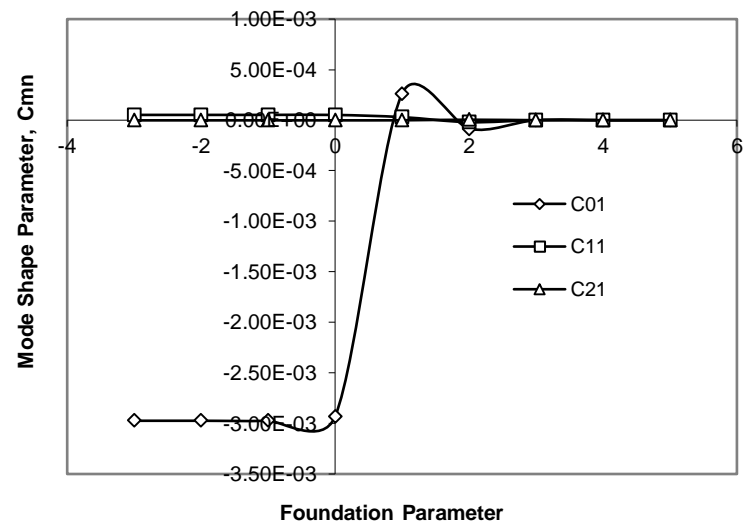


Fig. (ii)

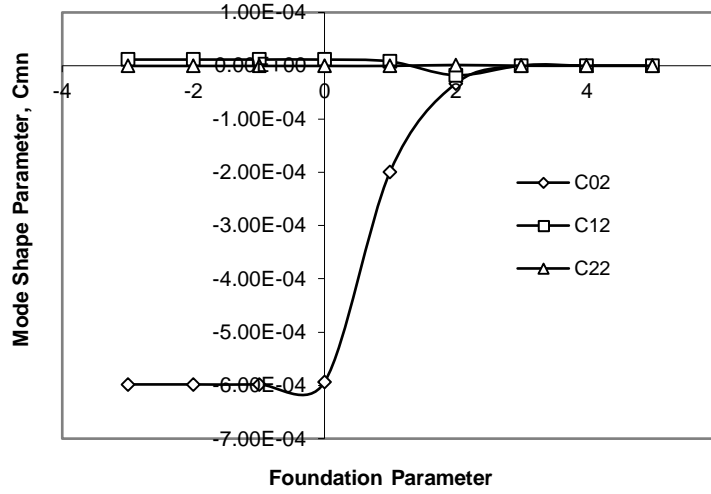


Fig. (iii)

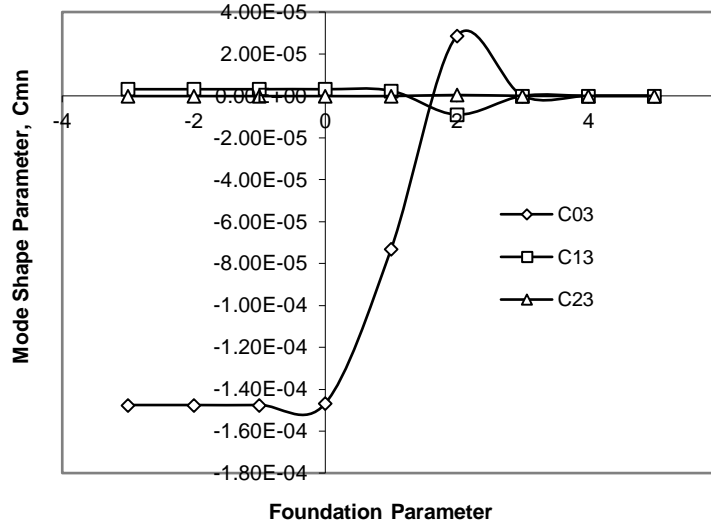


Fig. (iv)

Fig. 6.8a(i)-(iv) Mode shape parameters C_{mn} , for different foundation stiffness for $R_{11}=10$; $T_{11}=1000$ & $\nu=0.33$

Table 65b. Normalization constant A_{mn} , for different foundation stiffness for $R_{11}=10$; $T_{11}=1000$ & $\nu=0.33$

Log ξ	A_{00}	A_{10}	A_{20}	A_{01}	A_{11}	A_{21}
-3	1.83992	2.03944	3.22612	3.79138	5.12514	6.03747
-2	1.83992	2.03944	3.22612	3.79138	5.12514	6.03747
-1	1.83995	2.03903	3.22613	3.79142	5.12515	6.03747
0	1.84248	1.99862	3.22673	3.79606	5.12547	6.03756
1	2.18188	0.96898	3.28604	4.21271	5.15795	6.04621
2	3.89755	3.93822	4.1791	5.93975	5.84068	6.73167
3	7.0303	7.03049	7.03153	10.18614	10.18276	10.20726
4	11.35936	11.35947	11.36005	19.36193	19.35902	19.35027
5	22.47154	22.47153	22.47153	30.3033	30.30331	30.30333

continue

A_{02}	A_{12}	A_{22}	A_{03}	A_{13}	A_{23}
4.53473	5.60538	6.43609	5.11986	6.0409	6.81164
4.53473	5.60538	6.43609	5.11986	6.0409	6.81164
4.53474	5.60538	6.43609	5.11987	6.0409	6.81165
4.53587	5.60555	6.43615	5.12034	6.041	6.81168
4.64726	5.62242	6.44168	5.16732	6.05118	6.81532
6.01336	6.31526	6.99721	5.85822	6.76679	7.23276
9.93292	9.94438	9.98084	10.22036	10.22853	10.23447
16.78678	16.79039	16.79939	18.40884	18.40143	18.38568
31.68516	31.68495	31.68443	31.06873	31.06879	31.06892

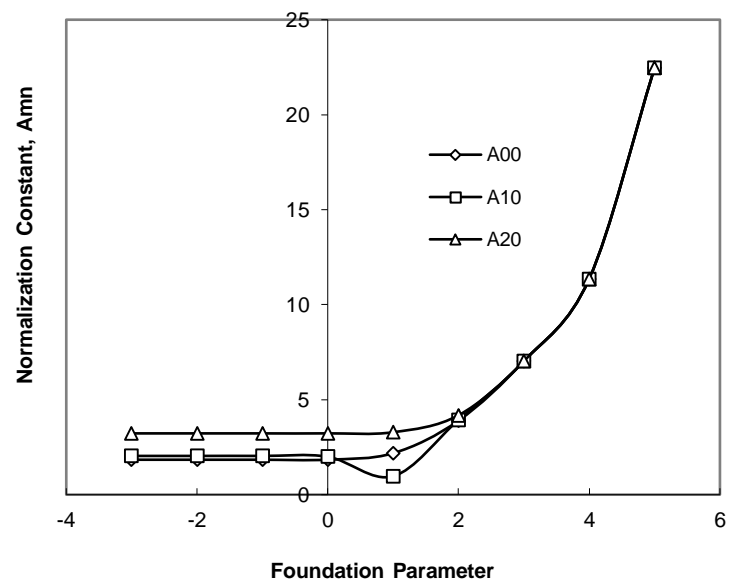


Fig. (i)

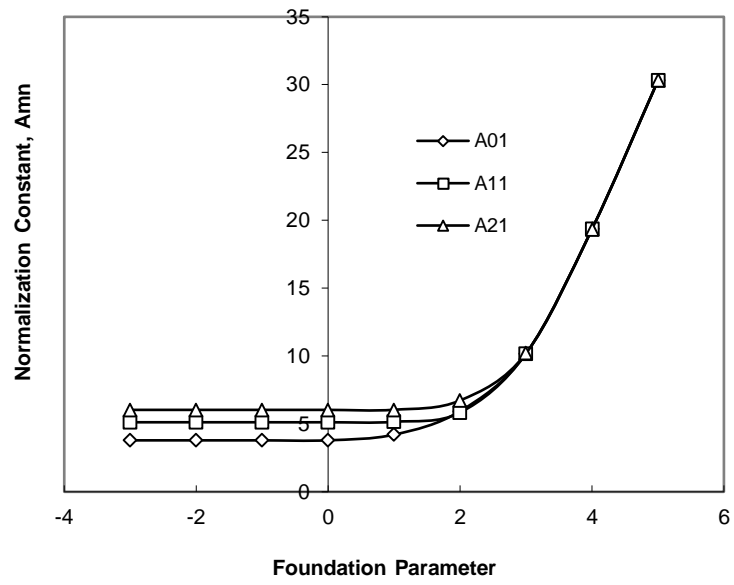


Fig. (ii)

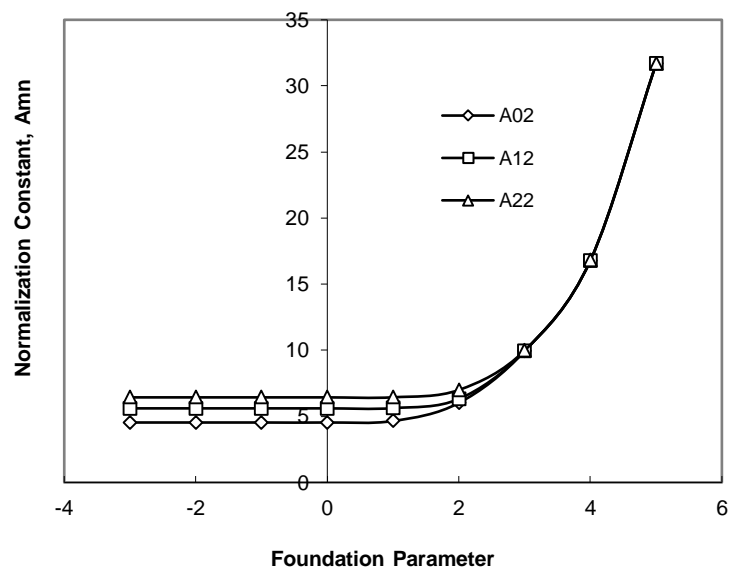


Fig. (iii)

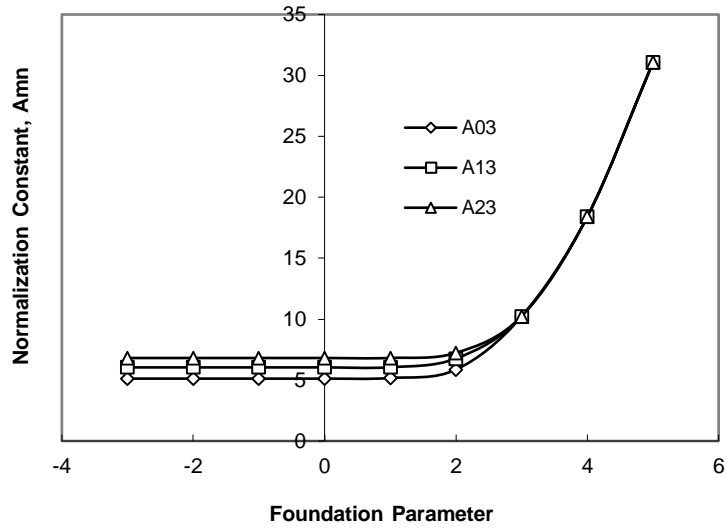


Fig. (iv)

Fig. 6.8b. Normalization constant A_{mn} , for different foundation stiffness for $R_{11}=10$; $T_{11}=1000$ & $\nu=0.33$

The eigenvalues for different plate materials, for various values of transverse, rotational and foundation parameters are computed and the results are given in Table 6.6. It is observed that for any value of foundation parameter (ξ), eigenvalues are independent on Poisson ratio, as shown in Fig. 6.9. And also it was observed that for any value of T_{11} , eigenvalues are independent on Poisson ratio. When $\xi=0$, then the frequency is 4.239 and this is in well agreement with the results (4.239) obtained by Andrei Zagrai [77].

Table 6.6 Eigenvalues for different set of Poisson ratio, R_{11} , T_{11} & ξ

ν	$R_{11}=1000, T_{11}=1000, \xi=1000$	$R_{11}=1000, T_{11}=100, \xi=10$	$R_{11}=1, T_{11}=1, \xi=10$	$R_{11}=1, T_{11}=1, \xi=100$
0	31.63347	4.92912	3.79959	10.02765
0.1	31.63347	4.92912	3.79959	10.02765
0.2	31.63347	4.92912	3.79959	10.02765
0.3	31.63347	4.92912	3.79959	10.02765
0.4	31.63347	4.92912	3.79959	10.02765
0.5	31.63347	4.92912	3.79959	10.02765
0.6	31.63347	4.92912	3.79959	10.02765
0.7	31.63347	4.92912	3.79959	10.02765
0.8	31.63347	4.92912	3.79959	10.02765
0.9	31.63347	4.92912	3.79959	10.02765

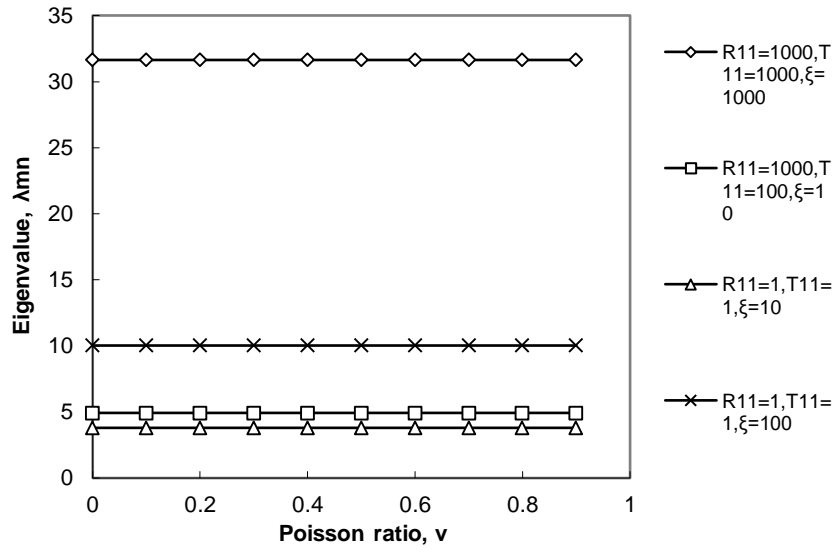


Fig. 6.9 Effect of Poisson ratio on Eigenvalues

Case: 2 Plates with edges elastically restrained against translation and rests on Winkler Foundation

For this case the set of Eqs, used are (6.28) and (6.29). The results are shown in Table 6.7.

The eigenvalues for the plate edge that is elastically restrained against translation and fully resting on the elastic foundation, at various values of the transverse stiffness ratios, are computed and the results are given in Table 6.7. As seen from the Table 6.7, eigenvalues increases with transverse stiffness ratios. The effects of the transverse stiffness ratios are clearly observed from Fig. 6.10. As seen from Fig. 6.10, eigenvalues increases with an increment in the transverse stiffness, and the plates become unstable in the region when the transverse stiffness exceeds a certain value, 100. The simply supported boundary conditions could be accounted for by setting $T_{11} \rightarrow \infty$ and $R_{11} \rightarrow 0$, as shown in Fig. 6.11. The frequency in this case is 2.23175 and this is in good agreement with the results published by C.Y. Wang [13].

Table 6. 7. Eigenvalues for different Translational stiffness ratio for $\xi=100$ & $\nu=0.33$

T_{11}	λ_{00}	λ_{10}	λ_{20}	λ_{01}	λ_{11}	λ_{21}
-3	10	10.0205	10.3517	10.10358	10.79568	12.46774
-2	10	10.02051	10.35171	10.10359	10.79568	12.46775
-1	10.00005	10.02061	10.3518	10.10368	10.79576	12.46779
0	10.00047	10.02162	10.35263	10.10462	10.79649	12.46827
1	10.003	10.03287	10.36125	10.11468	10.804	12.47302
2	10.00568	10.1199	10.46887	10.2319	10.89095	12.52351
3	10.00614	10.203	11.00421	10.49407	11.61576	13.1793
4	10.00619	10.21322	11.14468	10.53794	11.94459	14.15323
5	10.00619	10.21423	11.15725	10.54212	11.97273	14.2438
6	10.00619	10.21433	11.15849	10.54254	11.97546	14.25215
12	10.00619	10.21434	11.15862	10.54258	11.97576	14.25307

continue

02	λ_{12}	λ_{22}	λ_{03}	λ_{13}	λ_{23}
10.29701	11.43857	13.52984	10.63672	12.2505	14.67332
10.29702	11.43857	13.52985	10.63673	12.25051	14.67332
10.29711	11.43864	13.52989	10.63682	12.25056	14.67335
10.29803	11.43927	13.53026	10.63769	12.25109	14.67365
10.30745	11.44568	13.53403	10.64649	12.25645	14.67667
10.42003	11.5759	13.57333	10.74585	12.31326	14.70772
10.91134	12.27823	14.08459	11.41839	12.99719	15.0966
11.03916	12.88272	15.33948	11.70347	13.90786	16.53545
11.05093	12.93527	15.47979	11.72934	13.99516	16.74092
11.05209	12.94027	15.49231	11.73186	14.00329	16.75866
11.05222	12.94082	15.49369	11.73214	14.00418	16.7606

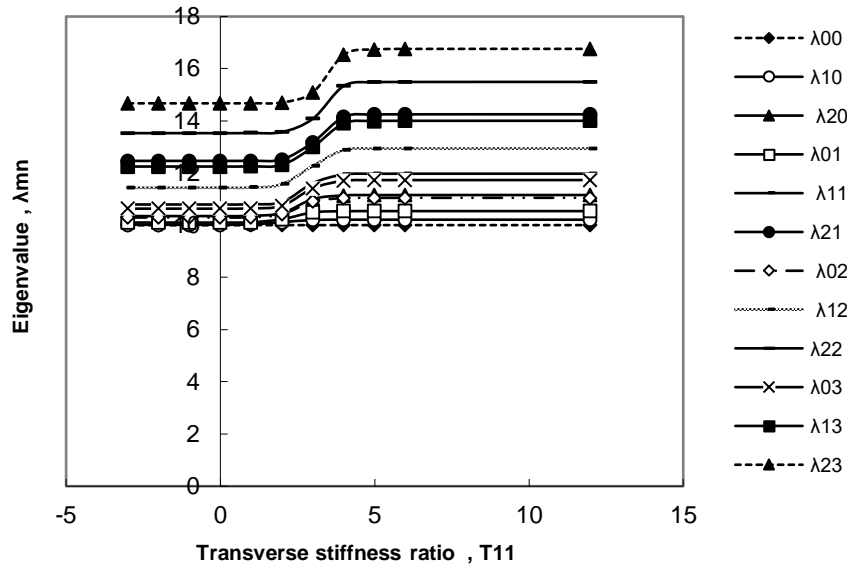


Fig. 6.10. Effect of translational constraint, T_{11} on eigenvalues, λ_{mn}

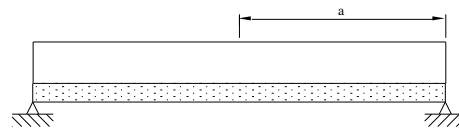


Fig. 6.11. A simply supported thin circular plate resting on full elastic foundation

The eigenvalues for the plate edge that is elastically restrained against translation and fully resting on the elastic foundation, at various values of the foundation stiffness ratios, are computed and the results are given in Table 6.8. As seen from the table 6.8, eigenvalues increases with foundation stiffness ratios. The effects of the foundation stiffness are clearly observed from Fig. 6.12. As seen from Fig. 6.12, eigenvalues increases with an increment in the foundation stiffness, and the plates become unstable in the region when the foundation stiffness exceeds a certain value, 10. As seen from the Table 6.7 and 6.8, the influence of foundation parameter on eigenvalue is more predominant than that of transverse stiffness parameter. As seen from Fig. 6.12, all the curves are stable up to certain region and beyond this all the curves tend to converge as the value of foundation stiffness increases.

Table 6.8. Eigenvalues for different Foundation stiffness ratio for $T_{11}=100$ & $\nu=0.33$

ξ	λ_{00}	λ_{10}	λ_{20}	λ_{01}	λ_{11}	λ_{21}
-3	2.18341	4.70075	6.69703	5.56683	7.98678	10.99197
-2	2.18341	4.70075	6.69703	5.56683	7.98678	10.99197
-1	2.18365	4.70077	6.69704	5.56684	7.98679	10.99197
0	2.20704	4.70315	6.69786	5.56827	7.98727	10.99216
1	3.3284	4.92488	6.77875	5.7064	8.03541	11.01074
2	10.00568	10.1199	10.46887	10.2319	10.89095	12.52351
3	31.62296	31.62664	31.63867	31.63037	31.6549	31.73756

λ_{02}	λ_{12}	λ_{22}	λ_{03}	λ_{13}	λ_{23}
6.50356	9.33292	12.43922	7.59879	10.67534	13.84974
6.50356	9.33292	12.43922	7.59879	10.67534	13.84973
6.50357	9.33292	12.43922	7.59879	10.67535	13.84974
6.50447	9.33323	12.43935	7.59936	10.67555	13.84983
6.5926	9.36352	12.45218	7.65514	10.69583	13.84914
10.42003	11.5159	13.57333	10.74585	12.31326	14.70772
31.63691	31.68259	31.81038	31.6491	31.72496	31.90972

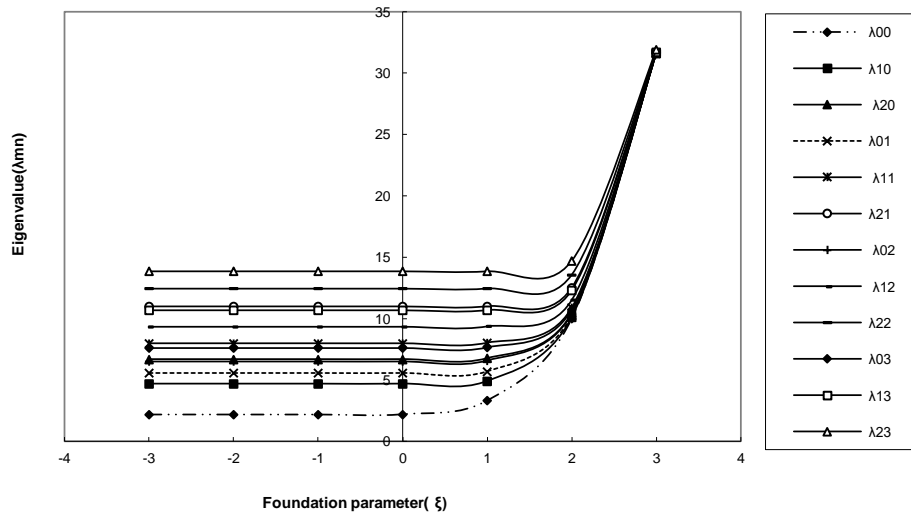


Fig. 6.12. Effect of Foundation constraint, ξ on eigenvalues, λ_{mn}

The eigenvalues for the plate edge that is elastically restrained against translation and fully resting on the elastic foundation, at various values of the transverse stiffness ratios and foundation stiffness ratios, are computed and the results are given in Table 6.9. As seen from

the table 6.9, eigenvalues increases with transverse and foundation stiffness ratios. The effects of the transverse and foundation stiffness ratios are clearly observed from Fig. 6.13. As seen from Fig. 6.13, eigenvalues increases with an increment in both the transverse and foundation stiffness ratios, and the plates become unstable in the region when the transverse and foundation stiffness exceeds a certain value. As observed from the Table 6.7 and 6.9, the influence of foundation parameter on eigenvalue is more predominant than that of transverse stiffness parameter alone. As observed from Table 6.7, 6.8 and 6.9, in Table 6.9, lower eigenvalues are recorded for lower values of foundation and transverse stiffness ratios together. As seen from Fig. 6.13, all the curves are stable up to certain region and beyond this all the curves tend to converge as the value of transverse and foundation stiffness ratios increases.

Table 6.9. Eigenvalues for different Translational and Foundation stiffness ratios for $\nu=0.33$

$\text{Log } T_{11} \text{ \& \& } \text{Log } \xi$	λ_{00}	λ_{10}	λ_{20}	λ_{01}	λ_{11}	λ_{21}
-3	0.2115	3.0115	6.2054	4.52915	7.73687	10.9091
-2	0.37648	3.01187	6.20544	4.52925	7.73689	10.90911
-1	0.67602	3.0156	6.20584	4.53032	7.73709	10.90918
0	1.30374	3.067	6.21074	4.54336	7.73963	10.91008
1	3.25317	3.90325	6.34932	4.87899	7.81237	10.93614
2	10.00568	10.1199	10.46887	10.2319	10.89095	12.52351
3	31.62297	31.62939	31.65958	31.63958	31.68744	31.78104

Continue.

λ_{02}	λ_{12}	λ_{22}	λ_{03}	λ_{13}	λ_{23}
5.93655	9.18564	12.3826	7.27469	10.57846	13.80849
5.93659	9.18566	12.38261	7.27471	10.57846	13.8085
5.93708	9.18578	12.38266	7.27499	10.57855	13.80854
5.94302	9.18733	12.38328	7.27834	10.57959	13.80899
6.10341	9.23131	12.40119	7.36838	10.60869	13.82199
10.42003	11.5152	13.57333	10.74585	12.31326	14.70772
31.65573	31.72292	31.85232	31.67796	31.76831	31.94926

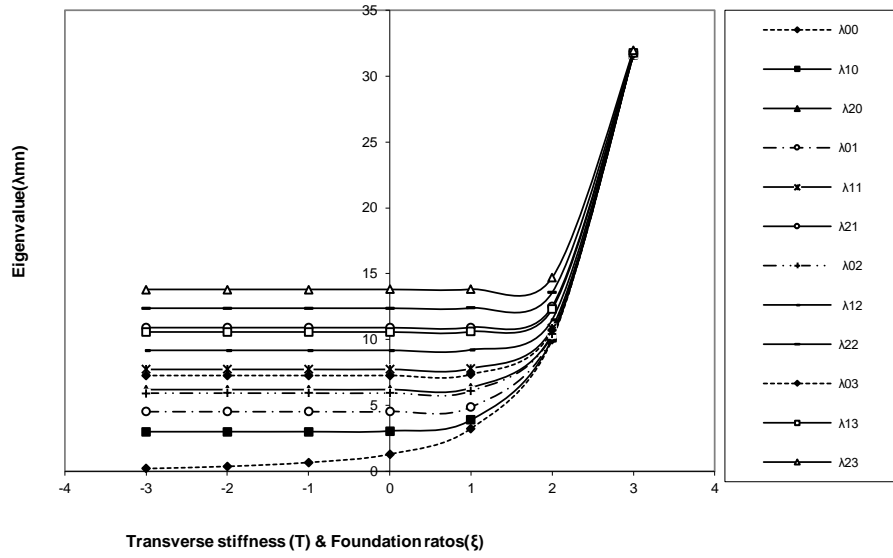


Fig. 6.13. Effect of translational, T_{11} and foundation, ξ constraints on eigenvalues, λ_{mn}

The eigenvalues for different plate materials, for various values of transverse and foundation parameters are computed and the results are given in Table 6.10. It was observed that for high ξ eigenvalues are independent on Poisson ratio, as shown in Fig. 6.14. And also it was observed that for any value of T_{11} , eigenvalues are independent on Poisson ratio.

Table 6.10. Eigenvalues for different Poisson ratios

ν	$T_{11}=1000, \xi=1000$	$T_{11}=100, \xi=10$	$T_{11}=10, \xi=1000$	$T_{11}=1, \xi=10$	$T_{11}=50, \xi=50$
0	31.62925	4.92456	10.03027	3.62553	7.28924
0.1	31.62929	4.92466	10.03111	3.64904	7.2896
0.2	31.62934	4.92476	10.0319	3.6708	7.28993
0.3	31.62938	4.92485	10.03265	3.69097	7.29025
0.4	31.62942	4.92494	10.03336	3.70974	7.29056
0.5	31.62946	4.92503	10.03404	3.72725	7.29085
0.6	31.62951	4.92511	10.03468	3.74361	7.29113
0.7	31.62955	4.92519	10.0353	3.75893	7.29139
0.8	31.62959	4.92527	10.03588	3.77332	7.29165
0.9	31.62962	4.92534	10.03644	3.78685	7.29189
1	31.62966	4.92541	10.03698	3.79959	7.29213

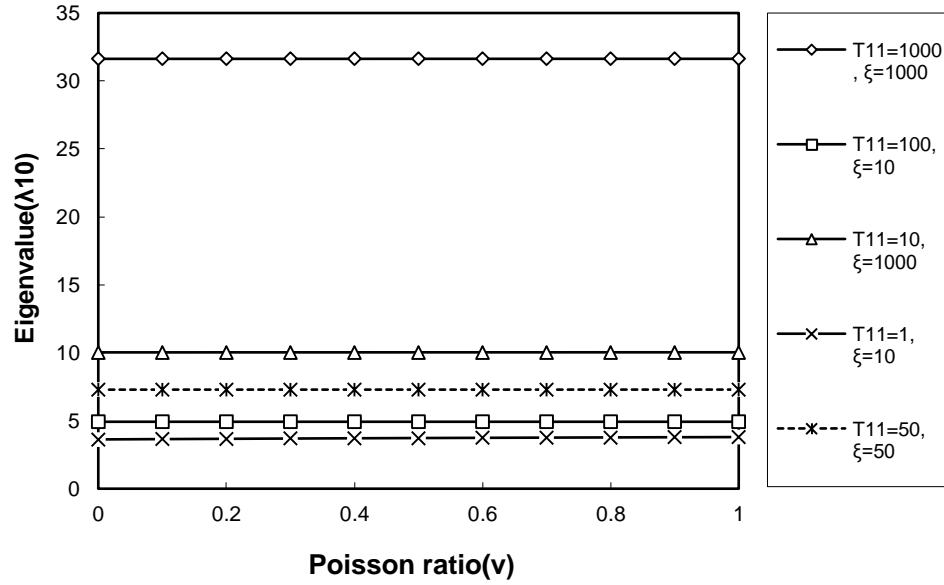


Fig. 6.14. Effect of Poisson ratio, ν on eigenvalues, λ_{mn}

Case: 3 Plates with edges elastically restrained against rotation and rests on Winkler foundation

The set of Eqs for this case are (6.34) and (6.35). The results are shown in Table 6.10. The eigenvalues for the plate edge that is elastically restrained against rotation and fully resting on the elastic foundation, at various values of the rotation stiffness ratios, are computed and the results are given in Table 6.10a. As seen from the Table 6.10a, eigenvalues increases with rotational stiffness ratios. The effects of the rotational stiffness ratios are clearly observed from Fig. 6.15. As seen from Fig. 6.15, eigenvalues increases with an increment in the rotational stiffness, and the plates become unstable in the region when the transverse stiffness exceeds a certain value, 10. The clamped boundary conditions could be accounted for by setting $K_{T1} \rightarrow \infty$ and $K_{R1} \rightarrow \infty$, as shown in Fig. 6.16. The frequency in this case is 3.19622 and this is in good agreement with the results published by C.Y. Wang [13]. The results with full foundation and without foundation are in well agreement with the results published by C.Y. Wang.

Table 6.10a. Eigenvalues for different Rotational stiffness ratio for $\xi=100$ & $\nu=0.33$

$\text{Log } R_{11}$	λ_{00}	λ_{10}	λ_{20}	λ_{01}	λ_{11}	λ_{21}
----------------------	----------------	----------------	----------------	----------------	----------------	----------------

-3	10.0062	10.21436	11.15865	10.04821	10.54261	11.9758
-2	10.00623	10.2145	11.15891	10.04829	10.54281	11.97608
-1	10.00655	10.21592	11.16151	10.04904	10.54486	11.97896
0	10.00926	10.22903	11.18599	10.05575	10.56402	12.00627
1	10.01911	10.29676	11.33578	10.08493	10.67237	12.18251
2	10.025	10.36081	11.52695	10.10703	10.79214	12.43485
3	10.02589	10.37253	11.56812	10.1107	10.81596	12.49334
4	10.02598	10.37379	11.57267	10.11109	10.81856	12.4999
5	10.02599	10.37392	11.57313	10.11113	10.81882	12.50056
6	10.02599	10.37393	11.57318	10.11113	10.81885	12.50063
12	10.02599	10.37393	11.57318	10.11113	10.81885	12.50063

continue

λ_{02}	λ_{12}	λ_{22}	λ_{03}	λ_{13}	λ_{23}
10.16057	11.05225	12.94086	10.37789	11.73217	14.00422
10.1607	11.0525	12.94115	10.37807	11.73246	14.00451
10.16198	11.05504	12.9441	10.37989	11.73529	14.00742
10.17355	11.0789	12.97232	10.39657	11.76206	14.03533
10.22995	11.22227	13.16185	10.48465	11.9305	14.22907
10.2808	11.40131	13.46114	10.57564	12.16352	14.56239
10.29003	11.43967	13.5355	10.59348	12.217	14.65081
10.29103	11.44392	13.54394	10.5943	12.22299	14.66098
10.29113	11.44435	13.5448	10.59563	12.2236	14.66201
10.29114	11.44439	13.54488	10.59565	12.22366	14.66212
10.29114	11.44439	13.54489	10.59565	12.22367	14.66213

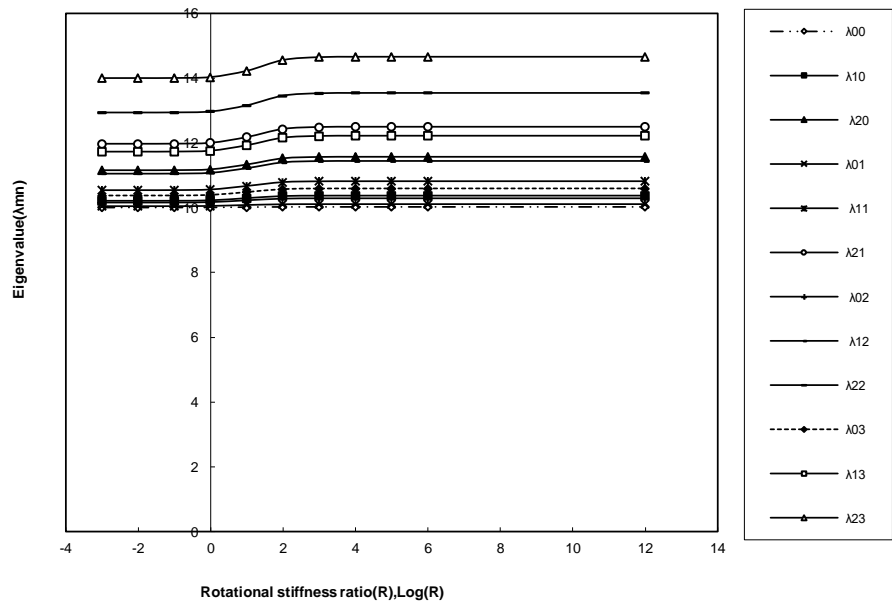


Fig. 6.15. Effect of Rotational constraint, T_{11} on eigenvalues, λ_{mn}

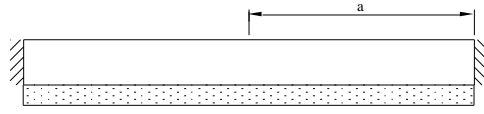


Fig. 6.16. A clamped thin circular plate resting on full elastic foundation

The eigenvalues for various values of the foundation stiffness ratios are computed and the results are given in Table 6.11. As seen from the Table 6.11, eigenvalues increases with foundation stiffness ratios. The effects of the foundation parameter are clearly observed from Fig. 6.17. As seen from Fig. 6.17, eigenvalues increases with an increment in the foundation stiffness, and the plates become unstable in the region when the foundation stiffness exceeds a certain value, 10. As seen from the Table 6.10 and 6.11, the influence of foundation parameter on eigenvalue is more predominant than that of transverse stiffness parameter. As seen from Fig. 6.17, all the curves are stable up to certain region and beyond this all the curves tend to converge as the value of foundation stiffness increases.

Table 6.11. Eigenvalues for different Foundation stiffness ratio for $R_{11}=100$ & $\nu=0.33$

ξ	λ_{00}	λ_{10}	λ_{20}	λ_{01}	λ_{11}	λ_{21}
-3	3.16533	6.24732	9.35364	4.56702	7.72726	10.85986
-2	3.16533	6.24732	9.35364	4.56702	7.72726	10.85986
-1	3.16541	6.24733	9.35364	4.56704	7.72726	10.85986
0	3.17318	6.24835	9.35394	4.56964	7.7278	10.86006
1	3.76242	6.34742	9.38404	4.80946	7.78088	10.87933
2	10.025	10.36081	11.52695	10.10703	10.79214	12.43485
3	31.62357	31.63481	31.68312	31.62622	31.65093	31.73217

continue

λ_{02}	λ_{12}	λ_{22}	λ_{03}	λ_{13}	λ_{23}
5.8503	9.11321	12.29268	7.07752	10.44219	13.67497
5.8503	9.11321	12.29268	7.07752	10.44219	13.67497
5.85032	9.11321	12.29269	7.07752	10.44219	13.67497
5.85155	9.11354	12.29282	7.07822	10.44241	13.67506
5.97135	9.14606	12.30612	7.147	10.46408	13.68473
10.2808	11.40131	13.46114	10.57564	12.16352	14.56239

31.63203	31.67716	31.80177	31.64259	31.71636	31.89569
----------	----------	----------	----------	----------	----------

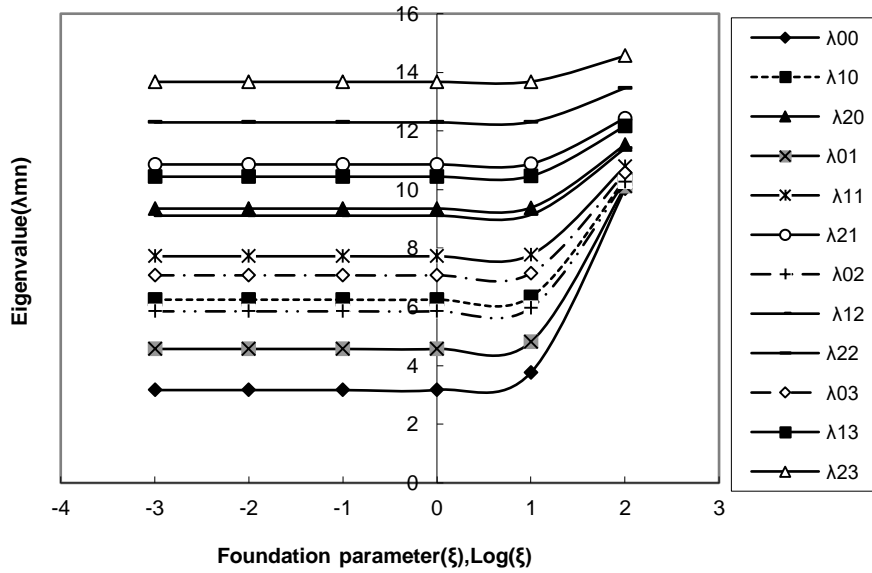


Fig. 6.17. Effect of Foundation constraint, ξ on eigenvalues, λ_{mn}

The eigenvalues for various values of the rotational and foundation stiffness ratios are computed and the results are given in Table 6.12. As seen from the Table 6.12, eigenvalues increases with rotational and foundation stiffness ratios. The effects of the rotational and foundation stiffness ratios are clearly observed from Fig. 6.18. As seen from Fig. 6.18, eigenvalues increases with an increment in both the rotational and foundation stiffness ratios, and the plates become unstable in the region when the rotational and foundation stiffness exceeds a certain value. As observed from the Table 6.10 and 6.12, the influence of foundation parameter on eigenvalue is more predominant than that of rotational stiffness parameter alone. As observed from Table 6.10, 6.11 and 6.12, in Table 6.12, lower eigenvalues are recorded for lower values of foundation and transverse stiffness ratios together. As seen from Fig. 6.18, all the curves are stable up to certain region and beyond

this all the curves tend to converge as the value of rotational and foundation stiffness ratios increases.

Table 6.12. Eigenvalues for different Rotational and Foundation stiffness ratios for $\nu = 0.33$

$\text{Log } R_{11} \text{ \& Log } \xi$	λ_{00}	λ_{10}	λ_{20}	λ_{01}	λ_{11}	λ_{21}
-3	2.23169	5.45487	8.61335	3.73321	6.96516	10.13936
-2	2.2346	5.45581	8.61392	3.7347	6.96587	10.13984
-1	2.26282	5.46515	8.61955	3.7494	6.97299	10.14457
0	2.48403	5.55041	8.67278	3.87679	7.0392	10.18964
1	3.64568	6.05133	9.01752	4.59051	7.44549	10.49385
2	10.025	10.36081	11.52695	10.10703	10.79214	12.43485
3	31.6236	31.63522	31.68511	31.62634	31.65187	31.73571

Continue

λ_{02}	λ_{12}	λ_{22}	λ_{03}	λ_{13}	λ_{23}
5.06457	8.37562	11.59012	6.32398	9.72535	12.98875
5.06561	8.3762	11.59053	6.32479	9.72585	12.98912
5.0759	8.38203	11.59464	6.3238	9.73082	12.99276
5.16829	8.43683	11.63398	6.40615	9.77787	13.02782
5.69517	8.78667	11.90841	6.83628	10.08876	13.27898
10.2808	11.40131	13.46114	10.57564	12.16352	14.56239
31.63235	31.67896	31.80746	31.64326	31.71939	31.90418

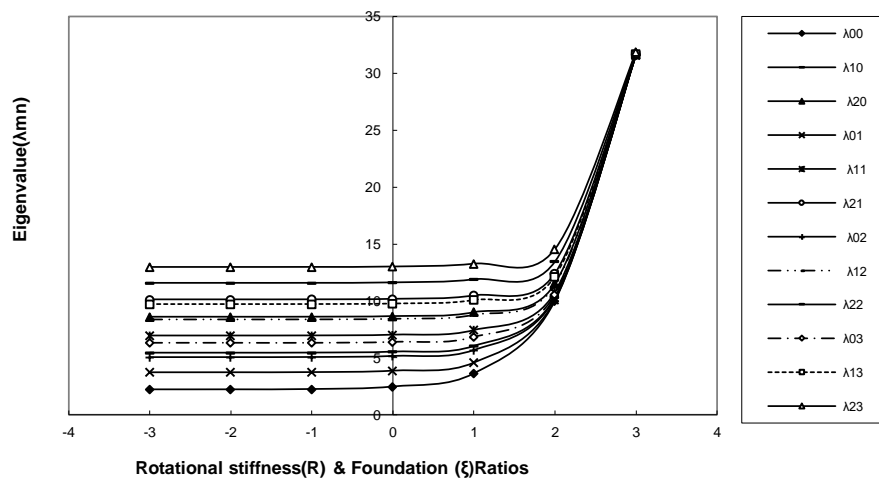


Fig. 6.18. Effect of Rotational, R and foundation, ξ constraints on eigenvalues, λ_{mn}

The eigenvalues for different plate materials, for various values have rotational and foundation parameters are computed and the results are given in Table 6.13. It was observed

that for high ξ eigenvalues are independent on Poisson ratio, as shown in Fig. 6.19. And also it was observed that for small values of T_{11} , eigenvalues are dependent on Poisson ratio.

Table 6.13. Eigenvalues for different Poisson ratios

ν	$R_{11}=1000,$ $\xi=1000$	$R_{11}=100,$ $\xi=10$	$R_{11}=1,$ $\xi=10$	$R_{11}=1, \xi$ $=100$	$R_{11}=50,$ $\xi=50$
0	31.63522	6.34725	5.66306	10.22445	7.93901
0.1	31.63522	6.3473	5.67136	10.22587	7.93911
0.2	31.63522	6.34735	5.67949	10.22726	7.9392
0.3	31.63522	6.3474	5.68746	10.22862	7.93929
0.4	31.63522	6.34746	5.69526	10.22997	7.93939
0.5	31.63522	6.34751	5.70292	10.23129	7.93948
0.6	31.63522	6.34756	5.71041	10.23259	7.93957
0.7	31.63522	6.34761	5.71776	10.23387	7.93966
0.8	31.63522	6.34767	5.72497	10.23513	7.93975
0.9	31.63522	6.34772	5.73204	10.23637	7.93984
1	31.63522	6.34777	5.73897	10.23759	7.93994

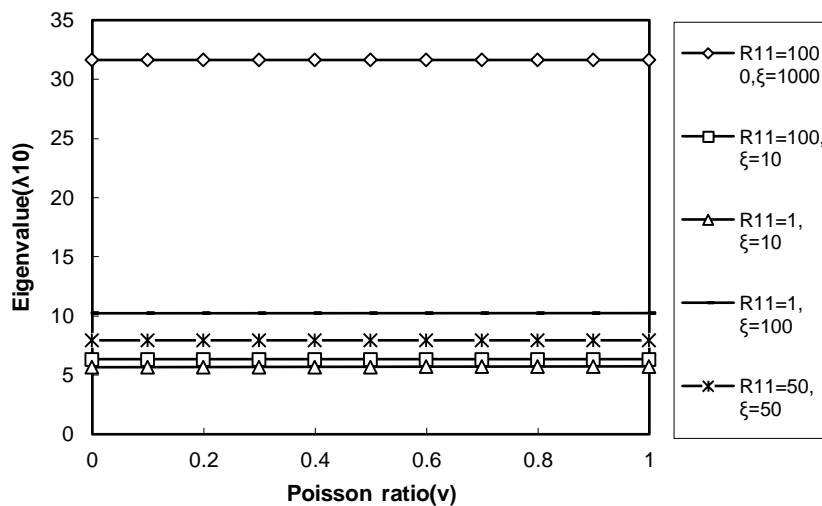


Fig. 6.19. Effect of Poisson ratio, ν on eigenvalues, λ_{mn}

Case: 4 Guided edge plate with Winkler foundation

The set of Eqs. for this case are (6.40) and (6.41). The eigenvalues for various values of the foundation stiffness ratios are computed and the results are given in Table 6.14. As seen from the Table 6.14, eigenvalues increases with foundation stiffness ratios. The effects of the foundation parameter are clearly observed from Fig. 6.20. As seen from Fig. 6.20, eigenvalues increases with an increment in the foundation stiffness, and the plates become

unstable in the region when the foundation stiffness exceeds a certain value. In guided edge plate lower eigenvalues are recorded for lower values of foundation as compare to the plate elastically restrained against translation and rotation. As seen from Fig.6.20, all the curves are stable up to certain region and beyond this all the curves tend to converge as the value of foundation stiffness increases. It is observed that the influence of foundation parameter on eigenvalues is more predominant than that of transverse stiffness parameter. The frequency in this case is 1.75563 and this is in good agreement with the results published by C.Y. Wang [13].

Table 6.14. Eigenvalues for different Foundation stiffness ratio for $\nu=0.33$

Log ξ	λ_{00}	λ_{10}	λ_{20}	λ_{01}	λ_{11}	λ_{21}
-3	0.03162	3.83171	7.01559	5.32915	8.53577	11.70579
-2	0.1	3.83171	7.01559	5.32915	8.53577	11.70579
-1	0.31623	3.83175	7.01559	5.32917	8.53577	11.7058
0	1	3.83614	7.01631	5.33081	8.53617	11.70595
1	3.16228	4.21474	7.08689	5.48717	8.57569	11.72135
2	10	10.05346	10.55728	10.19581	11.12329	13.0244
3	31.62278	31.62448	31.64191	31.62915	31.66466	31.77018

continue

λ_{02}	λ_{12}	λ_{22}	λ_{03}	λ_{13}	λ_{23}
6.70127	9.96806	13.16977	8.00845	11.34371	14.58483
6.70127	9.96806	13.16977	8.00845	11.34371	14.58483
6.70128	9.96806	13.16977	8.00846	11.34371	14.58484
6.7021	9.96831	13.16988	8.00894	11.34388	14.58492
6.78284	9.99321	13.1807	8.05669	11.3608	14.59289
10.46998	11.87313	14.14942	10.89952	12.76588	15.33135
31.63871	31.70054	31.85796	31.65525	31.75288	31.97458

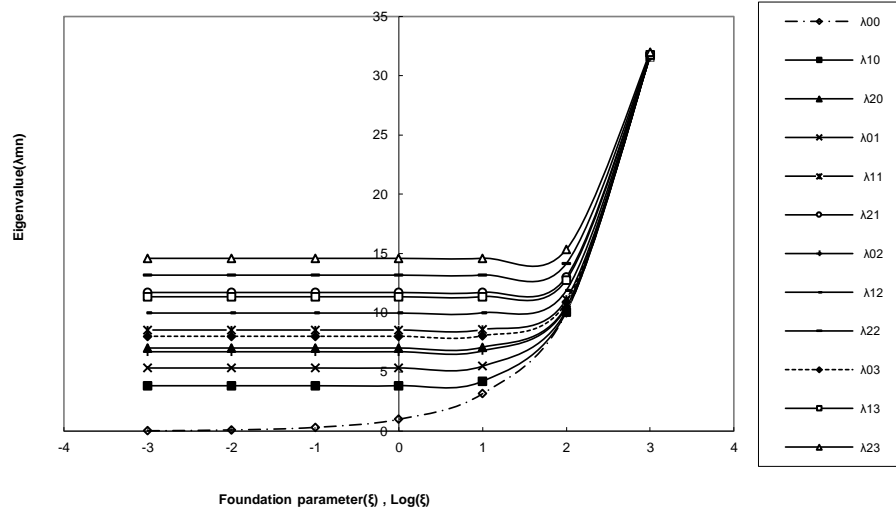


Fig. 6.20. Effect of Foundation constraint, ξ on eigenvalues, λ_{mn}

The eigenvalues for different plate materials, for various values of foundation parameters are computed and the results are given in Table 6.15. It is observed that for any value of foundation parameter (ξ), eigenvalues are independent on Poisson ratio, as presented in Fig. 6.21.

Table 6.15. Eigenvalues for different Poisson ratios

ν	$\xi=1$	$\xi=50$	$\xi=100$	$\xi=1000$	$\xi=1e+04$	$\xi=1e+05$
0	3.83614	7.2188	10.053	31.62448	100.0001	316.22777
0.1	3.83614	7.2188	10.053	31.62448	100.0001	316.22777
0.2	3.83614	7.2188	10.053	31.62448	100.0001	316.22777
0.3	3.83614	7.2188	10.053	31.62448	100.0001	316.22777
0.4	3.83614	7.2188	10.053	31.62448	100.0001	316.22777
0.5	3.83614	7.2188	10.053	31.62448	100.0001	316.22777
0.6	3.83614	7.2188	10.053	31.62448	100.0001	316.22777
0.7	3.83614	7.2188	10.053	31.62448	100.0001	316.22777
0.8	3.83614	7.2188	10.053	31.62448	100.0001	316.22777
0.9	3.83614	7.2188	10.053	31.62448	100.0001	316.22777
1	3.83614	7.2188	10.053	31.62448	100.0001	316.22777

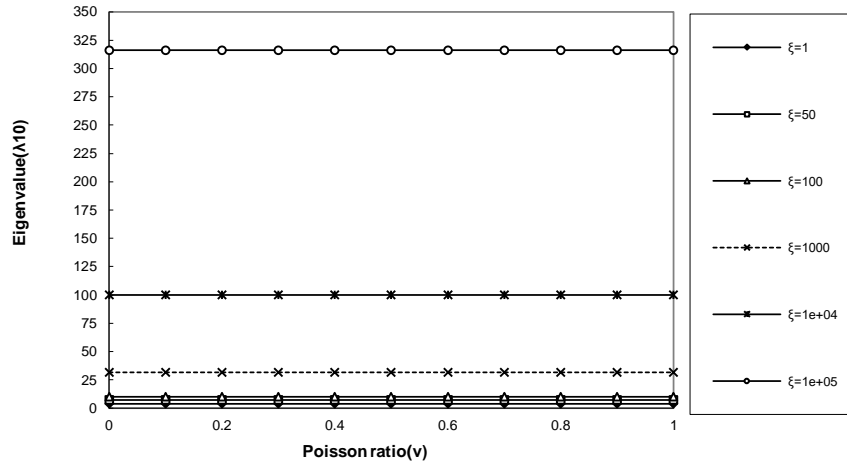


Fig. 6.21. Effect of Poisson ratio, ν on eigenvalues, λ_{mn}

It has been observed that eigenvalues changes desperately only in a limited range of constraints specific to each vibration mode and are stable elsewhere. By knowing the position of the region where eigenvalues change rigorously is rudiment for structural design in the field of aerospace, marine, mechanical and civil engineering applications and vibration control. It is observed that the influence of foundation parameter on eigenvalues is more predominant than that of translational parameter and rotational parameter.

CHAPTER 7

FREQUENCY ANALYSIS OF ANNULAR PLATES WITH ELASTICALLY RESTRAINED INNER AND OUTER EDGES AND RESTING ON ELASTIC FOUNDATION

7.1 Theoretical Background

Kim and Dickinson [87] have studied lateral vibration of thin annular plate subject to certain complicating effects. Kim and Dickinson [66] have also studied the flexural vibration of isotropic annular and circular plates with elastically restrained peripheries, using Rayleigh – Ritz method. Wang et al [88], Larrando et al [89] have studied free vibration of annular plates by differential quadrature method. It is accepted fact that the condition on a periphery often tends to be part way between the classical boundary conditions (free, clamped, simply supported) and may correspond more closely to some form of elastic restraints. The work presented here, are the results of investigation of vibrations of annular plate considering both the peripheries are elastically restrained against rotation and translation and also resting on elastic foundation.

7.2 Problem Definition

Consider a thin annular plate of radius R , uniform thickness h , Young's modulus E , density ρ , flexural rigidity D and Poisson's ratio ν , as shown in Fig. 7.1. The plate is also assumed to be made of linearly elastic, homogeneous and isotropic material. Moreover, the effects of shear deformation and rotary inertia are neglected. The edge of the annular plate is elastically restrained against rotation and translation at inner and outer periphery. The annular plate is supported by an elastic foundation as shown in Fig. 7.1. The present study is to determine the frequency of annular plate when both the peripheries are elastically restrained against rotation and translation and it is resting on elastic foundation.

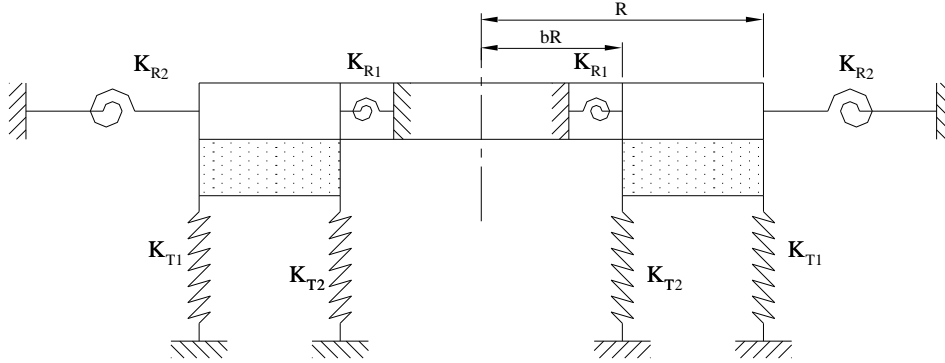


Fig. 7.1. Annular plate with Rotational and Translational Constraints at inner and outer edge and resting on elastic foundation

7.3 Derivation of Transverse Vibrations of Elastically Restrained edges

Consider an annular plate of outer radius, R and inner radius bR as shown in Fig. 7.1. The annular plate is supported by an elastic foundation. Let subscript I denote the annular portion $0 \leq \bar{r} \leq b$ and the subscript II denote the outer region $b \leq \bar{r} \leq 1$. Here, all lengths are normalized by R . In the classical plate theory, the following fourth order differential equation describes free flexural vibrations of an annular plate

$$D\nabla^4 w + \rho h \frac{\partial^2 w}{\partial t^2} = 0 \quad (7.1)$$

$$\text{Where } \nabla^2 = \frac{\partial^2}{\partial \bar{r}^2} + \frac{1}{\bar{r}} \frac{\partial}{\partial \bar{r}} + \frac{1}{\bar{r}^2} \frac{\partial^2}{\partial \theta^2} \quad (7.2)$$

Is the Laplace operator in the polar coordinates r and θ . The first studied of equation (7.1) were those of Poisson [16] and Kirchhoff [57] and the classical methods of finding the solutions of this equation is base on the separation of variables. After considering the foundation parameter the equation (7.1) becomes

$$D\nabla^4 w + \xi_1 w + \rho h \frac{\partial^2 w}{\partial t^2} = 0 \quad (7.3)$$

Where \bar{r} is the radial distance normalized by R . $D = Eh^3 / 12(1-\nu^2)$ is the flexural rigidity, $\bar{w} = w/R$, is normalized transverse displacement of the plate. $\xi_1 = R^4 k_w / D$ is non-dimensional foundation parameter. The general solution to the classical plate vibration equations in polar coordinates can be expressed as

$$\bar{w} = u(\bar{r}) \cos(n\theta) e^{i\omega t} \quad (7.4)$$

Where n is the number of nodal diameters, ω is the frequency. The function u is a linear combination of the Bessel functions $J_n(\bar{k}_1 \bar{r})$, $Y_n(\bar{k}_1 \bar{r})$, $I_n(\bar{k}_1 \bar{r})$ & $K_n(\bar{k}_1 \bar{r})$ and $\bar{k}_1 = R(\rho\omega^2 / D)^{1/4}$, is the square root of the non-dimensional frequency [17]. The annular plate of normalized radius at outer edge is 1 and the normalized radius at inner edge is b . There are two plate regions. The general solutions for the outer region are given by the following equation.

$$\bar{w}_I(\bar{r}, \theta) = [C_1 J_n(\bar{k}_1 \bar{r}) + C_2 Y_n(\bar{k}_1 \bar{r}) + C_3 I_n(\bar{k}_1 \bar{r}) + C_4 K_n(\bar{k}_1 \bar{r})] \cos(n\theta) \quad (7.5)$$

The boundary conditions at outer edges of the annular plate in terms of rotational stiffness (K_{R1}) and translational stiffness (K_{T1}) is given by the following expressions

$$M_r(\bar{r}, \theta) = K_{R1} \frac{\partial \bar{w}_I(\bar{r}, \theta)}{\partial \bar{r}} \quad (7.6)$$

$$V_r(\bar{r}, \theta) = -K_{T1} \bar{w}_I(\bar{r}, \theta) \quad (7.7)$$

The radial moment and the radial Kirchhoff shear at outer edge are defined as follows

$$M_r(\bar{r}, \theta) = -\frac{D}{R^3} \left[\frac{\partial^2 \bar{w}_I(\bar{r}, \theta)}{\partial \bar{r}^2} + \nu \left(\frac{1}{\bar{r}} \frac{\partial \bar{w}_I(\bar{r}, \theta)}{\partial \bar{r}} + \frac{1}{\bar{r}^2} \frac{\partial^2 \bar{w}_I(\bar{r}, \theta)}{\partial \theta^2} \right) \right] \quad (7.8)$$

$$V_r(\bar{r}, \theta) = -\frac{D}{R^3} \left[\frac{\partial}{\partial \bar{r}} \nabla^2 \bar{w}_I(\bar{r}, \theta) + (1-\nu) \frac{1}{\bar{r}} \frac{\partial}{\partial \theta} \left(\frac{1}{\bar{r}} \frac{\partial^2 \bar{w}_I(\bar{r}, \theta)}{\partial \bar{r} \partial \theta} - \frac{1}{\bar{r}^2} \frac{\partial \bar{w}_I(\bar{r}, \theta)}{\partial \theta} \right) \right] \quad (7.9)$$

From equations (7.6) and (7.8) yields the following

$$\left[\frac{\partial^2 \bar{w}_I(\bar{r}, \theta)}{\partial \bar{r}^2} + \nu \left(\frac{1}{\bar{r}} \frac{\partial \bar{w}_I(\bar{r}, \theta)}{\partial \bar{r}} + \frac{1}{\bar{r}^2} \frac{\partial^2 \bar{w}_I(\bar{r}, \theta)}{\partial \theta^2} \right) \right] = -\frac{K_{R1} R^2}{D} \frac{\partial^2 \bar{w}_I(\bar{r}, \theta)}{\partial \bar{r}^2} \quad (7.10)$$

$$\left[\frac{\partial^2 \bar{w}_I(\bar{r}, \theta)}{\partial \bar{r}^2} + \nu \left(\frac{1}{\bar{r}} \frac{\partial \bar{w}_I(\bar{r}, \theta)}{\partial \bar{r}} + \frac{1}{\bar{r}^2} \frac{\partial^2 \bar{w}_I(\bar{r}, \theta)}{\partial \theta^2} \right) \right] = -R_{11} \frac{\partial^2 \bar{w}_I(\bar{r}, \theta)}{\partial \bar{r}^2} \quad (7.11)$$

$$\text{where } R_{11} = \frac{K_{R1} R^2}{D} \quad (7.12)$$

From equations (7.7) and (7.9) yields the following

$$\left[\frac{\partial}{\partial \bar{r}} \nabla^2 \bar{w}_I(\bar{r}, \theta) + (1-\nu) \frac{1}{\bar{r}} \frac{\partial}{\partial \theta} \left(\frac{1}{\bar{r}} \frac{\partial^2 \bar{w}_I(\bar{r}, \theta)}{\partial \bar{r} \partial \theta} - \frac{1}{\bar{r}^2} \frac{\partial \bar{w}_I(\bar{r}, \theta)}{\partial \theta} \right) \right] = \frac{K_{T1} R^3}{D} \bar{w}_I(\bar{r}, \theta) \quad (7.13)$$

$$\left[\frac{\partial}{\partial \bar{r}} \nabla^2 \bar{w}_I(\bar{r}, \theta) + (1-\nu) \frac{1}{\bar{r}} \frac{\partial}{\partial \theta} \left(\frac{1}{\bar{r}} \frac{\partial^2 \bar{w}_I(\bar{r}, \theta)}{\partial \bar{r} \partial \theta} - \frac{1}{\bar{r}^2} \frac{\partial \bar{w}_I(\bar{r}, \theta)}{\partial \theta} \right) \right] = T_{11} \bar{w}_I(\bar{r}, \theta) \quad (7.14)$$

$$\text{where } T_{11} = \frac{K_{T1} R^3}{D} \quad (7.15)$$

Similarly, the boundary conditions at inner edge of the annular plate in terms of rotational stiffness (K_{R2}) and translational stiffness (K_{T2}) are given by the following expressions.

$$M_r(\bar{r}, \theta) = -K_{R2} \frac{\partial \bar{w}_I(\bar{r}, \theta)}{\partial \bar{r}} \quad (7.16)$$

$$V_r(\bar{r}, \theta) = K_{T2} \bar{w}_I(\bar{r}, \theta) \quad (7.17)$$

The radial moment and the radial Kirchhoff shear at inner edge are defined as follows

$$M_r(\bar{r}, \theta) = -\frac{D}{R^3} \left[\frac{\partial^2 \bar{w}_I(\bar{r}, \theta)}{\partial \bar{r}^2} + \nu \left(\frac{1}{\bar{r}} \frac{\partial \bar{w}_I(\bar{r}, \theta)}{\partial \bar{r}} + \frac{1}{\bar{r}^2} \frac{\partial^2 \bar{w}_I(\bar{r}, \theta)}{\partial \theta^2} \right) \right] \quad (7.18)$$

$$V_r(\bar{r}, \theta) = -\frac{D}{R^3} \left[\frac{\partial}{\partial \bar{r}} \nabla^2 \bar{w}_I(\bar{r}, \theta) + (1-\nu) \frac{1}{\bar{r}} \frac{\partial}{\partial \theta} \left(\frac{1}{\bar{r}} \frac{\partial^2 \bar{w}_I(\bar{r}, \theta)}{\partial \bar{r} \partial \theta} - \frac{1}{\bar{r}^2} \frac{\partial \bar{w}_I(\bar{r}, \theta)}{\partial \theta} \right) \right] \quad (7.19)$$

From equations (7.16) and (7.18) yields the following

$$\left[\frac{\partial^2 \bar{w}_I(\bar{r}, \theta)}{\partial \bar{r}^2} + \nu \left(\frac{1}{\bar{r}} \frac{\partial \bar{w}_I(\bar{r}, \theta)}{\partial \bar{r}} + \frac{1}{\bar{r}^2} \frac{\partial^2 \bar{w}_I(\bar{r}, \theta)}{\partial \theta^2} \right) \right] = \frac{K_{R2} R^2}{D} \frac{\partial^2 \bar{w}_I(\bar{r}, \theta)}{\partial \bar{r}^2} \quad (7.20)$$

$$\left[\frac{\partial^2 \bar{w}_I(\bar{r}, \theta)}{\partial \bar{r}^2} + \nu \left(\frac{1}{\bar{r}} \frac{\partial \bar{w}_I(\bar{r}, \theta)}{\partial \bar{r}} + \frac{1}{\bar{r}^2} \frac{\partial^2 \bar{w}_I(\bar{r}, \theta)}{\partial \theta^2} \right) \right] = R_{22} \frac{\partial^2 \bar{w}_I(\bar{r}, \theta)}{\partial \bar{r}^2} \quad (7.21)$$

$$\text{where } R_{22} = \frac{K_{R2} R^2}{D} \quad (7.22)$$

From equations (7.17) and (7.19) yields the following

$$\left[\frac{\partial}{\partial \bar{r}} \nabla^2 \bar{w}_I(\bar{r}, \theta) + (1-\nu) \frac{1}{\bar{r}} \frac{\partial}{\partial \theta} \left(\frac{1}{\bar{r}} \frac{\partial^2 \bar{w}_I(\bar{r}, \theta)}{\partial \bar{r} \partial \theta} - \frac{1}{\bar{r}^2} \frac{\partial \bar{w}_I(\bar{r}, \theta)}{\partial \theta} \right) \right] = -\frac{K_{T2} R^3}{D} \bar{w}_I(\bar{r}, \theta) \quad (7.23)$$

$$\left[\frac{\partial}{\partial \bar{r}} \nabla^2 \bar{w}_I(\bar{r}, \theta) + (1-\nu) \frac{1}{\bar{r}} \frac{\partial}{\partial \theta} \left(\frac{1}{\bar{r}} \frac{\partial^2 \bar{w}_I(\bar{r}, \theta)}{\partial \bar{r} \partial \theta} - \frac{1}{\bar{r}^2} \frac{\partial \bar{w}_I(\bar{r}, \theta)}{\partial \theta} \right) \right] = -T_{22} \bar{w}_I(\bar{r}, \theta) \quad (7.24)$$

$$\text{where } T_{22} = \frac{K_{T2} R^3}{D} \quad (7.25)$$

Case: (i) Plate *outer edges* are elastically restrained against rotation and translation

Boundary conditions when the outer edges are elastically restrained against rotation.

From equations (7.5) and (7.11) yields the following

$$\frac{\partial \bar{w}(\bar{r}, \theta)}{\partial \bar{r}} = \left[\frac{\bar{k}_1}{2} [J_{n-1}(\bar{k}_1 \bar{r}) - J_{n+1}(\bar{k}_1 \bar{r})] C_1 + \frac{\bar{k}_1}{2} [Y_{n-1}(\bar{k}_1 \bar{r}) - Y_{n+1}(\bar{k}_1 \bar{r})] C_2 + \right. \\ \left. \frac{\bar{k}_1}{2} [I_{n-1}(\bar{k}_1 \bar{r}) + I_{n+1}(\bar{k}_1 \bar{r})] C_3 - \frac{\bar{k}_1}{2} [K_{n-1}(\bar{k}_1 \bar{r}) + K_{n+1}(\bar{k}_1 \bar{r})] C_4 \right] \cos(n\theta) \quad (7.26)$$

$$\frac{\partial \bar{w}(\bar{r}, \theta)}{\partial \bar{r}} \Big|_{\bar{r}=1} = \left[\frac{\bar{k}_1}{2} [J_{n-1}(\bar{k}_1) - J_{n+1}(\bar{k}_1)] C_1 + \frac{\bar{k}_1}{2} [Y_{n-1}(\bar{k}_1) - Y_{n+1}(\bar{k}_1)] C_2 + \right. \\ \left. \frac{\bar{k}_1}{2} [I_{n-1}(\bar{k}_1) + I_{n+1}(\bar{k}_1)] C_3 - \frac{\bar{k}_1}{2} [K_{n-1}(\bar{k}_1) + K_{n+1}(\bar{k}_1)] C_4 \right] \cos(n\theta) \quad (7.27)$$

$$\frac{\partial \bar{w}(\bar{r}, \theta)}{\partial \bar{r}} \Big|_{\bar{r}=1} = \left[\frac{\bar{k}_1}{2} [T_1] C_1 + \frac{\bar{k}_1}{2} [U_1] C_2 + \frac{\bar{k}_1}{2} [V_1] C_3 - \frac{\bar{k}_1}{2} [W_1] C_4 \right] \cos(n\theta) \quad (7.28)$$

where $T_1 = J_{n-1}(\bar{k}_1) - J_{n+1}(\bar{k}_1)$; $U_1 = Y_{n-1}(\bar{k}_1) - Y_{n+1}(\bar{k}_1)$;

$V_1 = I_{n-1}(\bar{k}_1) + I_{n+1}(\bar{k}_1)$; $W_1 = K_{n-1}(\bar{k}_1) + K_{n+1}(\bar{k}_1)$;

$$\frac{\partial^2 \bar{w}(\bar{r}, \theta)}{\partial \bar{r}^2} = \left[\frac{\bar{k}_1^2}{4} [(J_{n-2}(\bar{k}_1 \bar{r}) - J_n(\bar{k}_1 \bar{r})) - (J_n(\bar{k}_1 \bar{r}) - J_{n+2}(\bar{k}_1 \bar{r}))] C_1 + \right. \\ \frac{\bar{k}_1^2}{4} [(Y_{n-2}(\bar{k}_1 \bar{r}) - Y_n(\bar{k}_1 \bar{r})) - (Y_n(\bar{k}_1 \bar{r}) - Y_{n+2}(\bar{k}_1 \bar{r}))] C_2 \\ + \frac{\bar{k}_1^2}{4} [(I_{n-2}(\bar{k}_1 \bar{r}) + I_n(\bar{k}_1 \bar{r})) + (I_n(\bar{k}_1 \bar{r}) + I_{n+2}(\bar{k}_1 \bar{r}))] C_3 + \\ \left. \frac{\bar{k}_1^2}{4} [(K_{n-2}(\bar{k}_1 \bar{r}) + K_n(\bar{k}_1 \bar{r})) + (K_n(\bar{k}_1 \bar{r}) + K_{n+2}(\bar{k}_1 \bar{r}))] C_4 \right] \cos(n\theta) \quad (7.29)$$

$$\frac{\partial^2 \bar{w}(\bar{r}, \theta)}{\partial \bar{r}^2} = \left[\begin{aligned} & \frac{\bar{k}_1^2}{4} [(J_{n-2}(\bar{k}_1 \bar{r}) + J_{n+2}(\bar{k}_1 \bar{r})) - 2J_n(\bar{k}_1 \bar{r})] C_1 + \\ & \frac{\bar{k}_1^2}{4} [(Y_{n-2}(\bar{k}_1 \bar{r}) + Y_{n+2}(\bar{k}_1 \bar{r})) - 2Y_n(\bar{k}_1 \bar{r})] C_2 + \\ & \frac{\bar{k}_1^2}{4} [(I_{n-2}(\bar{k}_1 \bar{r}) + I_{n+2}(\bar{k}_1 \bar{r})) + 2I_n(\bar{k}_1 \bar{r})] C_3 + \\ & \frac{\bar{k}_1^2}{4} [(K_{n-2}(\bar{k}_1 \bar{r}) + K_{n+2}(\bar{k}_1 \bar{r})) + 2K_n(\bar{k}_1 \bar{r})] C_4 \end{aligned} \right] \cos(n\theta) \quad (7.30)$$

$$\frac{\partial^2 \bar{w}(\bar{r}, \theta)}{\partial \bar{r}^2} \Big|_{\bar{r}=1} = \left[\begin{aligned} & \frac{\bar{k}_1^2}{4} [(J_{n-2}(\bar{k}_1) + J_{n+2}(\bar{k}_1)) - 2J_n(\bar{k}_1)] C_1 + \\ & \frac{\bar{k}_1^2}{4} [(Y_{n-2}(\bar{k}_1) + Y_{n+2}(\bar{k}_1)) - 2Y_n(\bar{k}_1)] C_2 + \\ & \frac{\bar{k}_1^2}{4} [(I_{n-2}(\bar{k}_1) + I_{n+2}(\bar{k}_1)) + 2I_n(\bar{k}_1)] C_3 + \\ & \frac{\bar{k}_1^2}{4} [(K_{n-2}(\bar{k}_1) + K_{n+2}(\bar{k}_1)) + 2K_n(\bar{k}_1)] C_4 \end{aligned} \right] \cos(n\theta) \quad (7.31)$$

$$\frac{\partial^2 \bar{w}(\bar{r}, \theta)}{\partial \bar{r}^2} \Big|_{\bar{r}=b} = \left[\begin{aligned} & \frac{\bar{k}_1^2}{4} [T_2 - 2J_n(\bar{k}_1)] C_1 + \frac{\bar{k}_1^2}{4} [U_2 - 2Y_n(\bar{k}_1)] C_2 + \\ & \frac{\bar{k}_1^2}{4} [V_2 + 2I_n(\bar{k}_1)] C_3 + \frac{\bar{k}_1^2}{4} [W_2 + 2K_n(\bar{k}_1)] C_4 \end{aligned} \right] \cos(n\theta) \quad (7.32)$$

where $T_2 = J_{n-2}(\bar{k}_1) + J_{n+2}(\bar{k}_1)$; $U_2 = Y_{n-2}(\bar{k}_1) + Y_{n+2}(\bar{k}_1)$;

$$V_2 = I_{n-2}(\bar{k}_1) + I_{n+2}(\bar{k}_1); W_2 = K_{n-2}(\bar{k}_1) + K_{n+2}(\bar{k}_1);$$

$$\frac{1}{\bar{r}} \frac{\partial \bar{w}(\bar{r}, \theta)}{\partial \bar{r}} = \frac{1}{\bar{r}} \left[\begin{aligned} & \frac{\bar{k}_1}{2} [J_{n-1}(\bar{k}_1 \bar{r}) - J_{n+1}(\bar{k}_1 \bar{r})] C_1 + \frac{\bar{k}_1}{2} [Y_{n-1}(\bar{k}_1 \bar{r}) - Y_{n+1}(\bar{k}_1 \bar{r})] C_2 + \\ & \frac{\bar{k}_1}{2} [I_{n-1}(\bar{k}_1 \bar{r}) + I_{n+1}(\bar{k}_1 \bar{r})] C_3 - \frac{\bar{k}_1}{2} [K_{n-1}(\bar{k}_1 \bar{r}) + K_{n+1}(\bar{k}_1 \bar{r})] C_4 \end{aligned} \right] \cos(n\theta) \quad (7.33)$$

$$\frac{1}{\bar{r}} \frac{\partial \bar{w}(\bar{r}, \theta)}{\partial \bar{r}} \Big|_{\bar{r}=1} = \left[\begin{aligned} & \frac{\bar{k}_1}{2} [J_{n-1}(\bar{k}_1) - J_{n+1}(\bar{k}_1)] C_1 + \frac{\bar{k}_1}{2} [Y_{n-1}(\bar{k}_1) - Y_{n+1}(\bar{k}_1)] C_2 + \\ & \frac{\bar{k}_1}{2} [I_{n-1}(\bar{k}_1) + I_{n+1}(\bar{k}_1)] C_3 - \frac{\bar{k}_1}{2} [K_{n-1}(\bar{k}_1) + K_{n+1}(\bar{k}_1)] C_4 \end{aligned} \right] \cos(n\theta) \quad (7.34)$$

$$\frac{1}{\bar{r}} \frac{\partial \bar{w}(\bar{r}, \theta)}{\partial \bar{r}} \Big|_{\bar{r}=1} = \left[\frac{\bar{k}_1}{2} [T_1] C_1 + \frac{\bar{k}_1}{2} [U_1] C_2 + \frac{\bar{k}_1}{2} [V_1] C_3 - \frac{\bar{k}_1}{2} [W_1] C_4 \right] \cos(n\theta) \quad (7.35)$$

$$\frac{\partial \bar{w}(\bar{r}, \theta)}{\partial \theta} = -n [C_1 J_n(\bar{k}_1 \bar{r}) + C_2 Y_n(\bar{k}_1 \bar{r}) + C_3 I_n(\bar{k}_1 \bar{r}) + C_4 K_n(\bar{k}_1 \bar{r})] \sin(n\theta) \quad (7.36)$$

$$\frac{\partial^2 \bar{w}(\bar{r}, \theta)}{\partial \theta^2} = -n^2 [C_1 J_n(\bar{k}_1 \bar{r}) + C_2 Y_n(\bar{k}_1 \bar{r}) + C_3 I_n(\bar{k}_1 \bar{r}) + C_4 K_n(\bar{k}_1 \bar{r})] \cos(n\theta) \quad (7.37)$$

$$\frac{1}{\bar{r}^2} \frac{\partial^2 \bar{w}(\bar{r}, \theta)}{\partial \theta^2} = -\frac{n^2}{\bar{r}^2} [C_1 J_n(\bar{k}_1 \bar{r}) + C_2 Y_n(\bar{k}_1 \bar{r}) + C_3 I_n(\bar{k}_1 \bar{r}) + C_4 K_n(\bar{k}_1 \bar{r})] \cos(n\theta) \quad (7.38)$$

$$\frac{1}{\bar{r}^2} \frac{\partial^2 \bar{w}(\bar{r}, \theta)}{\partial \theta^2} \bigg|_{\bar{r}=1} = -n^2 [C_1 J_n(\bar{k}_1) + C_2 Y_n(\bar{k}_1) + C_3 I_n(\bar{k}_1) + C_4 K_n(\bar{k}_1)] \cos(n\theta) \quad (7.39)$$

Substituting equations (7.28), (7.32), (7.35) and (7.39) into equation (7.11) yields the following equation, at $\bar{r} = 1$

$$\begin{aligned} & \left[\frac{\bar{k}_1^2}{4} T_2 + \frac{\bar{k}_1}{2} (\nu + R_{11}) T_1 - \left(\frac{\bar{k}_1^2}{2} + \nu^2 \right) J_n(\bar{k}_1) \right] C_1 + \left[\frac{\bar{k}_1^2}{4} U_2 + \frac{\bar{k}_1}{2} (\nu + R_{11}) U_1 - \left(\frac{\bar{k}_1^2}{2} + \nu^2 \right) Y_n(\bar{k}_1) \right] C_2 + \\ & \left[\frac{\bar{k}_1^2}{4} V_2 + \frac{\bar{k}_1}{2} (\nu + R_{11}) V_1 + \left(\frac{\bar{k}_1^2}{2} - \nu^2 \right) I_n(\bar{k}_1) \right] C_3 + \left[\frac{\bar{k}_1^2}{4} W_2 - \frac{\bar{k}_1}{2} (\nu + R_{11}) W_1 + \left(\frac{\bar{k}_1^2}{2} - \nu^2 \right) K_n(\bar{k}_1) \right] C_4 = 0 \end{aligned} \quad (7.40)$$

Boundary conditions when the outer edges are elastically restrained against translation.

From equations (7.5) and (7.14) yields the following

$$\frac{\partial}{\partial \bar{r}} \nabla^2 \bar{w}(\bar{r}, \theta) = \frac{\partial}{\partial \bar{r}} \left[\frac{\partial^2 w(\bar{r}, \theta)}{\partial \bar{r}^2} + \frac{1}{\bar{r}^2} \frac{\partial^2 w(\bar{r}, \theta)}{\partial \theta^2} + \frac{1}{\bar{r}} \frac{\partial w(\bar{r}, \theta)}{\partial \bar{r}} \right] \quad (7.41)$$

$$\frac{\partial}{\partial \bar{r}} \left[\frac{\partial^2 w(\bar{r}, \theta)}{\partial \bar{r}^2} \right] = \frac{\partial}{\partial \bar{r}} \left[\begin{aligned} & \frac{\bar{k}_1^2}{4} [(J_{n-2}(\bar{k}_1 \bar{r}) + J_{n+2}(\bar{k}_1 \bar{r})) - 2J_n(\bar{k}_1 \bar{r})] C_1 + \\ & \frac{\bar{k}_1^2}{4} [(Y_{n-2}(\bar{k}_1 \bar{r}) + Y_{n+2}(\bar{k}_1 \bar{r})) - 2Y_n(\bar{k}_1 \bar{r})] C_2 + \\ & \frac{\bar{k}_1^2}{4} [(I_{n-2}(\bar{k}_1 \bar{r}) + I_{n+2}(\bar{k}_1 \bar{r})) + 2I_n(\bar{k}_1 \bar{r})] C_3 + \\ & \frac{\bar{k}_1^2}{4} [(K_{n-2}(\bar{k}_1 \bar{r}) + K_{n+2}(\bar{k}_1 \bar{r})) + 2K_n(\bar{k}_1 \bar{r})] C_4 \end{aligned} \right] \cos(n\theta) \quad (7.42)$$

$$= \left\{ \begin{aligned} & \frac{\bar{k}_1^3}{8} [(J_{n-3}(\bar{k}_1 \bar{r}) - J_{n-1}(\bar{k}_1 \bar{r})) + (J_{n+1}(\bar{k}_1 \bar{r}) - J_{n+3}(\bar{k}_1 \bar{r})) - 2(J_{n-1}(\bar{k}_1 \bar{r}) - J_{n+1}(\bar{k}_1 \bar{r}))] C_1 + \\ & \frac{\bar{k}_1^3}{8} [(Y_{n-3}(\bar{k}_1 \bar{r}) - Y_{n-1}(\bar{k}_1 \bar{r})) + (Y_{n+1}(\bar{k}_1 \bar{r}) - Y_{n+3}(\bar{k}_1 \bar{r})) - 2(Y_{n-1}(\bar{k}_1 \bar{r}) - Y_{n+1}(\bar{k}_1 \bar{r}))] C_2 + \\ & \frac{\bar{k}_1^3}{8} [(I_{n-3}(\bar{k}_1 \bar{r}) + I_{n-1}(\bar{k}_1 \bar{r})) + (I_{n+1}(\bar{k}_1 \bar{r}) + I_{n+3}(\bar{k}_1 \bar{r})) + 2(I_{n-1}(\bar{k}_1 \bar{r}) + I_{n+1}(\bar{k}_1 \bar{r}))] C_3 - \\ & \frac{\bar{k}_1^3}{8} [(K_{n-3}(\bar{k}_1 \bar{r}) + K_{n-1}(\bar{k}_1 \bar{r})) + (K_{n+1}(\bar{k}_1 \bar{r}) + K_{n+3}(\bar{k}_1 \bar{r})) + 2(K_{n-1}(\bar{k}_1 \bar{r}) + K_{n+1}(\bar{k}_1 \bar{r}))] C_4 \end{aligned} \right\} \cos(n\theta) \quad (7.43)$$

$$= \left\{ \begin{aligned} & \frac{\bar{k}_1^3}{8} [(J_{n-3}(\bar{k}_1\bar{r}) - J_{n+3}(\bar{k}_1\bar{r})) - 3(J_{n-1}(\bar{k}_1\bar{r}) - J_{n+1}(\bar{k}_1\bar{r}))]C_1 + \\ & \frac{\bar{k}_1^3}{8} [(Y_{n-3}(\bar{k}_1\bar{r}) - Y_{n+3}(\bar{k}_1\bar{r})) - 3(Y_{n-1}(\bar{k}_1\bar{r}) - Y_{n+1}(\bar{k}_1\bar{r}))]C_2 + \\ & \frac{\bar{k}_1^3}{8} [(I_{n-3}(\bar{k}_1\bar{r}) + I_{n+3}(\bar{k}_1\bar{r})) + 3(I_{n-1}(\bar{k}_1\bar{r}) + I_{n+1}(\bar{k}_1\bar{r}))]C_3 - \\ & \frac{\bar{k}_1^3}{8} [(K_{n-3}(\bar{k}_1\bar{r}) + K_{n+3}(\bar{k}_1\bar{r})) + 3(K_{n-1}(\bar{k}_1\bar{r}) + K_{n+1}(\bar{k}_1\bar{r}))]C_4 \end{aligned} \right\} \cos(n\theta) \quad (7.44)$$

$$\frac{\partial}{\partial \bar{r}} \left[\frac{\partial^2 w(\bar{r}, \theta)}{\partial \bar{r}^2} \right]_{\bar{r}=1} = \left\{ \begin{aligned} & \frac{\bar{k}_1^3}{8} [(J_{n-3}(\bar{k}_1) - J_{n+3}(\bar{k}_1)) - 3(J_{n-1}(\bar{k}_1) - J_{n+1}(\bar{k}_1))]C_1 + \\ & \frac{\bar{k}_1^3}{8} [(Y_{n-3}(\bar{k}_1) - Y_{n+3}(\bar{k}_1)) - 3(Y_{n-1}(\bar{k}_1) - Y_{n+1}(\bar{k}_1))]C_2 + \\ & \frac{\bar{k}_1^3}{8} [(I_{n-3}(\bar{k}_1) + I_{n+3}(\bar{k}_1)) + 3(I_{n-1}(\bar{k}_1) + I_{n+1}(\bar{k}_1))]C_3 - \\ & \frac{\bar{k}_1^3}{8} [(K_{n-3}(\bar{k}_1) + K_{n+3}(\bar{k}_1)) + 3(K_{n-1}(\bar{k}_1) + K_{n+1}(\bar{k}_1))]C_4 \end{aligned} \right\} \cos(n\theta) \quad (7.45)$$

$$\frac{\partial}{\partial \bar{r}} \left[\frac{\partial^2 w(\bar{r}, \theta)}{\partial \bar{r}^2} \right]_{\bar{r}=1} = \left\{ \begin{aligned} & \frac{\bar{k}_1^3}{8} [T_3 - 3T_1]C_1 + \frac{\bar{k}_1^3}{8} [U_3 - 3U_1]C_2 + \\ & \frac{\bar{k}_1^3}{8} [V_3 + 3V_1]C_3 - \frac{\bar{k}_1^3}{8} [W_3 + 3W_1]C_4 \end{aligned} \right\} \cos(n\theta) \quad (7.46)$$

where $T_3 = J_{n-3}(\bar{k}_1) - J_{n+3}(\bar{k}_1); U_3 = Y_{n-3}(\bar{k}_1) - Y_{n+3}(\bar{k}_1);$

$$V_3 = I_{n-3}(\bar{k}_1) + I_{n+3}(\bar{k}_1); W_3 = K_{n-3}(\bar{k}_1) + K_{n+3}(\bar{k}_1);$$

$$\frac{\partial}{\partial \bar{r}} \left[\frac{1}{\bar{r}^2} \frac{\partial^2 w(\bar{r}, \theta)}{\partial \theta^2} \right] = \frac{1}{\bar{r}^2} \frac{\partial}{\partial \bar{r}} \left[\frac{\partial^2 w(\bar{r}, \theta)}{\partial \theta^2} \right] - \frac{2}{\bar{r}^3} \frac{\partial^2 w(\bar{r}, \theta)}{\partial \theta^2} \quad (7.47)$$

$$= \frac{1}{\bar{r}^2} \left\{ -n^2 \left[\begin{aligned} & \frac{\bar{k}_1}{2} [J_{n-1}(\bar{k}_1\bar{r}) - J_{n+1}(\bar{k}_1\bar{r})]C_1 + \frac{\bar{k}_1}{2} [Y_{n-1}(\bar{k}_1\bar{r}) - Y_{n+1}(\bar{k}_1\bar{r})]C_2 + \\ & \frac{\bar{k}_1}{2} [I_{n-1}(\bar{k}_1\bar{r}) + I_{n+1}(\bar{k}_1\bar{r})]C_3 - \frac{\bar{k}_1}{2} [K_{n-1}(\bar{k}_1\bar{r}) + K_{n+1}(\bar{k}_1\bar{r})]C_4 \end{aligned} \right] \cos(n\theta) \right\} - \quad (7.48)$$

$$\frac{2}{\bar{r}^3} \left\{ -n^2 [C_1 J_n(\bar{k}_1\bar{r}) + C_2 Y_n(\bar{k}_1\bar{r}) + C_3 I_n(\bar{k}_1\bar{r}) + C_4 K_n(\bar{k}_1\bar{r})] \cos(n\theta) \right\}$$

$$\begin{aligned} & \frac{\partial}{\partial \bar{r}} \left[\frac{1}{\bar{r}^2} \frac{\partial^2 w(\bar{r}, \theta)}{\partial \theta^2} \right]_{\bar{r}=1} = \\ & \left\{ -n^2 \left[\begin{aligned} & \frac{\bar{k}_1}{2} [J_{n-1}(\bar{k}_1) - J_{n+1}(\bar{k}_1)]C_1 + \frac{\bar{k}_1}{2} [Y_{n-1}(\bar{k}_1) - Y_{n+1}(\bar{k}_1)]C_2 + \\ & \frac{\bar{k}_1}{2} [I_{n-1}(\bar{k}_1) + I_{n+1}(\bar{k}_1)]C_3 - \frac{\bar{k}_1}{2} [K_{n-1}(\bar{k}_1) + K_{n+1}(\bar{k}_1)]C_4 \end{aligned} \right] \cos(n\theta) \right\} - \\ & 2 \left\{ -n^2 [C_1 J_n(\bar{k}_1) + C_2 Y_n(\bar{k}_1) + C_3 I_n(\bar{k}_1) + C_4 K_n(\bar{k}_1)] \cos(n\theta) \right\} \end{aligned} \quad (7.49)$$

$$\begin{aligned}
\frac{\partial}{\partial \bar{r}} \left[\frac{1}{\bar{r}^2} \frac{\partial^2 w(\bar{r}, \theta)}{\partial \theta^2} \right]_{\bar{r}=1} = & \\
-n^2 \left[\frac{\bar{k}_1}{2} [J_{n-1}(\bar{k}_1) - J_{n+1}(\bar{k}_1)] C_1 + \frac{\bar{k}_1}{2} [Y_{n-1}(\bar{k}_1) - Y_{n+1}(\bar{k}_1)] C_2 + \right. & \\
\left. \frac{\bar{k}_1}{2} [I_{n-1}(\bar{k}_1) + I_{n+1}(\bar{k}_1)] C_3 - \frac{\bar{k}_1}{2} [K_{n-1}(\bar{k}_1) + K_{n+1}(\bar{k}_1)] C_4 \right] \cos(n\theta) + & \\
2n^2 [C_1 J_n(\bar{k}_1) + C_2 Y_n(\bar{k}_1) + C_3 I_n(\bar{k}_1) + C_4 K_n(\bar{k}_1)] \cos(n\theta) &
\end{aligned} \tag{7.50}$$

$$\begin{aligned}
\frac{\partial}{\partial \bar{r}} \left[\frac{1}{\bar{r}^2} \frac{\partial^2 w(\bar{r}, \theta)}{\partial \theta^2} \right]_{\bar{r}=1} = -n^2 \left[\frac{\bar{k}_1}{2} [T_1] C_1 + \frac{\bar{k}_1}{2} [U_1] C_2 + \frac{\bar{k}_1}{2} [V_1] C_3 - \frac{\bar{k}_1}{2} [W_1] C_4 \right] \cos(n\theta) + & \\
2n^2 [C_1 J_n(\bar{k}_1) + C_2 Y_n(\bar{k}_1) + C_3 I_n(\bar{k}_1) + C_4 K_n(\bar{k}_1)] \cos(n\theta) &
\end{aligned} \tag{7.51}$$

$$\frac{\partial}{\partial \bar{r}} \left[\frac{1}{\bar{r}} \frac{\partial w(\bar{r}, \theta)}{\partial \bar{r}} \right] = \frac{1}{\bar{r}} \frac{\partial}{\partial \bar{r}} \left[\frac{\partial w(\bar{r}, \theta)}{\partial \bar{r}} \right] + \frac{\partial w(\bar{r}, \theta)}{\partial \bar{r}} \frac{\partial}{\partial \bar{r}} \left[\frac{1}{\bar{r}} \right] = \frac{1}{\bar{r}} \frac{\partial^2 w(\bar{r}, \theta)}{\partial \bar{r}^2} - \frac{1}{\bar{r}^2} \frac{\partial w(\bar{r}, \theta)}{\partial \bar{r}} \tag{7.52}$$

$$\begin{aligned}
= \frac{1}{\bar{r}} & \left[\frac{\bar{k}_1^2}{4} [(J_{n-2}(\bar{k}_1 \bar{r}) + J_{n+2}(\bar{k}_1 \bar{r})) - 2J_n(\bar{k}_1 \bar{r})] C_1 + \right. \\
& \frac{\bar{k}_1^2}{4} [(Y_{n-2}(\bar{k}_1 \bar{r}) + Y_{n+2}(\bar{k}_1 \bar{r})) - 2Y_n(\bar{k}_1 \bar{r})] C_2 + \\
& \frac{\bar{k}_1^2}{4} [(I_{n-2}(\bar{k}_1 \bar{r}) + I_{n+2}(\bar{k}_1 \bar{r})) + 2I_n(\bar{k}_1 \bar{r})] C_3 + \\
& \left. \frac{\bar{k}_1^2}{4} [(K_{n-2}(\bar{k}_1 \bar{r}) + K_{n+2}(\bar{k}_1 \bar{r})) + 2K_n(\bar{k}_1 \bar{r})] C_4 \right] \cos(n\theta) \\
- \frac{1}{\bar{r}^2} & \left[\frac{\bar{k}_1}{2} [J_{n-1}(\bar{k}_1 \bar{r}) - J_{n+1}(\bar{k}_1 \bar{r})] C_1 + \frac{\bar{k}_1}{2} [Y_{n-1}(\bar{k}_1 \bar{r}) - Y_{n+1}(\bar{k}_1 \bar{r})] C_2 + \right. \\
& \left. \frac{\bar{k}_1}{2} [I_{n-1}(\bar{k}_1 \bar{r}) + I_{n+1}(\bar{k}_1 \bar{r})] C_3 - \frac{\bar{k}_1}{2} [K_{n-1}(\bar{k}_1 \bar{r}) + K_{n+1}(\bar{k}_1 \bar{r})] C_4 \right] \cos(n\theta)
\end{aligned} \tag{7.53}$$

$$\begin{aligned}
\frac{\partial}{\partial \bar{r}} \left[\frac{1}{\bar{r}} \frac{\partial w(\bar{r}, \theta)}{\partial \bar{r}} \right]_{\bar{r}=1} = & \left[\frac{\bar{k}_1^2}{4} [(J_{n-2}(\bar{k}_1) + J_{n+2}(\bar{k}_1)) - 2J_n(\bar{k}_1)] C_1 + \right. \\
& \frac{\bar{k}_1^2}{4} [(Y_{n-2}(\bar{k}_1) + Y_{n+2}(\bar{k}_1)) - 2Y_n(\bar{k}_1)] C_2 + \\
& \frac{\bar{k}_1^2}{4} [(I_{n-2}(\bar{k}_1) + I_{n+2}(\bar{k}_1)) + 2I_n(\bar{k}_1)] C_3 + \\
& \left. \frac{\bar{k}_1^2}{4} [(K_{n-2}(\bar{k}_1) + K_{n+2}(\bar{k}_1)) + 2K_n(\bar{k}_1)] C_4 \right] \cos(n\theta) \\
- & \left[\frac{\bar{k}_1}{2} [J_{n-1}(\bar{k}_1) - J_{n+1}(\bar{k}_1)] C_1 + \frac{\bar{k}_1}{2} [Y_{n-1}(\bar{k}_1) - Y_{n+1}(\bar{k}_1)] C_2 + \right. \\
& \left. \frac{\bar{k}_1}{2} [I_{n-1}(\bar{k}_1) + I_{n+1}(\bar{k}_1)] C_3 - \frac{\bar{k}_1}{2} [K_{n-1}(\bar{k}_1) + K_{n+1}(\bar{k}_1)] C_4 \right] \cos(n\theta)
\end{aligned} \tag{7.54}$$

$$\frac{\partial}{\partial \bar{r}} \left[\frac{1}{\bar{r}} \frac{\partial w(\bar{r}, \theta)}{\partial \bar{r}} \right]_{\bar{r}=1} = \left[\frac{\bar{k}_1^2}{4} [T_2 - 2J_n(\bar{k}_1)] C_1 + \frac{\bar{k}_1^2}{4} [U_2 - 2Y_n(\bar{k}_1)] C_2 + \frac{\bar{k}_1^2}{4} [V_2 + 2I_n(\bar{k}_1)] C_3 + \frac{\bar{k}_1^2}{4} [W_2 + 2K_n(\bar{k}_1)] C_4 \right] \cos(n\theta) \quad (7.55)$$

$$- \left[\frac{\bar{k}_1}{2} [T_1] C_1 + \frac{\bar{k}_1}{2} [U_1] C_2 + \frac{\bar{k}_1}{2} [V_1] C_3 - \frac{\bar{k}_1}{2} [W_1] C_4 \right] \cos(n\theta)$$

$$\left[\frac{\partial^2 w(\bar{r}, \theta)}{\partial \bar{r} \partial \theta} \right] = \frac{\partial}{\partial \bar{r}} \left[\frac{\partial w(\bar{r}, \theta)}{\partial \theta} \right] = \frac{\partial}{\partial \bar{r}} \left\{ -n [C_1 J_n(\bar{k}_1 \bar{r}) + C_2 Y_n(\bar{k}_1 \bar{r}) + C_3 I_n(\bar{k}_1 \bar{r}) + C_4 K_n(\bar{k}_1 \bar{r})] \sin(n\theta) \right\} \quad (7.56)$$

$$= -n \left[\frac{\bar{k}_1}{2} [J_{n-1}(\bar{k}_1 \bar{r}) - J_{n+1}(\bar{k}_1 \bar{r})] C_1 + \frac{\bar{k}_1}{2} [Y_{n-1}(\bar{k}_1 \bar{r}) - Y_{n+1}(\bar{k}_1 \bar{r})] C_2 + \frac{\bar{k}_1}{2} [I_{n-1}(\bar{k}_1 \bar{r}) + I_{n+1}(\bar{k}_1 \bar{r})] C_3 - \frac{\bar{k}_1}{2} [K_{n-1}(\bar{k}_1 \bar{r}) + K_{n+1}(\bar{k}_1 \bar{r})] C_4 \right] \sin(n\theta) \quad (7.57)$$

$$\frac{1}{\bar{r}^2} \frac{\partial w(\bar{r}, \theta)}{\partial \theta} = \frac{-n}{\bar{r}^2} [C_1 J_n(\bar{k}_1 \bar{r}) + C_2 Y_n(\bar{k}_1 \bar{r}) + C_3 I_n(\bar{k}_1 \bar{r}) + C_4 K_n(\bar{k}_1 \bar{r})] \sin(n\theta) \quad (7.58)$$

From equations (7.57) and (7.58) yields the following

$$\begin{aligned} & \frac{\partial}{\partial \theta} \left[\frac{1}{\bar{r}} \frac{\partial^2 w(\bar{r}, \theta)}{\partial \bar{r} \partial \theta} - \frac{1}{\bar{r}^2} \frac{\partial w(\bar{r}, \theta)}{\partial \theta} \right] \\ &= -\frac{n^2}{\bar{r}} \left[\frac{\bar{k}_1}{2} [J_{n-1}(\bar{k}_1 \bar{r}) - J_{n+1}(\bar{k}_1 \bar{r})] C_1 + \frac{\bar{k}_1}{2} [Y_{n-1}(\bar{k}_1 \bar{r}) - Y_{n+1}(\bar{k}_1 \bar{r})] C_2 + \frac{\bar{k}_1}{2} [I_{n-1}(\bar{k}_1 \bar{r}) + I_{n+1}(\bar{k}_1 \bar{r})] C_3 - \frac{\bar{k}_1}{2} [K_{n-1}(\bar{k}_1 \bar{r}) + K_{n+1}(\bar{k}_1 \bar{r})] C_4 \right] \cos(n\theta) + \\ & \frac{n^2}{\bar{r}^2} [C_1 J_n(\bar{k}_1 \bar{r}) + C_2 Y_n(\bar{k}_1 \bar{r}) + C_3 I_n(\bar{k}_1 \bar{r}) + C_4 K_n(\bar{k}_1 \bar{r})] \cos(n\theta) \end{aligned} \quad (7.59)$$

Equation (7.59) can be written as

$$\begin{aligned} & (1-\nu) \frac{1}{\bar{r}} \frac{\partial}{\partial \theta} \left[\frac{1}{\bar{r}} \frac{\partial^2 w(\bar{r}, \theta)}{\partial \bar{r} \partial \theta} - \frac{1}{\bar{r}^2} \frac{\partial w(\bar{r}, \theta)}{\partial \theta} \right]_{\bar{r}=1} \\ &= (1-\nu) \left\{ -n^2 \left[\frac{\bar{k}_1}{2} [J_{n-1}(\bar{k}_1) - J_{n+1}(\bar{k}_1)] C_1 + \frac{\bar{k}_1}{2} [Y_{n-1}(\bar{k}_1) - Y_{n+1}(\bar{k}_1)] C_2 + \frac{\bar{k}_1}{2} [I_{n-1}(\bar{k}_1) + I_{n+1}(\bar{k}_1)] C_3 - \frac{\bar{k}_1}{2} [K_{n-1}(\bar{k}_1) + K_{n+1}(\bar{k}_1)] C_4 \right] \cos(n\theta) + \right. \\ & \quad \left. n^2 [C_1 J_n(\bar{k}_1) + C_2 Y_n(\bar{k}_1) + C_3 I_n(\bar{k}_1) + C_4 K_n(\bar{k}_1)] \cos(n\theta) \right\} \end{aligned} \quad (7.60)$$

$$= (1-\nu) \left\{ -n^2 \left[\frac{\bar{k}_1}{2} [T_1] C_1 + \frac{\bar{k}_1}{2} [U_1] C_2 + \frac{\bar{k}_1}{2} [V_1] C_3 - \frac{\bar{k}_1}{2} [W_1] C_4 \right] \cos(n\theta) + \right. \\ \left. n^2 [C_1 J_n(\bar{k}_1) + C_2 Y_n(\bar{k}_1) + C_3 I_n(\bar{k}_1) + C_4 K_n(\bar{k}_1)] \cos(n\theta) \right\} \quad (7.61)$$

Substituting $\bar{r}=1$ into equation (9.5) yields the following

$$\bar{w}_I(\bar{r}, \theta)_{\bar{r}=1} = [C_1 J_n(\bar{k}_1) + C_2 Y_n(\bar{k}_1) + C_3 I_n(\bar{k}_1) + C_4 K_n(\bar{k}_1)] \cos(n\theta) \quad (7.62)$$

Substituting equations (7.46), (7.51), (7.55), (7.61), (7.62) into equation (7.14) gives the following

$$\left[\frac{\bar{k}_1^3}{8} T_3 + \frac{\bar{k}_1^2}{4} T_2 - \frac{\bar{k}_1}{2} \left(\frac{3}{4} \bar{k}_1^2 + n^2(2-\nu) + 1 \right) T_1 + \left(n^2(3-\nu) - \frac{\bar{k}_1^2}{2} - T_{11} \right) J_n(\bar{k}_1) \right] C_1 + \\ \left[\frac{\bar{k}_1^3}{8} U_3 + \frac{\bar{k}_1^2}{4} U_2 - \frac{\bar{k}_1}{2} \left(\frac{3}{4} \bar{k}_1^2 + n^2(2-\nu) + 1 \right) U_1 + \left(n^2(3-\nu) - \frac{\bar{k}_1^2}{2} - T_{11} \right) Y_n(\bar{k}_1) \right] C_2 + \\ \left[\frac{\bar{k}_1^3}{8} V_3 + \frac{\bar{k}_1^2}{4} V_2 + \frac{\bar{k}_1}{2} \left(\frac{3}{4} \bar{k}_1^2 + n^2(-2+\nu) - 1 \right) V_1 + \left(n^2(3-\nu) + \frac{\bar{k}_1^2}{2} - T_{11} \right) I_n(\bar{k}_1) \right] C_3 + \\ \left[-\frac{\bar{k}_1^3}{8} W_3 + \frac{\bar{k}_1^2}{4} W_2 + \frac{\bar{k}_1}{2} \left(-\frac{3}{4} \bar{k}_1^2 + n^2(2-\nu) + 1 \right) W_1 + \left(n^2(3-\nu) + \frac{\bar{k}_1^2}{2} - T_{11} \right) K_n(\bar{k}_1) \right] C_4 = 0 \quad (7.63)$$

where

$$T_1 = J_{n-1}(\bar{k}_1) - J_{n+1}(\bar{k}_1); T_2 = J_{n-2}(\bar{k}_1) + J_{n+2}(\bar{k}_1); T_3 = J_{n-3}(\bar{k}_1) - J_{n+3}(\bar{k}_1); \\ U_1 = Y_{n-1}(\bar{k}_1) - Y_{n+1}(\bar{k}_1); U_2 = Y_{n-2}(\bar{k}_1) + Y_{n+2}(\bar{k}_1); U_3 = Y_{n-3}(\bar{k}_1) - Y_{n+3}(\bar{k}_1); \\ V_1 = I_{n-1}(\bar{k}_1) + I_{n+1}(\bar{k}_1); V_2 = I_{n-2}(\bar{k}_1) + I_{n+2}(\bar{k}_1); V_3 = I_{n-3}(\bar{k}_1) + I_{n+3}(\bar{k}_1); \\ W_1 = K_{n-1}(\bar{k}_1) + K_{n+1}(\bar{k}_1); W_2 = K_{n-2}(\bar{k}_1) + K_{n+2}(\bar{k}_1); W_3 = K_{n-3}(\bar{k}_1) + K_{n+3}(\bar{k}_1);$$

Case: (ii) Plate *inner edges* are elastically restrained against rotation and translation

Boundary conditions when the inner edges are elastically restrained against rotation.

From equation (7.5) and (7.21) yields the following

$$\frac{\partial \bar{w}(\bar{r}, \theta)}{\partial \bar{r}} = \left[\frac{\bar{k}_1}{2} [J_{n-1}(\bar{k}_1 \bar{r}) - J_{n+1}(\bar{k}_1 \bar{r})] C_1 + \frac{\bar{k}_1}{2} [Y_{n-1}(\bar{k}_1 \bar{r}) - Y_{n+1}(\bar{k}_1 \bar{r})] C_2 + \right. \\ \left. \frac{\bar{k}_1}{2} [I_{n-1}(\bar{k}_1 \bar{r}) + I_{n+1}(\bar{k}_1 \bar{r})] C_3 - \frac{\bar{k}_1}{2} [K_{n-1}(\bar{k}_1 \bar{r}) + K_{n+1}(\bar{k}_1 \bar{r})] C_4 \right] \cos(n\theta) \quad (7.64)$$

$$\frac{\partial \bar{w}(\bar{r}, \theta)}{\partial \bar{r}} \Big|_{\bar{r}=b} = \left[\frac{\bar{k}_1}{2} [J_{n-1}(\bar{k}_1 b) - J_{n+1}(\bar{k}_1 b)] C_1 + \frac{\bar{k}_1}{2} [Y_{n-1}(\bar{k}_1 b) - Y_{n+1}(\bar{k}_1 b)] C_2 + \right. \\ \left. \frac{\bar{k}_1}{2} [I_{n-1}(\bar{k}_1 b) + I_{n+1}(\bar{k}_1 b)] C_3 - \frac{\bar{k}_1}{2} [K_{n-1}(\bar{k}_1 b) + K_{n+1}(\bar{k}_1 b)] C_4 \right] \cos(n\theta) \quad (7.65)$$

$$\frac{\partial \bar{w}(\bar{r}, \theta)}{\partial \bar{r}} \Big|_{\bar{r}=b} = \left[\frac{\bar{k}_1}{2} [T_1'] C_1 + \frac{\bar{k}_1}{2} [U_1'] C_2 + \frac{\bar{k}_1}{2} [V_1'] C_3 - \frac{\bar{k}_1}{2} [W_1'] C_4 \right] \cos(n\theta) \quad (7.66)$$

where $T_1' = J_{n-1}(\bar{k}_1 b) - J_{n+1}(\bar{k}_1 b)$; $U_1' = Y_{n-1}(\bar{k}_1 b) - Y_{n+1}(\bar{k}_1 b)$;

$$V_1' = I_{n-1}(\bar{k}_1 b) + I_{n+1}(\bar{k}_1 b); W_1' = K_{n-1}(\bar{k}_1 b) + K_{n+1}(\bar{k}_1 b);$$

$$\frac{\partial^2 \bar{w}(\bar{r}, \theta)}{\partial \bar{r}^2} = \left[\begin{aligned} & \frac{\bar{k}_1^2}{4} [(J_{n-2}(\bar{k}_1 \bar{r}) - J_n(\bar{k}_1 \bar{r})) - (J_n(\bar{k}_1 \bar{r}) - J_{n+2}(\bar{k}_1 \bar{r}))] C_1 + \\ & \frac{\bar{k}_1^2}{4} [(Y_{n-2}(\bar{k}_1 \bar{r}) - Y_n(\bar{k}_1 \bar{r})) - (Y_n(\bar{k}_1 \bar{r}) - Y_{n+2}(\bar{k}_1 \bar{r}))] C_2 + \\ & \frac{\bar{k}_1^2}{4} [(I_{n-2}(\bar{k}_1 \bar{r}) + I_n(\bar{k}_1 \bar{r})) + (I_n(\bar{k}_1 \bar{r}) + I_{n+2}(\bar{k}_1 \bar{r}))] C_3 + \\ & \frac{\bar{k}_1^2}{4} [(K_{n-2}(\bar{k}_1 \bar{r}) + K_n(\bar{k}_1 \bar{r})) + (K_n(\bar{k}_1 \bar{r}) + K_{n+2}(\bar{k}_1 \bar{r}))] C_4 \end{aligned} \right] \cos(n\theta) \quad (7.67)$$

$$\frac{\partial^2 \bar{w}(\bar{r}, \theta)}{\partial \bar{r}^2} = \left[\begin{aligned} & \frac{\bar{k}_1^2}{4} [(J_{n-2}(\bar{k}_1 \bar{r}) + J_{n+2}(\bar{k}_1 \bar{r})) - 2J_n(\bar{k}_1 \bar{r})] C_1 + \\ & \frac{\bar{k}_1^2}{4} [(Y_{n-2}(\bar{k}_1 \bar{r}) + Y_{n+2}(\bar{k}_1 \bar{r})) - 2Y_n(\bar{k}_1 \bar{r})] C_2 + \\ & \frac{\bar{k}_1^2}{4} [(I_{n-2}(\bar{k}_1 \bar{r}) + I_{n+2}(\bar{k}_1 \bar{r})) + 2I_n(\bar{k}_1 \bar{r})] C_3 + \\ & \frac{\bar{k}_1^2}{4} [(K_{n-2}(\bar{k}_1 \bar{r}) + K_{n+2}(\bar{k}_1 \bar{r})) + 2K_n(\bar{k}_1 \bar{r})] C_4 \end{aligned} \right] \cos(n\theta) \quad (7.68)$$

$$\frac{\partial^2 \bar{w}(\bar{r}, \theta)}{\partial \bar{r}^2} \Big|_{\bar{r}=b} = \left[\begin{aligned} & \frac{\bar{k}_1^2}{4} [(J_{n-2}(\bar{k}_1 b) + J_{n+2}(\bar{k}_1 b)) - 2J_n(\bar{k}_1 b)] C_1 + \\ & \frac{\bar{k}_1^2}{4} [(Y_{n-2}(\bar{k}_1 b) + Y_{n+2}(\bar{k}_1 b)) - 2Y_n(\bar{k}_1 b)] C_2 + \\ & \frac{\bar{k}_1^2}{4} [(I_{n-2}(\bar{k}_1 b) + I_{n+2}(\bar{k}_1 b)) + 2I_n(\bar{k}_1 b)] C_3 + \\ & \frac{\bar{k}_1^2}{4} [(K_{n-2}(\bar{k}_1 b) + K_{n+2}(\bar{k}_1 b)) + 2K_n(\bar{k}_1 b)] C_4 \end{aligned} \right] \cos(n\theta) \quad (7.69)$$

$$\frac{\partial^2 \bar{w}(\bar{r}, \theta)}{\partial \bar{r}^2} \Big|_{\bar{r}=b} = \left[\begin{aligned} & \frac{\bar{k}_1^2}{4} [T_2' - 2J_n(\bar{k}_1 b)] C_1 + \frac{\bar{k}_1^2}{4} [U_2' - 2Y_n(\bar{k}_1 b)] C_2 + \\ & \frac{\bar{k}_1^2}{4} [V_2' + 2I_n(\bar{k}_1 b)] C_3 + \frac{\bar{k}_1^2}{4} [W_2' + 2K_n(\bar{k}_1 b)] C_4 \end{aligned} \right] \cos(n\theta) \quad (7.70)$$

where $T_2' = J_{n-2}(\bar{k}_1 b) + J_{n+2}(\bar{k}_1 b)$; $U_2' = Y_{n-2}(\bar{k}_1 b) + Y_{n+2}(\bar{k}_1 b)$;

$$V_2' = I_{n-2}(\bar{k}_1 b) + I_{n+2}(\bar{k}_1 b); W_2' = K_{n-2}(\bar{k}_1 b) + K_{n+2}(\bar{k}_1 b);$$

$$\frac{1}{\bar{r}} \frac{\partial \bar{w}(\bar{r}, \theta)}{\partial \bar{r}} = \frac{1}{\bar{r}} \left[\frac{\bar{k}_1}{2} [J_{n-1}(\bar{k}_1 \bar{r}) - J_{n+1}(\bar{k}_1 \bar{r})] C_1 + \frac{\bar{k}_1}{2} [Y_{n-1}(\bar{k}_1 \bar{r}) - Y_{n+1}(\bar{k}_1 \bar{r})] C_2 + \right. \\ \left. \frac{\bar{k}_1}{2} [I_{n-1}(\bar{k}_1 \bar{r}) + I_{n+1}(\bar{k}_1 \bar{r})] C_3 - \frac{\bar{k}_1}{2} [K_{n-1}(\bar{k}_1 \bar{r}) + K_{n+1}(\bar{k}_1 \bar{r})] C_4 \right] \cos(n\theta) \quad (7.71)$$

$$\frac{1}{\bar{r}} \frac{\partial \bar{w}(\bar{r}, \theta)}{\partial \bar{r}} \Big|_{\bar{r}=b} = \frac{1}{b} \left[\frac{\bar{k}_1}{2} [J_{n-1}(\bar{k}_1 b) - J_{n+1}(\bar{k}_1 b)] C_1 + \frac{\bar{k}_1}{2} [Y_{n-1}(\bar{k}_1 b) - Y_{n+1}(\bar{k}_1 b)] C_2 + \right. \\ \left. \frac{\bar{k}_1}{2} [I_{n-1}(\bar{k}_1 b) + I_{n+1}(\bar{k}_1 b)] C_3 - \frac{\bar{k}_1}{2} [K_{n-1}(\bar{k}_1 b) + K_{n+1}(\bar{k}_1 b)] C_4 \right] \cos(n\theta) \quad (7.72)$$

$$\frac{1}{\bar{r}} \frac{\partial \bar{w}(\bar{r}, \theta)}{\partial \bar{r}} \Big|_{\bar{r}=b} = \frac{1}{b} \left[\frac{\bar{k}_1}{2} [T_1'] C_1 + \frac{\bar{k}_1}{2} [U_1'] C_2 + \frac{\bar{k}_1}{2} [V_1'] C_3 - \frac{\bar{k}_1}{2} [W_1'] C_4 \right] \cos(n\theta) \quad (7.73)$$

$$\frac{\partial \bar{w}(\bar{r}, \theta)}{\partial \theta} = -n [C_1 J_n(\bar{k}_1 \bar{r}) + C_2 Y_n(\bar{k}_1 \bar{r}) + C_3 I_n(\bar{k}_1 \bar{r}) + C_4 K_n(\bar{k}_1 \bar{r})] \sin(n\theta) \quad (7.74)$$

$$\frac{\partial^2 \bar{w}(\bar{r}, \theta)}{\partial \theta^2} = -n^2 [C_1 J_n(\bar{k}_1 \bar{r}) + C_2 Y_n(\bar{k}_1 \bar{r}) + C_3 I_n(\bar{k}_1 \bar{r}) + C_4 K_n(\bar{k}_1 \bar{r})] \cos(n\theta) \quad (7.75)$$

$$\frac{1}{\bar{r}^2} \frac{\partial^2 \bar{w}(\bar{r}, \theta)}{\partial \theta^2} = -\frac{n^2}{\bar{r}^2} [C_1 J_n(\bar{k}_1 \bar{r}) + C_2 Y_n(\bar{k}_1 \bar{r}) + C_3 I_n(\bar{k}_1 \bar{r}) + C_4 K_n(\bar{k}_1 \bar{r})] \cos(n\theta) \quad (7.76)$$

$$\frac{1}{\bar{r}^2} \frac{\partial^2 \bar{w}(\bar{r}, \theta)}{\partial \theta^2} \Big|_{\bar{r}=1} = -\frac{n^2}{b^2} [C_1 J_n(\bar{k}_1 b) + C_2 Y_n(\bar{k}_1 b) + C_3 I_n(\bar{k}_1 b) + C_4 K_n(\bar{k}_1 b)] \cos(n\theta) \quad (7.77)$$

Substituting equations (7.66), (7.70), (7.73) and (7.77) into equation (7.21) gives the following equation, at $\bar{r} = b$

$$\left[\frac{\bar{k}_1^2}{4} T_2' + \frac{\bar{k}_1}{2} \left(\frac{\nu}{b} - R_{22} \right) T_1' - \left(\frac{\bar{k}_1^2}{2} + \frac{\nu m^2}{b^2} \right) J_n(\bar{k}_1 b) \right] C_1 + \left[\frac{\bar{k}_1^2}{4} U_2' + \frac{\bar{k}_1}{2} \left(\frac{\nu}{b} - R_{22} \right) U_1' - \left(\frac{\bar{k}_1^2}{2} + \frac{\nu m^2}{b^2} \right) Y_n(\bar{k}_1 b) \right] C_2 + \\ \left[\frac{\bar{k}_1^2}{4} V_2' + \frac{\bar{k}_1}{2} \left(\frac{\nu}{b} - R_{22} \right) V_1' + \left(\frac{\bar{k}_1^2}{2} - \frac{\nu m^2}{b^2} \right) I_n(\bar{k}_1 b) \right] C_3 + \left[\frac{\kappa^2}{4} W_2' - \frac{\bar{k}_1}{2} \left(\frac{\nu}{b} - R_{22} \right) W_1' + \left(\frac{\bar{k}_1^2}{2} - \frac{\nu m^2}{b^2} \right) K_n(\bar{k}_1 b) \right] C_4 = 0 \quad (9.78)$$

Boundary conditions when the inner edges are elastically restrained against translation.

From equation (7.5) and (7.24) yields the following

$$\frac{\partial}{\partial \bar{r}} \nabla^2 \bar{w}(\bar{r}, \theta) = \frac{\partial}{\partial \bar{r}} \left[\frac{\partial^2 \bar{w}(\bar{r}, \theta)}{\partial \bar{r}^2} + \frac{1}{\bar{r}^2} \frac{\partial^2 \bar{w}(\bar{r}, \theta)}{\partial \theta^2} + \frac{1}{\bar{r}} \frac{\partial \bar{w}(\bar{r}, \theta)}{\partial \bar{r}} \right] \quad (7.79)$$

$$\frac{\partial}{\partial \bar{r}} \left[\frac{\partial^2 w(\bar{r}, \theta)}{\partial \bar{r}^2} \right] = \frac{\partial}{\partial \bar{r}} \left[\begin{aligned} & \frac{\bar{k}_1^2}{4} [J_{n-2}(\bar{k}_1 \bar{r}) + J_{n+2}(\bar{k}_1 \bar{r}) - 2J_n(\bar{k}_1 \bar{r})] C_1 + \\ & \frac{\bar{k}_1^2}{4} [Y_{n-2}(\bar{k}_1 \bar{r}) + Y_{n+2}(\bar{k}_1 \bar{r}) - 2Y_n(\bar{k}_1 \bar{r})] C_2 + \\ & \frac{\bar{k}_1^2}{4} [I_{n-2}(\bar{k}_1 \bar{r}) + I_{n+2}(\bar{k}_1 \bar{r}) + 2I_n(\bar{k}_1 \bar{r})] C_3 + \\ & \frac{\bar{k}_1^2}{4} [K_{n-2}(\bar{k}_1 \bar{r}) + K_{n+2}(\bar{k}_1 \bar{r}) + 2K_n(\bar{k}_1 \bar{r})] C_4 \end{aligned} \right] \cos(n\theta) \quad (7.80)$$

$$= \left\{ \begin{aligned} & \frac{\bar{k}_1^3}{8} [(J_{n-3}(\bar{k}_1 \bar{r}) - J_{n-1}(\bar{k}_1 \bar{r})) + (J_{n+1}(\bar{k}_1 \bar{r}) - J_{n+3}(\bar{k}_1 \bar{r})) - 2(J_{n-1}(\bar{k}_1 \bar{r}) - J_{n+1}(\bar{k}_1 \bar{r}))] C_1 + \\ & \frac{\bar{k}_1^3}{8} [(Y_{n-3}(\bar{k}_1 \bar{r}) - Y_{n-1}(\bar{k}_1 \bar{r})) + (Y_{n+1}(\bar{k}_1 \bar{r}) - Y_{n+3}(\bar{k}_1 \bar{r})) - 2(Y_{n-1}(\bar{k}_1 \bar{r}) - Y_{n+1}(\bar{k}_1 \bar{r}))] C_2 + \\ & \frac{\bar{k}_1^3}{8} [(I_{n-3}(\bar{k}_1 \bar{r}) + I_{n-1}(\bar{k}_1 \bar{r})) + (I_{n+1}(\bar{k}_1 \bar{r}) + I_{n+3}(\bar{k}_1 \bar{r})) + 2(I_{n-1}(\bar{k}_1 \bar{r}) + I_{n+1}(\bar{k}_1 \bar{r}))] C_3 - \\ & \frac{\bar{k}_1^3}{8} [(K_{n-3}(\bar{k}_1 \bar{r}) + K_{n-1}(\bar{k}_1 \bar{r})) + (K_{n+1}(\bar{k}_1 \bar{r}) + K_{n+3}(\bar{k}_1 \bar{r})) + 2(K_{n-1}(\bar{k}_1 \bar{r}) + K_{n+1}(\bar{k}_1 \bar{r}))] C_4 \end{aligned} \right\} \cos(n\theta) \quad (7.81)$$

$$= \left\{ \begin{aligned} & \frac{\bar{k}_1^3}{8} [(J_{n-3}(\bar{k}_1 \bar{r}) - J_{n+3}(\bar{k}_1 \bar{r})) - 3(J_{n-1}(\bar{k}_1 \bar{r}) - J_{n+1}(\bar{k}_1 \bar{r}))] C_1 + \\ & \frac{\bar{k}_1^3}{8} [(Y_{n-3}(\bar{k}_1 \bar{r}) - Y_{n+3}(\bar{k}_1 \bar{r})) - 3(Y_{n-1}(\bar{k}_1 \bar{r}) - Y_{n+1}(\bar{k}_1 \bar{r}))] C_2 + \\ & \frac{\bar{k}_1^3}{8} [(I_{n-3}(\bar{k}_1 \bar{r}) + I_{n+3}(\bar{k}_1 \bar{r})) + 3(I_{n-1}(\bar{k}_1 \bar{r}) + I_{n+1}(\bar{k}_1 \bar{r}))] C_3 - \\ & \frac{\bar{k}_1^3}{8} [(K_{n-3}(\bar{k}_1 \bar{r}) + K_{n+3}(\bar{k}_1 \bar{r})) + 3(K_{n-1}(\bar{k}_1 \bar{r}) + K_{n+1}(\bar{k}_1 \bar{r}))] C_4 \end{aligned} \right\} \cos(n\theta) \quad (7.82)$$

$$\frac{\partial}{\partial \bar{r}} \left[\frac{\partial^2 w(\bar{r}, \theta)}{\partial \bar{r}^2} \right]_{\bar{r}=b} = \left\{ \begin{aligned} & \frac{\bar{k}_1^3}{8} [(J_{n-3}(\bar{k}_1 b) - J_{n+3}(\bar{k}_1 b)) - 3(J_{n-1}(\bar{k}_1 b) - J_{n+1}(\bar{k}_1 b))] C_1 + \\ & \frac{\bar{k}_1^3}{8} [(Y_{n-3}(\bar{k}_1 b) - Y_{n+3}(\bar{k}_1 b)) - 3(Y_{n-1}(\bar{k}_1 b) - Y_{n+1}(\bar{k}_1 b))] C_2 + \\ & \frac{\bar{k}_1^3}{8} [(I_{n-3}(\bar{k}_1 b) + I_{n+3}(\bar{k}_1 b)) + 3(I_{n-1}(\bar{k}_1 b) + I_{n+1}(\bar{k}_1 b))] C_3 - \\ & \frac{\bar{k}_1^3}{8} [(K_{n-3}(\bar{k}_1 b) + K_{n+3}(\bar{k}_1 b)) + 3(K_{n-1}(\bar{k}_1 b) + K_{n+1}(\bar{k}_1 b))] C_4 \end{aligned} \right\} \cos(n\theta) \quad (7.83)$$

$$\frac{\partial}{\partial \bar{r}} \left[\frac{\partial^2 w(\bar{r}, \theta)}{\partial \bar{r}^2} \right]_{\bar{r}=b} = \left\{ \begin{aligned} & \frac{\bar{k}_1^3}{8} [T_3' - 3T_1'] C_1 + \frac{\bar{k}_1^3}{8} [U_3' - 3U_1'] C_2 + \\ & \frac{\bar{k}_1^3}{8} [V_3' + 3V_1'] C_3 - \frac{\bar{k}_1^3}{8} [W_3' + 3W_1'] C_4 \end{aligned} \right\} \cos(n\theta) \quad (7.84)$$

where $T_3' = J_{n-3}(\bar{k}_1 b) - J_{n+3}(\bar{k}_1 b)$; $U_3' = Y_{n-3}(\bar{k}_1 b) - Y_{n+3}(\bar{k}_1 b)$;

$$V_3' = I_{n-3}(\bar{k}_1 b) + I_{n+3}(\bar{k}_1 b); W_3' = K_{n-3}(\bar{k}_1 b) + K_{n+3}(\bar{k}_1 b);$$

$$\frac{\partial}{\partial \bar{r}} \left[\frac{1}{\bar{r}^2} \frac{\partial^2 w(\bar{r}, \theta)}{\partial \theta^2} \right] = \frac{1}{\bar{r}^2} \frac{\partial}{\partial \bar{r}} \left[\frac{\partial^2 w(\bar{r}, \theta)}{\partial \theta^2} \right] - \frac{2}{\bar{r}^3} \frac{\partial^2 w(\bar{r}, \theta)}{\partial \theta^2} \quad (7.85)$$

$$= \frac{1}{\bar{r}^2} \left\{ -n^2 \left[\frac{\bar{k}_1}{2} [J_{n-1}(\bar{k}_1 \bar{r}) - J_{n+1}(\bar{k}_1 \bar{r})] C_1 + \frac{\bar{k}_1}{2} [Y_{n-1}(\bar{k}_1 \bar{r}) - Y_{n+1}(\bar{k}_1 \bar{r})] C_2 + \right. \right. \\ \left. \left. \frac{\bar{k}_1}{2} [I_{n-1}(\bar{k}_1 \bar{r}) + I_{n+1}(\bar{k}_1 \bar{r})] C_3 - \frac{\bar{k}_1}{2} [K_{n-1}(\bar{k}_1 \bar{r}) + K_{n+1}(\bar{k}_1 \bar{r})] C_4 \right] \cos(n\theta) \right\} - \quad (7.86)$$

$$\frac{2}{\bar{r}^3} \left\{ -n^2 [C_1 J_n(\bar{k}_1 \bar{r}) + C_2 Y_n(\bar{k}_1 \bar{r}) + C_3 I_n(\bar{k}_1 \bar{r}) + C_4 K_n(\bar{k}_1 \bar{r})] \cos(n\theta) \right\}$$

$$\frac{\partial}{\partial \bar{r}} \left[\frac{1}{\bar{r}^2} \frac{\partial^2 w(\bar{r}, \theta)}{\partial \theta^2} \right]_{\bar{r}=b} = \frac{1}{b^2} \left\{ -n^2 \left[\frac{\bar{k}_1}{2} [J_{n-1}(\bar{k}_1 b) - J_{n+1}(\bar{k}_1 b)] C_1 + \frac{\bar{k}_1}{2} [Y_{n-1}(\bar{k}_1 b) - Y_{n+1}(\bar{k}_1 b)] C_2 + \right. \right. \\ \left. \left. \frac{\bar{k}_1}{2} [I_{n-1}(\bar{k}_1 b) + I_{n+1}(\bar{k}_1 b)] C_3 - \frac{\bar{k}_1}{2} [K_{n-1}(\bar{k}_1 b) + K_{n+1}(\bar{k}_1 b)] C_4 \right] \cos(n\theta) \right\} - \quad (7.87)$$

$$\frac{2}{b^3} \left\{ -n^2 [C_1 J_n(\bar{k}_1 b) + C_2 Y_n(\bar{k}_1 b) + C_3 I_n(\bar{k}_1 b) + C_4 K_n(\bar{k}_1 b)] \cos(n\theta) \right\}$$

$$\frac{\partial}{\partial \bar{r}} \left[\frac{1}{\bar{r}^2} \frac{\partial^2 w(\bar{r}, \theta)}{\partial \theta^2} \right]_{\bar{r}=b} = -\frac{n^2}{b^2} \left[\frac{\bar{k}_1}{2} [J_{n-1}(\bar{k}_1 b) - J_{n+1}(\bar{k}_1 b)] C_1 + \frac{\bar{k}_1}{2} [Y_{n-1}(\bar{k}_1 b) - Y_{n+1}(\bar{k}_1 b)] C_2 + \right. \\ \left. \frac{\bar{k}_1}{2} [I_{n-1}(\bar{k}_1 b) + I_{n+1}(\bar{k}_1 b)] C_3 - \frac{\bar{k}_1}{2} [K_{n-1}(\bar{k}_1 b) + K_{n+1}(\bar{k}_1 b)] C_4 \right] \cos(n\theta) + \quad (7.88)$$

$$\frac{2n^2}{b^3} [C_1 J_n(\bar{k}_1 b) + C_2 Y_n(\bar{k}_1 b) + C_3 I_n(\bar{k}_1 b) + C_4 K_n(\bar{k}_1 b)] \cos(n\theta)$$

$$\frac{\partial}{\partial \bar{r}} \left[\frac{1}{\bar{r}^2} \frac{\partial^2 w(\bar{r}, \theta)}{\partial \theta^2} \right]_{\bar{r}=b} = -\frac{n^2}{b^2} \left[\frac{\bar{k}_1}{2} [T_1'] C_1 + \frac{\bar{k}_1}{2} [U_{11}'] C_2 + \frac{\bar{k}_1}{2} [V_{11}'] C_3 - \frac{\bar{k}_1}{2} [W_1'] C_4 \right] \cos(n\theta) + \quad (7.89)$$

$$\frac{2n^2}{b^3} [C_1 J_n(\bar{k}_1 b) + C_2 Y_n(\bar{k}_1 b) + C_3 I_n(\bar{k}_1 b) + C_4 K_n(\bar{k}_1 b)] \cos(n\theta)$$

$$\frac{\partial}{\partial \bar{r}} \left[\frac{1}{\bar{r}} \frac{\partial w(\bar{r}, \theta)}{\partial \bar{r}} \right] = \frac{1}{\bar{r}} \frac{\partial}{\partial \bar{r}} \left[\frac{\partial w(\bar{r}, \theta)}{\partial \bar{r}} \right] + \frac{\partial w(\bar{r}, \theta)}{\partial \bar{r}} \frac{\partial}{\partial \bar{r}} \left[\frac{1}{\bar{r}} \right] = \frac{1}{\bar{r}} \frac{\partial^2 w(\bar{r}, \theta)}{\partial \bar{r}^2} - \frac{1}{\bar{r}^2} \frac{\partial w(\bar{r}, \theta)}{\partial \bar{r}} \quad (7.90)$$

$$\begin{aligned}
&= \frac{1}{\bar{r}} \left[\frac{\bar{k}_1^2}{4} [(J_{n-2}(\bar{k}_1\bar{r}) + J_{n+2}(\bar{k}_1\bar{r})) - 2J_n(\bar{k}_1\bar{r})]C_1 + \right. \\
&\quad \frac{\bar{k}_1^2}{4} [(Y_{n-2}(\bar{k}_1\bar{r}) + Y_{n+2}(\bar{k}_1\bar{r})) - 2Y_n(\bar{k}_1\bar{r})]C_2 + \\
&\quad \frac{\bar{k}_1^2}{4} [(I_{n-2}(\bar{k}_1\bar{r}) + I_{n+2}(\bar{k}_1\bar{r})) + 2I_n(\bar{k}_1\bar{r})]C_3 + \\
&\quad \left. \frac{\bar{k}_1^2}{4} [(K_{n-2}(\bar{k}_1\bar{r}) + K_{n+2}(\bar{k}_1\bar{r})) + 2K_n(\bar{k}_1\bar{r})]C_4 \right] \cos(n\theta) \\
&- \frac{1}{\bar{r}^2} \left[\frac{\bar{k}_1}{2} [J_{n-1}(\bar{k}_1\bar{r}) - J_{n+1}(\bar{k}_1\bar{r})]C_1 + \frac{\bar{k}_1}{2} [Y_{n-1}(\bar{k}_1\bar{r}) - Y_{n+1}(\bar{k}_1\bar{r})]C_2 + \right. \\
&\quad \left. \frac{\bar{k}_1}{2} [I_{n-1}(\bar{k}_1\bar{r}) + I_{n+1}(\bar{k}_1\bar{r})]C_3 - \frac{\bar{k}_1}{2} [K_{n-1}(\bar{k}_1\bar{r}) + K_{n+1}(\bar{k}_1\bar{r})]C_4 \right] \cos(n\theta)
\end{aligned} \tag{7.91}$$

$$\begin{aligned}
\frac{\partial}{\partial \bar{r}} \left[\frac{1}{\bar{r}} \frac{\partial w(\bar{r}, \theta)}{\partial \bar{r}} \right]_{\bar{r}=b} &= \frac{1}{b} \left[\frac{\bar{k}_1^2}{4} [(J_{n-2}(\bar{k}_1b) + J_{n+2}(\bar{k}_1b)) - 2J_n(\bar{k}_1b)]C_1 + \right. \\
&\quad \frac{\bar{k}_1^2}{4} [(Y_{n-2}(\bar{k}_1b) + Y_{n+2}(\bar{k}_1b)) - 2Y_n(\bar{k}_1b)]C_2 + \\
&\quad \frac{\bar{k}_1^2}{4} [(I_{n-2}(\bar{k}_1b) + I_{n+2}(\bar{k}_1b)) + 2I_n(\bar{k}_1b)]C_3 + \\
&\quad \left. \frac{\bar{k}_1^2}{4} [(K_{n-2}(\bar{k}_1b) + K_{n+2}(\bar{k}_1b)) + 2K_n(\bar{k}_1b)]C_4 \right] \cos(n\theta) \\
&- \frac{1}{b^2} \left[\frac{\bar{k}_1}{2} [J_{n-1}(\bar{k}_1b) - J_{n+1}(\bar{k}_1b)]C_1 + \frac{\bar{k}_1}{2} [Y_{n-1}(\bar{k}_1b) - Y_{n+1}(\bar{k}_1b)]C_2 + \right. \\
&\quad \left. \frac{\bar{k}_1}{2} [I_{n-1}(\bar{k}_1b) + I_{n+1}(\bar{k}_1b)]C_3 - \frac{\bar{k}_1}{2} [K_{n-1}(\bar{k}_1b) + K_{n+1}(\bar{k}_1b)]C_4 \right] \cos(n\theta)
\end{aligned} \tag{7.92}$$

$$\begin{aligned}
\frac{\partial}{\partial \bar{r}} \left[\frac{1}{\bar{r}} \frac{\partial w(\bar{r}, \theta)}{\partial \bar{r}} \right]_{\bar{r}=b} &= \frac{1}{b} \left[\frac{\bar{k}_1^2}{4} [T_2' - 2J_n(\bar{k}_1b)]C_1 + \frac{\bar{k}_1^2}{4} [U_2' - 2Y_n(\bar{k}_1b)]C_2 + \right. \\
&\quad \left. \frac{\bar{k}_1^2}{4} [V_2' + 2I_n(\bar{k}_1b)]C_3 + \frac{\bar{k}_1^2}{4} [W_2' + 2K_n(\bar{k}_1b)]C_4 \right] \cos(n\theta) \\
&- \frac{1}{b^2} \left[\frac{\bar{k}_1}{2} [T_1']C_1 + \frac{\bar{k}_1}{2} [U_{1,1}']C_2 + \frac{\bar{k}_1}{2} [V_{1,1}']C_3 - \frac{\bar{k}_1}{2} [W_{1,1}']C_4 \right] \cos(n\theta)
\end{aligned} \tag{7.93}$$

$$\left[\frac{\partial^2 w(\bar{r}, \theta)}{\partial \bar{r} \partial \theta} \right] = \frac{\partial}{\partial \bar{r}} \left[\frac{\partial w(\bar{r}, \theta)}{\partial \theta} \right] = \frac{\partial}{\partial \bar{r}} \left\{ -n[C_1 J_n(\bar{k}_1\bar{r}) + C_2 Y_n(\bar{k}_1\bar{r}) + C_3 I_n(\bar{k}_1\bar{r}) + C_4 K_n(\bar{k}_1\bar{r})] \sin(n\theta) \right\} \tag{7.93a}$$

$$\begin{aligned}
&-n \left[\frac{\bar{k}_1}{2} [J_{n-1}(\bar{k}_1\bar{r}) - J_{n+1}(\bar{k}_1\bar{r})]C_1 + \frac{\bar{k}_1}{2} [Y_{n-1}(\bar{k}_1\bar{r}) - Y_{n+1}(\bar{k}_1\bar{r})]C_2 + \right. \\
&\quad \left. \frac{\bar{k}_1}{2} [I_{n-1}(\bar{k}_1\bar{r}) + I_{n+1}(\bar{k}_1\bar{r})]C_3 - \frac{\bar{k}_1}{2} [K_{n-1}(\bar{k}_1\bar{r}) + K_{n+1}(\bar{k}_1\bar{r})]C_4 \right] \cos(n\theta)
\end{aligned} \tag{7.94}$$

$$\frac{1}{\bar{r}^2} \frac{\partial w(\bar{r}, \theta)}{\partial \theta} = \frac{-n}{\bar{r}^2} [C_1 J_n(\bar{k}_1\bar{r}) + C_2 Y_n(\bar{k}_1\bar{r}) + C_3 I_n(\bar{k}_1\bar{r}) + C_4 K_n(\bar{k}_1\bar{r})] \sin(n\theta) \tag{7.95}$$

From equations (7.94) and (7.95) yields the following

$$\begin{aligned}
& \frac{\partial}{\partial \theta} \left[\frac{1}{\bar{r}} \frac{\partial^2 w(\bar{r}, \theta)}{\partial \bar{r} \partial \theta} - \frac{1}{\bar{r}^2} \frac{\partial w(\bar{r}, \theta)}{\partial \theta} \right] \\
&= -\frac{n^2}{\bar{r}} \left[\frac{\bar{k}_1}{2} [J_{n-1}(\bar{k}_1 \bar{r}) - J_{n+1}(\bar{k}_1 \bar{r})] C_1 + \frac{\bar{k}_1}{2} [Y_{n-1}(\bar{k}_1 \bar{r}) - Y_{n+1}(\bar{k}_1 \bar{r})] C_2 + \right. \\
&\quad \left. \frac{\bar{k}_1}{2} [I_{n-1}(\bar{k}_1 \bar{r}) + I_{n+1}(\bar{k}_1 \bar{r})] C_3 - \frac{\bar{k}_1}{2} [K_{n-1}(\bar{k}_1 \bar{r}) + K_{n+1}(\bar{k}_1 \bar{r})] C_4 \right] \cos(n\theta) + \\
&\quad \frac{n^2}{\bar{r}^2} [C_1 J_n(\bar{k}_1 \bar{r}) + C_2 Y_n(\bar{k}_1 \bar{r}) + C_3 I_n(\bar{k}_1 \bar{r}) + C_4 K_n(\bar{k}_1 \bar{r})] \cos(n\theta)
\end{aligned} \tag{7.96}$$

Equation (7.96) can be written as

$$\begin{aligned}
& (1-\nu) \frac{1}{\bar{r}} \frac{\partial}{\partial \theta} \left[\frac{1}{\bar{r}} \frac{\partial^2 w(\bar{r}, \theta)}{\partial \bar{r} \partial \theta} - \frac{1}{\bar{r}^2} \frac{\partial w(\bar{r}, \theta)}{\partial \theta} \right]_{\bar{r}=b} \\
&= (1-\nu) \left\{ -\frac{n^2}{b} \left[\frac{\bar{k}_1}{2} [J_{n-1}(\bar{k}_1 b) - J_{n+1}(\bar{k}_1 b)] C_1 + \frac{\bar{k}_1}{2} [Y_{n-1}(\bar{k}_1 b) - Y_{n+1}(\bar{k}_1 b)] C_2 + \right. \right. \\
&\quad \left. \frac{\bar{k}_1}{2} [I_{n-1}(\bar{k}_1 b) + I_{n+1}(\bar{k}_1 b)] C_3 - \frac{\bar{k}_1}{2} [K_{n-1}(\bar{k}_1 b) + K_{n+1}(\bar{k}_1 b)] C_4 \right] \cos(n\theta) + \\
&\quad \left. \frac{n^2}{b^3} [C_1 J_n(\bar{k}_1 b) + C_2 Y_n(\bar{k}_1 b) + C_3 I_n(\bar{k}_1 b) + C_4 K_n(\bar{k}_1 b)] \cos(n\theta) \right\}
\end{aligned} \tag{7.97}$$

$$\begin{aligned}
&= (1-\nu) \left\{ -\frac{n^2}{b} \left[\frac{\bar{k}_1}{2} [T_1'] C_1 + \frac{\bar{k}_1}{2} [U_{11}'] C_2 + \frac{\bar{k}_1}{2} [V_{11}'] C_3 - \frac{\bar{k}_1}{2} [W_1'] C_4 \right] \cos(n\theta) + \right. \\
&\quad \left. \frac{n^2}{b^3} [C_1 J_n(\bar{k}_1 b) + C_2 Y_n(\bar{k}_1 b) + C_3 I_n(\bar{k}_1 b) + C_4 K_n(\bar{k}_1 b)] \cos(n\theta) \right\}
\end{aligned} \tag{7.98}$$

Substituting $\bar{r} = b$ into equation (7.5) yields the following

$$\bar{w}_I(\bar{r}, \theta)_{\bar{r}=b} = [C_1 J_n(\bar{k}_1 b) + C_2 Y_n(\bar{k}_1 b) + C_3 I_n(\bar{k}_1 b) + C_4 K_n(\bar{k}_1 b)] \cos(n\theta) \tag{7.99}$$

Substituting equations (7.84), (7.89), (7.93), (7.98), (7.99) into equation (7.24) gives the following

$$\begin{aligned}
& \left[\frac{\bar{k}_1^3}{8} T_3' + \frac{\bar{k}_1^2}{4b} T_2' - \frac{\bar{k}_1}{2} \left(\frac{3}{4} \bar{k}_1^2 + n^2(2-\nu) + 1 \right) T_1' + \left(\frac{n^2(3-\nu)}{b^3} - \frac{\bar{k}_1^2}{2b} + T_{22} \right) J_n(\bar{k}_1 b) \right] C_1 + \\
& \left[\frac{\bar{k}_1^3}{8} U_3' + \frac{\bar{k}_1^2}{4b} U_2' - \frac{\bar{k}_1}{2} \left(\frac{3}{4} \bar{k}_1^2 + n^2(2-\nu) + 1 \right) U_1' + \left(\frac{n^2(3-\nu)}{b^3} - \frac{\bar{k}_1^2}{2b} + T_{22} \right) Y_n(\bar{k}_1 b) \right] C_2 + \\
& \left[\frac{\bar{k}_1^3}{8} V_3' + \frac{\bar{k}_1^2}{4b} V_2' + \frac{\bar{k}_1}{2} \left(\frac{3}{4} \bar{k}_1^2 + n^2(-2+\nu) - 1 \right) V_1' + \left(\frac{n^2(3-\nu)}{b^3} + \frac{\bar{k}_1^2}{2b} + T_{22} \right) I_n(\bar{k}_1 b) \right] C_3 + \\
& \left[-\frac{\bar{k}_1^3}{8} W_3' + \frac{\bar{k}_1^2}{4b} W_2' + \frac{\kappa}{2} \left(-\frac{3}{4} \bar{k}_1^2 + n^2(2-\nu) + 1 \right) W_1' + \left(\frac{n^2(3-\nu)}{b^3} + \frac{\bar{k}_1^2}{2b} + T_{22} \right) K_n(\bar{k}_1 b) \right] C_4 = 0
\end{aligned} \tag{7.100}$$

where

$$\begin{aligned}
T_1' &= J_{n-1}(\bar{k}_1 b) - J_{n+1}(\bar{k}_1 b); T_2' = J_{n-2}(\bar{k}_1 b) + J_{n+2}(\bar{k}_1 b); T_3' = J_{n-3}(\bar{k}_1 b) - J_{n+3}(\bar{k}_1 b); \\
U_1' &= Y_{n-1}(\bar{k}_1 b) - Y_{n+1}(\bar{k}_1 b); U_2' = Y_{n-2}(\bar{k}_1 b) + Y_{n+2}(\bar{k}_1 b); U_3' = Y_{n-3}(\bar{k}_1 b) - Y_{n+3}(\bar{k}_1 b); \\
V_1' &= I_{n-1}(\bar{k}_1 b) + I_{n+1}(\bar{k}_1 b); V_2' = I_{n-2}(\bar{k}_1 b) + I_{n+2}(\bar{k}_1 b); V_3' = I_{n-3}(\bar{k}_1 b) + I_{n+3}(\bar{k}_1 b); \\
W_1' &= K_{n-1}(\bar{k}_1 b) + K_{n+1}(\bar{k}_1 b); W_2' = K_{n-2}(\bar{k}_1 b) + K_{n+2}(\bar{k}_1 b); W_3' = K_{n-3}(\bar{k}_1 b) + K_{n+3}(\bar{k}_1 b); \\
\bar{k}_2 &= (\bar{k}_1^4 + \xi^2)^{1/4}
\end{aligned} \tag{7.101}$$

Where \bar{k}_1 is Frequency without foundation, \bar{k}_2 is Frequency with foundation

The following cases are considered for analysis.

CASE: 1 Annular plate when both the peripheries are elastically restrained against rotation and translation and also supporting on elastic foundation as shown in Fig. 7.1. The boundary conditions used for this case are Eqs. (7.11), (7.14), (7.21) and (7.24). The set of equations for this case are (7.40), (7.63), (7.78), and (7.100).

CASE: 2 Annular Plate when the outer periphery is elastically restrained against translation and the inner periphery is elastically restrained against rotation and translation and annular plate is resting on elastic foundation as shown in Fig. 7.2. Set $K_{R1} \rightarrow 0$ and

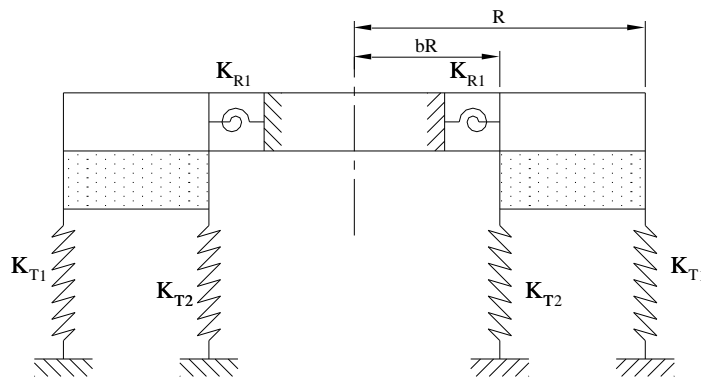


Fig. 7.2. Annular plate with Translational Constraints at inner edge and Rotational and Translational constraints at outer edge and resting on elastic foundation

Substituting $R_{11} \rightarrow 0$ into equation (7.6). Therefore, the boundary conditions from equations (7.6) and (7.7) are

$$M_r(\bar{r}, \theta) = 0 \quad (7.102)$$

$$V_r(\bar{r}, \theta) = -K_{T1} \bar{w}_I(\bar{r}, \theta) \quad (7.103)$$

The radial moment and the radial Kirchhoff shear at outer edge are defined as follows

$$M_r(\bar{r}, \theta) = -\frac{D}{R^3} \left[\frac{\partial^2 \bar{w}_I(\bar{r}, \theta)}{\partial \bar{r}^2} + \nu \left(\frac{1}{\bar{r}} \frac{\partial \bar{w}_I(\bar{r}, \theta)}{\partial \bar{r}} + \frac{1}{\bar{r}^2} \frac{\partial^2 \bar{w}_I(\bar{r}, \theta)}{\partial \theta^2} \right) \right] \quad (7.104)$$

$$V_r(\bar{r}, \theta) = -\frac{D}{R^3} \left[\frac{\partial}{\partial \bar{r}} \nabla^2 \bar{w}_I(\bar{r}, \theta) + (1-\nu) \frac{1}{\bar{r}} \frac{\partial}{\partial \theta} \left(\frac{1}{\bar{r}} \frac{\partial^2 \bar{w}_I(\bar{r}, \theta)}{\partial \bar{r} \partial \theta} - \frac{1}{\bar{r}^2} \frac{\partial \bar{w}_I(\bar{r}, \theta)}{\partial \theta} \right) \right] \quad (7.105)$$

From equations (7.102) and (7.104) yield

$$\left[\frac{\partial^2 \bar{w}_I(\bar{r}, \theta)}{\partial \bar{r}^2} + \nu \left(\frac{1}{\bar{r}} \frac{\partial \bar{w}_I(\bar{r}, \theta)}{\partial \bar{r}} + \frac{1}{\bar{r}^2} \frac{\partial^2 \bar{w}_I(\bar{r}, \theta)}{\partial \theta^2} \right) \right] = 0 \quad (7.106)$$

From equations (7.103) and (7.105) gives the following

$$\left[\frac{\partial}{\partial \bar{r}} \nabla^2 \bar{w}_I(\bar{r}, \theta) + (1-\nu) \frac{1}{\bar{r}} \frac{\partial}{\partial \theta} \left(\frac{1}{\bar{r}} \frac{\partial^2 \bar{w}_I(\bar{r}, \theta)}{\partial \bar{r} \partial \theta} - \frac{1}{\bar{r}^2} \frac{\partial \bar{w}_I(\bar{r}, \theta)}{\partial \theta} \right) \right] = \frac{K_{T1} R^3}{D} \bar{w}_I(\bar{r}, \theta) \quad (7.107)$$

$$\left[\frac{\partial}{\partial \bar{r}} \nabla^2 \bar{w}_I(\bar{r}, \theta) + (1-\nu) \frac{1}{\bar{r}} \frac{\partial}{\partial \theta} \left(\frac{1}{\bar{r}} \frac{\partial^2 \bar{w}_I(\bar{r}, \theta)}{\partial \bar{r} \partial \theta} - \frac{1}{\bar{r}^2} \frac{\partial \bar{w}_I(\bar{r}, \theta)}{\partial \theta} \right) \right] = T_{11} \bar{w}_I(\bar{r}, \theta) \quad (7.108)$$

$$\text{where } T_{11} = \frac{K_{T1} R^3}{D} \quad (7.109)$$

Equations (7.5) and (7.106) yields the following

$$\begin{aligned} & \left[\frac{\bar{k}_1^2}{4} T_2 + \frac{\bar{k}_1 \nu}{2} T_1 - \left(\frac{\bar{k}_1^2}{2} + m^2 \right) J_n(\bar{k}_1) \right] C_1 + \left[\frac{\bar{k}_1^2}{4} U_2 + \frac{\bar{k}_1 \nu}{2} U_1 - \left(\frac{\bar{k}_1^2}{2} + m^2 \right) Y_n(\bar{k}_1) \right] C_2 + \\ & \left[\frac{\bar{k}_1^2}{4} V_2 + \frac{\bar{k}_1 \nu}{2} V_1 + \left(\frac{\bar{k}_1^2}{2} - m^2 \right) I_n(\bar{k}_1) \right] C_3 + \left[\frac{\bar{k}_1^2}{4} W_2 - \frac{\bar{k}_1 \nu}{2} W_1 + \left(\frac{\bar{k}_1^2}{2} - m^2 \right) K_n(\bar{k}_1) \right] C_4 = 0 \end{aligned} \quad (7.110)$$

Therefore, the set of equations for this case are equations (7.110), (7.63), (7.78) and (7.100).

CASE: 3 Annular plate when the outer periphery is elastically restrained against Rotation and simply supported and the inner periphery is elastically restrained against rotation and translation and it is resting on elastic foundation as shown in Fig. 7.3.

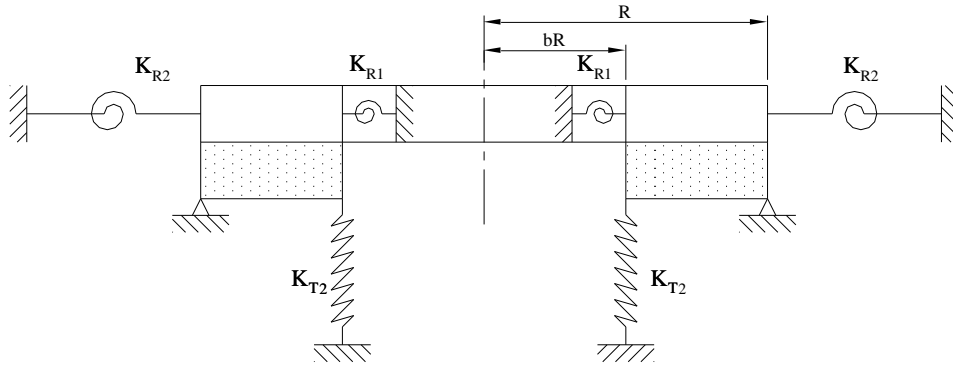


Fig. 7.3. Annular plate with Rotational Constraint and simply supported at inner edge and Rotational and Translational Constraints at outer edge and resting on elastic foundation

Set $K_T \rightarrow \infty$ and substitute this condition in equation (7.7). Therefore, the boundary conditions from equations (7.6) and (7.7) are

$$M_r(\bar{r}, \theta) = K_{R1} \frac{\partial \bar{w}_I(\bar{r}, \theta)}{\partial \bar{r}} \quad (7.111)$$

$$\bar{w}_I(\bar{r}, \theta) = 0 \quad (7.112)$$

Equations (7.6) and (7.107) yields the following

$$[J_n(\bar{k}_1)]C_1 + [Y_n(\bar{k}_1)]C_2 + [I_n(\bar{k}_1)]C_3 + [K_n(\bar{k}_1)]C_4 = 0 \quad (7.113)$$

Therefore, the set of equations for this are (7.40), (7.113), (7.78) and (7.100).

7.4 Solution

For the given values of $n, \nu, R_{11}, T_{11}, R_{22}, T_{22}$ & ξ the above set of equations, gives an exact characteristic equation for non-trivial solutions of the coefficients C_1, C_2, C_3 & C_4 . For non-trivial solution, the determinant of $[C]_{4 \times 4}$ must vanish. Using Mathematica, computer software with symbolic capabilities, solves this problem.

7.5 Results

The Poisson's ratio used in this work is $\nu=0.3$. The findings are presented in both tabular and graphical form.

CASE: 1 Annular plate when both the peripheries are elastically restrained against rotation and translation and resting on elastic foundation

The variation of the non-dimensional frequency parameter with rotational constraint is presented in Table 7.1. It is calculated for different values of non-dimensional rotational spring stiffness parameters R_{11} , and non-dimensional radii. i.e. from $b = 0.1$ to 0.9 by keeping $T_{11}, R_{22}, T_{22}, \& \xi$ constant. Fig. 7.4 shows the effect of rotational spring stiffness parameter on frequency parameter. It is observed from the Fig. 7.4 that the frequency increases with increase in rotational spring stiffness parameter. But it is observed that the influence of rotational spring stiffness parameter is very less. For a given radius parameter $b = 0.1$, the frequency parameter is increased by 8.55% when R_{11} increased from 0 to ∞ . Similarly for a given R_{11} (0 and ∞), the frequency parameter is increased by 86.27% and 71.66% respectively when b increased from 0.1 to 0.9. It was found that the $n=0$ axisymmetric mode gives the fundamental frequency. When $b=0$, the plate has full foundation support and the frequency is $\bar{k}_2=10.0056$. This is in well agreement with the results ($\bar{k}_2=10.00568$) obtained by Bhaskara Rao and Kameswara Rao [76]. Table 7.2, shows the comparison of results (for $R_{11}=20, T_{11}=R_{22}=T_{22}=100 \& \xi=0$), with the values obtained by Bhaskara Rao and Kameswara

Rao [90]. The variation of the non-dimensional frequency with translational spring stiffness parameter is presented in Table 7.3. It is calculated for different values of non-dimensional translational spring stiffness parameter T_{11} , and non-dimensional radii. i.e. from $b=0.1$ to 0.9 by keeping $R_{11}, R_{22}, T_{22}, \& \xi$ constant. The effect of translational spring stiffness parameter on frequency is plotted in Fig. 7.5. It is noticed from the Fig. 7.5, that the frequency increases with increase in translational spring stiffness parameter. For a given radius parameter $b=0.1$, the frequency parameter is increased by 27.35% when T_{11} increased from 0 to ∞ . Similarly for a given T_{11} (0 and ∞), the frequency parameter is increased by 74.39% and 417.66% respectively when b increased from 0.1 to 0.9. It is observed from Figs. 7.4 and 7.5, that in the former case the higher values of frequencies are recorded at lower values of R_{11} , but in the latter case lower frequency parameters are observed at lower values of T_{11} . Therefore, it is observed from the above, that the influence of T_{11} is more than that of R_{11} on frequency parameter. It was found that the $n=0$ axisymmetric mode gives the fundamental frequency. When $b=0$, the plate has full foundation support and the frequency is $\bar{k}_2=10$. This is in well agreement with the results ($\bar{k}_2=10$) obtained by Bhaskara Rao and Kameswara Rao [76].

Table 7.1 Frequency Parameter For Different Rotational Stiffness Parameters R_{11} , when $T_{11} = R_{22} = T_{22} = 100$ & $\xi = 10$ & $\nu = 0.3$

R_{11}	$b=0.1$	$b=0.2$	$b=0.3$	$b=0.4$	$b=0.5$	$b=0.6$	$b=0.7$	$b=0.8$	$b=0.9$
0	3.63258	3.84745	4.05488	4.27604	4.52517	4.82115	5.19732	5.73715	6.76639
5	3.80489	4.00748	4.19703	4.39537	4.61716	4.88213	5.22794	5.74634	6.76727
10	3.85428	4.05362	4.23774	4.42886	4.64223	4.89851	5.23655	5.7494	6.76768
15	3.87769	4.07551	4.25699	4.44457	4.65389	4.90609	5.24061	5.75093	6.76793
20	3.89135	4.08828	4.26819	4.45368	4.66062	4.91047	5.24296	5.75185	6.76808
50	3.92017	4.11525	4.29179	4.47278	4.67466	4.91958	5.24792	5.75385	6.76847
100	3.93126	4.12562	4.30084	4.48007	4.68	4.92304	5.24982	5.75464	6.76865
500	3.94076	4.13451	4.30859	4.48629	4.68454	4.92599	5.25144	5.75533	6.76881
1000	3.94199	4.13566	4.30959	4.4871	4.68513	4.92637	5.25165	5.75542	6.76883
2000	3.94261	4.13624	4.31009	4.4875	4.68543	4.92656	5.25176	5.75547	6.76884
10000	3.94311	4.1367	4.3105	4.48783	4.68566	4.92671	5.25184	5.7555	6.76885
1.00E+17	3.94323	4.13682	4.3106	4.48791	4.68572	4.92675	5.25187	5.75551	6.76885

Table 7.2 Comparison of Frequency Parameter for $R_{11} = 20, T_{11} = R_{22} = T_{22} = 100$ & $\xi = 0$

b	Thesis	Bhaskara Rao and Kameswara Rao [76]
0.1	3.3721	3.3721
0.3	3.90231	3.90231
0.5	4.39123	4.39123
0.7	5.06017	5.06017

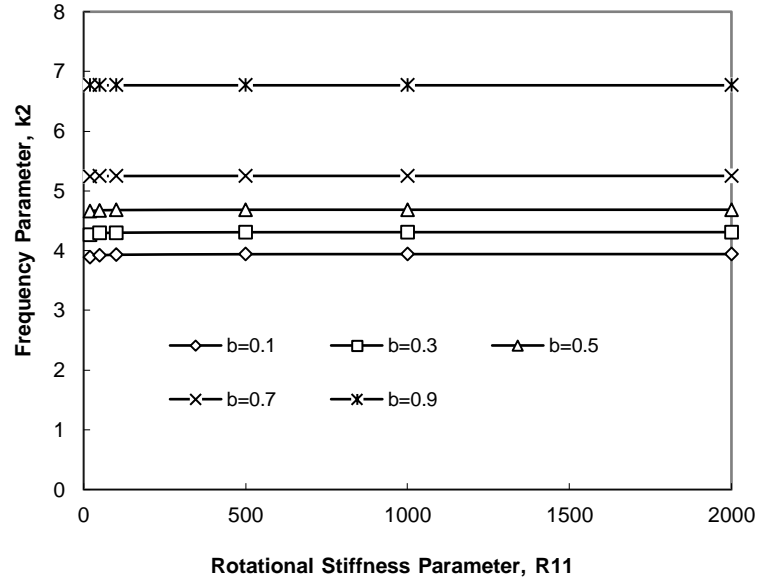


Fig. 7.4 Effect of Non-Dimensional Rotational Spring Stiffness R_{11} , on Frequency Parameter for $T_{11} = R_{22} = T_{22} = 100$ & $\xi = 10$

Table 7.3 Frequency for Different Translational stiffness Parameter T_{11} , when $R_{11} = R_{22} = T_{22} = 100$ & $\xi = 10$ & $\nu = 0.3$

T_{11}	$b = 0.1$	$b = 0.2$	$b = 0.3$	$b = 0.4$	$b = 0.5$	$b = 0.6$	$b = 0.7$	$b = 0.8$	$b = 0.9$
0	3.25945	3.33815	3.44098	3.5829	3.77362	4.02115	4.34404	4.80796	5.68426
5	3.34418	3.42658	3.52876	3.66636	3.85014	4.0903	4.40805	4.8713	5.75497
10	3.41781	3.50478	3.60749	3.74231	3.9209	4.15529	4.46899	4.93212	5.82315
15	3.4822	3.57443	3.67859	3.81186	3.98666	4.21658	4.52717	4.99065	5.88899
20	3.53878	3.63682	3.74316	3.87586	4.04802	4.27454	4.58283	5.04706	5.95267
50	3.7658	3.90366	4.03252	4.17484	4.34673	4.5682	4.87433	5.34908	6.29712
100	3.93126	4.12562	4.30084	4.48007	4.68	4.92304	5.24982	5.75464	6.76865
500	4.10705	4.39444	4.68777	5.02522	5.44109	5.96746	6.62394	7.46605	8.8894
1000	4.12919	4.42907	4.74195	5.11503	5.60356	6.28449	7.23442	8.47348	10.3016
2000	4.14008	4.44594	4.76834	5.1594	5.68758	6.46844	7.68424	9.48856	12.0056
10000	4.14868	4.45917	4.78897	5.19419	5.75453	6.62279	8.12828	11.0338	16.6507
1.00E+16	4.15081	4.46244	4.79405	5.20275	5.77108	6.66164	8.24751	11.5861	21.4874

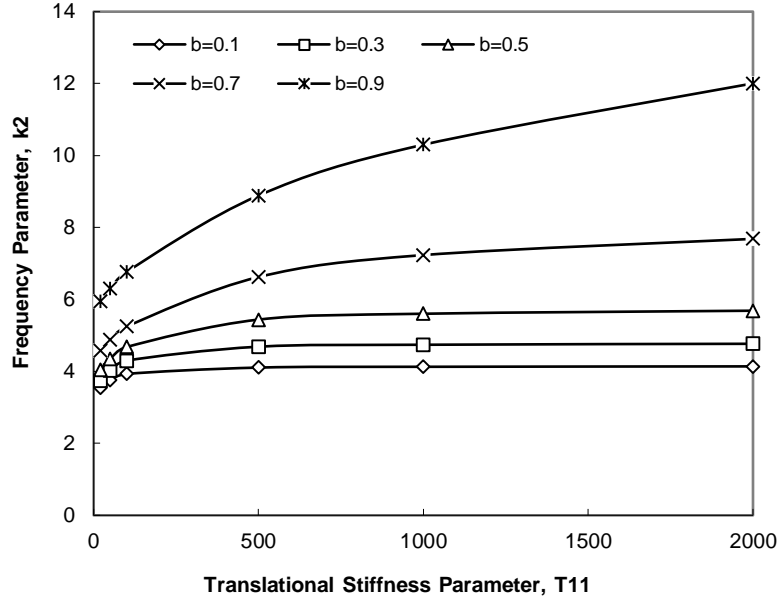


Fig. 7.5 Effect of Non-Dimensional Translational Spring Stiffness Parameter T_{11} , on Frequency Parameter for $R_{11} = R_{22} = T_{22} = 100$ & $\xi = 10$

The variation of the non-dimensional frequency with foundation constraint is presented in Table 7.4. It is calculated for different values of non-dimensional foundation stiffness parameter ξ , and non-dimensional radii. i.e. from $b = 0.1$ to 0.9 by keeping R_{11}, T_{11}, R_{22} & T_{22} constant. It is observed from the Fig. 7.6, the frequency increases with increase in foundation stiffness parameter. For a given radius parameter, the frequency increases with increase in foundation stiffness parameter. For a given radius parameter $b = 0.1$, the frequency parameter is increased by 192.32% when ξ increased from 0 to 100. Similarly for a given ξ (0 and 100), the frequency parameter is increased by 94.79% and 4.3% respectively when b increased from 0.1 to 0.9. As observed from Figs. 7.4, 7.5 and 7.6, the influence of foundation constraint is more on the frequency when compared to rotational and translational constraints. It was found that the $n = 0$ axisymmetric mode gives the fundamental frequency. When $b = 0$, the plate has full foundation support and the frequency is $\bar{k}_2 = 2.94751$. This is in well

agreement with the results ($\bar{k}_2=2.94751$) obtained by Bhaskara Rao and Kameswara Rao [76].

Table 7.4 Frequency for Different Foundation Stiffness Parameters ξ , when $T_{11} = R_{11} = R_{22} = T_{22} = 100$ & $\nu = 0.3$

ξ	$b=0.1$	$b=0.2$	$b=0.3$	$b=0.4$	$b=0.5$	$b=0.6$	$b=0.7$	$b=0.8$	$b=0.9$
0	3.43271	3.71125	3.94476	4.17163	4.41432	4.69863	5.06778	5.61871	6.68655
2.5	3.47071	3.74145	3.96997	4.19298	4.43238	4.71362	5.07974	5.6275	6.69177
5	3.57777	3.8279	4.04285	4.25517	4.48526	4.75776	5.11513	5.65362	6.70735
7.5	3.73736	3.96017	4.15622	4.35314	4.56944	4.8287	5.17254	5.69637	6.7331
10	3.93126	4.12562	4.30084	4.48007	4.68	4.92304	5.24982	5.75464	6.76865
12.5	4.1447	4.31276	4.46765	4.62888	4.81154	5.03689	5.34442	5.82705	6.81354
15	4.36748	4.51269	4.64904	4.79321	4.95893	5.16632	5.45362	5.91205	6.86724
17.5	4.59319	4.71912	4.8392	4.96788	5.11771	5.30771	5.57476	6.00798	6.92912
20	4.818	4.92787	5.03395	5.14891	5.28426	5.45795	5.70537	6.11326	6.99852
50	7.16727	7.20155	7.2364	7.27612	7.3255	7.39305	7.49735	7.68977	8.1899
100	10.0345	10.0471	10.06	10.0749	10.0936	10.1197	10.161	10.2404	10.4661
500	22.3638	22.3649	22.3661	22.3674	22.3692	22.3716	22.3754	22.3829	22.4052
1000	31.6239	31.6243	31.6247	31.6252	31.6258	31.6266	31.628	31.6307	31.6386
2000	44.7217	44.7219	44.722	44.7222	44.7224	44.7227	44.7232	44.7241	44.7269
10000	100	100	100	100	100	100	100	100	100
1.00E+17	1.00E+08	1.00E+08	1.00E+08	1.00E+08	1.00E+08	1.00E+08	1.00E+08	1.00E+08	1.00E+08

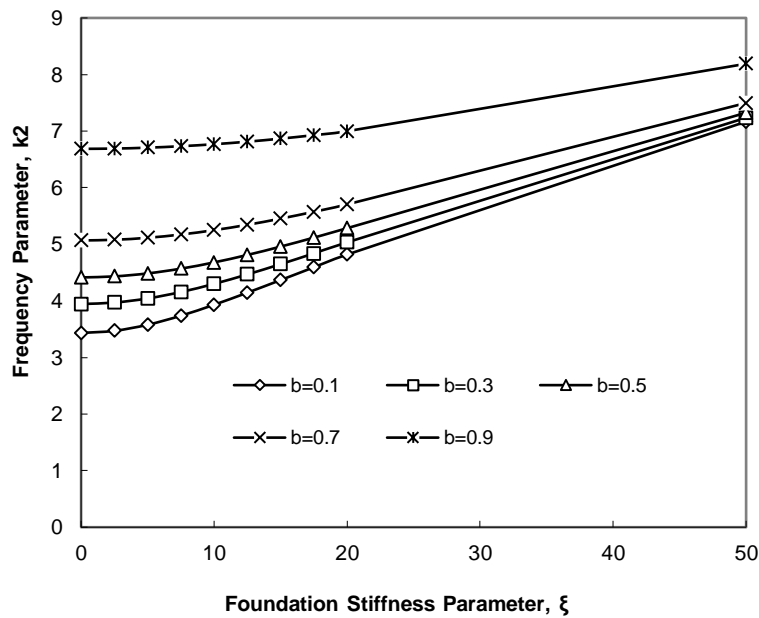


Fig. 7.6 Effect of Non-Dimensional Foundation Stiffness ξ , on Frequency Parameter for $R_{11} = T_{11} = R_{22} = T_{22} = 100$

The variation of the non-dimensional frequency with rotational, translational and foundation constraints is presented in Table 7.5. It is calculated for different values of non-

dimensional rotational, translational and foundation constraints and non-dimensional radii. i.e. from $b=0.1$ to 0.9 by keeping R_{22} & T_{22} constant. In Fig. 7.7, the effect of the three elastic constraints on frequency has been plotted and it is observed that the frequency increases with increase in the three elastic constraints. It is also shown frequency versus internal radius parameter in Fig. 7.8. For a given radius parameter $b=0.1$, the frequency parameter is increased by 161.19% when R_{11}, T_{11} & ξ increased from 0 to 20. Similarly for a given R_{11}, T_{11} & ξ (0 and 20), the frequency parameter is increased by 212.93% and 35.87% respectively when b increased from 0.1 to 0.9. It was found that the $n=0$ axisymmetric mode gives the fundamental. When $b=0$, the plate has full foundation support and the frequency is $\bar{k}_2=0.211466$. This is in well agreement with the results ($\bar{k}_2=0.211466$) obtained by Bhaskara Rao and Kameswara Rao [76]. Figs. 7.4, 7.5, 7.6, & 7.7 depict the variation of frequency as a function of the non-dimensional spring parameters i.e., both rotational and translational at inner and outer periphery of the annular plate and elastic foundation parameter.

Table 7.5 Frequency for Different Rotational R_{11} , Translational T_{11} , and Foundation ξ , Stiffness Parameters when $R_{22} = T_{22} = 100$ & $\nu = 0.3$

R_{11}, T_{11} & ξ	$b=0.1$	$b=0.2$	$b=0.3$	$b=0.4$	$b=0.5$	$b=0.6$	$b=0.7$	$b=0.8$	$b=0.9$
0	1.76955	2.02461	2.28783	2.59986	2.97468	3.41419	3.91811	4.53447	5.53745
2.5	2.23244	2.43938	2.65666	2.91404	3.22274	3.58906	4.02777	4.60166	5.58666
5	2.65932	2.80828	2.9742	3.18014	3.43748	3.7547	4.15021	4.69005	5.65138
7.5	3.05508	3.16621	3.29371	3.45733	3.66964	3.94209	4.2962	4.79985	5.73031
10	3.41743	3.50455	3.6055	3.73744	3.9133	4.14667	4.46175	4.92784	5.82182
12.5	3.75083	3.82204	3.90451	4.01317	4.16054	4.36122	4.64106	5.07014	5.92418
15	4.06014	4.1203	4.18954	4.28091	4.40616	4.58005	4.82904	5.22313	6.03568
17.5	4.34941	4.40154	4.46101	4.53932	4.6473	4.79934	5.02179	5.38367	6.15471
20	4.62181	4.6679	4.71995	4.78817	4.88251	5.01671	5.21651	5.54926	6.27984

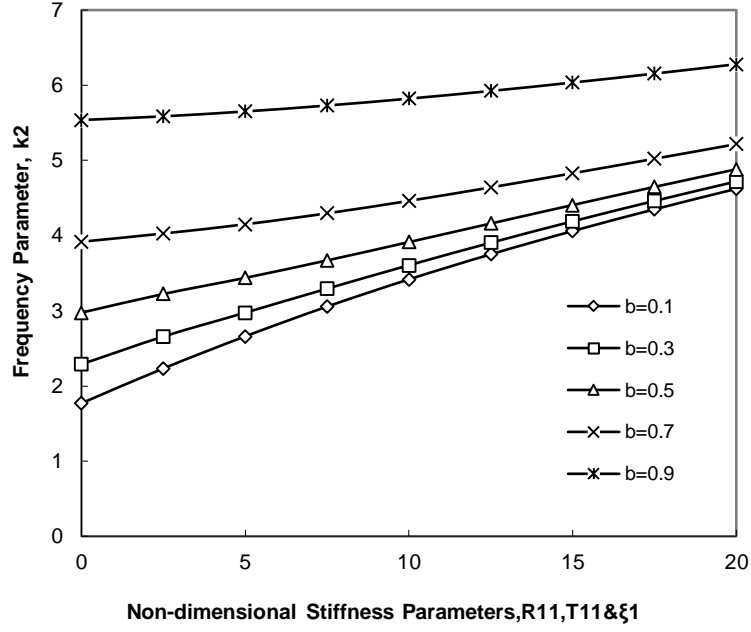


Fig. 7.7 Effect of Non-Dimensional Rotational R_{11} , Translational T_{11} , and Foundation ξ , Stiffness Parameters on Frequency Parameter for $R_{22} = T_{22} = 100$

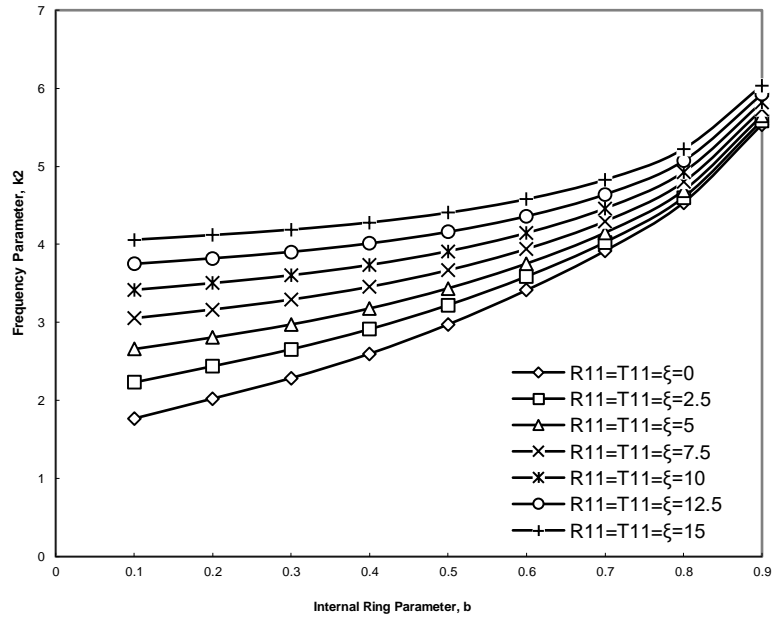


Fig. 7.8 Effect of Non-Dimensional Rotational Stiffness R_{11} , Translational Stiffness T_{11} , and Foundation Stiffness ξ , Parameters on Frequency Parameter for $R_{22} = T_{22} = 100$

The variation of the non-dimensional frequency parameter with rotational constraint R_{22} , is presented in Table 7.6. It is calculated for different values of non-dimensional rotational spring stiffness parameters R_{22} , and non-dimensional radii. i.e. from $b = 0.1$ to 0.9

by keeping $R_{11}, T_{11}, T_{22}, \&\xi$ constant. Fig. 7.9 shows the effect of rotational spring stiffness parameter on frequency parameter. It is observed from the Fig. 7.9 that the frequency increases with increase in rotational spring stiffness parameter. But it is observed that the influence of rotational spring stiffness parameter is very less. For a given radius parameter $b=0.1$, the frequency parameter is increased by 0.09% when R_{22} increased from 0 to ∞ . Similarly for a given R_{22} (0 and ∞), the frequency parameter is increased by 72.27% and 72.17% respectively when b increased from 0.1 to 0.9. It was found that the $n=0$ axisymmetric mode gives the fundamental frequency. The variation of the non-dimensional frequency with translational spring stiffness parameter T_{22} , is presented in Table 7.7. It is calculated for different values of non-dimensional translational spring stiffness parameter T_{22} , and non-dimensional radii. i.e. from $b=0.1$ to 0.9 by keeping $R_{11}, R_{22}, T_{11}, \&\xi$ constant. The effect of translational spring stiffness parameter on frequency is plotted in Fig. 7.10. It is noticed from the Fig. 7.10, that the frequency increases with increase in translational spring stiffness parameter. It was found that the $n=0$ axisymmetric mode gives the fundamental frequency. For a given radius parameter $b=0.1$, the frequency parameter is increased by 20.84% when T_{22} increased from 0 to ∞ . Similarly for a given T_{22} (0 and ∞), the frequency parameter is increased by 58.93% and 376.52% respectively when b increased from 0.1 to 0.9.

It is observed from the above discussion that the influence of foundation stiffness parameter is more on frequency than that of rotational and translational stiffness parameters at inner and outer edges $R_{11}, R_{22}, T_{11} \& T_{22}$. And also it observed that the influence of translational stiffness parameters is more on frequency than that of rotational stiffness parameters $R_{11} \& R_{22}$. It also noticed that the influence of elastic constraints at outer edge

R_{11} & T_{11} , on frequency is more predominant than that of elastic constraints at inner edge

R_{22} & T_{22} .

Table 7.6 Frequency For Different Rotational Stiffness Parameters R_{22} , when $R_{11} = T_{11} = T_{22} = 100$, $\xi = 10$ & $\nu = 0.3$

R_{22}	$b = 0.1$	$b = 0.2$	$b = 0.3$	$b = 0.4$	$b = 0.5$	$b = 0.6$	$b = 0.7$	$b = 0.8$	$b = 0.9$
0	3.92815	4.11186	4.2803	4.45695	4.65683	4.90211	5.23425	5.74694	6.76718
5	3.92939	4.1185	4.29092	4.46938	4.66965	4.91388	5.24286	5.75082	6.76773
10	3.92996	4.12099	4.29454	4.47338	4.67359	4.9174	5.24551	5.75219	6.768
15	3.93029	4.12229	4.29637	4.47535	4.67551	4.9191	5.24679	5.75289	6.76816
20	3.93051	4.12309	4.29747	4.47653	4.67664	4.9201	5.24755	5.75332	6.76827
50	3.93103	4.12489	4.29988	4.47907	4.67906	4.92222	5.24918	5.75426	6.76853
100	3.93126	4.12562	4.30084	4.48007	4.68	4.92304	5.24982	5.75464	6.76865
500	3.93147	4.12627	4.30168	4.48094	4.68081	4.92375	5.25037	5.75497	6.76875
1000	3.9315	4.12636	4.30179	4.48105	4.68092	4.92384	5.25044	5.75502	6.76877
2000	3.93152	4.1264	4.30185	4.48111	4.68097	4.92389	5.25047	5.75504	6.76878
10000	3.93153	4.12643	4.30189	4.48115	4.68101	4.92393	5.2505	5.75506	6.76878
1.00E+16	3.93153	4.12644	4.3019	4.48116	4.68102	4.92394	5.25051	5.75506	6.76878

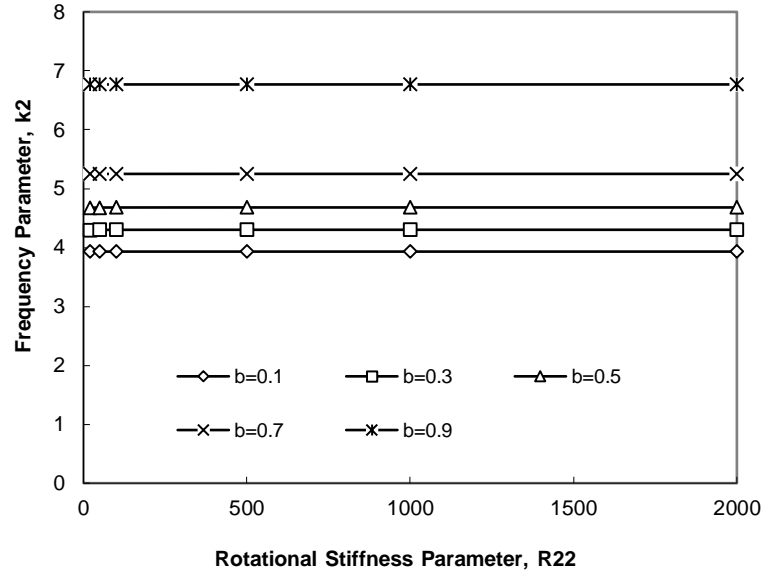


Fig. 7.9 Effect of Non-Dimensional Rotational Spring Stiffness R_{22} , on Frequency Parameter for $R_{11} = T_{11} = T_{22} = 100$ & $\xi = 10$

Table 7.7 Frequency for Different Translational Stiffness Parameters T_{22} when $R_{11} = R_{22} = T_{11} = 100$ & $\xi = 10$ & $\nu = 0.3$

T_{22}	$b = 0.1$	$b = 0.2$	$b = 0.3$	$b = 0.4$	$b = 0.5$	$b = 0.6$	$b = 0.7$	$b = 0.8$	$b = 0.9$
0	3.66318	3.73218	3.84143	3.98742	4.16619	4.37874	4.64501	5.03547	5.82194
5	3.68156	3.76209	3.87708	4.02468	4.20296	4.41524	4.68353	5.08024	5.88141
10	3.69925	3.79047	3.9108	4.06002	4.23809	4.45039	4.72087	5.12377	5.93911
15	3.7163	3.81743	3.94272	4.09359	4.27168	4.4843	4.75711	5.16611	5.99515
20	3.73274	3.84307	3.97298	4.1255	4.30384	4.51703	4.79232	5.20736	6.04965
50	3.81994	3.97338	4.12543	4.28801	4.47143	4.69216	4.98464	5.43465	6.34889
100	3.93126	4.12562	4.30084	4.48007	4.68	4.92304	5.24982	5.75464	6.76865
500	4.24848	4.46954	4.68681	4.94135	5.27003	5.71987	6.34349	7.22232	8.73899
1000	4.33208	4.54037	4.76481	5.04475	5.43192	6.00926	6.88341	8.13689	10.0868
2000	4.37837	4.57721	4.80527	5.09989	5.52379	6.19455	7.31088	9.08465	11.7285
10000	4.41683	4.6069	4.83787	5.14493	5.60137	6.36261	7.77088	10.6049	16.2457
1.00E+16	4.42655	4.61431	4.846	5.15625	5.62117	6.40691	7.90275	11.19	21.0936

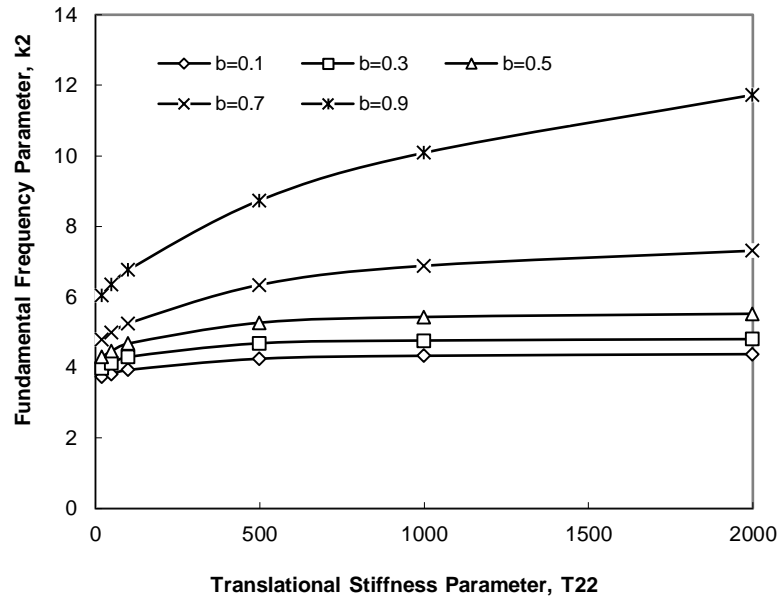


Fig. 7.10 Effect of Non-Dimensional Translational Spring Stiffness Parameter T_{22} , on Natural Frequency for $R_{11} = R_{22} = T_{11} = 100$ & $\xi = 10$

An investigation on the effect of Poisson's ratio, on the frequency is also studied. Each of the equations is reevaluated for values of Poisson's ratio between 0 and 0.5, and no significant variation is observed. Results are scarce in the literature. However, natural frequencies of two cases are determined to confirm the validation of certain results. Table 9.8, shows a comparison of results, in the case where both boundaries of the plate are rigidly clamped with the values obtained by Leissa, A. W. [17], Avalos, D. R. et al. [21]) and Amabili, M et al. [91]. However, in the reference (Avalos, D. R. et al. [21]), the results were obtained by approximate method.

Table 7.8. Comparison of Frequency Parameters when Both the Boundaries of the Plate are Rigidly Clamped

b	Present	Leissa, A. W. [17]	Avalos, D. R. et al. [21]	Amabili, M et al. [91]
0.1	27.280	27.3	27.67	27.280
0.3	45.346	45.2	45.37	45.346
0.5	89.250	89.2	89.31	89.250
0.7	248.399	248	248.9	248.40

Table 7.9, deals with the case where the inner boundary of the plate is simply supported and the outer boundary are rigidly clamped. Present results are compared with the results obtained by Leissa, A. W. [17] and Avalos, D. R. et al. [21]. [17] and [21] which correspond to the same Poisson's ratio ($\nu=1/3$). Also, the results are in good agreement with the results obtained by Amabili, M et al. [91] for the following two cases. (i) Annular plate with outer clamped edge and inner free edge as shown in Table 7.10 (ii) Annular plate with both edges free are shown in Table 7.11

Table 7.9 Comparison of Frequency Parameters when both the Inner Boundary of the Plate is Simply Supported and Outer Boundary of the Plate is Rigidly Clamped

b	Present	Leissa, A. W. [17]	Avalos, D. R. et al. [21]
0.1	22.595	22.58	22.83
0.3	33.663	33.66	33.66
0.5	63.977	64	63.94

Table 7.10 Comparison of Frequency Parameters when Outer Boundary is Clamped and Inner Boundary is Free

b	0	0.1	0.3	0.5	0.7
Present Work	3.19622	3.18736	3.37991	4.20886	6.56827
Amabili, M et al. [91]	3.19622	3.18736	3.37991	4.20886	6.56828

Table 7.11 Comparison of Frequency Parameters when Both Edges free ends

b	0	0.1	0.3	0.5	0.7
Present Work	3.00052	2.96219	2.89024	3.0518	3.62809
Amabili, M et al. [91]	3.00052	2.96219	2.89024	3.05180	3.62809

It is observed that, the influence of translational stiffness parameter on frequency is more predominant than that of rotational stiffness parameter. And also, it is observed that the influence of foundation parameter on frequency is more predominant than that of translational or rotational parameters. It is also noticed that the influence of elastic constraints

at outer edge R_{11} & T_{11} , on frequency is more predominant than that of elastic constraints at inner edge R_{22} & T_{22} . An investigation on the effect of Poisson's ratio, on the frequency is studied. Each of the equations is reevaluated for values of Poisson's ratio between 0 and 0.5, and no significant variation is observed. The wide range of values could be potentially used in vibration control and structural design.

CHAPTER 8

CONCLUSIONS

8.1 Conclusions

Research on easily understood engineering approaches for analysis of plates resting on elastic foundations has not been covered sufficiently in the literature. For particular plate problems, closed form solutions have been obtained. However, even for conventional plate analysis these solutions can only be applied to the problems with simple geometry, load and boundary conditions.

The first aim has been to review the governing differential equations of plate elements. After obtaining solutions of the governing differential equations, exact solutions have been derived by imposing boundary conditions.

It is important to know the natural frequencies for predicting the dynamic response of structures. The Kirchhoff's classical approach is used to derive the "exact frequency

equations” with necessary boundary conditions. It is observed that many researchers had considered only classical boundary conditions in determining the natural frequencies. However, in this thesis the effect of rotational and translational restraints are considered in determining the buckling loads and frequencies.

A wide range of complicated circular and annular plate problems (such as plate analysis, plate with elastically restrained edges and plate on elastic foundation) are solved by this exact solution. It has been verified the validity of our results with a broad range of applications such as buckling and vibration of plates with elastically restrained edges on elastic foundation and internal elastic ring supports.

From the derivations and applications of this dissertations some general points can be underlined as follows

In this dissertation the response of plates underlain by a Winkler foundation for the same problem was compared in many applications. From these results, it is inferred that presence of foundation parameter in the analysis is remarkably dominant. For instance, it gives smaller displacements so that smaller internal stresses, larger buckling loads and larger free vibration frequencies.

It is observed that the buckling load parameters increase as the foundation parameters increase. Also it is observed that the fundamental frequencies increase as the foundation parameters increase.

8.2 Future Scope of Studies

Some assumptions have been used throughout the present study. Under these assumptions, our solution strategy can be extended to many applications. The following assumptions are drawn.

1. In this solution, nonlinear effects of both plates and foundation are not included.

One can apply the solution to analyze plates with elastic foundation only if displacement field consists of small deflections.

2. Depth effect of foundation is ignored in response. Since properties of continuum may change significantly at a considerable depth, depth effect may be needed for certain types of problems.

3. Shear deformation, friction and torsional changes due to foundation parameters are not included.

4. The foundation parameters are assumed to be constant and equal in tension and compression. In the general case, the foundation behaves differently, cannot take any tension. An iterative technique can be adapted to this solution for plates on tensionless foundations.

5. In this study, the foundation parameters are assumed to be constants and their properties are not considered. Both experimental and theoretical studies must be performed.

6. This study could be extended to orthographic materials.

REFERENCES

1. Brush, D. O. and Almroth, B. O., 1975, "Buckling of bars, plates and shells", McGraw-Hill, New York.
2. Laura, P. A. A., Gutierrez, R. H., Sanzi, H. C., Elvira, G., 2000, "Buckling of circular, solids and annular plates with an intermediate circular support", *Ocean Engineering*, 27, pp. 749-755.
3. Wang, C. Y. and Wang, C. M., 2001, "Buckling of circular plates with an internal ring support and elastically restrained edges", *Thin-Walled Structures*, 39, pp. 821-825.
4. Reismann, H., 1952, "Bending and Buckling of an elastically restrained circular plate", *Journal of Applied Mechanics*, 19, pp. 167-172.
5. Kerr, A. D., 1962, "On the instability of circular plates", *Journal of aerospace Science*, 29, pp. 486-487.
6. Thevendran, V., Wang, C. M., 1996, "Buckling of annular plates elastically restrained against rotation along edges", *Thin-Walled Structures*, 25, pp. 231-246.
7. Yu, Y. Y., 1957, "Axisymmetrical Bending of Circular plates under simultaneous action of lateral load, Force in the middle plane, and Elastic Foundation", *Journal of Applied Mechanics*, 24, pp. 141-143.
8. Galletly, G. D., 1959, "Circular plates on a generalized elastic foundation", *Journal of Applied Mechanics*, 26, pp. 297.
9. Kline, L.V., and Hancock, J. O., 1965, "Buckling of circular plate on Elastic Foundation", *J. Eng. Ind.*, 87, pp. 323-324.
10. Wolkowisky, J. H., 1969, "Buckling of the circular plate Embedded in Elastic springs, an application to Geophysics", *Commun. Pure Appl. Math*, 22, pp. 367-667.
11. Elishakoff, I., Tang, J., 1988, "Buckling of polar orthographic circular plates on elastic-foundation by computerized symbolic algebra", *Computer Methods in Applied Mechanics and Engineering*, 68, pp. 229-247.

12. Wang, C. M., et al., 1997, "Relationships between buckling loads of Kirchhoff, Mindlin and Reddy polygonal plates on Pasternak foundation", *Journal of Engineering and Mechanics*, ASCE, 123(11), pp. 1134-1137.
13. Wang, C. Y., 2005, "On the Buckling of a Circular Plate on an Elastic Foundation", 72, pp. 795-796.
14. Yamaki, N., 1958, "Buckling of a Thin Annular Plate under Uniform Compression", *Journal of Applied Mechanics*, 25, pp. 267-273.
15. Chladni, E. F. F., 1803, *Die Akustik*, Leipzig.
16. Poisson, S. D., 1829, "Memories de l' Academie Rolyalesdes Sciences del' Institute de la France", ser. 28, 357. L'Equilibre et le mouvement des corps elastiques.
17. Leissa, A. W., 1969, *Vibration of plates*, SP-160, US Government Printing Office, Washington, DC.
18. Leissa, A. W., 1977, "Recent research in plate vibrations; classical theory", *Shock and Vibration Digest* 9, pp. 13-24.
19. Pardoen, G. C., 1978, "Asymmetric vibration and stability of circular plates".
20. Leissa, A. W., Laura, P.A. A., Gutierrez., 1979, "Transverse Vibrations of Circular Plates having non uniform edge Constraints", *Journal of Acoustical Society of America*, 66(1), pp. 180-184.
21. Avalos, D., Laura, P. A. A. and Bianchi, A. M., 1987, "Analytical and experimental investigation on Vibrating Circular Plate with Stepped thickness over a concentric circular region", *Journal of Acoustical Society of America*, 82(1), pp. 13-16.
22. Avalos, D., Laura, P. A. A., and Larrondo, H. A., 1988, "Vibrating Circular Plates with stepped thickness over a concentric circular region: a general approximate solution", *Journal of Acoustical Society of America*, 84(4), pp. 1181-1185.
23. Amabili, M., Pasqalini, A. and Dalpiaz, G., 1995, "Natural Frequencies and modes of free edge circular plates vibrating in vacuum or in contact with liquid", *Journal of Sound and Vibration*, 188, (5), pp. 685-699.
24. Kang, K. H. and Kim, K. J., 1996, "Modal properties of beams and plates on resilient supports with rotational and translational complex stiffness", *Journal of Sound and Vibration*, 190(2), pp. 207-220.

25. Kunukkasseril, V. X., Swamidas, A. S. J., 1974, "Vibrations of continuous circular plates", *International Journal of Solids and Structures*, 10, pp. 603-619.
26. Bodine, R. Y., 1967, "Vibration of a circular plate supported by a concentric ring of arbitrary radius", *Journal of the Acoustical Society of America*, 41, pp. 1551.
27. Singh, A. V., Mirza, S., 1976, "Free axisymmetric vibration of a circular plate elastically supported along two concentric circles", *Journal of Sound and Vibration*, 48, pp. 425-429.
28. Azimi, S., 1988, "Free Vibration of circular plates with elastic or rigid interior support", *Journal of Sound and Vibration*, 120(1), pp. 37-52.
29. Ding, Z., 1994, "Free vibration of arbitrarily shaped plated with concentric ring elastic and/or rigid supports", *Computers and Structures*, 50, pp. 685-692.
30. Chou, F. S., Wang, C. M., Chang, G. D., Olhoff, N., 1999, "Optimal design of internal ring supports for vibrating circular plates", *Journal of Sound and Vibration*, 219, pp. 525-537.
31. Wang, C. Y. and Wang, C. M., 2003, "Fundamental Frequencies of circular plates with internal elastic ring support", *Journal of Sound and Vibration*, 263, pp. 1071-1078.
32. Rdzanek Jr, W. P., Rdzanek, W. J. and Engel, Z., "Theoretical analysis of sound radiation of an elastically supported circular plate", *Journal of Sound and Vibration*, in press.
33. Itao, K. and Crandall, S. H., 1979, "Natural modes and natural frequencies of uniform, circular, free-edge plates", *Transactions of ASME, Journal of Applied Mechanics*, 46, pp. 448-453.
34. Southwell, R. V., 1922, "On the free transverse vibrations of uniform circular disc clamped at its center; and on the effects of rotation", *Proceedings of the Royal Society (London)* 101, pp. 133-153.
35. Hort, W and Koenig, M., 1922, "Studien U ber Schwingungen von Kreisplatten und Ringen", *Zeitschrift fur technische Physik (German)*, vol, 10, pp. 373.
36. Narayana Raju, P., 1962, "Vibrations of Annular Plates," *Journal of the Aeronautical Society of India*, vol. 14, pp.37.
37. Vogel, S. M., and Skinner, D. W., 1965, "Natural frequencies of transversely vibrating uniform annular plates", *Journal of Applied Mechanics*, 32, 926-931.
38. Winkler, E., 1867, "Die Lehre von der Elasticitaet und Festigkeit", Prag, Dominicus.

39. Hetenyi, M., 1946, "Beams on elastic foundations", University of Michigan Press.
40. Popov, E. P., 1951, "Successive approximation for beams on elastic foundations", Trans ASCE 116: pp. 1083-108.
41. Baker, A. L., 1957, "Raft foundations", Third ed. London: Concrete Publications Ltd.
42. Vesic, A. B., 1961, "Bending on beams resting on isotropic elastic solid", J. Eng Mech Div ASCE 2(87): pp. 35-53.
43. Kramrisch, F., Rogers, P., 1961, "Simplified design of combined footings", J. Soil Mech Div. ASCE 87(5): pp. 19-44.
44. Brown, C. B., Laurent, J. M., Tilton, J. R., 1977, "Beam – Plate system on Winkler foundation", J Eng Mech Div ASCE 103(4): pp. 589-600.
45. Dumir, P. C., 1988, "Large deflection axisymmetric analysis of orthotropic annular plates on elastic foundations", International Journal of Solids and Structures. 24, 777-787.
46. Smaile, J. S., 1991. "Large deflection response of annular plates on Pasternak foundations", "International Journal of Solids and Structures. 27(8), 1073-1084.
47. Weisensel, G. N, (1989) "Natural frequency for circular and annular plates", Journal of Sound and Vibration, Vol. 133, pp.129-134.
48. F. S. Chou, C. M. Wang, G. D. Cheng, N. Olhoff, 1999, "Optimal design of internal ring support for vibrating Circular plates", Journal of Sound and Vibration, 219 (3): 525-37.
49. A. W. Leissa, Vibration of Plates, Acoustical Society Of America, Sewickley. PA, 1993.
50. Leissa, A. W., 1993, "Vibration of plates, Acoustical Society of America", Sewickley, P.A.
51. Salari, M., Bert, C. M., Striz, A. G., 1987, "Free vibration of a solid circular plate free at its edge and attached to a Winkler foundation", Journal of Sound and Vibration, 118, pp. 188-191.
52. Laura, P. A. A, Gutierrez, R. H., Sanzi, H. C., Elvira, G., 1995, "The lowest axisymmetrical frequency of vibration of a circular plate partially embedded in a Winkler foundation", Journal of Sound and Vibration 185, pp. 915-919.
53. Celep, Z., 1988, "Circular plate on a tensionless Winkler foundation", Journal of Engineering Mechanics-ASCE114 (10), pp. 1723-1739.

54. Zheng, X. J., Zhou, Y. H., 1988, "Exact solution of nonlinear circular plate on elastic-foundation", *Journal of Engineering Mechanics-ASCE* 114, 1303-1316.
55. Ghosh, A. K., 1997, "axisymmetric dynamic response of a circular plate on an elastic foundation", *Journal of Sound and Vibration*, 105, pp. 112-120.
56. Bhaskara Rao. L & Kameswara Rao. C. "Vibrations Of Elastically Restrained Circular Plates Against Rotation and Supported by Partial Foundation", *Proceedings of Eight International Conference on Vibration Problems (ICOVP-2007)*, 31 Jan-3 Feb 2007, Bengal Engineering & Science University, Howrah, India.
57. Bhaskara Rao. L & Kameswara Rao. C. "Vibrations of Elastically Restrained Annular Plates on Elastic Foundation", *Fifteenth International Conference On Nuclear Engineering (ICONE15)*, ASME Paper ICONE15-10744, April 22-26, 2007, Japan.
58. Kirchhoff, G., 1876, *Vorlesungen iiber mathematische Physik*, Vol. 1, B. G. Teubner, Leipzig.
59. Love, A. E. H., 1944, "A Treatise on the Mathematical Theory of Elasticity", Dover Publications, Inc., New York, 1944.
60. Worch, G., 1956, "Elastische Scheiben", in *Beton-Kalender*, Vol.2, W. Ernst und Sohn, Berlin, pp. 31-120.
61. Bryan, G. H., 1891, "On the Stability of a Plane Plate under Thrust in its own Plane with Application to the Buckling of the Side of a Ship", *Proceedings, London Math Society*, 22, pp. 54-67.
62. Holanda, A. S., 2000, "Analysis of the Equilibrium and Stability of plates with contact Constraints", PhD thesis, Civil engineering Dept. PUC-Rio (in Portuguese).
63. Seide, P., 1958, "Compressive Buckling of a Long Simply Supported Plate on an Elastic Foundation", *Journal of Aerospace Sciences*, 25, pp. 382-394.
64. Warren, R. C., 1980, "Buckling of a Rectangular Plate on an Elastic Foundation. Compressed in Two Directions", Ph.D. thesis, Michigan State University.
65. Raju, K. K., and Rao, G. V., 1988, "Thermal Post-Buckling of Square Plate Resting on an Elastic Foundation by Finite Element Method", *Computers and Structures*, 28, pp. 195-199.
66. Kim, C. S. and Dickinson, S. M., 1990, "The Flectural Vibration of the Isotropic and Polar Orthotropic Annular and Circular Plates with Elastically Restrained Peripheries", *Journal of Sound and Vibration*, 143, pp. 171-179.

67. Wang, C. M., Xiang, Y., Kitipornchai, S., and Liew, K. M., 1993, "Axisymmetric Buckling of Circular Mindlin Plates with Ring Supports", *Journal of Structural Engineering*, 119(3), pp. 782-793.
68. Wang, C. M., and Tun Myint Aung, 2005, "Buckling of Circular Mindlin Plates with an Internal Ring Support and Elastically Restrained Edge", 131, pp. 359-366.
69. Wang, C. M., Wang, C. Y., and Reddy, J. N., 2005, *Exact Solutions for Buckling of Structural Members*, CRC Press, Boca Raton.
70. Bhaskara Rao, L and Kameswara Rao, C., 2007, "Buckling Of Circular Plates With an Internal Ring Support and Elastically Restrained Edge Against Rotation and Translation", Fifteenth International Conference On Nuclear Engineering (ICONE15), ASME Paper ICONE15-10864, April 22-26, 2007, Nagoya, Japan.
71. Mansfield, E. H., 1960, "On the Buckling of an Annular Plate", *Journal of Applied Mathematics*, 13, pp.16-23.
72. Timoshenko, S. P., Gere, J. M., 1961, "Theory of Elastic Stability", McGraw-Hill, New York.
73. Pflunger, A. 1964, "Stabilitats Probleme der Elastostatik", Berlin. Springer, pp. 448-453.
74. Westergaard, H. M., 1926, "Stresses in concrete pavements computed by theoretical analysis." *Public Roads*. 7(2), 23-35.
75. Huang, Y. H., 1974, "Finite element analysis of slabs on elastic solids", *Journal Ttrans. Engg.* , ASCE, 100(2).
76. Bhaskara Rao. L & Kameswara Rao. C., 2007, "Natural Frequency of Circular Plate Elastically Restrained Against Rotation and Resting on Winkler Foundation", *Proceedings of Eight International Conference on Vibration Problems (ICOVP-2007)*, 31 Jan-3 Feb 2007, p.p, 182-186, Bengal Engineering & Science University, Howrah, India.
77. Andrei Zagrai and Dimitri Donskoy, 2004, " A Soft Table for the Natural Frequencies and Modal Parameters of Uniform Plates with Elastic Edge Support", *Journal of Sound and Vibration*
78. Bhaskara Rao. L & Kameswara Rao. C. "Vibrations Of Elastically Restrained Circular Plates on Winkler-Pasternak Foundation", *Fifteenth International Conference On Nuclear Engineering (ICONE15)*, ASME Paper ICONE15-10340, April 22-26, 2007, Japan.
79. Bhaskara Rao. L & Kameswara Rao. C. "Buckling of Annular Plate With an Elastically Restrained Outer Edge Against Rotation And Simply Supported", *International Conference*

On Computer Aided Engineering 2007 (CAE 2007), December 13 -15, 2007, IIT Chennai, India.

80. Bhaskara Rao. L & Kameswara Rao. C. “Buckling Of Circular Plates with an Internal Elastic Ring Support and Elastically Restrained Guided Edge Against Translation”, International Conference On Vibration Engineering and Technology Of Machinery (VETOMAC-IV), December 17-19, 2007, pp. 393-400, Osmania University, Hyderabad, India.

81. A. W. Leissa 1973, *NASA SP-228*. Vibration of shells.

82. Bhaskara Rao. L & Kameswara Rao. C. “Vibrations Of Circular Plates on Elastic Foundation With an Internal Elastic Ring Support and Restrained Edge Against Rotation”, International Conference On Vibration Engineering and Technology Of Machinery (VETOMAC-IV), December 17-19, 2007, pp. 381-392, Osmania University, Hyderabad, India.

83. Bhaskara Rao. L & Kameswara Rao. C. “Buckling of Annular Plates with an Elastically Restrained Guided Edge Against Translation”, 16th International Conference on Nuclear Engineering (ICONE16), ASME Paper ICONE16-48427, May 11-15, 2008, Orlando, Florida, USA.

84. Bhaskara Rao. L & Kameswara Rao. C. “Natural Frequency of Elastically Restrained Circular Plates with Partial Winkler Foundation”, 16th International Conference on Nuclear Engineering (ICONE16), ASME Paper ICONE16-xxxxx, May 11-15, 2008, Orlando, Florida, USA.

85. Bhaskara Rao, L and Kameswara Rao, C., 2007, “Vibrations of Circular Plates with an Internal Ring Support and Flexible Edge Conditions”, Proc. of International Conference on Advances in Machine Design and Industry Automation (ICAMDIA-2007), COE, Pune, India, (2007) 182-186.

86. Bhaskara Rao. L & Kameswara Rao. C., 2008, “Frequency Analysis of Circular Plates With an Internal Elastic Ring Support and Flexible Edge”, 16th International Conference on Nuclear Engineering (ICONE16), May 11-15, 2008, Orlando, Florida, USA.

87. Kim, C. S. and Dickinson, S. M., 1989, “On the Lateral Vibration of Thin Annular and Circular Composite Plates Subject to Certain Complicating Effects,” Journal of Sound and Vibration, Vol. 130, pp 363-377.

88. Wang, X., Striz, A. G. and Bert, C. W., 1993, “Free Vibration Analysis of Annular Plates by the DQ method,” Journal of Sound and Vibration, Vol. 164, pp.173-175.

89. Larrando, H., Topalian, V., Avalor, D. R and Laura, P. A. A., 1994, “Free Vibration Analysis of Annular Plates by the DQ Method,” Journal of Sound and Vibration, Vol.177, pp. 137-139.

90. Bhaskara Rao. L & Kameswara Rao. C., "Frequency Analysis of Annular Plate With Internal and External Elastically Restrained Edge", Proceedings of International Conference on Advances in Machine Design and Industry Automation (ICAMDIA-2007), 10-12 Jan 2007, pp, 171-175, College of Engineering, Pune, India.
91. Amabili, M., Frosali, G., and Kwak, M. K, 1996, "Free Vibrations of Annular Plates Coupled with Fluids", Journal of Sound and Vibration, 191(5) pp. 825-846.